Stony Brook University

Design, synthesis and biological evaluation of new-generation taxoid-based tumor-targeting drug conjugates

A Dissertation Presented

by

Edison S. Zuniga

to

The Graduate School

in Partial Fulfillment of the

Requirements

for the Degree of

Doctor of Philosophy

in

Chemistry

Stony Brook University

May 2012

Stony Brook University

The Graduate School

Edison S. Zuniga

We, the dissertation committee for the above candidate for the

Doctor of Philosophy degree, hereby recommend

acceptance of this dissertation.

Iwao Ojima
Dissertation Advisor
Distinguished Professor, Department of Chemistry

Frank W. Fowler
Chairperson of Defense
Professor, Department of Chemistry

Kathlyn A. Parker
Third Member
Professor, Department of Chemistry

Susan B. Horwitz
Outside Member
Distinguished Professor, Department of Molecular Pharmacology
Albert Einstein College of Medicine

This dissertation is accepted by the Graduate School

Charles Taber
Interim Dean of the Graduate School

Abstract of the Dissertation

Design, synthesis and biological evaluation of new-generation taxoid-based tumor-targeting drug conjugates

by

Edison S. Zuniga

Doctor of Philosophy

in

Chemistry

Stony Brook University

2012

Over the past decades, chemotherapy has transitioned to an age of "targeted therapy." The development of Gleevec (Novartis) and Tarceva (Genentech and OSI Pharmaceuticals) has revolutionized the treatment of certain cancers, such as chronic myelogenous leukemia (CML), non-small cell lung cancer (NSCLC) and pancreatic cancer. Gleevec specifically targets the cancer cell-overexpressed Abl tyrosine kinase, and Tarceva targets the epidermal growth factor receptor that is mutated in different types of cancers. However, the use of these modern targeted-therapies is limited to specific cancer types. Therefore, considerable efforts have been made to find cancer-specific markers which can be exploited for tumor-specific delivery of more traditional chemotherapeutic drugs. A promising approach along this line is the development of tumor-targeting drug conjugates, which consists of one or multiple cytotoxic drugs (warheads) connected to a tumor-targeting module (TTM) via cleavable covalent bonds or cleavable linkers. The drug conjugates have been designed to remain inactive until they are specifically delivered to the tumor site, guided by the TTM and internalized, where the warhead is released from the carrier, restoring its original activity. New-generation taxoids have been developed by the Ojima laboratory via the β-lactam synthon method. These taxoids show orders of magnitude greater potency in a number of cancer cell lines compared to the parent compound paclitaxel. Thus, new-generation taxoids are promising candidates as warheads for tumor-targeting drug conjugates. Accordingly, a number of new-generation taxoid-based drug conjugates have been developed that contain polyunsaturated fatty acids (PUFAs), vitamins and monoclonal antibodies (mAbs) as TTM. The synthesis and biological evaluation of these novel drug conjugates will be discussed.

Dedication Page

The following is dedicated to the meals enjoyed and those missed in a day's work.

Table of Contents

Chapter 3
Polyunsaturated Fatty Acids as Tumor-Targeting Modules

Chapter 4
Mechanism-Based Cleavable Disulfide Linkers

Chapter 5
Vitamins as Tumor-Targeting Modules

Chapter 6
Design, Synthesis and Biological Evaluation of Novel Tumor-Targeting Drug Conjugates with Dual-Guiding Modules and Dual-Warheads. 1. Drug Conjugate with SB-T-1214 and Camptothecin.

Chapter 7
Design, Synthesis and Biological Evaluation of Novel Tumor-Targeting Drug Conjugates with Dual-Guiding Modules and Dual-Warheads. 2. Drug Conjugate with SB-T-1214 and Topotecan.

Chapter 8
Design, Synthesis and Biological Evaluation of Novel Tumor-Targeting Drug Conjugates with Dual-Guiding Modules and Dual-Warheads. 3. Drug Conjugate with Biotin and Folic Acid and Other Applications.

Chapter 9
Macromolecular Drug Delivery Systems

List of Figures

Figure **Page**

Chapter 1

Chapter 2

Chapter 3

Chapter 4

Chapter 5

Chapter 6

Chapter 7

Chapter 8

Chapter 9

List of Schemes

Scheme **Page**

Chapter 1

Chapter 3

Chapter 4

Chapter 5

Chapter 6

Chapter 7

Chapter 8

Chapter 9

List of Tables

Table **Page**

Chapter 1

Chapter 2

Chapter 3

Chapter 4

Chapter 5

Chapter 6

Chapter 7

List of Abbreviations

5-FU	5-Fluorouracil
10-DAB III	10-Deacetylbaccatin III
°C	Degrees Celsius
μM	Micromolar
ABC	ATP-binding cassette
Ac	Acetyl
Ad	Adenovirus
ADC	Antibody-drug conjugate
AIDS	Acquired immune deficiency syndrome
ALL	Acute lymphoblastic leukemia
Alloc	Allyloxycarbonyl
APC	Allophycocyanin
Arg	Arginine
Asp	Asparagine
ATP	Adenosine triphosphate
Az	Azide
BOC	*tert*-Butyl carbonate
Bu	Butyl
BuLi	Butyl lithium
CAM	Cerium-ammonium-molybdate
CAN	Ceric ammonium nitrate
CAR	Coxsackievirus-adenovirus receptor
Cbz	Carboxybenzyl
CD	Cluster of differentiation
CDC	Complement-dependent cytotoxicity
CDI	Carbonyldiimidazole
cDNA	Complementary DNA
CDR	Complementarity-determining region
CFM	Confocal microscopy
CI	Combination indices
Cit	Citruline
CMF	Cyclophosphamide, methotrexate and 5-fluorouracil
CML	Chronic myelogenous leukemia
COSY	Correlation spectroscopy
CPT	Camptothecin
CSC	Cancer stem cell
d	Day
DCC	*N*,*N*'-Dicyclohexylcabodiimide
DDS	Drug delivery system
DGA	Diglycolic acid
DHA	Docosahexaenoic acid
DIC	Diisopropylcarbodiimide
DIPEA	*N*,*N*-Diisopropylethylamine
DMAc	Dimethylacetamide

DMAP	4-Dimethylaminopyridine
DMF	Dimethylformamide
DMSO	Dimethyl sulfoxide
DNA	Deoxyribonucleic acid
DNase	Deoxyribonuclease
DPC	Di-2-pyridyl carbonate
DPBS	Dulbecco's Phosphate buffered saline
ECL	Enhanced chemiluminescence
EDC	1-Ethyl-3-(3-dimethylaminopropyl)carbodiimide
ee	Enantiomeric excess
EGFR	Epidermal growth factor receptor
EMEM	Eagle's minimal essential medium
EPA	Eicosapentaenoic acid
Et	Ethyl
EtOH	Ethanol
eV	Electonvolt
FA	Folic acid
Fab	Fragment of antigen binding
FACS	Fluorescence-activated cell sorting
FBS	Fetal Bovine Serum
Fc	Constant fragment
FDA	Food and drug administration
FITC	Fluorescein isothiocyanate
Fmoc	Fluorenylmethyloxycarbonyl
FR	Folate receptor
g	Gram
GABA	γ-Aminobutyric acid
Glc	Glucose
Glu	Glutamic acid
Gly	Glycine
gp60	glycoprotein 60
GSH	Glutathione
GSH-OEt	Glutathione ethyl ester
GTP	Guanosine-5'-triphosphate
h	Hours
HA	Hylauronic acid
HBTU	*O*-Benzotriazole-*N*,*N*,*N'*,*N'*-tetramethyluroniumhexafluorophosphate
HL	Hodgkin lymphoma
HOAc	Acetic acid
HObt	Hydroxybenzotriazole
HOSu	*N*-Hydroxysuccinimide
HPLC	High-performance liquid chromatography
HSA	Human serum albumin
Hz	Hertz
IC_{50}	Half maximal inhibitory concentration
Ig	Immunoglobin

IPA	Isopropanol
k	Kilo
L	Liter
Leu	Leucine
LiHMDS	Lithium bis(trimethylsilyl)amide and lithium hexamethyldisilazide
LNA	Linolenic acid
Luc	Luciferase transgene
Lys	Lysine
m	Meter
mAbs	Monoclonal antibodies
MACS	Magnetic activated cell sorting
MALDI	Matrix-assisted laser desoprtion/ionization
MATE	Multi-antimicrobial extrusion protein family
MDR	Multidrug resistance
Me	Methyl
MFS	Major facilitator superfamily
mg	Milligram
MHz	Megahertz
min	Minutes
mL	Milliliter
MMAE	Monomethylauristatin E
mmol	Millimole
MOI	Multiplicities of infection
MOMP	Mustard, oncovin, methotrexate and prednisone
MOPP	Mustard, oncovin, procarbazine and prednisone
m.p.	Melting point
MSCBM	Mesenchymal stem cell basal medium
Ms	Mesyl
MsCl	Mesyl chloride
MTT	3-(4,5-Dimethylthiazol-2-yl)-2,5-diphenyltetrazolium bromide
NCI	National Cancer Institute
NFPA	Nonfunctional pituitary adenoma
nM	Nanomolar
NMR	Nuclear magnetic resonance
NPC	Nuclear pore complex
NSCLC	Non-small-cell lung carcinoma
OC	Ovarian cancer
PBS	Phosphate buffer solution
PCR	Polymerase chain reaction
PE	Phycoerythrin
PEG	Polyethylene glycol
PET	Positron emission tomography
Pgp	P-glycoprotein
Ph	Phenyl
Phe	Phenylalanine
pM	Picomolar

PMA	Phosphomolybdic acid
PMP	p-Methoxyphenyl
Pr	Propyl
PUFA	Polyunsaturated fatty acid
py	Pyridine
r.t.	Room temperature
RGD	Arg-Gly-Asp
RME	Receptor-mediated endocytosis
RNA	Ribonucleic acid
RND	Resistance-nodulation-cell division superfamily
RPMI	Roswell Park Memorial Institute medium
s	Seconds
SAR	Structure-activity relationship
SB-T	Stony Brook taxoid
scFv	Single-chain variable fragment
SCID	Severe combined immune deficiency
SCLC	Small-cell lung carcinoma
SDS-PAGE	Sodium dodecyl sulfate polyacrylamide gel electrophoresis
SET	Single electron transfer
SMR	Small multidrug resistance family
SPARC	Secreted protein acidic and rich in cysteine
SPECT	Single-photon emission tomography
TBDMS	*tert*-Butyldimethylsilyl
TES	Triethylsilyl
TESCl	Triethylsilyl chloride
TFA	Trifluoroacetic acid
THF	Tetrahydrofuran
TIPS	Triisopropyl
TLC	Thin layer chromatography
topo I	Topoisomerase I
TIPS	Triisopropylsilyl
TIPSCl	Triisopropylsilyl chloride
TPPO	Triphenyphosphineoxide
TRAIL	THF related apoptosis inducing ligand
TTM	Tumor-targeting module
ULA	Ultra-low attachment
Val	Valine

Acknowledgments

It is with my utmost sincerity that I thank my advisor, Distinguished Professor Iwao Ojima, who has made the completion of this thesis and the work therein described a reality through an ardent devotion to his craft and undeniable chemical insight. Professor Ojima took a chance in accepting me into his laboratory, and though there were times when I have disappointed, he has shown patience and has been steadfast in offering guidance and advice throughout the years. He has provided opportunities that are unmatched among his colleagues and he has enveloped me in both medicinal and synthetic chemistry. Among all else, with discipline, resolve and an uncanny attention to detail, Professor Ojima has provided an invaluable educational environment for which I am wholeheartedly grateful for and indebted to him.

I would like to thank my committee members, Professor Frank Fowler and Professor Kathlyn Parker for their support and encouragement throughout the years. They have always been eager to help as I advanced in the Ph.D. program; guiding me through the corresponding nuances and allotting their time and efforts when I have requested it. I would especially like to thank Distinguished Professor Susan Horwitz for agreeing to be my "Outside Member" for my defense. I am absolutely honored that she, who has made remarkable contributions to medicinal chemistry and molecular biology, will attend my defense and critique my work.

When I applied for a degree in Chemistry, I never thought that I would have done so much cellular biology. This part of my research would not be possible without the help of Dr. Galina Botchkina, Rebecca Rowehl and Dr. Anne Savitt. Dr. Botchkina has welcomed me with open arms to work with her in her lab. She has taught me some invaluable lessons within and beyond the scope of molecular biology and cancer stem cell research. Rebecca Rowehl and Dr. Anne Savitt taught me the basics of cell culture and both continue to be extremely helpful and encouraging. Also, Dr. Guo-Wei Tian (Central Microscopy Imaging Center), the entire Research Flow Cytometry Core Facility Staff and Kathleen Hill (OSA Supply Center) have played a detrimental role in the completion of this dissertation.

In addition to Professor Iwao Ojima, I would like to thank Professors Isaac Carrico, Nancy Goroff, Kathlyn Parker and Jin Wang. I learned a great deal from their courses in my first year, which helped ease my transition to research. I again want to thank Professor Frank Fowler, as well as Professor Joseph Lauher, Professor Sampson, Dr. Susan Oatis, Dr. Rong Chen and Dr. Zachary Katsamanis for their support and guidance when I was a teaching assistant for the organic lecture course. Simply put, they made me famous.

It has been my esteemed pleasure to have worked with a number of remarkable individuals and collaborators within and outside the Ojima laboratory. Patricia Marinaccio will always be appreciated for everything she has done for me; large, small and otherwise. Where Professor Ojima is the brain of the laboratory, Pat is definitely the heart. Since my first day in the lab, she has always been generous and caring. I will never forget when she guided me through my 1st meeting; continuing to do so until my defense and beyond. I am indebted to her. Yoko Ojima is another person that has made life in Stony Brook welcoming during the years. She has been a gracious and lovely host for a number of Ojima group events. I am extremely thankful to my mentors Dr. Xianrui "Ray" Zhao and Dr. Liang Sun, who are both highly skilled and dedicated chemists that have helped me through my initial struggles in the lab. I was also fortunate to have worked with a number of individuals on the "cancer team." Ilaria Zanardi, Dr. Larisa Kuznetsova, Dr. Anushree Kamath, William T. Berger, Joshua D. Seitz, Tao Wang, Wen

Chen and Jacob G Vineberg have all played in integral part in my research and have provided a few laughs along the way. Professor Isaac Carrico, Dr. Partha Banerjee and I have collaborated on a project which is discussed in this dissertation; the National Cancer Institute (NCI), Dr. Stanislaus S. Wong and David Tan were also involved in other collaborations. All of their efforts are much appreciated.

It has also been a privilege to work with a number of Ojima group members throughout the years. We have all shared good times, good food and good discussion. Chi-Feng "Corey" Lin and I entered the Ojima lab together. He is the best chemist in the Ojima lab today and I am grateful for the time and discussion shared. Dr. Kunal Kumar and Alexandra A. Athan have made engaging company and good friends. Dr. Gary Teng, Chih-Wei Chien, Divya Awasthi, Bora Park, Yang Zang, Dr. Tadashi Honda, Dr. Suqing Zheng, Dr. Motohiro Takahashi, Roxanne Brockner and Dr. Béla Ruzsicska have all contributed to the completion of this dissertation. Dr. Jin Chen, Dr. Ce Shi, Dr. Stephen Chaterpaul, Dr. Santosh L. Yennurajalingam, Hiroki Moriwaki, Dr. Manisha Das, Dr. Joseph Kaloko, as well as the past and present Master's students and Ojima group members have also made contributions. I would also like to thank all of the visiting, undergraduate and high school students that I have mentored in the lab throughout the years. They have given me the opportunity to grow as an educator and have strengthened my understanding of organic chemistry. Lastly, I would like to thank all of the 7th floor chemistry groups, the Chemistry Class of 2006, the members of Chem Masters Int. and the folks at SVPS for the good time.

Stony Brook has been home for six years, and for that I thank Carol Brekke. Carol was the first person who I spoke with in Stony Brook and she is the main reason why I joined the Department of Chemistry. She will be remembered. Katherine Hughes has been an indispensable asset to me and the Department of Chemistry. Her tireless efforts are richly appreciated and detrimental to my advancement in the Ph.D. program. I would like to thank Heidi Ciolfi, Lizandia Perez, Barbara Schimmenti and Charmine Yapchin for their efforts in assuring that my administrative duties were completed and for providing a welcoming atmosphere in the Chemistry Main Office. The efforts put forth by Dr. Alvin Silverstein, Michael Teta and Dr. Deborah Stoner-Ma are duly noted and appreciated. All research will be at a standstill if it were not for their efforts in making the Chemistry building operational. Linda Dixon and Bradford Tooker have always provided encouraging words. Without NMR specialists Dr. James Marecek and Francis Picart, my research would be meaningless. A special thank you goes to Kathy Fortmueller, Maxine Purini as well as the rest of the custodial staff for also providing a warm and welcoming environment.

This dissertation would not be possible without the support of my family and friends. I especially thank my mom, dad, brother and the rest of my family. Without fail, they have always given me support and love when I most needed it. Without them, I am nothing. A big thank you goes to Winnie Situ for all of her help, as well as Christina B., Baaba B., Candace C., Ashley C., Brittany C., Kristen D., Diane F., Victoria G., Gabriel H., Blaine H., Suhani P., Penny P., Otessa W., Anni X. and the Satsri family for being there.

Vita

Education:

2004	B.A.	University of Washington
2004	B.S.	University of Washington
2012	Ph.D.	Stony Brook University

Publications:

Botchkina, G. I.; **Zuniga, E.S.**; Das, M.; Wang, Y.; Wang, H.; Zhu, S.; Savitt, A.; Rowehl, R.; Leyfman, Y.; Ju, J.; Shroyer, K.; Ojima, I. New-generation taxoid SB-T-1214 inhibits stem cell-related gene expression in 3D cancer spheroids induced by purified colon tumor-initiating cells. *Molecular Cancer* **2010**, *9*, 192-204.

Banerjee, P.S.; **Zuniga, E.S.**; Ojima, I.; Carrico, I.S. Targeted and armed oncolytic adenovirus via chemoselective modification. *Bioorg. Med. Chem. Lett.* **2011**, *21*, 4985-4988.

Reviews:

Ojima, I.; Das, M.; **Zuniga, E.** Novel taxoid-based tumour-targeting drug conjugates. *Chimica Oggi/Chemistry Today* **2009**, *27*, 54-56.

Ojima, I.; **Zuniga, E.S.**; Berger, W.T.; Seitz, J.D. Tumor-targeting drug delivery of new-generation taxoids. *Future Med. Chem.* **2012**, *4*, 33-50.

Selected Presentations:

Zuniga, E.S.; Shah, P.; Reimer, A.; Ojima, I. Towards novel tumor-targeting anticancer drug conjugates. 239th ACS National Meeting, San Francisco, CA, 2010

Zuniga, E.S.; Ojima, I. Novel tumor-targeting drug conjugate bearing a taxoid and topotecan. 240th ACS National Meeting, Boston, MA, 2010

Zuniga, E.S.; Ojima, I. Design, synthesis and biological evaluation of tumor-targeting drug conjugates bearing dual-warheads. 242nd ACS National Meeting, Denver, CO, 2011

Chapter 1

Synthesis and Biological Evaluation of New-Generation Taxoids

Chapter Contents

§ 1.1.0 Introduction

§ 1.1.1 Cancer

Cancer is a collection of diseases defined by the rapid proliferation of abnormal cells which have the tendency to invade surrounding tissue. Cancer cells use the machinery of normal, healthy cells to become immortal and self-sufficient. Cancer begins with a mutation in the genetic code causing a once healthy single cell to become abnormal. This abnormal cell grows self-sufficient in growth signals, becomes insensitive to anti-growth signals, develops sustained angiogenesis, divides with limitless potential, evades apoptosis, invades surrounding tissue and has the potential to metastasize (Figure 1.1).[1]

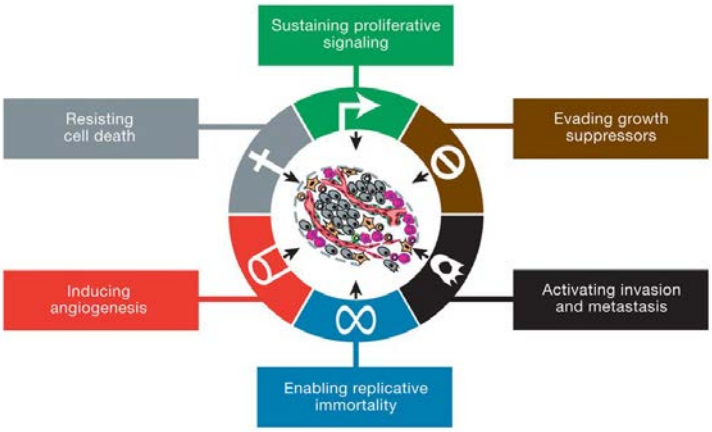

Figure 1.1: The hallmarks of cancer (adapted from [1])

Cancer is the leading cause of death in developed countries and is the second leading cause in developing countries.[2] Currently, one out of every four deaths in the United States is caused by cancer, and it has been estimated that there will be approximately 1.6 million new cancer cases and over half a million deaths from cancer in the United States in 2011.[3] Furthermore, it has been estimated that one in every two men and one in every three women living in North America will develop some form of cancer during their lifetime.[4]

Despite numerous medical advances, a cure for cancer has not been found. Furthermore, there is no cure-all treatment, as several treatment modes are employed and many of them are used in combination. These treatment modes are: (1) surgery, a physically invasive procedure which entails the removal of the cancerous tissue from the body; (2) radiation therapy, which is the use of high-energy light beam to irradiate cancerous tissues; (3) biological therapy, which attempts to use the body's natural defenses to recognize and destroy cancer; (4) gene therapy, which uses genes to activate an apoptotic pathway in cancer cells; (5) anti-angiogenic therapy, which involves blocking the blood supply to tumor tissues; and (6) chemotherapy, which entails the use of chemical agents to induce death in cancer cells.

Each treatment mode has its advantages and disadvantages. Chemotherapy is advantageous in that it is not invasive and the delivery of the chemotherapeutic agents is simple (e.g. orally or intravenously). Chemotherapeutics work on the premise that rapidly dividing cells can be identified and eradicated by inhibiting cell growth. There are several classes of chemotherapeutics each with different mechanisms of action. A large number of these

chemotherapeutic agents are plant alkaloids, and some function to block cell division by influencing microtubule dynamics (e.g. paclitaxel and vincristine) or interfere with the replication and transcription of DNA (e.g. topotecan).[5-8] Given their inhibitory activity, chemotherapeutic agents alter normal cellular machinery, inducing apoptosis in cells.

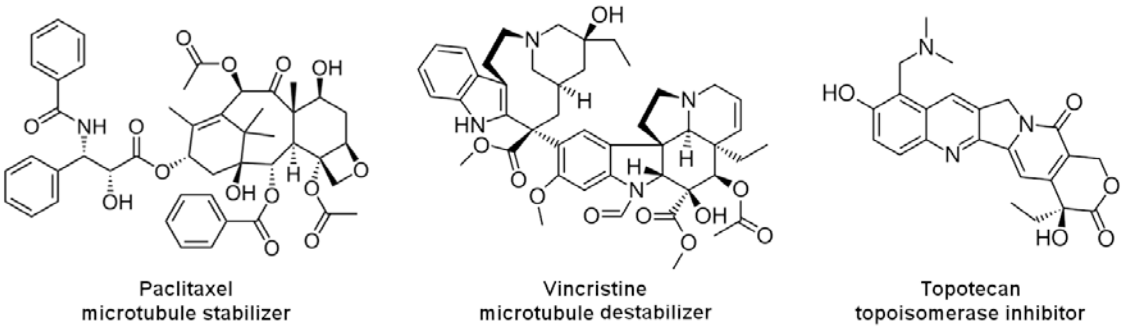

Figure 1.2: Examples of chemotherapeutic agents

§ 1.1.2 Paclitaxel

Paclitaxel and docetaxel, the semi-synthetic analog of paclitaxel, are two of the most widely used chemotherapeutic agents today. In 1962, extracts from the bark of the pacific yew tree, *Taxus brevifolia*, were found to have 9KB cytotoxic activity.[9] In the late 1960s, the active compound, isolated from plant extracts, was identified as taxol (paclitaxel). The isolation of taxol was guided by bioassay of the plant extracts.[9] At various steps along isolation, fractions were screened against the Walker WM tumor inhibition assay.[9] The structure of paclitaxel was reported in 1971.[10] The compound is a complex diterpene that consists of four fused rings, including a very rigid oxetane (D-ring), with an *N*-benzoylphenylisoserine side chain at the C-13 position of the A-ring.

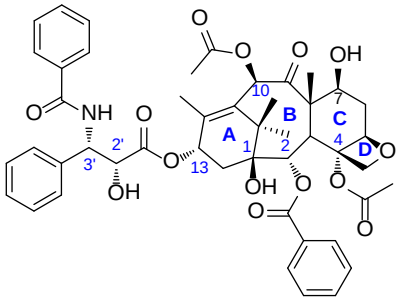

Figure 1.3: Paclitaxel

In 1979, Horwitz et al. discovered that paclitaxel is a microtubule assembly promoter, which induces microtubule polymerization, stabilizes the microtubules formed and prevents depolymerization, thereby inhibiting the normal dynamic reorganization of the microtubular network necessary for cell division, thus inducing apoptosis.[11, 12] Microtubules are the structural components of cytoskeleton that are formed by the polymerization of α and β tubulin heterodimers.[13] The α and β tubulin heterodimers polymerize by nucleation-elongation, where tubulin dimers are added at the ends of a short microtubule "nucleus".[14] The tubulin heterodimers lay head-to-tail, where an α-subunit of one dimer is in contact with the β-subunit of

another dimer. The resulting protofilaments comprise the backbone of the microtubule and each microtubule consists of 13 protofilaments arranged in an imperfect helix.[14] The assembly and disassembly of microtubules is essential in cell division, as microtubules are responsible for the formation of the mitotic spindle. Thus, microtubules play a vital role in the transportation of smaller organelles within cells. Tubulin is the target of several antitumor agents, such as colchicine and vinblastine (mitotic spindle formation inhibitors) or taxoids (mitotic spindle disassembly inhibitors).[14-17]

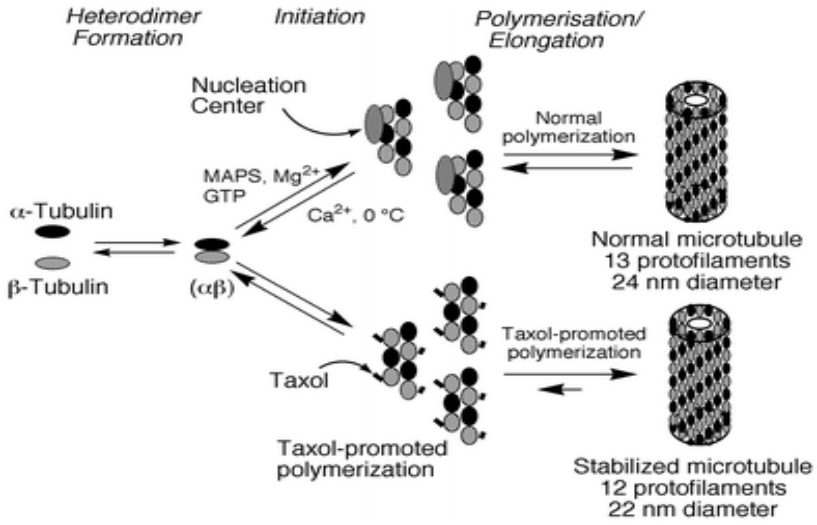

Figure 1.4: Microtubule formation in taxol and taxol-free cells (adapted from [11])

Taxoids promote microtubule assembly and stabilize the resulting microtubule formed, thereby inhibiting the disassembly of the mitotic spindle, stopping chromosome segregation and arresting mitosis in the G_2/M phase, eventually inducing apoptosis.[11, 12] Taxoids bind to the α,β-tubulin heterodimer aggregates in a 1:1 ratio to promote polymerization and stabilize the resulting microtubules in an irreversible manner (Figure 1.4). The resulting microtubule contains 12 protofilaments and is stabilized against depolymerization conditions. The effects that paclitaxel, as well as new-generation taxoids and discodermolide have on microtubule formation can be seen in the electromicrographs shown in Figure 1.5.[18]

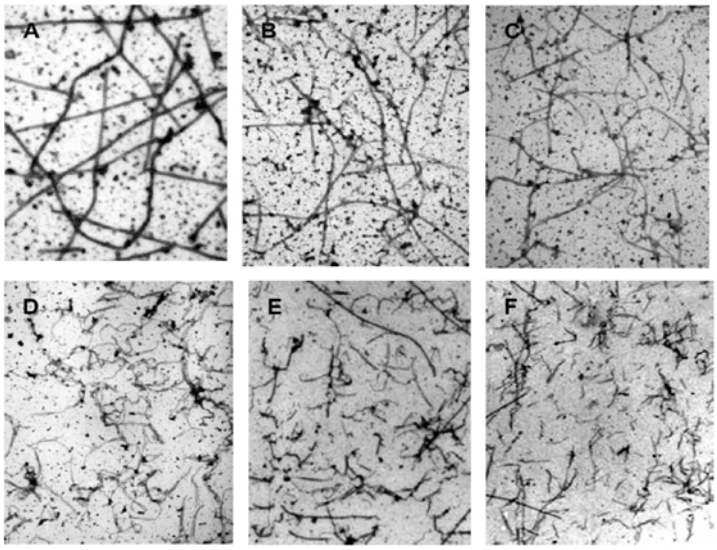

Figure 1.5: Electromicrograhs of microtubules (20000x) containing: (A) GTP; (B) paclitaxel; (C) SB-T-1214; (D) SB-T-121303; (E) SB-T-121213; (F) discodermolide (adapted from [18])

Figure 1.5 shows the electromicrographs of microtubules formed with GTP, paclitaxel, new-generation taxoids and discodermolide (a potent microtubule stabilizing agent).[18] As seen from the figure, GTP and paclitaxel form long and straight microtubules. In contrast, the microtubules formed with SB-T-1214 are shorter than those with GTP or paclitaxel.[18] Furthermore, the microtubules formed with SB-T-121203 and SB-T-121313 are shorter, more numerous and have more curvature. The microtubules formed with discoderomilde are similar to those formed with SB-T-121203 and SB-T-121313. These results suggest that the formation of short and numerous microtubules is related to the instantaneous rapid polymerization of tubulin.[18]

§ 1.1.3 Synthesis of Paclitaxel

Paclitaxel has been approved by the FDA for the treatment of advanced ovarian cancer (1992), breast cancer (1994), AIDS related Kaposi's sarcoma (1997) and non-small-cell lung cancer (1999). Docetaxel has also shown great promise in clinical trials. Offering excellent anticancer potency, the demand of paclitaxel greatly outweighs its supply. The pacific yew is a slow-growing coniferous tree found in the old-growth forest of the American Pacific Northwest.[19] Extracts of pacific yew bark is the only known natural source of paclitaxel, however, stripping the bark is fatal to the tree, making it a limited and nonrenewable source.

There have been a number of research groups that have attempted and successfully reported the total synthesis of paclitaxel. In 1994, Holton reported the first total synthesis of paclitaxel, which required more than 37 steps starting from patchoulene oxide.[20, 21] In the same year, Nicolaou published a synthetic route towards paclitaxel, which required the pre-assembly of 3 synthons. This total synthesis was published in 1995.[22-25] Other total syntheses have been reported by Danishefsky (1996),[26] Wender (1997),[27] Kuwajima (1998),[28] Mukaiyama (1999)[29] and Takahashi (2006).[30] It is worthy of note, that each synthetic route entails the synthesis of a baccatin III derivative followed by the Ojima-Holton β-lactam coupling method. Furthermore, each synthesis requires several steps resulting in low overall yield.

Although the total synthesis of paclitaxel proved to be a significant challenge for synthetic chemists, it was found that a semisynthetic precursor can be found in the leaves of *Taxus baccata* (European yew) or *Taxus wallichiana* (Himalayan yew).[31, 32] This was an important discovery because the yew leaves provided a readily renewable source for a key intermediate, 10-deacetylbaccatin III (10-DAB III) (Figure 1.6).

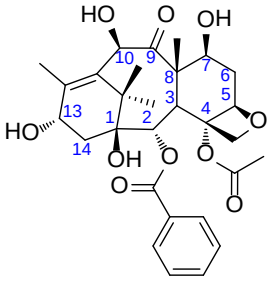

Figure 1.6: 10-Deacetylbaccatin III

In 1988, the first semi-synthetic route towards paclitaxel was reported using a 10-DAB III derivative by Greene and Potier (Scheme 1.1). However, epimerization occurred at the C-2' position of the side chain due to high reaction temperature (73 °C) and long reaction time (100 h).[31]

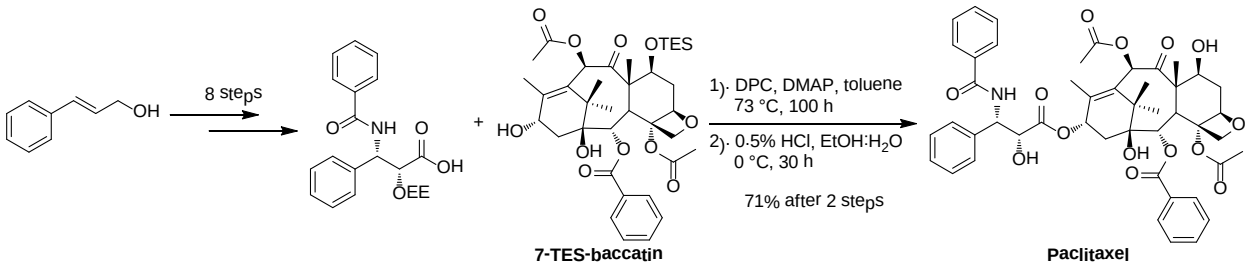

Scheme 1.1: Greene's semi-synthetic route towards paclitaxel

In 1984, the French pharmaceutical company Rhone-Poulenc Rorer (currently Sanofi-Aventis) developed docetaxel (Taxotére®).[32-34] This semi-synthetic analog of paclitaxel contains a *N-tert*-butoxycarbonyl moiety at the C-3' position and a free hydroxy moiety at the C-10 position. Docetaxel has the same mechanism of action as paclitaxel but was found to be twice as active. The FDA approved docetaxel for the treatment of breast cancer (1996) and non-small cell lung cancer (1999).[35]

§ 1.1.4 Application of the β-Lactam Synthon Method towards the Synthesis of Taxoids

With the readily available 10-DAB III, a substantial supply of paclitaxel can be obtained in a semi-synthetic means via the β-lactam synthon method.[36, 37] Enantiomerically enriched β-lactams can be used to efficiently introduce the C-13 side-chain, the (3*R*,4*S*)-*N*-benzoylphenylisoserine moiety, of paclitaxel. Changing the substituents of the β-lactam core modifies the C-13 side chain, thus giving a new series of paclitaxel analogs, which have orders of magnitude greater potency, better bioavailability and greater tumor specificity.

The β-lactam synthon method is a practical and versatile method for the semisynthesis of paclitaxel, docetaxel, and new taxoid analogs via 1-acyl-3-hydroxy β-lactams as key intermediates (Scheme 1.2).[36, 38, 39]

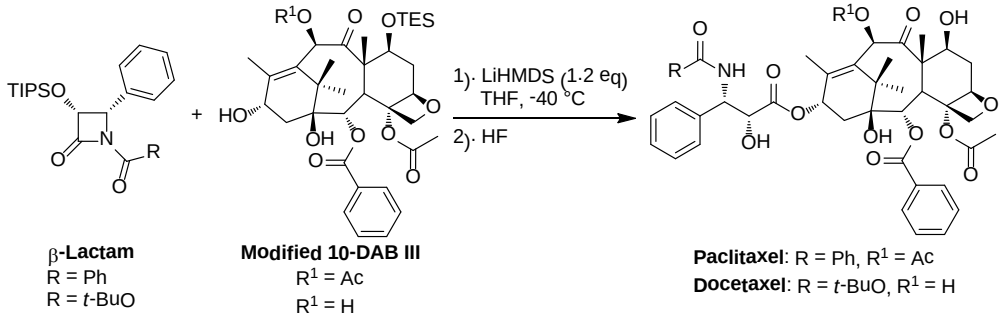

Scheme 1.2: The Ojima-Holton coupling protocol for the synthesis of taxoids

It was determined that 1-benzoyl-(3*R*,4*S*)-3-oxotriisopropylsilyl-4-phenyl-2-azetidinone serves as the key intermediate for the synthesis of paclitaxel and 1-*t*-Boc-(3*R*,4*S*)-3-oxotriisopropylsilyl-4-phenyl-2-azetidinone is an excellent intermediate towards the synthesis of docetaxel. Both of these β-lactams are readily derived from (3*R*,4*S*)-3-oxotriisopropylsilyl-4-phenyl-2-azetidinone, and can be coupled to modified baccatin III derivatives in excellent yields. The desired taxoid can be obtained after deprotection. Thus, the β-lactam synthon method is a highly efficient and practical route towards paclitaxel, docetaxel and new taxoid analogs.

Using this method, several new-generation taxoids have been prepared.[36, 39, 40] By incorporating fluorine-containing β-lactams, fluorine-containing taxoids can be prepared in the same manner.[41-43] Extensive structure-activity relationship (SAR) studies have been conducted on paclitaxel, docetaxel and their analogs. These findings are summarized in Figure 1.7.[44]

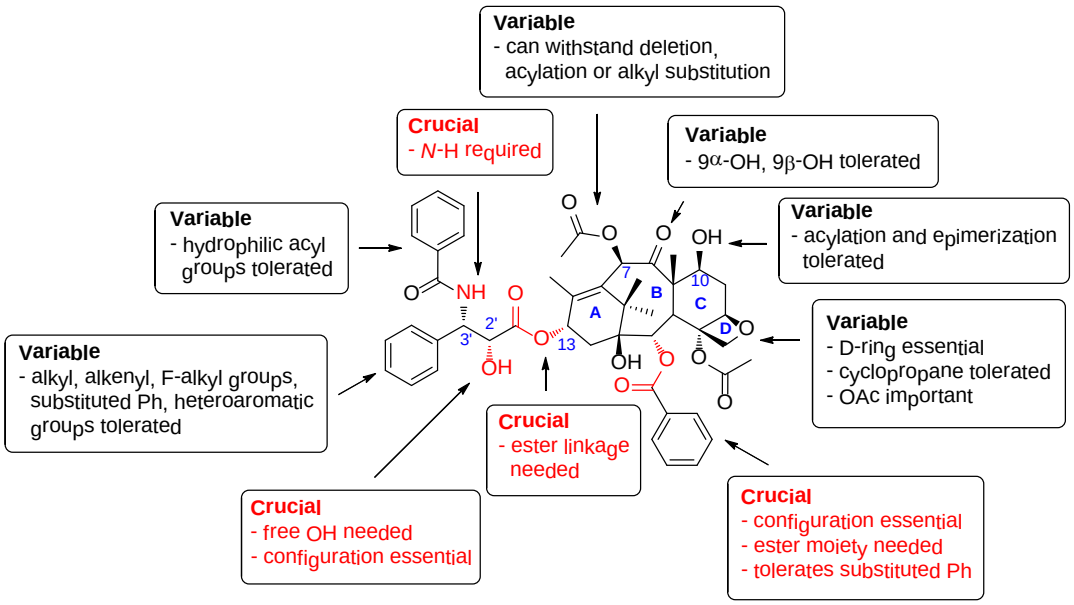

Figure 1.7: Summary of SAR studies of paclitaxel (adapted from [44])

Throughout the years, the Ojima laboratory has developed a series of highly potent new-generation taxoids through extensive SAR studies.[36, 39-43] A number of these taxoids posses 1 to 2 orders of magnitude greater potencies in drug-sensitive cancer cell lines and 2 to 3 orders of magnitude greater potencies in drug-resistant cell lines compared to that of paclitaxel and docetaxel. It was determined that introducing; (1) an alkenyl or alkyl group at the C-3' position, (2) a *t*-Boc moiety at the C-3'-*N*, (3) modifications at the C-10 position; and (4) substituted phenyl rings at the C-2 benzoate increase the anticancer activity of the taxoid. Some results of this SAR study are shown in Table 1.1.[45, 46]

Table 1.1: Structure and Cytotoxicity (IC_{50}, nM) of Selected New-Generation Taxoids against Various Cancer Cell Lines (adapted from [46])

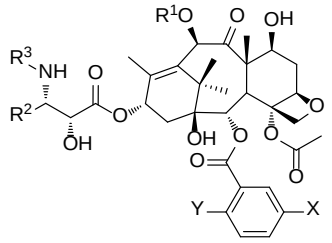

Taxane	R^1	R^2	R^3	X	Y
Paclitaxel	Ac	Ph	PhCO	H	H
Docetaxel	H	Ph	*t*-Boc	H	H
SB-T-1213	EtCO	*i*-butenyl	*t*-Boc	H	H
SB-T-1214	*c*-PrCO	*i*-butenyl	*t*-Boc	H	H
SB-T-1216	Me_2NCO	*i*-butenyl	*t*-Boc	H	H
SB-T-11033	EtCO	*i*-Bu	*t*-Boc	MeO	H
SB-T-121303	EtCO	*i*-butenyl	*t*-Boc	MeO	H
SB-T-121313	EtCO	*i*-butenyl	*t*-Boc	MeO	MeO
SB-T-121602	Me_2NCO	*i*-butenyl	*t*-Boc	Me	H

Taxane	MCF7[a]	NCI/ADR[b]	LCC6-MDR[c]	CFPAC-1[d]	HT-29[e]	DLD-1[f]
Paclitaxel	1.7	550	346	68	12	300
Docetaxel	1.0	723	120	-	-	-
SB-T-1213	0.18	4.0	-	4.6	0.37	3.9
SB-T-1214	0.20	3.9	-	0.38	0.73	3.8
SB-T-1216	0.13	7.4	-	0.66	0.052	5.4
SB-T-11033	0.36	0.61	0.80	-	-	-
SB-T-121303	0.36	0.79	0.90	0.89	-	-
SB-T-121313	0.30	-	-	0.025	0.56	-
SB-T-121602	0.08	-	-	0.31	0.003	0.46

[a] Human mammary cancer cell line (Pgp–). [b] Human ovarian cancer cell line (Pgp+). [c] *mdr1* transduced human breast cancer cell line (Pgp+); [d] Human pancreatic cancer cell line; [e] Human colon cancer cell line (Pgp-); [f] Human colon cancer cell line (Pgp+).

§ 1.1.5 Asymmetric Synthesis of β-Lactams

The β-lactam skeleton has attracted significant interest among synthetic and medicinal chemists over the years mainly because it is the core structure of natural and synthetic β-lactam antibiotics.[47] In addition, β-lactams have been playing an important role in organic synthesis as well. The use of β-lactams as synthons for compounds with biological and medicinal interests has been greatly advanced since the introduction of the "β-lactam synthon method" in late 1970s.[39, 48-55] Through the β-lactam synthon method, various β-lactams have been used as precursors to non-proteinogenic amino acids and amino alcohols, which are essential building blocks for the synthesis of peptides and peptidomimetics. Furthermore, the β-lactam synthon method has been applied to the synthesis of a variety of medicinally important compounds such as indolizidine and isoquinoline alkaloids, taxoids and other complex natural products.

The synthesis of these biologically important and stereochemically defined compounds can be facilitated by chemical transformations of enantiopure β-lactams (Figure 1.8). Enantioselective β-lactam synthesis can be accomplished using the following synthetic routes: (1) asymmetric ester enolate-imine cyclocondensation; (2) diastereoselective Staudinger ketene-imine cycloaddition reaction, followed by enzymatic resolution of enantiomers; or (3) asymmetric Staudinger [2+2] ketene-imine reaction. The chirality of these chiral β-lactams can be transferred directly to an array of synthetic intermediates, which are useful for the synthesis of enantiopure compounds of biological and medicinal significance.

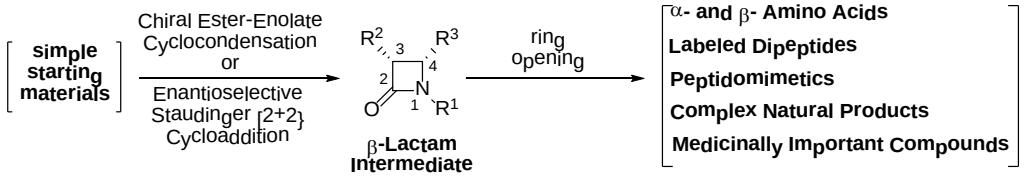

Figure 1.8: Biological transformations of β-lactams

Once β-lactams are obtained, any of the C-C and N-C bonds of the four-membered ring can be cleaved to yield useful chiral synthetic intermediates. The ring strain of the β-lactam ring promotes bond cleavage. The most widely exploited bond cleavage is that of the N1-C2 amide bond. This bond is susceptible to nucleophilic agents, as was described in the preparation of paclitaxel. The β-lactam synthon method has also been successfully applied to (1) the synthesis of biologically active oligopeptides, (2) the synthesis and stereoselective labeling of dipeptides, (3) the asymmetric synthesis of peptidomimetics, and (4) the synthesis of antimicrobial agents, complex natural products and highly potent taxoids (Figure 1.8).

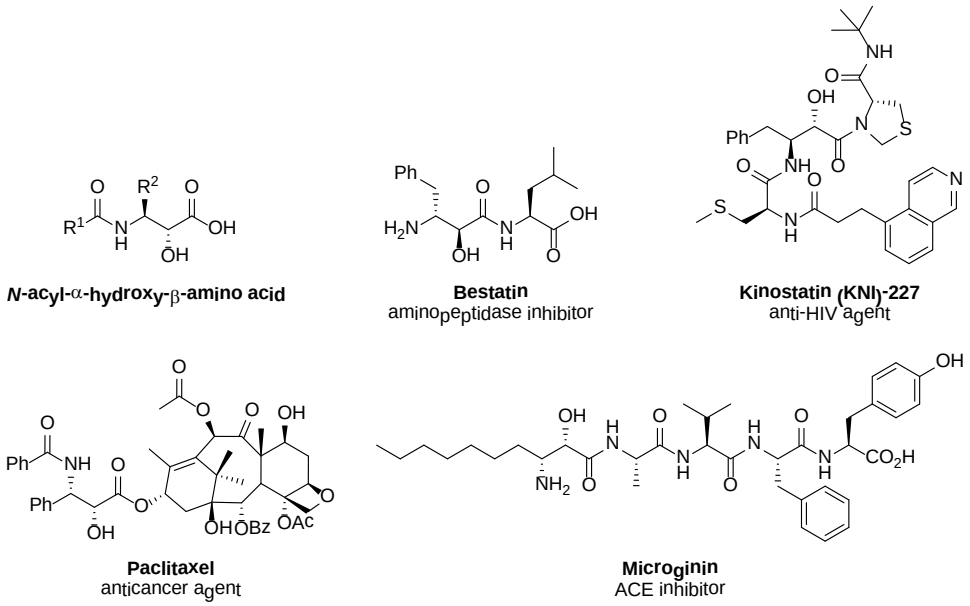

Figure 1.9: Medicinal important compounds obtained via β-lactam synthon method

§ 1.1.6 Staudinger [2+2] Ketene-Imine Cycloaddition Reaction

The first synthesis of β-lactams was reported by Staudinger in 1907, in which the Schiff base derived from aniline and benzaldehyde underwent thermal cycloaddition with diphenylketene to form 1,3,3,4-tetraphenylazetidin-2-one.[56] Since its introduction, the Staudinger [2+2] ketene-imine cycloaddition reaction has been regarded as the most direct and the most widely employed method for the synthesis of β-lactams. Although the Staudinger reaction has been documented for over a decade, uncertainties persist regarding the details of its mechanism. However, two recent reviews concerning this subject are available.[57, 58] The most widely accepted mechanism of the Staudinger ketene-imine cycloaddition involves the nucleophilic attack of an imine to a ketene or vice versa, thus generating a zwitterionic intermediate which undergoes conrotatory ring closure to give the 4-membered β-lactam ring, shown in Figure 1.10. When a mono-substituted ketene and an aldimine are used, the reaction produces two stereocenters in the β-lactam ring, hence *cis*- and/or *trans*-β-lactam products can be obtained exclusively or as a mixture in a variable ratio, depending on the substrate structures and reaction conditions.[57, 58] If there is no *Z* to *E* isomerization in the zwitterionic intermediate, the reaction gives *cis*-β-lactam as the exclusive product. Although Figure 1.10 only shows *E*-imine, the stereochemistry of the imine influences the stereochemistry of the resulting β-lactam, i.e., *E*-imines preferentially lead to the formation of *cis*-β-lactams, while *Z*-imines predominately give *trans*-β-lactams.[59-62] The studies conducted to establish the origin of *cis*/*trans* stereoselection revealed that the relative transition state energy in the rate-determining step is dictated by electronic torquoselectivity.[62-64]

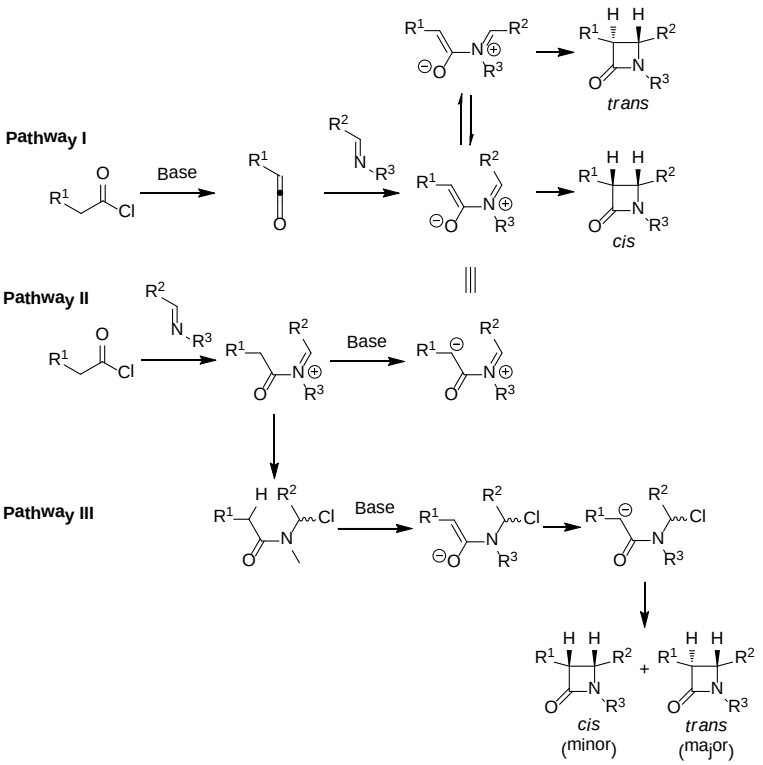

Figure 1.10: Proposed mechanistic pathways for β-lactam formation (adapted from [57, 58])

Also in Figure 1.10, two other pathways have also been proposed for the reaction, which involve mixing an acid chloride, a base and an imine all at once (pathways II and III). This reaction involves the acylation of the imine nitrogen, followed by deprotonation at the α-carbon by a base to generate the zwitterinonic intermediate as is generated in pathway I (pathway II). In another process, the chloride counter ion, generated in the first step, adds to the iminium bond to form the corresponding *N*-α-chloroalkylamide anion, which undergoes cyclization through an intramolecular S_N2 reaction (pathway III) that can accommodate the formation of *trans*-β-lactam as the major product under certain conditions.[57, 58]

It has been reported that reaction variables such as reaction temperature, solvent, base, additives and the order of addition of reactants influence the stereochemistry of the products. Nonpolar solvents are favorable for the formation of *cis*-β-lactams, whereas polar solvents are better for the formation of *trans*-β-lactams.[65] Presumably this effect is due to the stabilization of the zwitterionic intermediate in polar solvents, allowing isomerization of the double bond prior to ring closure. The stereoselectivity is also dependent on the order of addition of reactants, i.e., an acid chloride and an imine, which can be explained by the three pathways shown in Figure 1.10.

§ 1.1.7 Asymmetric Synthesis of β-Lactams through Enzymatic Kinetic Resolution

Enzymatic kinetic optical resolution of racemic β-lactams obtained by the Staudinger ketene-imine cycloaddition provides another route to enantiopure β-lactams. This protocol is especially useful for the synthesis of enantiopure 3-hydroxy-β-lactams.[66-72] Although half of the

racemic β-lactam cannot be converted to the desired enantiomer through this process, the starting materials are inexpensive. Furthermore, the other enantiomer can be used as a valuable and versatile synthon, thus may not be wasted.

Among various hydrolytic enzymes examined, Amano lipases and pig liver acetone powder (PLAP) have been found to provide the best results in the kinetic optical resolution of racemic *cis*-3-acetoxy-4-phenyl-β-lactams, yielding the corresponding (3*R*,4*S*)- and (3*S*,4*R*)-β-lactams with high enantiopurities.[66, 69] The "PS-Amano" lipase has been successfully applied to the kinetic resolution of racemic *cis*-3-acetoxy-4-(2-methylbut-2-enyl)azetidin-2-one.[70-72] The "PS-Amano" lipase preferentially hydrolyzes the acetate moiety at the C-3 position of this β-lactam. Therefore, (3*R*,4*S*)-β-lactam is obtained with extremely high enantiopurity (>99% ee) when the reaction is stopped over 50% conversion.

§ 1.2.0 Results and Discussion

§ 1.2.1 Synthesis of Enantiomerically-Enriched β-Lactam via Enzymatic Resolution

The synthesis of enantiopure *β*-lactams begins with the preparation of the four-membered heteocyclic ring core. This core is achieved *via* the Staudinger [2+2] cycloaddition between an imine and a ketene. The imine **1-1** is obtained in the condensation reaction of 3-methyl-2-butenal in the presence of *p*-anisidine and a drying reagent (Scheme 1.3).[73]

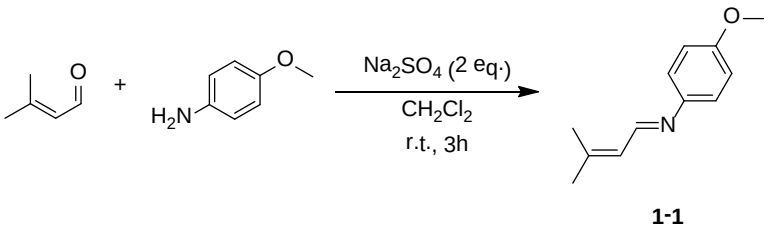

1-1

Scheme 1.3: Imine formation

The imine **1-1** is highly unstable, being sensitive to light and air. To prevent loss of the imine via decomposition or isomerization, the condensation reaction was done in the dark. Upon the completion of the reaction, the reaction mixture was filtered, the solvent was evaporated under vacuum pressure with low heat and the resulting material was used immediately without further purification. The [2+2] cycloaddition between the imine **1-1** and acetoxyacetyl chloride generated a racemic mixture of **1-2** (Scheme 1.4).[73]

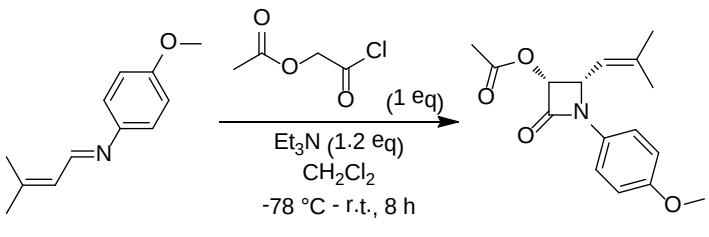

1-1 75% after 2 steps **(+/-) 1-2**

Scheme 1.4: Staudinger [2+2] ketene-imine cycloaddition

The cold -78 °C temperature was maintained to prevent *trans*-isomer formation of the *β*-lactam. This temperature was achieved using an acetone and dry ice bath or acetone with a cryocool. Acetoxyacetyl chloride was added against the sides of the reaction vessel to assure that the newly added reagent was cold and to assure slow addition. In addition, the temperature was held at -78 °C for at least 2 hours after the addition of the acid chloride. After 2 hours, the reaction was allowed to slowly warm to room temperature giving a racemic mixture of **1-2** in good yield (75% after 2 steps).

The two enantiomers of β-lactam **1-2** were resolved by enzymatic resolution using "PS-Amano" lipase (Scheme 1.5). "PS-Amano" lipase is derived from the bacteria *Burkholderia cepacia* and preferentially cleaves the acetate group of the (-) enantiomer leaving the (+) enantiomer intact.

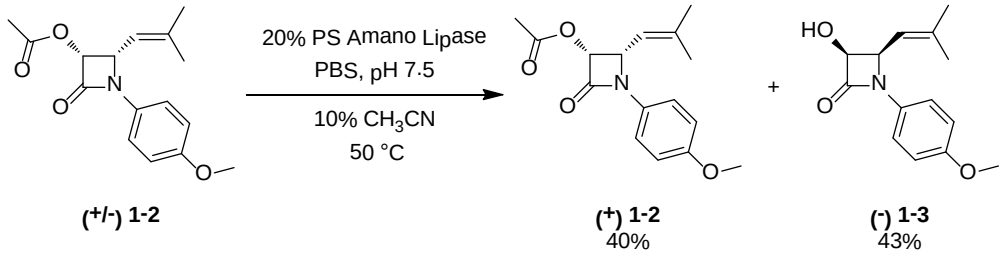

Scheme 1.5: Optical enzymatic resolution using "PS Amano" lipase

The enzymatic resolution reaction was monitored by NMR and was quenched when the ratio of the acetate to alcohol was 1 to 1.1 to ensure high enantioselectivity.[74] The desired (+) enantiomer was obtained in 40% isolated yield with >99% ee and the (-) enantiomer was obtained in 43% yield. Though the (+) enantiomer was used in subsequent steps, the (-) enantiomer was retained and can be used as a synthetic building block for other synthetic intermediates. It should be noted that at room temperature, the (-) enantiomer turns black over time. The desired **(+) 1-2** was converted to an alcohol *via* base-hydrolysis and the alcohol was protected with TIPS (Scheme 1.6).

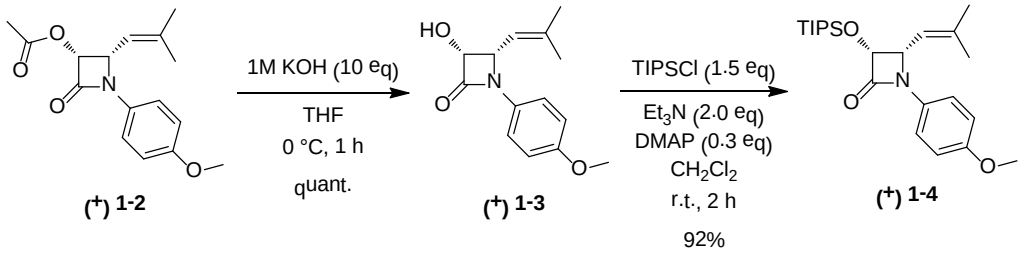

Scheme 1.6: Hydrolysis and TIPS-protection

Base hydrolysis of **(+) 1-2** is simple, efficient and straightforward, giving **(+) 1-3** in quantitative yield. The TIPS-protection also proceeded smoothly giving **(+) 1-4** in excellent yield (92%). However, it is worthy of note that the excess TIPSCl generates triisopropyldisiloxane which can be difficult to remove from the desired product. Further modification of **(+) 1-4** entails the deprotection of the *p*-methoxyphenyl (PMP) moiety in the presence of ceric ammonium nitrate (CAN) (Scheme 1.7).

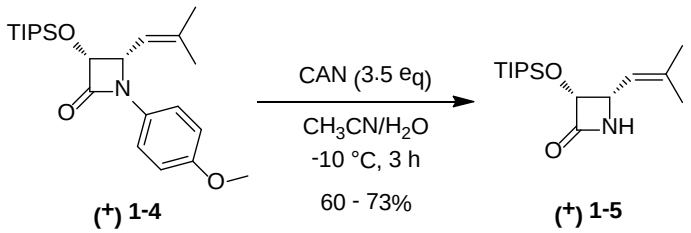

Scheme 1.7: PMP-deprotection using CAN

CAN-mediated PMP-deprotection is a finicky reaction that must be monitored frequently as the reaction proceeds. This reaction can be monitored via TLC, but after development the TLC plate must be stained with a cerium-ammonium-molybdate (CAM), phosphomolybdic acid (PMA) or vanillin stain. It is also important that the temperature of the CAN-mediated PMP-deprotection be maintained at -10 °C ± 2 °C. Ice formation will occur if temperatures drop well below -10 °C and the resulting ice may trap unreacted starting materials leading to a slow or no reaction. At elevated temperatures, the reaction gives undesired products. The temperature can be maintained using a mixture of ethanol and sodium chloride with ice or through the use of a cryocool. The CAN-mediated deprotection gave the desired **(+) 1-5** in moderate yield (60-73%). The mechanism for the removal of the PMP group involves two Single Electron Transfers (SET). The PMP group donates a single electron to cerium (IV) forming a radical cation intermediate that is susceptible to a nucleophilic attack by water. Donation of a second electron to another CAN molecule results in a quinone like radical which is then cleaved by the addition of a second water molecule producing the free amine, quinone and methanol as the primary products. The resulting **(+) 1-5** was treated with di-*tert*-butyl dicarbonate in the presence of base (Scheme 1.8).[37, 39]

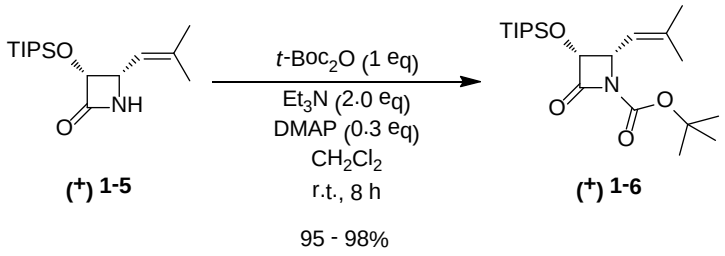

Scheme 1.8: Boc-protection of β-lactam

The amide-nitrogen was capped with a Boc moiety to yield the desired enantiopure **(+) 1-6** in excellent yields (95 – 98%). Following Boc protection, **(+) 1-6** can be coupled to baccatin III derivatives to yield 2nd-generation taxoids.

§ 1.2.2 Synthesis of New-Generation Taxoids

New-generation taxoids have the same mechanism of action as the parent compounds paclitaxel and docetaxel but 2-to-3 orders of magnitude greater potency than the parent compounds in MDR cancer cell lines. The synthesis of new-generation taxoids can be achieved using the β-lactam synthon method. Applying the β-lactam synthon method, the enantiopure β-

lactam **(+) 1-6** can be coupled to a baccatin III derivative to give new-generation taxoids, after deprotection. The synthesis of SB-T-1214 begins with the TES-protection of the C-7 alcohol of 10-DAB III (Scheme 1.9).[40]

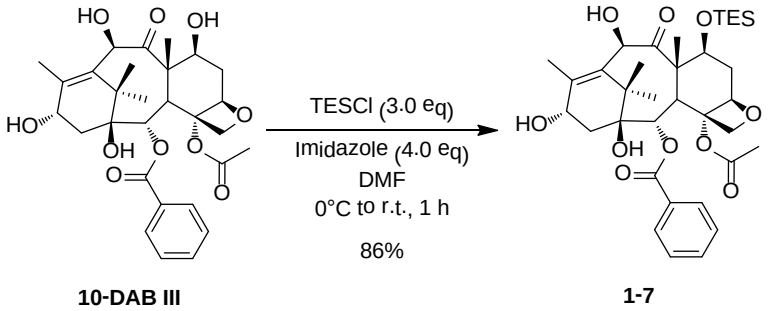

10-DAB III **1-7**

Scheme 1.9: Mono-TES-protection of 10-DAB III

The TES-protection was done at 0 °C and monitored closely to assure that multiple protections do not occur. Experiments have shown that it is possible to protect the C-10 and C-13 hydroxyl groups, in addition to the C-7 hydroxyl moiety. The mono-TES-protected **1-7** was obtained in good yield (86%). The functional group conversion of the C-10 hydroxyl to a cyclopropanecarbonyl moiety will afford SB-T-1214. This modification to the C-10 position was done in the presence of LiHMDS (Scheme 1.10).[40]

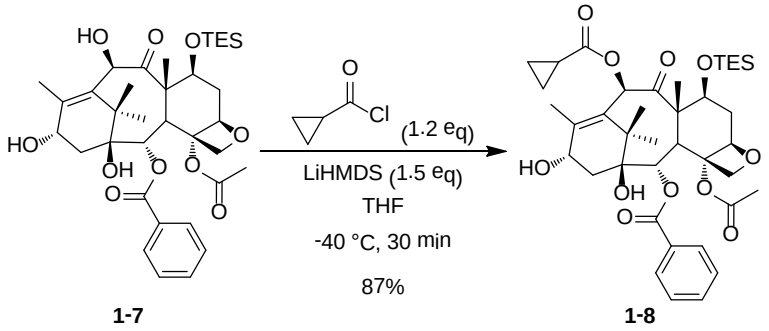

1-7 **1-8**

Scheme 1.10: Acylation of C-10 position

Again, the acylation of **1-7** was monitored closely to assure that multiple acylations do not occur. The addition of excess cyclopropanecarbonyl chloride and LiHMDS to **1-7** afforded **1-8** in good yield (87%). The resulting **1-8** was subjected to the Ojima-Holton coupling protocol in the presence of enantiopure β-lactam **(+)-1-6** and LiHMDS (Scheme 1.11).[40]

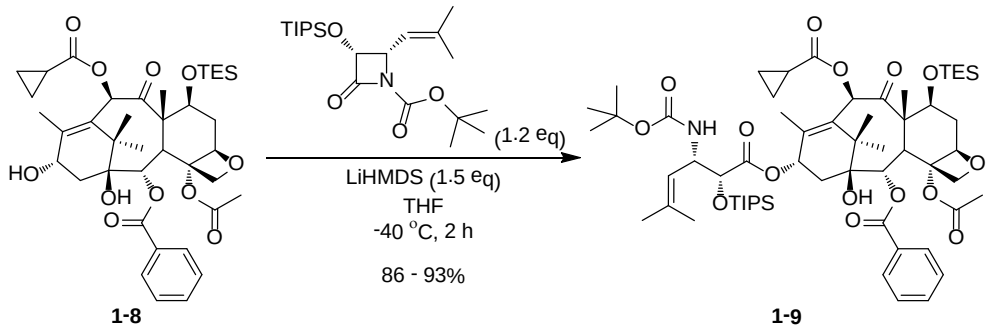

Scheme 1.11: Ojima-Holton β-lactam coupling

The nucleophilic hydroxide group at the C-13 position attacks the carbonyl carbon of the *β*-lactam ring, opening the ring while maintaining the stereochemistry. The Ojima-Holton coupling protocol gives **1-9** in excellent yield (86 - 93%). The final step towards SB-T-1214 involves the deprotection of the TIPS group at the C-2' position and the TES group at the C-7 position of **1-9** using HF/pyridine (Scheme 1.12).[40]

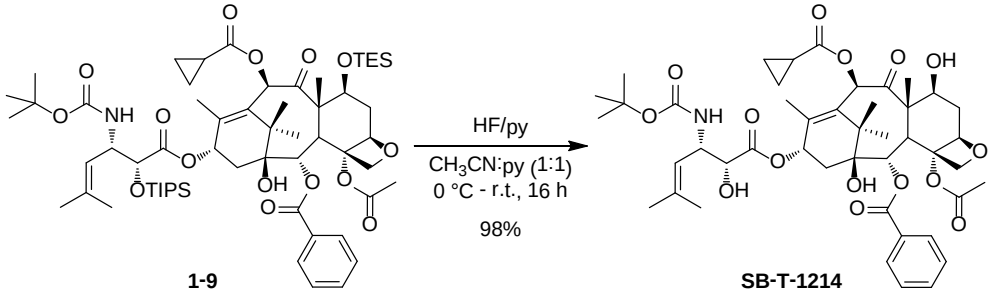

Scheme 1.12: Silyl group deprotection of taxoid

The addition of excess HF in pyridine (0.01 mL/mg) to **1-9** gave **SB-T-1214** in excellent yield (98%). SB-T-1214 is a new-generation taxoid which contains a cyclopropanecarbonyl moiety at the C-10 position, an isobutenyl moiety at the C-3' position and a BOC moiety at the C-3'-*N*. The biological activity of SB-T-1214, as well as other new-generation taxoids was evaluated against a variety of cancer cell lines.

§ 1.2.3 Biological Evaluation of New-Generation Taxoids

Based on SAR studies the Ojima research group has developed a series of highly potent new-generation taxoids (Table 1.2).[18, 40, 75-81] These new-generation taxoids have been synthesized using the Ojima-Holton β-lactam synthon method. The biological activity of these taxoids was evaluated in a variety of cancer cell lines using an MTT-assay to measure inhibitory concentrations. The results of the biological assay are shown in Table 1.3.

Table 1.2: New-Generation Taxoids

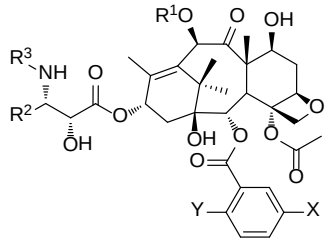

Taxane	R^1	R^2	R^3	X	Y
Paclitaxel	Ac	Ph	PhCO	H	H
SB-T-1213[a]	EtCO	CH_2=CH	*t*-Boc	H	H
SB-T-121312[a]	EtCO	CH_2=CH	*t*-Boc	Me	Me
SB-T-121313[a]	EtCO	CH_2=CH	*t*-Boc	MeO	MeO
SB-T-1214	*c*-PrCO	CH_2=CH	*t*-Boc	H	H
SB-T-121402[a]	*c*-PrCO	CH_2=CH	*t*-Boc	Me	H
SB-T-121403[a]	*c*-PrCO	CH_2=CH	*t*-Boc	MeO	H
SB-T-121413[a]	*c*-PrCO	CH_2=CH	*t*-Boc	MeO	MeO
SB-T-1216[b]	Me_2NCO	CH_2=CH	*t*-Boc	H	H
SB-T-121602[a]	Me_2NCO	CH_2=CH	*t*-Boc	Me	H
SB-T-121603[a]	Me_2NCO	CH_2=CH	*t*-Boc	MeO	H
SB-T-121613[a]	Me_2NCO	CH_2=CH	*t*-Boc	MeO	MeO
SB-T-12854[b]	Me_2NCO	CF_2=CH	*t*-Boc	H	H

[a] taxoid synthesized by Joshua D. Seitz; [b] taxoid synthesized by Ilaria Zanardi

Table 1.3: Cytotoxicity of New-Generation Taxoids against Various Bulk Cancer Cell Lines

Taxane	IC_{50} (nM)								
	A2780 (ovarian cancer)	CFPac-1 (pancreatic cancer)	DLD-1 (colon cancer)	HT-29 (colon cancer)	ID8 (ovarian cancer)	MCF-7 (breast cancer)	Panc-1 (pancreatic cancer)	PC3 (prostate cancer)	PC3MM2 (prostate cancer)
Paclitaxel	16.2 ± 8.28	68.0 ± 22.9	29.5 ± 10.8	11.6 ± 3.57	14.5 ± 5.88	6.25 ± 0.76	1.97 ± 0.76	1.68 ± 0.84	0.48 ± 0.08
SB-T-1213	0.041 ± 0.020	4.58 ± 2.58	>5000	0.37 ± 0.22	8.92 ± 1.61	0.20 ± 0.11	1.11 ± 0.52	0.44 ± 0.04	0.39 ± 0.06
SB-T-121312	8.97 ± 3.44	3.09 ± 1.39	>5000	52.9 ± 19.1	82.8 ± 14.6	37.7 ± 2.06	49.8 ± 10.2	4100 ± 360	4050 ± 254
SB-T-121313	1.46 ± 0.32	0.025 ± 0.001	13.2 ± 0.64	3.60 ± 1.35	0.016 ± 0.003	0.30 ± 0.01	0.56 ± 0.39	0.43 ± 0.11	0.26 ± 0.15
SB-T-1214	0.36 ± 0.03	0.38 ± 0.14	0.38 ± 0.21	0.73 ± 0.30	2.51 ± 1.24	0.35 ± 0.11	0.35 ± 0.14	0.38 ± 0.10	0.47 ± 0.02
SB-T-121402	0.40 ± 0.01	3.36 ± 0.10	1.19 ± 0.12	2.11 ± 0.94	0.53 ± 0.01	0.54 ± 0.25	0.27 ± 0.14	0.23 ± 0.11	0.27 ± 0.16
SB-T-121403	0.41 ± 0.03	1.79 ± 0.59	14.3 ± 4.86	19.0 ± 3.00	0.071 ± 0.01	6.05 ± 0.78	0.34 ± 0.14	0.45 ± 0.01	3.68 ± 1.90
SB-T-121413	0.14 ± 0.03	1.88 ± 0.14	>5000	45.5 ± 7.26	0.66 ± 0.24	3.76 ± 2.81	0.31 ± 0.14	0.26 ± 0.06	0.43 ± 0.33
SB-T-1216	0.96 ± 0.46	0.66 ± 0.46	0.54 ± 0.19	0.052 ± 0.012	5.49 ± 2.51	0.34 ± 0.20	3.29 ± 2.12	0.47 ± 0.04	0.43 ± 0.03
SB-T-121602	0.29 ± 0.17	0.31 ± 0.10	0.046 ± 0.011	0.003 ± 0.002	3.79 ± 2.10	0.08 ± 0.05	2.82 ± 1.58	0.46 ± 0.05	0.45 ± 0.06
SB-T-121603	0.25 ± 0.11	3.74 ± 1.21	4.50 ± 1.32	0.003 ± 0.002	4.02 ± 2.71	0.18 ± 0.09	3.70 ± 0.83	0.066 ± 0.039	0.37 ± 0.22
SB-T-121613	39.6 ± 7.38	58.1 ± 20.0	>5000	34.1 ± 10.1	40.6 ± 24.3	3.29 ± 1.47	>5000	0.16 ± 0.04	0.49 ± 0.17
SB-T-12854	3.13 ± 1.93	0.35 ± 0.15	0.25 ± 0.18	0.54 ± 0.03	0.28 ± 0.15	0.51 ± 0.32	6.02 ± 0.86	5.08 ± 2.43	32.5 ± 26.3

- Cells were suspended in RPMI with L-glutamine (Lonza BioWhittaker, BW12-702F), with 5% FBS (Thermo Scientific, HyClone, SH3007003), 5% Nu Serum (BD Biosciences, 355100) and 1% Penn Strip before administration of taxoid
- Cells were incubated for 48 hours at 37 °C with 5% CO_2 after administration of taxoid
- The optical density was determined using Acsent Multiskan optical density reader
- The reported values are a calculated averages of IC_{50} values determined from three individual experiments
- IC_{50} values were calculated using SigmaPlot v 10.0
- All IC_{50} values are report in nM scale unless otherwise noted

As seen from Table 1.2, a number of new-generation taxoids show orders of magnitude greater activity in different cancer cell lines compared to the parent compound, paclitaxel. The majority of the new-generation taxoids show sub-nanomolar IC_{50} values. It is worthy of note that these taxoids show selective activity against this series of cancer cell lines tested. For example, SB-T-1213 demonstrated substantial activity against HT-29 (colon), MCF-7 (breast), PC3 (prostate) and PC3MM2 (prostate) cancer cell lines, showing subnanomolar inhibitory concentrations against each of the cell lines. However, in comparing the ovarian cancer cell lines A2780 and ID-8, SB-T-1213 has 200 times greater activity against A2780 (IC_{50} of 0.041 nM) than in ID-8 (IC_{50} of 8.92 nM). Furthermore, SB-T-121312, an analog of SB-T-1213 containing a dimethyl-substituted phenyl ring of the C-2 benzoate, shows less potency against the series of cancer cell lines evaluated compared to SB-T-1213. Whereas, SB-T-121313 shows excellent activity against CFPac-1 (pancreatic), ID-8 (ovarian), MCF-7 (breast), Panc-1 (pancreatic), PC3 (prostate) and PC3MM2 (prostate) cancer cell lines, with slightly lower IC_{50} values compared to SB-T-1213.

Also shown in Table 1.2, SB-T-1214 demonstrated subnanomolar activity in all cancer cell lines evaluated except in ID-8 (IC_{50} of 2.51 nM). SB-T-121402 and SB-T-121403, the substituted benzoate derivates of SB-T-1214, showed decreased potency against all of the cancer cell lines. However, SB-T-121403 performed substantially well against ID-8 cancer cells with an IC_{50} value of 0.071 nM. SB-T-121413, the dimethoxy-substituted benzoate, showed excellent activity in A2780 (IC_{50} of 0.14 nM), ID-8 (IC_{50} of 0.66 nM, almost 10 times more active than SB-T-1214), Panc-1, PC3 and PC3MM2 cancer cell lines.

Much like SB-T-1214, SB-T-1216 shows excellent activity against all cell lines, being least active in ID-8 and Panc-1 cells with IC_{50} values of 5.49 nM and 3.29 nM, respectively. However, it is worthy of note that SB-T-121602 and SB-T-121603, the substituted benzoate derivates of SB-T-1216, showed extremely potent activity in a number of cell lines. SB-T-121602 showed picomolar activity in DLD-1 (IC_{50} of 46 pM), HT-29 (IC_{50} of 3 pM) and MCF-7 (IC_{50} of 80 pM). Similarly, SB-T-121603, the methoxy-substituted phenyl derivative of SB-T-1216, showed picomolar activity in HT-29 (IC_{50} of 3 pM) and PC3 (IC_{50} of 66 pM). SB-T-121613 showed less potent activity against the cell lines evaluated but performed well against PC3 (IC_{50} of 0.16 nM) and PC3MM2 (IC_{50} of 0.49 nM). SB-T-12854, the difluoro-derivative of SB-T-1216, showed subnanomolar activity in a number of cancer cell lines evaluated but decreased potency in A2780, Panc-1, PC3 and PC3MM2 cell lines was also observed.

New-generation taxoids show magnitudes greater activity in a series of cancer cell lines compared to paclitaxel. In most cases, the IC_{50} of the new-generation taxoids is subnanomolar with some taxoids possessing picomolar activity. Thus, new-generation taxoids are promising candidates for possible use as chemotherapeutic agents and for use as warhead for tumor-targeting drug conjugates.

§ 1.3.0 Summary

Paclitaxel is one of the most significant drugs in current cancer treatment. Paclitaxel, which alters the assembly and disassembly of microtubules, has been used to treat a number of different cancers for the past decades. Furthermore, the total synthesis of paclitaxel is still highly sought after in current synthetic chemistry research. The β-lactam synthon method has proven to

be an efficient method to synthesize taxoids. β-Lactams with high enantiomeric excess were synthesized via an enzymatic kinetic resolution of β-lactam obtained by Staudinger [2+2] ketene-imine cycloaddition. The synthesized β-lactam was used for the synthesis of new-generation taxoid SB-T-1214. The biological activity of SB-T-1214 in addition to other new-generation taxoids was evaluated *in vitro*. A number of these new-generation taxoids show more than 1-to-2 orders of magnitude greater activity against various cancer cell lines. SB-T-1214 showed excellent activity against all of the cancer cell lines evaluated. In addition, SB-T-121602 and SB-T-121603 had picomolar activity in HT-29 (human colon) cancer cell line. Thus, new-generation taxoids are promising candidates as warheads for tumor-targeting drug conjugate development.

§ 1.4.0 Experimental

Caution

Taxoids have been established as a potent cytotoxic agent. Thus, they and all structurally related compounds and derivatives must be considered as mutagens and potential reproductive hazards for both males and females. Appropriate precautions (i.e. use of gloves, goggles, lab coat and fume hood) must be taken while handling these compounds.

General information

All chemical were obtained from either Sigma-Aldrich, Fisher Scientific or VWR International, and used as is unless otherwise noted. All reactions were carried out under nitrogen in oven dried glassware using standard Schlenk techniques unless otherwise noted. Reactions were monitored by thin layer chromatography (TLC) using E. Merck 60F254 precoated silica gel plates and alumina plate depending on the compounds. Dry solvents were degassed under nitrogen and were dried using the PURESOLV system (Inovatative Technologies, Newport, MA). Tetrahydrofuran was freshly distilled from sodium metal and benzophenone. Dichloromethane was also distilled immediately prior to use under nitrogen from calcium hydride. Toluene was also distilled immediately prior to use under nitrogen from calcium hydride. Yields refer to chromatographically and spectroscopically pure compounds. Flash chromatography was performed with the indicated solvents using Fisher silica gel (particle size 170-400 Mesh). ^{1}H, ^{13}C and ^{9}F data were obtained using either 300 MHz Varian Gemni 2300 (75 MHz ^{13}C, 121 MHz ^{19}F) spectrometer, the 400 MHz Varian INOVA 400 (100 MHz ^{13}C) spectrometer or the 500 MHz Varian INOVA 500 (125 MHz ^{13}C) in $CDCl_3$ as solvent unless otherwise stated. Chemical shifts (δ) are reported in ppm and standardized with solvent as internal standard based on literature reported values.[82] Melting points were measured on Thomas Hoover Capillary melting point apparatus and are uncorrected. Optical rotations were measured on Perkin-Elmer Model 241 polarimeter.

Experimental procedure

N-(4-Methoxyphenyl)-3-methyl-2-butenaldimine (1-1)[73]

To 6.3 g (50 mmol) *p*-anisidine, recrystallized from hot hexanes, and 15 g (100 mmol) anhydrous Na_2SO_4 dissolved in CH_2Cl_2 (100 mL) was added 6.8 mL (60 mmol) 3-methylbut-2-enal, dropwise. The mixture was stirred at room temperature for 3 hours in the dark producing a dark red solution. The solvent was evaporated to yield **1-1**, which was used immediately in the

subsequent step without further purification: crude ^{1}H NMR (300 MHz, $CDCl_3$, ppm) δ 2.024 (s, 3 H), 2.081 (s, 3 H), 3.878 (s, 3 H), 6.255 (d, 1 H, *J* = 3.9 Hz), 6.941-6.981 (m, 2 H), 7.157-7.209 (m, 2 H), 8.438 (d, *J* = 9.6 Hz, 1 H).

(±)-1-(4-Methoxyphenyl)-3-acetoxyl-4-(2-methylprop-1-enyl)azetidin-2-one (1-2)[73]

To the resulting **1-1** dissolved in CH_2Cl_2 (200 mL) was added 11 mL (100 mmol) Et_3N. The mixture was cooled to -78 ˚C for 30 minutes. To the mixture was added 6.8 mL (60 mmol) acetoxyacetyl chloride, dropwise along the side of the flask, producing an orange solution. The mixture was stirred vigorously and the temperature was maintained at -78 ˚C for 2 hours. The solution was warmed to room temperature. After 10 hours, the reaction was quenched with CH_2Cl_2 (250 mL). The organic layer was washed three times with brine, dried over anhydrous $MgSO_4$, and concentrated *in vacuo*. The resulting crude was purified via column chromatography on silica gel (hexanes:ethyl acetate = 3:1) to yield racemic β-lactam, **1-2** (11.7 g, 78% yield after two steps), as a white solid: ^{1}H NMR (300 MHz, $CDCl_3$, ppm) δ 1.599 (s, 1 H), 1.793 (s, 3 H), 1.823 (s, 3 H), 2.115 (s, 3 H), 3.783 (s, 3 H), 4.946-4.993 (dd, *J* = 10.2 Hz, 4.8 Hz, 1 H), 5.113-5.153 (m, 1 H), 5.794 (d, *J* = 4.8 Hz, 1 H), 6.842 (d, *J* = 9 Hz, 2 H), 7.300 (d, *J* = 9 Hz, 2 H). All data are consistent with literature values.[73]

Enantioselective hydrolysis of β-lactam (1-2)[83]

To 11 g (0.04 mol) **1-2** dissolved in CH_3CN (50 mL) and 1.3 L of 0.2 M sodium phosphate buffer (pH 7.4) heated to 50 °C was added 2.4 g of "PS Amano" lipase. The mixture was stirred vigorously with a mechanical stirrer and the temperature was maintained at 50 ^{o}C. As the reaction progressed, the solution changed in color from yellow to red. The reaction was monitored via TLC and ^{1}H-NMR. After 26 hours, the reaction reached 50% conversion based on ^{1}H-NMR, and the reaction was quenched with ethyl ether (400 mL). The residual lipase was filtered over Celite and washed with ethyl ether. The filtrate was extracted using ethyl ether (3 x 100 mL). The organic layers were washed three times with brine, dried over anhydrous $MgSO_4$, and concentrated *in vacuo*. The resulting crude was purified via column chromatography on silica gel (hexanes:ethyl acetate = 3:1 and then 1:1) to yield **(+)-1-2** (4.76 g, 40% yield with >99% ee), as a white solid, and (-)-**1-2** (4.42 g, 43% yield), as an orange solid. To measure optical purity, to 25 mg **(+)-1-2** dissolved in THF, cooled to 0 °C, was added 1 M KOH. After 1 h, the reaction was quenched with 5 mL saturated NH_4Cl and extracted with CH_2Cl_2 (4 x 10 mL). The organic layers were collected, dried over $MgSO_4$ and concentrated *in vacuo* to yield **(+) 1-3**. The resulting white solid was dissolved in isopropanol and analyzed for optical purity using HPLC (column: OD-H; method: isocratic program, flow rate 0.6 mL/min, eluent 85%/15% hexanes/isoproanol).

(3*R*,4*S*)-1-(4-Methoxyphenyl)-3-hydroxy-4-(2-methylprop-1-enyl)azetidin-2-one [(+) 1-3][37, 84]

To 4 g (0.01 mol) **(+) 1-2** dissolved in THF (240 mL), cooled to 0 °C, was added 1 M KOH (140 mL) in 165 mL THF. The mixture was stirred at 0 °C and the reaction was monitored via TLC. After 2 h, the reaction was quenched with 200 mL saturated NH_4Cl and extracted with CH_2Cl_2 (4 x 100 mL). The organic layers were collected, dried over $MgSO_4$ and concentrated *in vacuo* to yield **(+) 1-3** (3.47 g, 100% yield), as a white solid without further purification: ^{1}H NMR (300 MHz, $CDCl_3$, ppm) δ 1.255 (br s, 1 H), 1.432 (s, 1H), 1.859 (s, 3 H), 1.864 (s, 3 H), 3.781 (s, 3 H), 4.865 (dd, J_1 = 10.2 Hz, J_2 = 4.8 Hz, 1 H), 5.091 (d, *J* = 5.1 Hz, 1 H), 5.242-5.289 (m, 1 H),

6.832 (d, J = 15 Hz, 2 H), 7.300 (d, J = 9 Hz, 1 H). All data are consistent with literature values.[37, 84]

1-*p*-Methoxyphenyl-3-triisopropylsiloxy-4-(2-methylpropen-2-yl)azetidin-2-one [(+) 1-4][37, 84]

To a solution of 3.55 g (14 mmol) **(+) 1-3** and 0.4 g (3 mmol) DMAP dissolved in CH_2Cl_2 (60 mL) was added 9 mL (65 mmol) Et_3N followed by the dropwise addition of 4.62 mL (21 mmol) chlorotriisopropylsilane, producing a yellow solution. The mixture was stirred at room temperature and the reaction was monitored via TLC. After 14 hours, the reaction was quenched with saturated NH_4Cl (100 mL) and extracted with ethyl ether (3 x 100 mL). The organic layer was washed three times with brine, dried over anhydrous $MgSO_4$, and concentrated *in vacuo*. The resulting crude was purified via flash column chromatography on silica gel (hexanes:ethyl acetate = 15:1) to yield **(+) 1-4** (5.35 g, 92% yield), as a white solid: ^{1}H NMR δ (300 MHz, $CDCl_3$, ppm) 1.059-1.115 (m, 21 H), 1.794 (s, 3 H), 1.845 (s, 3 H), 3.772 (s, 3 H) , 4.780-4.830 (dd, J_1 = 10.2 Hz, J_2 = 4.8 Hz, 1 H), 5.048 (d, J = 5.1 Hz, 1 H), 5.310-5.352 (m, 1 H), 6.820 (d, J = 9 Hz, 2 H), 7.303 (d, J = 9 Hz, 2 H). All data are consistent with literature values.[37, 84]

3-Triisopropylsilyloxy-4-(2-methylpropen-2-yl)azetidin-2-one [(+) 1-5][37, 84]

A solution of 500 mg (1 mmol) **(+) 1-4** dissolved in CH_3CN:H_2O (1:1, 30 mL of each) was cooled to -10 °C. After 10 minutes at -10 °C, to the solution was added 2.4 g (4 mmol) of cerium ammonium nitrate (CAN) dissolved in H_2O (5 mL) via addition funnel. The mixture was stirred at -10 °C and the reaction was monitored via TLC. After 3 h, the reaction was quenched with saturated $NaHSO_3$ (10 mL). The aqueous layer was filtered over Celite and the filtrate was extracted with ethyl acetate (3 x 100 mL). The organic layer was washed with brine (2 x 100 mL), collected, dried over $MgSO_4$ and concentrated *in vacuo*.The resulting crude was purified via column chromatography on silica gel (hexanes/ethyl acetate = 5/1) to yield **(+) 1-5** (270 mg, 73% yield), as a white solid: m.p. 84-86 °C; ^{1}H NMR (300 MHz, $CDCl_3$, ppm) δ 1.103-1.148 (m, 21 H), 1.755 (s, 3 H), 1.829 (s, 3 H), 4.487-4.539 (dd, J_1 = 10.2 Hz, J_2 = 5.1 Hz, 1 H), 5.051-5.078 (m, 1 H), 5.370 (d, J = 10 Hz, 1 H), 6.001 (br s, 1 H). All data are in agreement with literature values.[37, 84]

1-(*tert*-Butoxycarbonyl)-3-triisopropylsiloxy-4-(2-methylpropen-2-yl)azetidin-2-one [(+) 1-6][37, 84]

To a solution of 270 mg (0.9 mmol) **(+) 1-5**, 28 mg (0.2 mmol) DMAP and 0.4 mL (2.8 mmol) Et_3N dissolved in CH_2Cl_2 (4 mL) was added 208 mg (9.5 mmol) di-*tert*-butyl dicarbonate dissolved in CH_2Cl_2 (1 mL) producing a yellow mixture. The mixture was stirred at room temperature and the reaction was monitored via TLC. After 16 hours, the reaction was quenched with saturated NH_4Cl (5 mL). The residue was extracted with ethyl acetate (4 x 50 mL). The organic layer was washed with brine (2 x 50 mL), collected, dried over $MgSO_4$, and concentrated *in vacuo*. The resulting crude was purified via flash column chromatography on silica gel (hexanes:ethyl acetate = 25:1) to yield **(+) 1-6** (360 mg, 100% yield), as a yellow oil: ^{1}H NMR (300 MHz, $CDCl_3$, ppm) δ 1.018-1.108 (m, 21 H), 1.478 (s, 9 H), 1.761 (s, 3 H), 1.786 (s, 3 H), 4.723-4.775 (dd, J_1 = 10.2, J_2 = 5.7, 1 H), 4.952 (d, J = 5.7 Hz, 1 H), 5.249-5.300 (m, 1.0 Hz, 1 H). All data are in agreement with literature values.[37, 84]

10-Deacetyl-7-triethylsilylbaccatin III (1-7)[40]

A solution of 400 mg (0.7 mmol) 10-deacetylbaccatin III and 0.2 g (3.0 mmol) imidazole dissolved in DMF (6.75 mL) was cooled to 0 °C in an acetone/dry-ice bath. To the mixture was added 0.31 mL (1.8 mmol) chlorotriethylsilane. The mixture was stirred at 0 °C and the reaction was monitored via TLC. After 1 hour, the reaction was quenched with saturated NH_4Cl (15 mL) and the organics were extracted with ethyl acetate (3 x 50 mL). The organic layers were collected, dried over anhydrous $MgSO_4$ and concentrated *in vacuo*. The resulting crude was purified via flash column chromatography on silica gel (hexanes:ethyl acetate = 2:1) to yield **1-7** (433 mg, 86% yield), as a white solid: ^{1}H NMR (300 MHz, $CDCl_3$, ppm) δ 0.506-0.598 (m, 6 H), 0.911-0.964 (m, 9 H), 1.084 (s, 6 H), 1.258 (m, 2 H), 1.573 (m, 1H), 1.735 (s, 3H), 1.856-1.947 (m, 1 H), 2.043 (s, 1H), 2.087 (s, 3 H), 2.252 (s, 1 H), 2.285 (s, 3 H), 2.426-2.527 (m, 1 H), 3.942 (d, J = 7.1 Hz, 1 H), 4.148 (d, J = 8.3 Hz, 1 H), 4.254 (s, 1 H), 4.298 (d, J = 8.3 Hz, 1 H), 4.380-4.438 (dd, J_1 = 10.5 Hz, J_2 = 6.4 Hz, 1 H), 4.843-4900 (m, 1 H), 4.933-4.973 (m, 1 H), 5.172 (s, 1 H), 5.590 (d, J = 7.0 Hz, 1 H), 7.472 (t, J = 7.5 Hz, 2 H), 7.602 (t, J = 7.5 Hz, 1 H), 8.092 (d, J = 7.3 Hz, 2 H). All data are consistent with the reported values.[40]

10-Cyclopropanecarbonyl-10-deacetyl-7-triethylsilylbaccatin III (1-8)[40]

A solution of 192 mg (0.29 mmol) **1-7** dissolved in THF (5.4 mL) was cooled to -40 °C in an acetone bath using a cryocool. After 10 minutes, to the solution was added 0.061 mL (0.32 mmol) LiHMDS in 1.0 M THF. The mixture was stirred for an additional 10 minutes then to the solution was added 0.034 mL (0.37 mmol) cyclopropanecarboxylic acid chloride, dropwise, producing a yellow solution. The mixture was stirred at -40 °C and the reaction was monitored via TLC. After 30 minutes, the reaction was quenched with saturated NH_4Cl (5 mL) and the organic material was extracted with ethyl acetate (3 x 50 mL). The organic layers were collected, dried over anhydrous $MgSO_4$ and concentrated *in vacuo*. The resulting crude was purified via column chromatography on silica gel (hexanes:ethyl acetate = 3:1 then 2:1) to yield **1-8** (185 mg, 87% yield), as a white solid: ^{1}H NMR (300 MHz, $CDCl_3$, ppm) δ 0.474-0.590 (m, 6 H), 0.861-0.914 (m, 9 H), 0.999 (s, 3 H), 1.155 (s, 3 H), 1.642 (s, 3 H), 1.803-1.874 (m, 1 H), 1.989 (s, 3 H), 2.043 (s, 1 H), 2.193 (s, 3 H), 2.281 (s, 3 H), 2.466-2.573 (m, 1 H), 3.872 (d, J = 7.6 Hz, 1 H), 4.132 (d, J = 8.2 Hz, 1 H), 4.88 (d, J = 8.0 Hz, 1 H), 4.452-4.480 (dd, J_1 = 10.2, J_2 = 6.7 Hz, 1 H), 4.837 (t, J = 7.6 Hz, 1 H), 4.944 (d, J = 8.8 Hz, 1 H), 5.624 (d, J = 6.8 Hz, 1 H), 6.463 (s, 1 H), 7.473 (t, J = 8.0 Hz, 2 H), 7.602 (t, J = 7.2 Hz, 1 H), 8.121 (d, J = 7.2 Hz, 1 H). All data are consistent with the reported values.[40]

2'-Triisopropylsilyl-3'-dephenyl-10-(cyclopropanecarbonyl)-3'-(2-methyl-2-propenyl)docetaxel (1-9)[40]

A mixture of 100 mg (0.14 mmol) **1-8** and 80 mg (0.20 mmol) **(+) 1-6** dissolved in THF (7 mL) was cooled to -40 °C in an acetone bath using a cryocool. After 10 minutes, to the solution was added 0.2 mL LiHMDS in 1.0 M THF, dropwise, producing a yellow solution. The mixture was stirred at -40 °C and the reaction was monitored via TLC. After 1.5 hours, the reaction was quenched with saturated NH_4Cl (3 mL). The mixture was extracted using ethyl acetate (3 x 50 mL) and the organic layer was washed with saturated NH_4Cl (1 x 25 mL) and brine (2 x 50 mL), collected, dried over $MgSO_4$, and concentrated *in vacuo*. The resulting crude was purified via column chromatography on silica gel (hexanes:ethyl acetate = 5:1) to yield **1-9** (144 g, 93% yield), as a white solid: ^{1}H NMR (300 MHz, $CDCl_3$, ppm) δ 0.512-0.598 (m, 6 H), 0.888-0.940 (m, 9 H), 1.10 (s, 3 H), 1.115 (s, 3 H), 1.193 (s, 3 H), 1.233 (s, 3 H), 1.687 (s, 3 H), 1.754 (s, 3 H), 1.795 (s, 3 H), 1.839-1.924 (m, 1 H), 2.009 (s, 3 H), 2.354 (s, 3 H), 3.833 (d, J = 6.6 Hz, 1

H), 4.182 (d, *J* = 8.4 Hz, 1 H), 4.288 (d, *J* = 8.4 Hz, 1 H), 4.463-4.502 (m, 1 H), 4.763-4.849 (m, 1 H), 4.924 (d, J = 8.7 Hz, 1 H), 5.320-5.357 (m, 1 H), 5.676 (d, *J* = 6.8 Hz, 1 H), 6.085 (m, 1 H), 6.479 (s, 1 H), 7.456 (t, *J* = 7.5 Hz, 2 H), 7.599 (t, *J* = 7.8 Hz, 1 H), 8.095 (d, *J* = 7.5 Hz, 1 H). All data were in agreement with literature values.[40]

3'-Dephenyl-10-(cyclopropanecarbonyl)-3'-(2-methyl-2-propenyl)docetaxel (SB-T-1214)[40]

A solution of 107 mg (0.09 mmol) **1-9** dissolved in CH_3CN:pyridine (1:1, 3 mL each) was cooled to 0 °C in an ice-bath. To the solution was added 1.2 mL HF/pyridine, dropwise, producing a colorless solution. The mixture was stirred at room temperature and the reaction was monitored via TLC. After 16 hours, the reaction was quenched with saturated $NaHCO_3$ (5 mL) and diluted with ethyl acetate (10 mL). The organic layer was washed with saturated $CuSO_4$ (3 x 30 mL) and with brine (3 x 30 mL), collected, dried over $MgSO_4$, and concentrated *in vacuo*. The resulting crude was purified via flash column chromatography on silica gel (hexanes:ethyl acetate = 1:1) to yield **SB-T-1214** (79 mg, 98% yield), as a white solid: m.p. 160-161 °C; ^{1}H NMR (300 MHz, $CDCl_3$, ppm) δ 0.989-1.034 (m, 2 H), 1.160 (s, 3 H), 1.263 (s, 3 H), 1.354 (s, 9 H), 1.583 (s, 3 H), 1.672 (s, 3 H), 1.767 (s, 3 H), 1.901 (s, 3 H), 2.046 (s, 1 H), 2.356 (s, 3 H), 2.490-2.593 (m, 2 H), 3.361 (br s, 1 H), 3.798 (d, *J* = 7.2 Hz, 1 H), 4.196 (d, *J* = 7.2 Hz, 1 H), 4.295 (d, J = 7.2 Hz, 1 H), 4.397-4.450 (m, 1 H), 4.758 (m, 2 H), 4.945-4.983 (m, 1 H), 5.306-5.329 (m, 1 H), 5.657 (d, J = 7.2 Hz, 1 H), 6.138-6.206 (m, 1 H), 6.300 (s, 1 H), 7.476 (t, *J* = 7.2 Hz, 2 H), 7.613 (t, *J* = 7.5 Hz, 1 H), 8.094 (d, *J* = 7.2 Hz, 2 H). All data are consistent with the reported values.[40]

Cell culture system for MTT assay[85]

Cell lines (obtained from ATCC unless otherwise noted and maintained at SBU Cell Culture/Hybridoma Facility) were cultured in RPMI-1640 with L-glutamine (Lonza BioWhittaker, BW12-702F: A2780, DLD-1, ID-8, MCF-7, PC3, PC3MM2), DMEM (Lonza BioWhittaker, BW12-604F: CFPac-1, MDA MB 231, Panc-1) or McCoy's 5A (Gibco #16600: HT-29) supplemented with 5% FBS (Thermo Scientific, HyClone, SH3007003), 5% Nu Serum (BD Biosciences, 355100) and 1% Penn Strip, at 37 °C in a humidified incubator with 5% CO_2. The cells were washed with DPBS and dissociated using TrypLE. The cells were incubated at 37 °C until the cells were detached from the plate, transferred to a centrifuge vial and pelleted via centrifugation at 1500 rpm for 5 min. The cells were counted per 1 mL media. The desired amount of media was added to the cell solution so that 8,000 cells can be added to each well of a 96-well plate in 200 μL aliquots. After the addition, the cells were incubated at 37 °C with 5% CO_2.

Drug treatment for MTT assay[86]

A serial dilution of the drug compound dissolved in sterile DMSO was prepared by the addition of fully-supplemented RPMI-1640. The residual medium in each well was aspirated and the different drug-concentration solutions were added to each well of every column of the 96-well plate in 100 μL aliquots. After the addition of the drug solution, the cells were incubated at 37 °C for 48 hours. After the incubation period, the medium was aspirated and the cells were washed with DPBS and then 40 μL of 0.5 mg/mL MTT (3-(4,5-dimethylthiazol-2-yl)-2,5-diphenyltetrazolium bromide) in DPBS was added to each well. The cells were then incubated at 37 °C for 3 hours. After the incubation period, the MTT solution was aspirated and the remaining crystals were dissolved using a 40 μL of 0.4 M HCl in isopropanol. The plates were

shaken for 10 minutes to assure that all of the crystals are dissolved. The optical density was determined from the resulting solutions using the Acsent Multiskan optical density reader. Each experiment was run in triplicate.

Data analysis for MTT assay[86]

The optical density data was used to calculate IC_{50} values for each drug on a given cell line using the Hill slope equation. The optical density values obtained from each concentration of drug solution were divided by the optical density value obtained from the cells with zero drug concentration. Using SigmaPlot v.10, the ratios were plotted versus the drug concentration and the IC_{50} values were calculated from the plot using the pre-programmed calculation within the SigmaPlot program.

§ 1.5.0 References

1. Hanahan, D.; Weinberg, R. A. Hallmarks of Cancer: The Next Generation. *Cell* **2011,** 144, 646-674.
2. Jemal, A., Bray, F., Center, M.M., Ferlay, J., Ward, E., Forman, D. Global Cancer Statistics. *CA Cancer J. Clin.* **2011,** 61, 69-90.
3. Siegel, R., Ward, E., Brawley, O., Jemal, A. Cancer Statistics, 2011. *CA Cancer J. Clin.* **2011,** 61, 212-236.
4. Jernal, A.; Siegel, R.; Ward, E.; Murray, T.; Xu, J.; Smigal, C.; Thun, M. J. Cancer Statistics, 2006. *CA Cancer J Clin* **2006,** 56, 106-130.
5. Adams, D. J.; Wahl, M. L.; Flowers, J. L.; Sen, B.; Colvin, M.; Dewhirst, M. W.; Manikumar, G.; Wani, M. C. Camptothecin analogs with enhanced activity against human breast cancer cells. II. Impact of the tumor pH gradient. *Cancer Chemo. and Pharm.* **2005,** 57, 145-154.
6. Ulukan, H.; Swaan, P. W. Camptothecins, a review of their chemotherapeutical potential. *Drugs* **2002,** 62, 2039-2057.
7. Wall, M. E.; Wani, M. C.; Cook, C. E.; Palmer, K. H.; McPhail, A. T.; Sim, G. A. Plant antitumor agents. I. The isolation and structure of camptothecin, a novel alkaloidal leukemia and tumor inhibitor from camptotheca acuminate. *J. Am. Chem. Soc.* **1966,** 88, 3888-3890.
8. Li, Q.-Y.; Zu, Y.-G.; Shi, R.-Z.; Yao, L.-P. Review Camptothecin: Current Perspectives. *Curr. Med. Chem.* **2006,** 13, 1-19.
9. Wall, M. E.; Wani, M. C. Camptothecin and Taxol: Discovery to Clinic-Thirteenth Bruce F. Cain Memorial Award LEcture. *Cancer Res.* **1995,** 55, 753-760.
10. Wani, M. C.; Taylor, H. L.; Wall, M. E.; Coggon, P.; McPhail, A. T. Plant antitumor agents. VI. Isolation and structure of taxol, a novel antileukemic and antitumor agent from Taxus brevifolia. *J. Am. Chem. Soc.* **1971,** 93, 2325-2327.
11. Schiff, P. B.; Fant, J.; Horwitz, S. B. Promotion of microtubule assembly in vitro by taxol. *Nature* **1979,** 277, 665-667.
12. Schiff, P. B.; Horwitz, S. B. Taxol Stabilizes Microtubules in Mouse Fibroblast Cells. *Proc. Natl. Acad. Sci. U.S.A.* **1980,** 77, 1561-1565.
13. Downing, K. H.; Nogales, E. Tubulin and microtubule structure. *Curr. Opin. Cell Biol.* **1998,** 10, 16-22.

14. Jordan, M. A.; Wilson, L. Microtubules as a target for anticancer drugs. *Nat. Rev. Cancer* **2004,** 4, 253-265.
15. Jordan, M. A. Mechanism of action of antitumor drugs that interact with microtubules and tubulin. *Curr. Med. Chem.: Anti-Cancer Agents* **2002,** 2, 1-17.
16. Margolis, R. L.; Rauch, C. T.; Wilson, L. Mechanism of colchicine-dimer addition to microtubule ends: implications for the microtubule polymerization mechanism. *Biochemistry* **1980,** 19, 5550-5557.
17. Hadfield, J. A.; Ducki, S.; Hirst, N.; McGown, A. T. Tubulin and microtubules as targets for anticancer drugs. *Prog. Cell Cycle Res.* **2003,** 5, 309-325.
18. Ojima, I., Chen, J., Sun, L., Borella, C. P., Wang, T., Miller, M. L., Lin, S., Geng, X., Kuznetsova, L., Qu, C., Gallagher, G., Zhao, X., Zanardi, I., Xia, S., Horwitz, S.B., St. Clair, J. M., Guerriero, J.L., Bar-Sagi, D., Veith, J. M., Pera, P., Bernacki, R. J. Design, Synthesis, and Biological Evaluation of New-Generation Taxoids. *J. Med. Chem.* **2008,** 51, 3203-3221.
19. Nicolaou, K. C.; Dai, W.-M.; Guy, R. K. Chemistry and Biology of Taxol. *Angew. Chem., Int. Ed. Engl.* **1994,** 33, 15-44.
20. Holton, R. A.; Somoza, C.; Kim, H. B.; Liang, F.; Biediger, R. J.; Boatman, P. D.; Shindo, M.; Smith, C. C.; Kim, S.; Nadizadeh, H.; Suzuki, Y.; Tao, C.; Vu, P.; Tang, S.; Zhang, P.; Murthi, K. K.; Gentile, L. N.; Liu, J. H. First total synthesis of taxol. 1. Functionalization of the B ring. *J. Am. Chem. Soc.* **1994,** 116, 1597-1598.
21. Holton, R. A.; Somoza, C.; Kim, H. B.; Liang, F.; Biediger, R. J.; Boatman, P. D.; Shindo, M.; Smith, C. C.; Kim, S.; Nadizadeh, H.; Suzuki, Y.; Tao, C.; Vu, P.; Tang, S.; Zhang, P.; Murthi, K. K.; Gentile, L. N.; Liu, J. H. First total synthesis of taxol. 2. Completion of the C and D rings. *J. Am. Chem. Soc.* **1994,** 116, 1599-1600.
22. Nicolaou, K. C.; Nantermet, P. G.; Ueno, H.; Guy, R. K.; Couladouros, E. A.; Sorensen, E. J. Total Synthesis of Taxol. 1. Retrosynthesis, Degradation, and Reconstitution. *J. Am. Chem. Soc.* **1995,** 117, 624-633.
23. Nicolaou, K. C.; Liu, J. J.; Yang, Z.; Ueno, H.; Sorensen, E. J.; Claiborne, C. F.; Guy, R. K.; Hwang, C. K.; Nakada, M.; Nantermet, P. G. Total Synthesis of taxol. 2. Construction of A and C ring intermediates and initial attempts to construct the ABC ring system. *J. Am. Chem. Soc.* **1995,** 117, 634-644.
24. Nicolaou, K. C.; Yang, Z.; Liu, J. J.; Nantermet, P. G.; Claiborne, C. F.; Renaud, J.; Guy, R. K.; Shibayama, K. Total Synthesis of Taxol. 3. Formation of Taxol's ABC Ring Skeleton. *J. Am. Chem. Soc.* **1995,** 117, 645-652.
25. Nicolaou, K. C.; Ueno, H.; Liu, J. J.; Nantermet, P. G.; Yang, Z.; Renaud, J.; Paulvannan, K.; Chadha, R. Total Synthesis of Taxol. 4. The Final Stages and Completion of the Synthesis. *J. Am. Chem. Soc.* **1995,** 117, 653-659.
26. Danishefsky, S. J.; Masters, J. J.; Young, W. B.; Link, J. T.; Snyder, L. B.; Magee, T. V.; Jung, D. K.; Isaacs, R. C. A.; Bornmann, W. G.; Alaimo, C. A.; Coburn, C. A.; Di Grandi, M. J. Total Synthesis of Baccatin III and Taxol. *J. Am. Chem. Soc.* **1996,** 12, 2843-2859.
27. Wender, P. A.; Badham, N. F.; Conway, S. P.; Floreancig, P. E.; Glass, T. E.; Granicher, C.; Houze, J. B.; Janichen, J.; Lee, D.; Marquess, D. G.; McGrane, P. L.; Meng, W.; Mucciaro, T. P.; Muhlebach, M.; Natchus, M. G.; Paulsen, H.; Rawlins, D. B.; Satkofsky, J.; Shuker, A. J.; Sutton, J. C.; Taylor, R. E.; Tomooka, K. The Pinene Path to Taxanes. 5. Stereocontrolled Synthesis of a Versatile Taxane Precursor. *J. Am. Chem. Soc.* **1997,** 119, 2755-2756.

28. Morihira, K.; Hara, R.; Kawahara, S.; Nishimori, T.; Nakamura, N.; Kusama, H.; Kuwajima, I. Enantioselective Total Synthesis of Taxol. *J. Am. Chem. Soc.* **1998,** 120, 12980-12981.
29. Mukaiyama, T.; Shiina, I.; Iwadare, H.; Saitoh, M.; Nishimura, T.; Ohkawa, N.; Sakoh, H.; Nishimura, K.; Tani, Y.-i.; Hasegawa, M.; Yamada, K.; Saitoh, K. Asymmetric Total Synthesis of Taxol. *Chem. Eur. J.* **1999,** 5, 121-161.
30. Doi, T.; Fuse, S.; Miyamoto, S.; Nakai, K.; Sasuga, D.; Takahashi, T. A Formal Total Synthesis of Taxol Aided by an Automated Synthesizer. *Chem. Asian. J.* **2006,** 1, 370-383.
31. Denis, J. N.; Greene, A. E.; Guenard, D.; Gueritte-Voegelein, F.; Mangatal, L.; Potier, P. Highly efficient, practical approach to natural taxol. *J. Am. Chem. Soc.* **1988,** 110, 5917-5919.
32. Guénard, D.; Guéritte-Voegelein, F.; Potier, P. Taxol and taxotére: discovery, chemistry, and structure-activity relationships. *Acc. Chem. Res.* **1993,** 26, 160-167.
33. Colin, M.; Guénard, D.; Guéritte-Voegelein, F.; Potier, P. Taxotére, European Patent Application. Eur. Pat. Appl. 1988.
34. Guéritte-Voegelein, F.; Mangatal, L.; Guénard, D.; Potier, P.; Guilhem, J.; Cesario, M.; Pascard, C. Structure of a Synthetic Taxol Precursor: *N-tert*-Butoxycarbonyl-10-deacetyl-*N*-debenzoyltaxol. *Acta Crystallogr.* **1990,** C46, 781-784.
35. Bissery, M.; Guéritte-Voegelein, F.; Guénard, D.; Lavelle, F. Experimental Antitumor Activity of Taxotére (RP 56976, NSC 628503), a Taxol Analog. *Cancer Res.* **1991,** 51, 4845-4852.
36. Ojima, I. Recent Advances in the β-Lactam Synthon Method. *Acc. Chem. Res.* **1995,** 28, 383-389.
37. Ojima, I.; Sun, C. M.; Zucco, M.; Park, Y. H.; Duclos, O.; Kuduk, S. D. A Highly Efficient Route to Taxotère by The β-Lactam Synthon Method. *Tetrahedron Lett.* **1993,** 34, 4149-4152.
38. Ojima, I.; Habus, I.; Zhao, M. Efficient and Practical Asymmetric Synthesis of the Taxol C-13 Side Chain, N-Benzoyl-(2R,3S)-3-phenylisoserine, and Its Analogues via Chiral 3-Hydroxy-4-aryl-β-lactams through Chiral Ester Enolate-Imine Cyclocondensation. *J. Org. Chem.* **1991,** 56, 1681-1683.
39. Ojima, I.; Habus, I.; Zhao, M.; Zucco, M.; Park, Y. H.; Sun, C. M.; Brigaud, T. New and Efficient Approaches to the Semisynthesis of Taxol and Its C-13 Side Chain Analogs by Means of β-Lactam Synthon Method. *Tetrahedron* **1992,** 48, 6985-7012.
40. Ojima, I., Slater, J. C., Michaud, E., Kuduk, S. D., Bounaud, P. Y., Vrignaud, P., Bissery, M. C., Veith, J. M., Pera, P., Bernacki, R. J. Syntheses and Structure-Activity Relationships of the Second-Generation Antitumor Taxoids: Exceptional Activity against Drug-Resistant Cancer Cells. *J. Med. Chem.* **1996,** 39, 3889-3896.
41. Ojima, I.; Kuznetsova, L.; Ungureanu, I. M.; Pepe, A.; Zanardi, I.; Chen, J. Fluoro-β-lactams as Useful Building Blocks for the Synthesis of Fluorinated Amino Acids, Dipeptides, and Taxoids. In *Fluorine-containing Synthons*, Soloshonok, V. A., Ed. American Chemical Society/Oxford University Press: Washington, D.C., 2005; pp 544-561.
42. Ojima, I.; Slater, J. C. Synthesis of Novel 3`-Trifluoromethyl Taxoids Through Effective Kinetic Resolution of Racemic 4-CF_3-β-Lactams With Baccatins. *Chirality* **1997,** 9, 487-494.
43. Ojima, I.; Kuduk, S. D.; Slater, J. C.; Gimi, R. H.; Sun, C. M. Syntheses of New Fluorine-Containing Taxoids by Means of β-Lactam Synthon Method. *Tetrahedron* **1996,** 52, 209-224.

44. Kingston, D. G. I. Recent Advances in the Chemistry of Taxol1,2. *J. Nat. Prod.* **2000,** 63, 726-734.
45. Ojima, I. Tumor-targeting drug delivery of chemotherapeutic agents. *Pure Appl. Chem.* **2011,** 83, 1685-1698.
46. Ojima, I.; Zuniga, E. S.; Berger, W. T.; Seitz, J. D. Tumor-targeting drug delivery of new-genreation taxoids. *Future Med. Chem.* **2012,** 4, 33-50.
47. Georg, G. I. *The Organic Chemistry of b-Lactams and refereces cited therein*. VCH: New York, 1992.
48. Ojima, I. β-Lactam Synthon Method – Enantiomerically Pure β-Lactams as Synthetic Intermediates. In *The Organic Chemistry of β-Lactams and β-Lactam Antibiotics*, Georg, G. I., Ed. VCH Publishers: New York, 1992; pp 197-255.
49. Hatanaka, N.; Abe, R.; Ojima, I. β-Lactam as Synthetic Intermediate: Synthesis of Leucine-Enkephalin. *Chem. Lett.* **1981**, 1297-1298.
50. Hatanaka, N.; Ojima, I. Effective Method for the Asymmetric Synthesis of Bis-β-lactams by the Cycloaddition of Azidoketen to Benzylideneamines Bearing a Chiral β-Lactam Backbone. *J. Chem. Soc., Chem. Commun.* **1981**, 344-346.
51. Ojima, I.; Yamato, T.; Nakahashi, K. Synthesis of Novel and Chiral Bisazetidines by the Hydroalane Reduction of Bis-β-lactams. *Tetrahedron Lett.* **1985,** 26, 2035-2038.
52. Ojima, I.; Qiu, X. Asymmetric Alkylation of Chiral β-Lactam Ester Enolates. A New Approach to the Synthesis of α-Alkylated α-Amino Acids. *J. Am. Chem. Soc.* **1987,** 109, 6537-6538.
53. Ojima, I.; Shimizu, N.; Qiu, X.; Chen, H.-J. C.; Nakahashi, K. New Aspects of β-Lactam Chemistry: β-Lactams as Chiral Building Blocks. *Bull. Soc. Chim. France* **1987**, 649-658.
54. Cossio, F. P.; Lopez, C.; Oiarbide, M.; Palomo, C.; Aparicio, D.; Rubiales, G. Synthetic utility of azetidin-2,3-diones: a new approach to 3-hydroxyethyl-β-lactams and α-amino acid derivatives. *Tetrahedron Lett.* **1988,** 29, 3133-3136.
55. Ojima, I.; Park, Y. H.; Sun, C. M.; Zhao, M.; Brigaud, T. New and Efficient Routes to Norstatine and Its Analogs with High Enantiomeric Purity by β-Lactam Synthon Method. *Tetrahedron Lett.* **1992,** 33, 5739-5742.
56. Staudinger, H. Zur Kenntniss der Ketene. Diphenylketen. *Justus Liebigs Ann. Chem.* **1907,** 356, 51-123.
57. Cossio, F. P.; Arrieta, A.; Sierra, M. A. The Mechanism of the Ketene-Imine (Staudinger) Reaction in its Centennial: Still an Unsolved Problem? *Acc. Chem. Res.* **2008,** 41, 925-936.
58. Venturini, A.; Gonzalez, J. Mechanistic Aspects of the Ketene-Imine Cycloaddition Reactions. *Mini Rev. Med. Chem.* **2006,** 3, 185-194.
59. Dumas, S.; Hegedus, L. S. Electronic Effects on the Stereochemical Outcome of the Photochemical Reaction of Chromium Carbene Compleses with Imines to Form β-Lactams. *J. Org. Chem.* **1994,** 59, 4967-4971.
60. Georg, G. I.; Ravikumar, V. T. Stereocontrolled ketene-imine cycloaddition reactions. In *Organic Chemistry β-lactams*, G.I., G., Ed. VCH Publishing: New York, NY, 1993; pp 295-368.
61. Hegedus, L. S.; Montgomery, J.; Narukawa, Y.; Snustad, D. C. A contribution to the confusion surrounding the reaction of ketenes with imines to produce β-lactams. A comparison of stereoselectivity dependence on the method of ketene generation: acid chloride/triethylamine s photolysis of chromium carbene complexes. *J. Am. Chem. Soc.* **1991,** 113, 5784-5791.

62. Cossio, F. P.; Ugalde, J. M.; Lopez, X.; Lecea, B.; Palomo, C. A semiempirical theoretical study on hte formation of 5784-5791-lactams from ketenes and imine. *J. Am. Chem. Soc.* **1993,** 115, 995-1004.
63. Lopez, R.; Sordo, T. L.; Sordo, J. A.; Gonzalez, J. Torquoelectronic effect in the control of the stereoselectivity of ketene-imine cycloaddition reactions. *J. Org. Chem.* **1993,** 58, 7036-7037.
64. Cossio, F. P.; Arrieta, A.; Lecea, B.; Ugalde, J. M. Chiral Control in the Staudinger Reaction between Ketenes and Imines. A Theoretical SCF-MO Study on Asymmetric Torquoselectivity. *J. Am. Chem. Soc.* **1994,** 116, 2085-2093.
65. Wang, Y.; Liang, Y.; Jiao, L.; Du, D.-M.; Xu, J. Do Reaction Conditions Affect the Stereoselectivity in the Staudinger Reaction? *J. Org. Chem.* **2006,** 71, 6983-6990.
66. Brieva, R.; Crich, J. Z.; Sih, C. J. Chemoenzymic synthesis of the C-13 side chain of taxol: optically active 3-hydroxy-4-phenyl β-lactam derivatives. *J. Org. Chem.* **1993,** 58, 1068-1075.
67. Banik, B. K.; Manhas, M. S.; Bose, A. K. Stereospecific Glycosylation via Ferrier Rearrangement for Optical Resolution. *J. Org. Chem.* **1994,** 59, 4714-4716.
68. Patel, R. N. Enzymic processes for the resolution of enantiomeric mixtures of compounds useful as intermediates in the preparation of taxanes. 1995.
69. Holton, R. A.; Vu, P. Enzymatic process for the resolution of enantiomeric mixtures of b-lactams. 2001029245, 2001.
70. Kuznetsova, L.; Ungureanu, I.; Pepe, A.; Zanardi, I.; Wu, X.; Ojima, I. Trifluoromethyl- and difluoromethyl-β-lactams as useful building blocks for the synthesis of fluorinated amino acids, dipeptides, and fluoro-taxoids. *J Fluor. Chem* **2004,** 125, 487-500.
71. Chen, J.; Kuznetsova, L.; Ungureanu, I.; Ojima, I. Recent Advances in the Synthesis of α-Hydroxy-β-amino Acids and Their Use in the SAR Studies of Taxane Anticancer Agents. In *Enantioselective Synthesis of Amino Acids, Second Edition*, Juaristi, E.; Soloshonok, V., Eds. John Wiley: New York, 2005; pp 447-476.
72. Kuznetsova, L. V.; Pepe, A.; Ungureanu, I. M.; Pera, P.; Bernacki, R. J.; Ojima, I. Syntheses and structure-activity relationships of novel 3'-difluoromethyl and 3'-trifluoromethyl-taxoids. *J. Fluor. Chem.* **2008,** 129, 817-828.
73. Lin, S.; Geng, X.; Qu, C.; Tynebor, R.; Gallagher, D.; Pollina, E.; Rutter, J.; Ojima, I. Synthesis of Highly Potent Second-Generation Taxoids Through Effective Kinetic Resolution Coupling of Racemic β-Lactams with Baccatins. *Chirality* **2000,** 12, 431-441.
74. Geney, R.; Sun, L.; Pera, P.; Bernacki, R. J.; Xia, S.; Horwitz, S. B.; Simmerling, C. L.; Ojima, I. Use of the Tubulin Bound Paclitaxel Conformation for Structure-Based Rational Drug Design. *Chem. & Bio.* **2005,** 12, 339-348.
75. Ojima, I.; Slater, J. C.; Kuduk, S. D.; Takeuchi, C. S.; Gimi, R. H.; Sun, C. M.; Park, Y. H.; Pera, P.; Veith, J. M.; Bernacki, R. J. Syntheses and Structure-Activity Relationships of Taxoids Derived from 14-beta-Hydroxy-10-deacetylbaccatin III. *J. Med. Chem.* **1997,** 40, 267-278.
76. Ojima, I.; Wang, T.; Miller, M. L.; Lin, S.; Borella, C. P.; Geng, X.; Pera, P.; Bernancki, R. J. Synthesis and structure-activity relationships of new second-generation taxoids. *Bioorg. Med. Chem. Lett.* **1999,** 9, 3423-3428.
77. Ojima, I.; Songnian, L.; Wang, T. Recent Advances in the Medicinal Chemistry of Taxoids with Novel -Amino Acid Side Chains. *Curr. Med. Chem.* **1999,** 6, 927-954.

78. Ferlini, C., Distefano, M., Pignatelli, F., Lin, S., Riva, A., Bombardelli, E., Mancuso, S., Ojima, I., Scambia, G. Antitumor activity of novel taxanes that act as the same time as cytotoxic agents and P-glycoprotein inhibitors. *Brit. J. Cancer* **2000,** 83, 1762-1768.
79. Geney, R.; Chen, J.; Ojima, I. Recent Advances in the New Generation Taxane Anticancer Agents *Med. Chem.* **2005,** 1, 125-139.
80. Ehrlichova, M., Vaclavikova, R., Ojima, I., Pepe, A., Kuznetsova, L.V., Chen, J., Truksa, J., Kovar, J., Gut, I. Transport and cytotoxicity of paclitaxel, docetaxel, and novel taxanes in human breast cancer cells. *Arch Pharmacol* **2005,** 372, 95-105.
81. Kovar, J., Ehrlichova, M., Smejkalova, B., Zanardi, I., Ojima, I., Gut, I. Comparison of cell death-inducing effect of novel taxane SB-T-1216 and paclitaxel in breast cancer cells. *Anticancer Res.* **2009,** 29, 2951-2960.
82. Gottlieb, H. E.; Kotlyar, V.; Nudelman, A. NMR Chemical Shifts of Common Laboratory Solvents as Trace Impurities. *J. Org. Chem.* **1997,** 62, 7512-7515.
83. Brieva, R.; Crich, J. Z.; Sih, C. J. Chemoenzymic synthesis of the C-13 side chain of taxol: optically active 3-hydroxy-4-phenyl .beta.-lactam derivatives. *J. Org. Chem.* **1993,** 58, 1068-1075.
84. Ojima, I.; Habus, I.; Zhao, M.; Zucco, M.; Park, Y. H.; Sun, C. M.; Brigaud, T. New and efficient approaches to the semisynthesis of taxol and its C-13 side chain analogs by means of [beta]-lactam synthon method. *Tetrahedron* **1992,** 48, 6985-7012.
85. Cree, I. A. Principles of Cancer Cell Culture. In *Methods in Molecular Biology*, Cree, I. A., Ed. Springer Science + Business Media, LLC: 2011; Vol. 731, pp 13-26.
86. Mosmann, T. Rapid colorimetric assay for cellular growth and survival: Application to proliferation and cytotoxicity assays. *J. Immunological Methods* **1983,** 65, 55-63.

Chapter 2

Biological Evaluation of New-Generation Taxoid SB-T-1214 against Cancer Stem Cells

Chapter Contents

§ 2.1.0 Introduction

§ 2.1.1 Cancer Stem Cells

There are many types of cancers, but all forms of cancer share one common characteristic: the rapid proliferation of affected cells. Two basic therapies for treating cancer have been developed: (1) differentiation therapy, which induces differentiation;[1-4] and (2) destruction therapy, which stops malignant proliferation.[4] Despite success in some cases, these therapies do not completely cure cancer, as second malignancies arise after treatment. The ineffectiveness of these therapies has been attributed to the existence of a rare drug-resistant and slow-proliferating, tumor-initiating cell: cancer stem cells (CSCs).[5]

Stem cells have the ability to self-renew and generate all of the cell lineages in corresponding tissues. Stem cells divide asymmetrically. When stem cells divide producing two daughter cells, one daughter remains a stem cell and the other becomes a progenitor cell that undergoes differentiation into specialized cells.[6, 7] CSCs are very similar to normal stem cells. CSCs are tumor-initiating cells that possess the capacity to self-renew and differentiate into non-stem cell cancer progeny.[8-10]

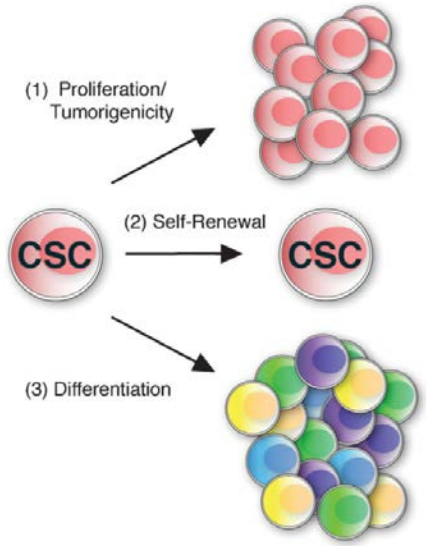

Figure 2.1: Hallmarks of CSCs (adapted from [11])

The origin of CSCs remains unknown. However, several theories are currently being investigated. One theory is that CSCs originated from normal stem cells which have undergone genetic or epigenetic mutations.[12-15] Similarly, CSCs may arise from an intrinsic mutation of the stem cell niche.[4] The stem cell niche is an anchoring site for stem cells which functions to: (1) maintain stem cells, (2) generate factors that control stem cell number, proliferation and fate determination, and (3) control normal asymmetric division of stem cells.[16, 17] Another theory is that cancer cells de-differentiated or re-differentiated to stem-like cells.[18] A similar concept is based on a tumor hierarchy model. In this model, tumors are comprised of different types of stem cells: one type of stem cell that is optimal to the specific environment and a secondary type that can adjust to another environment and adapt.[8]

§ 2.1.2 Identifying and Isolating CSCs

Cancer stem cells contain certain markers on the cell surface, which can be used to identify and verify the "stemness" of a cancer cell.[11] CD133, also known as prominin-1, is a cell membrane protein that has been widely used as a marker for the identification and isolation of CSCs from normal and cancer tissues.[19] Also, stemness verification can be made using a combination of markers. For example, CSCs can be identified by using both CD133 and CD44 as markers.[20-28] CD44 is a glycoprotein involved in stemness and tumor development, in part via β-catenin and Wnt signaling activation of the CD44 gene transcription.[29, 30] It was demonstrated that the full range of CD44 alternatively spliced variants is widely expressed in normal and tumor colonic cells located in the crypt base known as a colonic stem cell niche. [31] Numerous studies have demonstrated that both $CD133^+$ and $CD44^+$ cells are highly tolerant to anti-cancer therapies.[28, 32-39] Moreover, the number of CSCs can be significantly increased after treatment.[34, 40-44] The ratio of $CD133^+$ cells correlates with tumor aggressiveness, histological grade and clinical outcome.[35, 45-48] Similar data were reported for CD44-positive cells.[28]

Through the years, CSCs have been identified and isolated by sorting cells for the presence of stem cell markers. In 1994, Dick et al. reported the existence of CSCs by showing that leukemia-initiating stem cells, cells expressing a $CD34^+/CD38^-$ phenotype, induced acute myeloid leukemia (AML) in SCID mice.[49] In 2003, Clarke et al. reported the existence of tumor-initiating cells, cells expressing a $CD44^+/CD24^{-/low}$ phenotype, in breast cancer.[45] In recent years, many types of CSCs from brain,[35, 50] kidney,[51] liver,[52, 53] colon,[54, 55] and pancreatic[56] cancers have been identified, isolated and enriched by exploiting cancer cell surface markers.

§ 2.1.3 Targeting CSCs

Traditional therapies act against the bulk population of tumor cells with the underlying premise that cancer cells have unlimited proliferative potential and can acquire the ability to metastasize. However, small numbers of disseminated cancer cells found at sites distant from the primary tumor site do not generate a secondary tumor (i.e. the disseminated cells are not metastatic).[57, 58] It has been proposed that most cancer cells lack the ability to form a new tumor and only disseminated CSCs are responsible for metastasis.[59] This may be the reason as to why current drugs fail to eradicate solid tumors. Though current drugs are effective against metastatic tumors, the effects are often temporary thus leading to further tumor growth.[60, 61]

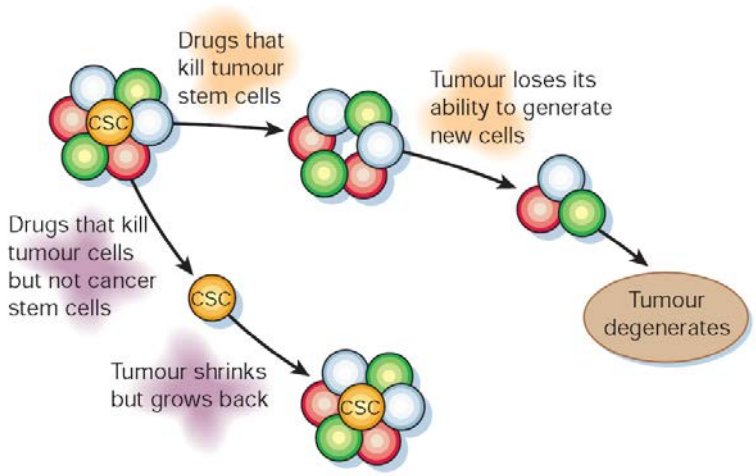

Figure 2.2: CSCs as targets for anticancer therapy (adapted from [59])

CSCs are exclusively endowed with tumor-initiating capacity in the majority of cancer types, and are responsible for tumor recurrence, metastasis and drug resistance. CSCs give rise to a hierarchy of actively proliferating, but progressively differentiating tumor cells, which contribute to the cellular heterogeneity of human cancers. Furthermore, CSCs are more resistant to chemotherapy than mature cells from the same tumor tissue.[62] This resistance is due to multiple mechanisms, including their relative quiescence, profound capacity for DNA repair, activation of the ATP-binding cassette (ABC) transporters that efflux anticancer agents, resistance to apoptosis and others.[63-65] Accordingly, novel chemotherapeutic agents should be designed to specifically target CSCs. To develop CSC-targeting drugs, CSCs need to be isolated for a gene-expression profiling. This will provide insight into how CSCs are tumor-initiating, and based on the biochemical pathways involved in tumorigenesis, CSC targets can be identified and new chemotherapeutics can be developed.

§ 2.2.0 Results and Discussion

Colon cancer is inherently drug-resistant due to various unknown mechanisms, thus both CSCs and the variably differentiated cells that comprise the proliferative pool of the colon cancer can potentially contribute to drug resistance. CSCs are biologically distinct from differentiated cancer cells, thus targeting CSCs entails determining and targeting the differences in gene expression between CSCs and normal cancer cells.

§ 2.2.1 Biological Activity of Chemotherapeutic Agents against CSCs

HCT-116 cells were selected to compare the cytotoxic activity of traditional chemotherapeutic agents with those of new-generation taxoids in CSC-enriched cell culture. As shown in the previous chapter, a number of new-generation taxoids exhibited 2-3 orders of magnitude higher cytotoxicity than the parent compound, paclitaxel against a series of cancer cell lines. One compound that performed well against all cancer cell lines was SB-T-1214. With such promising antitumor activity, it was hypothesized that SB-T-1214 may specifically target

tumor-specific CSCs by inhibiting some stemness-related signalling pathways and/or promoting their differentiation. Since CSC-enriched CD133+ and CD44+ cell populations are more resistant to conventional therapies compared to differentiated cells, evaluating the cytotoxic effect of SB-1214 against CD133+ and CD44+ cell phenotypes is of significant importance.[28, 32-39]

It was found that HCT-116 cells grown at standard adherent conditions express moderate levels of stem cell markers, CD133 and CD44. However, cytotoxicity assay experiments require not only enriched CSCs, but also culture conditions that allow for the retaining of the stem-like phenotype during drug treatment. Kirkland reported that collagen type I inhibits cell differentiation and promotes stemness in human colon cancer.66 We have found that additional purification of CD133high/CD44high cell population by repeated sets of cell sorting followed by culturing at low cell density on type I collagen in serum-free stem cell medium led to significantly higher *in vivo* tumorigenic potential and sphere forming capacity of this cell phenotype.[26, 27]

Accordingly, HCT-116 cells were twice sorted for the CD133 phenotype using magnetic-activated cell sorting (MACS). The sorted cells were cultured on collagen type I-coated plates before being split into collagen-coated 96-well plates and treated with drug. The cytotoxicity of cisplatin, doxorubicin, methotrexate, topotecan, paclitaxel, SB-T-1214, SB-T-1216, SB-T-121602 and SB-T-12854 was evaluated. The results of this experiment are shown in Table 2.1.

Table 2.1: Biological Evaluation of Chemotherapeutic Agents against CSC-Enriched Cancer Cells

Cisplatin

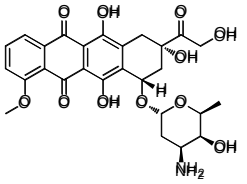

Doxorubicin

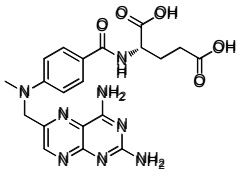

Methotrexate

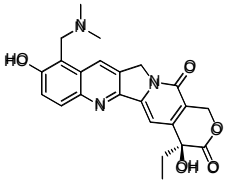

Topotecan

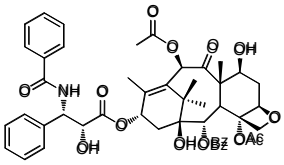

Paclitaxel

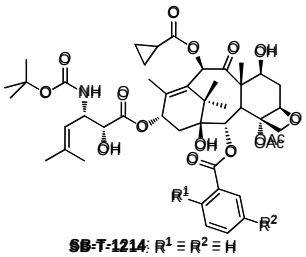

SB-T-1214: $R^1 \equiv R^2 \equiv H$

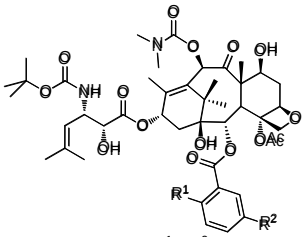

SB-T-1216: $R^1 \equiv R^2 \equiv H$
SB-T-121602: $R^1 \equiv H$, $R^2 \equiv CH_3$

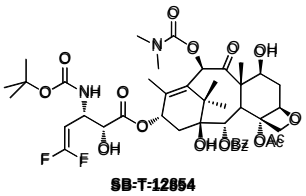

SB-T-12854

Cancer Cell Line	Drug	Average IC_{50} (nM)
HCT-116 ++ ($CD133^+$ colon)	Cisplatin	4540 ± 276
	Doxorubicin	78.0 ± 28.2
	Methotrexate	32.7 ± 11.2
	Paclitaxel	33.8 ± 3.33
	Topotecan	451 ± 12
	SB-T-1214	0.28 ± 0.10
	SB-T-1216[a]	0.83 ± 0.05
	SB-T-121602[b]	0.24 ± 0.13
	SB-T-12854[b]	0.14 0.05

[a] taxoid synthesized by Ilaria Zanardi; [b] taxoid synthesized by Joshua D. Seitz

- Cells were suspended in MSCBM hMSC Basal Medium (Lonza BioWhittaker, PT-3238) supplemented with MSCGM hMSC SingleQuot Kit (Lonza BioWhittaker, PT-4105) and cultured on collagen-coated plates before administration of taxoid
- Cells were incubated for 48 hours at 37 °C with 5% CO_2 after administration of taxoid
- The optical density was determined using Acsent Multiskan optical density reader
- The reported values are a calculated averages of IC_{50} values determined from three individual experiments
- IC_{50} values were calculated using SigmaPlot v 10.0
- All IC_{50} values are report in nM scale unless otherwise noted

As seen from Table 2.1, methotrexate and paclitaxel showed the best activity against the CSC-enriched cell line (IC50 values of 32.7 nM and 33.8 nM, respectively) when compared to the other traditional chemotherapeutic agents. All of the new-generation taxoids showed subnanomolar activity. These promising results suggest that new-generation taxoids may not only inhibit CSC growth but also may inhibit the tumorigenic and metastatic properties of CSCs.

§ 2.2.2 Biological Activity of SB-T-1214 against CSC-Enriched Colon Cancer Cells

To study the effects of SB-T-1214 against colon CSCs, DLD-1, HCT-116 and HT-29 cell lines were chosen. As mentioned above with HCT-116, the majority (bulk) of all types of DLD-1 and HT-29 cells expressed moderate levels of stem cell markers, CD133 and CD44, when grown in standard adherent conditions. However, all three cell lines were comprised of a small subpopulation of cells which expressed the highest levels of CD133 and CD44 (CD133high/CD44high; dotted squares on Figure 2.3 A-C). These cells were previously reported to possess profound self-renewing capacity in vivo and in vitro and the 3D spheroids induced by these cells possessed stem-like features.[26, 27]

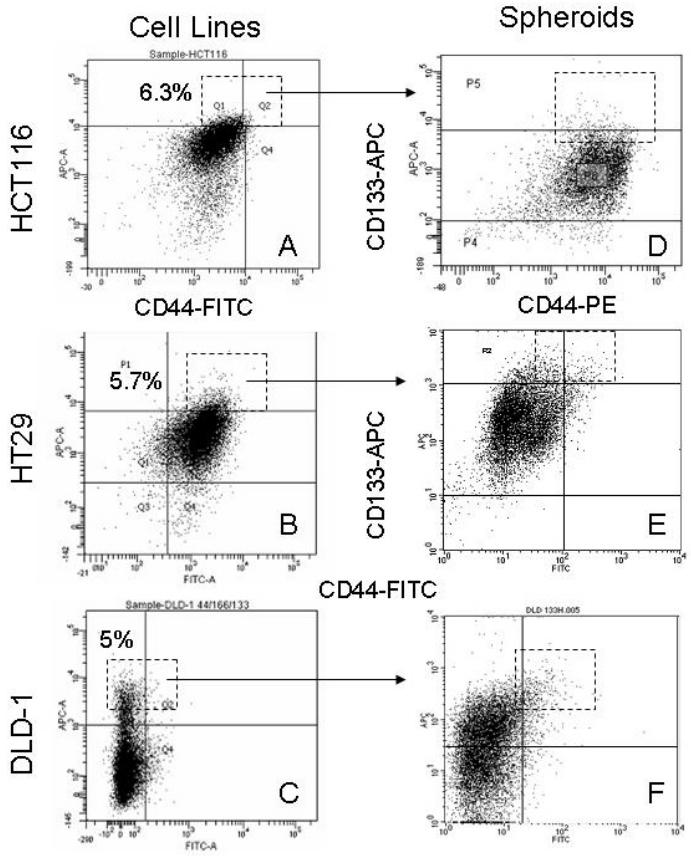

Figure 2.3: The CD133^{high}/CD44^{high} phenotypic cell population in three colon cancer cell lines (adapted from [5])

It was also found that the isolated CD133high/CD44high cells derived from all three colon cancer cell lines were capable of forming dense floating multicellular spheroids in non-adherent cultures with serum-free medium. The HCT-116 cells revealed higher efficiency (1 of 66 cells induced 3D spheroids) compared to DLD-1 (1 of 118 cells) and HT-29 (1 of 175 cells). Dissociated spheroid cells retained an original cell phenotype and expressed widely studied stem cell markers.5 The expression of stem-cell related genes and effects of CSC-related activity

induced by SB-T-1214 in these 3D spheroids was studied and compared to that of bulk cells using PCR array assay.

As mentioned previously, the purification of CD133high/CD44high cell populations and culturing at low density on collagen-type I in serum-free medium promotes the expression of stem-like phenotype in human colon cancer cells and increases the expression of CD133.66 These approaches were used for growing 3D spheroids enriched with highly tumorigenic and clonogenic cells to be able to reveal genomic differences between these relatively rare cells in comparison to their bulk counterparts. They were also used as a target population for studying CSC-specific drug effects.

In our first study, the fluorescence activated cell sorting (FACS) sorted CD133high/CD44high cells were plated on type I collagen-coated plates and cultured in MSCB serum-free medium for 2 days before treatment with SB-T-1214. After 48 h incubation with the drug, a majority (89-96%) of all cell types underwent apoptosis (Figure 2.4 A-C). The 4-11% surviving cells showed multiple abnormalities, such as enlarged size (Figure 2.4 G-I, K), multiple nuclei (Figure 2.4 E, G-I), a significant increase in the number of long (Figure 2.4 J) and knobby (Figure 2.4 F, I) projections and severe vacuolization (Figure 2.4 K). Furthermore, many cells showed signs of mitotic catastrophe (Figure 2.4 G-I).

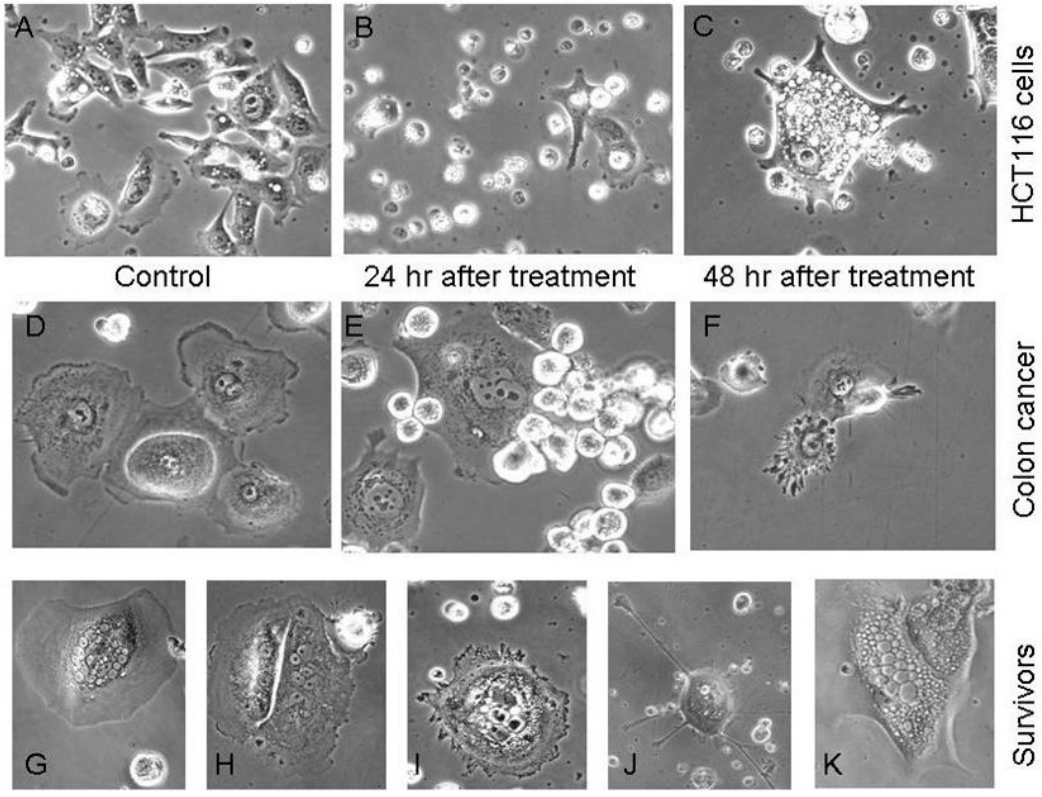

Figure 2.4: Cytotoxic effects of SB-T-1214 against colon CSC-enriched cell populations grown on type I collagen-coated surfaces (adapted from [5])

Next, we studied the activity of SB-T-1214 against colon cancer spheroids induced by $CD133^{high}/CD44^{high}$ cells in 3D cultures. Spheroids were treated with 0.1-1 μM SB-T-1214 for 48 h (Figure 2.5 A-C). Confocal microscopy (CFM) images show that FITC-labeled taxoid

penetrated the spheroids (Figure 2.5 B). Treatment with the drug induced loss of integrity of the floating spheroids and apoptosis in more than 90% of the spheroid cells. It is worthy of note that the surviving cells significantly loss the ability to form secondary spheroids, indicating that the CSC population was critically affected and the drug induced a loss of stemness (Figure 2.5 F). Thus, 1000 of untreated HCT-116 primary spheroid cells induced 125 ± 6 secondary spheroids, 1000 HT-29 primary spheroid cells induced 75 ± 7 secondary spheroids and 1000 DLD-1 cells gave rise to 93 ± 6 secondary spheroids, whereas SB-T-1214-treated spheroid cells produced 1.5 ± 0.3, 4 ± 0.6 and 3 ± 0.4 secondary spheroids, respectively.

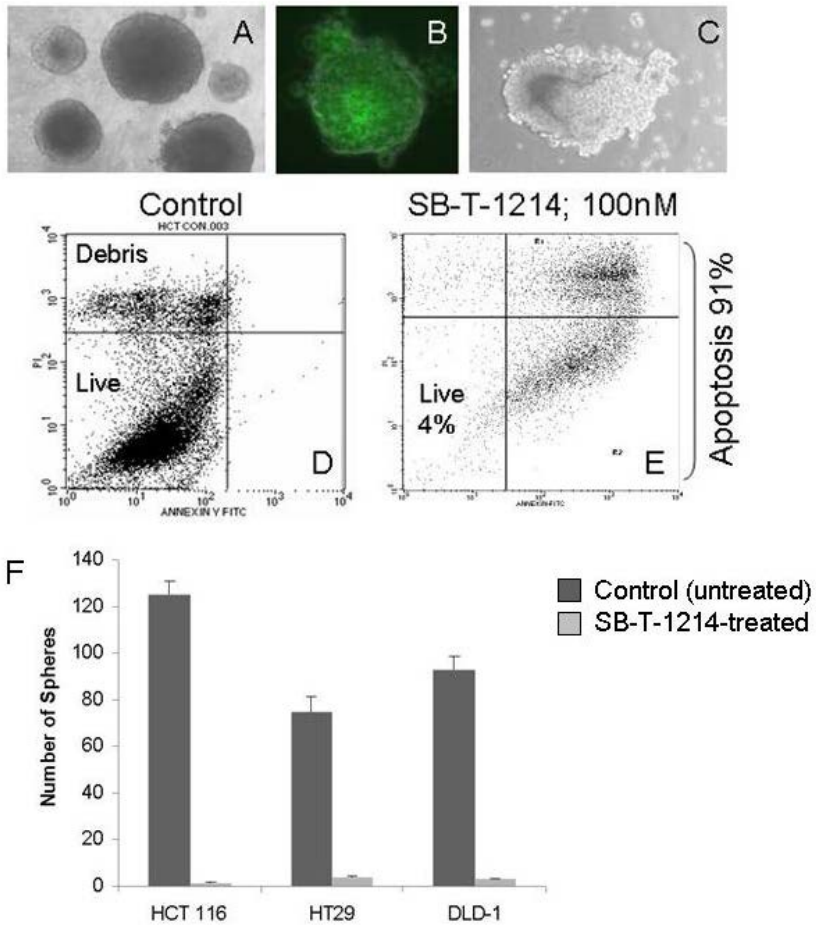

Figure 2.5: Biological activity of SB-T-1214 against colonospheres grown in 3D culture (adapted from [5])

The $CD133^{high}/CD44^{high}$ cell populations derived from the three analyzed colon cancer cell lines were characterized with the stem cell pathway-specific PCR Array assay (*SA*Biosciences). Each array contains SYBR Green-based real-time PCR gene-specific assays for a set of 84 genes. Using filtering criteria of a 1.5 or greater fold-change in expression, we have analyzed differentially expressed genes in HCT-116, DLD-1 and HT-29 types of floating colonospheres compared to their bulk differentiated adherent counterparts, as well as before and after treatment with SB-T-1214 (Figure 2.6).

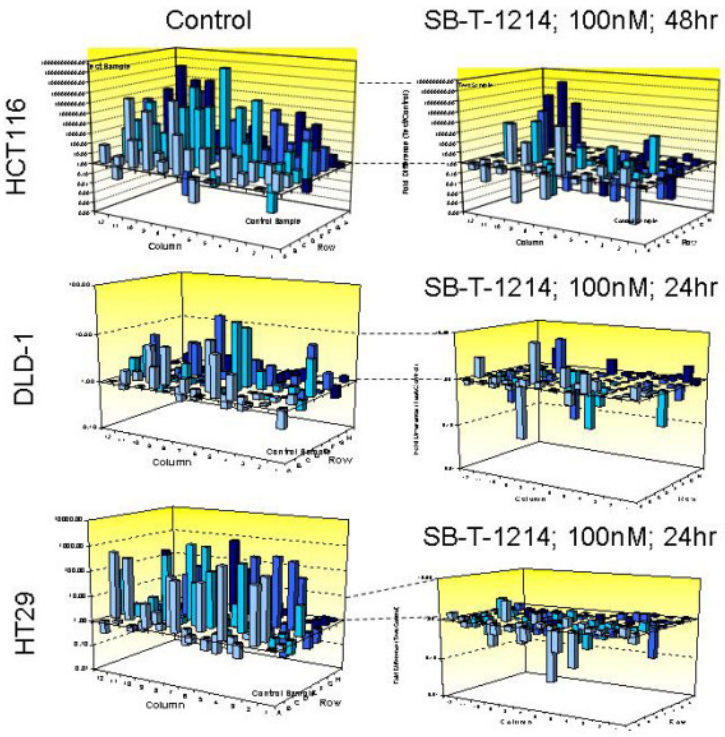

Figure 2.6: SB-T-1214-induced alteration in stem cell-related gene expression profiles (adapted from [5])

The most profound differences were observed in HCT-116 spheroids grown from $CD133^{high}/CD44^{high}$ cells. Approximately one-fourth of the analyzed stem cell-related genes were commonly up-regulated in all three types of spheroids, however, HCT-116 spheroids showed significantly higher levels of stem cell-related gene expression, including Wnt and Notch pathway genes responsible for self-renew and cell cycle regulation. Furthermore, 6 out of 6 analyzed genes responsible for stem cell self-renewal (*SOX1*, *SOX2*, *MYST1*, *MYST2*, *NEUROG2* and *HSPA9*) and 3 out of 5 genes which regulate symmetrical/asymmetrical cell division (*NOTCH1*, *NOTCH2* and *PARD6A*) were significantly up-regulated in the HCT-116 $CD133^{high}/CD44^{high}$ colonospheres compared to their bulk counterparts. The most significantly up-regulated genes in HT-29 spheroids were *ACAN*, *ALPI*, *APC*, *ASCL2*, *CCND2*, *CD3D*, *CD4*, *CD8A*, *CD8B*, *COL2A1*, *COL9A1*, *DHH*, *DLL3*, *DTX1 FGF1*, *GJA1*, *S100B*, *SOX2*, *T*, *TERT* and *WNT1*. The genes up-regulated in DLD-1 spheroids *were ALDH1A1*, *ASCL2*, *CCND2*, *CD4*, *COL1A1*, *DLL1*, *DTX1*, *FGF1*, *GJA1*, *IGF1*, *JAG1*, *MME*, *NCAM1*, and *NOTCH1*.

It is worthy of note that relatively low concentrations of SB-T-1214 (100 nM-1 μM for 24 or 48 hr) induced dramatic down-regulation of stemness in the majority of stem cell-related genes in all three types of colonospheres. Though SB-T-1214 showed subnanomolar activity in monolayer MTT assay, CSCs are a much more aggressive and drug resilient cell population, thus a concentration greater than experimentally obtained IC_{50} concentration was used. The most significant drug-induced down-regulation of gene expression was detected in: (1) HCT-116 spheroids for *SOX1*, *RPL13A*, *BMP3*, *NEUROG2*, *GJB1*, *GJA1*, *ASCL2*, *CTNNA1*, *GDF2*, *ALPI*, *S100B*, *CD8B1*, *ACTB*, *CCND1*, *FGF1*, *PARD6A*, *DVL1*, *GDF3*, *ISL1*, *CD3D*, *MME*, *FGFR1*, *RB1*, *BMP1*, *AIN1*, *ALDH1A1*, *CD8A*, *PPARD*, *FZD1*, *NUMB*, *ABCG2*; (2) HT-29 spheroids for *ACAN*, *ALPI*, *BMP3*, *CD3D*, *CD4*, *CD8A*, *CD8B*, *CDH2*, *COL2A1*, *COL9A1*, *DHH*, *DLL1*,

DLL3, DTX1, FGF1, FGF3, FZD1, GDF2, IGF1, MME, MYOD, NCAM1, NEUROG2, S100B, SOX2, and *TERT*; and (3) DLD-1 spheroids for *CD4, CDH2, COL1A1, DLL1, DTX1, IGF1, FGF3, FZD1, JAG1, KRT15, MSX1, NCAM1* and *NOTCH1*. Many of these genes are related to the stem cell self-renewal, regulation of symmetric/asymmetric division and pluripotency.

§ 2.3.0 Summary

There is some evidence that suggests that the majority of tumors are comprised of a small population of tumor-initiating cancer stem cells (CSCs). CSCs are responsible for tumor development, cancer cell maintenance and drug resistance. CSCs can be identified and isolated based on specific cell surface markers which verify the stemness of a cancer cell. Stem cell-enriched populations of DLD-1, HCT-116 and HT-29 (human colon) cancer cell lines were isolated by sorting bulk cancer cells which expressed high levels of CD133 and CD44. These CD133high/CD44high sorted cells were used to induce 3D colon cancer spheroids. New-generation taxoids showed excellent activity against CSC-enriched HCT-116 CD133high cells. Furthermore, SB-T-1214 showed substantial activity against colon cancer spheroids and efficiently inhibited the expression of a majority of stem cell-related genes. This data indicates that the previously observed long-term efficacy of SB-T-1214 against drug resistant colon tumors in vivo may be explained by the down-regulation of multiple stem cell-related genes in the tumorigenic population.

§ 2.4.0 Experimental

Caution

Cisplatin, doxorubicin, methotrexate, topotecan and paclitaxel have been established as potent cytotoxic agents. Thus, they and all structurally related compounds and derivatives must be considered as mutagens and potential reproductive hazards for both males and females. Appropriate precautions (i.e. use of gloves, goggles, lab coat and fume hood) must be taken while handling these compounds.

General information

DLD-1, HCT-116 and HT-29 (ATCC) were maintained at SBU Cell Culture/Hybridoma Facility. Prior to sorting, cells were grown cultured in DMEM (Lonza BioWhittaker, BW12-604F) supplemented with 10% FBS (Thermo Scientific, HyClone, SH3007003) and 1% Penn Strip, at 37 °C in a humidified incubator with 5% CO_2. Isolated CSCs were counted, resuspended in serum-free Mesenchymal stem cell medium (MSCBM; Lonza BioWhittaker PT-3238) and cultured in: (1) adherent culture on type I collagen (Rat tail, BD Biosciences, 354236); or (2) non-adherent, ultra-low attachment (ULA) culture.

CSC purification and antibodies

Cells were labeled with fluorescence-labeled stem cell markers: anti-human CD133/2-APC (Miltenyi Biotec, clone 293C3); CD166-PE (R&D Systems, clone 105902); CD44-FITC (Invitrogen/Biosource, clone F10-44-2); CD44-PE (Invitrogen/Biosources, clone F10-44-2); CD44v6-FITC (R&D Systems, clone 2F10); *h*EpCAM-FITC (Miltenyi Biotec, 130-080-031).

Antibodies were diluted in buffer containing 5% BSA (Miltenyi Biotec, 130-091-376), 1 mM EDTA and 15-20% blocking reagent (Miltenyi Biotec, 130-059-901) to inhibit unspecific binding to non-target cells. After 15 min incubation at 4 °C, stained cells were sorted with multiparametric flow cytometry with BD FACS Aria cell sorter (BD Biosciences) in sterile conditions.
For immunohistochemical analysis, *h*EpCAM-FITC, biotin-conjugated human CD133 as primary Abs (Miltenyi Biotec, 130-097-049) and streptavidin-FITC (BD Pharmingen, 554060) as a secondary Abs were used.

Generation of floating multicellular spheroids
Four hundred cells of a particular phenotype were seeded on each well of ULA 6-well plate (Corning, Lowell, 3471) in serum-free MSCBM containing 10-25% Matrigel matrix (BD Biosciences, 356234) and examined after 1 week of culturing at 37 °C with 5% CO_2. Fresh medium was added after one week of culturing every third day.

Sphere propagation
After initial culturing on ULA plates, primary spheres were gently disaggregated by repeated pipetting and transferred into ULA flasks for further propagation and maintenance.

Sphere formation assay
Clonogenic potential of different phenotypic subpopulations was determined before and after treatment with SB-T-1214. Cells were counted, resuspended in MSCBM/Matrigel and plated on 48-well plates at a final count of 300 cells per well. One to two weeks after initiation, the plates were inspected for colony (sphere) growth, the number of colonies within each well was quantified by phase contrast microscopy and representative fields were photographed. Isolation of the CSC populations from peritoneal wash of colon cancer patients and solid tumors, as well as induction of the mouse tumor xenografts were carried out as we described previously.[26, 27]

Drug treatment

***In vivo* cytotoxicity**
All experiments involving the use of animals were performed in accordance with SBU institutional animal welfare guidelines. Initially, the SB-T-1214 was evaluated for its efficacy against a drug-resistant human colon tumor xenograft (Pgp+) DLD-1 in severe combined immune deficient mice (SCID). Taxoid was administered intravenously at three doses 3 times using 3 day regimens (q3d × 3, on day 5, 8, and 11), starting from day 5 after DLD-1 subcutaneous tumor implantation. Cell death was analyzed with flow cytometry using either Annexin V/PI staining (BD PharMingen) or Live/Dead assay (BioVision, CA) as recommended by the manufacturers.

***In vitro* cytotoxicity** was studied in two settings: a) using adherent type-I collagen monolayer cultures of freshly isolated $CD133^{high}/CD44^{high}$ cells; and b) three-dimensional cultures of floating multicellular spheroids induced by $CD133^{high}/CD44^{high}$ and CD133-negative cells.

Adherent to type I collagen cultures

The $CD133^{high}/CD44^{high}$ cells ($4\text{-}5 \times 10^3$ cells/well) were seeded onto the type I collagen-coated 6-well plates, and the experiments were initiated 24 h later, upon sub-confluency. The regular MSCB medium was replaced with treatment media containing SB-T-1214 at selected concentrations (0.001-0.1 μg/ml). Treatment media was removed 24 hr later, followed by washing with regular MSCBM and dissociation of cells with an Enzyme-free dissociating reagent (Chemicon International). Upon termination (48 hr from start), cell viability and cell death was analyzed through flow cytometry.

Cell culture system for MTT assay

Cells were plated and resuspended in serum-free mesenchymal stem cell medium (MSCBM; Lonza BioWhittaker PT-3238) supplemented with MSCGM hMSC SingleQuot Kit, and incubated at 37 °C in a humidified 5% CO_2 incubator for 2 to 3 days. The cells were washed with DPBS and dissociated using TrypLE. The cells were allowed to sit at room temperature until the cells were detached from the plate, transferred to a centrifuge vial and pelleted via centrifugation at 1500 rpm for 5 min. Media was added to the pellet and the pellet was disrupted. The cells were counted per 1 mL. The desired amount of media was added so that 10,000 cells were added to each well of a 96-well plate. After the addition, the cells were incubated at 37 °C for 1 day.

Drug treatment for MTT assay

A serial dilution of the drug compound dissolved in sterile DMSO was prepared by the addition of fully-supplemented RPMI. The residual media in each well was aspirated and the different drug concentrations were added to each well of every column of the 96-well plate in 100 μL aliquots. After the addition of the drug solution, the cells were incubated at 37 °C for 48 hours. After the incubation period, the medium was aspirated and the cells were washed with DPBS and then 40 μL of 0.5 mg/mL MTT (3-(4,5-dimethylthiazol-2-yl)-2,5-diphenyltetrazolium bromide) in DPBS was added to each well. The cells were then incubated at 37 °C for 3 hours. After the incubation period, the MTT solution was aspirated and the remaining crystals were dissolved using a 40 μL of 0.4 M HCl in isopropanol. The plates were shaken for 10 minutes to assure that all of the crystals are dissolved. The optical density was determined from the resulting solutions using the Acsent Multiskan optical density reader. Each experiment was run in triplicate.

Data analysis for MTT assay

The optical density data was used to calculate IC_{50} values for each drug on a given cell line using the Hill slope equation. The optical density values obtained from each concentration of drug solution were divided by the optical density value obtained from the cells with zero drug concentration. Using SigmaPlot v.10, the ratios were plotted versus the drug concentration and the IC_{50} values were calculated from the plot using the pre-programmed calculation within the SigmaPlot program.

3D culture

Cytotoxicity studies were carried out when floating spheroids induced by different cell phenotypes reached about 400-500 μm in diameter. Spheres were resuspended in the drug-containing MSCBM (0.01-0.1 μg/ml) and either plated on ULA 48-well plates (5-10 spheres/well) for microscopy or remained in ULA flasks if a larger number of sphere cells was required for FACS, PCR array, western blot and other analyses. After treatment with the drug for

48 hours, spheroids/cells were rinsed twice in DPBS, centrifuged for 5 min at 1,000 rpm, and incubated in regular MSCBM for 24 hr. Then, rinsed spheroids/cells were dissociated with an Enzyme-free dissociating reagent and single cell suspensions were further analyzed.

PCR array assay

Stem cell-specific gene expression profiles were studied with the PCR Array assay (SABiosciences, CA) in accordance with the manufacturer's recommendations. Briefly, total RNA was isolated from different cell populations or whole floating spheroids using PARIS kit (Ambion). Up to 1 μg of total RNA was treated with DNase and cDNA was prepared using RT^2 First Strand kit. For each analysis, pairs of the test and control cDNA samples were mixed with RT^2 qPCR Master mix and distributed across the PCR array 96-well plates, each of which contained 84 stem cell-related probes and control housekeeping genes. After cycling with real-time PCR (Opticon MJ Research or ABI 7300, Applied Biosystems), obtained amplification data (fold-changes in C_t values of all the genes) was analyzed with SABiosciences software.

Western blotting

Cell pellets were suspended in Lysis Buffer (Active Motif, CA) and incubated for 10 min on ice on a rocking platform. After brief vortexing, cell lysates were centrifuged at 4,000 g for 30 min at 4°C. The protein content in the supernatant was determined by a Bradford method, and equivalent amounts of total proteins (10 μg) were resolved on 10% SDS-PAGE gel. After transferring to a polyvinylidene fluoride membrane, levels of various proteins were determined by Western blot analysis using antibodies specific for Oct4, Sox2, Nanog, Lin-28, c-Myc, GAPDH and β-actin, respectively (1:500 dilution, 4°C, overnight). Following incubation with peroxidase-conjugated secondary Abs (anti-rabbit IgG; ECL, UK) for 1 hr at 25°C, blots were developed using the enhanced chemiluminescence (ECL) reagents. Alternatively, the blots were washed three times with PBST and incubated with AlexaFluor 680-conjugated goat anti-rabbit secondary antibody (Invitrogen) for 1 hr. Blots were then washed three times with PBST, twice with water, and the image captured on an Odyssey Infrared Imaging System (Li-Cor Biosciences).

Statistical analysis

The statistical significance of differences was determined using Student's *t*-test. $P < 0.05$ was considered statistically significant.

§ 2.5.0 References

1. Pierce, G. B.; Speers, W. C. Tumors as Caricatures of the Process of Tissue Renewal: Prospects for Therapy by Directing Differentiation. *Cancer Res.* **1988,** 48, 1996-2004.
2. Beere, H. M.; Hickman, J. A. Differentiation: a suitable strategy for cancer chemotherapy? *Anti-cancer Drug Design* **1993,** 8, 299-322.
3. Leszczyniecka, M.; Roberts, T.; Dent, P.; Grant, S.; Fisher, P. B. Differentiation therapy of human cancer: basic science and clinical applications. *Pharmacol. Ther.* **2001,** 90, 105-156.
4. Li, L.; Neaves, W. B. Normal Stem Cells and Cancer Stem Cells: The Niche Matters. *Cancer Res.* **2006,** 66, 4553-4557.

5. Botchkina, G. I., Zuniga, E.S., Das, M.,, Wang, Y., Wang, H., Zhu, S., Savitt, A.G., Rowehl, R.A., Leyfman, Y., Ju, J., Shroyer, K., Ojima, I. New-generation taxoid SB-T-1214 inhibits stem cell-related gene expression in 3D cancer spheriods induced by purified colon tumor-initiating cells. *Mol. Cancer* **2010,** 9, 192-204.
6. Becker, A. J.; McCulloch, E. A.; Till, J. E. Cytological Demonstration of the Clonal Nature of Spleen Colonies Derived from Transplanted Mouse Marrow Cells. *Nature* **1963,** 197, 452-454.
7. Siminovitch, L.; McCulloch, E. A.; Till, J. E. The distribution of colony-forming cells among spleen colonies. *J. Cell. Comp. Physiol.* **1963,** 62, 327-336.
8. Clarke, M. F.; Dick, J. E.; Dirks, P. B.; Eaves, C. J.; Jamieson, C. H. M.; Jones, D. L.; Visvader, J.; Weissman, I. L.; Wahl, G. M. Cancer Stem Cells—Perspectives on Current Status and Future Directions: AACR Workshop on Cancer Stem Cells. *Cancer Res.* **2006,** 66, 9339-9344.
9. Al-Hajj, M.; Wicha, M. S.; Benito-Hernandez, A.; Morrison, S. J.; Clarke, M. F. Prospective identification of tumorigenic breast cancer cells. *Pcot Natl Acad Sci USA* **2003,** 100, 3983-3988.
10. Al-Hajj, M.; Clarke, M. F. Self-renewal and solid tumor stem cells. *Oncogene* **2004,** 23, 7274-7282.
11. Schatton, T.; Frank, N. Y.; Frank, M. H. Identification and targeting of cancer stem cells. *BioEssays* **2009,** 32, 1037-1049.
12. Bonnet, D.; Dick, J. E. Human acute myeloid leukemia is organized as a hierarchy that originates from a primitive hematopoietic cell. *Nature Med.* **1997,** 3, 730-737.
13. Miyamoto, T.; Weissman, I. L.; Akashi, K. AML1/ETO-expressing nonleukemic stem cells in acute myelogenous leukemia with 8;21 chromosomal translocation. *Proc. Natl. Acad. Sci. U.S.A.* **2000,** 97, 7521-7526.
14. George, A. A.; Franklin, J.; Kerkof, K.; Shah, A. J.; Price, M.; Tsark, E.; Bockstoce, D.; Yao, D.; Hart, N.; Carcich, S.; Parkman, R.; Crooks, G. M.; Weinberg, K. Detection of leukemic cells in the CD34+ CD38− bone marrow progenitor population in children with acute lymphoblastic leukemia. *Blood* **2001,** 97, 3925-3930.
15. Mauro, M. J.; Drucker, B. J. Chronic myelogenous leukemia. *Curr. Opin. Oncol.* **2001,** 13, 3-7.
16. Li, L.; Xie, T. Stem cell niche: structure and function. *Annu. Rev. Cell. Dev. Biol.* **2005,** 21, 605-631.
17. Spradling, A.; Drummond-Barbosa, D.; Kai, T. Stem cells find their niche. *Nature* **2001,** 414, 98-104.
18. Kirchner, T.; Müller, S.; Hattori, T.; Mukaisyo, K.; Papadopulos, T.; Brabletz, T.; Jung, A. Metaplasia, intraepithelial neoplasia and early cancer of the stomach are related to dedifferentiated epithelial cells defined by cytokeratin-7 expression in gastritis *Virchows Archiv.* **2001,** 439, 512-522.
19. Shmelkov, S. V.; Clair, R.; Lyden, D.; Rafii, S. AC133/CD133/Prominin-1. *Int. J. Biochem. Cell Biol.* **2005,** 37, 715-719.
20. Collin, A. T.; Berry, P. A.; Hyde, C.; Stower, M. J.; Maitland, N. J. Prospective identification of tumorigenic prostate cancer stem cells. *Cancer Res.* **2005,** 65, 10946-10951.
21. Jin, L.; Hope, K. J.; Zhai, Q.; Smadja-Joffe, F.; Dick, J. E. Targeting of CD44 eradicates human acute myeloid leukemic stem cells. *Nat. Med.* **2006,** 10, 167-174.

22. Krause, D. S.; Lazarides, K.; von Andrian, U. H.; Van Etten, R. A. Requirement for CD44 in homing and engraftment of BCR-ABL-expressing leukemic stem cells. *Nat. Met.* **2006,** 10, 1175-1180.
23. Patrawala, L.; Calhoun, T.; Schneider-Broussard, R.; Li, H.; Bhatia, B.; Tang, S.; Reilly, J. G.; Chandra, D.; Zhou, J.; Claypool, K.; Coghlan, L.; Tang, D. G. Highly purified CD44+ prostate cancer cells from xenograft human tumors are enriched in tumorigenic and metastatic progenitor cells. *Oncogene* **2006,** 25, 1696-1708.
24. Dalerba, P.; Dylla, S. J.; Park, I. K.; Liu, R.; Wang, X.; Cho, R. W.; Hoey, T.; Gurney, A.; Huang, E. H.; Simeone, D. M.; Shelton, A. A.; Parmiani, G.; Castelli, C.; Clarke, M. F. Phenotypic characterization of human colorectal cancer stem cells. *PNAS* **2007,** 104, 10158-10163.
25. Haraguch, M.; Ohkuma, M.; Sakashita, H.; Matsuzaki, S.; Tanaka, F.; Mimori, K.; Kamohara, Y.; Inoue, H.; Mori, M. CD133+CD44+ Population Efficiently Enriches Colon Cancer Initiating Cells. *Ann. Surgical Oncol.* **2008,** 15, 2927-2933.
26. Rowehl, R. H.; Crawford, H.; Dufour, A.; Leyfman, Y.; Ju, J.; Botchkina, G. I. Genomic Analysis of Prostate Cancer Stem Cells Isolated from Highly Metastatic Cell Line. *Cancer Genomics and Proteomics* **2008,** 5, 301-309.
27. Botchkina, I. L.; Rowehl, R. A.; Rivadeneira, D. E.; Karpeh, M. S. J.; Crawford, H.; Dufour, A.; Ju, J.; Weng, Y.; Leyfman, Y.; Botchkina, G. I. Phenotypic Subpopulations of Metastatic Colon Cancer Stem Cells. *Cancer Geno. Proteo.* **2009,** 6, 19-30.
28. Hong, S. P.; Wen, J.; Bang, S.; Park, S.; Song, S. Y. CD44-positive cells are responsible for gercitabine resistance in pancreatic cancer cells. *Int. J. Cancer* **2009,** 125, 2323-2331.
29. Ponta, H.; Sherman, L.; Herrlich, P. A. CD44: From adhesion molecules to signalling regulators. *Nat. Rev. Mol. Cell Biol.* **2003,** 4, 33-45.
30. Marhaba, R.; Zoller, M. CD44 in cancer progression: adhesion, migration and growth regulation. *J. Mol. Histol.* **2004,** 35, 211-231.
31. Gotley, D. C.; Fawcett, J.; Walsh, M. D.; Reeder, J. A.; Simmons, D. L.; Antalis, T. M. Alternatively spliced variants of the cell adhesion molecule CD44 and tumour progression in colorectal cancer. *Brit. J. Cancer* **1996,** 74, 342-351.
32. Frank, N. Y.; Pendse, S. S.; Lapchak, P. H.; Margaryan, A.; Shlain, D.; Doeing, C.; Sayegh, M. N.; Frank, M. H. Regulation of progenitor cell fusion of ABCB5 P-glycoprotein, a novel human ATP-binding cassette transporter. *J. Biol. Chem.* **2005,** 278, 47156-47165.
33. Frank, N. Y.; Margaryan, A.; Huang, Y.; Schatton, T.; Waaga-Gasser, A. M.; Gasser, M.; Sayegh, M. H.; Sadee, W.; Frank, M. H. ABCB5-meditated doxorubicin transport and chemoresistance in human malignant melanoma. *Cancer Res.* **2005,** 65, 4320-4333.
34. Bao, S.; Wu, Q.; McLendon, R. E.; Hao, Y.; Shi, Q.; Hjelmelad, A. B.; Dewhirst, M. W.; Bigner, D. D.; Rich, J. N. Glioma stem cells promote radioresistance by preferential activation of the DNA damage response. *Nature* **2006,** 444, 756-760.
35. Liu, G.; Yuan, X.; Zeng, Z.; Tunici, P.; Ng, H.; Abdulkadir, I. R.; Lu, L.; Irvin, D.; Black, K. L.; Yu, J. S. Analysis of gene expression and chemoresistance of CD133+ cancer stem cells in glioblastoma. *Mol. Cancer* **2006,** 5, 67-79.
36. Bertolini, G.; Roz, L.; Perego, P.; Tortoreto, M.; Fontanella, E.; Gatti, L.; Pratesi, G.; Fabbri, A.; Andriani, F.; Tinelli, S.; Roz, E.; Caserini, R.; Lo Vullo, S.; Camerini, T.; Mariani, L.; Delia, D.; Calabro, E.; Pastorino, U.; Sozzi, G. Highly tumorigenic lung cancer CD133+ cells display stem-like features and are spared by cisplatin treatment. *Proc. Natl. Acad. Sci. U.S.A.* **2009,** 106, 16281-16286.

37. Dallas, N. A.; Xia, L.; Fan, F.; Gray, M. J.; Gaur, P.; van Buren, G.; Samuel, S.; Kim, M. P.; Lim, S. J.; Ellis, L. M. Chemoresistant colorectal cancer cells, the cancer stem cell phenotype, and increased sensitivity to insulin-like growth factor-1 receptor inhibition. *Cancer Res.* **2009,** 69, 1951-1957.
38. Vlashi, E.; McBride, W. H.; Pajonk, F. Radiation responses of cancer stem cells. *J. Cell. Biochem.* **2009,** 108, 339-342.
39. Liu, Q.; Nguyen, D. H.; Dong, Q.; Shitaku, P.; Chung, K.; Liu, O. Y.; Tso, J. L.; Liu, J. Y.; Konkankit, V.; Cloughesy, T. F.; Mischel, P. S.; Lane, T. F.; Liau, L. M.; Nelson, S. F.; Tso, C. L. Molecular properties of CD133+ glioblastoma stem cells derived from treatment-refractory recurrent brain tumors. *J. Neurooncol.* **2009,** 94, 1-19.
40. Dirks, P. B. Cancer: Stem cells and brain tumours. *Nature* **2006,** 444, 687-688.
41. Eramo, A.; Ricci-Vitiani, L.; Zeuner, A.; Pallini, R.; Lotti, F.; Sette, G.; Pilozzi, E.; Larocca, L. M.; Peschle, C.; De Maria, R. Chemotherapy resistance of glioblastoma stem cells. *Cell Death Differ.* **2006,** 13, 1238-1241.
42. Woodward, W. A.; Chen, M. S.; Behbod, F.; Alfaro, M. P.; Buchholz, T. A.; Rosen, J. M. WNT/β-catenin mediates radiation resistance of mouse mammary progenitor cells. *Proc. Natl. Acad. Sci. U.S.A.* **2007,** 104, 618-623.
43. Todaro, M.; Alea, M. P.; Stefano, A. B.; Cammareri, P.; Vermeulen, L.; Lovino, F.; Tripodo, C.; Russo, A.; Gulotta, G.; Medema, J. P.; Stassi, G. Colon cancer stem cells dictate tumor growth and resist cell death by production of interleukin-4. *Cell Stem Cell* **2007,** 1, 389-402.
44. Bleau, A. M.; Hambardzumyan, D.; Ozawa, T.; Fomchenko, E. I.; Huse, J. T.; Brennan, C. W.; Holland, E. C. PTEN/PI3K/Akt pathway regulates the side population phenotype and ABCG2 activity in glimoa tumor stem-like cells. *Cell Stem Cell* **2009,** 4, 226-235.
45. Al-Hajj, M.; Wicha, M. S.; Benito-Hernandez, A.; Morrison, S. J.; Clarke, M. F. Prospective identification of tumorigenic breast cancer cells. *PNAS USA* **2003,** 100, 3983-3988.
46. Zeppernick, F.; Ahmadi, R.; Campos, B.; Dictus, C.; Helmke, B. M.; Becker, N.; Lichter, P.; Unterberg, A.; Radlwimmer, B.; Herold-Mende, C. C. Stem Cell Marker CD133 Affects Clinical Outcome in Glioma Patients. *Clin. Cancer Res.* **2008,** 14, 123-129.
47. Maeda, S.; Shinchi, H. H.; Kurahara, H. Y.; Mataki, Y.; Maemura, K.; Sato, M.; Natsugoe, S.; Aikou, T.; Takao, S. S. CD133 expression is correlated with lymph node metastasis and vascular endothelial growth factor-C expression in pancreatic cancer. *Brit. J. Cancer* **2008,** 98, 1389-1397.
48. Horst, D.; Kriegl, L.; Engel, J.; Kirchner, T.; Jung, A. CD13 expression is an independent prognostic marker for low survival in colorectal cancer. *Brit. J. Cancer* **2008,** 99, 1285-1289.
49. Lapidot, T.; Sirard, C.; Vormoor, J.; Murdoch, B.; Hoang, T.; Caceres-Cortes, J.; Minden, M.; Paterson, B.; Caligiuri, M. A.; Dick, J. E. A cell initiating human acute myeloid leukaemia after transplanation into SCID mice. *Nature* **1994,** 367, 645-648.
50. Singh, S. K.; Clarke, I. D.; Terasaki, M.; Bonn, V. E.; Hawkins, C.; Squire, J.; Dirks, P. B. Identification of a cancer stem cell in human brain tumors. *Cancer Res.* **2003,** 63, 5821-5828.
51. Bussolati, B.; Bruno, S.; Grange, C.; Buttiglieri, S.; Deregibus, M. C.; Cantino, D.; Camussi, G. Isolation of renal progenitor cells from adult human kidney. *Am. J. Pathol.* **2005,** 166, 545-555.
52. Suetsugu, A.; Nagaki, M.; Aoki, H.; Motohashi, T.; Kunisada, T.; Moriwaki, H. Characterization of CD133+ hepatocellular carcinoma cells as cancer stem/progenitor cells. *Biochem. and Biophys. Res. Comm.* **2006,** 351, 820-824.

53. Yin, S.; Li, J.; Hu, C.; Chen, X.; Yao, M. CD133 positive hepatocellular carcinoma cells possess high capacity for tumorigenicity. *Int. J. Cancer* **2007,** 120, 1444-1450.
54. O'Brien, C. A.; Pollett, A.; Gallinger, S.; Dick, J. A human colon cancer cell capable of initiating tumor growth in immunodeficient mice. *Nature* **2007,** 445, 106-110.
55. Ricci-Vitiani, L.; Lombardi, D. G.; Pilozzi, E.; Biffoni, M.; Todaro, M.; Peschle, C.; De Maria, R. Identification and expansion of human colon-cancer-initiating cells. *Nature* **2007,** 445, 111-115.
56. Hermann, P. C.; Huber, S. L.; Herrler, T.; Aicher, A.; Ellwart, J. W.; Guba, M.; Bruns, C. J.; Heeschen, C. Distinct populations of cancer stem cells determine tumor growth and metastatic activity in human pancreatic cancer. *Cell Stem Cell* **2007,** 1, 313-323.
57. Southam, C. M.; Brunschwig, A. Quantitative studies of autotransplantation of human cancer. *Cancer* **1961,** 14, 971-978.
58. Salsbury, A. J. The significance of the circulating cancer cell. *Cancer Treat. Rev.* **1975,** 2, 55-72.
59. Reya, T.; Morrison, S. J.; Clarke, M. F.; Weissman, I. L. Stem cells, cancer, and cancer stem cells. *Nature* **2001,** 414, 105-111.
60. Stockler, M.; Wilcken, N. R. C.; Chersi, D.; Simes, R. J. Systematic reviews of chemotherapy and endocrine therapy in metastatic breast cancer. *Cancer Treat. Rev.* **2000,** 26, 151-168.
61. Park, C. H.; Bergsagal, D. E.; McCulloch, E. A. Mouse myeloma tumor stem cells: a primary cell culture assay. *J. Natl. Cancer Inst.* **1971,** 46, 411-422.
62. Harrison, D. E.; Lerner, C. P. Most primitive hematopoietic stem cells are stimulated to cycle rapidly after treatment with 5-fluorouracil. *Blood* **1991,** 78, 1237-1240.
63. Dean, M.; Fojo, T.; Bates, S. Tumor stem cell and drug resistance. *Nat. Rev. Cancer* **2005,** 5, 275-284.
64. Donnenberg, V. S.; Donnenberg, A. D. Multiple drug resistance in cancer revisited: the cancer stem cell hypothesis. *J. Clin. Pharmacol.* **2005,** 45, 872-877.
65. Mimeault, M.; Hauke, R.; Mehra, P. P.; Batra, S. K. Recent advances in cancer stem/progenitor cell research: therapeutic implications for overcoming resistance to the most aggressive cancers. *J. Cell. Mol. Med.* **2007,** 11, 981-1011.
66. Kirkland, S. C. Type I collagen inhibits differentiation and promotes a stem cell-like phenotype in human colorectal carcinoma cells. *Brit. J. Cancer* **2009,** 101, 320-326.

Chapter 3

Polyunsaturated Fatty Acids as Tumor-Targeting Modules

Chapter Contents

§ 3.1.0 Introduction

§ 3.1.1 Prevailing Issues in Chemotherapeutic Treatment

Multidrug resistance (MDR) and lack of tumor specificity are two major obstacles that may lead to the failure of many forms of chemotherapy. Multidrug resistance is the principal mechanism in which cancer cells develop resistance to chemotherapeutic drugs.[1] Tumors are comprised of a heterogeneous population of cells. Chemotherapeutic drugs kill drug-sensitive cells but are ineffective against drug-resistant cells. These residual cells render drug treatment unsuccessful as the remaining tumor cells are resistant to the drug, thus the tumor continues to grow.

MDR may arise from decreased cell wall permeability of the drug, altered drug-target sites, increased mutation rates caused by drug treatment or through an efflux mechanism. Efflux transporters are classified into five major superfamilies: the major facilitator superfamily (MFS); the ATP-binding cassette superfamily (ABC); the small multidrug resistance family (SMR); the resistance-nodulation-cell division superfamily (RND); and the Multi-antimicrobial extrusion protein family (MATE).[2] The overexpression of superfamily proteins allow for the efflux of a number of diverse types of drugs resulting in a loss of efficacy.[3] Therefore, new drugs are being developed with increased efficacy against MDR cancer.

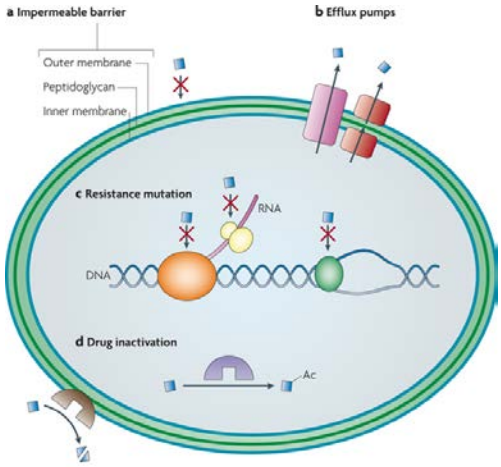

Figure 3.1: Mechanisms of MDR (adapted from [4])

Whereas MDR renders a drug ineffective, a lack of tumor specificity can have devastating effects on patients receiving chemotherapeutic drugs. Conventional chemotherapy works on the premise that rapidly proliferating cells, such as tumor cells, are more likely to be killed than normal cells. However, this is not the case, as it is a well known and established fact that the lack of specificity in conventional chemotherapeutic agents can lead to undesired and potentially severe side effects, such as myelosuppression and depression of the immune system. In addition, chemotherapeutic drugs may cause nausea, vomiting, malnutrition and hair loss. Therefore, tumor specific drug delivery protocols and drug delivery systems (DDS) have been developed.

Recently, chemotherapy has transitioned into the age of "targeted therapy."[5] For example, in 2001 imatinib mesylate (Gleevec ®) received FDA approval for the treatment of chronic

myelogenous leukemia (CML).[6] Imatinib specifically targets the Bcr-Abl complex; a tyrosine kinase that is overexpressed in CML cells.[7, 8] Furthermore, brentuximab vedotin is an antibody-drug conjugate that targets CD30, a defining marker of Hodgkin's lymphoma (HL).[9, 10] Imatinib and brentuximab vedotin are just two effective examples of tumor-targeting chemotherapy.

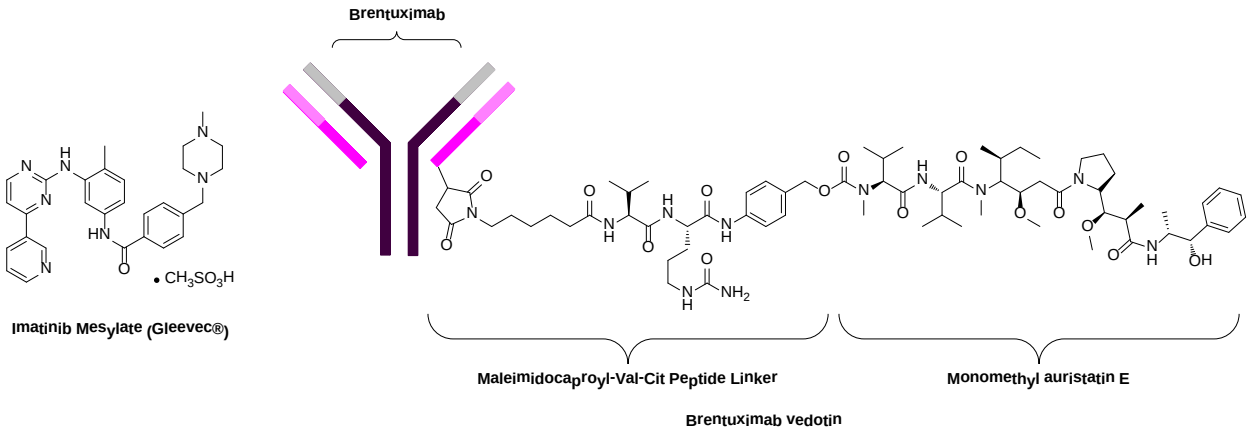

Figure 3.2: Tumor-targeting chemotherapeutic agents

§ 3.1.2 Tumor-Targeting Modules

The idea of selectively targeting cancer was introduced by Paul Ehrlich in the early twentieth century. Ehrlich envisioned treating cancer with a "magic bullet" that would specifically target cancer cells, while leaving normal tissues and cells unharmed. Though imatinib specifically targets CML cells, in other cancer types there are multiple abnormalities that must be targeted. Tyrosine kinases play a major role in cellular signal transduction. However, cell signaling pathways within cancer cells are extremely complex. Blocking the activity of one protein in the signaling pathway does not guarantee a complete inhibition of the pathway, as several other pathways may exist which bypass the effects of inhibiting the one protein. Thus, there is a need to modify existing highly-potent chemotherapeutic drugs to specifically target tumor cells.

A promising approach along this line is the development of tumor-targeting prodrugs, which contain a cytotoxic drug conjugated to a tumor-targeting module (TTM). The basic premise of tumor-targeting prodrugs is that the drug conjugate is inactive until it is delivered to the tumor site by the TTM and internalized into tumor cells. After the drug conjugate is internalized, the cytotoxic agent is released from its carrier to restore its original activity. Tumor-targeting prodrugs can be classified into a number of groups based on TTM. These TTMs include polyunsaturated fatty acids (PUFA), hylauronic acids (HA), vitamins, oligopeptides and monoclonal antibodies (mAbs). Some of these drug conjugates gave promising preclinical results.[9-12] However, limited success has been achieved due to inherent pitfalls of the TTM and other reasons.[13, 14]

§ 3.1.3 Polyunsaturated Fatty Acids as Tumor-Targeting Modules

Omega-3 polyunsaturated fatty acids (PUFA) such as docosahexaenoic acid (DHA), eicosapentaenoic acid (EPA) and linolenic acid (LNA) are naturally occurring compounds found in vegetable oils, cold-water fish and meat (Figure 3.3). Single-arterial perfusion studies have shown that some PUFAs are taken up more rapidly by tumor cells than normal cells.[15] In addition, some omega-3 PUFAs have exhibited anticancer activity against CFPAC-1, Mia-Pa-Ca-2 and Panc-1 pancreatic and HL-60 leukemia cell lines in both clinical and preclinical trials.[16, 17] It has also been shown that PUFAs are readily incorporated into the lipid bilayer of tumor cells thereby disrupting the morphology of the cell and presumably influencing the susceptibility of the tumor cells to anticancer agents.[18, 19]

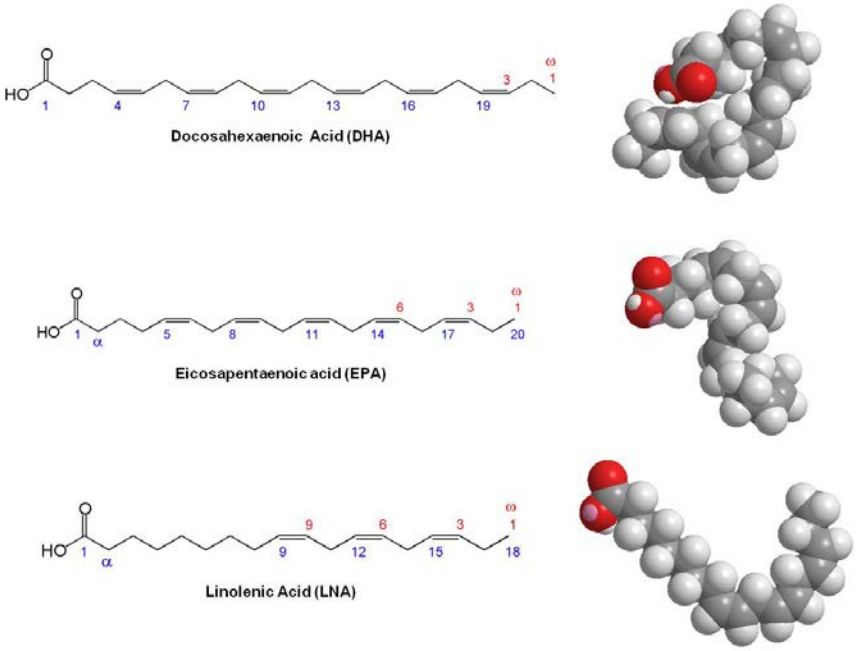

Figure 3.3: Linear and space-filling models of essential PUFAs

Polyunsaturated fatty acids are utilized as cellular membrane components, energy resources and signaling molecules. It has also been shown that PUFAs affect a number of cellular processes involved in human disease. Furthermore, PUFAs are readily taken up by malignant cells, thus making PUFAs ideal TTMs for drug conjugation. The conjugation of cytotoxic drugs to PUFAs has been found to substantially alter the pharmacokinetics and distribution of the cytotoxic drugs, resulting in the accumulation of the cytotoxic agent in cancer cells.[20] The solubility of PUFA-drug conjugates is increased compared to the free drug, as the PUFA component of the drug conjugate readily binds to human serum albumin (HSA) to form an HSA-drug conjugate complex. There is evidence to suggest that glycoprotein 60 (gp60) and "secreted protein acidic and rich in cysteine" (SPARC) play a crucial role in the transport of HSA-bound complexes from tumor blood vessels to the tumor interstitium leading to an accumulation of the HSA-bound complexes in the tumor cells (Figure 3.4).[20-22]

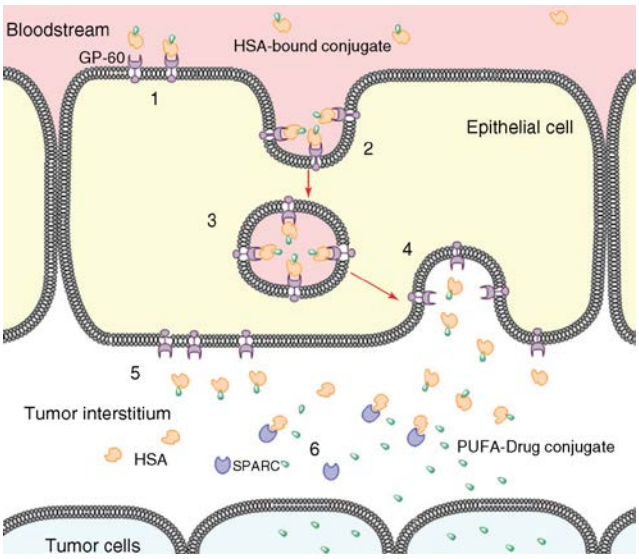

Figure 3.4: gp60-Mediated transcytosis (adapted from [20])

It is very likely that PUFA-drug conjugates accumulate into tumor tissue and then to tumor cells, wherein the PUFA-drug linkage would be cleaved, releasing the PUFA and the free drug. It is possible that once internalized, certain PUFAs and their metabolites affect a number of vital signaling pathways, resulting in synergism with cytotoxic drugs.[23] Thus, conjugation of drugs to PUFAs results in improved tumor specificity, increased drug-accumulation and enhanced drug efficacy.

§ 3.1.4 The Influence of Polyunsaturated Fatty Acids against Drug Resistant Cancer Cells

Drug resistance in cancer cells is due to malfunctions in signaling pathways involved in apoptosis and cell cycle progression. Certain PUFAs have been shown to moderate these malfunctions in a dose-dependent manner, as certain PUFAs moderate inflammation, cellular adhesion and metabolism.[20] It has been suggested that supplementing dietary PUFAs during the administration of chemotherapeutics may help protect healthy tissue while simultaneously increasing the efficacy of the chemotherapeutics.[23] Thus, synergism between PUFAs and cytotoxic drugs has been observed in a variety of cancer cell lines.[24] For example, a synergistic effect was observed in SGC7901 gastric cancer cells coadministered with 1-to-1 ratio of DHA and 5-fluorouracil (40 μg/mL of each).[25] A similar effect was observed with DHA and clioquinol (5 μM with 100 μM DHA) against A2780 (human ovarian cancer) cell line. Synergism was also observed between EPA and TNP-470, an angiogenesis inhibitor (EPA, 221 μg/mL; TNP-470, 34.2 μg/mL), as well as EPA and genistein, a potent tyrosine kinase inhibitor (genistein 93 and 176 μM; EPA 211 and 609 μM, respectively), against two breast cancer cell lines.[26, 27] The coadministeration of γ-LNA with vinorelbine or paclitaxel also showed synergistic activity in various cancer cell lines.[28] This synergistic cytotoxicity and potential use as TTMs, make PUFAs highly attractive candidates for drug conjugation and tumor-targeted chemotherapy.

DHA-paclitaxel, which advanced to Phase III clinical trials against a number of cancer types, has shown to have better pharmacokinetic properties and increased efficacy than the parent compound paclitaxel (Figure 3.5).[29] However, it is unlikely that DHA-paclitaxel would be effective against MDR tumors that overexpress (Pgp), as paclitaxel is a known P-gp substrate.[11]

DHA-paclitaxel is less cytotoxic than the parent compound by one or two orders of magnitude, until the ester linkage is cleaved.[12] In addition, the high levels of serum protein binding significantly reduce clearance rate and volume distribution, resulting in less systemic toxicity hence reduced side-effects.[11] Another advantage of DHA-paclitaxel over paclitaxel is that the DHA-drug conjugate exhibits a wider therapeutic window, and therefore allows the delivery of higher concentrations of paclitaxel to the tumor.

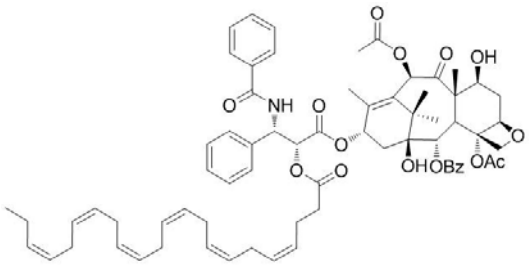

Figure 3.5: DHA-paclitaxel (Taxoprexin)

As mentioned previously, new-generation taxoids exhibit 2-3 orders of magnitude better activity than paclitaxel against MDR cancer cell lines.[30-32] Thus, PUFA conjugates with a new-generation taxoid as a warhead should be more efficacious than DHA-paclitaxel against MDR cell lines. Accordingly, novel PUFA-taxoid conjugates were synthesized and assayed *in vivo* for their efficacy against different drug-resistant and drug sensitive human tumor xenografts in severe combined immune deficiency (SCID) mice.[33] Several of these drug conjugates led to a complete regression of the tumor in all surviving mice with minimal systemic toxicity. Remarkably, DHA-SB-T-1214 led to a complete regression of the highly drug-resistant DLD-1 colon tumor xenograft in 5 of 5 mice without recurrence of tumor growth for more than 190 days after treatment. Again, little systemic toxicity was observed, implying the tumor specificity of the PUFA-drug conjugates (Figure 3.6). As a result, DHA-SB-T-1214 is currently undergoing the last stage preclinical evaluations, and an Investigational New Drug (IND) application to the FDA will be filed in the near future.

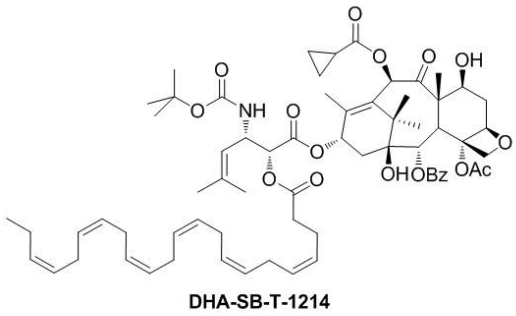

DHA-SB-T-1214

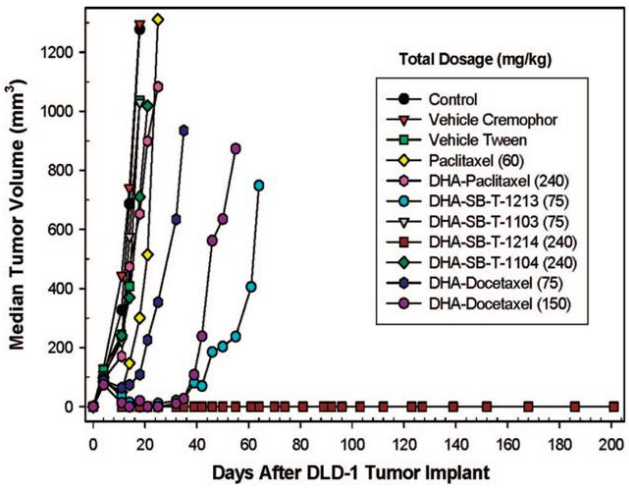

Figure 3.6: DHA-taxoid drug conjugate, DHA-SB-T-1214, and effect of DHA-taxoid drug conjugates on human colon tumor xenograft DLD-1 (adapted from [33])

§ 3.2.0 Results and Discussion

§ 3.2.1 Internalization of PUFA-FITC Conjugates

The exact mechanism of PUFA-internalization into cancer cells is unknown. However, there is evidence to suggest that HSA and SPARC are involved in PUFA and PUFA-conjugate cellular internalization. To evaluate the internalization of DHA- and LNA-conjugates into cells, both DHA-FITC and LNA-FITC conjugates (William T. Berger, Ojima laboratory) were synthesized and their internalization into various human cancer cells and normal human cells was evaluated using FACS (Figure 3.7).

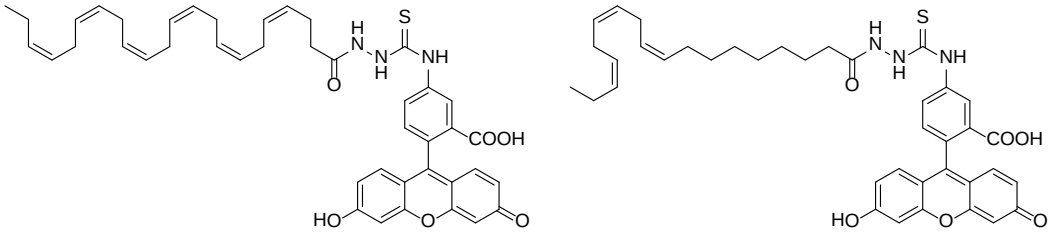

Figure 3.7: PUFA-FITC conjugates

The PUFA-FITC conjugates were prepared by first converting the PUFA-free acid into PUFA-hydrazide. The resulting PUFA-hydrazide was coupled to the thioisocynate moiety of FITC to give the desired FITC-labeled PUFA conjugates. To evaluate internalization, PUFA-FITC conjugates were administered into various cancer cell lines, A2780 (human ovarian), DLD-1 (human colon), HT-29 (human colon), MCF-7 (human breast) and Panc-1 (human pancreatic). To evaluate tumor cell-specificity, HS-27 (normal human foreskin) cells were administered with PUFA-conjugates. The internalization of these conjugates was evaluated using FACS (Figure 3.8).

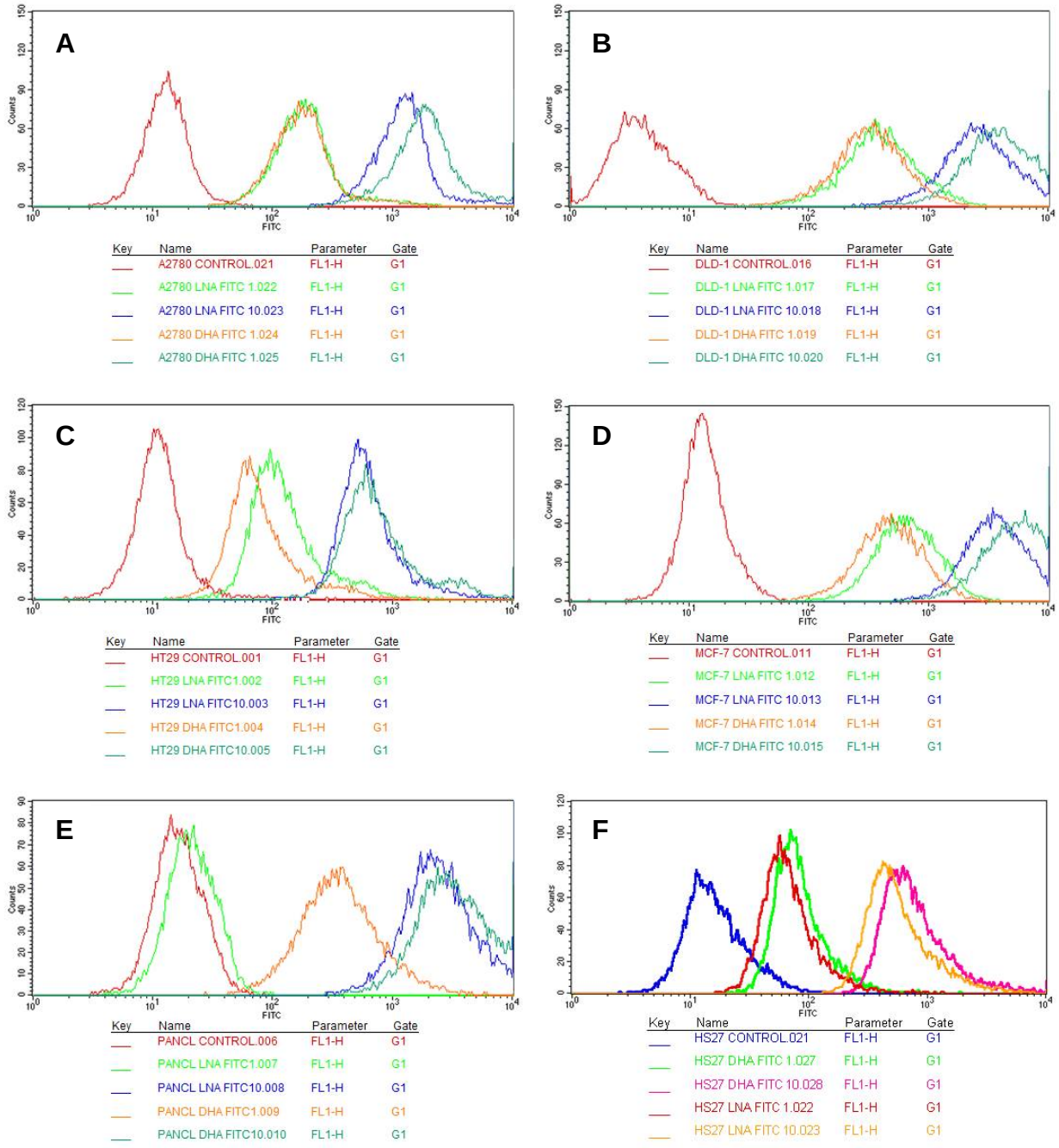

Figure 3.8: FACS analysis and histogram overlays evaluating internalization of PUFA-FITC (1 µM and 10 µM concentration) incubated in different cell lines for 1 hour at 37 °C. (A) A2780 human ovarian cancer; (B) DLD-1 human colon cancer; (C) HT-29 human colon cancer; (D) MCF-7 human breast cancer; (E) Panc-1 human pancreatic cancer; (F) HS-27 normal human skin fibroblast.

The cells were resuspended in RPMI supplemented with FBS and antibiotics. Following incubation at 37 °C with 5% CO_2, the cells were administered with PUFA-FITC conjugate at two different concentrations, 1 µM and 10 µM, for 1 hour. After the incubation period, the cells were washed and analyzed using FACS. As seen from Figure 3.8, in general when the cells are incubated with a higher concentration of PUFA-FITC probe (10 µM), there is an increase in

internalization observed compared to the cells incubated with 1 μM probe, as depicted in the green (1 μM) and blue (10 μM) lines in the histograms of cancer cell lines and the green (1 μM) and pink (10 μM) lines in the histogram of the normal cell line. Furthermore, the internalization of LNA-FITC and DHA-FITC (at the same concentration) is comparable in all of the cell lines evaluated. However, as shown in Figure 3.8E, LNA-FITC did not internalize in Panc-1 cells. This result is most likely caused by experimental error, i.e. the cells were not treated with the precise concentration of 1 μM LNA-FITC. In addition, comparing HS-27 (normal human foreskin) with the cancer cell lines, internalization of both PUFA-FITC probes in the cancer cell lines is greater than the internalization observed in the normal cell line, as depicted in Figure 3.8E where the observed fluorescence is an order of magnitude less than those observed in the cancer cell lines treated with the same concentration of PUFA-FIT probe. This difference of internalization is prominent in A2780, DLD-1, MCF-7 and Panc-1, as shown in Figure 3.8 A, B, C and D. These results suggest that both DHA and LNA may be more specific towards cancer cells. Furthermore, it is worthy of note that both DHA-FITC and LNA-FITC conjugates have similar internalization rates into both human cancer and normal cells, i.e. probe internalization was observed within 1 hour of incubation in cells.

§ 3.2.2 Synthesis and Biological Evaluation of PUFA-Taxoid Drug Conjugate

The synthesis of PUFA-taxoid drug conjugates is achieved through the coupling of a free taxoid to the PUFA in the presence of DIC and DMAP. The PUFA is coupled at the 2'-position of the taxoid, however the 7-position of the baccatin core is also a coupling site. If the coupling reaction is prolonged and if excess PUFA were used in the reaction, PUFA coupling at both 2'- and C7-positions is observed. Following this coupling protocol, LNA-SB-T-1214 was synthesized (Scheme 3.1).

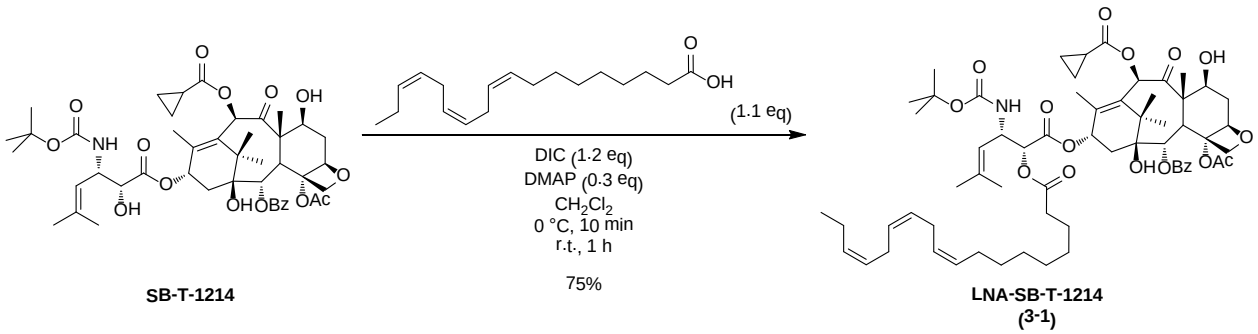

Scheme 3.1: Synthesis of LNA-SB-T-1214

The coupling reaction proceeded smoothly affording **3-1** in good yield (75%). In this instance, coupling at both the 2'- and 7-position was observed. Once the bis-coupled product was formed based on TLC, the reaction was quenched and purified to obtain the desired LNA-SB-T-1214. To prevent bis-coupling from occurring, the reaction temperature should be maintained at 0 °C for the duration of the reaction or the reaction time at room temperature should be decreased. Furthermore, linolenic acid was chosen as the PUFA, as it is less likely to be oxidized when compared to DHA, thus the PUFA-taxoid drug conjugate can be stored without decomposition over a longer period of time.

Two other PUFA-taxoid conjugates, DHA-SB-T-1214 (Chem Masters Int.) and DHA-SB-T-12854 (Dr. Yuan Li, Ojima laboratory), were synthesized (Table 3.1) and the biological activity of each PUFA-taxoid drug conjugate was evaluated in various cancer cell lines using MTT assay (Table 3.2).

Table 3.1: New-Generation Taxoids and PUFA-Taxoid Drug Conjugates

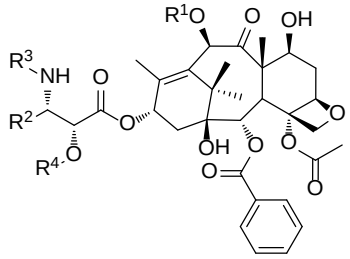

Taxane	R^1	R^2	R^3	R^4
Paclitaxel	Ac	Ph	PhCO	H
SB-T-1214	*c*-PrCO	CH_2=CH	*t*-Boc	H
DHA-SB-T-1214[a]	*c*-PrCO	CH_2=CH	*t*-Boc	DHA
LNA-SB-T-1214	*c*-PrCO	CH_2=CH	*t*-Boc	LNA
SB-T-12854[b]	Me_2NCO	CF_2=CH	*t*-Boc	H
DHA-SB-T-12854[c]	Me_2NCO	CF_2=CH	*t*-Boc	DHA

[a] taxoid synthesized by Chem Masters Int.; [b] taxoid synthesized by Ilaria Zanardi; [c] taxoid synthesized by Dr. Yuan Li

Table 3.2: Cytotoxicity of New-Generation Taxoids and PUFA-Taxoid Drug Conjugates in Various Bulk Cancer Cell Lines

	IC_{50} (nM)									
Taxane	**A2780 (ovarian cancer)**	**CFPac-1 (pancreatic cancer)**	**DLD-1 (colon cancer)**	**HT-29 (colon cancer)**	**ID8 (ovarian cancer)**	**MCF-7 (breast cancer)**	**MDA MB 231 (breast cancer)**	**Panc-1 (pancreatic cancer)**	**PC3 (prostate cancer)**	**PC3MM2 (prostate cancer)**
Paclitaxel	16.2 ± 8.28	68.0 ± 22.9	29.5 ± 10.8	11.6 ± 3.57	14.5 ± 5.88	6.25 ± 0.76	14.5 ± 5.55	3.84 ± 0.85	1.68 ± 0.84	0.48 ± 0.08
SB-T-1214	0.36 ± 0.03	0.38 ± 0.14	0.38 ± 0.21	0.73 ± 0.30	2.51 ± 1.24	0.35 ± 0.11	28.9 ± 26.7	0.35 ± 0.14	0.38 ± 0.10	0.47 ± 0.02
DHA-SB-T-1214	51.8 ± 3.88	5.79 ± 3.35	132 ± 65	201 ± 57	526 ± 91	20.8 ± 2.2	27.1 ± 2.2	59.4 ± 8.2	7.73 ± 4.01	5.38 ± 3.40
LNA-SB-T-1214	12100 ± 1160	705 ± 116	>50000	>50000	1170 ± 30	24500 ± 6510	260 ± 140	552 ± 120	391 ± 147	522 ± 366
SB-T-12854	3.13 ± 1.93	0.35 ± 0.15	0.25 ± 0.18	0.54 ± 0.03	0.28 ± 0.15	0.51 ± 0.32	0.52 ± 0.32	6.02 ± 0.86	5.08 ± 2.43	32.5 ± 26.3
DHA-SB-T-12854	213 ± 130	59.1 ± 22.0	216 ± 52.2	555 ± 18.1	216 ± 68.5	111 ± 11.3	273 ±166	136 ± 18.7	0.23 ± 0.11	0.27 ± 0.16

- Cells were suspended in RPMI with L-glutamine (Lonza BioWhittaker, BW12-702F), with 5% FBS (Thermo Scientific, HyClone, SH3007003), 5% Nu Serum (BD Biosciences, 355100) and 1% Penn Strip before administration of taxoid
- Cells were incubated for 48 hours at 37 °C with 5% CO_2 after administration of taxoid
- The optical density was determined using Acsent Multiskan optical density reader
- The reported values are a calculated averages of IC_{50} values determined from three individual experiments
- IC_{50} values were calculated using SigmaPlot v 10.0
- All IC_{50} values are report in nM scale unless otherwise noted

As seen from Table 3.2, all of the PUFA-taxoid conjugates show several orders of magnitude greater IC_{50} values compared to their parent new-generation taxoid in each of the cancer cell lines evaluated. Of the two PUFA-SB-T-1214 drug conjugates, DHA-SB-T-1214 showed higher potency compared to LNA-SB-T-1214 in each cancer cell line. However, the activity of DHA-SB-T-1214 is magnitudes less potent than SB-T-1214. Furthermore, the decrease in cytotoxicity shown by LNA-SB-T-1214 may also suggest a decrease in systemic toxicity. Thus, LNA-SB-T-1214 may have the ability to effectively kill cancer cells and leave normal tissues unharmed. DHA-SB-T-12854 also displayed a decrease in potency in most of the cancer cell lines. However, DHA-SB-T-12854 performed very well against the prostate cancer cell lines, PC3 and PC3MM2, with subnanomolar IC_{50} values of 0.23 nM and 0.27 nM, respectively. The free taxoid SB-T-12854 displayed several orders of magnitude less potency in both PC3 and PC3MM2, 5.08 nM and 32.5 nM, respectively. This result may be caused by the decomposition of SB-T-12854 in storage or experimental error in treating the cells with the taxoid, i.e. cells were not treated with the correct concentration of taxoid. Nonetheless, it is reasonable to assume that an intracellular esterase cleaves the ester bond connecting the taxoid to the PUFA, releasing the taxoid in its active form. Thus, it is also reasonable to assume that some cancer cell lines have a higher concentration of intracellular esterase, resulting in higher observed potency. For example, when comparing the cancer cell lines treated with DHA-SB-T-1214, the drug conjugate displayed nanomolar activity against CFPac-1, PC3 and PC3MM2 cancer cell lines, but orders of magnitude lower potency in the other cancer cell lines evaluated. Thus, the cleavage of the ester bond was accelerated in these three cell lines, possibly due to an endogenous esterase. However, the stark difference between the activities of DHA-SB-T-1214 and LNA-SB-T-1214 against all cancer cell lines is at the moment unexplainable. One explanation is that the rate in which the cleavage of the ester bond between LNA and taxoid is slower due to the free rotation of the sp3 C-C bonds of LNA which may block an esterase from cleaving the bond. Further work along this line is currently being done in the Ojima laboratory.

The *in vitro* activities of PUFA-taxoid drug conjugates were also evaluated in doxorubicin-resistant ovarian cancer cell line A2780-DX3. The results from this experiment are shown in Table 3.3.

Table 3.3: Biological Evaluation of PUFA-Taxoid Drug Conjugate against A2780 Cell Lines

	IC_{50} (nM)	
Drug	**A2780 (wild type ovarian cancer)**	**A2780-DX3 (DX resistant ovarian cancer)**
Doxorubicin	8087 ± 92	>50000
Paclitaxel	26.1 ± 1.99	>50000
SB-T-1214	0.36 ± 0.06	13.3 ± 4.60
DHA-SB-T-1214[a]	580 ± 30	32.3 ± 1.40
LNA- SB-T-1214	12133 ± 737	559 ± 73
SB-T-12854[b]	2.47 ± 0.20	1.57 ± 0.29
DHA-SB-T-12854[c]	286 ± 66	12.4 ± 3.49

[a] taxoid synthesized by Chem Masters Int.; [b] taxoid synthesized by Ilaria Zanardi; [c] taxoid synthesized by Dr. Yuan Li

- Cells were suspended in RPMI with L-glutamine (Lonza BioWhittaker, BW12-702F), with 5% FBS (Thermo Scientific, HyClone, SH3007003), 5% Nu Serum (BD Biosciences, 355100) and 1% Penn Strip before administration of taxoid
- Cells were incubated for 48 hours at 37 °C with 5% CO_2 after administration of taxoid
- The optical density was determined using Acsent Multiskan optical density reader
- The reported values are a calculated averages of IC_{50} values determined from three individual experiments
- IC_{50} values were calculated using SigmaPlot v 10.0
- All IC_{50} values are report in nM scale unless otherwise noted

As seen from Table 3.3, a similar trend is seen between the *in vitro* activities of DHA-taxoid and LNA-taxoid drug conjugates (i.e. an observed lower cytotoxicity for LNA drug conjugates). It is worthy of note that the PUFA-taxoid drug conjugates showed higher cytotoxicity against the DX-resistant cell line, A2780-DX3, compared to the wild type cell line. Of the PUFA-taxoid drug conjugates examined, DHA-SB-T-12854 showed the best cytotoxicity in both A2780 and A2780-DX3 cell lines with IC_{50} values of 286 nM and 12.4 nM, respectively.

The activity of PUFA-taxoid drug conjugates was also evaluated against normal human cell lines, HS-27 (foreskin fibroblast) and WI-38 (lung fibroblast). The results from this experiment are shown in Table 3.4.

Table 3.4: Biological Activity of PUFA-Taxoid Drug Conjugates against Normal Human Cell Lines

Drug	Incubation time with drug (h)	IC_{50} (nM) HS-27 (human foreskin fibroblast)	IC_{50} (nM) WI-38 (human lung fibroblast)
Paclitaxel	24	>5000	580 ± 30
-	48	>5000	35.9 ± 5.0
-	72	>5000	9.70 ± 1.61
SB-T-1214	24	4.68 ± 0.16	3.05 ± 0.33
-	48	3.40 ± 0.60	1.57 ± 0.60
-	72	0.20 ± 0.04	0.71 ± 0.17
DHA-SB-T-1214[a]	24	0.52 ± 0.02	52.2 ± 3.0
-	48	0.39 ± 0.13	3.62 ± 1.74
-	72	0.36 ± 0.09	3.18 ± 1.06
LNA- SB-T-1214	24	>10000	>5000
-	48	>10000	128 ± 40
-	72	>10000	33.4 ± 10.1
SB-T-12854[b]	24	5.86 ± 1.30	2.11 ± 0.24
-	48	6.11 ± 0.21	0.25 ± 0.05
-	72	2.38 ± 0.88	0.27 ± 0.03
DHA-SB-T-12854[c]	24	0.77 ± 0.05	44.1 ± 3.5
-	48	0.64 ± 0.09	55.6 ± 6.3
-	72	0.28 ± 0.07	42.0 ± 8.26

[a] taxoid synthesized by Chem Masters Int.; [b] taxoid synthesized by Ilaria Zanardi; [c] taxoid synthesized by Dr. Yuan Li

- Cells were suspended in RPMI-1640 with L-glutamine (Lonza BioWhittaker, BW12-702F: HS-27), or EMEM (Lonza BioWhittaker, BW12-125: WI-38) supplemented with 5% FBS (Thermo Scientific, HyClone, SH3007003), 5% Nu Serum (BD Biosciences, 355100) and 1% Penn Strip before administration of taxoid
- Cells were incubated for 48 hours at 37 °C with 5% CO_2 after administration of taxoid
- The optical density was determined using Acsent Multiskan optical density reader; the reported values are a calculated averages of IC_{50} values determined from three individual experiments; IC_{50} values were calculated using SigmaPlot v 10.0; all IC_{50} values are report in nM scale unless otherwise noted

As seen from Table 3.4, in general the PUFA-taxoid drug conjugates demonstrated significant potency after 48 h incubation against both normal cell lines. However, LNA-SB-T-1214 did not show activity in HS-27 after 72 h. Likewise, LNA-SB-T-1214 possesses less activity in WI-38 cells compared to DHA-SB-T-1214 and DHA-SB-T-12854. The lower activity demonstrated by LNA-SB-T-1214 drug conjugate against cancer and normal cells may be a result of the cells ability to grow without LNA, i.e. LNA is not as essential as DHA for cell growth, therefore LNA-taxoid drug conjugate is not readily cleaved inside the cell compared to DHA-taxoid drug conjugates. Similarly, LNA drug conjugates may diffuse back out of the cell without delivering the free taxoid, whereas DHA drug conjugates are held within the cell via protein-binding with Fatty Acid Binding Protein (FABP). The effects of HSA with LNA-taxoid drug conjugates are currently being investigated in the Ojima laboratory.

§ 3.2.3 Internalization of PUFA-Taxoid-Fluorescein Conjugates

The internalization of PUFA-FITC conjugates was evaluated using FACS. From these experiments it was shown that both DHA-FITC and LNA-FITC conjugates are internalized into cancer cells. Standard MTT assays show a significant decrease in cytotoxicity of the PUFA-taxoid drug conjugates compared to the parent new-generation taxoid. To evaluate the internalization of these PUFA-taxoid drug conjugates into cancer cells, the fluorescence-labeled drug conjugates were prepared. Two drug conjugate, DHA-SB-T-1214-Fluoresein and LNA-SB-T-1214-Fluorescein (Dr. Larisa Kuznetsova, Ojima laboratory) were synthesized (Figure 3.9).

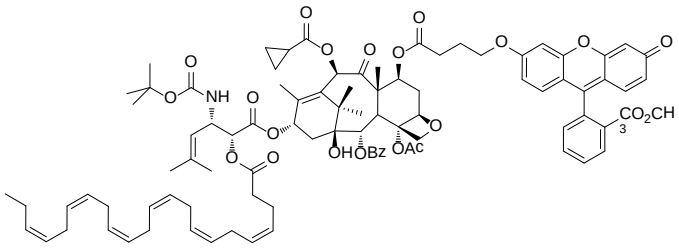

DHA-SB-T-1214-fluorescein

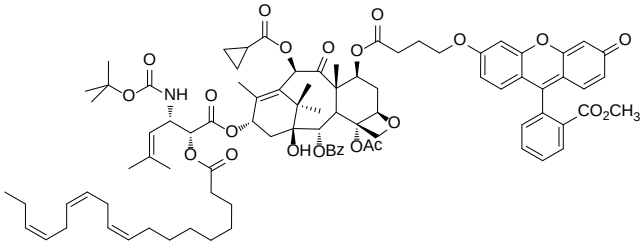

LNA-SB-T-1214-fluorescein

Figure 3.9: PUFA-taxoid-fluorescein

For the synthesis of these fluorescein-labeled PUFA-taxoid drug conjugates, fluorescein was coupled to the C7-position of 2'-TBDMS-protected SB-T-1214 via a 4-hydroxybutanoic acid spacer. After deprotection of the silyl moiety, PUFA was coupled to the free 2'-position of the taxoid in the presence of DIC and DMAP to give the desired PUFA-SB-T-1214-fluorescein drug conjugates. The internalization of these drug conjugates was evaluated in A2780 (human ovarian cancer), DLD-1 (human colon cancer), HT-29 (human colon cancer), MCF-7 (human breast cancer) and HS-27 (normal human foreskin) cell lines using FACS (Figure 3.10).

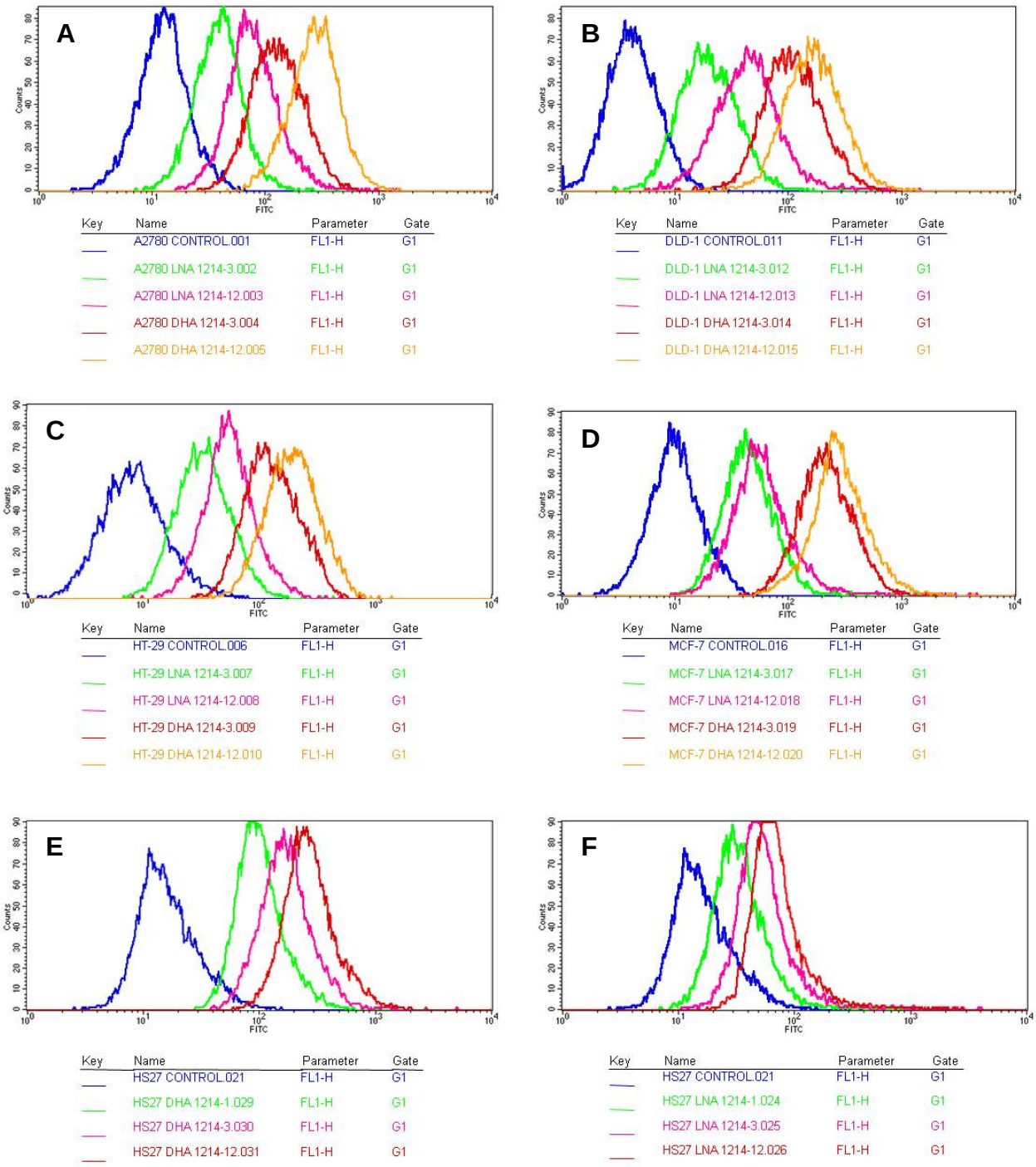

Figure 3.10: FACS analysis and histogram overlays evaluating internalization of 1 µM PUFA-Taxoid-Fluorescein incubated in different cell lines for 3 h or 12 h at 37 °C. (A) A2780 human ovarian cancer; (B) DLD-1 human colon cancer; (C) HT-29 human colon cancer; (D) MCF-7 human breast cancer; (E) Panc-1 human pancreatic cancer; (F) HS-27 normal human skin fibroblast.

The cells were resuspended in RPMI supplemented with FBS and antibiotics. Following incubation at 37 °C with 5% CO_2, the cells were administered with PUFA-SB-T-1214-Fluorescein drug conjugate at 1 µM concentration for 3 hour or 12 hour incubation periods. After

the incubation period, the cells were washed and analyzed using FACS. As can be seen from the FACS charts, as the amount of time in which the cells are incubated with PUFA-SB-T-1214-fluorescein drug conjugate there is an increase in internalization (i.e., the red, pink and orange lines shift to the right). It appears that at least 12 hours of incubation is required to for complete internalization of the fluorescein-labeled PUFA-taxoid drug conjugate into cancer cells, as indicated by the FACS analysis [i.e. the orange line (in cancer cells) and red line (normal cells) are completely separate from the blue line (control)]. In addition, comparing HS-27 cells, there appears to be greater internalization of the DHA-SB-T-1214-fluorescein drug conjugate into the normal cell line compared to the internalization of LNA-SB-T-1214-fluorescein. However, based on the number of cells in which the fluorescein-labeled PUFA-taxoid drug conjugate was internalized, there is a greater tumor-specificity shown by DHA-SB-T-1214-fluorescein when comparing human cancer cells to normal human cells.

§ 3.2.4 Synthesis of PUFA-NSC 706744 Drug Conjugate

The compound NSC 706744 was obtained from the National Cancer Institute (NCI) with the purpose of evaluating the biological activity of tumor-targeting drug conjugates containing the drug. NSC 706744 is a non-camptothecin, topoisomerase I inhibitor that contains an aminol moiety, which increases the polarity of the compound making the compound soluble in water.[34-36] In addition, the compound does not contain the lactone ring that is present in camptothecin. Under certain conditions, it has been shown that this lactone ring can open to yield a carboxylate-CPT which has no biological activity.[37-40] Thus the structure of NSC 706744 does look promising.

As previously mentioned, some polyunsaturated fatty acids have shown anticancer activity in several cancer cell lines. In addition, some tumor cells readily uptake some PUFA. Drug conjugates containing PUFA as the targeting module may provide powerful weapons in anticancer therapy. The two PUFAs used for conjugate synthesis were DHA and LNA. Both are omega-3 fatty acids and provide nutritional benefits in humans. PUFA-NSC 706744 drug conjugates with DHA and LNA as TTM were prepared using standard DIC coupling conditions (Scheme 3.2).

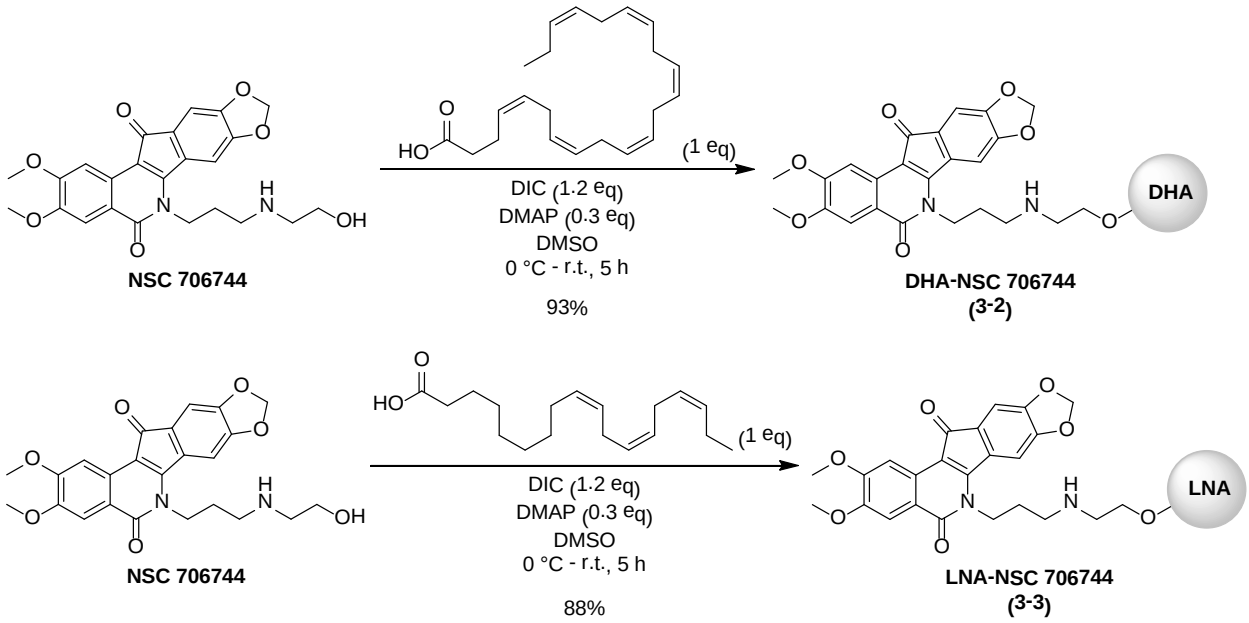

Scheme 3.2: Synthesis of PUFA-NSC 706744 drug conjugates

The PUFA-drug coupling proceeded nicely in both DHA and LNA cases, as both drug conjugates were obtained in high yield (93% and 88%, respectively). Though an additional side-product was formed and isolated (for both DHA and LNA couplings), pure PUFA-NSC 706744 drug conjugates were obtained after column chromatography. HPLC analysis of both conjugated showed >96% purity. However, after 1 month in storage under nitrogen at -4 to 0 °C, decomposition of both DHA- and LNA-NSC 706744 drug conjugates was observed.

§ 3.3.0 Summary

Multidrug resistance and lack of tumor specificity are two major hurdles which render chemotherapeutic agents ineffective. A promising approach to combat these dilemmas is the development of tumor-targeting prodrugs, which contains a cytotoxic drug conjugated to a tumor-targeting module (TTM). Tumor-targeting prodrugs are designed to remain inactive until it is delivered to the tumor site by the TTM and internalized into tumor cells. After the drug conjugate is internalized, the cytotoxic agent is released from its carrier to restore its original activity. Apart from providing health benefits, polyunsaturated fatty acids are utilized as cellular membrane components, energy resources and signaling molecules. Furthermore, PUFAs are readily taken up by malignant cells, as observed in FACS experiments. Thus, PUFAs make ideal TTMs for tumor-targeting prodrug synthesis. Accordingly, LNA-SB-T-1214 was synthesized. The biological activity of LNA-SB-T-1214 was evaluated in a series of cancer cell lines and compared to other PUFA-taxoid drug conjugates previously developed in the Ojima laboratory. A common trend was observed, in that the LNA-taxoid drug conjugate showed lower *in vitro* activity compared to DHA-taxoid. A similar trend was observed in wild type A2780 (human ovarian) and doxorubicin-resistant A2780 cancer cell lines. DHA-SB-T-12854 showed the best activity among the PUFA-taxoid drug conjugates tested against these two cell lines. These results suggest that PUFA-taxoid drug conjugates have encouraging anticancer activity and are

promising preclinical/clinical drug candidates. The synthesis of PUFA-NSC 706744 drug conjugates was also discussed.

§ 3.4.0 Experimental

Caution

Taxoids and NSC 706744 have been established as a potent cytotoxic agent. Thus, they and all structurally related compounds and derivatives must be considered as mutagens and potential reproductive hazards for both males and females. Appropriate precautions (i.e. use of gloves, goggles, lab coat and fume hood) must be taken while handling these compounds.

General information

All chemical were obtained from either Sigma-Aldrich, Fisher Scientific or VWR International, and used as is unless otherwise noted. All reactions were carried out under nitrogen in oven dried glassware using standard Schlenk techniques unless otherwise noted. Reactions were monitored by thin layer chromatography (TLC) using E. Merck 60F254 precoated silica gel plates and alumina plate depending on the compounds. Dry solvents were degassed under nitrogen and were dried using the PURESOLV system (Inovatative Technologies, Newport, MA). Tetrahydrofuran was freshly distilled from sodium metal and benzophenone. Dichloromethane was also distilled immediately prior to use under nitrogen from calcium hydride. Toluene was also distilled immediately prior to use under nitrogen from calcium hydride. Yields refer to chromatographically and spectroscopically pure compounds. Flash chromatography was performed with the indicated solvents using Fisher silica gel (particle size 170-400 Mesh).^{1}H, ^{13}C and ^{9}F data were obtained using either 300 MHz Varian Gemni 2300 (75 MHz ^{13}C, 121 MHz ^{19}F) spectrometer, the 400 MHz Varian INOVA 400 (100 MHz ^{13}C) spectrometer or the 500 MHz Varian INOVA 500 (125 MHz ^{13}C) in $CDCl_3$ as solvent unless otherwise stated. Chemical shifts (δ) are reported in ppm and standardized with solvent as internal standard based on literature reported values.[41] Melting points were measured on Thomas Hoover Capillary melting point apparatus and are uncorrected. Optical rotations were measured on Perkin-Elmer Model 241 polarimeter. NSC 706744 was obtained from NCI.

Experimental procedure

LNA-SB-T-1214 (3-1)

To a solution of SB-T-1214 (100 mg, 0.1 mmol), DMAP (5 mg, 0.03 mmol) and LNA (33 mg, 0.1 mmol) dissolved in CH_2Cl_2 [0.1 M] was added DIC (0.02 mL, 0.11 mmol). The mixture was stirred at room temperature and the reaction was monitored using TLC. After 1 hour, the SB-T-1214 starting material was consumed, the reaction solvent was evaporated. The resulting crude was dissolved in 10 mL of ethyl ether. The organic layer was washed with aqueous NH_4Cl (3 x 10 mL), then with water (3 x 10 mL), dried over $MgSO_4$ and concentrated *in vacuo*. The resulting crude was purified using flash column chromatography on silica gel (hexanes:ethyl acetate = 3:1) to yield **3-1** (110 mg, 75% yield) as a waxy white solid: ^{1}H NMR (400 MHz, $CDCl_3$, ppm) δ 0.876-1.029 (m, 6 H), 1.251 (s, 4 H), 1.338 (s, 16 H), 1.660 (m, 6 H), 1.831-1.895 (m, 1 H), 1.923 (s, 3 H), 2.040-2.094 (m, 2 H), 2.290 (m, 1 H), 2.371 (s, 3 H), 2.423-2.449 (m, 2 H), 2.515-2.559 (m, 1 H), 2.603 (br s, 1 H), 2.804 (t, *J* = 6 Hz, 2 H), 3.800 (d, *J* = 7.2 Hz, 1

H), 4.169-4.317 (dd, J_1 = 8.4 Hz, J_2 = 42 Hz, 2 H), 4.437 (m, 1 H), 4.784 (s, 1 H), 4.924-4.983 (m, 3 H), 5.171 (d, J = 8 Hz), 5.297-5.408 (m, 3 H), 5.660 (d, J = 2.8 Hz, 1 H), 6.187 (m, 1 H), 6.294 (m, 1 H), 7.473 (t, J = 7.6 Hz, 2 H), 7.602 (t, J = 7.2 Hz, 1 H), 8.100 (d, J = 7.6 Hz, 2 H); ^{13}C NMR (400 MHz, $CDCl_3$, ppm) δ 9.287, 9.492, 9.750, 13.187, 14.432, 14.963, 18.719, 20.738, 22.445, 22.597, 24.935, 25.731, 25.815, 25.929, 26.915, 27.386, 28.418, 29.230, 29.290, 29.359, 29.784, 33.965, 35.627, 35.741, 43.382, 45.849, 49.226, 58.704, 71.832, 72.333, 74.579, 75.482, 75.626, 75.695, 76.598, 79.550, 80.006, 81.204, 84.695, 120.247, 127.305, 127.980, 128.428, 128.511, 128.853, 129.528, 130.401, 132.161, 132.693, 133.785, 138.126, 143.711, 155.086, 167.213, 168.571, 169.831, 173.109, 175.287, 204.283; LC-MS MS (ESI) *m/z* calcd for $C_{63}H_{87}NO_{16}$ $(M+H)^+$ 1114.6, found 1114.6.

DHA-NSC 706744 (3-2)

To NSC 706744 (10 mg, 0.02 mmol) and DMAP (0.1 mg, 0.003 mmol) dissolved in DMSO [0.5 M] cooled to 0 °C was added DHA (7 mg, 0.016 mmol). The mixture was stirred for 10 min at 0 °C. To the mixture was added DIC (0.005 mL, 0.02 mmol). The mixture was stirred and allowed to warm to room temperature and the reaction was monitored via TLC. After 5 h, the reaction mixture was diluted with ethyl acetate producing a purple precipitate. The precipitate was collected and dissolved in ethyl acetate. The organic layer was washed with water, dried over $MgSO_4$ and concentrated *in vacuo*. The resulting crude was purified using flash column chromatography on silica gel (hexanes:ethyl acetate = 3:1) to yield **3-2** (15 mg, 93% yield), as a waxy purple solid. This reaction was repeated on a 100 mg scale to yield 85 mg (51% isolated yield) of **2-2**. After re-purification on silica gel 21 mg of the conjugate was recovered in addition to 3 fractions of decomposed material. ^{1}H NMR (500 MHz, $CDCl_3$, ppm) δ 0.985 (t, J = 7.5 Hz, 3 H), 1.170 (d, J = 6.5 Hz, 2 H), 1.272 (s, 2 H), 1.800 (br s, 1 H), 2.084 (m, 6 H), 2.384 (s, 5 H), 2.483 (s, 2 H), 2.840 (br s, 12 H), 3.665 (m, 4 H), 3.995 (s, 3 H), 4.059 (s, 3 H), 4.242 (m, 2 H), 4.525-4.552 (m, 1 H), 5.377 (m, 12 H), 6.099 (s, 2 H), 7.072 (s, 1 H), 7.115 (s, 1 H), 7.635 (s, 1 H), 8.031 (s, 1 H); ^{13}C NMR (400 MHz, $CDCl_3$, ppm) δ 14.455, 18.621, 20.746, 22.764, 23.235, 23.660, 25.815, 27.978, 29.882, 33.047, 34.086, 41.766, 42.449, 42.783, 43.724, 45.469, 46.456, 46.623, 56.230, 56.480, 58.651, 61.823, 102.854, 103.203, 104.334, 105.252, 105.579, 105.897, 108.121, 117.144, 119.891, 121.287, 127.191, 127.707, 128.048, 128.253, 128.466, 128.671, 128.762, 129.323, 129.801, 130,568, 132.222, 132.693, 137.564, 149.076, 149.327, 149.737, 151.808, 153.132, 155.132, 162.599, 172.897, 173.185, 189.774.

LNA-NSC 706744 (3-3)

To NSC 706744 (10 mg, 0.02 mmol) and DMAP (0.1 mg, 0.003 mmol) dissolved in DMSO [0.5 M] cooled to 0 °C was added LNA (0.006 mL, 0.016 mmol). The mixture was stirred for 10 min at 0 °C. To the mixture was added DIC (0.005 mL, 0.02 mmol). The mixture was stirred and allowed to warm to room temperature and the reaction was monitored via TLC. After 5 h, the reaction mixture was diluted with ethyl acetate producing a purple precipitate. The precipitate was collected and dissolved in ethyl acetate. The organic layer was washed with water, dried over $MgSO_4$ and concentrated *in vacuo*. The resulting crude was purified using flash column chromatography on silica gel (hexanes:ethyl acetate = 3:1) to yield **3-3** (15 mg, 88% yield), as an oily purple solid. This reaction was repeated on a 100 mg scale to yield 99 mg (60% isolated yield) of **3-3**. After re-purification on silica gel 46 mg of the conjugate was recovered in addition to 2 fractions of decomposed material. ^{1}H NMR (500 MHz, $CDCl_3$, ppm) δ 0.901 (m, 6 H), 3.500 (s, 2 H), 3.598-3.640 (q, J_1 = 7 Hz, J_2 = 7.5 Hz, J_3 = 7 Hz, 6 H), 3.835-3.855 (m, 3 H),

3.942 (s, 4 H), 3.997 (s, 4 H), 4.574 (br s, 4 H), 4.625-4.652 (m, 4 H), 6.147 (s, 2 H), 7.034 (s, 1 H), 7.235 (s, 1 H), 7.613 (s, 1 H), 7.950 (s, 1 H), DMSO and ethyl acetate also present.

Cell culture system for MTT assay

Cell lines (obtained from ATCC unless otherwise noted and maintained at SBU Cell Culture/Hybridoma Facility) were cultured in RPMI-1640 with L-glutamine (Lonza BioWhittaker, BW12-702F: A2780, DLD-1, HS-27, ID-8, MCF-7), DMEM (Lonza BioWhittaker, BW12-604F: CFPac-1 Panc-1), EMEM (Lonza BioWhittaker, BW12-125: WI-38) or McCoy's 5A (Gibco #16600: HT-29) supplemented with 5% FBS (Thermo Scientific, HyClone, SH3007003), 5% Nu Serum (BD Biosciences, 355100) and 1% Penn Strip and incubated at 37 °C in a humidified incubator with 5% CO_2. The cells were washed with DPBS and dissociated using TrypLE. The cells were incubated at 37 °C until the cells were detached from the plate, transferred to a centrifuge vial and pelleted via centrifugation at 1500 rpm for 5 min. The cells were counted per 1 mL media. The desired amount of media was added to the cell solution so that 8,000 cells can be added to each well of a 96-well plate in 200 μL aliquots. After the addition, the cells were incubated at 37 °C with 5% CO_2.

Drug treatment for MTT assay

A serial dilution of the free taxoid and LNA-SB-T-1214 drug conjugate dissolved in sterile DMSO was prepared by the addition of fully-supplemented RPMI-1640. The residual medium in each well was aspirated and the different drug concentrations were added to each well of every column of the 96-well plate in 100 μL aliquots. After the addition of the drug solution, the cells were incubated at 37 °C for 48 hours. After the incubation period, the medium was aspirated and the cells were washed with DPBS and then 40 μL of 0.5 mg/mL MTT (3-(4,5-dimethylthiazol-2-yl)-2,5-diphenyltetrazolium bromide) in DPBS was added to each well. The cells were then incubated at 37 °C for 3 hours. After the incubation period, the MTT solution was aspirated and the remaining crystals were dissolved using a 40 μL of 0.4 M HCl in isopropanol. The plates were shaken for 10 minutes to assure that all of the crystals are dissolved. The optical density was determined from the resulting solutions using the Acsent Multiskan optical density reader. Each experiment was run in triplicate.

Data analysis for MTT assay

The optical density data was used to calculate IC_{50} values for each drug on a given cell line using the Hill slope equation. The optical density values obtained from each concentration of drug solution were divided by the optical density value obtained from the cells with zero drug concentration. Using SigmaPlot v.10, the ratios were plotted versus the drug concentration and the IC_{50} values were calculated from the plot using the pre-programmed calculation within the SigmaPlot program.

Cell culture system for PUFA-FITC conjugate internalization

Target cells plated and were resuspended in RPMI with L-glutamine (Lonza BioWhittaker, BW12-702F) supplemented with 5% FBS (Thermo Scientific, HyClone, SH3007003), 5% Nu Serum (BD Biosciences, 355100) and 1% Penn Strip, and incubated at 37 °C in a humidified 5% CO_2 incubator for 2 to 3 days. The cells were washed with DPBS and dissociated using TrypLE. The cells were allowed to sit at room temperature until the cells were detached from the plate,

transferred to a centrifuge vial and pelleted via centrifugation at 1500 rpm for 5 min. Media was added to the pellet and the pellet was disrupted. The cells were counted per 1 mL. The desired amount of media was added so that 50,000 cells could be added to each well of a 6-well plate. After the addition, the cells were resuspended supplemented RPMI and incubated at 37 °C for 1 day. After the incubation period, the cells were treated with 1 μM and 10 μM of PUFA-FITC conjugate and incubated for 1 hour. After this incubation period, the media was aspirated, the cells were washed with DPBS and then dissociated using Hank's Enzyme Free Dissociation Solution. The dissociated cells were transferred to a centrifuge tube and pelleted via centrifugation at 1500 rpm for 5 min. The resulting pellet was washed twice with DPBS (10 mL then 1 mL). After the final wash, internalization was monitored using FACS. Flow cytometry analysis of treated cells was performed with a FACSCalibur flow cytometer (SBU Medical Center Core facility laboratory), operating at a 488 nm excitation wavelength and detecting emission wavelengths with a 530/30 nm bandpass filter. Cell samples suspended in 2% formulin in DPBS were count with a minimal 10,000 cells per sample using CellQuest 3.3 software (Becton Dickinson) and the distribution of FITC fluorescence was analyzed using WinMDI 2.9 freeware (Joseph Trotter, Scripps Research Institute).

Cell culture system for PUFA-SB-T-1214-Fluorescein drug conjugate internalization

Target cells plated and were resuspended in RPMI with L-glutamine (Lonza BioWhittaker, BW12-702F) supplemented with 5% FBS (Thermo Scientific, HyClone, SH3007003), 5% Nu Serum (BD Biosciences, 355100) and 1% Penn Strip, and incubated at 37 °C in a humidified 5% CO_2 incubator for 2 to 3 days. The cells were washed with DPBS and dissociated using TrypLE. The cells were allowed to sit at room temperature until the cells were detached from the plate, transferred to a centrifuge vial and pelleted via centrifugation at 1500 rpm for 5 min. Media was added to the pellet and the pellet was disrupted. The cells were counted per 1 mL. The desired amount of media was added so that 50,000 cells could be added to each well of a 6-well plate. After the addition, the cells were resuspended supplemented RPMI and incubated at 37 °C for 1 day. After the incubation period, the cells were treated with 1 μM of PUFA-SB-T-1214-Fluorescein drug conjugate and incubated for 1, 3 and 12 hour time periods. After this incubation period, the media was aspirated, the cells were washed with DPBS and then dissociated using Hank's Enzyme Free Dissociation Solution. The dissociated cells were transferred to a centrifuge tube and pelleted via centrifugation at 1500 rpm for 5 min. The resulting pellet was washed twice with DPBS (10 mL then 1 mL). After the final wash, internalization was monitored using FACS. Flow cytometry analysis of treated cells was performed with a FACSCalibur flow cytometer (SBU Medical Center Core facility laboratory), operating at a 488 nm excitation wavelength and detecting emission wavelengths with a 530/30 nm bandpass filter. Cell samples suspended in 2% formulin in DPBS were count with a minimal 10,000 cells per sample using CellQuest 3.3 software (Becton Dickinson) and the distribution of FITC fluorescence was analyzed using WinMDI 2.9 freeware (Joseph Trotter, Scripps Research Institute).

§ 3.5.0 References

1. Gottesman, M. M., Pastan, I. Biochemistry of multidrug resistance mediated by the multidrug transporter. *Annu. Rev. Biochem.* **1993,** 62, 385-427.

2. Jack, D. L.; Yang, N. M.; Saier, M. H. J. The drug/metabolite transporter superfamily. *Eur. J. Biochem.* **2001,** 268, 3620-3639.
3. Ferlini, C., Distefano, M., Pignatelli, F., Lin, S., Riva, A., Bombardelli, E., Mancuso, S., Ojima, I., Scambia, G. Antitumor activity of novel taxanes that act as the same time as cytotoxic agents and P-glycoprotein inhibitors. *Brit. J. Cancer* **2000,** 83, 1762-1768.
4. Allen, H. K.; Donao, J.; Wang, H. H.; Cloud-Hansen, K. A.; Davies, J.; Handelsman, J. Call of the wild: antibiotic resistance genes in natural environments. *Nature Rev. Microbio.* **2010,** 8, 251-259.
5. Devita Jr., V. T.; Chu, E. A History of Cancer Chemotherapy. *Cancer Res.* **2008,** 68, 8643-8653.
6. Druker, B. J.; Lydon, N. B. Lessons learned from the development of an Abl tyrosine kinase inhibitor for chronic myelogenous leukemia. *J. Clin. Invest.* **2000,** 105, 3-7.
7. Drucker, B. J.; Tamura, S.; Buchdunger, E.; Ohno, S.; Segal, G. M.; Fanning, S.; Zimmerman, J.; Lydon, N. B. Effects of a selective inhibitor of the Abl tyrosine kinase on the growth of Bcr-Abl positive cells. *Nat. Med.* **1996,** 2, 561-566.
8. Krause, D. S.; Van Etten, R. A. Tyrosine kinases as targets for cancer therapy. *N. Engl. J. Med.* **2005,** 2, 172-187.
9. Doronina, S. O., Mendelsohn, B.A., Bovee, T.D., Cerveny, C.G., Alley, S.C., Meyer, D.L., Oflazoghu, E., Toki, B.E., Sanderson, R.J., Zabinski, R.F., Wahl, A.F., Senter, P.D. Enhanced Activity of Monomethylauristatin F through Monoclonal Antibody Delivery: Effects of Linker Technology on Efficacy and Toxicity. *Bioconjugate Chem.* **2006,** 17, 114-124.
10. Beck, A., Haeuw, J.F., Wurch, T., Goetsch, L., Bailly, C., Corvaia, N. The next generation of antibody-drug conjugates comes of age. *Discov. Med.* **2010,** 10, 329-339.
11. Bradley, M. O., Webb, N.L., Anthony, F.H., Devanesan, P., Wittman, P.A., Hemamalini, S., Chander, M.C., Baker, S.D., He, L., Horwitz, S.B., Swindell, C.S. Tumor targeting by covalent conjugation of a natural fatty acid to taxol. *Clin. Cancer Res.* **2001,** 7, 3229-3238.
12. Whelan, J. Targeted taxane therapy for cancer. *Drug Discovery Today* **2002,** 7, 90-92.
13. Wahl, A. F.; Donaldson, K. L.; Mixan, B. J.; Trail, P. A.; Siegall, C. B. Selective tumor sensitization to taxanes with the mAb-drug conjugate cBR96-doxorubicin. *Int. J. Cancer* **2001,** 4, 590-600.
14. Hamann, P. R.; Hinman, L. M.; Beyer, C. F.; Lindh, D.; Upeslacis, J.; Flowers, D. A.; Bernstein, I. An Anti-CD33 Antibody−Calicheamicin Conjugate for Treatment of Acute Myeloid Leukemia. Choice of Linker. *Bioconjugate Chem.* **2002,** 13, 40-46.
15. Sauer, L. A., Dauchy, R.T., Blask, D.E. Mechanism for the antitumor and anticachectic effects of n-3 fatty acids. *Cancer Res.* **2000,** 60, 5289-5295.
16. Wigmore, S. J., Ross, J.A., Falconer, J.S., Plester, C.E., Tisdale, M.J., Carter, D.C., Fearon, K.C.H. The effect of polyunsaturated fatty acids on the progress of cachexia in patients with pancreatic cancer. *Nutrition* **1996,** 12, S27-S30.
17. Hawkins, R. A.; Sangster, K.; Arends, M. J. Apoptotic death of pancreatic cancer cells induced by polyunsaturated fatty acids varies with double bond number an involves an oxidative mechanism. *J. Pathol.* **1998,** 185, 61-70.
18. Grammatikos, S. I., Subbaiah, P.V., Victor, T.A., Miller, W.M. n-3 and n-6 fatty acid processing and growth effects in neoplastic and non-cancerous human mammary epithelial cell lines. *Brit. J. Cancer* **1994,** 70, 219-227.

19. Diomede, L., Colotta, F., Piovani, B., Re, F., Modest, E.J., Salmona, M. Induction of apoptosis in human leukemic cells by the ether lipid 1-octadecyl-2-methyl-racglycero-3-phosphocholine. A possible basis for its selective action. *Int. J. Cancer Res.* **1993,** 53, 124-130.
20. Seitz, J. D.; Ojima, I. Drug Conjugates with Polyunsaturated Fatty Acids. In *Drug Delivery in Oncology: From Basic Research to Cancer Therapy*, 1st ed.; Kratz, F.; Senter, P.; Steinhagen, H., Eds. Wiley-VCH Verlag GmbH & co. KGaA.: 2010; Vol. 3, pp 1323-1360.
21. Ibrahim, N. K., Desai, N., Legha, S., Soon-Shiong, P., Theriault, R.L., Rivera, E., Esmaeli, B., Ring, S.E., Bedikian, A., Hortobagyi, G.N., Ellerhorst, J.A. Phase I and pharmacokinetic study ABI-007, a cremophor-free, protein-stabilized nanoparticle formulation of paclitaxel. *Clin. Cancer Res.* **2002,** 8, 1038-1044.
22. Desai, N., Trieu, V., Yao, Z., Louie, L., Ci, S., Yang, A., Tao, C., De, T., Beals, B., Dykes, D., Noker, P., Yao, R., Labao, E., Hawkins, M., Soon-Shiong, P. Increased antitumor activity, intratumor paclitaxel concentrations, and endothelial cell transport of cremophor-free, albumin-bound paclitaxel, ABI-007, compared with cremophor-based paclitaxel. *Clin. Cancer Res.* **2006,** 12, 1317-1324.
23. Rose, D. P.; Connolly, J. M. Omega-3 fatty acids as cancer chemopreventive agents. *Pharmacol. Ther.* **1999,** 83, 217-244.
24. Tuller, E. R.; Brock, A. L.; Yu, H.; Lou, J. R.; Benbrook, D. M.; Ding, W.-Q. PPARα signaling mediates the synergistic cytotoxicity of clioquinol and docosahexaenoic acid in human cancer cells. *Biochem. Pharmacol.* **2009,** 77, 1480-1486.
25. Zhuo, Z.; Zhang, L.; Mu, Q.; Lou, Y.; Gong, Z.; Shi, Y.; Quyang, G.; Zhang, Y. The effect of combination treatment with docosahexaenoic acid and 5-fluorouracil on the mRNA expression of apoptosis-related genes, including the novel gene BCL2L12, in gastric cancer cells. *In Vitro Cell. Dev. Biol. Anim.* **2009,** 45, 69-74.
26. Yamamoto, D.; Kiyozuka, Y.; Adachi, Y.; Takada, H.; Hioki, K.; Tsubura, A. Synergistic action of apoptosis induced by eicosapentaenoic acid and TNP-470 on human breast cancer cells. *Breast Cancer Res. Treat.* **1999,** 55, 149-160.
27. Nakagawa, H.; Yamamoto, D.; Kiyozuka, Y.; Tsuta, K.; Uemura, Y.; Hioki, K.; Tsutsui, Y.; Tsubura, A. Effects of genistein and synergistic action in combination with eicosapentaenoic acid on the growth of breast cancer cell lines. *J. Cancer Res. Clin. Oncol.* **2000,** 126, 448-454.
28. Menendez, J. A.; Ropero, S.; del Mar Barbacid, M.; Montero, S.; Solanas, M.; Escrich, E.; Cortes-Funes, H.; Colmer, R. Synergistic interaction between vinorelbine and gamma-linolenic acid in breast cancer cells. *Eur. J. Cancer* **2001,** 37, 402-413.
29. Ojima, I.; Zuniga, E. S.; Berger, W. T.; Seitz, J. D. Tumor-targeting drug delivery of new-genreation taxoids. *Future Med. Chem.* **2012,** 4, 33-50.
30. Ojima, I.; Slater, J. C.; Michaud, E.; Kuduk, S. D.; Bounaud, P.-Y.; Vrignaud, P.; Bissery, M.-C.; Veith, J.; Pera, P.; Bernacki, R. J. Syntheses and structure–activity relationships of the second generation antitumor taxoids. Exceptional activity against drug-resistant cancer cells. *J. Med. Chem.* **1996,** 39, 3889-3896.
31. Ojima, I.; Slater, J. C.; Kuduk, S. D.; Takeuchi, C. S.; Gimi, R. H.; Sun, C. M.; Park, Y. H.; Pera, P.; Veith, J. M.; Bernacki, R. J. Syntheses and Structure-Activity Relationships of Taxoids Derived from 14-beta-Hydroxy-10-deacetylbaccatin III. *J. Med. Chem.* **1997,** 40, 267-278.
32. Ojima, I., Slater, J. C., Michaud, E., Kuduk, S. D., Bounaud, P. Y., Vrignaud, P., Bissery, M. C., Veith, J. M., Pera, P., Bernacki, R. J. Syntheses and Structure-Activity Relationships of

the Second-Generation Antitumor Taxoids: Exceptional Activity against Drug-Resistant Cancer Cells. *J. Med. Chem.* **1996,** 39, 3889-3896.
33. Ojima, I. Guided Molecular Missiles for Tumor-Targeting Chemotherapy-Case Studies Using the Second-Generation Taxoid as Warheads. *Acc. Chem. Res.* **2008,** 41, 108-119.
34. Cushman, M.; Jayaraman, M.; Vroman, J. A.; Fukunaga, A. K.; Fox, B. M.; Kohlhagen, G.; Strumberg, D.; Pommier, Y. Synthesis of new indeno[1,2-c]isoquinolines: cytotoxic non-camptothecin topoisomerase I inhibitors. *J. Med. Chem.* **2000,** 43, 3688-3698.
35. Anthony, S.; Jayaraman, M.; Laco, G.; Kohlhagen, G.; Kohn, K. W.; Cushman, M.; Pommier, Y. Differential Induction of Topoisomerase I-DNA Cleavage Complexes by the Indenoisoquinoline MJ-III-65 (NSC 706744) and Camptothecin: Base Sequence Analysis and Activity against Camptothecin-Resistant Topoisomerases I. *Cancer Res* **2003,** 63, 7428-7435.
36. Xiao, X.; Antony, S.; Kohlhagen, G.; Pommier, Y.; Cushman, M. Design, synthesis, and biological evaluation of cytotoxic 11-aminoalkenylindenoisoquinoline and 11-diaminoalkenylindeoisoquinoline topoisomerase I inhibitors. *Bioorg. & Med. Chem.* **2004,** 12, 5147-5160.
37. Hertzberg, R. P.; Caranfa, M. J.; Holden, K. G.; Jakas, D. R.; Gallagher, D.; Mattern, M. R.; Mong, S.-M.; Bartus, J.-O.; Johnson, R. K.; Kingsbury, W. D. Modification of the hydroxylactone ring of camptothecin: inhibition of mammalian topoisomerase I and biological activity. *J. Med. Chem.* **1989,** 32, 715-720.
38. Hsiang, Y. H.; Lihou, M. G.; Liu, F. Arrest of replication forks by drug-stabilized topoisomerase I-DNA cleavable complexes as a mechanism of cell killing by camptothecin. *Cancer Res.* **1989,** 49, 5077-5082.
39. Giovanella, B. C.; Hinz, H. R.; Kozielski, A. J.; Stehlin Jr., J. S.; Silber, R.; Potmesil, M. Complete growth inhibition of human cancer xenografts in nude mice by treatment with 20-(S)-Camptothecin. *Cancer Res.* **1991,** 51, 3052-3055.
40. Wani, M. C.; Ronman, P. E.; Lindley, J. T.; Wall, M. E. Plant antitumor agents. 18. Synthesis and biological activity of camptothecin analogs. *J. Med. Chem.* **1980,** 23, 554-560.
41. Gottlieb, H. E.; Kotlyar, V.; Nudelman, A. NMR Chemical Shifts of Common Laboratory Solvents as Trace Impurities. *J. Org. Chem.* **1997,** 62, 7512-7515.

Chapter 4

Mechanism-Based Cleavable Disulfide Linkers

Chapter Contents

§ 4.1.0 Introduction

§ 4.1.1 Tumor-Targeted Chemotherapy

Chemotherapy has been ushered into an age of tumor targeted therapy.[1] A promising approach along this line is the development of tumor-targeting drug conjugates. Tumor-targeting drug conjugates are inactive until they are delivered to the tumor site, guided by a tumor-targeting module (TTM). Once internalized, the cytotoxic drug is cleaved from its carrier to restore its original activity. An area which has been widely explored in tumor-targeting drug design is the development of novel cleavable spacers and linkers. Cleavable spacers and linkers have been used to conjugate drug molecules, small molecules and delivery systems to targeting modules.[2-8] Spacers and linkers have also been employed in sensor molecules to fluorophores or imaging agents to peptides.[9-11] In addition, the application of cleavable spacers and linkers has been explored in nanotechnology and dendrimeric systems, which led to amplified drug or imaging agent release.[5, 12, 13]

In general, there are two major classes of linkers which have been employed in drug conjugate design: (1) cleavable linkers, which are linkers cleaved by the intracellular environment releasing the drug in its active form; and (2) noncleavable linkers, which leave linker components attached to the drug with no adverse effects to the potency of the drug.[14] Cleavable linkers can be subcategorized based on their mechanism of cleavage, (1) chemically labile linkers are cleaved based on the differential properties between the plasma and cytoplasmic compartments, and (2) enzyme-labile linkers are cleaved by the action of intracellular proteases.[14] Depending on the TTM and drug used for the drug conjugate, each linker has advantages and disadvantages. For example, chemically labile linkers suffer from limited plasma stability, thus may undergo cleavage at off-target sites. However, using hindered linkers increases the stability, thus limiting off-target toxicity. Noncleavable linkers have the highest stability but the residual linker components left after cleavage must be designed as to not alter the activity of the original drug. There being no universal linker for a given combination of TTM and drug, each linker has to be optimized for the chosen delivery system.

§ 4.1.2 Cleavable Linkers

Cleavable linkers are stable during systemic circulation but can be cleaved by certain intracellular conditions, such as low pH inside the cell or the presence of an intracellular protein. For example, hydrazone linkers are relatively stable at neutral pH (7.3 – 7.5), but undergo hydrolysis after internalization into endosomes (pH 5.0 – 6.5) and lysosomes (pH 4.5 – 5.0).[14, 15] Hydrazone linkers contain two cleavable bonds, a hydrazone, which is the cleavage site, and a sterically hindered disulfide. This linker was used to conjugate doxorubicin, a potent intercalating agent, to humanized mAb BR96.[16] However, it was found that the hydrazone linker prematurely cleaved under physiological pH, illustrating the instability of the linker in circulation.[17]

Chemically labile linkers, such as the hydrazone linker, often have limited plasma stability, thus may result in off-target drug release. Accordingly, peptide linkers have been developed to increase plasma stability and to better control intracellular drug release. Peptide linkers are designed for rapid lysosomal hydrolysis induced by the presence of an intracellular

enzyme. Tetrapeptide Gly-Phe-Leu-Gly, as well as dipeptides Phe-Lys and Val-Cit have been employed for drug delivery systems and immunoconjugates.[18-20] For example, brentuximab vedotin (Seattle Genetics) is an antibody-drug conjugate (ADC) that conjugates anti-CD30 mAb and monomethylauristatin (MMAE) via a valine-citruline dipeptide linker (Figure 4.1).[21, 22] This linker, containing unnatural amino acid citruline, was chosen to confer added stability to the mAb-drug conjugate in blood circulation, while maintaining the ability to release MMAE by the action of cathepsin B upon internalization into CD30-expressing tumor cells.

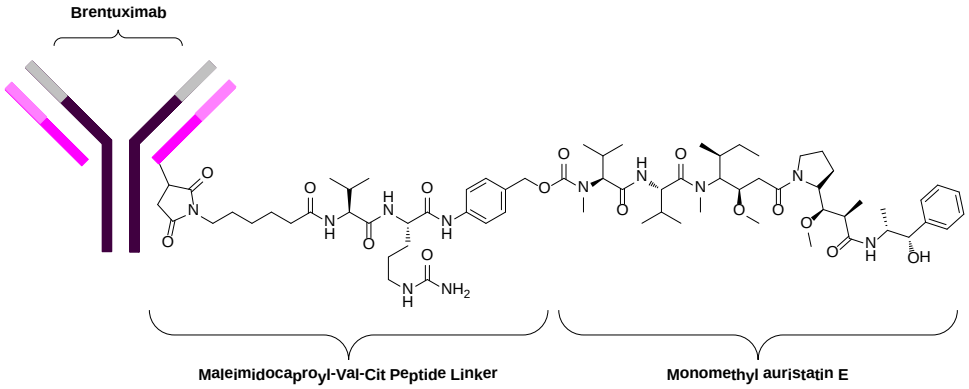

Figure 4.1: Brentuximab vedotin immunoconjugate

Disulfide linkers are another alternative to acid-labile and enzyme-labile linkers. The cleavage of disulfide linkers is attributed to the abundance of intracellular glutathione, which is present in micromolar concentrations in the blood but in millimolar concentrations in the cytoplasma.[14] Disulfide linkers have exhibited excellent efficacy in a number of tumor xenografts in preclinical models.[23-25] For example, DM1 and DM4, thiol-containing derivatives of maytansine, were conjugated to humanized mAbs including HuC242 and anti-CD44v6.[26-28] A number of these ADCs are in phase I and II clinical studies.[26, 29] It is worthy of note that ADCs with cleavable linkers may also be active when they are not fully internalized into tumor cells.[30] One reason for this is that when the linker is cleaved in the extracellular space, the drug freely penetrates the cell membrane to reach its target.[14] Thus, tumor-targeting drug conjugates which contain a cleavable linker have the potential to kill adjacent cells within the tumor that are not targeted by the TTM.[31]

§ 4.1.3 Noncleavable Linkers

Thioether bonds have been employed to conjugate maytansinoids, such as DM1, to a number of mAbs, including cantuzumab, trastuzumab and lapatinib (Figure 4.2).[25, 28, 32] Surprisingly, these thioether linked immunoconjugates showed superior activity in breast cancer therapy compared to unconjugated trastuzumab or trastuzumab-maytansinoid drug conjugates linked through disulfide linkers.[32]

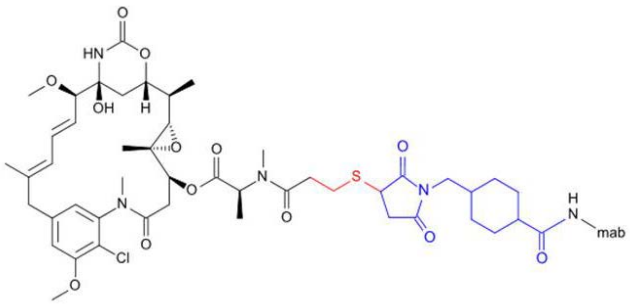

Figure 4.2: Trastuzumab-DM1 is a phase III clinical candidate

It is believed that drug release occurs after internalization of the ADC followed by degradation of the mAb in the lysosome, resulting in the release of the maytansinoid still attached to the linker.[14] Though the linker residue is still attached, the activity of the drug is not diminished. Recently, an alternative mechanism of drug cleavage was reported.[33] Fishkin et al. reported a novel pathway for *ex vivo* maytansinoid release from a thioether linker. This mechanism entails a chemical oxidation of the thioether moiety followed by sulfoxide elimination.[33] It is worthy of note that drug conjugates comprised of noncleavable linkers must be internalized and degraded within the cell to become active, as the released drug does not penetrate the cell membrane.[14]

§ 4.1.4 Self-Immolative Disulfide Linkers

Self-immolative linker moieties are widely employed in the synthesis of drug conjugates to link an amino- or hydroxyl-containing drug to a TTM. In these drug conjugates, the TTM transports and delivers anticancer drugs to cancer cells and the active form of the drug is released due to an intramolecular destruction or cleavage of the linker generated by the intracellular environment, such as pH or the presence of various proteins. However, the linker must be stable, after being coupled to a chemotherapeutic agent and tumor-targeting module, for an extended period of time in storage and in blood circulation. After internalization, the linker must be readily cleaved releasing the active drug compound.

Previously, the Ojima research group designed and synthesized taxoid-based ADCs (Figure 4.3), which exhibited promising results against human cancer xenografts in SCID mice (Figure 4.4).[4, 34] These *in vivo* results demonstrated the tumor-specific delivery of a taxoid anticancer agent, as all animals were cured without any noticeable toxicity to the animals. For these ADCs, an alkyl disulfide linker was employed as the linker. This linker was stable in blood circulation but was efficiently cleaved by intracellular reducing substances in cancer cells. However, in this first-generation ADC, the original taxoid molecule was not released. The taxoid released contained a sulfhydrylpropanoyl moiety at the C10 position: remnants of the disulfide linker that was not completely cleaved. Thus, the cytotoxicity of the taxoid released (SB-T-12136-SH) was 8 times weaker than the parent taxoid (SB-T-1213).[4]

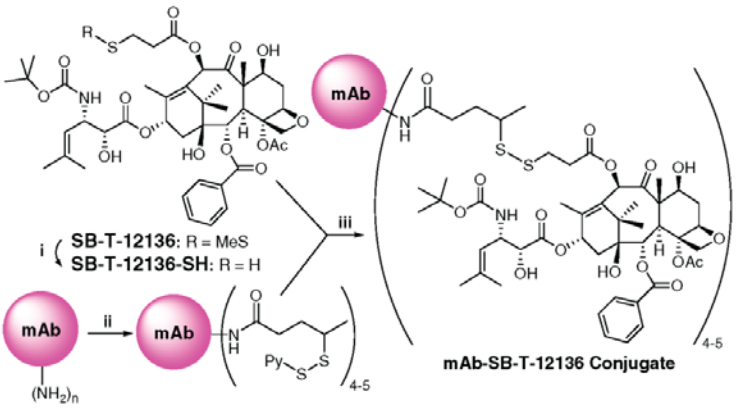

[a] (i) DTT; (ii) SPP (10 equiv in ethanol), 50 mM potassium phosphate buffer, pH 6.5, NaCl (50 mM), EDTA (2 mM), 90 min; (iii) 50 mM potassium phosphate buffer, pH 6.5, NaCl (50 mM), EDTA (2 mM), SB-T-12136-SH (1.7 equiv per dithiopyridyl group, in EtOH), 24 h.

Figure 4.3: 1st-generation mAb-linker-taxoid drug conjugate synthesis (adapted from [35])

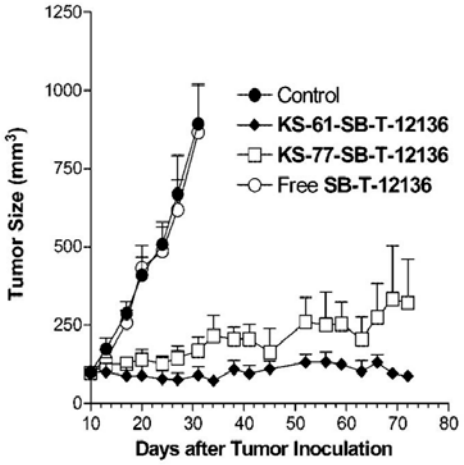

Figure 4.4: *In vivo* activity of anti-EGFR mAb-taxoid conjugates against A431 xenografts (adapted from [35])

Accordingly, second-generation, self-immolative bifunctional disulfide linkers were developed and used to conjugate taxoids to mAbs. These disulfide linkers can efficiently release a taxoid inside cancer cells when the disulfide bond is cleaved by an intracellular thiol, such as glutathione (GSH), which is 1,000 times greater in concentration in cancer cells than in blood plasma.[36] The TTM guides the drug conjugate to the receptors on the surface of the tumor and the entire conjugate is internalized via receptor-mediated endocytosis (RME). As the disulfide bond is cleaved, the drug is released to attack target proteins via a thiolactonization process (Figure 4.5). To promote this thiolactonization process, a phenyl moiety was placed to direct the cleavage of the disulfide bond by an intracellular thiol, generating a sulfyhydrylphenyl or thiopphenylate species which attacks the linker-drug ester bond. The mechanism-based drug-release of the 2nd-generation disulfide linkers was validated in a model system using fluorine-labeled compounds and monitoring by ^{19}F NMR, as well as in a real system cancer cells using fluorescence-labeling and confocal fluorescence microscopy (CFM).[5, 8, 34, 35]

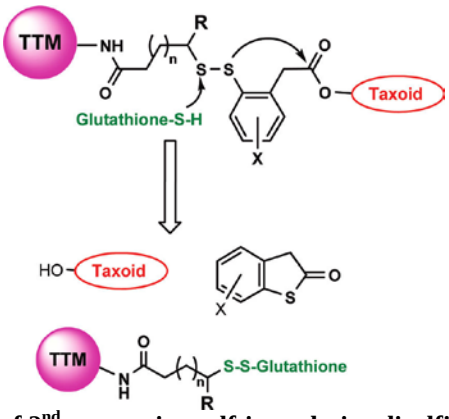

Figure 4.5: Thiolactonization of 2nd-generation self-immolative disulfide linker (adapted from [35])

The Ojima laboratory has employed 2nd-generation self-immolative disulfide linkers into the synthesis of tumor-targeting drug conjugates and DDS.[5, 8, 35, 37-39] Using fluorescently labeled probes of these drug conjugates and DDS, the Ojima group has successfully validated the mechanism of tumor-targeting drug delivery, drug conjugate/DDS internalization into cancer cells and intracellular drug release and drug binding to target proteins.[5, 8, 35, 37, 38]

§ 4.2.0 Results and Discussion

§ 4.2.1 Synthesis of Disulfide Linker Intermediates

The synthesis of the self-immolative disulfide linkers begins with key intermediate synthesis. These intermediates are needed for the two thiol-disulfide exchange reactions required to prepare the desired linker. The desired thiolactone, **4-1**, can be prepared via the oxidation of the boronic acid moiety in the presence of hydrogen peroxide,[40] followed by basic hydrolysis of the thiolactone (Scheme 4.1).

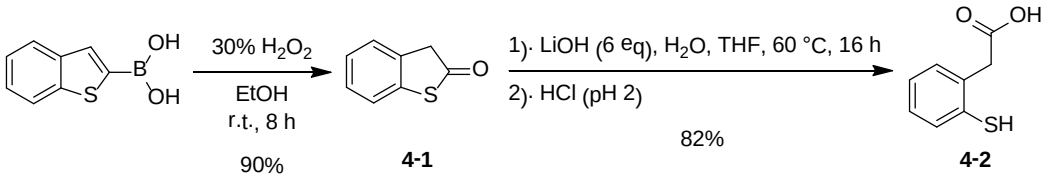

Scheme 4.1: Synthesis of key intermediate sulfhydrylphenylacetic acid

The first intermediated, **4-2**, was prepared from the oxidation of thianaphthene 2-boronic acid in the presence of hydrogen peroxide to produce the thiolactone **4-1** in excellent yield (90%). Thiolactone **4-1** is then treated with LiOH and acidified with aqueous HCl to produce **4-2** in good yield (82%) after extraction and purification. The thiolactone is also the byproduct formed after the self-immolation of the disulfide linker. The next step is the base-mediated ring-opening of the thiolactone followed by acidic work-up via the addition of 1 N HCl yielding the free sulfhydryl and the free carboxylic acid. Purification of both **4-1** and **4-2** can be achieved without the use of flash column chromatography. Extraction of organic materials from aqueous

layer and subsequent treatment with Norit and filtering over Celite and silica gel affords pure **4-1** and **4-2**, respectively, in high yields as mentioned above.

It is worthy of note that the boronic acid stating material may decompose in storage, as observed by a change in color from white to red solid. Thus, to avoid use of the boronic acid, another synthetic route towards the thiolactone was attempted which entails the boronation of benzothiophene. This is done in the presence *n*-butyl lithium, followed by the treatment of tributylborate to yield **4-3**, which can be oxidized in the presence of hydrogen peroxide (Scheme 4.2).[40]

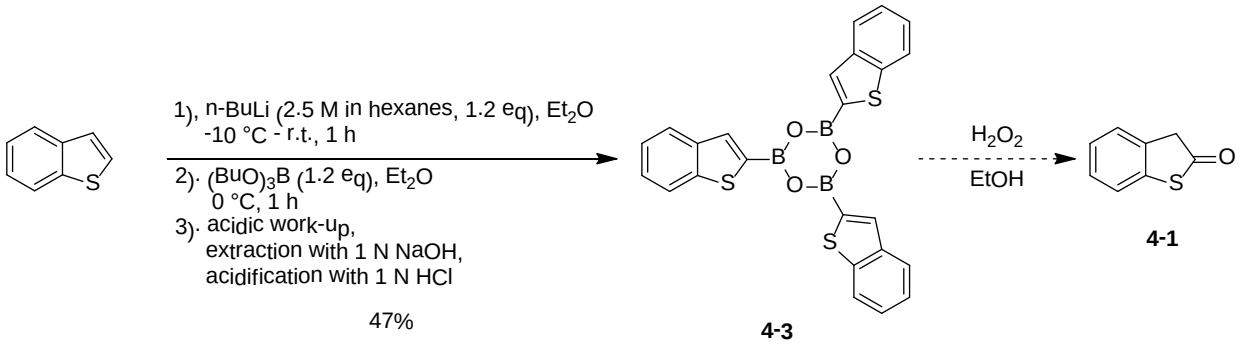

Scheme 4.2: Trioxatriborinane preparation towards thiolactone

The desired trioxatriborinane **4-3** was obtained in low yield (47%). The low yield may be attributed to incomplete formation of benzothiophene anion in the 1st step or an incomplete formation of the trioxatriborinane complex in the 2nd step. The second intermediate, **4-4**, is prepared via the oxidation of pyridine-2-thiol in the presence of $KMnO_4$ (Scheme 4.3).[41]

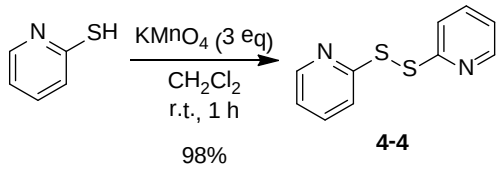

Scheme 4.3: Synthesis of pyridinal-2,2-disulfanylpyridine

This reaction is facile and produces the desired **4-4** in high yields (>90%) with minimal impurities. The starting material is commercially available. The addition of $KMnO_4$ is done very slowly; added in small allotments over the course of thirty minutes. Upon reaction completion, the reaction mixture was filtered over celite, and the organic solvent was concentrated to yield the desired product.

§ 4.2.2 Synthesis of Propanoic Acid-Based Disulfide Linker

The thiol-disulfide exchange reaction is essential in the cleavage of the disulfide bond of the 2nd-generation disulfide linker. Furthermore, the thiol-disulfide exchange is a widely employed method for the synthesis of asymmetric disulfides. The desired propanoic acid-based disulfide linker is obtained from the thiol-disulfide exchange between **4-6** and **4-2**. The thiol-disulfide exchange reaction between **4-4** and commercially available 3-sulfhydrylpropanoic acid gives **4-5**. The resulting free acid is TIPS-protected in the presence of TIPSCl and base. A

second thiol-disulfide exchange reaction of the resulting TIPS-protected **4-6** with **4-2** affords the asymmetric disulfide linker **4-7** (Scheme 4.4).[41, 42]

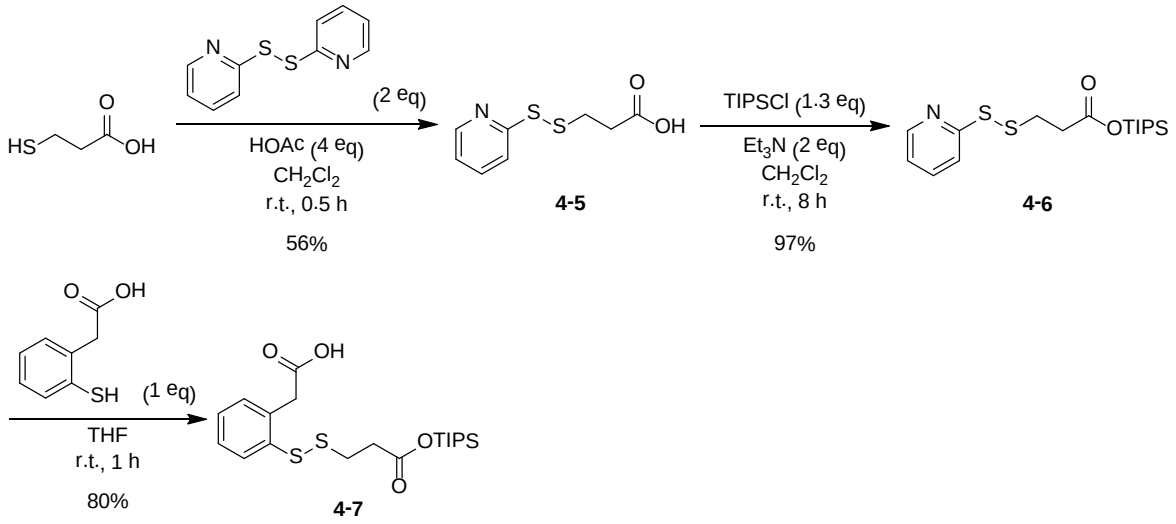

Scheme 4.4: Synthesis of propanoic acid-based disulfide linker

The thiol-disulfide exchange reaction of 3-sulfhydrylpropanoic acid and **4-4** gives **4-5** in moderate yield (56%). This yield may be improved by increasing the temperature of the reaction and by increasing the equivalents of **4-4** used. Furthermore, the use of flash column chromatography on both alumina and silica gels is not needed if AcOH were excluded from the reaction mixture. The following TIPS-protection and second thiol-disulfide exchange afford compounds **4-6** and **4-7** in good yields, 97% and 80%, respectively.

§ 4.2.3 Synthesis of Methyl-Branched Disulfide Linker

The methyl-branched disulfide linker can be obtained using two different routes starting from γ-valerolactone. The first procedure requires a ring-opening in the presence of boron tribromide,[43] followed by a nucleophilic substitution using thiourea to yield **4-9**, as a salt.[44] The **4-9** salt is then subjected to hydrolysis under relatively harsh conditions to yield the desired 4-sulfhydrylpentanoic acid, **4-10**. The thiol-disulfide exchange with **4-4**, TIPS protection and final thiol-disulfide exchange with **4-2** yields the desired methyl-branched linker **4-13** (Scheme 4.5).

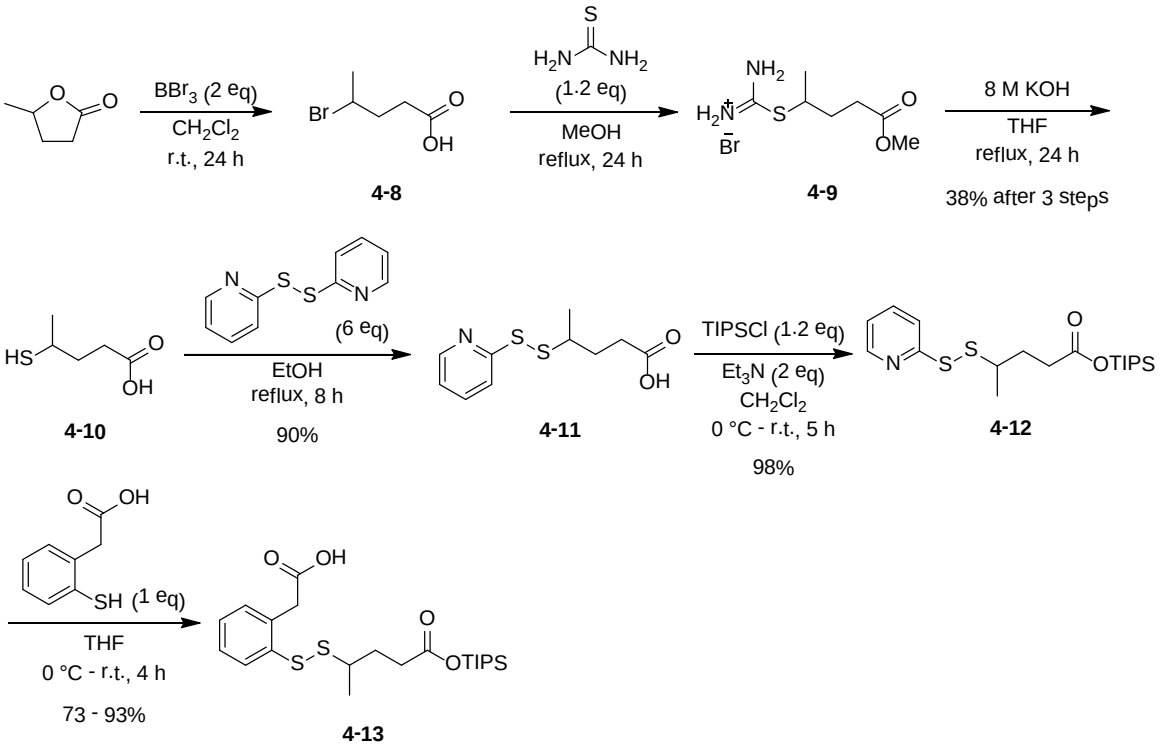

Scheme 4.5: 1st route towards methyl-branched disulfide linker

The ring-opening substitution was achieved to give crude containing **4-8**, which was treated with thiourea without purification to give **4-9**. The hydrolysis of **4-9** in the presence of 8 M KOH afforded a crude mixture of **4-10** with other impurities in fair yield (38% after 3 steps). Purification of **4-10** was not done and the material was used in the thiol-disulfide exchange to give **4-11** in high yield (90%). The sequential TIPS-protection followed by another thiol-disulfide exchange gives **4-13** in good yields, 98% and >73%, respectively. To increase the yield and simplify the formation of **4-10**, a new procedure was employed. Based on literature precedence, the desired sulfhydryl-containing compound **4-10** can be obtained from γ-valerolactone using HBr in the presence of thiourea, followed by hydrolysis (Scheme 4.6).[43]

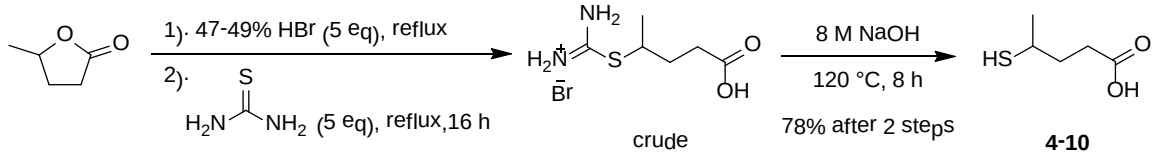

Scheme 4.6: Cleaner route towards 4-sufhydrylpentanoic acid

In a one-pot reaction, γ-valerolactone is stirred under reflux conditions with HBr, activating the lactone for nucleophilic attack by thiourea, which was added after reflux was established. The resulting salt was then hydrolyzed under extremely harsh conditions to yield pure **4-10** as a color-less oil (78% yield as opposed to impure 38% yield over 3 steps via the previous method). It has been observed that the ratio of HBr to thiourea should be 1 to 1. In addition, five equivalents of HBr and thiourea gave higher yields in comparison to lower amounts. Increasing the amount of HBr and thiourea used may increase the overall yield further, but recovery of unreacted starting material becomes a problem and is currently being

investigated. The hydrolysis can also be modified. Using such extreme conditions is very dangerous. Lowering the concentration of base used can be done, but the reaction time needs to be increased. The next step in the synthesis of the methyl-branched disulfide linker entails the thiol-disulfide exchange reaction between **4-10** and **4-4** to obtain **4-11** (Scheme 4.7).

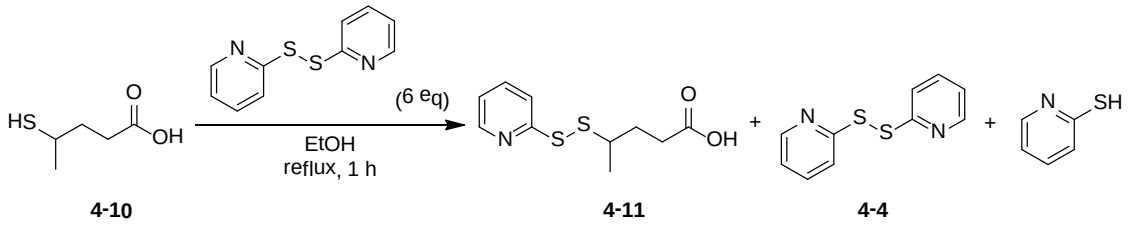

4-10 **4-11** **4-4**

Scheme 4.7: 1st thiol-disulfide exchange towards methyl-branched disulfide linker intermediate

Excess amount pyridinyldisulfanylpyridine is required for the disulfide exchange to occur in high yields (>90%). However, separating the unreacted pyridinyldisulfanylpyridine (solid) from the desired product (oil) and the generated 2-thiopyridone (solid) is difficult using column chromatography. With a gradient eluent system pure **4-11** can be isolated in high yield (93%), as well as unreacted pyridinyldisulfanylpyridine and generated 2-thiopyridone. The use of chromatography can be avoided by evaporating the reaction solvent upon completion of the reaction, then precipitating the excess material with the addition of hexanes. The precipitate can be filtered off and retained for other use; the filtrate contains a mixture of **4-11** and the 2-thiopyridone (which is also recycled) that can be separated using flash column chromatography or used in the next step without further purification. The 2-thiopyridone does not react in the subsequent TIPS protection reaction, thus treating the mixture with TIPSCl in the presence of base yields a mixture containing the desired **4-12** and 2-thiopyridone (Scheme 4.8). Both compounds can be easily separated using flash column chromatography affording **4-12** in high yields (98% after 2 steps).

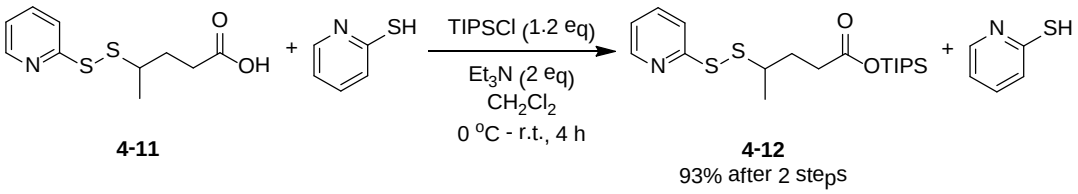

4-11

4-12
93% after 2 steps

Scheme 4.8: Methyl-branched disulfide linker intermediate TIPS protection

The final step towards the methyl-branched disulfide linker entails a second thiol-disulfide exchange between **4-12** and **4-2**. It has been determined that making the reaction more concentrated and keeping the reaction between -10 - 0 °C for the entirety of the reaction increases the reaction yield (Scheme 4.9).

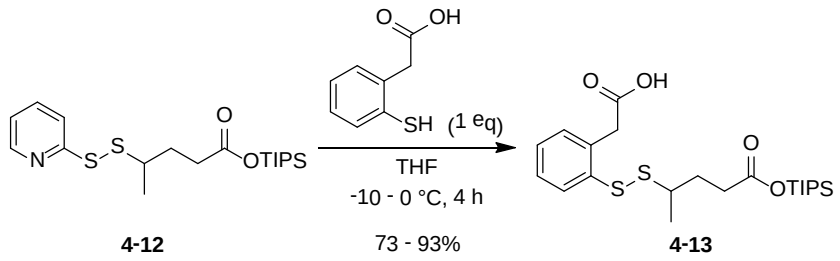

Scheme 4.9: 2nd thiol-disulfide exchange towards methyl-branched disulfide linker

A concentrated reaction solution allows for greater interaction of starting materials, thus driving the thiol-disulfide exchange. It has also been observed experimentally that keeping the TIPS-protected product with the phenylacetic acid moiety for an extended period of time at room temperature leads to the deprotection of the TIPS moiety. Thus, the higher concentration and cooler reaction conditions were used. The desired asymmetric disulfide linker was obtained in good to excellent yields (73 - 93%). Pure linker **4-13** can be stored for a short period of time under N_2 or argon at -20 °C or below without significant decomposition. However, impurities and prolonged storage at elevated temperatures will result in decomposition.

§ 4.2.4 Synthesis of Dimethyl-Branched Disulfide Linker

For the synthesis of a more stable disulfide linker, it was hypothesized that the incorporation of a second methyl branch would further prolong linker stability, as an additional methyl moiety alpha to the disulfide bond may prevent premature cleavage of the drug from the linker. The synthesis of the dimethyl-branched linker begins with the opening of the thiirane ring in the presence of acetonitrile and *n*-butyl lithium. The resulting mixture is then treated with NaOH to convert the nitrile moiety into a carboxylate which is protonated during acidic work-up (Scheme 4.10).[27, 45]

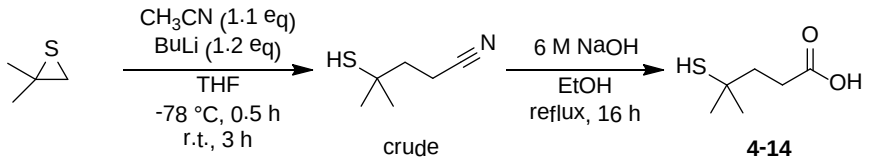

Scheme 4.10: Synthesis of dimethyl-branched sulfhydrylpentanoic acid

These reactions were messy based on TLC. More interesting was the fact that during the extraction of the 3-sulfhydryl-3-methylbutanenitrile, the organic layer being washed turned black. It was reported that the compound is unstable, thus after the initial extractions and evaporation of the organic solvent, the crude mixture was immediately treated with base to yield **4-14** with some impurity. The mixture containing **4-14** was then treated with pyridinyl-disulfanyl-pyridine for the first thiol-disulfide exchange followed by TIPS protection (Scheme 4.11).

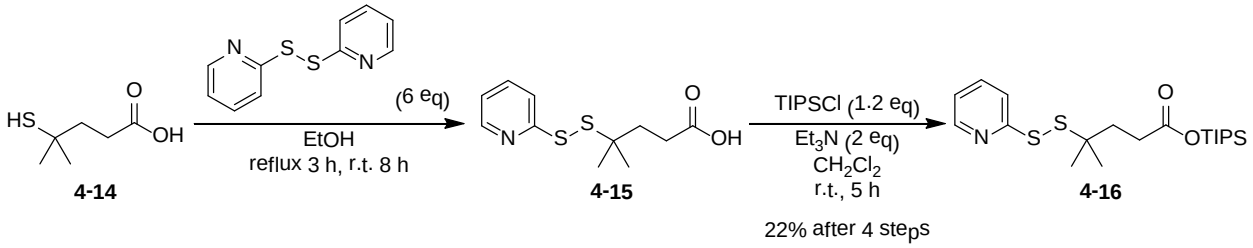

Scheme 4.11: 1st thiol-disulfide exchange and TIPS protection of dimethyl-branched disulfide linker

The first thiol-disulfide exchange proceeded smoothly despite using an impure mixture of **4-14**. TIPS-protection of the mixture containing **4-15** afforded **4-16** in 22% yield after 4 steps. The second thiol-disulfide exchange reaction of **4-16** with **4-2** was attempted to prepare the desired dimethyl-branched disulfide linker (Scheme 4.12).

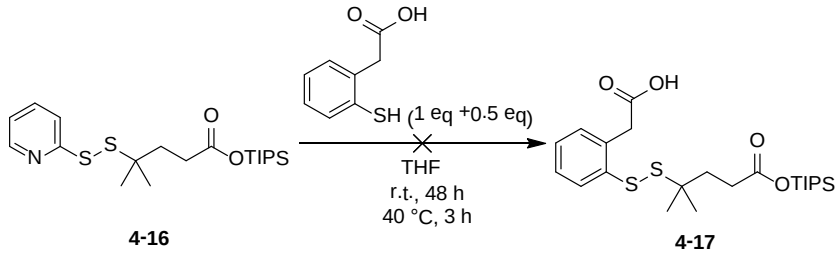

Scheme 4.12: 2nd thiol-disulfide exchange towards dimethyl-branched disulfide linker

However, the reaction did not proceed as expected. After 24 hours, based on TLC, the reaction did not produce the desired **4-17**. At this moment another 0.5 equivalent of the sulfhydrylphenylacetic acid was added to drive the reaction. Despite the addition, the reaction did not produce **4-17**. Thus, the reaction was heated, but gave no desired product. It is believed that the steric bulk generated by the two methyl moieties alpha to the disulfide bond prevented the thiol-disulfide exchange from occurring. It is worthy of note that the addition of a base did not push the exchange to occur, thus no product was obtained. This thiol-disulfide exchange is currently being examined.

§ 4.2.5 Synthesis of SB-T-1214-Me-Linker-OSu "Coupling-Ready Construct"

The drug-linker coupling-ready construct contains all of the necessary moieties to prepare tumor-targeting drug conjugates. The drug-linker compound can be conjugated to any TTM bearing free amine(s). The synthesis of the coupling-ready construct begins with the synthesis of the appropriate linker, followed by drug coupling and ending with carboxylic acid activation. The SB-T-1214-linker compound **4-18** is obtained from the DMAP-catalyzed and DIC-mediated coupling of SB-T-1214 and the methyl-branched disulfide linker **4-13** (Scheme 4.13). The C-2' position of is the most reactive site of the taxoid and is the position which the linker is coupled.

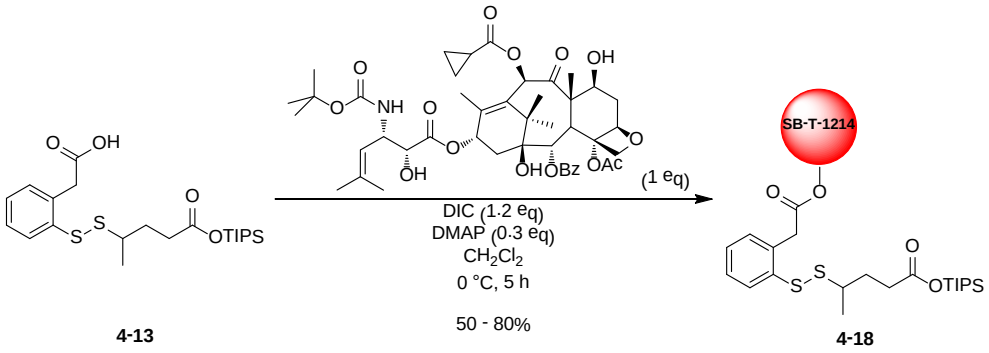

Scheme 4.13: DIC-mediated SB-T-1214-methyl-branched disulfide linker coupling

It has been observed that extending the reaction time gives **4-18** in moderate to low yields (<50%). In addition, dilute conditions and warming the reaction temperature leads to poor yields. For this reason, the reaction temperature is maintained at 0 °C and the reaction is done with a concentration of 0.5 M. Upon completion, the reaction mixture is immediately purified via flash column chromatography. Maintaining cool reaction temperatures and concentrated conditions yields the desired **4-18** in good yields (75-80%). The SB-T-1214-Me-linker-OSu "coupling-ready construct" can be prepared via deprotection of the TIPS moiety and OSu-activation (Scheme 4.14).

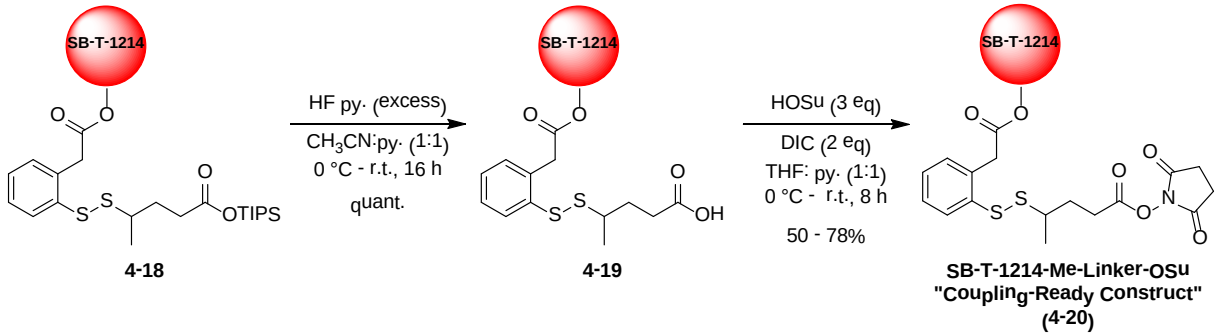

Scheme 4.14: Deprotection and activation towards SB-T-1214-Me-linker-OSu "coupling-ready construct"

Silyl-deprotection using HF in pyridine afforded **4-19** in quantitative yield after extraction and removal of excess pyridine. The activation of the free carboxylic acid in the presence of HOSu and DIC gave **4-20** in moderate yield (50%). This yield was improved with longer reaction times, i.e. increasing the time at room temperature from 16 to 26 hours, gave **4-20** in 65% to 78% yield in separate attempts. High purity of SB-T-1214-Me-linker-OSu "coupling-ready construct" (**4-20**) is necessary for the synthesis of tumor-targeting drug conjugates.

§ 4.2.6 Synthesis of Camptothecin-Linker-OSu "Coupling-Ready Construct"

Following the same coupling protocol as described above, the disulfide linkers **4-7** and **4-13** were coupled to the commercially available topoisomerase I inhibitor, camptothecin. Using standard peptide coupling conditions, camptothecin-linker compounds **4-21a** and **4-21b** were

prepared. Deprotection of the silyl moiety was done using HF/py to give the free carboxylic acid which was then activated via esterification with HOSu (Scheme 4.15).

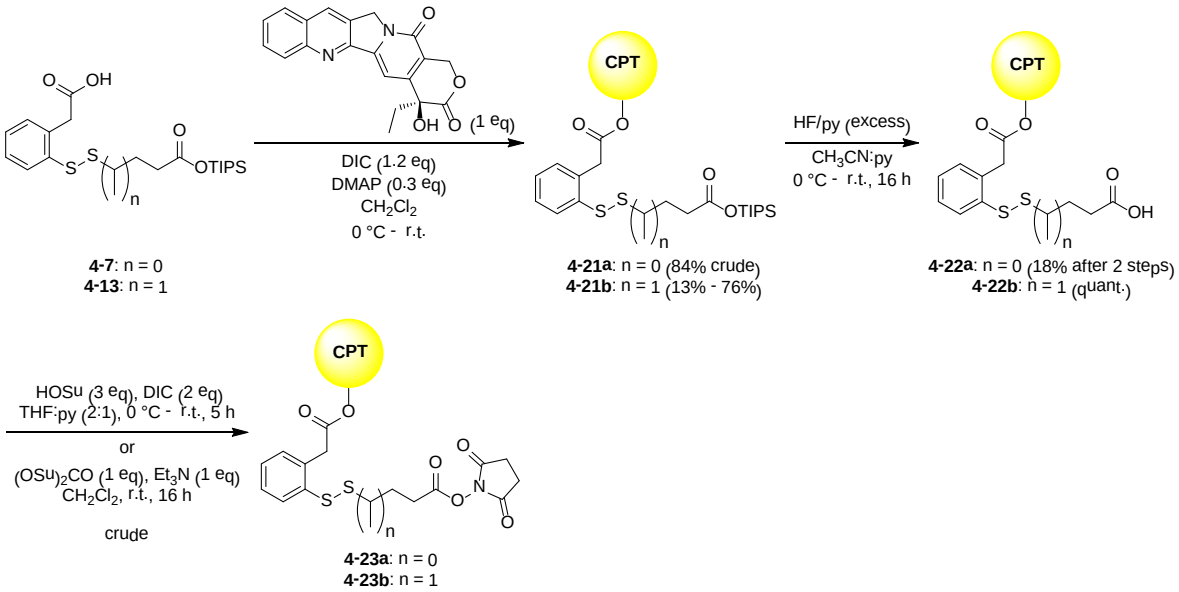

Scheme 4.15: Synthesis of camptothecin-linker

Low solubility is a serious drawback when using camptothecin for chemical synthesis. Furthermore, the only reactive hydroxyl moiety of camptothecin is sterically hindered, which slows coupling at that position. Lastly, the cyclic ester which bears the reactive hydroxyl is susceptible to acidic and basic conditions. As such, coupling of disulfide linkers **4-7** and **4-17** to camptothecin afforded **4-21a** as a crude mixture in DIU (84% crude) and **4-21b** with inconsistent yields ranging from 13 – 84% on multiple attempts. Deprotection of the TIPS moiety proceeds smoothly in the presence of HF giving **4-22a-b** in near quantitative yields. Activation of the free carboxylic acid to an activated-OSu ester was attempted in two ways, (1) peptide coupling in the presence of HOSu or (2) treatment of free carboxylic acid to OSu-carbonate, which was obtained from the treatment of *N*-hydroxysuccinimide with triphosgene (Scheme 4.16).[46]

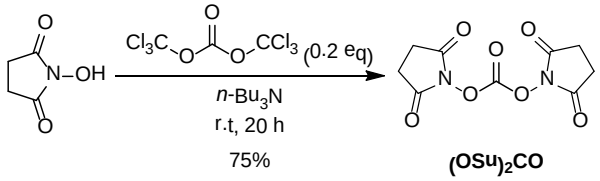

Scheme 4.16: Preparation of OSu-carbonate

The activation using a coupling reagent is preferred as the OSu-carbonate is air and moisture sensitive. It is worthy of note that the use of coupling reagents does result in a messier reaction (e.g. the generation of urea), thus additional attention should be given during purification.

§ 4.2.7 Synthesis and Biological Evaluation of PUFA-Me-Linker-Taxoid Drug Conjugate

As previous mentioned, linolenic acid (LNA) is an essential polyunsaturated fatty acid (PUFA) which plays a crucial role in many metabolic processes. LNA is readily incorporated into the lipid bilayer of tumor cells resulting in the disruption of the membrane structure thereby influencing the chemosensitivity of the tumor cells.[47-49] Furthermore, the Ojima laboratory has synthesized PUFA-taxoid conjugates which contain DHA or LNA covalently bonded to the C-2' position of the taxoid. Though these PUFA-taxoid conjugates performed well in both *in vitro* and *in vivo* assays, it was hypothesized that even higher potency can be achieved if the taxoid were cleaved from the PUFA via our 2nd-generation disulfide linker. Accordingly, LNA-Me-linker-SB-T-1214 was prepared. Following similar synthetic routes as detailed above, LNA-hydrazide was prepared (Scheme 4.17 and 4.18) and coupled to **4-20** (Scheme 4.19).

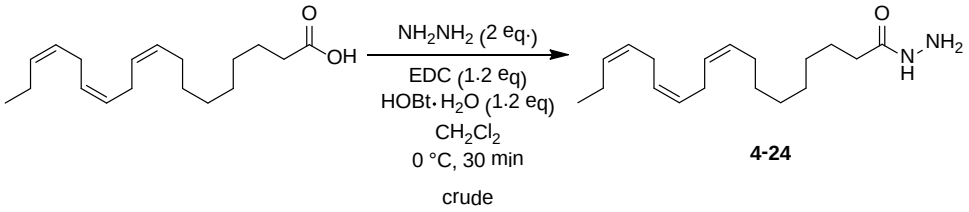

Scheme 4.17: Synthesis of LNA-hydrazide

LNA-hydrazide (**4-24**) can be obtained via standard peptide coupling in the presence of hydrazine, EDC and HOBt. However, these conditions gave a messy reaction which is not easily purified, as LNA-hydrazide is a polar and water-soluble oil. Thus, crude **4-24** was used, which leads to low yields in the subsequent coupling. An alternative route towards LNA-hydrazide is the conversion of commercially available methyl linolenoate to the corresponding hydrazide. This conversion is achieved easily and cleanly by treating methyl linolenoate (LNA methyl ester) with hydrazine at elevated temperature (Scheme 4.18).

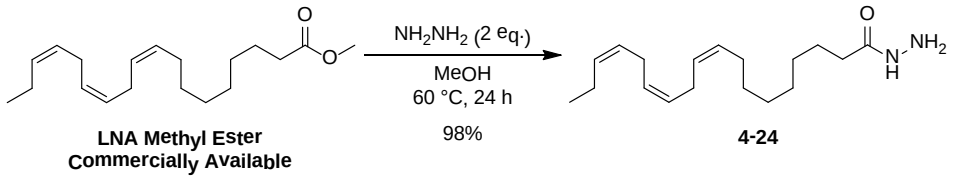

Scheme 4.18: Conversion of LNA methyl ester to LNA-hydrazide

LNA methyl ester is colorless oil that has a high boiling point, thus is stable in reaction conditions which require heating up to 192 °C. Thus, heating LNA methyl ester in the presence of hydrazine and methanol gives pure **4-24** in excellent yield (98%). Treating SB-T-1214-Me-linker-OSu (**4-20**) with **4-24** in the presence of DIPEA affords LNA-Me-linker-SB-T-1214 (Scheme 4.19).

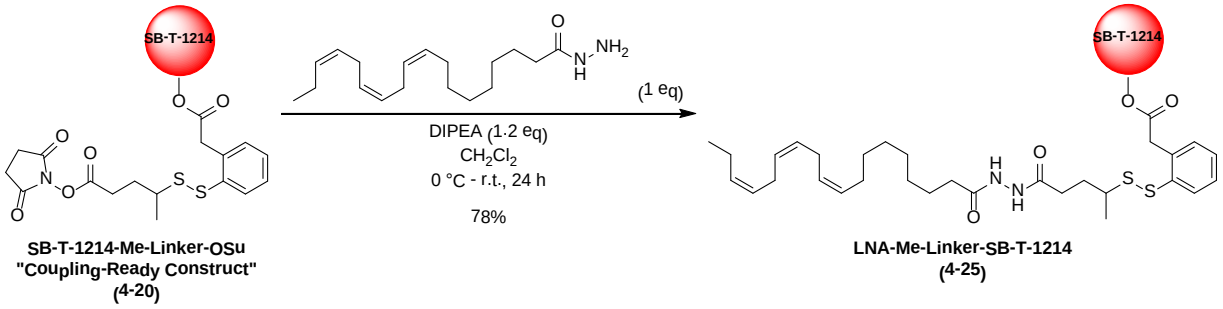

Scheme 4.19: Synthesis of LNA-Me-linker-SB-T-1214 drug conjugate

The desired LNA-Me-linker-SB-T-1214 drug conjugate was obtained in good yield (78%). The biological activity of **4-25** was evaluated *in vitro* against A2780 (human ovarian), DLD-1 (human colon), HT-29 (human colon) and MCF-7 (human breast) cancer cell lines with the addition of glutathione ethyl ester (GSH-OEt). These results are show in Table 4.1. These cell lines were chosen because internalization studies using LNA-FITC gave promising results, as was discussed in Chapter 3.

Table 4.1: Biological Evaluation of LNA-Me-linker-SB-T-1214 against Various Cancer Cell Lines

Taxane	Time of Incubation with drug (h)	Time of Incubation with GSH-OEt (h)	IC_{50} (nM) A2780	DLD-1	HT-29	MCF-7
Paclitaxel	**48**	-	16.2 ± 8.28	29.5 ± 10.8	11.6 ± 3.57	6.25 ± 0.76
SB-T-1214	**48**	-	0.36 ± 0.03	0.38 ± 0.21	0.73 ± 0.30	0.35 ± 0.11
LNA-SB-T-1214	**48**	-	12100 ± 1160	>50000	>50000	24500 ± 6510
LNA-linker-SB-T-1214	**1**	**48**	4.37 ± 2.60	>5000	1.31 ± 0.11	4.98 ± 0.99

- Cells were suspended in RPMI with L-glutamine (Lonza BioWhittaker, BW12-702F), with 5% FBS (Thermo Scientific, HyClone, SH3007003), 5% Nu Serum (BD Biosciences, 355100) and 1% Penn Strip before administration of taxoid
- Cells were incubated for 48 hours at 37 °C with 5% CO_2 after administration of taxoid (paclitaxel, SB-T-1214 and LNA-SB-T-1214); cells incubated for 1 hour at 37 °C with 5% CO_2 after administration of LNA-Me-linker-SB-T-1214, washed with DPBS, resuspended in RPMI with 2 eq. GSH-OEt and incubated for 48 hours at 37 °C with 5% CO_2
- The optical density was determined using Acsent Multiskan optical density reader
- The reported values are a calculated averages of IC_{50} values determined from three individual experiments
- IC_{50} values were calculated using SigmaPlot v 10.0
- All IC_{50} values are report in nM scale unless otherwise noted

LNA-Me-linker-SB-T-1214 (**4-25**) was incubated with the cells for 1 hour at 37 °C with 5% CO_2. After washing the cells thoroughly with DPBS, the cells were resuspended in RPMI containing 2 molar equivalents of GSH-OEt to assure cleavage of the disulfide bond, and incubated for 48 hours at 37 °C with 5% CO_2. As seen from Table 4.1, the *in vitro* activity of **4-25** is approximately 1 order of magnitude less potent than the free taxoid, SB-T-1214, against A2780, HT-29 and MCF-7 cancer cell lines. Furthermore, **4-25** did not show substantial activity against DLD-1, which is congruent to the *in vitro* activity of LNA-SB-T-1214. DLD-1 cancer cells are more resistant to cytotoxic agents and this resistance may be demonstrated with the observed low potency of the **4-25** and LNA-SB-T-1214. In general, drug conjugate **4-25** outperformed LNA-SB-T-1214 and paclitaxel, showing greater potency in the cancer cell lines evaluated. This result suggests that the taxoid is cleaved from the linker as a faster rate than the PUFA-taxoid ester bond is cleaved.

§ 4.3.0 Summary

Drug conjugates with a tumor-targeting module are guided by the TTM to the tumor site. These drug conjugates are inactive while in circulation. Once internalized, the cytotoxic drug is cleaved from its carrier to restore its original activity. There are two major classes of linkers, cleavable and noncleavable, which are employed to conjugate a cytotoxic drug to a TTM. Cleavable linkers are cleaved by the intracellular environment or by an intracellular protein, whereas noncleavable linkers are not fully cleaved from the drug yet the residual linker does not affect the activity of the drug. Disulfide linkers have been employed in a number of tumor-targeting drug conjugates. The cleavage of disulfide linkers is attributed to the abundance of intracellular glutathione found in cancer cells. The Ojima laboratory has developed second-generation, self-immolative bifunctional disulfide linkers, which have been employed in the development of taxoid-based ADCs, tumor-targeting drug conjugates and DDSs. In model systems and using fluorescently labeled probes, intracellular disulfide linker cleavage and drug release has been validated in vitro. The synthesis of 2nd-generation disulfide linkers was discussed. In addition, the preparation of drug-linker coupling-ready constructs has been highlighted. These coupling-ready constructs can be coupled to any TTM bearing a free amine. For example, the synthesis of LNA-Me-linker-SB-T-1214 was achieved by coupling SB-T-1214-Me-linker coupling-ready construct to linolenic acid. The LNA-linker-taxoid drug conjugate showed 4 orders of magnitude greater activity than the LNA-taxoid drug conjugate. Accordingly, PUFA-linker-taxoid drug conjugates with different PUFAs, such as DHA and EPA, as TTM may also demonstrate significant anticancer activity, thus would make a promising carrier for the tumor-specific delivery of highly potent taxoids.

§ 4.4.0 Experimental

Caution

Taxoids and camptothecin have been established as a potent cytotoxic agent. Thus, they and all structurally related compounds and derivatives must be considered as mutagens and potential reproductive hazards for both males and females. Appropriate precautions (i.e. use of gloves, goggles, lab coat and fume hood) must be taken while handling these compounds.

General information

All chemical were obtained from either Sigma-Aldrich, Fisher Scientific or VWR International, and used as is unless otherwise noted. All reactions were carried out under nitrogen in oven dried glassware using standard Schlenk techniques unless otherwise noted. Reactions were monitored by thin layer chromatography (TLC) using E. Merck 60F254 precoated silica gel plates and alumina plate depending on the compounds. Dry solvents were degassed under nitrogen and were dried using the PURESOLV system (Inovatative Technologies, Newport, MA). Tetrahydrofuran was freshly distilled from sodium metal and benzophenone. Dichloromethane was also distilled immediately prior to use under nitrogen from calcium hydride. Toluene was also distilled immediately prior to use under nitrogen from calcium hydride. Yields refer to chromatographically and spectroscopically pure compounds. Flash

chromatography was performed with the indicated solvents using Fisher silica gel (particle size 170-400 Mesh). ^{1}H, ^{13}C and ^{9}F data were obtained using either 300 MHz Varian Gemni 2300 (75 MHz ^{13}C, 121 MHz ^{19}F) spectrometer, the 400 MHz Varian INOVA 400 (100 MHz ^{13}C) spectrometer or the 500 MHz Varian INOVA 500 (125 MHz ^{13}C) in $CDCl_3$ as solvent unless otherwise stated. Chemical shifts (δ) are reported in ppm and standardized with solvent as internal standard based on literature reported values.[50] Melting points were measured on Thomas Hoover Capillary melting point apparatus and are uncorrected. Optical rotations were measured on Perkin-Elmer Model 241 polarimeter.

Experimental procedure

3*H*-Benzo[*b*]thiophen-2-one (**4-1**):[40, 51]
To a solution of thianaphthene-2-boronic acid (1.5 g, 8 mmol) dissolved in EtOH [0.2 M] was added 2.8 mL of 30% hydrogen peroxide, dropwise. The mixture was stirred at room temperature and the reaction was monitored via TLC. After 16 h, the mixture was diluted with water and extracted with $CHCl_3$ (3 x 50 mL). The organic layers were combined, dried over $MgSO_4$ and concentrated *in vacuo*. The resulting crude was purified using flash column chromatography on silica gel (hexanes:ethyl acetate = 3:1) to yield **4-1** (1.1 g, 90% yield), a brown solid: m.p. 48-49 °C (m.p. lit. 50-51 °C); ^{1}H NMR (300 MHz, $CDCl_3$, ppm) δ 3.850 (s, 2 H), 7.168-7.267 (m, 4 H). All data are consistent with literature values.[40, 51]

2-Sulfhydrylphenylacetic acid (4-2):[52]
To a solution of **4-1** (300 mg, 2 mmol) dissolved in THF [0.5 M] warmed to 60 °C was added a solution of LiOH (500 mg, 12 mmol) dissolved in 10 mL water, dropwise, producing a cloudy white mixture. The mixture was stirred overnight at 60 °C and the reaction was monitored via TLC. After 16 hours, the mixture was removed from heat and cooled to room temperature. At room temperature, the mixture was diluted with 2 mL water and 10 mL diethyl ether. The pH was adjusted to pH 2 using 1 M HCl producing a white precipitate. The organic layer was extracted with CH_2Cl_2 (3 x 50 mL), washed with brine, dried over $MgSO_4$, and concentrated *in vacuo*. The resulting crude was purified using flash column chromatography on silica gel (hexanes:ethyl acetate = 1:1) to yield **4-2** (230 mg, 82% yield), as a yellow solid: m.p. 85-86 °C (m.p. lit. 90-92 °C); ^{1}H NMR (300 MHz, $CDCl_3$, ppm) δ 3.492 (s, 1 H), 3.823 (s, 2 H), 7.153-7.248 (m, 2 H), 7.383-7.424 (m, 2 H). All data are consistent with literature values.[52]

2,4,6-Tribenzo[*b*]thiophen-2-yl-1,3,5,2,4,6-trioxatriborinane (4-3)[40]
This compound was prepared following the literature procedure described by Bordwell and Fried. To benzo[*b*]thiophene (500 mg, 3.7 mmol) dissolved in 8 mL dry ether at 0 °C was added 2.5 M *n*-butyllithium in hexanes (1.7 mL, 3.7 mmol) over a period of 3 minutes. The solution was stirred at room temperature for 1 hour during which the solution became yellow in color. After 1 hour, the solution was cooled to 0 °C. To the cooled solution was added *n*-butyl borate (1 g, 4 mmol) dissolved in 2 mL ether dropwise over a period of 5 minutes. The mixture was stirred for 1 hour and quenched with ethanol and then with 0.1 M HCl. The organic layer was collected and the aqueous layer was extracted three times with ether. The organic layers were combined and extracted three times with aqueous 1 M KOH. The pH of the combined aqueous layers was adjusted to 2 using 1 M HCl. The acidic solution was extracted three times with ether. The organic layers were combined, dried over $MgSO_4$ and concentrated *in vacuo* yielding yellow oil.

The oil was triturated with hexanes to yield **3-3** (630 mg, 47% yield), as an off-white solid: m.p. > 235 °C (m.p. lit. > 270 °C).[40]

2,2'-Dipyridyl disulfane (4-4):[41]
To a solution of pyridine-2(1*H*)-thione (2.8 g, 20 mmol) dissolved in CH_2Cl_2 [0.1 M] was added $KMnO_4$ (12 g, 60 mmol) over a period of 20 minutes. The mixture was stirred vigorously and the reaction was monitored via TLC. After 1 hour, the solution was filtered over celite and concentrated *in vacuo* to yield **4-4** (2.71 g, 98% yield), as a white solid without further purification: m.p. 67-68 °C (m.p. lit. 58 °C); ^{1}H NMR (300 MHz, $CDCl_3$, ppm) δ 7.089-7.134 (m, 2 H), 7.604 (d, *J* = 2.8 Hz, 2 H), 7.623-7.631 (m, 2 H), 8.455-8.480 (m, 2 H). All data are consistent with literature values.[41]

3-(Pyridin-2-yldisulfanyl)propanoic acid (4-5):[42]
To a solution of **4-4** (2.2 g, 10 mmol) and 0.25 mL HOAc dissolved in EtOH [0.2 M] cooled to 0 °C, was added 3-mercaptopropanoic acid (0.43 mL, 5 mmol), dropwise, producing a yellow solution. The mixture was stirred at room temperature and the reaction was monitored via TLC. After 16 hours, the reaction solvent was evaporated. The resulting crude was dissolved in CH_2Cl_2 and purified using neutral alumina gel column (CH_3OH:CH_2Cl_2 = 1:1 with 3% HOAc) to yield starting material and crude containing **4-5**. The resulting crude was further purified using flash column chromatography on silica gel (hexanes:ethyl acetate = 1:1) to yield **4-5** (1.20 g, 56% yield), as a yellow oil: ^{1}H NMR (300 MHz, $CDCl_3$, ppm) δ 2.604 (t, *J* = 9.6 Hz, 2 H), 2.857 (t, *J* = 9.6 Hz, 2 H), 7.002 (t, *J* = 2.8 Hz, 1 H), 7.555-7.634 (m, 2 H), 8.318 (m, 1 H), 11.131 (s, 1 H). All data are consistent with literature values.[42]

Tri*iso*propylsilyl 3-(pyridin-2-yldisulfanyl)propanoate (4-6):
To a solution of **4-5** (900 mg, 4 mmol) and Et_3N (1.1 mL, 8 mmol) dissolved in CH_2Cl_2 [0.5 M] and cooled to 0 °C was added chlorotriisopropylsilane (1.2 mL, 6 mmol), dropwise, producing a yellow-orange solution. The mixture was stirred at room temperature and the reaction was monitored via TLC. After 2 hours, the reaction was quenched with aqueous $NaHCO_3$ and diluted with ethyl ether (25 mL). The organic layer was washed with brine (3 x 10 mL), collected, dried over $MgSO_4$ and concentrated *in vacuo*. The resulting crude was purified using flash column chromatography on silica gel (hexanes:ethyl acetate = 5:1) to yield **4-6** (1.55 g, 97% yield), as a colorless liquid: ^{1}H NMR (300 MHz, $CDCl_3$, ppm) δ 0.949-1.053 (m, 21 H), 2.272 (t, *J* = 9.2 Hz, 2 H), 3.007 (t, *J* = 9.2 Hz, 2 H), 7.067 (t, *J* = 1.6 Hz, 1 H), 7.612-7.713 (m, 2 H), 8.421 (m, 1 H); FIA-MS MS (ESI) *m/z* calcd for $C_{17}H_{29}NO_2S_2Si$ (M+) 371.6, found 371.1.

2-(2-((3-Oxo-3-(tri*iso*propylsilyloxy)propyl)disulfanyl)phenyl)acetic acid (4-7):
To a solution of **4-6** (348 mg, 0.9 mmol) dissolved in THF [0.3 M] and cooled to 0 °C was added **4-2** (156 mg, 0.9 mmol) dissolved in THF [0.3 M], dropwise. The yellow mixture was stirred vigorously at 0 °C, and the reaction was monitored via TLC. After 4 hours, the reaction solvent was evaporated. The resulting crude was purified using flash column chromatography on silica gel (hexanes:ethyl acetate = 1:1) to yield **4-7** (143 mg, 80% yield), as a very viscous yellow oil. The oil was stored in a freezer purged with nitrogen before use in subsequent step: ^{1}H NMR (300 MHz, $CDCl_3$, ppm) δ 1.051-1.090 (m, 21 H), 2.753 (t, *J* = 9.6 Hz, 2 H), 2.92 (t, *J* = 9.6 Hz, 2 H), 3.894 (s, 2 H), 7.241-7.308 (m, 3 H), 7.750 (d, *J* = 1.2 Hz, 1 H); FIA-MS MS (ESI) *m/z* calcd for $C_{20}H_{32}O_4S_2Si$ $(M+H)^+$ 429.6, found 429.1.

4-Bromopentanoic acid (4-8)[43]

To a solution of γ-valerolactone (1 mL, 10 mmol) dissolved in CH_2Cl_2 [0.2 M] and cooled to 0 °C was added BBr_3 (2 mL, 20 mmol) dissolved in CH_2Cl_2 [0.2 M], dropwise via an additional funnel. The mixture was stirred at room temperature. After 24 h, the reaction vessel was chilled in an ice-bath and the reaction solution was diluted with ice-water. The pH was adjusted to 2 using 1 M HCl. The solution was extracted with CH_2Cl_2 (3 x 50 mL). The organic layers were combined washed with brine (3 x 50 mL), dried under $MgSO_4$ and concentrated *in vacuo* to yield crude containing **4-8** (2.1 g), as a brown oil: ^{1}H NMR (500 MHz, $CDCl_3$, ppm) δ 1.689 (d, J = 1.5 Hz, 3 H), 2.123 (m, 2H), 2.502 (m, 2 H), 4.124 (m, 1 H), 11.702 (s, 1 H). Starting material, γ-valerolactone, was also present. All data are consistent with literature values.[43]

2-(5-Methoxy-5-oxopentan-2-yl)isothiouronium bromide (4-9)

To the crude sample of **4-8** (~8 mmol) dissolved in 30 mL CH_3OH was added thiourea (480 mg, 6.7 mmol). The mixture was stirred under reflux conditions. The reaction was monitored by LC/MS. After 20 h, the reaction solvent was evaporated and the resulting crude was washed with CH_2Cl_2 to yield crude containing **4-9** (1.37 g), as an off-white solid which was used in the next step without further purification.

4-Sulfhydrylpentanoic acid (4-10)

Method 1[27, 53]

The resulting **4-9** was dissolved in 20 mL 8.0 M KOH and stirred at 60 °C. The reaction was monitored by LC/MS. After 20 h, the reaction was allowed to cool to room temperature. The pH was adjusted to 1 with 1 M HCl. The aqueous layer was extracted with ether (3 x 50 mL). The organic layers were combined, washed with brine (2 x 50 mL), then washed with water (2 x 50 mL), dried over $MgSO_4$ and concentrated *in vacuo* to yield **4-10** (463 mg, 38% yield after 3 steps), as a yellow oil with strong stench:

Method 2

To a solution of γ-valerolactone (5.25 g, 52 mmol) dissolved in 30% HBr in water [2.0 M] and heated to 70 °C was added thiourea (11.2 g, 156 mmol). The mixture was stirred under reflux conditions. After 24 h, the reaction was allowed to cool to 60 °C. At this temperature, the reaction was diluted with water. The aqueous layer was extracted with CH_2Cl_2 (3 x 50 mL), then with ethyl ether (3 x 50 mL). The aqueous layer was kept which contains **4-9**. The pH of the aqueous layer containing **4-9** was adjusted to 14 with 8 M NaOH. The solution turned pink-red during basification. A stir bar was added and the reaction mixture was stirred under reflux conditions. Upon completion, the mixture was cooled to room temperature, diluted with ice-cold water and the pH was adjusted to 2 with 1 M HCl. The acidified solution was extracted with CH_2Cl_2 (3 x 50 mL). The organic layers were collected, dried over $MgSO_4$ and concentrated *in vacuo* to yield **4-10** (5.2 g, 78% yield), as a yellow oil with a strong stench:

^{1}H NMR (300 MHz, $CDCl_3$, ppm) δ 1.323 (d, J = 3.5 Hz, 3 H), 1.417 (d, J = 3.5, 1 H), 1.696-1.792 (m, 1 H), 1.900-1.951 (m, 1H), 2.461-2.501 (m, 2 H), 2.904-2.950 (m, 1H), 10.5 (br s, 1 H). All data are consistent with reported values.[27, 53]

4-(Pyridin-2-yldisulfanyl)pentanoic acid (4-11)[27, 53]

Method 1

To a solution of **4-4** (1.0 g, 4.5 mmol) dissolved in EtOH [0.2 M] was slowly added **4-10** (100 mg, 0.8 mmol) dropwise. The mixture stirred under reflux conditions and the reaction was monitored via TLC. After 1 h, the reaction solution was evaporated. The resulting yellow oil was dissolved in CH_2Cl_2 and purified using flash column chromatography on silica gel (hexanes:ethyl acetate = 3:1) to yield **4-11** (177 mg, 90% yield), as a thick, yellow oil:
Method 2
To a solution of **4-4** (6 g, 24 mmol) dissolved in EtOH [0.1 M] and stirred under reflux conditions was slowly added **4-10** (500 mg, 4 mmol) dissolved in EtOH [0.4 M], dropwise. The reaction was allowed to stir under reflux conditions and monitored via TLC. After 2 h, the reaction solution was evaporated. The resulting crude was triturated with hexanes to afford yellow precipitate. The precipitate was collected and washed with hexanes. The mother liquor was retained and concentrated *in vacuo* to yield yellow-orange oil containing **4-11** and pyridine-2-thiol:
^{1}H NMR (400 MHz, $CDCl_3$, ppm) δ 1.300 (d, J = 6.8 Hz, 3 H), 1.832 (m, 2 H), 2.487 (t, J = 8 Hz, 2 H), 2.960-3.011(m, 1 H), 7.058 (t, J = 5.2 Hz, 1 H), 7.619 (t, J = 7.6, 1 H), 7.713 (m, 1H), 8.420 (d, J = 4.4 Hz, 1 H), 10.077 (s, 1 H). All data are consistent with reported values.[27, 53]

Triisopropylsilyl 4-(pyridin-2-yldisulfanyl)pentanoate (4-12)
Method 1
To **4-11** (160 mg, 0.7 mmol) and Et_3N (0.2 mL, 1.4 mmol) dissolved in CH_2Cl_2 [0.2 M] and cooled to 0 °C was added chlorotriisopropylsilane (0.17 mL, 0.8 mmol), dropwise. The mixture was stirred at room temperature and the reaction was monitored via TLC. After 5 hours, the reaction solvent was evaporated and the resulting crude was purified using flash column chromatography on silica gel (hexanes:ethyl acetate =5:1) to yield **4-12** (259 mg, 98% yield), as a colorless oil:
Method 2
The oil containing **4-11** was dissolved in 10 mL methylene chloride and cooled to 0 °C. To the cooled solution was added 0.8 mL chlorotriisopropylsilane followed by 0.7 mL Et_3N, dropwise. The mixture was stirred at room temperature and the reaction was monitored via TLC. After 4 hours, the reaction was purified immediately using flash column chromatography on silica gel to yield **4-12** (1.3 g, 93% after 2 steps), as a yellow oil and pyridine-2-thiol:
^{1}H NMR (300 MHz, $CDCl_3$, ppm) δ 1.007 (m, 21 H), 1.300 (m, 3 H), 1.866 – 2.004 (m, 2 H), 2.253 – 2.468 (m, 2 H), 2.960 – 3.011 (m, 1 H), 7.058 (t, J = 5.2 Hz, 1 H), 7.563 (m, 1H), 7.619 (t, J = 7.6, 1 H), 7.688 – 7.721 (dt, 1 H), 8.396 – 8.421 (dq, 1 H); FIA-MS MS (ESI) *m/z* calcd for $C_{19}H_{33}NO_2S_2Si$ $(M+H)^+$ 400.1, found 400.2.

2-(5-Oxo-5-triisopropylsilyloxypentan-2-yl)disulfanylphenylacetic acid (4-13)
To a solution of **4-12** (700 mg, 1.8 mmol) dissolved in THF [0.6 M] cooled to -10 °C was added a solution of **4-2** (295 mg, 1.8 mmol) dissolved in THF [0.6 M], dropwise. The yellow mixture was stirred, the temperature was maintained and the reaction was monitored via TLC. After 4 hours, the reaction solvent was evaporated *in vacuo* without heat and the resulting crude was purified immediately using flash column chromatography on silica gel (hexanes:ethyl acetate = 3:1) to yield **4-13** (750 mg, 93% yield), as a very viscous yellow oil. The oil was stored in a vial purged with nitrogen at 0 °C before use in subsequent step. This reaction was repeated with yields ranging from 73 - 93%: ^{1}H NMR (400 MHz, $CDCl_3$, ppm) δ 1.060 (m, 21 H), 1.235 – 1.310 (m, 3 H), 1.805 – 1.840 (m, 1 H), 1.917 – 1.954 (m, 1 H), 2.388 – 2.435 (m, 2 H), 2.884 –

2.918 (m, 1 H), 3.896 (s, 2 H), 7.178 – 7.211 (m, 1 H), 7.267 – 7.297 (m, 1H), 7.784 – 7.803 (d, J = 7.6 Hz, 1 H); FIA-MS MS (ESI) *m/z* calcd for $C_{22}H_{36}O_4S_2Si$ $(M)^+$ 456.7, found 456.2.

3-Sulfhydryl-3-methylbutanoic acid (4-14)[27]

This compound was prepared based on the literature reported procedure of Widdison, et. al. To 20 mL of dry THF cooled to -78 °C was added 10 mL 2.5 M n-butyllithium in hexanes. To the solution was added 1.25 mL acetonitrile dropwise over a period of 3 minutes. The mixture was stirred for 30 minutes, as a white precipitate formed. To the mixture was added isobutylene sulfide (2 mL, 20 mmol) dissolved in 13 mL of dry THF dropwise via addition funnel over a period of 20 minutes. The mixture was stirred at room temperature for 3 hours. After 3 hours, the reaction vessel was placed in an ice-bath and the reaction was quenched with 0.1 M HCl. The THF layer was retained and the aqueous layer was washed twice with ethyl acetate. The THF and ethyl acetate layers were combined, dried over $NaSO_4$ and concentrated *in vacuo*. The resulting crude oil was dissolved in 4 mL of ethanol. To the solution was added aqueous 7 M NaOH. The mixture was stirred under reflux conditions overnight. After 16 hours, the reaction was cooled to room temperature and diluted with water. The aqueous layer was extracted two times with ethyl acetate. The pH of the aqueous layer was adjusted to 2 using 1 M HCl and then extracted three additional times with ethyl acetate. All of the organic layers were collected, dried over $MgSO_4$ and concentrated *in vacuo* to yield a crude orange liquid containing **4-14** (2.15 g): crude ^{1}H NMR (400 MHz, $CDCl_3$, ppm) δ 1.162 – 1.210 (m, 2 H), 1.314 (s, 6 H), 1.523 (s, 1H), 1.971 – 1.992 (m, 2 H), 2.417 – 2.472 (m, 2 H). All data are consistent with reported values.[27]

3-Methyl-3-(pyridin-2-yldisulfanyl)butanoic acid (4-15)

A solution of pyridinyldisulfanylpyridine (20 g, 90 mmol) dissolved in EtOH [0.1 M] was stirred under reflux conditions. To the mixture was slowly added 2 g of crude liquid containing **4-14** dissolved in 30 mL of EtOH via addition funnel. The reaction was stirred under reflux conditions and monitored via TLC. After 4 h, the reaction solution was evaporated. The resulting crude was triturated with hexanes to afford yellow precipitate. The precipitate was collected and washed with hexanes. The mother liquor was retained and concentrated *in vacuo* to yield orange oil containing **4-15** and pyridine-2-thiol, which was used in the subsequent step without further purification.

Triisopropylsilyl 3-methyl-3-(pyridin-2-yldisulfanyl)butanoate (4-16)

The oil containing **4-15** was dissolved in 8 mL methylene chloride and cooled to 0 °C. To the cooled solution was added 1 mL TIPSCl followed by 1 mL Et_3N dropwise. The mixture was stirred at room temperature and the reaction was monitored via TLC. After 8 hours, the reaction was purified immediately using column chromatography on silica gel to yield **4-16** (1.8 g, 22% yield after 4 steps), as a yellow oil and pyridine-2-thiol: ^{1}H NMR (400 MHz, $CDCl_3$, ppm) δ 1.010 – 1.046 (m, 21 H), 1.199 – 1.277 (m, 9 H), 1.893 – 1.934 (m, 2 H), 2.412 – 2.452 (m, 2 H), 6.997 – 7.027 (td, 1 H), 7.546 – 7.589 (td, 1H), 7.693 – 7.713 (d, J = 8 Hz, 1 H), 8.381 – 8.391 (d, J = 4 Hz, 1 H); FIA-MS MS (ESI) *m/z* calcd for $C_{20}H_{35}NO_2S_2Si$ $(M+H)^+$ 414.7, found 414.2.

Attempted synthesis of dimethyl-branched disulfide linker (4-17)

To a solution of **4-16** (500 mg, 1.5 mmol) dissolved in THF [0.6 M] cooled to 0 °C was added a solution of sulfhydrylphenylacetic acid (250, 1.5 mmol) dissolved in THF [0.6 M], dropwise. The yellow mixture was stirred at room temperature and the reaction was monitored via TLC.

After 24 hours, there was no reaction based on TLC. At this point, sulfhydrylphenylacetic acid (50 mg, 0.3 mmol) was added. The reaction was stirred for an additional 24 hours, but no reaction was observed. At this point, the reaction was heated to 40 °C and stirred for 3 hours. After 3 hours, a loss of TIPS was observed resulting in the formation of **3-17** and no formation of desired product. To push the reaction, 2 equivalents of Et_3N were added. No desired product was formed.

SB-T-1214-Me-linker-TIPS ester conjugate (4-18)

To a mixture of SB-T-1214 (100 mg, 0.1 mmol), **4-13** (57 mg, 0.12 mmol) and DMAP (1 mg, 0.03 mmol) dissolved in CH_2Cl_2 [0.05 M] and cooled to 0 °C was added DIC (0.02 mL, 0.12 mmol), dropwise. The mixture was stirred at room temperature and the reaction was monitored via TLC. After 8 hours, the reaction mixture was purified using column chromatography on silica gel to yield 20 mg SB-T-1214 and **4-18** (70 mg, 50% yield), as a white solid. This reaction was repeated affording **4-18** in yields ranging from 75 – 80%: m.p. 162-163 °C; ^{1}H NMR (500 MHz, $CDCl_3$, ppm) δ 0.988 (m, 2 H), 1.046 (m, 21 H), 1.079 (m, 2 H), 1.147 (m, 3 H), 1.255 (m, 8 H), 1.358 (s, 6 H), 1.663 (s, 2 H), 1.717 (s, 2 H), 1.775 (m, 3 H), 1.903 (m, 2 H), 2.041 (s, 3 H), 2.380 (m, 4 H), 2.540 (m, 1 H), 3.784 (s, 1 H), 4.125 (s, 2 H), 4.183 (m, 1 H), 4.313 (m, 1 H), 4.407 (m, 1 H), 4.981 (m, 2 H), 5.142 (m, 1 H), 5.678 (d, *J* = 7 Hz, 1 H), 6.221 (m, 1 H), 6.295 (d, *J* = 7 Hz, 1 H), 7.298 (m, 1 H), 7.587 – 7.616 (t, *J* = 5 Hz, 1 H), 7.784 – 7.822 (t, *J* = 11 Hz, 1 H), 8.094 – 8.110 (d, *J* = 6.4 Hz, 1 H).

SB-T-1214-Me-linker-carboxylic acid conjugate (4-19)

To **4-18** (24 mg, 0.04 mmol) dissolved in a 1:1 mixture of CH_3CN:py [0.01 M] cooled to 0 °C was added HF/pyridine (0.1 mL per 10 mg), dropwise. The mixture was stirred at room temperature and the reaction was monitored via TLC. After 16 hours, the reaction was quenched with 10% citric acid (5 mL) and diluted with ethyl acetate (5 mL). The organic layer was extracted and washed with aqueous $CuSO_4$ (3 x 30 mL), then washed with brine (3 x 30 mL), dried over $MgSO_4$, and concentrated *in vacuo* to yield **4-19** (20 mg, quantitative yield), as a white solid. This reaction was repeated to afford **4-19** with yields >89%: m.p. 85-86 °C; ^{1}H NMR (500 MHz, $CDCl_3$, ppm) δ 0.988 (m, 2 H), 1.079 (m, 2 H), 1.147 (m, 3 H), 1.255 (m, 8 H), 1.358 (s, 6 H), 1.663 (s, 2 H), 1.717 (s, 2 H), 1.775 (m, 3 H), 1.903 (m, 2 H), 2.041 (s, 3 H), 2.380 (m, 4 H), 2.540 (m, 1 H), 3.784 (s, 1 H), 4.125 (s, 2 H), 4.183 (m, 1 H), 4.313 (m, 1 H), 4.407 (m, 1 H), 4.981 (m, 2 H), 5.142 (m, 1 H), 5.678 (d, *J* = 7 Hz, 1 H), 6.221 (m, 1 H), 6.295 (d, *J* = 7 Hz, 1 H), 7.298 (m, 1 H), 7.587 – 7.616 (t, *J* = 5 Hz, 1 H), 7.784 – 7.822 (t, *J* = 11 Hz, 1 H), 8.094 – 8.110 (d, *J* = 6.4 Hz, 1 H); HRMS EI+ *m/z* calcd for $C_{58}H_{73}NO_{18}S_2$ $(M+H)^+$ 1136.4269, 1136.4344 (Δ 7.5 ppm).

SB-T-1214-Me-linker-OSu coupling-ready construct (4-20)

To a mixture of **4-19** (20 mg, 0.02 mmol) and HOSu (0.1 mmol) dissolved in pyridine [0.1 M] was added DIC (0.024 mmol). The reaction was stirred at room temperature and monitored via TLC and LC/MS. After 16 h, the reaction mixture was quenched with NH_4Cl and washed with brine. The combined organic layers were dried with $MgSO_4$ and concentrated *in vacuo* resulting in a crude mixture. The resulting crude was purified using column chromatography on silica gel to yield **4-20** (10 mg, 50% yield), as a white solid. This reaction was repeated to afford **4-20** in yields ranging from 65 – 78%: m.p. 80-82 °C; ^{1}H NMR (500 MHz, $CDCl_3$, ppm) δ 0.988 (m, 2 H), 1.079 (m, 2 H), 1.147 (m, 3 H), 1.255 (m, 8 H), 1.358 (s, 6 H), 1.656 (s, 4 H), 1.725 (m, 7 H), 1.899 (s, 3 H), 2.076 (s, 5 H), 2.347 (m, 5 H), 2.656 (m, 1 H), 2.824 (s, 3 H), 2.957 (m, 11

H), 3.803 (m, 1 H), 4.083 (s, 2 H), 4.187 (m, 1 H), 4.287 (m, 1 H), 4.407 (m, 1 H), 4.974 (m, 2 H), 5.678 (m, 1 H), 6.221 (m, 1 H), 6.279 (s, 1 H), 7.316 (m, 1 H), 7.594 (t, *J* = 5 Hz, 1 H), 7.784 (m, 1 H), 8.015 (s, 1 H), 8.097 – 8.115 (d, *J* = 9 Hz, 1 H); HRMS EI+ *m/z* calcd for $C_{62}H_{76}N_2O_{20}S_2$ $(M+H)^+$ 1233.4433, found 1233.4524 (Δ 9.1 ppm).

General procedure for camptothecin-linker-drug coupling

An equimolar ratio drug and **4-7** or **4-13** with 0.3 equivalent of DMAP were dissolved in CH_2Cl_2 and cooled to 0 °C. After 10 min, to the mixture was added 1.2 equivalents of DIC, dropwise. The mixture was stirred at room temperature and the reaction was monitored via TLC. After 16 hours, the reaction solvent was evaporated and the resulting crude was purified using flash column chromatography on silica gel (hexanes:ethyl acetate = 1:1 followed by 5% CH_3OH in CH_2Cl_2) to yield **4-21**:

4-21a (36 mg, 84% crude yield)**,** as a white solid with a small trace of dicyclohexyl urea: ^{1}H NMR (400 MHz, $CDCl_3$, ppm) δ 0.95 (s, 1 H), 1.00-1.02 (m, 21 H) (H on TIPS group), 1.220 (m, 8 H) (H of DCU), 2.159-2.2 (m, 2 H), 2.272-2..32 (m, 2 H), 2.618 (t, J = 3.6 Hz, 2 H), 2.838 (t, J = 3.6 Hz, 2H), 2.93 (s, 2 H), 3.992 (s, 2 H), 5.265 (s, 3 H), 5.360-5.402 (d, J = 8 Hz, 2 H), 5.613-5.656 (d, J = 8 Hz, 2 H), 7.667-7.699 (m, 3 H), 7.825-7.863 (m, 2 H), 7.922-7.942 (m, 1 H), 8.222-8.263 (m, 1 H), 8.363 (m, 2 H); ^{13}C NMR ($CDCl_3$, 400 MHz) 7.771, 12.058, 12.111, 17.894, 17.947, 20.846, 32.016, 33.852, 35.506, 38.792, 50.205, 67.325, 96.708, 120.414, 128.192, 128.276, 128.374, 128.389, 128.420, 128.564, 128.693, 129.953, 130.818, 131.068, 131.265, 131.387, 133.512, 136.661, 145.972, 146.412, 149.106, 152.559, 157.597, 167.508, 170.156, 171.591; FIA-MS MS (ESI) *m/z* calcd for $C_{40}H_{46}N_2O_7S_2Si$ $(M+H)^+$ 759.0, found 758.3.

4-21b: (44 mg, 13% - 76% yield range from several attempts), as a yellow solid: ^{1}H NMR (500 MHz, $CDCl_3$, ppm) δ 1.046 (m, 21 H), 1.179 (m 4 H), 1.266 (m, 3 H), 1.744 (m, 1 H), 1.876 (m, 2 H), 2.127 (m, 1 H), 2.368 (m, 3 H), 2.414 (m, 1 H), 2.877 (m, 1 H), 3.480 – 3.998 (dq, 1 H), 4.217 (m, 1 H), 5.285 (s, 3 H), 5.395 (m, 1 H), 5.651 (m, 1 H), 7.101 (m, 1 H), 7.238 (m, 3 H), 7,688 (m, 2 H), 7.787 (m, 1 H), 7.869 (m, 1 H), 7.934 (m, 1 H), 8.251 (m, 1 H), 8.393 (m, 1 H); FIA-MS MS (ESI) *m/z* calcd for $C_{42}H_{50}N_2O_7S_2Si$ $(M+H)^+$ 786.3, found 787.3.

General procedure for camptothecin-linker-CO_2H conjugate (4-22a and 4-22b)

4-21(a-b) was dissolved in a 1:1 mixture of CH_3CN:py [0.01 M] and cooled to 0 °C. To the mixture was added HF pyridine (0.1 mL per 10 mg substrate). The mixture was stirred at room temperature and the reaction was monitored via TLC. After 16 h, the reaction was quenched with 0.2 M citric acid (5 x amount of HF pyridine used) and extracted with CH_2Cl_2 (2 x). The organic layers were washed with $CuSO_4$ (3 x), then washed with brine (3 x), collected, dried over $MgSO_4$ and concentrated *in vacuo* to yield **4-22**:

4-22a (18 mg, 71% after 2 steps), as a yellow solid: ^{1}H NMR (400 MHz, $CDCl_3$, ppm) δ 0.95 (s, 1 H), 2.159-2.2 (m, 2 H), 2.272-2..32 (m, 2 H), 2.618 (t, *J* = 3.6 Hz, 2 H), 2.838 (t, *J* = 3.6 Hz, 2H), 2.93 (s, 2 H), 3.992 (s, 2 H), 5.265 (s, 3 H), 5.360-5.402 (d, *J* = 8 Hz, 2 H), 5.613-5.656 (d, *J* = 8 Hz, 2 H), 7.667-7.699 (m, 3 H), 7.825-7.863 (m, 2 H), 7.922-7.942 (m, 1 H), 8.220-8.263 (m, 1 H), 8.363 (m, 2 H); FIA-MS MS (ESI) *m/z* calcd for $C_{31}H_{26}N_2O_7S_2$ $(M+H)^+$ 603.6, found 603.3.

4-22b (42 mg, quantitative), as an off-white solid: ^{1}H NMR (500 MHz, $CDCl_3$, ppm) δ 0.876 (m, 1 H), 0.977 (m, 2 H), 1.043 (t, *J* = 6.5 Hz, 1 H), 1.205 (m 1 H), 1.266 (m, 3 H), 1.744 (m, 1 H), 1.876 (m, 2 H), 2.127 (m, 1 H), 2.368 (m, 3 H), 2.414 (m, 1 H), 2.877 (m, 1 H), 3.480-3.998 (m, 1 H), 4.217 (m, 1 H), 5.285 (s, 3 H), 5.395 (m, 1 H), 5.651 (m, 1 H), 7.101 (m, 1 H), 7.238 (m, 3

H), 7,688 (m, 2 H), 7.787 (m, 1 H), 7.869 (m, 1 H), 7.934 (m, 1 H), 8.251 (m, 1 H), 8.393 (m, 1 H); FIA-MS MS (ESI) *m/z* calcd for $C_{33}H_{30}N_2O_7S_2$ $(M)^+$ 630.7, found 630.1.

CPT-linker-OSu conjugate (4-23a and 4-23b)

Method 1

A mixture of HOSu (8 g, 70 mmol) and triphosgene (4.125 g, 14 mmol) was dissolved in THF [1 M] and cooled to 0 °C. To the mixture was added *n*-Bu_3N in THF [4 M] (20 mL, 84 mmol), dropwise through an addition funnel. After the addition, the solution turned yellow and precipitate formed. The mixture was stirred at room temperature. After 18 h, the mixture was cooled in an ice-bath for 30 minutes. The chilled slurry was filtered and washed with THF to yield **$(OSu)_2CO$** (6.65 g, 75% yield), as a white solid with trace amounts of *N*-hydroxysuccinimide: ^{1}H NMR (300 MHz, $CDCl_3$, ppm) δ 2.847 (s, 8 H). All data are consistent with literature values.[46] To a mixture of **4-22a** (10 mg, 0.01 mmol) and **$(OSu)_2CO$** (7 mg, 0.01 mmol) dissolved in CH_2Cl_2 [0.1 M] was added Et_3N(0.1 mL, 0.01 mol). The mixture was stirred at room temperature and the reaction was monitored via TLC and LC/MS. After 16 h, the reaction mixture was quenched with NH_4Cl (5 mL) and washed with brine (1 x). The organic layer was dried over $MgSO_4$ and concentrated *in vacuo* resulting in a crude mixture of **4-23a** and HOSu (11 mg): crude ^{1}H NMR (300 MHz, $CDCl_3$, ppm) δ 0.822-0.934 (m, 2 H), 1.252 (m, 6 H), 1.585 (m, 2 H), 2.341 (s, 2 H), 2.839 (s, 4 H), 3.118-3.504 (m, 1 H), 3.700 (s, 1 H), 5.026 (m, 1 H), 5.799 (s, 1 H).

Method 2

To a mixture of **4-22b** (35 mg, 0.01 mmol) and HOSu (32 mg, 0.01 mmol) dissolved in pyridine was added DIC (0.01 mL, 0.02 mmol). The mixture was stirred at room temperature and the reaction was monitored via TLC and LC/MS. After 5 h, the reaction solvent was evaporated and the resulting crude was purified using flash column chromatography (10% CH_3OH in CH_2Cl_2) to yield **4-23b** (30 mg, 75% yield): ^{1}H NMR (400 MHz, $CDCl_3$, ppm) δ 0.894-0.929 (m, 5 H), 1.037 (t, *J* = 4.5 Hz, 2 H), 1.115-1.127 (m, 2 H), 1.209-1.312 (m, 18 H), 1.618 (m, 2 H), 1.969-2.005 (m, 1H), 2.034 (m, 1 H), 2.380-2.410 (m, 2 H), 2.589 (br s, 4 H), 2.674 (s, 1 H), 2.893 (s, 4 H), 4.331 (s, 1 H), 5.314 (s, 1 H), 5.386 (d, *J* = 9.9 Hz, 1 H), 5.587 (d, *J* = 9.9 Hz, 1 H), 7.411-7.430 (m, 1 H), 7.639 (s, 1 H), 7.763-7.794 (m, 1 H), 8.031-8.050 (m, 1 H), 8.076 (s, 1 H).

(*9Z,12Z,15Z*)-Octadeca-9,12,15-trienehydrazide (4-24)

Method 1

To LNA (40 mg, 0.03 mmol) with EDC (0.036 mmol) and HOBt monohydrate (0.036 mmol) dissolved in CH_2Cl_2 [0.03 M] and cooled to 0 °C was added hydrazine (0.06 mmol), dropwise. The temperature was maintained and the reaction was stirred for 30 minutes. After 30 minutes, the reaction solvent was evaporated and the resulting crude was washed with acetonitrile and isopropanol to yield a crude mixture containing **4-24** which was used without further purification:

Method 2

To methyl linolenoate (0.5 mL, 1.5 mmol) dissolved in dry CH_3OH [0.2 M] was added anhydrous hydrazine (3 mmol). The mixture was stirred at 60 °C for 16 h. After 16 h, the reaction solvent and unreacted hydrazine were evaporated. The resulting crude was concentrated *in vacuo* to yield **4-24** (450 mg, 98% yield) as colorless oil without further purification:

^{1}H NMR (500 MHz, $CDCl_3$, ppm) δ 0.994 (t, *J* = 8 Hz, 3 H), 1.364-1.270 (m, 11 H), 1.652 (m, 4 H), 2.111-2.048 (m, 4), 2.160 (t, *J* = 8 Hz, 2 H), 2.823 (s, 4 H), 3.681 (s, 1 H), 3.914 (s, 1 H), 5.425-5.321 (m, 6 H), 6.747 (s, 1 H).

SB-T-1214-linker-LNA drug conjugate (4-25)

To a solution of **4-20** (40 mg, 0.03 mmol) dissolved in CH_2Cl_2 [0.1 M] and cooled to 0 °C was added **4-24** (0.03 mmol) dissolved in CH_2Cl_2 [0.1 M], followed by the dropwise addition of DIPEA (0.036 mmol). The mixture was stirred and allowed to warm to room temperature. The reaction was monitored via TLC. After 24 h, the reaction solvent was evaporated and the resulting crude was purified using flash column chromatography on silica gel (hexanes:ethyl acetate = 1:1) to yield **4-25** (30 mg, 78% yield) as a white solid: m.p. 89-90 °C; ^{1}H NMR (400 MHz, $CDCl_3$, ppm) δ 0.954-0.992 (m, 3 H), 1.134-1.150 (m, 12 H), 1.251-1.336 (m, 22 H), 1.654-1.743 (m, 14 H), 1.886 (d, *J* = 5.6 Hz, 4 H), 2.043-2.095 (m, 3 H), 2.335 (br s, 4 H), 2.335 (m, 2 H), 3.39 (t, *J* = 5.6 Hz, 3 H), 3.789-3.887 (m, 2 H), 4.150-4.169 (m, 2 H), 4.295 (d, *J* = 8.4 Hz, 1 H), 4.408 (br s, 1 H), 4.947 (d, *J* = 8.8 Hz, 3 H), 5.058 (br s, 1 H), 5.298-5.400 (m, 3 H), 5.652 (d, *J* = 6.8 Hz, 1 H), 6.201 (t, *J* = 8 Hz, 1 H), 6.269 (s, 1 H), 7.470 (t, *J* = 7.2 Hz, 2 H), 7.605 (t, *J* = 7.6 Hz, 1 H), 7.789 (m, 1 H), 8.089 (d, *J* = 7.2 Hz, 2 H); ^{13}C NMR (400 MHz, $CDCl_3$, ppm) δ 9.355, 9.552, 9.742, 13.203, 14.978, 20.746, 22.370, 22.628, 23.629, 24.259, 25.815, 26.900, 27.408, 28.433, 29.131, 29.306, 29.488, 29.784, 35.596, 36.879, 38.928, 42.517, 43.360, 45.902, 58.651, 72.333, 74.807, 75.125, 79.580, 81.212, 84.672, 127.312, 127.972, 128.511, 128.830, 129.414, 130.317, 132.177, 157.173, 157.591, 167.251, 175.356, 204.177; LC-MS MS (ESI) *m/z* calcd for $C_{76}H_{103}N_3O_{18}S_2$ $(M+H)^+$ 1410.7, found 1410.7.

Cell culture system for MTT assay

Cell lines (obtained from ATCC unless otherwise noted and maintained at SBU Cell Culture/Hybridoma Facility) were cultured in RPMI-1640 with L-glutamine (Lonza BioWhittaker, BW12-702F: A2780, DLD-1, MCF-7) or McCoy's 5A (Gibco #16600: HT-29) supplemented with 5% FBS (Thermo Scientific, HyClone, SH3007003), 5% Nu Serum (BD Biosciences, 355100) and 1% Penn Strip, at 37 °C in a humidified incubator with 5% CO_2. The cells were washed with DPBS and dissociated using TrypLE. The cells were incubated at 37 °C until the cells were detached from the plate, transferred to a centrifuge vial and pelleted via centrifugation at 1500 rpm for 5 min. The cells were counted per 1 mL media. The desired amount of RPMI-1640 was added to the cell solution so that 8,000 cells can be added to each well of a 96-well plate in 200 μL aliquots. After the addition, the cells were incubated at 37 °C with 5% CO_2.

Drug treatment for MTT assay

A serial dilution of the free taxoid and LNA-SB-T-1214 drug conjugate dissolved in sterile DMSO was prepared by the addition of fully-supplemented RPMI-1640. The residual medium in each well was aspirated and the different drug-concentration solutions were added to each well of every column of the 96-well plate in 100 μL aliquots. After the addition of the drug solution, the cells were incubated at 37 °C for 48 hours. After the incubation period, the medium was aspirated and the cells were washed with DPBS and then 40 μL of 0.5 mg/mL MTT (3-(4,5-dimethylthiazol-2-yl)-2,5-diphenyltetrazolium bromide) in DPBS was added to each well. The cells were then incubated at 37 °C for 3 hours. After the incubation period, the MTT solution was aspirated and the remaining crystals were dissolved using a 40 μL of 0.4 M HCl in

isopropanol. The plates were shaken for 10 minutes to assure that all of the crystals are dissolved. The optical density was determined from the resulting solutions using the Acsent Multiskan optical density reader. Each experiment was run in triplicate.

A serial dilution of LNA-Me-linker-SB-T-1214 dissolved in sterile DMSO was prepared by the addition of fully-supplemented RPMI-1640. The residual medium in each well was aspirated and the different drug-concentration solutions were added to each well of every column of the 96-well plate in 100 μL aliquots. After the addition of the drug solution, the cells were incubated at 37 °C for 1 hour. After the incubation period, the medium was aspirated and the cells were washed with DPBS. To the washed cells 2 equivalents of GSH-OEt dissolved in RPMI-1640 was added to each well. After the addition of GSH-OEt, the cells were incubated at 37 °C for 48 hours. After the incubation period, the medium was aspirated and the cells were washed with DPBS and then 40 μL of 0.5 mg/mL MTT in DPBS was added to each well. The cells were then incubated at 37 °C for 3 hours. After the incubation period, the MTT solution was aspirated and the remaining crystals were dissolved using a 40 μL of 0.4 M HCl in isopropanol. The plates were shaken for 10 minutes to assure that all of the crystals are dissolved. The optical density was determined from the resulting solutions using the Acsent Multiskan optical density reader. Each experiment was run in triplicate.

Data analysis for MTT assay

The optical density data was used to calculate IC_{50} values for each drug on a given cell line using the Hill slope equation. The optical density values obtained from each concentration of drug solution were divided by the optical density value obtained from the cells with zero drug concentration. Using SigmaPlot v.10, the ratios were plotted versus the drug concentration and the IC_{50} values were calculated from the plot using the pre-programmed calculation within the SigmaPlot program.

§ 4.5.0 References

1. Devita Jr., V. T.; Chu, E. A History of Cancer Chemotherapy. *Cancer Res.* **2008,** 68, 8643-8653.
2. Mauger, A. B.; Burke, P. J.; Somani, H. H.; Friedlos, F.; Knox, R. J. Self-Immolative Prodrugs: Candidates for Antibody-Directed Enzyme Prodrug Therapy in Conjunction with a Nitroreductase Enzyme. *J. Med. Chem.* **1994,** 37, 3452-3458.
3. Schmidt, F.; Florent, J. C.; Monneret, C.; Straub, R.; Czech, J.; Gerken, M.; Bosslet, K. Glucuronide prodrugs of hydroxy compounds for antibody directed enzyme prodrug therapy (ADEPT) : A phenol nitrogen mustard carbamate. *Bioorg. Med. Chem. Lett.* **1997,** 7, 1071-1076.
4. Ojima, I., Geng, X., Wu, X., Qu, C., Borella, C. P., Xie, H., Wilhelm, S. D., Leece, B. A., Bartle, L. M., Goldmacher, V. S., Chari, R. V. J. Tumor-Specific Novel Taxoid-Monoclonal Antibody Conjugates. *J. Med. Chem.* **2002,** 45, 5620-5623.
5. Chen, J., Chen, S., Zhao, X., Kuznetsova, L., Wong, S.S., Ojima, I. Functionalized Single-walled Carbon Nanotubes as Rationally Designed Vehicles for Tumor-Targeted Drug Delivery. *J. Am. Chem. Soc.* **2008,** 130, 16778-16785.
6. Burke, P. J.; Senter, P. D.; Meyer, D. W.; Miyamoto, J. B.; Anderson, M.; Toki, B. E.; Manikumar, G.; Wani, M. C.; Kroll, D. J.; Jeffery, S. C. Design, Synthesis, and Biological

Evaluation of Antibody−Drug Conjugates Comprised of Potent Camptothecin Analogues. *Bioconjugate Chem.* **2009,** 20, 1242-1250.
7. Vlahov, I. R.; Vite, G. D.; Kleindi, P. J.; Wang, Y.; Santhapuram, H. K. R.; You, F.; Howard, S. J.; Kim, S.-H.; Lee, F. F. Y.; Leamon, C. P. Regioselective synthesis of folate receptor-targeted agents derived from epothilone analogs and folic acid. *Bioorg. Med. Chem. Lett.* **2010,** 20, 4578-4581.
8. Chen, S., Zhao, X., Chen, J., Chen, J., Kuznetsova, L., Wong, S.S., Ojima, I. Mechanism-based tumor-targeting drug delivery system. Validation of efficient vitamin receptor-mediated endocytosis and drug release. *Bioconjugate Chem.* **2010,** 21, 979-987.
9. Meyer, Y.; Richard, J.-A.; Massonneau, M.; Renard, P.-Y.; Romieu, A. Development of a New Nonpeptidic Self-Immolative Spacer. Application to the Design of Protease Sensing Fluorogenic Probes. *Org. Lett.* **2008,** 10, 1517-1520.
10. Zhang, X.-B.; Waibel, M.; Hasserodt, J. An Autoimmolative Spacer Allows First-Time Incorporation of a Unique Solid-State Fluorophore into a Detection Probe for Acyl Hydrolases. *Chem. Eur. J.* **2010,** 16, 792-795.
11. Antunes, I. F.; Haisma, H. J.; Elsinga, P. H.; Dierckx, R. A.; de Vries, E. F. J. Synthesis and Evaluation of [18F]-FEAnGA as a PET Tracer for β-Glucuronidase Activity. *Bioconjugate Chem.* **2010,** 21, 911-920.
12. Amir, R. J.; Pessah, N.; Shamis, M.; Shabat, D. Self-Immolative Dendrimers. *Angew. Chem., Int. Ed.* **2003,** 42, 4494-4499.
13. Avital-Shmilovici, M.; Shabat, D. Self-immolative dendrimers: A distinctive approach to molecular amplification. *Soft Matter* **2010,** 6, 1073-1080.
14. Ducry, L.; Stump, B. Antibody-drug conjugates: linking cytotoxic payloads to monoclonal antibodies. *Bioconjugate Chem.* **2010,** 21, 5-13.
15. Hamann, P. R.; Hinman, L. M.; Beyer, C. F.; Lindh, D.; Upeslacis, J.; Flowers, D. A.; Bernstein, I. An Anti-CD33 Antibody−Calicheamicin Conjugate for Treatment of Acute Myeloid Leukemia. Choice of Linker. *Bioconjugate Chem.* **2002,** 13, 40-46.
16. Trail, P. A.; Willner, D.; Lasch, S. J.; Henderson, A. J.; Hofstead, S.; Casazza, A. M.; Firestone, R. A.; Hellström, I.; Hellström, K. E. Cure of xenografted human carcinomas by BR96-doxorubicin immunoconjugates. *Science* **1993,** 261, 212-215.
17. Kaneko, T.; Willner, D.; Monkovic, I.; Knipe, J. O.; Braslawsky, G. R.; Greenfield, R. S.; Vyas, D. M. New hydrazone derivatives of Adriamycin and their immunoconjugates - a correlation between acid stability and cytotoxicity. *Bioconjugate Chem.* **1991,** 2, 133-141.
18. Rejmanová, P.; Kopeček, J.; Duncan, R.; Lloyd, J. B. Stability in rat plasma and serum of lysosomally degradable oligopeptide sequences in N-(2-hydroxypropyl) methacrylamide copolymers. *Biomaterials* **1985,** 6, 45-48.
19. Dalton King, H.; Dubowchik, G. M.; Mastalerz, H.; Willner, D.; Hofstead, S. J.; Firestone, R. A.; Lasch, S. J.; Trail, P. A. Monoclonal Antibody Conjugates of Doxorubicin Prepared with Branched Peptide Linkers: Inhibition of Aggregation by Methoxytriethyleneglycol Chains. *J. Med. Chem.* **2002,** 45, 4336-4343.
20. Dubowchik, G. M.; Firestone, R. A.; Padilla, L.; Willner, D.; Hofstead, S.; Mosure, K.; Knipe, J. O.; Lasch, S. J.; Trail, P. A. Cathepsin B-Labile Dipeptide Linkers for Lysosomal Release of Doxorubicin from Internalizing Immunoconjugates: Model Studies of Enzymatic Drug Release and Antigen-Specific In Vitro Anticancer Activity. *Bioconjugate Chem.* **2002,** 13, 855-869.

21. Doronina, S. O., Mendelsohn, B.A., Bovee, T.D., Cerveny, C.G., Alley, S.C., Meyer, D.L., Oflazoghu, E., Toki, B.E., Sanderson, R.J., Zabinski, R.F., Wahl, A.F., Senter, P.D. Enhanced Activity of Monomethylauristatin F through Monoclonal Antibody Delivery: Effects of Linker Technology on Efficacy and Toxicity. *Bioconjugate Chem.* **2006,** 17, 114-124.
22. Beck, A., Haeuw, J.F., Wurch, T., Goetsch, L., Bailly, C., Corvaia, N. The next generation of antibody-drug conjugates comes of age. *Discov. Med.* **2010,** 10, 329-339.
23. Liu, C.; Tadayoni, B. M.; Bourret, L. A.; Mattocks, K. M.; Derr, S. M.; Widdison, W. C.; Kedersha, N. L.; Ariniello, P. D.; Goldmacher, V. S.; Lambert, J. M.; Blätter, W. A.; Chari, R. V. Eradication of large colon tumor xenografts by targeted delivery of maytansinoids. *Proc. Natl. Acad. Sci. U.S.A.* **1996,** 93, 8618-8623.
24. Chari, R. V. J. Targeted Delivery of chemotherapeuitcs: tumor-activated prodrug therapy. *Adv. Drug Deliv. Rev.* **1998,** 31, 89-104.
25. Chari, R. V. J. Targeted cancer therapy: conferring specificity to cytotoxic drugs. *Acc. Chem. Res.* **2008,** 41, 98-107.
26. Tolcher, A. W.; Ochoa, L.; Hammond, L. A.; Patnaik, A.; Edwards, T.; Takimoto, C.; Smith, L.; de Bono, J.; Schwartz, G.; Mays, T.; Jonak, Z. L.; Johnson, R.; DeWitte, M.; Martino, H.; Audette, C.; Maes, K.; Chari, R. V.; Lambert, J. M.; Rowinsky, E. K. Cantuzumab Mertansine, a Maytansinoid Immunoconjugate Directed to the CanAg Antigen: A Phase I, Pharmacokinetic, and Biologic Correlative Study *J. Clin. Oncol.* **2003,** 21, 211-222.
27. Widdison, W. C.; Wilhelm, S. D.; Cavanagh, E. E.; Whiteman, K. R.; Leece, B. A.; Kovtun, Y.; Goldmacher, V. S.; Xie, H.; Steeves, R. M.; Lutz, R. J.; Zhao, R.; Wang, L.; Blattler, W. A.; Chari, R. V. J. Semisynthetic Maytansine Analogues for the Targeted Treament of Cancer. *J. Med. Chem.* **2006,** 49, 4392-4408.
28. Erickson, H. K.; Park, P. U.; Widdison, W. C.; Kovtun, Y. V.; Garrett, L. M.; Hoffman, K.; Lutz, R. J.; Goldmacher, V. S.; Blätter, W. A. Antibody-Maytansinoid conjugates are activated in targeted cancer cells by lysosomal degradation and linker-dependent intracellular processing. *Cancer Res.* **2006,** 66, 4426-4433.
29. Ranson, M.; Sliwkowski, M. X. Perspectives on anti-HER monoclonal antibodies. *Oncology* **2002,** 63, 17-24.
30. Polson, A. G.; Calemine-Fenaux, J.; Chan, P.; Chang, W.; Christensen, E.; Clark, S.; de Sauvage, F. J.; Eaton, D.; Elkins, K.; Elliott, J. M.; Frantz, G.; Fuji, R. N.; Gray, A.; Harden, K.; Ingle, G. S.; Kljavin, N. M.; Koeppen, H.; Nelson, C.; Prabhu, S.; Raab, H.; Ross, S.; Stephan, J.-P.; Scales, S. J.; Spencer, S. D.; Vandlen, R.; Wranik, B.; Yu, S.-F.; Zheng, B.; Ebens, A. Antibody-drug conjugates for the treatment of non-Hodgkin's lymphoma: Target and linker-drug selection. *Cancer Res.* **2009,** 69, 2358-2364.
31. Kovtun, Y. V.; Audette, C. A.; Ye, Y.; Xie, H.; Ruberti, M. F.; Phinney, S. J.; Leece, B. A.; Chittenden, T.; Blätter, W. A.; Goldmacher, V. S. Antibody-drug conjugates designed to eradicate tumors with homogenous and heterogeneous expression of the target antigen. *Cancer Res.* **2006,** 66, 3214-3221.
32. Lewis Phillips, G. D.; Li, G.; Dugger, D. L.; Crocker, L. M.; Parsons, K. L.; Mai, E.; Blätter, W. A.; Lambert, J. M.; Chari, R. V.; Lutz, R. J.; Wong, W. L. T.; Jacobson, F. S.; Koeppen, H.; Schwall, R. H.; Kenkare-Mitra, S. R.; Spencer, S. D.; Sliwkowski, M. X. Targeting HER2-Positive Breast Cancer with Trastuzumab-DM1, an Antibody–Cytotoxic Drug Conjugate. *Cancer Res.* **2008,** 68, 9280-9290.

33. Fishkin, N.; Maloney, E. K.; Chari, R. V. J.; Singh, R. A novel pathway for maytansinoid release from thioether linked antibody-drug conjugates (ADCs) under oxidative conditions. *Chem. Commun.* **2011,** 47, 10752-10754.
34. Ojima, I. Use of Fluorine in the Medicinal Chemistry and Chemical Biology of Bioactive Compounds-A Case Study on Fluorinated Taxane Anticancer Agents. *ChemBioChem* **2004,** 5, 628-635.
35. Ojima, I. Guided Molecular Missiles for Tumor-Targeting Chemotherapy-Case Studies Using the Second-Generation Taxoid as Warheads. *Acc. Chem. Res.* **2008,** 41, 108-119.
36. Kigawa, J., Minagawa, Y., Kanamori, Y., Itamochi, H., Cheng, X., Okada, M., Oisho, T., Terakawa, N. Glutathione concentration may be a useful predictor of response to second-line chemotherapy in patients with ovarian cancer. *Cancer* **1998,** 82, 697-702.
37. Ojima, I. Tumor-targeting drug delivery of chemotherapeutic agents. *Pure Appl. Chem.* **2011,** 83, 1685-1698.
38. Ojima, I.; Zuniga, E. S.; Berger, W. T.; Seitz, J. D. Tumor-targeting drug delivery of new-genreation taxoids. *Future Med. Chem.* **2012,** 4, 33-50.
39. Banerjee, P. S.; Zuniga, E. S.; Ojima, I.; Carrico, I. S. Targeted and armed oncolytic adenovirus via chemoselective modification. *Bioorg. & Med. Chem. Lett.* **2011,** 21, 4985-4988.
40. Bordwell, F. G., Fried, H.E. Heterocyclic aromatic anions with 4n + 2 pi-electrons. *J. Org. Chem.* **1991,** 56, 4218-4223.
41. Shaabani, A.; Tavasoli-Rad, F.; Lee, D. G. Potassium Permanganate Oxidation of Organic Compounds. *Syn. Comm.* **2005,** 35, 571 - 580.
42. Samukov, V. V. A Simple Preparation of 3-(2-Pyridyldithio)-Propionic Acid. *Syn. Comm.* **1998,** 28, 3213 - 3217.
43. Olah, G.; Karpeles, R.; Narang, S. Synthetic methods and reactions: 107. Preparation of omega-haloalkylcarboxylic acids and esters or related compounds from lactones and boron trihalides. *Synthesis* **1982,** 11, 963-965.
44. Crabb, T.; Trethewey, A. Compounds with bridgehead nitrogen. Part 54. The stereochemistry of some derivatives of perhydrothiazolo[3,4-a]pyridine and the synthesis of 9-methylperhydro-3,8,methano-1,3-thiazocines. *J. Chem. Soc., Perkin Trans I* **1988,** 5, 1173-1178.
45. Sobik, P.; Grunenberg, J.; Brczky, K.; Laatsch, H.; Wagner-Dbler, I.; Schulz, S. Identification, synthesis, and conformation of tri- and tetrathiacycloalkanes from Marine Bacteria. *J. Org. Chem.* **2007,** 72, 3776-3782.
46. Pereira, D.; Hai, T. T.; Nelson, D. A Convenient Large Scale Synthesis of N,N'-Disuccinimidyl Carbonate. *Syn. Comm.* **1998,** 28, 4019-4024.
47. Sauer, L. A., Dauchy, R.T., Blask, D.E. Mechanism for the antitumor and anticachectic effects of n-3 fatty acids. *Cancer Res.* **2000,** 60, 5289-5295.
48. Grammatikos, S. I., Subbaiah, P.V., Victor, T.A., Miller, W.M. n-3 and n-6 fatty acid processing and growth effects in neoplastic and non-cancerous human mammary epithelial cell lines. *Brit. J. Cancer* **1994,** 70, 219-227.
49. Diomede, L., Colotta, F., Piovani, B., Re, F., Modest, E.J., Salmona, M. Induction of apoptosis in human leukemic cells by the ether lipid 1-octadecyl-2-methyl-racglycero-3-phosphocholine. A possible basis for its selective action. *Int. J. Cancer Res.* **1993,** 53, 124-130.
50. Gottlieb, H. E.; Kotlyar, V.; Nudelman, A. NMR Chemical Shifts of Common Laboratory Solvents as Trace Impurities. *J. Org. Chem.* **1997,** 62, 7512-7515.
51. Dickinson, R. P., Iddon, B. Condensed Thiophen Ring Systems. Part III. A New Synthesis of Benzo[b]thiophen-2(3H)- and - 3(2H)-ones and Some Reactions of

Benzo[b]thiophen-2(3H)-one with Dimethyl Sulphate in the Presence of Base. *J. Chem. Soc.* **1970,** 14, 1926-1928.
52. Charles, M. Überführung des Oxindols in das 2-Keto-dihydro-1-thionaphthen (»Thio-oxindol«). *Chem. Ber*. **1912,** 45, 1481-1485.
53. Chari, R. V. J.; Widdison, W. C. Methods for preparation of cytotoxic conjugates of maytansinoids and cell binding agents. 2003.

Chapter 5

Vitamins as Tumor-Targeting Modules

Chapter Contents

§ 5.1.0 Introduction

§ 5.1.1 Vitamins

The lack of tumor-specificity in conventional chemotherapeutic agents has been a longstanding problem, resulting in undesirable and severe side effects. A solution to this problem lays in the unique biological properties of tumor cells, as a number of oncogenes, suppressor oncogenes and signaling pathways have been identified, which can be exploited as tumor-specific drug targets. One means in which targeted chemotherapy can be achieved is through the development of tumor-targeting drug conjugates. Tumor-targeting drug conjugates consists of one or multiple cytotoxic drugs connected to a tumor-targeting module (TTM) via cleavable covalent bonds or cleavable linkers. The drug conjugate has been designed to remain inactive until it is specifically delivered to the tumor site by the TTM and internalized, where the warhead is released from the carrier and restored to its original activity. Many cancer cells overexpress tumor-specific receptors that have been used as targets to deliver warheads. For example, monoclonal antibodies (mAbs),[1-5] transferrin[6-8] and vitamins, such as biotin[9-15] and folic acid,[16-20] have been used as TTMs in drug conjugate development, as each targets a specific protein receptor on tumor cell surface.

Vitamins are required by all living cells for survival, but cancer cells in particular need certain vitamins and nutrients to sustain their rapid growth and proliferation, e.g., vitamin B12, folic acid, biotin and ribofravin are all essential for cell division. Therefore, the vitamin receptors are overexpressed on the cancer cell surface for uptake of necessary vitamins.[9] Accordingly, these vitamin receptors serve as useful targets for tumor-targeting drug delivery as well as biomarkers for identification and imaging of cancer cells. Among vitamin receptors, folate and biotin receptors have been shown to be important and relevant targets in a number of cancer cell lines.

§ 5.1.2 Folic Acid

Folic acid (vitamin B_9), mostly in the form of folate, is essential for DNA synthesis, DNA repair, DNA methylation, RNA synthesis, as well as a number of other biological processess.[21] Furthermore, folate is important in cell division and cell proliferation. It is worthy of note that folate becomes biologically active only after it is converted to dihydrofolic acid in the liver. Tetrahydrofolate and other folate derivatives are responsible for the biological activity of folate.

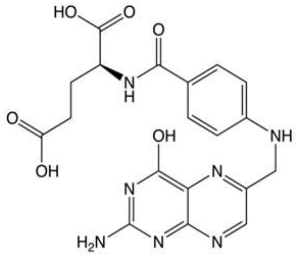

Folic Acid

Figure 5.1: Chemical structure of folic acid

Folate is not endogenously produced in mammalian cells. Thus, most mammalian cells obtain folate through low affinity reduced folate carriers, proton-coupled folate transporters or folate receptor on the cell surface.[20, 22] Various cancer cells overexpress the folate receptor, as a consequence of their increased requirement for folic acid. The folate receptor was recognized as an excellent target for tumor-targeting drug delivery.[16, 19, 20, 23-25] Accordingly, folate has been used as the TTM for the development of a number of drug conjugates, thereby enhancing the tumor-specific delivery of cytotoxic agents, such as paclitaxel, mitomycin, and maytansine, among others.[16, 25-31]

Folate-targeting ^{99m}Tc-based radioimaging was used to evaluate which cancer cells aggressively up-regulate the folate receptor (Table 5.1).[19] It was found that ovarian, lung, kidney, endometrial, breast, brain, colon carcinomas and myeloid cells of hematopoetic lineage regularly overexpress the folate receptor. It is worthy of note that folate-drug conjugates retain a high binding affinity towards the folate receptor, but do not have affinity towards the low affinity reduced folate carriers and proton-coupled folate transporters found on the majority of normal cells.

Table 5.1: Evaluation of Folate Receptor Up-Regulation in Various Cancer Cells (adapted from [19])

cancer	% FR^+	number of cases examined
ovarian	82	488
lung (NSCLC: non-small-cell carcinoma)	66	511
endometrial	64	148
renal cell carcinoma (RCC)	64	310
colorectal	34	314
breast	29	380
nonfunctional pituitary adenoma (NFPA)	100	20
thyroid	48	23
cervical	30	23
lung metastases	30	23
lung (SCLC: small-cell lung carcinoma)	25	24
mesothelioma	21	38

§ 5.1.3 Biotin

Biotin (vitamin B_7 or vitamin H) is essential for cell division, cell growth, fatty acid production, metabolism of fats and amino acids and plays a role in energy production,[32] which makes it essential for rapidly dividing cancer cells. Biotin is not naturally produced in mammalian cells and is obtained through external sources via intestinal absorption. Rapidly dividing cells readily uptake vitamins, such as biotin, to maintain their rapid proliferation. In contrast to the folate receptors, the biotin receptors have not been studied until it was reported in 2004 that these receptors were even more overexpressed than the folate and vitamin B_{12} receptors in a variety of cancer cells.[9] Thus, the biotin receptor has emerged as a new target for tumor-targeting drug delivery.

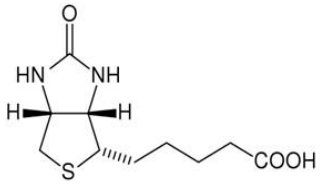

Biotin

Figure 5.2: Chemical structure of biotin

It has been shown that many types of cancer cells overexpress the receptor for biotin.[9] Russell-Jones et al. examined the uptake of vitamin-targeted rhodamine-labeled polymers in various cancer cell lines. These vitamins included folate, vitamin B12 (Cbl) and biotin. The results from this experiment are presented in Table 5.2.

Table 5.2: The Internalization of Vitamin-Targeted Rhodamine-Labeled Polymers in Various Cancer Cell Lines (adapted from [9])

Tumor	Mouse	Type	Folate	Vitamin B_{12}	Biotin
O157	Balb/C	Bcell lymph	+/-	+/-	+/-
BW5147	AKR/J	Lymphoma	+/-	+/-	+/-
HCT-116	Balb/C-Nu	Colon	-	-	-
L1210	DBA/2	Leukemia	+/-	+/-	-
L1210FR	DBA/2	Leukemia	++	+++	+++
Ov 2008	Balb/C-Nu	Ovarian	+++	-	++
ID-8	C57/B1	Ovarian	+++	-	++
Ovcar-3		Ovarian	+++	-	++
Colo-26	Balb/C	Colon	+/-	++	+++
P815	DBA/2	Mastocytoma	+/-	++	+++
M109	Balb/C	Lung	+	+++	+++
RENCA	Balb/C	Renal Cell	+	+++	+++
RD995	C3H/HeJ	Renal Cell	+	++	+++
4T1	Balb/C	Breast	+	++	+++
JC	Balb/C	Breast	+	++	+++
MMT060562	Balb/C	Breast	+	++	+++

As shown on the table O157, BW5147 and HCT-116 cell lines showed no enhancement of uptake with any of the targeting agents, whereas, L1210FR, Ov2008, ID-8 and Ovcar-3 cell lines showed enhanced uptake of folate and biotin-targeted polymers.[9] Furthermore, Colo-26, P815, M109, RENCA, RD995, 4T1, JC and MMT060562 cell lines showed enhanced uptake of vitamin B12 and biotin-labeled polymers.[9] It is worthy of note that cells which overexpress the folate receptor or the vitamin B12 receptor, also overexpress the biotin receptor.

It has been established that biotin receptors are overexpressed on the cell surfaces of a number of cancer cell lines. Accordingly, biotin has been incorporated into a number of tumor-targeting conjugates as TTM. For example, biotin-PEG-camptothecin drug conjugates were prepared which significantly enhanced the in vitro cytotoxic activity of camptothecin by enhancing the drug conjugate uptake via the sodium-dependent multivitamin transporter.[33] Furthermore, biotin has been conjugated to catchol polymers for the tumor specific delivery of bortezomib to cancer cells.34 Biotin has also been used as the TTM for nanoparticle- and

PAMAM dendrimer-based drug delivery systems (DDSs).[35-37] The Ojima laboratory previously developed taxoid-based drug conjugates and SWNT-based DDSs that contain biotin as TTM.[11-15] These drug conjugates and DDSs were shown to be internalized into cancer cells via receptor-mediated endocytosis (RME), specifically delivering the cytotoxic taxoids to cancer cells.

§ 5.1.4 Receptor-Mediated Endocytosis

Vitamin-drug conjugates should be internalized into cancer cells via RME (Figure 5.3).[11, 15] The binding of the vitamin module to its receptor initiates a signaling cascade, which leads to the formation of a membrane invagination. The vitamin-receptor complex is encapsulated into a coated vesicle and individual vesicles fuse to form the early endosome. In the endosome, the vitamin-drug conjugate is released from the receptors and the receptors are recycled to the cell surface. In the endosome or lysosome, the vitamin-drug linkage is cleaved by endogenous enzymes, lower pH or reducing substances, such as glutathione, to release the drug in its active form. Then, the drug released from lysosome attacks its target protein.

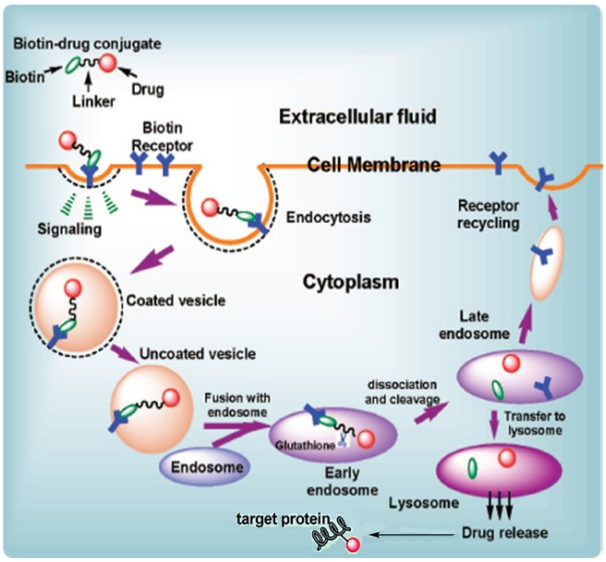

Figure 5.3: Receptor-Mediated Endocytosis (adapted from [11])

The Ojima lab has conducted a mechanistic study for the validation of tumor-targeting drug delivery by monitoring the internalization through receptor-mediated endocytosis and drug release of several fluorescence-labeled biotin conjugates.[11, 13-15] For this study, biotin-fluorescein was designed and synthesized to observe RME. A biotin-linker-coumarin conjugate was designed and synthesized to confirm internalization via RME and release of coumarin after internalization via disulfide cleavage, as coumarin becomes fluorescent when it is released as a free molecule. A third conjugate, biotin-SB-T-1214-fluorescein conjugate was designed and synthesized to validate the internalization of a biotin-drug conjugation via RME and drug release via the GSH-mediated self-immolation of the disulfide linker, in which the taxoid-fluorescein molecule is released to target microtubules.

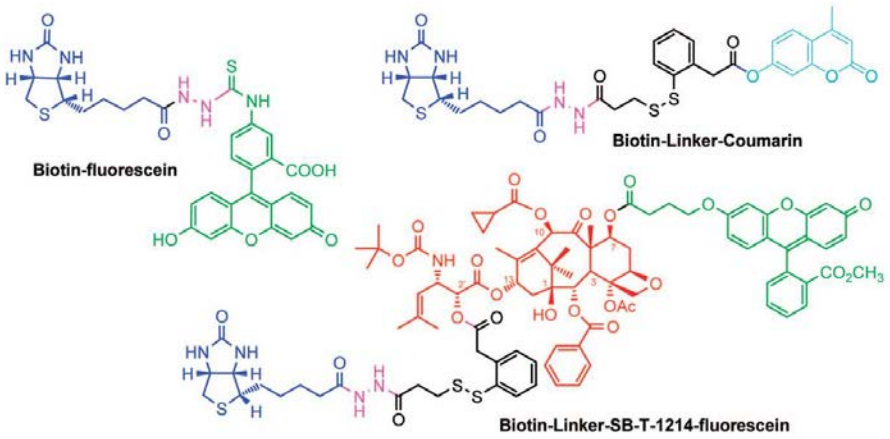

Figure 5.4: Fluorescein-labeled probes for evaluation of biotin-receptor overexpression (adapted from [11, 13-15])

The cellular uptake of the fluorescently labeled conjugates was monitored by confocal fluorescence microscopy (CFM) and fluorescence activated cell sorting (FACS).[11, 13-15] After the administration of 100 nM biotin-fluorescein to L1210FR cells at 37 °C for 3 h, and thorough washing with DPBS, CFM analysis shows the internalization of this fluorescent probe into the leukemia cells. To confirm that endocytosis is an energy-dependent process, L1210FR cells were treated with 100 nM biotin-fluoresein and incubated at 4 °C for 3 h. Both CFM and FACS analysis show a decrease of fluorescence-activity in the cells, which clearly indicates that the fluorescence probe was internalized through endocytosis. To further confirm that probe internalization was done through RME, excess 2 mM free biotin molecules were preincubated for 1 h to saturate the biotin receptors on the cancer cell surface, followed by the addition of 100 nM biotin-fluorescein probe at 37 °C for 3 h. Both CFM and FACS analysis show an almost complete absence of fluorescence, which confirms that probes were internalized via RME.[11, 13-15]

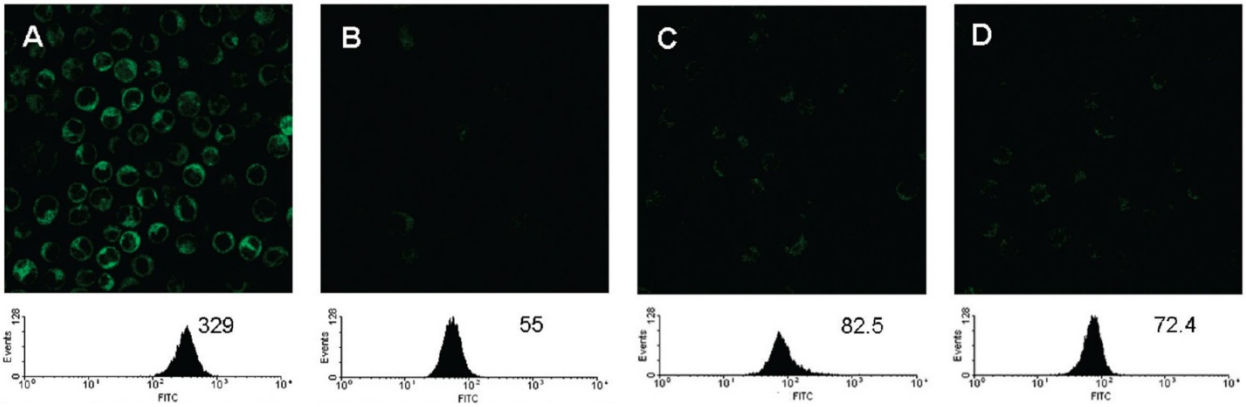

Figure 5.5: CFM images and FACS analysis of biotin-fluorescein in L1210FR cells. (A) 100 nM biotin-fluorescein incubated in L1210FR cells at 37 °C for 3 h; (B) 100 nM biotin-fluoresein incubated in L1210FR cells at 4 °C for 3 h; (C-D) 2 mM biotin incubated in L1210FR cells at 37 °C for 1 h then incubated with 100 nM biotin-fluorescein at 37 °C for 3 h (adapted from [11, 13-15])

To evaluate biotin-linker conjugate internalization and linker cleavage 1 μM biotin-linker-coumarin conjugate was incubated with L1210FR at 37 °C for 3 h.[11, 13-15] After washing thoroughly with DPBS, 2 mM glutathione ethyl ester was added to the medium, to assure

cleavage of the disulfide bond, and cells were incubated for an additional 2 h at 37 °C. As shown from the CFM image, coumarin molecules were released in the leukemia cells, as indicated by the blue fluorescence. This result confirms that the intracellular drug release via cleavage of the disulfide linkage by glutathione and the subsequent thiolactonization took place.[11, 13-15]

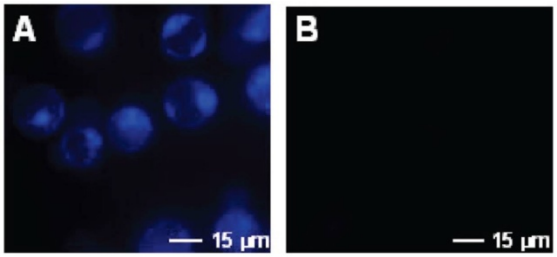

Figure 5.6: CFM image of biotin-linker-coumarin in L1210FR cells. (A) 1 µM biotin-linker-coumarin incubated with L1210FR at 37 °C for 3 h, followed by addition of 2 nM GSH-ethyl ester; (B) 1 µM biotin-linker-coumarin incubated with L1210FR at 37 °C for 3 h with no GSH added (adapted from [11, 13-15])

To evaluate biotin-drug conjugate internalization and drug release, L1210FR cells were treated with 20 µM biotin–linker–SB-T-1214-fluorescein conjugate and incubated at 37 °C for 3 h.[11, 13-15] As CFM images show, the biotin-drug conjugate was internalizied via RME. To mediate disulfide linker cleavage via thiolactonization, 2 mM glutathione ethyl ester was added to the medium and the cells were incubated for an additional 1 h to assure drug release. The CFM image indicates that released fluorescence-labeled taxoid binds to the microtubules.[11, 13-15]

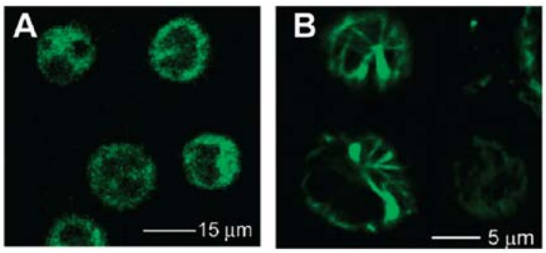

Figure 5.7: CFM image of biotin-linker-SB-T-1214-fluorescein in L1210FR cells. (A) 20 µM biotin–linker–SB-T-1214-fluorescein incubated with L1210FR at 37 °C for 3 h; (B) 20 µM biotin–linker–SB-T-1214-fluorescein incubated with L1210FR at 37 °C for 3 h, followed by addition of 2 mM GSH-ethyl ester (adapted from [11, 13-15])

Using these three fluorescence-labeled biotin conjugates, the Ojima research group confirmed that biotin is internalized into cancer cells via RME.[11, 13-15] Furthermore, biotin-linker-drug conjugates also internalize via RME and in the presence of a free thiol-containing molecule, the 2nd-generation disulfide linker is cleaved releasing the drug. Thus the mechanism-based drug release and tumor-targeting drug delivery and internalization have been validated, making disulfide linkers a suitable linker moiety and biotin a suitable TTM.

§ 5.2.0 Results and Discussion

§ 5.2.1 Synthesis and Biological Evaluation of Biotin-Me-Linker-Taxoid Drug Conjugate

Biotin, a commercially available compound that is stable in a number of chemical transformations, contains a valeric acid moiety attached to a fused ring system. Conversion of biotin into biotin-hydrazide begins with the conversion of the free carboxylic acid into a methyl ester in the presence of methanol and thionyl chloride, followed by treatment with hydrazine to afford biotin-hydrazide (Scheme 5.1).

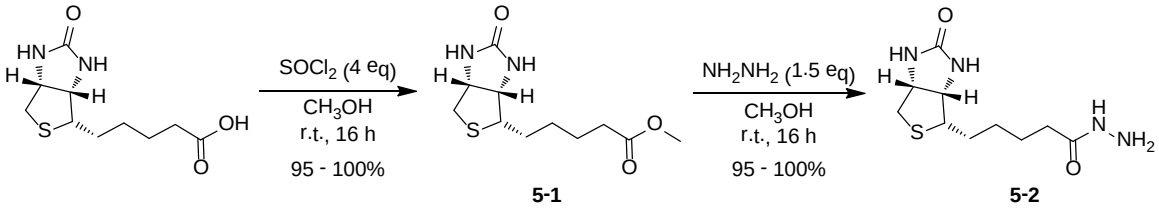

Scheme 5.1: Synthesis of biotin-hydrazide

Biotin methyl ester (**5-1**) was obtained in excellent to quantitative yields after distillation of excess methanol and thionyl chloride. Conversion of **5-1** to biotin-hydrazide (**5-2**) was also obtained in excellent yields. Both **5-1** and **5-2** can be stored under N_2 at room temperature for long periods of time without any sign of decomposition. Treatment of SB-T-1214-Me-linker-OSu (**4-20**) with **5-2** gives tumor-targeting drug conjugate biotin-Me-linker-SB-T-1214 (**5-3**) (Scheme 5.2).

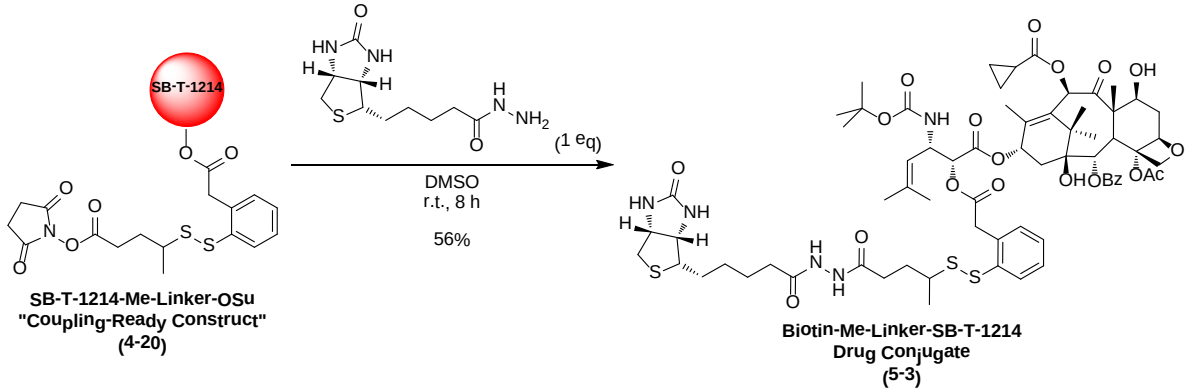

Scheme 5.2: Synthesis of biotin-Me-linker-SB-T-1214 drug conjugate

Due to a lack of solubility of **5-2**, the coupling reaction was done using DMSO as solvent. Excess **4-20** was used for the coupling, however, the reaction was slow and gave the desired drug conjugate **5-3** in moderate yield (56%). Using dichloromethane and pyridine as co-solvents for the reaction may increase the rate of the reaction and conversion to **5-3**. The use of this co-solvent system has been explored in similar coupling reactions to be mentioned later. The biological evaluation of **5-3** was evaluated against CT-26 (murine colon) and these results were compared with those obtained for MX-1 (human breast) cancer cell lines. These results are listed in Table 5.3. CT-26, also known as Colo-26, was chosen as a control cell line because it was shown that CT-26 cells overexpress the biotin receptor.[9]

Table 5.3: Biological Evaluation of Biotin-Me-Linker-SB-T-1214 against Various Cancer Cell Lines

Taxane	Time of Incubation with drug (h)	Time of Incubation with GSH-OEt (h)	IC_{50} (nM) CT-26	IC_{50} (nM) MX-1
Paclitaxel[a]	**48**	**-**	>5000	0.54 ± 0.19
SB-T-1214[a]	**48**	**-**	0.41 ± 0.15	0.38 ± 0.17
biotin-linker-SB-T-1214[a]	**48**	**-**	16.4 ± 5.1	0.33 ± 0.04
biotin-linker-SB-T-1214[b]	**72**	**-**	4.92 ± 0.25	0.27 ± 0.03
biotin-linker-SB-T-1214[c]	**6**	**48**	413 ± 76	0.15 ± 0.05

[a] Cells were incubated for 48 hours at 37 °C with 5% CO_2 after administration of taxoid; [b] Cells were incubated for 72 hours at 37 °C with 5% CO_2 after administration of taxoid; [c] Cells incubated for 6 hour at 37 °C with 5% CO_2 after administration of biotin-Me-linker-SB-T-1214, washed with DPBS, resuspended in RPMI with 2 eq. GSH-OEt and incubated for 48 hours at 37 °C with 5% CO_2

- Cells were suspended in RPMI-1640 Medium 10 x (Sigma Aldrich, R1145) supplemented with tissue culture grade water, 0.3 g/L L-glutamine, 2.0 g/L sodium bicarbonate, 10% FBS, and 1% Penn Strep before administration of taxoid
- The optical density was determined using Acsent Multiskan optical density reader
- The reported values are a calculated averages of IC_{50} values determined from three individual experiments
- IC_{50} values were calculated using SigmaPlot v 10.0
- All IC_{50} values are report in nM scale unless otherwise noted

As seen from Table 5.3, biotin-Me-linker-SB-T-1214 (**5-3**) shows good activity in CT-26 and excellent activity against MX-1 after 48 and 72 hour incubations, suggesting that the drug conjugate was successfully internalized via biotin receptor-mediated endocytosis and that both cell lines have enough intracellular GSH or thiol-containing protein to cleave the disulfide bond, thereby, eliciting the potent activity of free SB-T-1214. Surprisingly, the addition of glutathione ethyl ester (GSH-OEt), an additive meant to assure linker cleavage, quenched the activity of **5-3** against CT-26 cells. This result indicates that glutathione may have beneficial and life-prolonging affects in the murine cancer cell line. Whereas, the activity of **5-3** is amplified when GSH-OEt was added to MX-1 cells previously incubated with the drug conjugate. The results obtained from MX-1 suggest: (1) MX-1 cells overexpress the biotin receptor; (2) the activity of **5-3** is greater than paclitaxel and on par with SB-T-1214, without the addition of GSH, thus marking the possible use of **5-3** for in vivo assays; and (3) the addition of GSH-OEt to MX-1 cells previously incubated with **5-3** increased the activity of the drug conjugate, which clearly indicates that the excess GSH cleaved the disulfide bond, releasing the free taxoid inside the cell.

§ 5.2.2 Synthesis of Folate-Me-Linker-NSC 706744 Drug Conjugate

As mentioned in Chapter 3, NSC 706744 is a non-camptothecin, topoisomerase I inhibitor, which was supplied by NCI with the purpose of preparing and evaluating the biological activity of tumor-targeting drug conjugates containing the drug.[38-40] The synthesis of PUFA-NSC 706744 drug conjugates was difficult due to the instability of the PUFA and drug conjugate. To counter this problem, vitamins were chosen as TTM, as they are not susceptible to oxidation and can withstand harsh reaction conditions. The synthesis of Folate-Me-linker-NSC 706744 drug conjugate begins with the coupling of NSC 706744 to 2nd-generation disulfide linker, **4-13**, using DIC-mediated coupling conditions (Scheme 5.3).

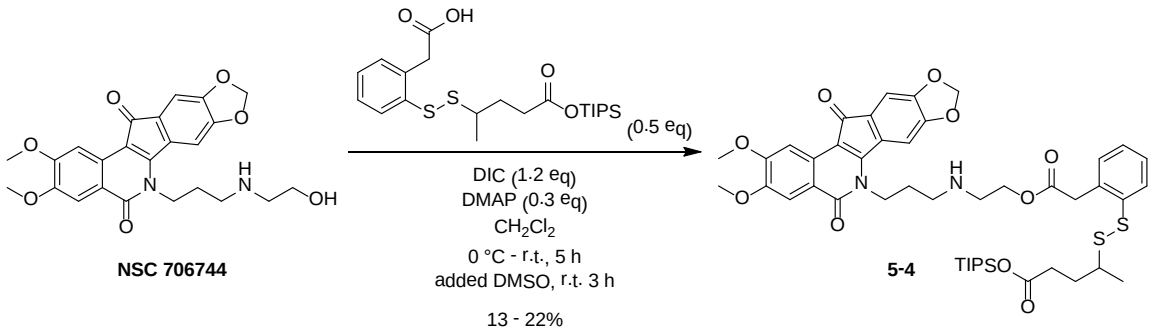

Scheme 5.3: NSC 706744-Me-linker coupling

Due to the poor solubility of NSC 706744, DMSO was used as a co-solvent for the reaction. Despite the addition of DMSO, NSC 706744 was not completely dissolved, as the reaction mixture was cloudy throughout its duration. Furthermore, the reaction is messy resulting in the generation of several side products. The coupled drug-linker product **5-4** was obtained in low yields (13-22%) on multiple attempts. Some unreacted starting material can be obtained via filtration of the reaction mixture. Additional starting material can be obtained through lyophilization of the filtrate, however recovered material is impure and difficult to purify. The product **5-4** is soluble in organic solvents such as dichloromethane, acetonitrile and ethyl acetate, thus can be purified via column chromatography.

The deprotection of the TIPS ester was investigated using two fluoride sources: (1) CsF which may provide a faster deprotection and an easier work-up after the reaction is complete (Scheme 5.4); and (2) HF in pyridine, a standard silyl group deprotection reagent, which requires removal of pyridine (Scheme 5.5).

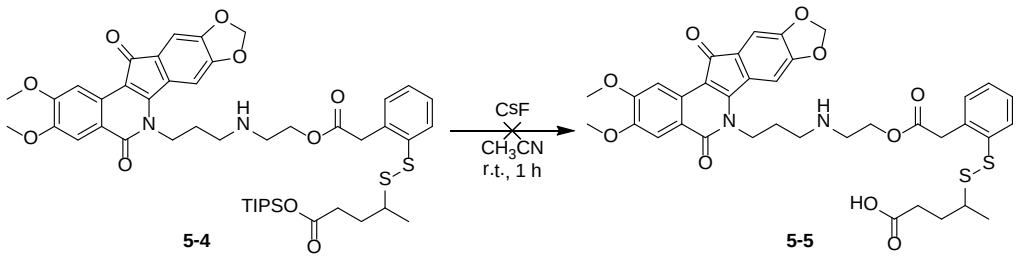

Scheme 5.4: Attempted deprotection of NSC 706744-Me-linker-TIPS

Silyl-deprotection using CsF proved to be a messy reaction resulting in the formation of the desired product and two additional side products based on TLC. These products were not isolated due to the scale of the reaction. However, the use of HF in pyridine yielded the deprotected product **5-5** with minimal impurities (Scheme 5.5).

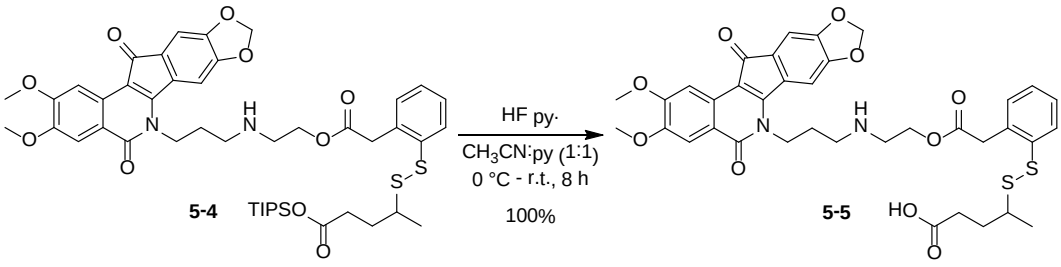

Scheme 5.5: 2nd attempted deprotection of NSC 706744-Me-linker-TIPS

The silyl-deprotection of **5-4** using HF in pyridine afforded **5-5** in quantitative yield. Removal of excess pyridine was done via extraction with $CuSO_4$. Following aqueous wash and concentration of organic materials **5-5** was obtained and used in the subsequent step without further purification. Conversion of the carboxylic acid **5-5** to activated ester **5-6** was achieved using standard peptide coupling conditions in the presence of HOSu (Scheme 5.6).

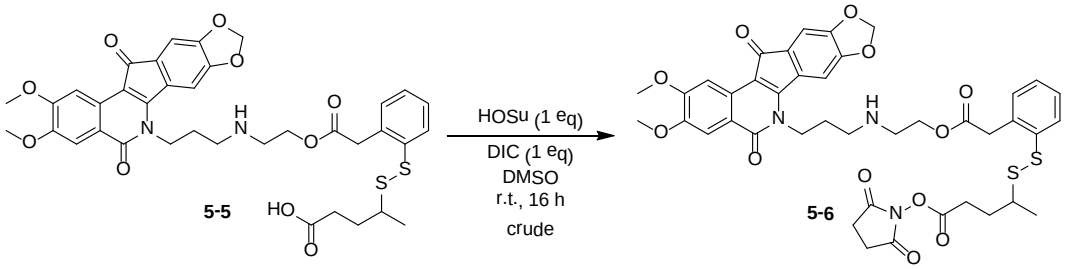

Scheme 5.6: NSC 706744-Me-linker OSu activation

The esterification of **5-5** was slow and messy, leading to unreacted starting material and the formation of diisopropylurea, each having similar R_f values on TLC, making purification difficult. Accordingly, **5-6** was used crude without purification in the coupling with folate-hydrazide (Scheme 5.7).

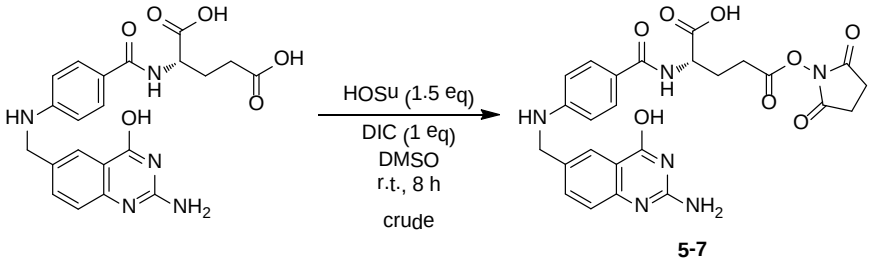

Scheme 5.7: Folic acid OSu activation

It is well understood that folic acid is synthetically difficult to work with, as it is insoluble in most organic solvents and only soluble in DMSO. Thus the conversion of folic acid to folate-OSu **5-7** was done in DMSO. Purification of reaction crude was done by washing with ethyl acetate (to wash off the diisopropylurea) and THF (to wash off the unreacted HOSu). Despite the washes, ^{1}H NMR of the compound showed the presence of both the urea and HOSu. Thus, the compound was used crude in the conversion to folate-hydrazide amide using hydrazine (Scheme 5.8).

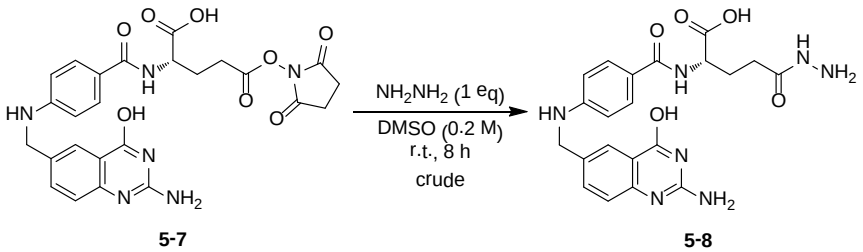

Scheme 5.8: Synthesis of folate-hydrazide

The formation of **5-8** and complete conversion of folate-OSu was confirmed via mass spectroscopy. However, **5-8** was not isolated. It is worthy of note that isolation can be achieved via lyophilization of reaction solvent and purification can be done via washing with organic solvents. Accordingly, the reaction solution containing **5-8** was directly added dropwise to a DMSO solution containing crude **5-6** (Scheme 5.9).

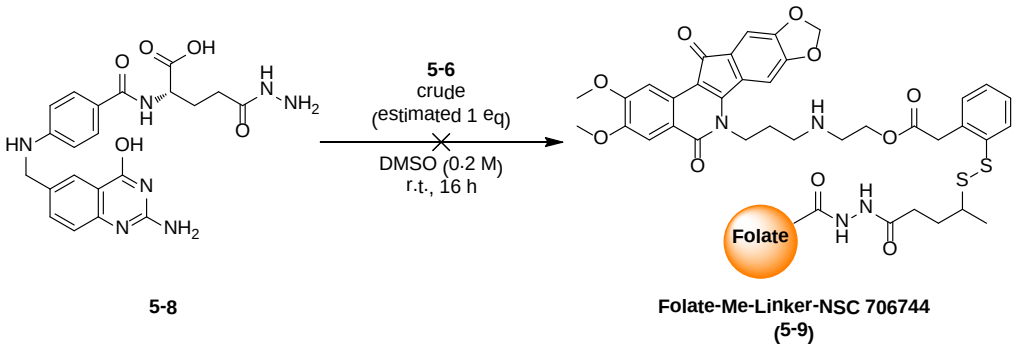

Scheme 5.9: Attempted synthesis of folate-Me-linker-NSC 706744 drug conjugate

The coupling of **5-8** to **5-6** was monitored by mass spectroscopy. However, after 16 hours no desired product was observed. Due to difficulties in handling folic acid, NSC 706744 and their derivatives, biotin was chosen as an alternative TTM for the development of vitamin-linker-NSC 706744 drug conjugate. The synthesis of **5-9** may be improved by the use of preparative HPLC for intermediate purification. However, low solubility of both folic acid and NSC 706744 may also make HPLC purification difficult. The improved synthesis and purification of folic acid derivatives is currently being investigated.

§ 5.2.3 Synthesis of Biotin-Me-Linker-NSC 706744 Drug Conjugate

The use of DMSO as a solvent is problematic considering the fact that any unreacted starting material will be difficult to recover. Accordingly, the preparation of the biotin-linker-NSC 706744 conjugate was done by first attaching biotin onto the linker moiety and then conjugating the drug compound onto the biotin-linker. Biotin-hydrazide (**5-2**) was coupled to **5-10** [**5-10** was obtained by treating 3-methyl-3-(pyridin-2-yldisulfanyl)butanoic acid (**4-15**) with DIC in the presence of HOSu] (Scheme 5.10).

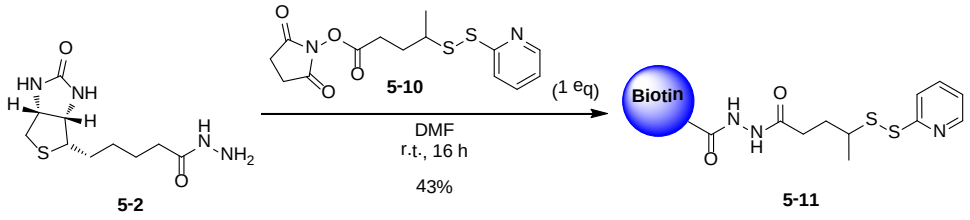

Scheme 5.10: Synthesis of biotinylated linker intermediate

The coupling of **5-2** to **5-10** afforded **5-11** in moderate yield (43%). The pyridinyl moiety provides a good leaving good for a thiol-disulfide exchange. However, the incorporation of

biotin changes the solubility of the compound. This has ramifications in the subsequent thiol-disulfide exchange. However, treating **5-11** with sulfhydrylphenylacetic acid yields the desired biotinylated disulfide linker (Scheme 5.11).

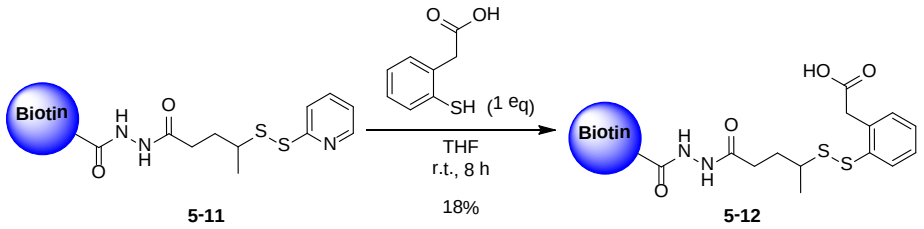

Scheme 5.11: Synthesis of biotin-linker

The thiol-disulfide exchange afforded the biotinylated disulfide linker, **5-12**, in low yield (18%). If is reasonable to assume that the low solubility of **5-11** in THF resulted in the low yield. In addition, the biotin side-chain may have hindered the reaction, as the "long-chain" **5-11** may have folded back on itself, thus blocking the reactive sulfide bond. The coupling of **5-12** to NSC 706744 was done in the presence of DIC and DMAP in DMSO (Scheme 5.12).

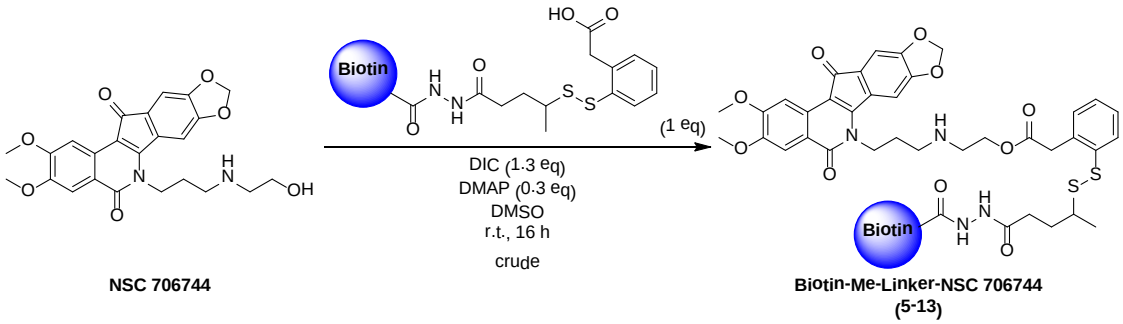

Scheme 5.12: Synthesis of biotin-linker-NSC 706744 drug conjugate

The coupling of **5-12** to NSC 706744 was messy resulting in the formation of seven products based on TLC. As with other NSC 706744 derivatives, the isolation and purification of **5-13** was difficult, as isolated fractions were analyzed by mass spectroscopy, however the desired mass peak was not a major peak. Thus, no further purification was attempted. We hypothesize that the polyamine side chain of NSC 706744 hinders the reactivity of the compound and alters the stability of conjugates formed with the compound. Accordingly, changing the side chain to bear different heteroatoms may increase the reactivity of NSC 706744 towards coupling reaction conditions.

§ 5.3.0 Summary

Vitamins, such as biotin and folic acid, are vital for the longevity and maintenance of rapidly dividing cells. Both biotin and folic acid are not endogenously produced in mammalian cells. Thus, rapidly dividing cells, such as cancer cells, greedily uptake biotin and folic acid obtained through external sources. Through experiments using fluorescently-labeled folate and

biotin, it has been shown that various cancer cells overexpress the folate receptor and the biotin receptor, making both vitamin receptors an excellent target for tumor-targeting drug delivery. Accordingly, folate and biotin have been used as TTMs for the development of drug conjugates which enhance the tumor-specific delivery of cytotoxic agents. Vitamin-drug conjugates are internalized via receptor-mediated endocytosis, as confirmed by the Ojima laboratory using fluorescence-labeled biotin conjugates. Based on these findings, biotin-linker-SB-T-1214 drug conjugate was easily prepared via coupling biotin-hydrazide to taxoid-linker coupling-ready construct. The biological activity of the biotin-linker-taxoid drug conjugate was evaluated against two cancer cell lines. It was shown that the biotin-linker-taxoid drug conjugate demonstrated excellent activity against the cell lines tested. Thus, biotin-linker-SB-T-1214 may also demonstrate excellent activity in preclinical *in vivo* assays. Furthermore, vitamin-linker is a promising carrier for the tumor-specific delivery of cytotoxic agents. The attempted syntheses of vitamin-linker-NSC 706744 drug conjugate were also discussed.

§ 5.4.0 Experimental

Caution

Taxoids and NSC 706744 have been established as a potent cytotoxic agent. Thus, they and all structurally related compounds and derivatives must be considered as mutagens and potential reproductive hazards for both males and females. Appropriate precautions (i.e. use of gloves, goggles, lab coat and fume hood) must be taken while handling these compounds.

General information

All chemical were obtained from Sigma-Aldrich, Fisher Scientific or VWR International, and used as is unless otherwise noted. All reactions were carried out under nitrogen in oven dried glassware using standard Schlenk techniques unless otherwise noted. Reactions were monitored by thin layer chromatography (TLC) using E. Merck 60F254 precoated silica gel plates and alumina plate depending on the compounds. Dry solvents were degassed under nitrogen and were dried using the PURESOLV system (Inovatative Technologies, Newport, MA). Tetrahydrofuran was freshly distilled from sodium metal and benzophenone. Dichloromethane was also distilled immediately prior to use under nitrogen from calcium hydride. Toluene was also distilled immediately prior to use under nitrogen from calcium hydride. Yields refer to chromatographically and spectroscopically pure compounds. Flash chromatography was performed with the indicated solvents using Fisher silica gel (particle size 170-400 Mesh).1H, 13C and 9F data were obtained using either 300 MHz Varian Gemni 2300 (75 MHz 13C, 121 MHz 19F) spectrometer, the 400 MHz Varian INOVA 400 (100 MHz 13C) spectrometer or the 500 MHz Varian INOVA 500 (125 MHz 13C) in CDCl3 as solvent unless otherwise stated. Chemical shifts (δ) are reported in ppm and standardized with solvent as internal standard based on literature reported values.41 Melting points were measured on Thomas Hoover Capillary melting point apparatus and are uncorrected. Optical rotations were measured on Perkin-Elmer Model 241 polarimeter.

Experimental procedure

Biotin methyl ester (5-1)[15, 42]

An emulsion of biotin (100 mg, 0.4 mmol) in CH_3OH [0.1 M] was cooled to 0 °C. To the emulsion was added thionyl chloride (1.6 mmol), dropwise. After the addition was complete, the reaction solution became clear, and the mixture was stirred at room temperature. The reaction was monitored via TLC. After 16 h, the reaction solvent was evaporated to yield **5-1** (110 mg, quant. yield), as an off-white/yellow solid which was used in the next step without further purification: m.p. 164-165 °C (m.p. lit. 166 °C); ^{1}H NMR (300 MHz, CD_3OD, ppm) δ 1.575-1.867 (m, 6 H), 2.473-2.521 (t, J = 3.75 Hz, 2 H), 2.902-2.942 (d, J = 6 Hz, 2 H), 3.108-3.168 (dd, $J_1 = J_2$ = 2.4 Hz, 1 H), 3.415-3.490 (m, 1 H), 3.800 (s, 3 H), 4.575-4.616 (m, 1 H), 4.771-4.813 (m, 1 H), 6.048 (s, 1 H). All data are consistent with literature values.[15, 42]

Biotin-hydrazide (5-2)[15, 42]

To a solution of **5-1** (110 mg, 0.4 mmol) dissolved in CH_3OH [0.2 M] was added anhydrous hydrazine (2 mmol). The mixture was stirred at room temperature and the reaction was monitored via TLC. After 16 h, the reaction solvent was evaporated. The resulting crude was diluted with water and washed with $CHCl_3$ (5 x 20 mL). The aqueous layer was collected and concentrated *in vacuo* to yield **5-2** (110 mg, quant. yield), as a white solid: ^{1}H NMR (400 MHz, DMSO-d_6, ppm) δ 1.223-1.313 (m, 2 H), 1.402-1.612 (m, 4 H), 1.964 (t, J = 7.2 Hz, 2 H), 2.518 (d, J = 12.4 Hz, 1 H), (d, J = 6 Hz, 2 H), 3.108-3.168 (dd, $J_1 = J_2$ = 2.4 Hz, 1 H), 3.415-3.490 (m, 1 H), 4.575-4.616 (m, 1 H), 2.757-2.801 (dd, J_1 = 12.4 Hz, J_2 = 5.2 Hz, 1 H), 3.026-3.073 (m, 1 H), 4.068-4.100 (m, 3 H), 4.246-4.278 (m, 1 H), 6.311 (s, 1 H), 6.380 (s, 1 H), 8.870 (s, 1 H); ^{13}C NMR (500 MHz, DMSO-d_6, ppm) δ 25.886, 28.673, 28.881, 33.894, 55.569, 56.069, 59.853, 61.696, 163.354, 172.169. All data are consistent with literature values.[15, 42]

Biotin-Me-linker-SB-T-1214 drug conjugate (5-3)[15]

To a solution of **4-20** (140 mg, 0.1 mmol) dissolved in DMSO [0.2 M] was added **5-2** (30 mg, 0.1 mmol) dissolved in DMSO [0.2 M], dropwise. The mixture was stirred at room temperature and the reaction was monitored via TLC. After 8 h, the reaction was diluted with water resulting in a white precipitate. The precipitate was collected and purified using flash column chromatography on silica gel (10% CH_3OH in CH_2Cl_2) to yield **5-3** (10 mg, 56% yield), as a white solid: ^{1}H NMR (400 MHz, $CDCl_3$, ppm) δ 0.834-0.868 (m, 2 H), 0.926-0.975 (m, 8 H), 1.086-1.134 (m, 8 H), 1.226-1.344 (m, 36 H), 1.637-1.694 (m, 21 H), 1.890 (s, 4 H), 2.017 (s, 3 H), 2.143-2.481 (m, 10 H), 2.635 (m, 3 H), 2.947 (m, 3 H), 3.611 (t, J = 8.5 Hz, 1 H), 3.766 (d, J = 7.2 Hz, 1 H), 3.968 (br s, 2 H), 4.131 (d, J = 8.8 Hz, 1 H), 4.257 (d, J = 8.8 Hz, 1 H), 4.349-4.394 (m, 1 H), 4.915-5.118 (m, 4 H), 5.640 (d, J = 8.5 Hz, 1 H), 6.141 (m, 1 H), 6.304 (s, 1 H), 7.422-7.492 (m, 2 H), 7.562-7.580 (m, 1 H), 7.767 (m, 1 H), 8.066 (d, J = 7.2 Hz, 2 H), 8.930 (br s, 1 H), 9.338 (s, 1 H); ^{13}C NMR (500 MHz, $CDCl_3$, ppm) δ 1.210, 9.380, 9.499, 9.881, 13.291, 13.662, 14.995, 18.724, 22.207, 22.724, 25.296, 26.008, 26.831, 27.928, 28.492, 28.601, 29.890, 33.166, 33.500, 35.706, 35.979, 38.930, 40.212, 43.419, 46.167, 55.483, 58.598, 61.399, 62.792, 72.036, 75.223, 75.691, 79.302, 81.291, 84.645, 128.145, 128.836, 129.498, 130.323, 130.540, 131.354, 132.910, 133.375, 133.827, 136.999, 142.840, 164.392, 167.096, 168.627, 170.027, 170.822, 172.238, 175.040, 204.046; HRMS ES+ *m/z* calcd for $C_{68}H_{89}N_5O_{19}S_3$ $(M+)^+$ 1375.5314, found 1375.5388 (Δ 7.4 ppm). All data are in agreement with literature values.[15]

NSC 706744-Me-linker-TIPS (5-4)

To a mixture of **4-13** (25 mg, 0.05 mmol), DMAP (0.015 mmol) and NSC 706744 (0.1 mmol) dissolved in CH_2Cl_2 [0.1 M] and cooled to 0 °C was added DIC (0.06 mmol) dropwise. The mixture was allowed to warm to room temperature. After 5 h, no reaction was observed on TLC and NSC 706744 starting material precipitate was present in reaction mixture. DMSO was added to the mixture until NSC 706744 dissolved. The mixture was stirred at room temperature and the reaction was monitored via TLC. After 3 h, the reaction mixture was diluted with water to produce a precipitate. The precipitate was collected and purified using flash column chromatography on silica gel (hexanes:ethyl acetate = 1:1) to yield **5-4** (13 mg, 13 - 22% yield) as a purple solid: ^{1}H NMR (500 MHz, $CDCl_3$, ppm) δ 1.022-1.080 (m, 21 H), 2.401 (m, 4 H), 3.007 (m, 3 H), 3.617-4.127 (m, 14 H), 4.501 (m, 2 H), 6.083 (s, 2 H), 7.077-7.154 (m 4 H), 7.198-7.203 (m, 2 H), 7.647 (s, 1 H), 7.753 (s, 1 H), 8.047 (s, 1 H).

NSC 706744-Me-linker-CO_2H (5-5)

Method 1

To a cooled solution of **5-4** (10 mg, 0.01 mmol) dissolved in CH_3CN [0.1 M] was added CsF (0.02 mmol). The mixture was stirred at room temperature and the reaction was monitored via TLC. After 2 h, starting material was present in addition to 3 products. No compound isolation was attempted given reaction scale.

Method 2

To a cooled solution of **5-4** (8 mg, 0.008 mmol) dissolved in a 1:1 mixture of CH_3CN:py was added 0.08 mL HF:pyridine. The mixture was allowed to warm to room temperature. After 8 h, the reaction mixture was diluted with $NaCO_3$. The mixture was extracted with ethyl acetate (3 x 20 mL). The organic layers were combined and washed with $CuSO_4$ (3 x 20 mL) then washed with brine (3 x 20 mL). The organic layer was collected, dried over $MgSO_4$ and concentrated *in vacuo* to yield **5-5** (7 mg, quant. yield), as a purple solid: ^{1}H NMR (500 MHz, $CDCl_3$, ppm) δ 2.401 (m, 4 H), 3.007 (m, 3 H), 3.617-4.127 (m, 14 H), 4.501 (m, 2 H), 6.083 (s, 2 H), 7.077-7.154 (m 4 H), 7.198-7.203 (m, 2 H), 7.647 (s, 1 H), 7.753 (s, 1 H), 8.047 (s, 1 H); FIA-MS MS (ESI) *m/z* calcd for $C_{37}H_{38}N_2O_{10}S_2$ $(M+H)^+$ 735.8, found 735.2.

NSC 706744-Me-linker-OSu (5-6)

To a mixture of **5-5** (5 mg, 0.006 mmol) and HOSu (0.006 mmol) dissolved in DMSO [0.1 M] and cooled to 0 °C was added DIC (0.0072 mmol). The mixture was allowed to warm to room temperature and the reaction was monitored via TLC. After 5 h, the reaction was diluted with water to produce a precipitate. The precipitate was collected and washed with ethyl acetate to yield a crude mixture containing **5-6** with HOSu which was used in the following reaction without further purification.

Folate-OSu (5-7)[43]

To a mixture of folic acid (100 mg, 0.23 mmol) and HOSu (0.23 mmol) in DMSO [0.2 M] was added DIC (0.28 mmol). The mixture was stirred at room temperature. After 8 h, the reaction mixture was diluted with water to produce an orange precipitate. The precipitate was collected via vacuum filtration and washed with ethyl acetate and then washed with CH_3OH to yield a crude mixture containing **5-7** with HOSu which was used in the following reaction without further purification: ^{1}H NMR (500 MHz, DMSO-d_6, ppm) δ 2.513-2.606 (m, 4 H), 2.814 (br s, 4 H), 3.623-3.664 (m, 1 H), 4.508 (s, 2 H), 4.566-4.578 (d, J = 6 Hz, 1 H), 5.479 (d, J = 8 Hz, 1

H), 6.671-6.753 (m, 2 H), 6.906-7.019 (m, 2 H), 7.660-7.698 (m, 2 H), 8.657 (m, 1 H), 11.455 (br s, 1 H). All data are consistent with literature values.[43]

Folate-NH_2NH_2 (5-8)[44]

To a solution of 10 mg crude **5-7** dissolved in DMSO [0.1 M] was added 1 equivalent of hydrazine. The mixture was stirred at room temperature and the reaction was monitored via FIA. Upon complete conversion of starting material to **5-8**, the reaction crude mixture was directly used in the next step; FIA-MS MS (ESI) *m/z* calcd for $C_{21}H_{23}N_7O_5$ $(M+H)^+$ 454.4, found 454.2.

Folic acid-Me-linker-NSC 706744 drug conjugate (5-9)

To a solution of 7 mg crude **5-6** in DMSO [0.2 M] was added the reaction solution containing **5-8** [0.1 M]. The mixture was stirred at room temperature and the reaction was monitored via TLC. After 6 h, **5-6** was consumed. The reaction mixture was diluted with water to produce a red precipitate which was purified using column chromatography on silica gel to yield 8 mg of a brown solid. No desired product was isolated.

Biotinylated pyridinyl-disulfanylpentanoic acid (5-11)

To a mixture of **4-15** (100 mg, 0.4 mmol) and HOSu (138 mg, 1.2 mmol) dissolved in CH_2Cl_2:pyridine (9:1) was added DIC (0.01 mL, 0.02 mmol). The mixture was stirred at room temperature and the reaction was monitored via TLC. After 8 h, the reaction solvent was evaporated and the resulting crude was purified using flash column chromatography (hexanes:ethyl acetate = 3:1) to yield **5-10** (106 mg, 76% yield). To a solution of **5-10** (75 mg, 0.22 mmol) dissolved in DMF [0.4 M] was added **5-2** (0.22 mmol) dissolved in DMF [0.4 M]. The mixture was stirred at room temperature and the reaction was monitored via TLC. As the reaction proceeded, white precipitate formed. After 16 h, the reaction mixture was filtered and the organic layer was collected, diluted with 25 mL ethyl acetate and washed with water (3 x 20 mL). The organic layers were combined, dried over $MgSO_4$ and concentrated *in vacuo*. The resulting crude was purified using flash column chromatography on silica gel to yield **5-11** (60 mg, 43% yield), as a yellow-orange oil: ^{1}H NMR (400 MHz, $CDCl_3$, ppm) δ 1.230-1.310 (m, 4 H), 1.781-1.935 (m, 3 H), 2.102 (m, 1 H), 2.280-2.317 (m, 2 H), 2.380-2.407 (m, 1 H), 2.522-2.570 (m, 1 H), 2.646 (s, 2 H), 2.960 – 3.011 (m, 1 H), 7.058 (t, *J* = 5.2 Hz, 1 H), 7.619 (t, *J* = 7.6, 1 H), 7.713 (m, 1H), 8.420 (d, *J* = 4.4 Hz, 1 H), 10.077 (s, 1 H); FIA-MS MS (ESI) *m/z* calcd for $C_{21}H_{31}N_7O_4S_3$ $(M+H)^+$ 542.7, found 542.1.

Biotin-Me-linker-CO_2H (5-12)

To a solution of **5-11** (50 mg, 0.1 mmol) dissolved in THF [0.2 M] and cooled to 0 °C was added **4-2** (0.1 mmol), dropwise. The mixture was allowed to warm to room temperature and the reaction was monitored via TLC. After 8 h, the reaction solution was evaporated and the resulting oil was triturated with ethyl acetate to yield **5-12** (10 mg, 18% yield), as an orange oil: ^{1}H NMR (400 MHz, $CDCl_3$, ppm) δ 1.230-1.310 (m, 4 H), 1.781-1.935 (m, 3 H), 2.102 (m, 1 H), 2.280-2.317 (m, 2 H), 2.380-2.407 (m, 1 H), 2.522-2.570 (m, 1 H), 2.646 (s, 2 H), 2.830-2.904 (m, 1 H), 3.804 (s, 2 H), 7.208 (m, 2 H), 7.730-7.760 (m, 1 H), 7.996-8.034 (m, 1 H); FIA-MS MS (ESI) *m/z* calcd for $C_{24}H_{34}N_6O_6S_3$ $(M+H)^+$ 599.8, found 599.3.

Biotin-linker-NSC 706744 drug conjugate (5-13)

To a mixture of **5-12** (5 mg, 0.01 mmol), DMAP (0.003 mmol) and NSC 706744 (0.01 mmol) dissolved in DMSO [0.01 M] was added DIC (0.012 mmol). The mixture was stirred at room temperature and the reaction was monitored via TLC. After 16 h, the reaction mixture was diluted with water producing a purple precipitate. The precipitate was collected and recrystalized from CH_3OH and CH_2Cl_2 to yield **5-13** (6 mg, 60% crude yield) as a purple solid: crude ^1H NMR (400 MHz, $CDCl_3$, ppm) δ 0.844 (m, 1 H), 1.154-1.403 (m, 24 H), 1.792-2.136 (m, 18 H), 2.387-2.459 (m, 3 H), 2.665-3.015 (m, 5 H), 3.446 (s, 1 H), 3.607-3.692 (m, 2 H), 3.943-4.007 (m, 6 H), 4.425 (m, 2 H), 6.019 (m, 1 H), 7.008-7.052 (m, 2 H), 7.582-7.789 (m, 4 H), 7.968-8.005 (m, 1 H), 8.405 (m, 1 H); FIA-MS MS (ESI) *m/z* calcd for $C_{48}H_{56}N_8O_{12}S_3$ $(M+H)^+$ 1033.2, found 1034.1 (minor peak).

Cell culture system for MTT assay

Cell lines (obtained from ATCC unless otherwise noted and maintained at SBU Cell Culture/Hybridoma Facility) were cultured in RPMI-1640 with L-glutamine (Lonza BioWhittaker, BW12-702F: CT-26) or DMEM (Lonza BioWhittaker, BW12-604F: MX-1) at 37 °C with 5% CO_2.The cells were washed with DPBS and dissociated using TrypLE. The cells were incubated at 37 °C until the cells were detached from the plate, transferred to a centrifuge vial and pelleted via centrifugation at 1500 rpm for 5 min. The cells were counted per 1 mL media. The desired amount of RPMI-1640 Medium 10 x (Sigma Aldrich, R1145) was added to the cell solution so that 8,000 cells can be added to each well of a 96-well plate in 200 μL aliquots. After the addition, the cells were resuspended in RPMI-1640 Medium 10 x (Sigma Aldrich, R1145) supplemented with tissue culture grade water, 0.3 g/L L-glutamine, 2.0 g/L sodium bicarbonate, 10% FBS, and 1% Penn Strep and incubated at 37 °C with 5% CO_2.

Drug treatment for MTT assay

A serial dilution of biotin-Me-linker-SB-T-1214 dissolved in sterile DMSO was prepared by the addition of fully-supplemented RPMI-1640 Medium 10 x. The residual medium in each well was aspirated and the different drug-concentration solutions were added to each well of every column of the 96-well plate in 100 μL aliquots. After the addition of the drug solution, the cells were incubated at 37 °C for 48 or 72 hour periods. After the incubation period, the medium was aspirated and the cells were washed with DPBS and then 40 μL of 0.5 mg/mL MTT (3-(4,5-dimethylthiazol-2-yl)-2,5-diphenyltetrazolium bromide) in DPBS was added to each well. The cells were then incubated at 37 °C for 3 hours. After the incubation period, the MTT solution was aspirated and the remaining crystals were dissolved using a 40 μL of 0.4 M HCl in isopropanol. The plates were shaken for 10 minutes to assure that all of the crystals are dissolved. The optical density was determined from the resulting solutions using the Acsent Multiskan optical density reader. Each experiment was run in triplicate.

For cells treated with GSH-OEt: After the addition of the drug solution, the cells were incubated at 37 °C for 6 hours. To the washed cells 2 equivalents of GSH-OEt dissolved in RPMI-1640 Medium 10 x was added to each well. After the addition of GSH-OEt, the cells were incubated at 37 °C for 48 hours. After the incubation period, the medium was aspirated and the cells were washed with DPBS and then 40 μL of 0.5 mg/mL MTT in DPBS was added to each well. The cells were then incubated at 37 °C for 3 hours. After the incubation period, the MTT solution was aspirated and the remaining crystals were dissolved using a 40 μL of 0.4 M HCl in isopropanol. The plates were shaken for 10 minutes to assure that all of the crystals are

dissolved. The optical density was determined from the resulting solutions using the Acsent Multiskan optical density reader. Each experiment was run in triplicate.

Data analysis for MTT assay

The optical density data was used to calculate IC_{50} values for each drug on a given cell line using the Hill slope equation. The optical density values obtained from each concentration of drug solution were divided by the optical density value obtained from the cells with zero drug concentration. Using SigmaPlot v.10, the ratios were plotted versus the drug concentration and the IC_{50} values were calculated from the plot using the pre-programmed calculation within the SigmaPlot program.

§ 5.5.0 References

1. Chari, R. V. J. Targeted Delivery of chemotherapeuitcs: tumor-activated prodrug therapy. *Adv. Drug Deliv. Rev.* **1998,** 31, 89-104.
2. Ojima, I., Geng, X., Wu, X., Qu, C., Borella, C. P., Xie, H., Wilhelm, S. D., Leece, B. A., Bartle, L. M., Goldmacher, V. S., Chari, R. V. J. Tumor-Specific Novel Taxoid-Monoclonal Antibody Conjugates. *J. Med. Chem.* **2002,** 45, 5620-5623.
3. Wu, X.; Ojima, I. Tumor specific novel taxoid-monoclonal antibody conjugates. *Curr. Med. Chem.* **2004,** 11, 429-438.
4. Doronina, S. O., Mendelsohn, B.A., Bovee, T.D., Cerveny, C.G., Alley, S.C., Meyer, D.L., Oflazoghu, E., Toki, B.E., Sanderson, R.J., Zabinski, R.F., Wahl, A.F., Senter, P.D. Enhanced Activity of Monomethylauristatin F through Monoclonal Antibody Delivery: Effects of Linker Technology on Efficacy and Toxicity. *Bioconjugate Chem.* **2006,** 17, 114-124.
5. Beck, A., Haeuw, J.F., Wurch, T., Goetsch, L., Bailly, C., Corvaia, N. The next generation of antibody-drug conjugates comes of age. *Discov. Med.* **2010,** 10, 329-339.
6. Wagner, E.; Curiel, D.; Cotten, M. Delivery of drugs, proteins and genes into cells using transferrin as a ligand for receptor-mediated endocytosis. *Adv. Drug Delivery Rev.* **1994,** 14, 113-135.
7. Oh, S.; Kim, B. S.; Singh, N. P.; Lai, H.; Sasaki, T. Synthesis and Anti-cancer Activity of Covalent Conjugates of Artemisinin and a Transferrin-receptor Targeting Peptide. *Cancer Lett.* **2008,** 272, 110-121.
8. Nakase, I.; Gallis, B.; Takatani-Nakase, T.; Oh, S.; Lacoste, E.; Singh, N. P.; Goodlet, D. R.; Tanaka, S.; Futaki, S.; Lai, H.; Sasaki, T. Transferrin receptor-dependent cyotoxicity of artemisinin-transferrin conjugates on prostate cancer cells and induction of apoptosis. *Cancer Lett.* **2009,** 274, 290-298.
9. Russell-Jones, G., McTavish, Kirsten, McEwan, John, Rice, John, Nowotnik, David. Vitamin-mediated targeting as a potential mechanism to increase drug uptake by tumours. *J. of Inorg. Biochem.* **2004,** 98, 1625-1633.
10. Chen, S.; Zhao, X.; Chen, J.; Chen, J.; Kuznetsova, L.; Wong, S. S.; Ojima, I. Mechanism-based tumor-targeting drug delivery system. Validation of efficient vitamin receptor-mediated endocytosis and drug release. *Bioconjugate Chem.* **2010,** 21, 979-987.
11. Ojima, I. Guided Molecular Missiles for Tumor-Targeting Chemotherapy-Case Studies Using the Second-Generation Taxoid as Warheads. *Acc. Chem. Res.* **2008,** 41, 108-119.

12. Chen, J., Chen, S., Zhao, X., Kuznetsova, L., Wong, S.S., Ojima, I. Functionalized Single-walled Carbon Nanotubes as Rationally Designed Vehicles for Tumor-Targeted Drug Delivery. *J. Am. Chem. Soc.* **2008,** 130, 16778-16785.
13. Ojima, I. Tumor-targeting drug delivery of chemotherapeutic agents. *Pure Appl. Chem.* **2011,** 83, 1685-1698.
14. Ojima, I.; Zuniga, E. S.; Berger, W. T.; Seitz, J. D. Tumor-targeting drug delivery of new-genreation taxoids. *Future Med. Chem.* **2012,** 4, 33-50.
15. Chen, S., Zhao, X., Chen, J., Chen, J., Kuznetsova, L., Wong, S.S., Ojima, I. Mechanism-based tumor-targeting drug delivery system. Validation of efficient vitamin receptor-mediated endocytosis and drug release. *Bioconjugate Chem.* **2010,** 21, 979-987.
16. Leamon, C. P.; Reddy, J. A. Folate-targeted chemotherapy. *Adv. Drug Delivery Rev.* **2004,** 56, 1127-1141.
17. Y., L.; Low, P. S. Folate-mediated delivery of macromolecular anticancer therapeutic agents. *Adv. Drug Delivery Rev.* **2002,** 54, 675-693.
18. Lee, J. W.; Lu, J. Y.; Low, P. S.; Fuchs, P. L. Synthesis and evaluation of taxol-folic acid conjugates as targeted antineoplastics. *Bioorg. & Med. Chem.* **2002,** 10, 2397-2414.
19. Xia, W.; Low, P. S. Folate-targeted therapies for cancer. *J. Med. Chem.* **2010,** 53, 6811-6824.
20. Reddy, J. A.; Leamon, C. P. Folate receptor targeted cancer chemotherapy. In *Targeted Drug Strategies for Cancer and Inflammation*, Jackman, A. L.; Leamon, C. P., Eds. Springer Science+Buisness Media, LLC: 2011; pp 135-150.
21. Weinstein, S. J.; Hartman, T. J.; Stolzenberg-Solomon, R.; Pietinen, P.; Barrett, M. J.; Taylor, P. R.; Virtamo, J.; Albanes, D. Null Association between Prostate Cancer and Serum Folate, Vitamin B6, Vitamin B12, and Homocysteine. *Cancer Epidemiol., Biomarkers & Prevention* **2003,** 12, 1271-1272.
22. Sabharanjak, S.; Mayor, S. Folate receptor endocytosis and trafficking. *Adv. Drug Deliv. Rev.* **2004,** 56, 1099-1109.
23. Lu, Y.; Low, P. S. Folate-mediated delivery of macromolecular anticancer therapeutic agents. *Adv. Drug Deliv. Rev.* **2002,** 54, 675-693.
24. Lu, Y.; Sega, E.; Leamon, C. P.; Low, P. S. Folate receptor-targeted immunotherapy of cancer: Mechanism and therapeutic potential. *Adv. Drug Deliv. Rev.* **2004,** 56, 1161-1176.
25. Reddy, J. A.; Westrick, E.; Vlahov, I.; Howard, S. J.; Santhapuram, H. K.; Leamon, C. P. Folate receptor specific anti-tumor activity of folate-mitomycin conjugates. *Cancer Chemother. Pharmacol.* **2006,** 58, 229-236.
26. Satyam, A. Design and synthesis of releasable folate–drug conjugates using a novel heterobifunctional disulfide-containing linker. *Bioorg. Med. Chem. Lett.* **2008,** 18, 3196-3199.
27. Ladino, C. A.; Chari, R. V. J.; Bourret, L. A.; Kedersha, N. L.; Goldmacher, V. S. Folate-maytansinoids: target-selective drugs of low molecular weight. *Int. J. Cancer* **1997,** 73, 859-864.
28. Lee, J. W.; Lu, J. Y.; Low, P. S.; Fuchs, P. L. Synthesis and evaluation of taxol-folic acid conjugates as targeted antineoplastics. *Bioorg. Med. Chem.* **2002,** 10, 2397-2414.
29. Steinberg, G.; Borch, R. F. Synthesis and evaluation of pteroic acid-conjugated nitroheterocyclic phosphoramigates as folate receptor-targeted alkylating agents. *J. Med. Chem.* **2001,** 44, 69-73.
30. Aronov, O.; Horowitz, A. T.; Gabizon, A.; Gibson, D. Folate-targeted PEG as a potential carrier for Carboplatin analogs. Synthesis and *in vitro* studies. *Bioconjugate Chem.* **2003,** 14, 563-574.

31. Liu, J.; Kolar, C.; Lawson, T. A.; Gmeiner, W. H. Targeted drug delivery to chemoresistant cells: folic acid derivatization of FdIMP[10] enhances cytotoxicity toward 5-FU-resistant human colorectal tumor cells. *J. Org. Chem.* **2001,** 66, 5655-5663.
32. Zempleni, J.; Wijeratne, S. S.; Hassan, Y. I. Biotin. *Biofactors* **2009,** 35, 36-46.
33. Minko, T.; Paranjpe, P. V.; Qiu, B.; Lalloo, A.; Won, R.; Stein, S.; Sinko, P. J. Enhancing the anticancer efficacy of camptothecin using biotinylated poly(ethylene glycol) conjugates in sensitive and multidrug-resistant human ovarian carcinoma cells. *Cancer Chemother. Pharmacol.* **2002,** 50, 143-150.
34. Su, J.; Chen, F.; Cryns, V. L. Catechol Polymers for pH-Responsive, Targeted Drug Delivery to Cancer Cells. *J. Amer. Chem. Soc.* **2011,** 133, 11850-11853.
35. Kim, S. Y.; Cho, S. H.; Lee, Y. M.; Chu, L.-Y. Biotin-Conjugated Block Copolymeric Nanoparticles as Tumor-Targeted Drug Delivery Systems. *Macromolecular Res.* **2007,** 15, 646-655.
36. Yellepeddi, V. K.; Kuman, A.; Palakurthi, S. Biotinylated Poly(amido)amine (PAMAM) Dendrimers as Carriers for Drug Delivery to Ovarian Cancer Cells *In Vitro*. *Anticancer Res.* **2009,** 29, 2933-2944.
37. Heo, D. N.; Yang, D. H.; Moon, H.-J.; Lee, J. B.; Bae, M. S.; Lee, S. C.; Lee, W. J.; Sun, I.-C.; Kwon, I. K. Gold nanoparticles surface-functionalized with paclitaxel drug and biotin receptor as theranostic agents for cancer therapy. *Biomaterials* **2012,** 33, 856-866.
38. Cushman, M.; Jayaraman, M.; Vroman, J. A.; Fukunaga, A. K.; Fox, B. M.; Kohlhagen, G.; Strumberg, D.; Pommier, Y. Synthesis of new indeno[1,2-c]isoquinolines: cytotoxic non-camptothecin topoisomerase I inhibitors. *J. Med. Chem.* **2000,** 43, 3688-3698.
39. Anthony, S.; Jayaraman, M.; Laco, G.; Kohlhagen, G.; Kohn, K. W.; Cushman, M.; Pommier, Y. Differential Induction of Topoisomerase I-DNA Cleavage Complexes by the Indenoisoquinoline MJ-III-65 (NSC 706744) and Camptothecin: Base Sequence Analysis and Activity against Camptothecin-Resistant Topoisomerases I. *Cancer Res* **2003,** 63, 7428-7435.
40. Xiao, X.; Antony, S.; Kohlhagen, G.; Pommier, Y.; Cushman, M. Design, synthesis, and biological evaluation of cytotoxic 11-aminoalkenylindenoisoquinoline and 11-diaminoalkenylindeoisoquinoline topoisomerase I inhibitors. *Bioorg. & Med. Chem.* **2004,** 12, 5147-5160.
41. Gottlieb, H. E.; Kotlyar, V.; Nudelman, A. NMR Chemical Shifts of Common Laboratory Solvents as Trace Impurities. *J. Org. Chem.* **1997,** 62, 7512-7515.
42. Corey, E. J.; Mehrotra, M. M. A simple and enantioselective synthesis of (+)-biotin. *Tetrahedron Lett.* **1988,** 29, 57-60.
43. Pasut, G.; Canal, F.; Dalla Via, L.; Arpicco, S.; Veronese, F. M.; Schiavon, O. Antitumoral activity of PEG-gemcitabine prodrugs targeted by folic acid. *J. Control. Release* **2008,** 127, 239-248.
44. Anbharasi, V.; Cao, N.; Feng, S.-S. Doxorubicin conjugated to D-α-tocopheryl polyethylene glycol succinate and folic acid as a prodrug for targeted chemotherapy. *J. Biomed. Mater. Res. A* **2010,** 94A, 730-743.

Chapter 6

Design, Synthesis and Biological Evaluation of Novel Tumor-Targeting Drug Conjugates with Dual-Guiding Modules and Dual-Warheads. 1. Drug Conjugate with SB-T-1214 and Camptothecin.

Chapter Contents

§ 6.1.0 Introduction

§ 6.1.1 Combination Chemotherapy

Currently, there are a number of methods which are used to treat cancer. These methods include but are not limited to (1) surgery, (2) radiation therapy, (3) biological therapy, (4) gene therapy (5) anti-angiogenic therapy (6) hematopoietic/stem cell or bone marrow transplantation (7) hyperthermia and (8) chemotherapy. Most cancers are treated by using a combination of the treatment methods. For example, surgery with chemotherapy or radiation with chemotherapy are widely employed treatment modes. Chemotherapeutic drugs may be used to shrink the tumor, rendering removal of the shrunken tumor via local therapies, such as surgery or radiation, less destructive. This method is called neoadjuvant chemotherapy. In adjuvant chemotherapy, chemotherapeutic drugs are given after the tumor has been removed via local therapy, to kill any remaining cancer cells at or extended from the original tumor site. A similar approach to utilizing a local therapy with chemotherapy is the use of combination chemotherapy. Combination chemotherapy employs the use of different drugs simultaneously to shrink the tumor and kill cancer cells.

Over the past decades, anticancer treatment has significantly improved through the use of newly developed drugs and the combination of drugs. For example, the development of irinotecan (a potent, water-soluble camptothecin analog) and capecitabine (a prodrug of 5-fluorouracil) have increased the mean survival time in patients receiving therapy for colon cancer.[1, 2] Furthermore, the use of fluorouracil-leucovorin, oxaliplatin and irinotecan in combination has also increased the overall survival in patients treated for advanced colon cancer.[3] The use of drug combinations results in (1) a decrease in systemic toxicity for the patient, as the drugs can be administered below their tolerated doses; and (2) increased cell kill of the tumor cell population, as each drug inhibits tumor growth at different stages of the cell cycle.[4] Also, the likelihood of the tumor developing resistance to the drug combination is decreased with the simultaneous administration of the drugs.

§ 6.1.2 A Brief History of Combination Chemotherapy

Frei, Holland and Freireich hypothesized that cancer chemotherapy should follow the strategy of anti-tuberculosis therapy, i.e. the use of a combination of drugs, each with a different mechanism of action.[5-7] The use of combination therapy led to promising results for the treatment of various types of leukemia and Hodgkin's disease in the 1960s.[7-11] In 1963, Scott reported the use of chlorambucil (a DNA alkylating agent) as maintenance chemotherapy following treatment with nitrogen mustard in patients with advanced Hodgkin's disease.[8] The results were promising, as patients who received chlorambucil averaged 35 weeks to relapse and those who were not given chlorambucil averaged 12 weeks. Also in the 1960s, researchers at NCI developed a new combination chemotherapy, known as MOMP, which consisted of nitrogen mustard, oncovin (vincristine), methotrexate and prednisone.[9, 10] This regimen yielded a high complete remission rate and proved to be relatively safe with no toxic synergistic effects.[9, 10] The MOMP protocol was modified by substituting methotrexate with procarbazine (a potent monoamine oxidase inhibitor), thus creating MOPP. The change showed excellent antitumor activity in several lymphomas and Hodgkins' disease with decreased adverse side effects

compared to MOMP.[9, 10] With refinements to the MOPP regimen, acute lymphoblastic leukemia (ALL) in children is a curable disease, as well as Hodgkin's and non-Hodgkin's lymphoma.[11]

The use of combination chemotherapy in advanced breast cancer was also evaluated in the early 1960s.[12] The combination of methotrexate and thiotepa gave promising results.[12] However, at the time the combination was not applicable in the adjuvant situation.[11] The schedule of the cyclophosphamide, methotrexate and 5-fluorouracil (CMF) regimen was designed to mimic the highly successful MOPP regimen.[13, 14] The therapeutic and toxicologic effects of the CMF regimen was first evaluated at the Instituto Nazionale Tumori of Milan as an adjuvant treatment in patients with node-positive breast cancer.[11, 13, 14] The evaluation gave exceptional results, as the CMF protocol was active in patients with metastatic cancer leading to an overall response rate over 50% and approximately 20% of patients attainted complete remission.[13, 14] The results of this trial made a substantial impact on the standard care for breast cancer, as the CMF regimen is still widely employed for not only the treatment of breast cancer, but also for colorectal and other types of tumors.[11] To date, a large number of chemotherapy regimens have been developed and are currently being used to treat different cancers. Furthermore, new drug combinations are being developed and evaluated in clinical trials against a variety of cancer types.

§ 6.1.3 Camptothecins

In general, most cytotoxic drugs target proteins involved in cell division or DNA synthesis. For example paclitaxel targets microtubules and inhibit the G_2/M phase of mitosis, whereas capecitabine, a prodrug derivative of 5-fluorouracil, works by inhibiting thymidylate synthase, which plays a role in DNA replication. It is worthy of note that the combination of paclitaxel and capecitabine is in phase II clinical trials.[15, 16] As single agents both drugs exhibit activity in various cancer cell lines, however, the combination of paclitaxel and capecitabine was shown to be a highly active and well-tolerated regimen for the treatment of metastatic breast cancer.[15, 16] Furthermore, the combination of a taxoid and a camptothecin also proved to be well-tolerated, causing minimal clinical side effects.[17, 18] In several preclinical studies, it was found that simultaneous exposure of a taxane and a camptothecin exhibited an additive or synergistic effect.[19, 20]

Camptothecin (CPT) is a quinoline alkaloid that inhibits DNA topoisomerase I. CPT was first discovered in 1966 by Wani and Wall. The compound was isolated from the bark and stem of Camptotheca, *Camptotheca acuminate*.[21] In preliminary clinical trials, CPT showed excellent anticancer activity. However, the compound also showed low solubility and adverse side effects. The anticancer activity of CPT has been attributed to its planar structure.[22, 23] CPT contains a planar pentacyclic ring structure and one chiral center with (S) configuration. Two camptothecin derivatives, irinotecan and topotecan have been approved by the FDA for the treatment of cancer (Figure 6.1).

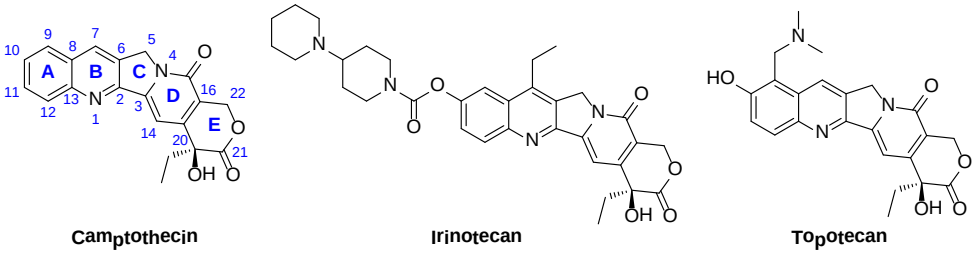

Figure 6.1: Camptothecin and camptothecin derivatives

The camptothecins are DNA topoisomerase I inhibitors, thus influence DNA replication. Topoisomerase I (topo I) relieves the tension generated from the winding and unwinding of DNA during DNA replication. The activity of topo I allows for the rotation of one DNA strand over the other (ligation). During DNA replication, topo I wraps around DNA and nicks the DNA backbone permitting the double helix to unwind (Figure 6.2).[24]

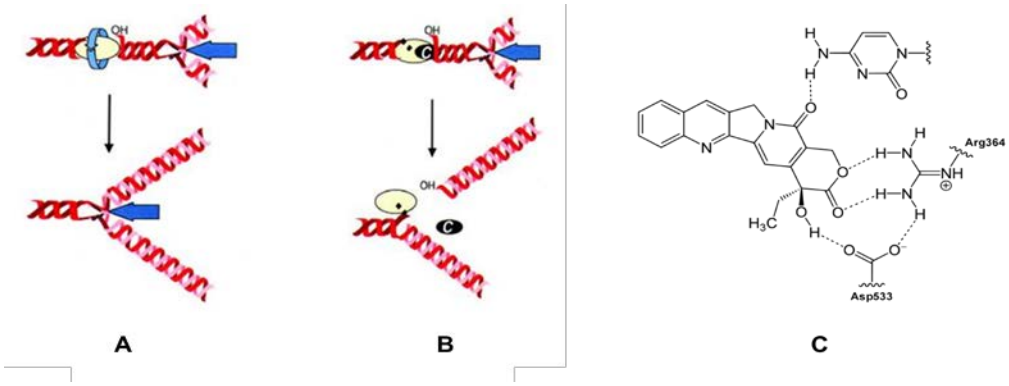

Figure 6.2: Mechanism of action of camptothecins. (A) DNA replication without camptothecin present; (B) camptothecin binds to topoisomerase I, as DNA replication proceeds, the replication fork collides with camptothecin-topoisomerase I complex resulting in double strand break (adapted from [24, 25])

In the presence of camptothecins, the drug is bound to the topo I-nicked DNA complex, forming a stabile ternary complex.[25] This complex is formed mainly by the interaction of the E-ring with the topo I enzyme. The lactone is bonded with two hydrogen bonds to the amino groups on Arg364.[25] The hydroxyl moiety at the C-20 position forms a hydrogen bond to Asp533.[25] It is worthy of note that C-20 be in *S*-configuration as the *R*-configuration is an inactive form of camptothecins. The binding of camptothecins to topo I inhibits the relegation of the nicked strand and the release of the enzyme. As replication continues, the replication fork collides with the camptothecin-topoisomerase I complex resulting in double strand break during the S-phase of the cell cycle and induces apoptosis.[24, 25]

§ 6.1.4 Synergistic Activity of Taxoids and Camptothecins

Isobologram and combination index (CI) analyses are commonly used methods for evaluating drug interactions in combination chemotherapy. The isobologram method evaluates the interaction at a chosen effect level, thus is useful to investigate the drug interaction at the corresponding concentration.[26-28] CI analysis, a more widely used method, provides qualitative information on the nature of drug interaction, and the extent of drug interaction (e.g. synergism,

summation and antagonism) is quantified via a calculated CI value.[29] For mutually exclusive (drugs with a similar mechanism of action) or nonexclusive drugs (those with different mechanisms of action), synergy is indicated when CI < 1, summation is indicated when CI =1 and antagonism is indicated when CI > 1.[29] To analyze the combined drug effect via CI analysis, cells are treated with a combination of drugs, where the combined drug regimen evaluated is equal to the ratio of the IC_{50} value for each drug. The data obtained from these experiments can be processed using dose-effect analyzer software, such as CalcuSyn (Biosoft, Cambridge, UK), to calculate CI using the median effect method according to Chou and Talalay.[29]

The extent of drug interaction between paclitaxel and a camptothecin have been evaluated in a variety of cancer cell lines. Kaufman et al. observed that the combination of paclitaxel and topotecan had antagonistic effects against A549 (non-small cell lung) cancer cells simultaneously treated with paclitaxel and topotecan for 7 days (CI = 1.7 ± 0.2).[30] For this experiment, cells were treated with a fixed ratio of both drugs simultaneously at doses that corresponded to 1/2, 5/8, 3/4, 7/8, 1 and 1.5 times the individual IC_{50} values and the data was analyzed by the method developed by Chou and Talalay.[30] Using an isobologram method, Kano et al. found that simultaneous administration of paclitaxel and SN-38 (the active metabolite of irinotecan) was sub-additive or protective for MCF-7 (breast), A549 and WiDr (colon) cancer cell lines, and produced additive effects in PA1 (ovarian) cancer cell line.[31] However, they also found that the sequential exposure of paclitaxel (24 h) followed by SN-38 (24 h) produced additive effects in all four cell lines.[31] For simultaneous exposure, the cells were incubated with solutions of paclitaxel and SN-38 for 24 h, and then the cells were washed, resuspended in culture medium without drugs and incubated for an additional 4 days.[31] For sequential exposure, the cells were incubated with one drug for 24 h, washed and then incubated with the second drug for 24 h. After the second incubation period, the cells were washed and resuspended in fresh culture medium and incubated for 3 days.[31]

Madden et al. found that treatment with paclitaxel followed by a camptothecin is synergistic, while reversing the order of drug treatment or treating the cells with the taxane and the camptothecin simultaneously results in no more than additive effects.[32] They found that a 90-minute exposure of a sub-lethal concentration of paclitaxel produces a ten-fold reduction in the concentration of camptothecin required to reduce cellular proliferation by 50%. Following Madden's results, Murren et al. administered irinotecan to advanced cancer patients as a 90-minute infusion immediately after the administration of paclitaxel (75 mg/m^2, 1 h).[17] Patients were treated for 4 weeks, followed by a 2-week rest. Following this regime, Murren et al. found that the combined treatment of irninotecan and paclitaxel is well-tolerated and devoid of significant gastrointestinal or neurologic toxicities observed when each drug is used as a single agent. Furthermore, prolonged stabilization of disease (6 months or more) was observed in 5 of the 21 patients.

In a separate study, Murren et al. found that the combination of docetaxel (a semi-synthetic analog of paclitaxel) and irinotecan showed promising activity in the treatment of non-small cell lung cancer (NSCLC).[33] In this phase I study, escalating doses of docetaxel (25 mg/m^2 up to 40 mg/m^2) were given to patients before irinotecan (50 mg/m^2) for 4 weeks followed by a 2-week rest.[33] Of the 5 patients with NSCLC evaluated, one gave partial response to the treatment program. These results suggested that the combination of docetaxel and irinotecan has promise as a treatment of NSCLC.[33]

A phase II study of docetaxel and irinotecan in metastatic or recurrent esophageal cancer also gave promising results.[34] However, the regimen evaluated needs to be modified to reduce

side effects. Treatment with docetaxel (40 mg/m^2/d) and irinotecan (100 mg/m^2/d) in 21 day intervals also showed modest antineoplastic activity in patients with metastatic adenocarcinoma of the esophagus, gastroesophageal junction and gastric cardia in another phase II study. Similarly, paclitaxel (100 mg/m^2) and irinotecan (225 mg/m^2) in 3 week intervals showed promising activity in metastatic adenocarcinoma of the esophagus and gastric cardia.[35] In an *in vitro* study, Ohtsu et al. synthesized five paclitaxel-camptothecin drug conjugates conjugated by an ester and an imine linkage which exhibited potent activity in a series of cancer cell lines.[36]

§ 6.1.5 Design of a Tumor-Targeting Drug Conjugate Bearing a Taxoid and Camptothecin

As mentioned in previous chapters, the lack of tumor-specificity in conventional chemotherapeutic agents, such as taxoids and camptothecins, has been a longstanding problem, resulting in undesirable and severe side effects. A promising approach to combat the limitation of chemotherapeutics is through the development of tumor-targeting drug conjugates. Tumor-targeting drug conjugates consists of one or multiple cytotoxic drugs connected to a tumor-targeting module (TTM) via cleavable covalent bonds or cleavable linkers. Based on this design, the drug conjugate is inactive until it is specifically delivered to the tumor site by the TTM, such as biotin and folic acid, and internalized, where the warhead is released from the carrier, restoring its original activity.

Accordingly, a novel tumor-targeting drug conjugate bearing dual-warheads has been designed and synthesized utilizing biotin as the TTM. The warheads chosen were SB-T-1214, a new-generation taxoid that inhibits microtubule depolymerization, and camptothecin, a potent DNA replication inhibitor (Figure 6.3). This drug conjugate will enable the tumor-specific delivery of both SB-T-1214 and camptothecin, drugs with synergistic activity, through a single drug molecule, thus circumventing complicated pharmacokinetics issues associated with combination chemotherapy.

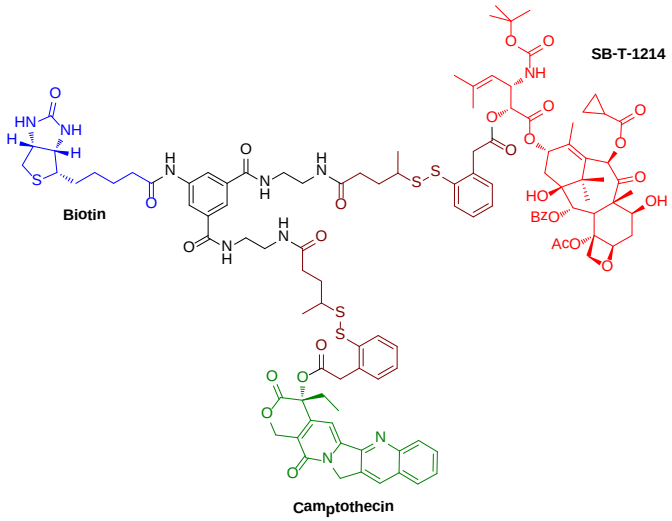

Figure 6.3: Tumor-targeting drug conjugate bearing dual-warheads

SB-T-1214 demonstrated greater potency in various cancer cell lines compared to the parent compounds and a combination of a taxoid and camptothecin has shown excellent synergistic activity in a number of clinical trials. Thus, it is reasonable to assume that the dual

mechanism of action makes the drug conjugate highly efficacious. Furthermore, the presence of biotin increases tumor-specificity of the drug conjugate, as cancer cells overexpress biotin receptors. Based on the published studies on single-warhead conjugates from the Ojima laboratory, the drug conjugate should be specifically delivered to cancer cells and internalized via receptor-mediated endocytosis (RME).[37-40] Once internalized, the drug moieties should be released in their active form through the self-immolation of disulfide linkers triggered by the presence of an intracellular thiol to target microtubules (SB-T-1214) and topoisomerase I (camptothecin).

§ 6.2.0 Results and Discussion

§ 6.2.1 Biological Evaluation of a Taxoid and Camptothecin

The drug conjugate bearing dual-warheads, SB-T-1214 and camptothecin, has been designed to specifically deliver one molecule of each warhead. SB-T-1214 and camptothecin have different mechanisms of action and the combination of both is absent of cross-resistance.[41] As mentioned earlier, sequential treatment with a taxoid and a camptothecin as single agents exhibited additive to synergistic effects against different cancer cell lines.[30-32] For these experiments isobologram and CI analyses were employed to quantitatively assess drug interaction. To evaluate the interaction of SB-T-1214 with camptothecin *in vitro*, MTT assays were performed in which an equimolar mixture of SB-T-1214 and camptothecin (conditions mimicking warhead delivery of the drug conjugate with dual-warheads) was administered to various cancer cell lines. The cells were incubated with the drug combination for 48 hours at 37 °C. The IC_{50} values obtained from these experiments are listed in Table 6.1. As seen from the data in Table 6.1, the combination of SB-T-1214 with camptothecin showed substantial activity against MCF-7 (human breast) cancer cell line. The equimolar combination of SB-T-1214 and camptothecin displayed one order of magnitude greater potency against human ovarian cancer cell lines A2780 and ID-8 compared to camptothecin as a single drug. The combination of SB-T-1214 and camptothecin did not show significant activity against the human pancreatic (CFPac-1 and Panc-1) and human colon (DLD-1 and HT-29) cancer cell lines when compared to the single drugs. With these preliminary results, the activity of SB-T-1214 with camptothecin was screened in various breast cancer cell lines. These results are listed in Table 6.2.

Table 6.1: Biological Evaluation of Equimolar Combination of a Taxoid and Camptothecin against Various Cancer Cell Lines

Drug	IC_{50} (nM)						
	A2780 (ovarian cancer)	CFPac-1 (pancreatic cancer)	DLD-1 (colon cancer)	HT-29 (colon cancer)	ID8 (ovarian cancer)	MCF-7 (breast cancer)	Panc-1 (pancreatic cancer)
Paclitaxel	16.2 ± 8.28	68.0 ± 22.9	29.5 ± 10.8	11.6 ± 3.57	14.5 ± 5.88	6.25 ± 0.76	1.97 ± 0.76
SB-T-1214	0.36 ± 0.03	0.38 ± 0.14	0.38 ± 0.21	0.73 ± 0.30	2.51 ± 1.24	0.35 ± 0.11	0.35 ± 0.14
Camptothecin	39.2 ± 13.5	38.6 ± 5.8	131 ± 118	66.2 ± 10.1	196 ± 21	159 ± 63	73.2 ± 5.0
SB-T-1214:CPT	7.61 ± 1.61	38.6 ± 10.8	153 ± 38	66.8 ± 9.4	31.6 ± 2.89	0.34 ± 0.14	0.35 ± 0.14

Table 6.2: Biological Evaluation of Equimolar Combination of a Taxoid and Camptothecin against Various Breast Cancer Cell Lines

Drug	IC_{50} (nM)					
	BT20	LCC6 wt	LCC6 MDR	MCF-7	MDA MB 231	SkBr3
SB-T-1214	0.20 ± 0.06	0.68 ± 0.33	0.86 ± 0.15	0.35 ± 0.11	2.89 ± 2.67	0.48 ± 0.03
Camptothecin	230 ± 25	2.43 ± 1.48 µM	381 ± 98	159 ± 63	503 ± 8	705 ± 277
SB-T-1214:CPT	475 ± 8	324 ± 78	492 ± 5	0.34 ± 0.14	406 ± 140	3.74 ± 1.15

- Cells were suspended in RPMI with L-glutamine (Lonza BioWhittaker, BW12-702F), with 5% FBS (Thermo Scientific, HyClone, SH3007003), 5% Nu Serum (BD Biosciences, 355100) and 1% Penn Strip before administration of drug
- Cells were incubated for 48 hours at 37 °C with 5% CO_2 after administration of taxoid:camptothecin mixture
- The optical density was determined using Acsent Multiskan optical density reader
- The reported values are a calculated averages of IC_{50} values determined from three individual experiments
- IC_{50} values were calculated using SigmaPlot v 10.0
- All IC_{50} values are report in nM scale unless otherwise noted

As seen from Table 6.2, there is further selectivity amongst the breast cancer cell lines. The combination of SB-T-1214 and camptothecin showed excellent activity against MCF-7 and SkBr3 breast cancer cell lines with IC_{50} values of 0.34 and 3.74 nM, respectively. Furthermore, the combination resulted in greater potency against BT20, LCC6 wt, LCC6 MDR and MDA MB 231 cancer cell lines compared to treatment with camptothecin as a single drug.

To evaluate the effects that sequential drug incubation has in the combination of SB-T-1214 with camptothecin, cancer cells were treated with SB-T-1214 and incubated for 24 hours at 37 °C followed by the treatment with camptothecin and an additional incubation period of 24 hours at 37 °C. Also, the order of addition was switched, i.e. treating with camptothecin (24 h) followed by SB-T-1214 (24 h). In addition, the activities of SB-T-1214 and camptothecin as single agents were evaluated for 24 and 48 hour incubation periods. For these experiments MCF-7, MDA MB 231 and SkBr3 human breast cancer cell lines were used. These results are listed in Table 6.3.

Table 6.3: Biological Evaluation of Single Drug Administration and Sequential Administration of Drug Combination against Various Breast Cancer Cell Lines

Taxane	Time of Incubation (h)	IC_{50} (nM) MCF-7	MDA MB 231	SkBr3
SB-T-1214	**24**	26.8 ± 9.61	23.2 ± 12.5	33.2 ± 19.2
SB-T-1214	**48**	0.56 ± 0.34	2.89 ± 2.67	0.48 ± 0.03
Camptothecin	**24**	>5000	>5000	>5000
Camptothecin	**48**	48.3 ± 3.46	503 ± 8	705 ± 277
SB-T-1214:CPT*	**-**	0.36 ± 0.17	3.47 ± 2.04	3.22 ± 0.47
CPT:SB-T-1214‡	**-**	27.7 ± 8.86	556 ± 125	230 ± 117

* Cells were treated with SB-T-1214 for 24 hours at 37 °C with 5% CO_2 then treated with camptothecin for an additional 24 hours at 37 °C with 5% CO_2: total incubation time with drug is 48 hours

‡ Cells were treated with camptothecin for 24 hours at 37 °C with 5% CO_2 then treated with SB-T-1214 for an additional 24 hours at 37 °C with 5% CO_2: total incubation time with drug is 48 hours

- Cells were suspended in RPMI with L-glutamine (Lonza BioWhittaker, BW12-702F), with 5% FBS (Thermo Scientific, HyClone, SH3007003), 5% Nu Serum (BD Biosciences, 355100) and 1% Penn Strip before administration of taxoid and/or camptothecin
- Cells were incubated for 24 or 48 hours at 37 °C with 5% CO_2 after administration of drug
- The optical density was determined using Acsent Multiskan optical density reader
- The reported values are a calculated averages of IC_{50} values determined from three individual experiments
- IC_{50} values were calculated using SigmaPlot v 10.0
- All IC_{50} values are report in nM scale unless otherwise noted

As seen from Table 6.3, in general, a longer incubation period with single drugs leads to lower IC_{50} values. Also listed in the table, when the cancer cells are treated sequentially with SB-T-1214 followed by camptothecin, there is a significant increase in activity against MCF-7 and MDA MB 231 cancer cell lines compared to treatment with SB-T-1214 as a single agent. The IC_{50} value of the sequentially administered drug combination against MCF-7 is 0.36 nM compared to 0.56 nM, the IC_{50} value of SB-T-1214 alone (48 h incubation). The IC_{50} value of SB-T-1214 with camptothecin is one order of magnitude more potent than SB-T-1214 alone (48 h incubation). The combination of SB-T-1214 and camptothecin demonstrated more potency against SkBr3 (IC_{50} 3.22 nM) compared to camptothecin as a single drug. Lastly, the treatment of camptothecin followed by SB-T-1214 quenched the activity of the combination in all three of the breast cancer cell lines evaluated. Kano et al. suggests that the difference in activity observed

when a taxoid and a camptothecin are administered simultaneously versus sequentially are a result of the effect on the cell cycle that each drug possess.[31, 42] Taxoids induce a G2-M arrest and camptothecins effects the cells in the S phase. Thus, when the drugs are administered simultaneously, one agent may limit the efficacy of the other by preventing cells from entering the specific phase in which the other agent is active.[31, 42] Kano et al. further suggest that for the sequential administration of drugs, the cell cycle arrest may result in cell synchronization, thus leading to increased drug sensitivity.[42] Regardless, the *in vitro* results show the benefits of treating cells with an equimolar combination of SB-T-1214 and camptothecin. Furthermore, these results merit the assessment of drug interaction between SB-T-1214 and camptothecin in a variety of cancer cell lines using the method developed by Chou and Talalay.

§ 6.2.2 Chemical Modifications of Small-Molecule Splitter Modules

Trisubstituted small-molecule splitter modules were designed based on commercially available 1-amino-3,5-dicarboxylic acid and 3,5-diaminobenzoic acid. Different substituents were introduced to the aromatic compounds to test the reactivity of the compounds towards different reaction conditions. Boc-protection of 1-aminobenzene-3,5-dicarboxylic acid and commercially available 1-aminobenzene-3,5-dicarboxylic acid dimethyl ester was achieved by treating both with di-*tert*-butyl dicarbonate in the presence of base. Conversion of the dicarboxylic acid or dimethyl ester moieties to the corresponding hydrazide was attempted using hydrazine under reflux conditions (Scheme 6.1).

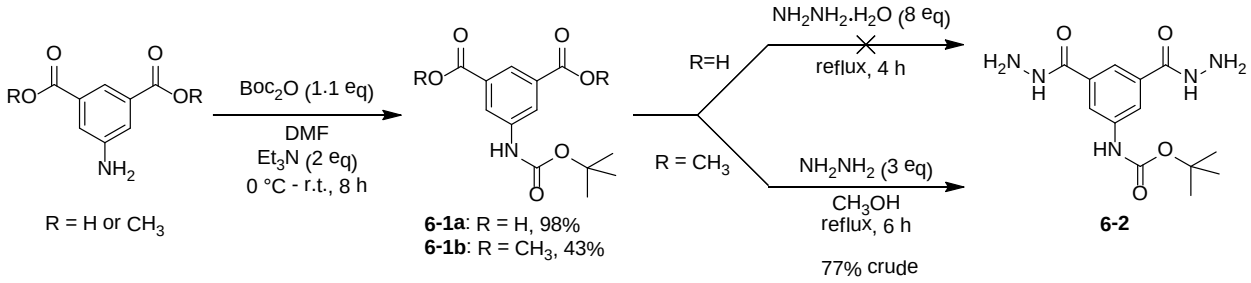

Scheme 6.1: Testing the reactivity of 1-amino-3,5-dicarboxylic acid

The electron withdrawing 3,5-dicarboxylic acids or methyl esters did not hinder the nucleophilicity of the amino moiety, as Boc-protection of the amine afforded **6-1a** (98%) and **6-1b** (43%). However, treating dicarboxylic acid **6-1a** with neat hydrazine monohydrate did not afford **6-2**.[43] **6-2** was obtained in 77% crude by treating **6-1b** with anhydrous hydrazine in refluxing methanol.[44] Relative ease in chemical modification rendered 1-amino-3,5-dicarboxylic acid a possible candidate as a small-molecule splitter module.

Selective modification of 3,5-diaminobenzoic acid did not proceed as desired. Boc-protection of 3,5-diaminobenzoic acid methyl ester (**6-3**) afforded a mixture of bis- and mono-Boc protected product (Scheme 6.2).

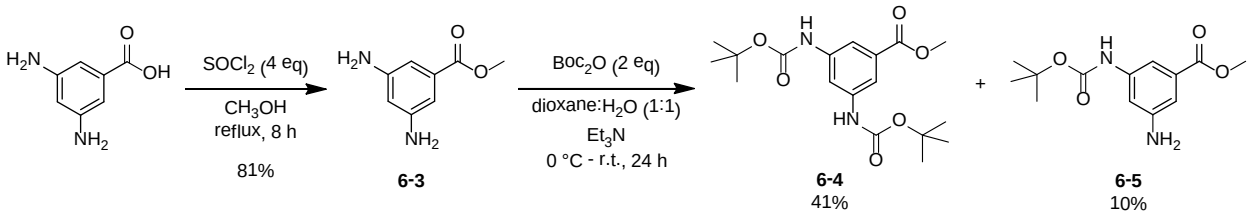

Scheme 6.2: Modifications of 3,5-diaminobenzoic acid

Esterification of 3,5-diaminobenzoic acid in the presence of thionyl chloride and refluxing methanol afforded **6-3** in good yield (81%). Subsequent Boc-protection resulted in the formation of two products, **6-4** (41%) and **6-5** (10%), as well as unreacted **6-3**. **6-4** was then treated with hydrazine in refluxing methanol to afford **6-6**, which was then treated with commercially available biotin-OSu to give **6-7** (Scheme 6.3).

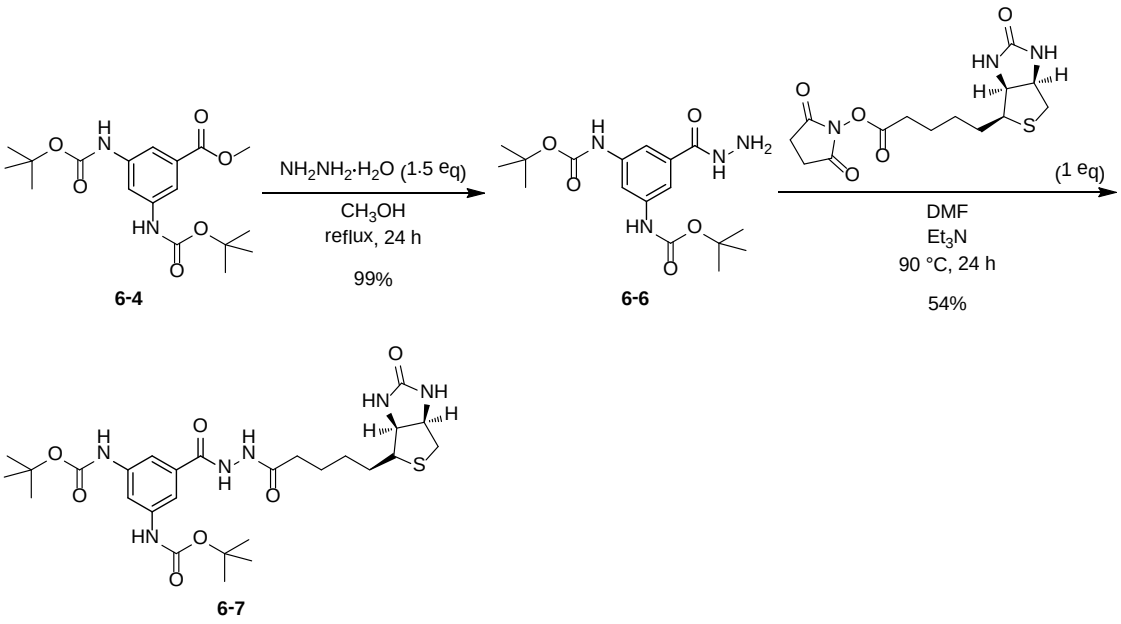

Scheme 6.3: Biotinylation of modified 3,5-diaminobenzoic acid

The conversion of carboxylic acid **6-4** to hydrazide **6-6** was accomplished in excellent yield (99%). To explore the reactivity of **6-6**, biotin-OSu was coupled to the resulting hydrazide to give **6-7** in moderate yield (54%). Although **6-7** was prepared, the resulting low yields for Boc-deprotection and biotinylation steps suggested that 1-aminobenzene-3,5-dicarboxylic acid or derivative be the preferred starting material to prepare a small-molecule splitter module.

§ 6.2.3 1st Attempted Synthesis of Drug Conjugate Bearing Dual-Warheads

Based on the experiment described above, a small-molecule splitter module was developed based on sequential, chemical modifications of commercially available 1-aminobenzene-3,5-dicarboxylic acid. Coupling of biotin to 1-aminobenzene-3,5-dicarboxylic acid was achieved using two methods: (1) standard peptide coupling conditions (i.e. treating with DCC and DMAP) (Scheme 6.4); and (2) coupling of biotin acid chloride to 1-amino-3,5-

dicarboxylic acid dimethyl ester (Scheme 6.5).[45] Dihydrazide formation of the resulting biotinylated-3,5-dicarboxylic acid **6-8** was accomplished using hydrazine in refluxing methanol (Scheme 6.4).

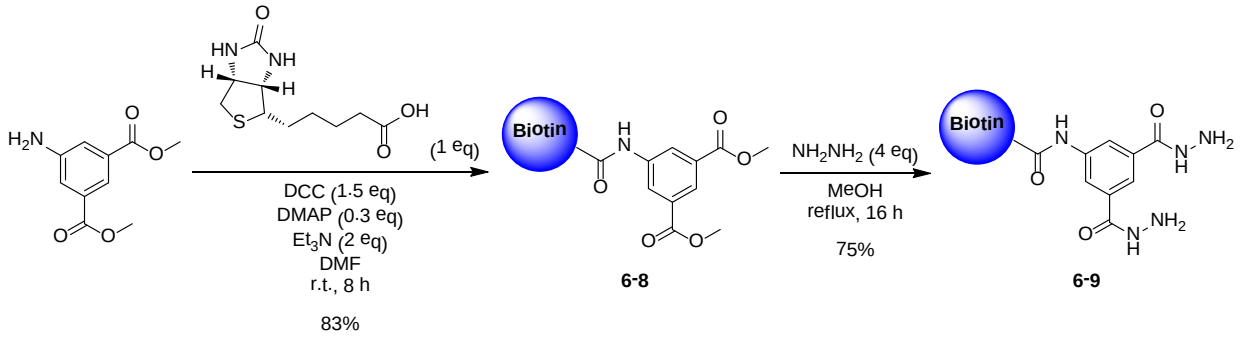

Scheme 6.4: Dihydrazide formation of biotin splitter

The coupling of biotin with 1-aminobenzene-3,5-dicarboxylic acid dimethyl acid in the presence of DCC, DMAP and Et_3N afforded **6-8** in high yield (83%) after purification via column chromatography. However, an alternative route was examined, as to limit the need for column chromatography. Modifying the protocol described by Kluger et al., **6-8** was obtained in high yields and purified via recrystallization (Scheme 6.5).[45]

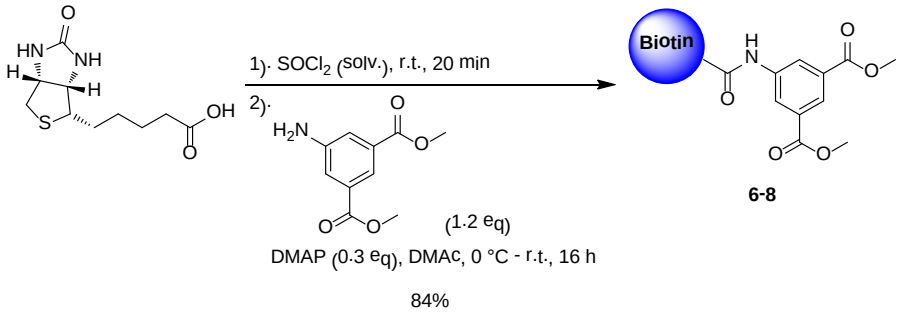

Scheme 6.5: Biotinylation of 1-amino-3,5-dicarboxylic acid dimethyl ester

This alternative route entails the conversion of biotin to biotin acid chloride in the presence of thionyl chloride. As this reaction proceeds, the biotin acid chloride crashes out of the solution. The excess thionyl chloride is removed via distillation, then 1-aminobenzene-3,5-dicarboxylic acid dimethyl ester is added to the resulting crude biotin acid chloride. Recrystallization from DMF and water afforded **6-8** in high yield (84%). This efficient method of biotinylation can be employed on large scales without the use of other reagents. However, caution should be given to the distillation of thionyl chloride. As mentioned previously, treating **6-8** with hydrazine affords the dihydrazide **6-9**, which was used for the coupling with CPT-linker compounds **4-22a** (free acid) and **4-23a** (activated ester) (Scheme 6.6).

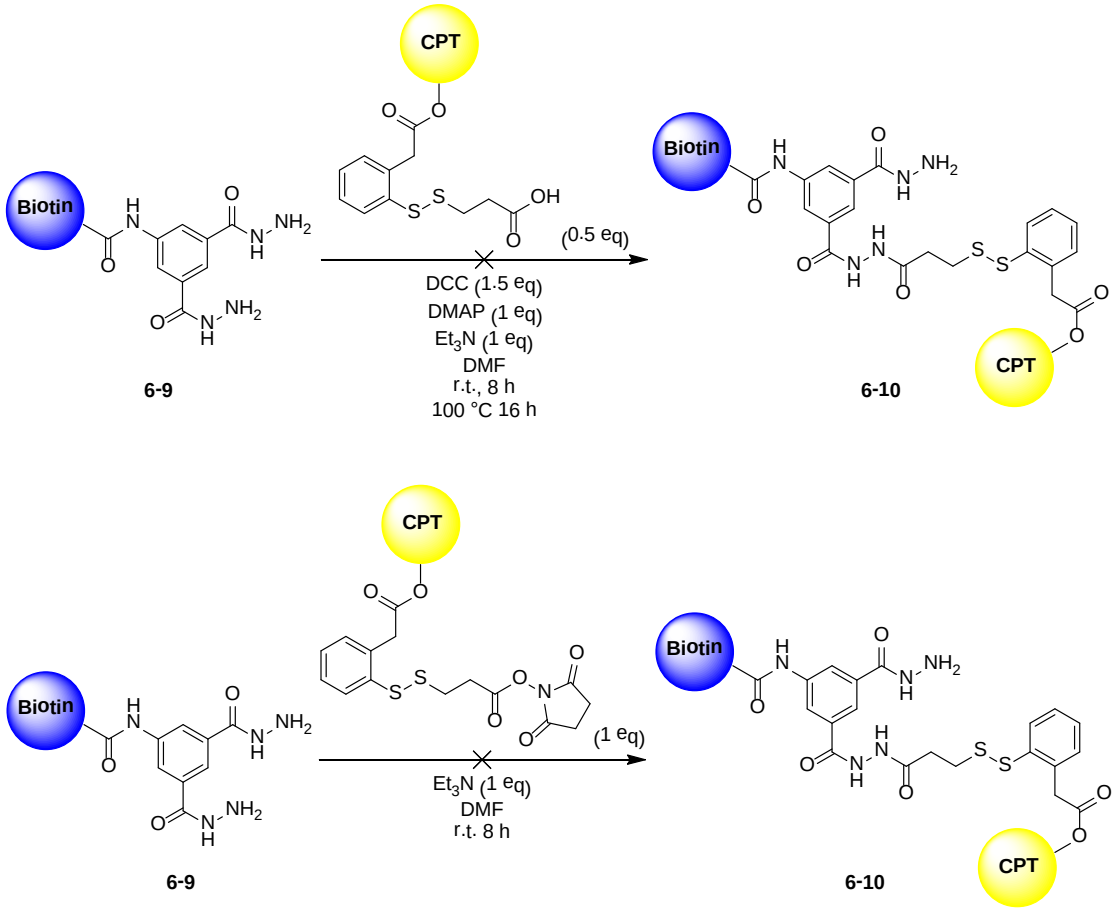

Scheme 6.6: 1st attempted coupling of camptothecin-linker to biotin splitter module

The coupling of CPT-linker to biotin-splitter **6-9** was attempted using two methods: (1) peptide coupling in the presence of DCC and DMAP; and (2) coupling via treatment with an activated ester. However, neither route afforded the desired compound **6-10**. Surprisingly, free CPT was obtained when **6-9** was treated with **4-22a** in the presence of DCC and DMAP. The release of CPT may have been caused by the basic conditions of the reaction, resulting in the cleavage of the drug from the linker. Furthermore, sterics may have been the cause for both coupling reactions to fail. Accordingly, **6-8** was treated with ethylenediamine to extend the reactive amines from the splitter module (Scheme 6.7).

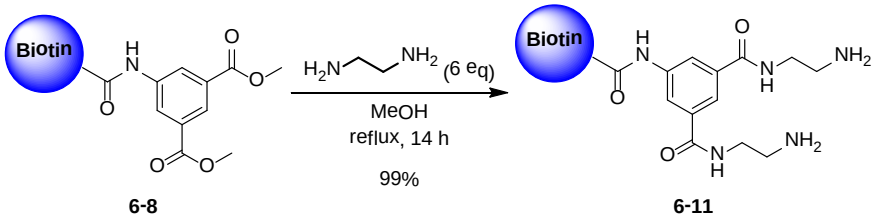

Scheme 6.7: Amine extension of biotin splitter

The addition of excess ethylenediamine to **6-8** in refluxing methanol afforded **6-11** in excellent yield (99%). The diamine was obtained in good yields; however selective modification of the symmetric splitter would be difficult. The selective couplings of **6-11** with paclitaxel-

linker-CO_2H (obtained from Dr. Xianrui Zhao) and **4-22a** were attempted in the presence of DCC and DMAP (Scheme 6.7).

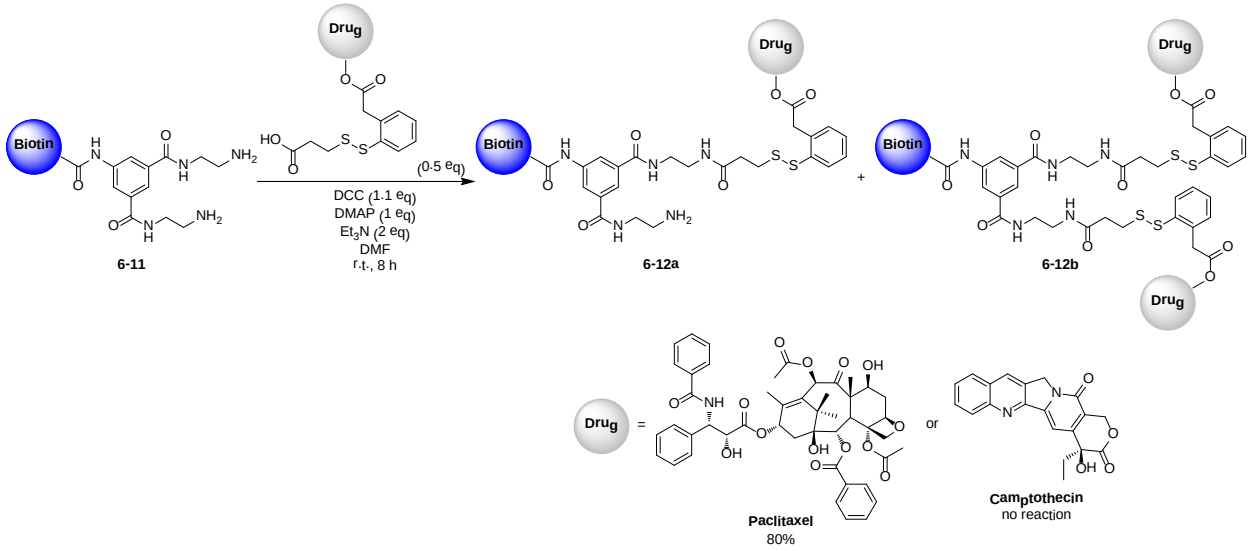

Scheme 6.8: 1st attempted selective drug-linker coupling

For the coupling reaction, drug-linker-CO_2H was used as the limiting reagent (0.5 equivalents) and the addition of the compound to **6-11** in dilute conditions was slow. However, selective coupling was not observed as both amines were functionalized with the drug-linker compound in the cases where paclitaxel was the drug. No reaction was observed when CPT-linker-CO_2H was used. Though the conditions could be modified such that (1) a large excess of **6-11** is used, or (2) an equimolar concentration of SB-T-1214-linker-CO_2H and CPT-linker-CO_2H, or their corresponding activated esters, is added to **6-11**. These conditions were not employed, as various attempts of splitter module desymmetrization through selective chemical modifications were explored.

§ 6.2.4 Desymmetrization of Small-Molecule Splitter Modules

The first attempt of splitter module desymmetrization was based on the mono-Boc-protection of ethylenediamine. The addition of di-*tert*-butyl carbonate to an excess amount of ethylenediamine affords *N*-Boc-ethylenediamine (**6-13**) in excellent yields (>90%) (Scheme 6.9).[46] Similar Boc-protection conditions were employed to biotin-splitter **6-11** in an attempt to install a Boc-moiety on one amine moiety while leaving one amine free (Scheme 6.10).

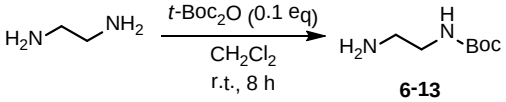

Scheme 6.9: Boc-protection of ethylene diamine

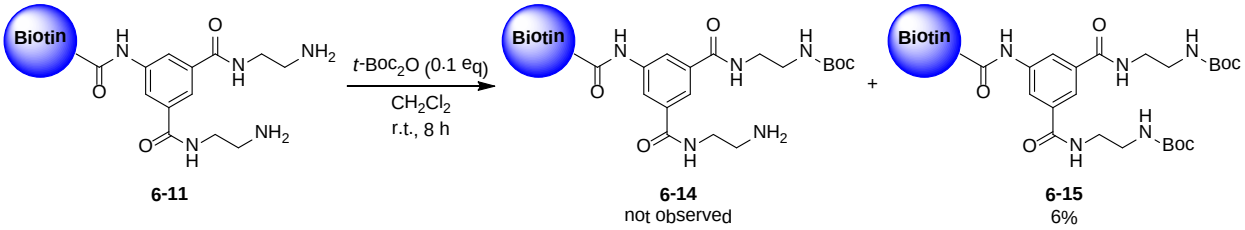

Scheme 6.10: Attempted selective Boc-protection of biotin-splitter

The slow addition of di-*tert*-butyl carbonate to excess **6-11** (10 equivalents) in dilute reaction conditions afforded the bis-Boc-protected splitter **6-15** and no formation of the desired **6-14**. This result led to alternative routes towards desymmetrization, mono-amide conversion of biotin-splitter via: (1) selective saponofication of **6-8** followed by conversion of the free acid to the corresponding amide (Scheme 6.11);[47] and (2) direct and selective amide formation of **6-8** as shown in Scheme 6.13.

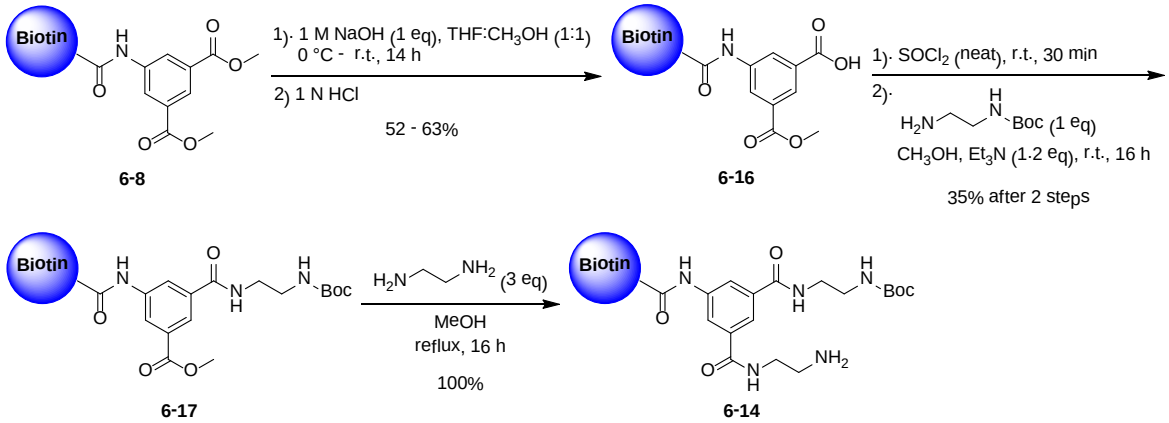

Scheme 6.11: Selective saponofication and amide formation of splitter module

Selective saponofication was accomplished by treating **6-8** with 1 M NaOH to give **6-16** in moderate yields (52 – 63%).[47] The coupling of **6-13** to the resulting carboxylic acid **6-16** was done by converting the carboxylic acid to the corresponding acid chloride followed by the addition of **6-13** to give **6-17** in fair yield (35% after 2 steps). Treatment of **6-17** with ethylenediamine in refluxing methanol afforded **6-14** in quantitative yield. The coupling of **6-13** to **6-16** was also achieved using different peptide coupling conditions. These results are listed in Table 6.4.

Table 6.4: Methods towards Selective Amide Formation of 6-17

6-16 (mmol)	Coupling Reagent	Additional Reagent	Solvent [0.1 M]	Temp (°C)	Reaction time with coupling reagents (h)	**6-13** (mmol)	Reaction time with **6-13** (h)[a]	Isolated yield (%)[b]
0.06 mmol	$SOCl_2$	Et_3N	-	0 °C	0.5	0.06	8	35% (12 mg)
2.4 mmol	CDI (2.8 mmol)	-	THF	50 °C	1	2.4	24	15% (200 mg)
1.2 mmol	DIC (1.4 mmol)	HOSu (1.2 mmol)	THF:pyridine (1:1)	r.t.	16	1.2	16	90% (600 mg)

[a] reactions with **6-13** were done at room temperature; [b] all yields reported are isolated yields after 2 steps

As listed in Table 6.4, the conversion of **6-16** to **6-17** was obtained in high yield (90% after 2 steps) using DIC and HOSu. The OSu activation followed by amide formation gave the best result. The attempted coupling using CDI gave **6-17** in low yield (15%). This low yield may have resulted from the lack of **6-16** activation initiated by CDI. Although the conversion of **6-16** to the acid chloride using $SOCl_2$ followed by amide formation in the presence of base to afford **6-17** in fair yield (35%) proved to be the cleanest reaction conditions. However, caution should be given to the distillation of excess thionyl chloride, as well as the quenching of any resulting acid generated by reacted thionyl chloride. The residual acid may remove the Boc moiety of **6-13**. During our exploration of splitter desymmetrization procedures, 3-amino-5-(methoxycarbonyl)benzoic acid became a commercially available product. As such, biotinylation of 3-amino-5-(methoxycarbonyl)benzoic acid using the protocol described by Kluger et al. afforded **6-16** (Scheme 6.12).[45]

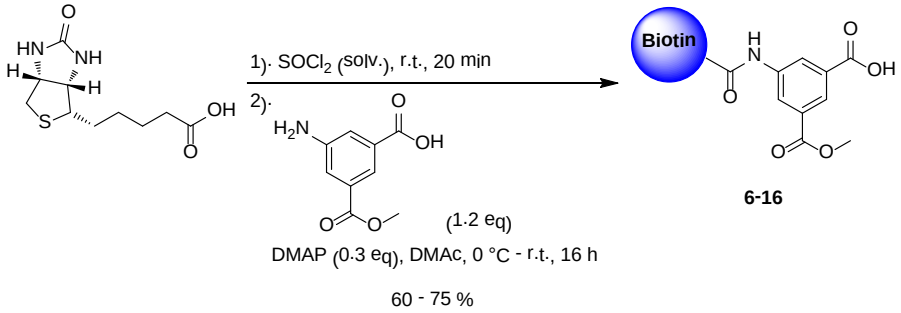

Scheme 6.12: Biotinylation of 3-amino-5-(methoxycarbonyl)benzoic acid

As with previous biotinylation reactions, the Kluger protocol afforded **6-16** in fair to good yields (60 – 75%). Purification was again done using recrystallization from DMF and water. This procedure is applicable to large scale preparation of **6-16** which was further modified as described above. Also mentioned previously, in a final attempt to generate **6-17** directly, **6-9** was treated with **6-13** in methanol (Scheme 6.13).

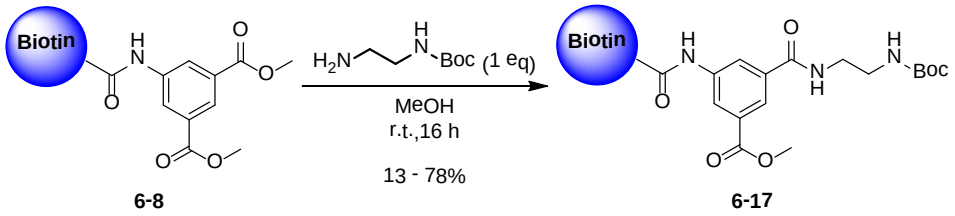

6-8 **6-17**

Scheme 6.13: Direct and selective amide formation of splitter module

Surprisingly, the reaction between **6-8** and **6-13** yielded **6-17** at room temperature, as formation of **6-17** was monitored using thin-layer chromatography (TLC) and mass spectroscopy. However, **6-17** was obtained with inconsistent yields (13 – 78%) on multiple attempts. It is worthy of note that this reaction condition was the cleanest among all conditions employed.

§ 6.2.5 2nd Attempted Synthesis of Drug Conjugate Bearing Dual-Warheads

As mentioned above, the treatment of **6-17** with ethylenediamine in refluxing methanol give **6-14** in excellent yield. Splitter **6-14** was used in coupling reactions CPT-linker compounds **4-22a** (free acid) and **4-23b** (activated ester) (Scheme 6.14).

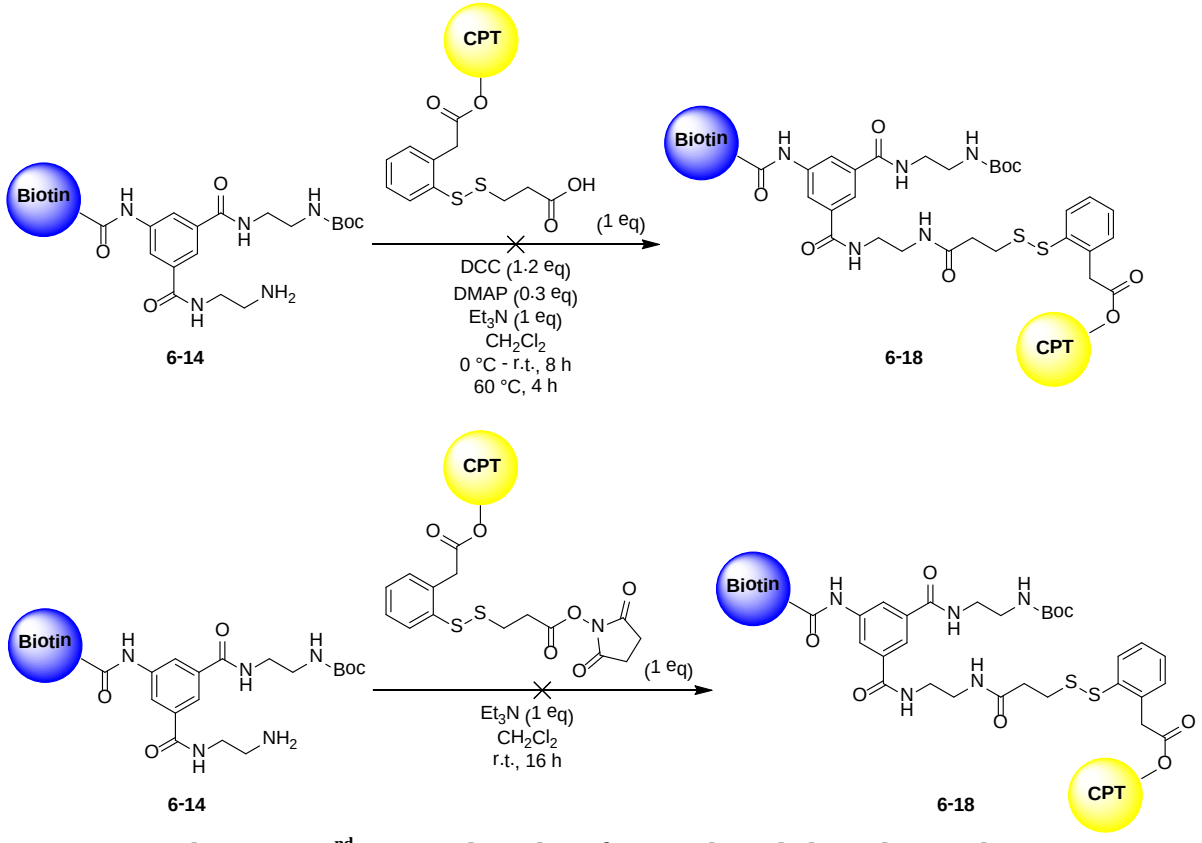

6-14 **6-18** **6-14** **6-18**

Scheme 6.14: 2nd attempted coupling of camptothecin-linker to biotin splitter

Similar to the other CPT-linker coupling reactions mentioned above, the coupling of **6-14** to CPT-linker compounds **4-22a** (free acid) and **4-23a** (activated ester) did not generate the desired **6-18**. Likewise, free CPT was again recovered from the reaction with **4-22a**, suggesting that CPT was again prematurely cleaved from the linker. Unreacted **4-23a** was obtained in the second reaction. These results suggest that the propanoic acid linker is not suitable for the coupling conditions employed, as the short alkyl chain linker may be: (1) unstable under basic conditions, resulting in the premature cleavage of CPT; and (2) sterically crowded at the activated ester for nucleophile to attack. Accordingly, **6-14** was treated with CPT-Me-Linker-OSu coupling-ready construct **4-23b** (Scheme 6.15).

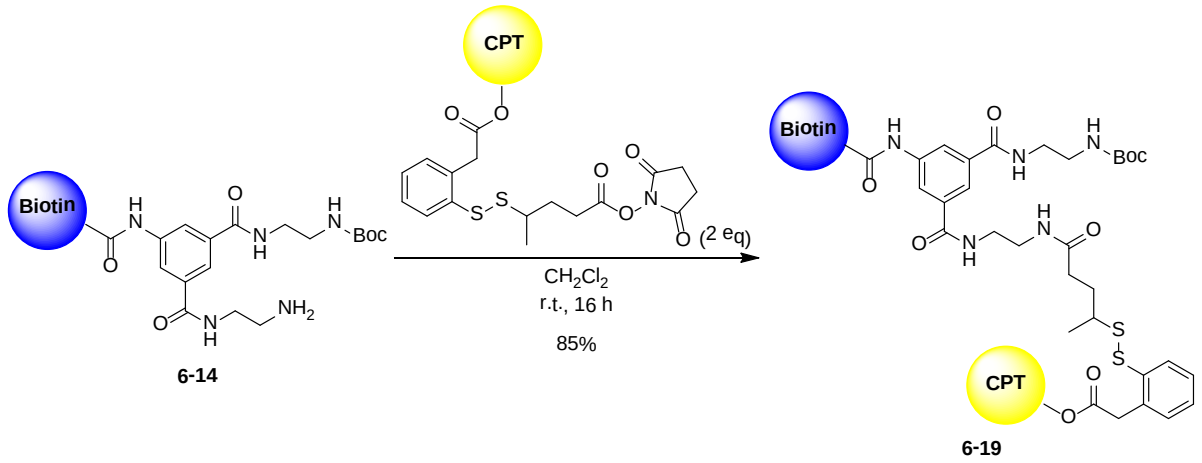

6-14 **6-19**

Scheme 6.15: 3rd attempted coupling of camptothecin-linker to biotin splitter

The addition of **6-14** to excess **4-23b** gave the coupled product **6-19** in good yield (85%). The reaction was monitored by TLC and mass spectroscopy. Throughout the duration of the reaction, the formation of free CPT was not observed. This result suggests that the propanoic disulfide-linker was indeed unsuitable for coupling due to instability or sterics. Subsequent removal of the Boc-protecting group and treatment with **4-20** afforded **DW-1**, a tumor-targeting drug conjugate bearing dual-warheads (Scheme 6.16).

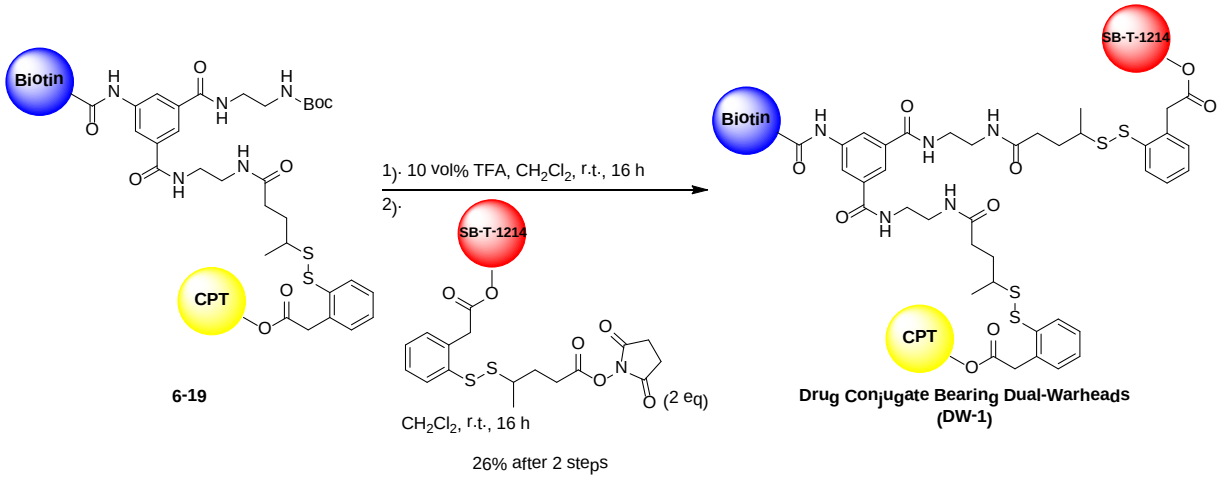

6-19 **Drug Conjugate Bearing Dual-Warheads (DW-1)**

Scheme 6.16: Synthesis of 1st-generation tumor-targeting drug conjugate bearing dual-warheads

The Boc moiety was removed by treating **6-19** with TFA. This deprotection step was monitored by mass spectroscopy. Quenching with aqueous sodium bicarbonate, filtration and concentration of the filtrate afforded the free amine, which was added to **4-20** to give **DW-1** in low yield (26% after 2 steps). This low yield may have been caused by sterics, as the free amine is buried within both biotin- and CPT-linker side-chains. The biological activity of DW-1 was evaluated against MCF-7, MDA MB 231 and SkBr3 (human breast) cancer cell lines. These results are listed in Table 6.5 and compared with results listed in Table 6.3.

Table 6.5: Biological Evaluation of Drug Conjugate DW-1

Taxane	Time of Incubation (h)	IC_{50} (nM) MCF-7	MDA MB 231	SkBr3
SB-T-1214	**24**	26.8 ± 9.61	23.2 ± 12.5	33.2 ± 19.2
SB-T-1214	**48**	0.56 ± 0.34	2.89 ± 2.67	0.48 ± 0.03
Camptothecin	**24**	>5000	>5000	>5000
Camptothecin	**48**	48.3 ± 3.46	503 ± 7.57	705 ± 277
SB-T-1214:CPT*	**-**	0.36 ± 0.17	3.47 ± 2.04	3.22 ± 0.47
CPT:SB-T-1214‡	**-**	27.7 ± 8.86	556 ± 125	230 ± 117
DW-1	**48**	3.51 ± 1.95	4.89 ± 0.26	2.72 ± 2.07

* Cells were treated with SB-T-1214 for 24 hours at 37 °C with 5% CO_2 then treated with camptothecin for an additional 24 hours at 37 °C with 5% CO_2: total incubation time with drug is 48 hours

‡ Cells were treated with camptothecin for 24 hours at 37 °C with 5% CO_2 then treated with SB-T-1214 for an additional 24 hours at 37 °C with 5% CO_2: total incubation time with drug is 48 hours

- Cells were suspended in RPMI with L-glutamine (Lonza BioWhittaker, BW12-702F), with 5% FBS (Thermo Scientific, HyClone, SH3007003), 5% Nu Serum (BD Biosciences, 355100) and 1% Penn Strip before administration of taxoid and/or camptothecin
- Cells treated with DW-1 were resuspended in RPMI-1640 Medium 10 x (Sigma Aldrich, R1145) supplemented with tissue culture grade water, 0.3 g/L L-glutamine, 2.0 g/L sodium bicarbonate, 10% FBS, and 1% Penn Strep before administration of taxoid
- Cells were incubated for 24 or 48 hours at 37 °C with 5% CO_2 after administration of drug
- The optical density was determined using Acsent Multiskan optical density reader
- The reported values are a calculated averages of IC_{50} values determined from three individual experiments
- IC_{50} values were calculated using SigmaPlot v 10.0
- All IC_{50} values are report in nM scale unless otherwise noted

As listed in Table 6.5, the activity of **DW-1** is within standard deviation of the *in vitro* activity observed when the cells were treated with SB-T-1214 then with camptothecin against MDA MB 231 and SkBr3 cancer cell lines. The activity of **DW-1** is one order of magnitude less active compared to the activity observed when the cells were treated with the taxoid then camptothecin in MCF-7 cells (IC_{50} = 0.36 nM) or when the cells were treated with a 1-to-1 mixture of taxoid:camptothecin (IC_{50} = 0.34 nM, see Table 6.2). This observed lower activity may have been caused by the uncoordinated cleavage of the two disulfide bonds (i.e. in some **DW-1** molecules the disulfide bond of the CPT-linker was cleaved before the disulfide bond of the taxoid is cleaved), thus CPT was released first then SB-T-1214 was cleaved. These results also suggest that the intracellular concentration of GSH of the three breast cancer cell lines tested is high enough to cleave the disulfide bonds, releasing the free drugs in their active form.

§ 6.3.0 Summary

Combination chemotherapy has led the great advances in anticancer treatment, resulting in the "cure" for acute lymophoblastic leukemia (ALL), as well as Hodgkin's and non-Hodgkin's lymphoma. Furthermore, combined chemotherapy has prolonged the survival rate in patients treated for breast cancer and currently, most cancers are treated using a combination of chemotherapeutic agents. For example, the combination of a taxoid and a camptothecin has shown promising results in a number of clinical trials. The beneficial (i.e. additive and synergistic) effects of a taxoid and a camptothecin have been demonstrated in different cancer cell lines using isobologram and CI analyses. These findings were shown in an *in vitro* biological evaluation using an MTT assay against a number of cancer cell lines. These experiments demonstrated that the combination of SB-T-1214, a potent new-generation taxoid, and camptothecin have increased potent in certain cancer cell lines. The combination of SB-T-1214 and camptothecin showed excellent activity in three breast cancer cell lines (MCF-7, MDA MB 231 and SkBr3). Based on these findings, a novel tumor-targeting drug conjugate bearing dual-warheads (both SB-T-1214 and camptothecin) was designed and synthesized utilizing biotin as the TTM. This drug conjugate specifically delivers SB-T-1214 and camptothecin to cancer cells through a single drug molecule, thus circumventing complicated pharmacokinetics issues associated with combination chemotherapy. The synthesis and biological evaluation of a drug conjugate bearing dual-warheads were discussed. Much like the free agents, the drug conjugate bearing SB-T1214 and camptothecin showed excellent *in vitro* activity. However, there are a few limitations in the design of the drug conjugate, which will be discussed in the next chapter.

§ 6.4.0 Experimental

Caution

Taxoids and camptothecin have been established as a potent cytotoxic agent. Thus, they and all structurally related compounds and derivatives must be considered as mutagens and potential reproductive hazards for both males and females. Appropriate precautions (i.e. use of gloves, goggles, lab coat and fume hood) must be taken while handling these compounds.

General information

All chemical were obtained from Sigma-Aldrich, Fisher Scientific or VWR International, and used as is unless otherwise noted. All reactions were carried out under nitrogen in oven dried glassware using standard Schlenk techniques unless otherwise noted. Reactions were monitored by thin layer chromatography (TLC) using E. Merck 60F254 precoated silica gel plates and alumina plate depending on the compounds. Dry solvents were degassed under nitrogen and were dried using the PURESOLV system (Inovatative Technologies, Newport, MA). Tetrahydrofuran was freshly distilled from sodium metal and benzophenone. Dichloromethane was also distilled immediately prior to use under nitrogen from calcium hydride. Toluene was also distilled immediately prior to use under nitrogen from calcium hydride. Yields refer to chromatographically and spectroscopically pure compounds. Flash chromatography was performed with the indicated solvents using Fisher silica gel (particle size 170-400 Mesh).^{1}H, ^{13}C and ^{9}F data were obtained using either 300 MHz Varian Gemni 2300 (75 MHz ^{13}C, 121 MHz ^{19}F) spectrometer, the 400 MHz Varian INOVA 400 (100 MHz ^{13}C) spectrometer or the 500

MHz Varian INOVA 500 (125 MHz ^{13}C) in $CDCl_3$ as solvent unless otherwise stated. Chemical shifts (δ) are reported in ppm and standardized with solvent as internal standard based on literature reported values.[48] Melting points were measured on Thomas Hoover Capillary melting point apparatus and are uncorrected. Optical rotations were measured on Perkin-Elmer Model 241 polarimeter.

Experimental procedure

1-Boc-aminobenzene-3,5-dicarboxylic acid (6-1a)[49]

To a mixture of 1-aminobenzene-3,5-dicarboxylic acid (1.0 g, 5.5 mmol) and Et_3N (1.5 mL, 11 mmol) dissolved in DMF [0.1 M] and cooled to 0 °C was added di-*tert*-butyl dicarbonate (1.3 g, 6 mmol) dissolved in DMF (1 mL), dropwise, producing a cloudy, white solution. The mixture was stirred at room temperature and the reaction was monitored via TLC. After 8 h, the reaction solvent was evaporated yielding **6-1a** (1.5 g, 98% yield), as an off-white solid: ^1H NMR (300 MHz, CD_3OD, ppm) δ 1.339 (s, 9 H), 8.260 (s, 1 H), 8.500 (s, 1 H), 9.854 (s, 1 H). All data are consistent with literature values.[49]

1-Boc-aminobenzene-3,5-dicarboxylic acid dimethyl ester (6-1b)

To a mixture of 1-aminobenzene-3,5-dicarboxylic acid dimethyl ester (1.0 g, 4.8 mmol) and Et_3N (1.3 mL, 9.6 mmol) dissolved in DMF [0.1 M] and cooled to 0 °C was added di-*tert*-butyl dicarbonate (1.2 g, 5 mmol) dissolved in DMF (1 mL), dropwise, producing a yellow-cloudy solution. The mixture was stirred at room temperature and the reaction was monitored via TLC. After 8 h, the reaction solvent was evaporated. The resulting crude was dissolved in CH_2Cl_2 and purified using flash column chromatography on silica gel (hexanes:ethyl acetate = 6:1) to yield **6-1b** (632 mg, 43% yield), as a white solid: ^1H NMR (300 MHz, $CDCl_3$, ppm) δ 1.533 (s, 9 H), 3.933 (s, 6 H), 6.711 (br s, 1 H), 8.248 (s, 1 H), 8.354 (s, 1 H); HRMS MS ES+ *m/z* calcd for $C_{15}H_{19}NO_6$ $(M+H)^+$ 310.1212, found 310.1289 (Δ 7.7 ppm).

1-Boc-aminobenzene-3,5-dihydrazide (6-2)

Method 1

To **6-1a** (500 mg, 1.8 mmol) was added 0.7 mL hydrazine monohydrate. The mixture was stirred under reflux conditions and the reaction was monitored via TLC. After 12 h, formation of **6-2** was not observed.

Method 2

To **6-1b** (535 mg, 1.7 mmol) dissolved in CH_3OH [0.3 M] was added anhydrous hydrazine (0.17 mL, 5 mmol), dropwise. The mixture was stirred under reflux conditions and the reaction was monitored via TLC. After 6 h, the reaction solvent was evaporated yielding a white solid. The solid was dissolved in CH_2Cl_2 and purified using flash column chromatography on silica gel (hexanes:ethyl acetate = 2:1) to yield crude containing **6-2** (414 mg, 77% yield crude), which was used in the next step without further purification.

Methyl 3,5-diaminobenzoate (6-3)[50]

To 3,5-diaminobenzoic acid (2.5 g, 16 mmol) dissolved in dry methanol [0.1 M] cooled to 0 °C in an ice-bath was added thionyl chloride (5 mL, 64 mmol) dropwise. The mixture was stirred at 0 °C for 30 minutes producing a grey emulsion. The mixture was removed from the ice-bath and stirred under reflux conditions. The reaction was monitored via TLC. After 8 h, the reaction

was allowed to cool slowly to room temperature. The reaction solvent was evaporated and the resulting crude was diluted with ethyl acetate. The organic layer was washed with $NaHSO_3$ (3 x 50 mL) and with brine (2 x 50 mL). The organic layer was collected, dried over $MgSO_4$ and concentrated *in vacuo* to yield **6-3** (2.2 g, 81% yield), as an orange-red solid: m.p. 131-132 °C; ^{1}H NMR (300 MHz, $CDCl_3$, ppm) δ 3.667 (bs, 4 H), 3.856 (s, 3 H), 6.175-6.190 (m, 1 H), 6.772 (s, 2 H); ^{13}C NMR (300 MHz, $CDCl_3$, ppm) δ 11.680, 52.275, 105.913, 107.215, 147.786. All data are consistent with literature values.[50]

Methyl 3,5-bis(*N*-Boc-amino)benzoate (6-4) and methyl 3-amino-5-(*N*-Boc-amino)benzoate (6-5)

To a solution of **6-3** (1 g, 6 mmol) and Et_3N (1.5 mL, 12 mmol) dissolved in a 1-to-1 mixture of dioxanes:H_2O [0.1 M] cooled to 0 °C was added di-*tert*-butyl dicarbonate (2.6 g, 12 mmol) dissolved in 5 mL dioxanes:H_2O (1:1). The mixture was stirred at room temperature and the reaction was monitored *via* TLC. After 24 h, the reaction solvent was evaporated and the resulting crude was diluted with ethyl acetate. The organic layer was washed with 10% citric acid (3 x 50 mL), H_2O (1 x 50 mL) and then with brine (1 x 50 mL). The organic layer was collected, dried over $MgSO_4$ and concentrated *in vacuo*. The resulting crude was purified using flash column chromatography on silica gel (hexanes:ethyl acetate = 4:1) to yield **6-4** (910 mg, 41% yield) as an orange solid and (hexanes:ethyl acetate = 2:1) and **6-5** (160 mg, 10% yield) as a yellow solid:

6-4: m.p. 220-221 °C; ^{1}H NMR (300 MHz, $CDCl_3$, ppm) δ 1.515 (s, 18 H), 3.888 (s, 3 H), 6.561 (s, 2 H), 7.657-7.665 (m, 2 H), 7.820 (m, 1 H); HRMS MS ES+ *m/z* calcd for $C_{15}H_{19}NO_6$ $(M+H)^+$ 367.1791, found 367.1869 (Δ 7.8 ppm).

6-5: m.p. 132-134 °C; ^{1}H NMR (300 MHz, $CDCl_3$, ppm) δ 1.457 (s, 9 H), 2.489 (s, 3 H), 3.319 (br s, 3 H), 7.034-7.046 (m, 1 H), 7.250-7.236 (m, 1 H), 7.312 (s, 1 H); HRMS MS ES+ *m/z* calcd for $C_{13}H_{18}N_2O_4$ $(M+H)^+$ 267.1267, found 267.1345 (Δ 7.8 ppm).

3,5-Bis(*N*-Boc-amino)-1-benzohydrazide (6-6)

To a solution of **6-4** (460 mg, 1 mmol) dissolved in CH_3OH [0.04 M] was added hydrazine monohydrate (0.1 mL, 1.5 mmol). The mixture was stirred under reflux conditions and the reaction was monitored *via* TLC. After 24 h, the reaction solvent was evaporated and the resulting solid was washed with CH_2Cl_2 to yield **6-6** (456 mg, 99% yield), as a white solid: m.p. 218-219 °C; ^{1}H NMR (300 MHz, $CDCl_3$, ppm) δ 1.515 (s, 18 H), 6.561 (s, 2 H), 7.657-7.665 (m, 2 H), 7.820 (m, 1 H).

3,5-Bis(*N*-Boc-amino)-1-biotinylbenzohydrazide (6-7)

To a mixture of **6-6** (74 mg, 0.2 mmol) and Et_3N (0.05 mL, 0.4 mmol) dissolved in DMF [0.1 M] was added biotin-OSu (108 mg, 0.2 mmol) dissolved in 1 mL DMF. The mixture was stirred at 90 °C and the reaction was monitored via TLC and FIA. After 24 h, the reaction solvent was evaporated. The resulting crude purified using flash column chromatography on silica gel (5% CH_3OH in CH_2Cl_2) to yield **6-7** (65 mg, 54% yield), as an off-white solid: ^{1}H NMR (300 MHz, $CDCl_3$, ppm) δ 1.226-1.488 (m, 2 H), 1.493 (s, 9 H), 1.622 (m, 4 H), 2.283-2.346 (m, 2 H), 2.674 (s, 3 H), 2.878 (s, 1 H), 2.956 (s, 1 H), 4.294 (m, 1 H), 4.472 (m, 1 H), 6.125 (bs, 1 H), 6.701 (bs, 1 H), 7.400 (m, 1 H), 7.737 (m, 1 H), 7.882 (s, 1 H), 9.632 (bs, 1 H); HRMS MS ES+ *m/z* calcd for $C_{27}H_{40}N_6O_7S$ $(M+H)^+$ 593.2679, found 593.2757 (Δ 7.8 ppm).

1-Biotinylaminobenzene-3,5-dicarboxylic acid dimethyl ester (6-8)

Method 1

To mixture of biotin (50 mg, 0.2 mmol), DCC (64 mg, 0.3 mmol) and DMAP (7 mg, 0.06 mmol) dissolved in DMF [1 M] was added Et_3N (0.03 mL, 0.2 mmol) dropwise followed by the dropwise addition of dimethyl 5-aminoisophthalate (43 mg, 0.2 mmol) dissolved in 1 mL DMF. The mixture was stirred at room temperature and the reaction was monitored via TLC. After 8 hours, the solvent was evaporated. The crude was dissolved in CH_2Cl_2 and purified using flash column chromatography on silica gel to yield **6-8** (75 mg, 83% yield)**,** as an off-white/orange solid:

Method 2

In a 0 °C ice-bath, biotin (200 mg, 0.8 mmol) was dissolved in $SOCl_2$ [0.2 M]. The mixture was stirred at room temperature. As the reaction progressed a yellow precipitate began to form. After 30 min, the excess $SOCl_2$ was evaporated to yield crude biotin-chloride. The resulting crude biotin-chloride was dissolved in 1 mL DMA and cooled to 0 °C. In a separate vessel, dimethyl 5-aminoisophthalate (224 mg, 1 mmol) and DMAP (30 mg, 0.2 mmol) were dissolved in DMAc [1 M] and cooled to 0 °C. The isophthalate mixture was added to the biotin-chloride mixture dropwise. The mixture was warmed slowly to room temperature for 8 h, and then heated at 90 °C for an additional 2 h. Upon heating the solution turned red. After heating, the reaction was allowed to cool to room temperature and then diluted with water producing a precipitate. The orange precipitate was filtered and collected. The collected precipitate was dissolved in DMF and precipitated out with water. The resulting precipitate was washed with chloroform, dried and collected to yield **6-8** (300 mg, 84% yield), as an orange solid:

All data are consistent for each reaction: m.p. 123-126 °C; ^{1}H NMR (300 MHz, CD_3OD, ppm) δ 1.442-1.824 (m, 6 H), 2.346-2.372 (t, J = 3.9 Hz, 2 H), 2.675-2.717 (d, J = 6.3 Hz, 1 H), 2.892-2.950 (dd, J_1 = 2.4 Hz, J_2 = 2.4 Hz, 1 H), 3.289-3.311 (m, 1 H), 4.575-4.616 (m, 1 H), 4.771-4.813 (m, 1 H), 6.048 (s, 1 H) 7.488 (s, 1 H), 8.450 (m, 2 H); HRMS MS ES+ *m/z* calcd for $C_{20}H_{25}N_3O_6S$ $(M+H)^+$ 436.1464, found 436.1542 (Δ 7.8 ppm).

5-Biotinylamino-isophthalyl-dihydrazide (6-9)

In a two-necked round bottomed flask, **6-8** (75 mg, 0.17 mmol) was dissolved in CH_3OH [0.5 M]. To the mixture was added hydrazine, dropwise (0.03 mL, 0.68 mmol). The mixture was stirred under reflux conditions and the reaction was monitored via TLC. After 16 h, the mixture was allowed to cool to room temperature. The solvent was evaporated *in vacuo* to yield **6-9** (45 mg, 75% yield), as a sticky, yellow solid without further purification: ^{1}H NMR (400 MHz, CD_3OD, ppm) δ 1.219-1.493 (m, 2 H), 1.632-1.859 (m, 4 H), 2.351-2.387 (t, *J* = 3.6 Hz, 2 H), 2.681-2.713 (d, *J* = 6.4 Hz, 1 H), 2.899-2.943 (dd, $J_1 = J_2$ = 2.4 Hz, 1 H), 3.292-3.304 (m, 1 H), 4.280-4.311 (m, 1 H), 4.470-4.500 (m, 1 H); ^{13}C NMR (400 MHz, CD_3OD, ppm) δ 21.178, 28.812, 29.237, 29.753, 34.739, 35.999, 37.509l 38.290, 43.823, 54.545, 58,038, 59.645, 61.071, 64.403, 66.027, 158.615, 168.829, 175.690.

Attempted synthesis of 3-biotinyl-5-CPT-linker-1-benzohydrazide (6-10)

Method 1

A mixture of **6-9** (6 mg, 0.01 mmol), DCC (6 mg, 0.015 mmol) and DMAP (1 mg, 0.0025 mmol) was dissolved in DMF [0.2 M]. To the solution was added Et_3N (0.01 mL, 0.01 mmol) followed by the dropwise addition of **4-22a** (8 mg, 0.005 mmol) in DMF [0.01 M]. The mixture was stirred at room temperature and the reaction was monitored via TLC. After 8 h, TLC showed no reaction. The mixture was then stirred at 100 °C. Based on TLC, the starting material was

consumed. The reaction mixture was purified directly using flash column chromatography on silica gel to yield unreacted CPT-Linker-CO_2H and 2 mg free CPT.
Method 2
A mixture of **6-9** (7 mg, 0.01 mmol) and **4-23a** (10 mg, 0.01 mmol) was dissolved in DMF [0.1 M]. To the mixture was added Et_3N (0.01 mL, 0.01 mmol). The mixture was stirred at room temperature and the reaction was monitored via TLC. After 8 h, TLC and FIA analysis of the mixture showed no reaction. The reaction mixture was purified using flash column chromatography on silica gel to yield 8 mg unreacted **4-23a** and 5 mg unreacted **6-9**.

***N*^{1},*N*^{3}-Bis(2-aminoethyl)-5-biotinylaminoisophthalamide (6-11)**
To **6-8** (120 mg, 0.28 mmol) dissolved in CH_3OH [1 M] was added ethylenediamine (0.07 mL, 1.7 mmol), dropwise. The mixture was stirred under reflux conditions and the reaction was monitored via FIA. After 14 h, the solvent was evaporated, and the resulting solid was washed with chloroform to yield **6-11** (133 mg, 99% yield), as a sticky, yellow solid, which was used without further purification: ^{1}H-NMR (500 MHz, CD_3OD, ppm) δ 1.279-1.403 (m, 2 H), 1.487-1.669 (m, 4 H), 2.432 (t, *J* = 7 Hz, 2 H), 2.890 (t, *J* = 6.5 Hz, 4 H), 2.915-2.941 (m, 1 H), 3.213-3.230 (m, 2 H), 3.339 (s, 2 H), 3.487 (t, *J* = 6.5 Hz, 4 H), 4.307 (dd, J_1 = 8 Hz, J_2 = 4.5 Hz, 1 H), 4.484 (dd, *J*1 = 7.5 Hz, *J*2 = 5 Hz, 1 H), 7.994 (s, 1 H), 8.158 (s, 1 H), 8.278-8.367 (m, 1 H); HRMS MS ES+ *m/z* calcd for $C_{22}H_{33}N_7O_4S$ $(M+H)^+$ 492.2315, found 492.2405 (Δ 0.9 ppm).

General procedure for 1st attempted drug-linker-splitter coupling (6-12a and 6-12b)
To a solution of **6-11**, drug-linker-CO_2H (2 eq.) and DMAP (1 eq.) dissolved in CH_2Cl_2 [0.01 M] was added DCC (1.1 eq.) dissolved in CH_2Cl_2. The mixture was stirred at room temperature and the reaction was monitored via TLC, using ninhydrin as a staining reagent. After 16 h, the reaction solvent was evaporated and the mixture was diluted with 5 mL ethyl acetate. The organic layer was washed with water (5 x 5 mL) and then with brine (1 x 5 mL). The organic layer was collected, dried over $MgSO_4$ and concentrated in vacuo. The resulting crude was purified using flash column chromatography on silica gel (hexanes:ethyl acetate = 3:1) to yield:
6-12a: none obtained.
6-12b [drug = paclitaxel; **6-11** (4 mg, 0.009 mmol), paclitaxel-linker-CO_2H (20 mg, 0.018 mmol), DMAP (1 mg, 0.009 mmol), DCC (8 mg, 0.01 mmol)]: 20 mg, 80% yield, as yellow-oil; ^{1}H NMR (500 MHz, $CDCl_3$, ppm) δ 0.849-0.827 (m, 4 H), 0.862-0.890 (m, 4 H), 0.981-1.002 (m, 4 H), 1.115-1.362 (m, 35 H), 1.366-1.433 (m, 6 H), 1.657-1.726 (m, 22 H), 1.746-1.769 (m, 5 H), 1.893 (s, 6 H), 2.038 (s, 4 H), 2.244 (s, 1 H), 2.350-2.360 (m, 6 H), 2.523 (s, 2 H), 2.604 (s, 2 H), 2.827 (t, *J* = 3 Hz, 2 H), 2.876 (s, 2 H), 2.928 (t, *J* = 4 Hz, 1 H), 2.949 (s, 2 H), 2.999 (t, *J* = 3 Hz, 2 H), 3.081 (t, *J* = 3 Hz, 1 H), 3.796 (d, *J* = 3 Hz, 2 H), 3.979-4.077 (m, 1 H), 4.095-4.138 (m, 3 H), 4.168-4.185 (m, 2 H), 4.238-4.266 (m, 2 H), 4.289-4.306 (m, 2 H), 4.359-4.379 (m, 1 H), 4.415-4.424 (m, 2 H), 4.822 (s, 2 H), 4.900-4.967 (m, 6 H), 5.072 (s, 2 H), 5.667 (d, *J* = 2 Hz, 2 H), 6.183 (t, *J* = 4 Hz, 2 H), 6.283 (s, 2 H), 7.096-7.103 (m, 1 H), 7.283-7.336 (m, 5 H), 7.451-7.482 (m, 4 H), 7.529 (s, 1 H), 7.578-7.619 (m, 2 H), 7.682 (s, 1 H), 7.771 (d, *J* = 4 Hz, 1 H), 8.007 (s,1 H), 8.108 (d, *J* = 4 Hz, 4 H), 8.457-8.463 (m, 1 H).
6-12b: [drug = camptothecin; **6-11** (15 mg, 0.03 mmol), CPT-linker-CO_2H (10 mg, 0.015 mmol), DMAP (2 mg, 0.01 mmol), DCC (7 mg, 0.01 mmol)]: not obtained.

***N*-Boc-ethylenediamine (6-13)[46]**

To ethylenediamine (13 mL, 0.2 mol) dissolved in CH_2Cl_2 [0.1 M] was added di-*tert*-butyl dicarbonate (5 g, 0.02 mol) dissolved in 5 mL CH_2Cl_2, dropwise via an addition funnel. Upon addition, white precipitate formed. After 8 h, the reaction solvent was evaporated, diluted with water and extracted with $CHCl_3$ (3 x 50 mL). The organic layers were collected, dried over $MgSO_4$ and concentrated *in vacuo* to yield **6-13** (3 g, quantitative yield) without further purification: ^{1}H NMR (300 MHz, $CDCl_3$, ppm) δ 1.140 (s, 2 H), 1.180 (s, 9 H), 2.502-2.532 (t, *J* = 2.25 Hz, 2 H), 2.871-2.912 (m, 2 H), 5.554 (s, 1 H); ^{13}C NMR (300 MHz, CD_3OD, ppm) δ 28.403, 41.865, 43.458, 78.753, 156.407. All data are consistent with literature values.[46]

Attempted synthesis of N^1-(Boc-ethylenediamine)-N^3-ethyleneamine-5-biotinylaminobenzohydrazide (6-14) and (6-15)

Method 1

To **6-11** (58 mg, 0.1 mol) dissolved in a 1-to-1 mixture of CH_2Cl_2:DMF [0.1 M] was added di-*tert*-butyl dicarbonate (2.5 g, 0.01 mol) dissolved in 2 mL CH_2Cl_2, dropwise via an addition funnel. Upon addition, white precipitate formed. After 8 h, the reaction solvent was evaporated, diluted with water and extracted with $CHCl_3$ (3 x 50 mL). The organic layers were collected, dried over $MgSO_4$ and concentrated *in vacuo* to yield **6-11** (40 mg, 69% recovered) and **6-15** (6 mg, 6% yield), bis-Boc-protected product, without formation of **6-14**.

Method 2

To **6-17** (100 mg, 0.18 mmol) dissolved in CH_3OH [1 M] was added ethylenediamine (0.07 mL, 0.6 mmol). The mixture was stirred under reflux conditions. The reaction was monitored via TLC. After 16 h, the reaction solvent was evaporated, diluted with chloroform, and washed with water. The organic layer was collected, dried over $MgSO_4$ and concentrated *in vacuo*. The resulting crude was purified using flash column chromatography on silica gel to yield **6-14** (100 mg, quant. yield), as a yellow oily foam.

All data are consistent for each reaction: ^{1}H-NMR (500 MHz, $CDCl_3$, ppm): δ 1.236 (m, 2 H), 1.435 (s, 9 H), 1.822 (m, 4 H), 2.329-2.337 (m, 2 H), 2.816 (br s, 4 H), 3.183-3.221 (m, 4 H), 4.273 (m, 1 H), 4.457 (m, 1 H), 5.932 (s, 1 H), 8.158 (s, 1 H), 8.430 (m, 3 H); HRMS MS ES+ *m/z* calcd for $C_{27}H_{41}N_7O_6S$ $(M+H)^+$ 592.2839, found 592.2916 (Δ 7.7 ppm).

3-Biotinylamino-5-benzoic acid methyl ester (6-16)

Method 1

To **6-8** (100 mg, 0.2 mmol) dissolved in a 1:1 mixture of THF:MeOH [0.2 M] cooled to 0 °C was added 1 M NaOH (0.2 mL, 0.02 mmol). The mixture was allowed to warm slowly to room temperature and the reaction was monitored via TLC. After 16 hours, the reaction solvent was adjusted to pH 2 with 1 M HCl. The acidified solution was extracted with ethyl acetate (3 x 50 mL). The organic layers were collected, dried over $MgSO_4$ and concentrated *in vacuo* to yield **6-16** (50 mg, 50% yield) without further purification:

Method 2

In a 0 °C ice-bath, biotin (200 mg, 0.8 mmol) was dissolved in $SOCl_2$ [0.2 M]. The mixture was stirred at room temperature. As the reaction progressed a yellow precipitate began to form. After 30 min, the excess $SOCl_2$ was evaporated to yield crude biotin-chloride. The resulting crude biotin-chloride was dissolved in 1 mL DMAc and cooled to 0 °C. In a separate vessel, monomethyl 5-aminoisophthalate (224 mg, 1 mmol) and DMAP (30 mg, 0.02 mmol) were dissolved in DMAc [1 M] and cooled to 0 °C. The isophthalate mixture was added to the biotin-chloride mixture dropwise. The mixture was warmed slowly to room temperature for 8 h, and

then heated at 90 °C for an additional 2 h. Upon heating the solution turned red. After heating, the reaction was allowed to cool to room temperature. At room temperature, the reaction mixture was diluted with water. Upon dilution, the product precipitated out. The orange precipitate was filtered and collected. The collected precipitate was dissolved in DMF and precipitated out with water. The resulting precipitate was washed with $CHCl_3$, dried and collected to yield **6-16** (260 mg, 75% yield), as an orange solid:
All data are consistent for each reaction: ^{1}H NMR (500 MHz, CD_3OD, ppm) δ 1.442-1.824 (m, 6 H), 2.289-2.355 (m, 2 H), 2.930-2.940 (dd, J_1 = 2.4 Hz, J_2 = 2.4 Hz, 2 H), 3.182-3.247 (m, 1 H), 3.929 (s, 3 H), 4.285-4.321 (m, 1 H), 4.468-4.482 (m, 1 H), 8.346 (s, 1H), 8.447 (s, 1 H), 8.708 (s, 1 H); HRMS MS ES+ *m/z* calcd for $C_{19}H_{23}N_3O_6S$ $(M+H)^+$ 422.1308, found 422.1395 (Δ 8.7 ppm).

3-(*N*-Boc-ethylenediamino)-5-biotinylamino-1-benzoic acid methyl ester (6-17)
Method 1
In a 0 °C ice-bath, **6-16** (25 mg, 0.06 mmol) was dissolved in $SOCl_2$ [0.06 M]. The mixture was stirred at room temperature. After 30 min, the excess $SOCl_2$ was evaporated. The resulting acid chloride was dissolved in 1 mL CH_3OH and cooled to 0 °C. To this solution was added **6-13** (0.01 mg, 0.06 mmol) in 0.5 mL CH_3OH. The mixture was stirred and allowed to warm to room temperature. The reaction was monitored via TLC. After 8 h, the solvent was evaporated, the resulting crude was diluted with $CHCl_3$, washed with water (3 x 20 mL) and then with brine (3 x 20 mL). The organic layers were collected, dried over $MgSO_4$ and concentrated *in vacuo* to yield **6-17** (12 mg, 35% after 2 steps):
Method 2
A mixture of **6-16** (1 g, 2.4 mmol) and CDI (2.8 mmol) was dissolved in THF. The reaction was stirred under reflux conditions and monitored via TLC. After 1 hour, the reaction mixture was cooled to 50 °C, upon which Boc-protected ethylene diamine (2.4 mmol) dissolved in THF was added. The reaction was stirred under reflux conditions and monitored by TLC. After 24 h, the reaction was diluted with water and extracted with ethyl acetate (3 x 50 mL). The organic layers were combined, dried over $MgSO_4$ and concentrated *in vacuo*. The resulting crude material was recrystalized using ethyl acetate and hexanes, and then by CH_3OH and CH_2Cl_2 to yield **6-17** (200 mg, 15% yield), as a brown foam and unreacted starting material:
Method 3
A mixture of **6-16** (500 mg, 1.2 mmol), HOSu (1.2 mmol) and DIC (1.4 mmol) was dissolved in a 1:1 mixture of THF:pyridine [0.1 M] and cooled to 0 °C. The reaction was stirred at room temperature and monitored via TLC. After 16 hours, the reaction was diluted with water to produce a precipitate. The precipitate was collected and washed with ethyl acetate to yield a crude mixture contained OSu-activated biotin-splitter. The resulting crude was dissolved in THF. To the solution was added Boc-protected ethylene diamine (1.2 mmol) dissolved in THF. The reaction was stirred at room temperature and monitored by TLC. After 16 h, the reaction was diluted with water and extracted with ethyl acetate (3 x 50 mL). The organic layers were combined, dried over $MgSO_4$ and concentrated *in vacuo*. The resulting crude material was recrystalized using ethyl acetate and hexanes, and then by CH_3OH and CH_2Cl_2 to yield **6-17** (600 mg, 90% yield after 2 steps), as brown foam:
Method 4
To **6-8** (100 mg, 0.2 mmol) dissolved in CH_3OH [0.1 M] was added **6-13** (4 mg, 0.2 mmol) dissolved in CH_3OH [0.2 M]. The mixture was stirred at room temperature and the reaction was monitored via TLC. After 16 h, the reaction solvent was evaporated, diluted with water and

extracted with $CHCl_3$ (3 x 50 mL). The organic layers were collected, dried over $MgSO_4$ and concentrated *in vacuo*. The resulting crude was purified using flash column chromatography on silica gel to yield **6-17** (100 mg, 78% yield), as light-brown foam:
All data are consistent for each reaction: ^{1}H-NMR (500 MHz, $CDCl_3$, ppm): δ 1.211-1.234 (m, 2 H), 1.397 (s, 9 H), 1.627-1.766 (m, 4 H), 2.366-2.415 (t, *J* = 3.9 Hz, 2 H), 2.722 (m, 4 H), 2.941-2.915 (m, 1 H), 3.085-3.192 (m, 4 H), 3.888 (s, 3 H), 4.304 (m, 1 H), 4.494 (m, 1 H), 5.000 (br s, 3 H), 5.932 (s, 1 H), 6.708 (s, 1 H), 8.286 (s, 1 H), 8.439 (m, 3 H), 9.200 (s, 1 H); HRMS MS ES+ *m/z* calcd for $C_{26}H_{37}N_5O_7S$ $(M+H)^+$ 564.2414, found 564.2490 (Δ 7.6 ppm).

2nd Attempted synthesis of CPT-linker biotin-splitter coupling (6-18)
Method 1
A mixture of **4-22a** (26 mg, 0.04 mmol), DCC (13 mg, 0.048 mmol) and DMAP (2 mg, 0.0012 mmol) was dissolved in CH_2Cl_2 (0.1M) and cooled to 0 °C. To the mixture was added 1 equivalent (0.01 mL) of Et_3N, followed by the dropwise addition of **6-14** (33 mg, 0.04 mmol) dissolved in CH_2Cl_2 [0.1 M]. The mixture was allowed to warm to room temperature. After 8 h, the reaction was monitored via TLC. TLC showed no reaction. The mixture was heated at 60 °C and the reaction monitored via TLC. After heating for 4 h, the reaction was allowed to cool to room temperature. The solvent was diluted with aqueous NH_4Cl, extracted $CHCl_3$ (3 x 50 mL). The organic layers were collected washed with water (3 x 20 mL) and then with brine (3 x 20 mL), dried over $MgSO_4$ and concentrated *in vacuo*. The resulting crude was purified using flash column chromatography on silica gel to yield 5 mg camptothecin and no desired product.
Method 2
To **4-23a** (10 mg, 0.06 mmol) crude was dissolved in CH_2Cl_2 [0.1 M] and cooled to 0 °C. To the mixture was added Et_3N (0.01 mL, 0.06 mmol) followed by the dropwise addition of **6-13** (40 mg, 0.06 mmol) dissolved in CH_2Cl_2 [0.1 M]. The mixture was allowed to warm to room temperature. After 8 h, the reaction was monitored via TLC. The solvent was diluted with aqueous NH_4Cl, extracted with $CHCl_3$ (3 x 20 mL). The organic layers were collected washed with water (3 x 20 mL) and then with brine (3 x 20 mL), dried over $MgSO_4$ and concentrated *in vacuo*. The resulting crude was purified using flash column chromatography on silica gel to yield 33 mg **6-14**, 5 mg **4-23a** and no desired product.

CPT-Me-linker-biotin-splitter (6-19)
To **4-23b** (10 mg, 0.01 mmol) dissolved in CH_2Cl_2 [0.1 M] was added **6-14** (10 mg, 0.01 mmol) dissolved in CH_2Cl_2 [0.1 M]. The mixture was stirred at room temperature and the reaction was monitored via TLC. After 16 h, the solvent was evaporated resulting in crude which was purified using flash column chromatography on silica gel to yield **6-19** (26 mg, 85% yield), as a yellow solid: ^{1}H NMR (500 MHz, $CDCl_3$, ppm) δ 0.861 (m, 1 H), 1.486 (m, 3 H), 1.636 (m, 2 H), 1.779 (m, 3 H), 1.978 (s, 2 H), 2.028 (s, 3 H), 3.118-3.458 (m, 20 H), 3.895 (s, 6 H), 4.362 (m, 1 H), 4.531 (m, 1 H), 5.098 (br s, 1 H), 5.286 (s, 3 H), 5.373 (m, 1 H), 5.461-5.591 (m, 4 H), 6.037 (s, 1 H), 6.352 (2 H), 6.521 (m, 1 H), 6.799 (m, 1 H), 7.122 (m, 1 H), 7.656 (m, 1 H), 7.807 (m, 1 H), 7.911-7.939 (t, *J* = 6.5 Hz, 1 H), 8.045 (m, 1 H), 8.214-8.240 (m, 1 H), 8.325 (s, 1 H), 8.462 (s, 2 H), 9.131 (s, 1 H), 11.085 (br s, 1 H); ^{13}C NMR (400 MHz, $CDCl_3$ ppm): δ 8.809, 18.522, 23.280, 25.640, 28.488, 28.357, 28.547, 29.875, 34.003, 34.777, 35.505, 36.113, 36.795, 37.319, 40.605, 41.060, 46.213, 51.958, 52.094, 53.618, 53.627, 55.759, 58.590, 60.722, 62.392, 70.686, 79.868, 125.028, 125.886, 128.352, 131.266, 139.500, 155.413, 157.151,

159.207, 164.641, 166.378, 170.347, 172.555, 172.730, 173.451, 173.557; LC-MS MS (ESI) *m/z* calcd for $C_{60}H_{69}N_9O_{12}S_3$ $(M+H)^+$ 1204.4, found 1204.4.

Drug Conjugate Bearing Dual-Warheads SB-T-1214 and Camptothecin (DW-1)

6-19 (15 mg, 0.01 mmol) was dissolved in 2 mL of 10% TFA in CH_2Cl_2. After the addition, the reaction solution turned bright yellow. The mixture was stirred at room temperature. After 16 h, the reaction was quenched with $NaHCO_3$ and filtered over cotton. The filtrate was evaporated resulting in 10 mg of Boc-deprotected **6-19**, as yellow-brown oil which was used without further purification. The resulting oil was dissolved in CH_2Cl_2 [0.05 M]. This solution was added dropwise to a solution of **4-20** (10 mg, 0.02 mmol) dissolved in CH_2Cl_2 [0.05 M]. The mixture was stirred at room temperature and the reaction was monitored via TLC. After 16 h at room temperature, the mixture was directly purified using flash column chromatography on silica gel to yield **DW-1** (8 mg, 26% after 2 steps) as a yellow solid: ^{1}H NMR (500 MHz, $CDCl_3$, ppm) δ 0.845-0.913 (m, 6 H), 0.994-1.471 (m, 68 H), 1.742 (m, 14 H), 1.922 (m, 9 H), 2.350-2.447 (m, 14 H), 2.528-2.576 (m, 4 H), 2.661 (s, 2 H), 2.723 (s, 10 H), 2.808 (s, 1 H), 2.906 (s, 2 H), 2.981 (2 H), 3.457-3.543 (m, 2 H), 3.717 (t, *J* = 4 Hz, 2 H), 3.796-3.819 (m, 2 H), 3.954 (s, 2 H), 4.949-5.034 (m, 6 H), 5.169 (m, 2 H), 5.689 (d, *J* = 7 Hz, 1 H), 6.196-6.260 (m, 2 H), 6.302 (d, *J* = 7 Hz, 1 H), 7.490 (t, *J* = 7.5 Hz, 4 H), 7.606-7.637 (m, 2 H), 7.805-7.849 (m, 2 H), 8.038 (s, 1 H), 8.117-8.132 (m, 4 H); MALDI-TOF *m/z* calcd for $C_{113}H_{132}N_{10}O_{27}S_5$ $(M+Na+H)^+$ 2222.6, found 2246.6.

Cell culture system for MTT assay

Cell lines (obtained from ATCC unless otherwise noted and maintained at SBU Cell Culture/Hybridoma Facility) were cultured in RPMI-1640 with L-glutamine (Lonza BioWhittaker, BW12-702F: A2780, DLD-1, ID-8, LCC6 MDR, LCC6 wt, MCF-7), DMEM (Lonza BioWhittaker, BW12-604F: BT-20, CFPac-1, MDA MB 231, Panc-1) or McCoy's 5A (Gibco #16600: HT-29, SkBr3) supplemented with 5% FBS (Thermo Scientific, HyClone, SH3007003), 5% Nu Serum (BD Biosciences, 355100) and 1% Penn Strip, at 37 °C in a humidified incubator with 5% CO_2. Cell lines treated with drug conjugate **DW-1** were cultured in RPMI-1640 Medium 10 x (Sigma Aldrich, R1145) supplemented with tissue culture grade water, 0.3 g/L L-glutamine, 2.0 g/L sodium bicarbonate, 10% FBS, and 1% Penn Strep. The cells were washed with DPBS and dissociated using TrypLE. The cells were incubated at 37 °C until the cells were detached from the plate, transferred to a centrifuge vial and pelleted via centrifugation at 1500 rpm for 5 min. The cells were counted per 1 mL media. The desired amount of cell media was added to the cell solution so that 8,000 cells can added to each well of a 96-well plate in 200 μL aliquots. After the addition, the cells were incubated at 37 °C with 5% CO_2.

Single drug MTT assay

A serial dilution of the drug compound (SB-T-1214 or camptothecin) dissolved in sterile DMSO was added using fully-supplemented RPMI. The residual medium in each well was aspirated and 100 μL of the different drug-concentration solutions were added to each well of every column of the 96-well plate. After the addition of the drug solution, the cells were incubated at 37 °C for 48 hours. After the incubation period, the media was aspirated and the cells were washed with DPBS. To the washed cells 0.5 μL of a solution of 5 mg MTT (3-(4,5-dimethylthiazol-2-yl)-2,5-diphenyltetrazolium bromide) per 10 mL color-less media or DPBS

were added. The cells were then incubated at 37 °C for 3 hours. After the incubation period, the MTT solution was aspirated and the remaining crystals were washed with DPBS. The crystals were dissolved using a 0.5 μL of 0.4 M HCl in isopropanol. The plates were shaken for 10 minutes to assure that all of the crystals are dissolved. The optical density was determined from the resulting solutions using the Acsent Multiskan optical density reader. Each experiment was run in triplicate.

Simultaneous-drug treatment MTT assay

Cells were resuspended in 200 μL medium with approximately 8000 to 10,000 cells per well of a 96-well plate and incubated at 37 °C with 5% CO_2 for 24 hours before drug treatment. A serial dilution of a 1-to-1 mixture of SB-T-1214 and camptothecin was dissolved in sterile DMSO was added using media. The residual media in each well were aspirated and the different drug solutions were added to each well of every column of the 96-well plate. After the addition of the drug solution, the cells were incubated at 37 °C for 48 hours. After the incubation period, the media was aspirated and the cells were washed with DPBS. To the washed cells 0.5 μL of a solution of 5 mg MTT per 10 mL color-less media or DPBS were added. The cells were then incubated at 37 °C for 3 hours. After the incubation period, the MTT solution was aspirated and the remaining crystals were washed with DPBS. The crystals were dissolved using a 0.5 μL of 0.4 M HCl in isopropanol. The plates were shaken for 10 minutes to assure that all of the crystals are dissolved. The optical density was determined from the resulting solutions using the Acsent Multiskan optical density reader. Each experiment was run in triplicate.

Sequential drug treatment MTT assay

Cells were resuspended in 200 μL medium with approximately 8000 to 10,000 cells per well of a 96-well plate and incubated at 37 °C with 5% CO_2 for 24 hours before drug treatment. Two sets of serial dilutions of SB-T-1214 and camptothecin dissolved in sterile DMSO were added using media. The residual media in each well were aspirated and the different drug solutions were added to each well of every column of the 96-well plate. After the addition of the first drug solution, the cells were incubated at 37 °C for 24 hours. After the incubation period, the second drug solution was added followed by an additional 24 hour incubation period at 37 °C. After the second incubation period, the media was aspirated and the cells were washed with DPBS. To the washed cells 0.5 μL of a solution of 5 mg MTT per 10 mL color-less media or DPBS were added. The cells were then incubated at 37 °C for 3 hours. After the incubation period, the MTT solution was aspirated and the remaining crystals were washed with DPBS. The crystals were dissolved using a 0.5 μL of 0.4 M HCl in isopropanol. The plates were shaken for 10 minutes to assure that all of the crystals are dissolved. The optical density was determined from the resulting solutions using the Acsent Multiskan optical density reader. Each experiment was run in triplicate.

Drug conjugate MTT assay

A serial dilution of **DW-1** dissolved in sterile DMSO was prepared by the addition of fully-supplemented RPMI-1640 Medium 10 x. The residual medium in each well was aspirated and the different drug-concentration solutions were added to each well of every column of the 96-well plate in 100 μL aliquots. After the addition of the drug solution, the cells were incubated at 37 °C for 48 or 72 hour periods. After the incubation period, the medium was aspirated and the cells were washed with DPBS and then 40 μL of 0.5 mg/mL MTT in DPBS was added to each

well. The cells were then incubated at 37 °C for 3 hours. After the incubation period, the MTT solution was aspirated and the remaining crystals were dissolved using a 40 μL of 0.4 M HCl in isopropanol. The plates were shaken for 10 minutes to assure that all of the crystals are dissolved. The optical density was determined from the resulting solutions using the Acsent Multiskan optical density reader. Each experiment was run in triplicate.

Data analysis for MTT assay

The optical density data was used to calculate IC_{50} values for each drug on a given cell line using the Hill slope equation. The optical density values obtained from each concentration of drug solution were divided by the optical density value obtained from the cells with zero drug concentration. Using SigmaPlot v.10, the ratios were plotted versus the drug concentration and the IC_{50} values were calculated from the plot using the pre-programmed calculation within the SigmaPlot program.

§ 6.5.0 References

1. Conti, J. A.; Kemeny, N. E.; Saltz, L. B.; Huang, Y.; Tong, W. P.; Chou, T. C.; Sun, M.; Pulliam, S.; Gonzalez, C. Irinotecan is an active agent in untreated patients with metastatic colorectal cancer. *J. Clin. Oncol.* **1996,** 14, 709-715.
2. Twelves, C.; Scheithauer, W.; McKendrick, J.; Seitz, J.-F.; Van Hazel, G.; Wong, A.; Diaz-Rubio, E.; Gilberg, F.; Cassidy, J. Capecitabine versus 5-fluorouracil/folinic acid as adjuvant therapy for stage III colon cancer: final results from the X-ACT trial with analysis by age and preliminary evidence of a pharmacodynamic marker of efficacy *Ann Oncol* **2011,** Sept. 6, 1-9.
3. Grothey, A.; Sargent, D.; Goldberg, R. M.; Schmoll, H.-J. Survival of Patients With Advanced Colorectal Cancer Improves With the Availability of Fluorouracil-Leucovorin, Irinotecan, and Oxaliplatin in the Course of Treatment *J. Clin. Oncol.* **2004,** 22, 1209-1214.
4. Mross, K.; Kratz, F. Limits of Conventional Cancer Chemotherapy. In *Drug Delivery in Oncology*, Kratz, F.; Senter, P.; Steinhagen, H., Eds. Wiley-VCH Verlag GmbH & co. KGaA: Weinheim, Germany, 2012; Vol. 1, pp 3-31.
5. Frei III, E.; Holland, J. F.; Schneiderman, M. A.; Pinkel, D.; Selkirk, G.; Freireich, E. J.; Silver, R. T.; Gold, G. L.; Regelson, W. A Comparative Study of Two Regimens of Combination Chemotherapy in Acute Leukemia. *Blood* **1958,** 13, 1126-1148.
6. Frei III, E.; Freireich, E. J.; Gehan, E.; Pinkel, D.; Holland, J. F.; Selawry, O.; Haurani, F.; Spurr, C.; Hayes, D. M.; James, G. W.; Rothberg, H.; Sodee, B.; Rundles, R. W.; Schroeder, L. R.; Hoogstraten, B.; Wolman, I. J.; Traggis, D. G.; Cooper, T.; Ebaugh, F.; Taylor, R. Studies of Sequential and Combination Antimetabolite Therapy in Acute Leukemia: 6-Mercaptopurine and Methotrexate. *Blood* **1961,** 18, 431-454.
7. Frei III, E.; Karon, M.; Levin, R. H.; Freireich, E. J.; Taylor, R. J.; Hananian, J.; Selawry, O.; Holland, J. F.; Hoogstraten, B.; Wolman, I. J.; Abir, E.; Sawitsky, A.; Lee, S.; Mills, S. D.; Burgert Jr., E. O.; Spurr, C. L.; Patterson, R. B.; Ebaugh, F. G.; James III, G. W.; Moon, J. H. The Effectiveness of Combinations of Antileukemic Agents in Inducing and Maintaining Remission in Children with Acute Leukemia. *Blood* **1965,** 26, 642-656.
8. Scott, J. L. The effect of nitrogen mustard and maintenance chlorambucil in the treatment of advanced Hodgkin's disease. *Cancer Chemother. Rep.* **1963,** 27, 27-32.

9. DeVita Jr., V. T.; Serpick, A. A.; Carbone, P. P. Combination chemotherapy in the treatment of advanced Hodgkin's disease. *Ann. Intern. Med.* **1970,** 73, 881-895.
10. Devita, V. T.; Lewis, B. J.; Rozencweig, M.; Muggia, F. M. The chemotherapy of Hodgkin's diesease: past experiences and future directions. *Cancer* **1978,** 42(2 suppl), 979-990.
11. Devita Jr., V. T.; Chu, E. A History of Cancer Chemotherapy. *Cancer Res.* **2008,** 68, 8643-8653.
12. Greenspan, E. M.; Fieber, M.; Lesnick, G.; Edelman, S. Response of advanced breast cancer to the combination of the anti-metabolite methotrexate and the alkylating agent thiotepa. *J. Mt Sinai Hosp.* **1963,** 30, 246-267.
13. Canellos, G. P.; Pocock, S. J.; Taylor III, S. G.; Sears, M. E.; Klassen, D. J.; Band, P. R. Combination chemotherapy for metastatic breast carcinoma. Prospective comparison of multiple drug therapy with L-phenylalanine mustard. *Cancer* **1976,** 38, 1882-1886.
14. Bonadonna, G.; Brusamolino, E.; Valagussa, P.; Rossi, A.; Brugnatelli, L.; Brambilla, C.; De Lena, M.; Tancini, G.; Bajetta, E.; Musumeci, R.; Veronesi, U. Combination chemotherapy as an adjuvant treatment in operable brease cancer. *N. Engl. J. Med.* **1976,** 294, 405-410.
15. Gradishar, W. J.; Meza, L. A.; Amin, B.; Samid, D.; Hill, T.; Chen, Y.-M.; Lower, E. E.; Marcom, P. K. Capecitabine plus paclitaxel as front-line combination therapy for metastatic breast cancer: a multicenter phase II study. *J. Clin. Oncol.* **2004,** 22, 2321-2327.
16. Blum, J. L.; Dees, E. C.; Chacko, A.; Doane, L.; Ethirajan, S.; Hopkins, J.; McMahon, R.; Merten, S.; Negron, A.; Neubauer, M.; Ilegbodu, D.; Boehm, K. A.; Asmar, L.; O.Shaughnessy, J. A. Phase II trial of capecitabine and weekly paclitaxel as first-line therapy for metastatic breast cancer. *J. Clin. Oncol.* **2006,** 24, 4384-4390.
17. Murren, J. R.; Peccerillo, K.; DiStasio, S. A.; Li, X.; Leffert, J. J.; Pizzorno, G.; Burtness, B. A.; McKeon, A.; Cheng, Y.-c. Dose escalation and pharamacokinetic study of irinotecan in combination with paclitaxel in patients with advanced cancer. *Cancer Chemother. Pharmacol.* **2000,** 45, 43-50.
18. Lilenbaum, R. C.; Ratain, M. J.; Miller, A. A.; Hargis, J. B.; Hollis, D. R.; Rosner, G. L.; O'Brien, S. M.; Brewster, L.; Green, M. R.; Schilsky, R. L. Phase I study of paclitaxel and topotecan in patients with advanced tumors: a Cancer and Leukemia Group B study. *J. Clin. Oncol.* **1995,** 13, 2230-2237.
19. Bissery, M. C.; Vrignaud, P.; Lavelle, F. In vivo evaluation of the docetaxel-irinotecan combination. *Proc. Am. Assoc. Cancer Res.* **1996,** 37, 378.
20. Langer, C. J. Irinotecan/Taxane combinations in advanced non-small-cell lung cancer. *Clin. Lung Cancer* **2002,** 4, S10-S14.
21. Wall, M. E.; Wani, M. C. Camptothecin and Taxol: Discovery to Clinic-Thirteenth Bruce F. Cain Memorial Award Lecture. *Cancer Research* **1995,** 55, 753-760.
22. Ulukan, H.; Swaan, P. W. Camptothecins, a review of their chemotherapeutical potential. *Drugs* **2002,** 62, 2039-2057.
23. Lu, A. J.; Zheng, Z. S.; Zou, H. J.; Luo, X. M.; Jiang, H. L. 3D-QSAR study of 20 (S)-camptothecin analogs. *Euro. J. Med. Chem.* **2007,** 42, 307-314.
24. Rivory, L. P. New drugs for the colorectal cancer-mechanisms of action. *Australian Prescriber* **2002,** 25, 108-110.
25. Redinbo, M. R.; Stewart, L.; Kuhn, P.; Champoux, J. J.; Hol, W. G. J. Crystal structure of human topoisomerase I in covalent and noncovalent complexes with DNA. *Science* **1998,** 279, 1504-1513.

26. Fraser, T. R. The antagonism between the actions of active substances. *Br. Med. J.* **1872,** 2, 485-487.
27. Zhao, L.; Wientjes, M. G.; Au, J. L.-S. Evaluation of Combination Chemotherapy Integration of Nonlinear Regression, Curve Shift, Isobologram, and Combination Index Analyses. *Clin. Cancer Res.* **2004,** 10, 7994-8004.
28. Steel, G. G.; Peckham, M. J. Exploitable mechanisms in combined radiotherapy-chemotherapy. The concept of additivity. *Int. J. Radiat. Oncol. Biol. Phys.* **1979,** 5, 85-93.
29. Chou, T.-C.; Talalay, P. Quantitative analysis of dose-effect relationships: the combined effects of multiple drugs or enzyme inhibitors. *Adv. Enzyme Regul.* **1984,** 22, 27-55.
30. Kaufmann, S. H.; Peereboom, D.; Buckwalter, C. A.; Svingen, P. A.; Grochow, L. B.; Donehower, R. C.; Rowinsky, E. K. Cytotoxic effects of topotecan combined with various anticancer agents in human cancer cell lines. *J. Natl. Cancer Inst.* **1996,** 88, 734-741.
31. Kano, Y.; Akutsu, M.; Tsunoda, S.; Mori, K.; Suzuki, K.; Adachi, K. I. *In vitro* schedule-dependent interaction between paclitaxel and SN-38 (the active metabolite or irinotecan) in human carcinoma cell lines. *Cancer Chemother. Pharmacol.* **1998,** 42, 91-98.
32. Madden, T.; Newman, R. A.; Antoun, G.; Johansen, M. J.; Ali-Osman, F. Low-level taxane exposure increases the activity of topoisomerase I targeted agents. *Proc. Am. Assoc. Cancer Res.* **1998,** 39, 527.
33. Adjei, A. A.; Argiris, A.; Murren, J. R. Docetaxel and irinotecan, alone and in combination, in the treatment of non-small cell lung cancer. *Semin. Oncol.* **1999,** 26 (5 Suppl 16), discussion 41-42.
34. Govindan, R.; Read, W.; Faust, J.; Trinkaus, K.; Ma, M. K.; Baker, S. D.; McLeod, H. L.; Perry, M. C. Phase II study of docetaxel and irinotecan in metastatic or recurrent esophageal cancer: a preliminary report. *Oncology (Williston Park)* **2003,** 17 (9 Suppl 8), 27-31.
35. Hecht, J. R.; Blanke, C. D.; Benson III, A.; Lenz, H. J. Irinotecan and paclitaxel in metastatic adenocarcinoma of the esophagus and gastric cardia. *Oncology (Williston Park)* **2003,** 17 (9 Suppl 8), 13-15.
36. Ohtsu, H.; Nakanishi, Y.; Bastow, K. F.; Lee, F.-Y.; Lee, K.-H. Antitumor agents 216. Synthesis and evaluation of paclitaxel–camptothecin conjugates as novel cytotoxic agents. *Bioorg. & Med. Chem.* **2003,** 11, 1851-1857.
37. Ojima, I. Guided Molecular Missiles for Tumor-Targeting Chemotherapy-Case Studies Using the Second-Generation Taxoid as Warheads. *Acc. Chem. Res.* **2008,** 41, 108-119.
38. Ojima, I. Tumor-targeting drug delivery of chemotherapeutic agents. *Pure Appl. Chem.* **2011,** 83, 1685-1698.
39. Ojima, I.; Zuniga, E. S.; Berger, W. T.; Seitz, J. D. Tumor-targeting drug delivery of new-genreation taxoids. *Future Med. Chem.* **2012,** 4, 33-50.
40. Chen, S., Zhao, X., Chen, J., Chen, J., Kuznetsova, L., Wong, S.S., Ojima, I. Mechanism-based tumor-targeting drug delivery system. Validation of efficient vitamin receptor-mediated endocytosis and drug release. *Bioconjugate Chem.* **2010,** 21, 979-987.
41. Jensen, P. B.; Holm, B.; Sorensen, M.; Christensen, I. J.; Sehested, M. *In vitro* cross-resistance and collateral sensitivity in seven resistant small-cell lung cancer cell lines: preclinical identification of suitable drug partners to taxotere, taxol, topotecan and gemcitabin. *Br. J. Cancer* **1997,** 75, 869-877.
42. Shah, M. A.; Schwartz, G. K. The relevance of drug sequence in combination chemotherapy. *Drug Resist. Update* **2000,** 3, 335-356.

43. Ishida, H.; Qi, Z.; Sokabe, M.; Donowaki, K.; Inoue, Y. Molecular Design and Synthesis of Artificial Ion Channels Based on Cyclic Peptides Containing Unnatural Amino Acids. *J. Org. Chem.* **2001,** 66, 2978-2989.
44. Toda, F.; Hyoda, S.; Okada, K.; Hirotsu, K. Isolation of Anhydrous Hydrazine as Stable Inclusion Complexes with Hydroquinone and p-Methoxyphenol, and their Solid State Reaction with Esters which gives Pure Hydrazides. *J. Chem. Soc., Chem. Commun.* **1995**, 1531-1532.
45. Crapatureanu, S.; Serbanescu, R.; Brevitt, S. B.; Kluger, R. Molecular Necklaces. Cross-Linking Hemoglobin with Reagents Containing Covalently Attached Ligands. *Bioconjugate Chem.* **1999,** 10, 1058-1067.
46. Ravikumar, V. T. A Convenient Large Scale Synthesis of *N*-BOC-Ethylenediamine. *Synth. Comm.* **1994,** 24, 1767-1772.
47. Stachel, S. J.; Coburn, C. A.; Steele, T. G.; Jones, K. G.; Loutzenhiser, E. F.; Gregro, A. R.; Rajapakse, H. A.; Lai, M.-T.; Crouthamel, M.-C.; Xu, M.; Tugusheva, K.; Lineberger, J. E.; Pietrak, B. L.; Espeseth, A. S.; Shi, X.-P.; Chen-Dodson, E.; Holloway, M. K.; Munshi, S.; Simon, A. J.; Kuo, L.; Vacca, J. P. Structure-Based Design of Potent and Selective Cell-Permeable Inhibitors of Human β-Secretase (BACE-1). *J. Med. Chem.* **2004,** 47, 6447-6450.
48. Gottlieb, H. E.; Kotlyar, V.; Nudelman, A. NMR Chemical Shifts of Common Laboratory Solvents as Trace Impurities. *J. Org. Chem.* **1997,** 62, 7512-7515.
49. Kubik, S.; Bitta, J. Cyclic Hexapeptides with Free Carboxylate Groups as New Receptors for Monosaccharides. *Org. Lett.* **2001,** 3, 2637-2640.
50. Yoshiizumi, K.; Nakajima, F.; Dobashi, R.; Nishimura, N.; Ikeda, S. 2,4-Bis(octadecanoylamino)benzenesulfonic acid sodium salt as a novel scavenger receptor inhibitor with low molecular weight. *Bioorg. Med. Chem. Lett.* **2004,** 14, 2791-2795.

Chapter 7

Design, Synthesis and Biological Evaluation of Novel Tumor-Targeting Drug Conjugates with Dual-Guiding Modules and Dual-Warheads. 2. Drug Conjugate with SB-T-1214 and Topotecan.

Chapter Contents

§ 7.1.0 Introduction

§ 7.1.1 Novel Tumor-Targeting Drug Conjugate Bearing Dual-Warheads

As discussed in the previous chapter, a novel tumor-targeting drug conjugate with dual-warheads (**DW-1**) was developed using a trisubstituted small-molecule splitter module based on 1-aminobenzene-3,5-dicarboxylic acid and utilizing biotin as the tumor-targeting module (TTM). The warheads chosen were SB-T-1214, a 2nd-generation taxoid that shows excellent activity in a variety of cancer cell lines, and camptothecin, a potent alkaloid that inhibits DNA topoisomerase I. It was shown that **DW-1** demonstrated potent activity against three different breast cancer cell lines. These results suggest that the drug conjugate was guided to the cancer cell surface by biotin and internalized via receptor-mediated endocytosis (RME), thereby releasing the synergistic combination of drugs from the carrier. However, there are limitations to the originally developed drug conjugate **DW-1**. One major limitation is insolubility, as both SB-T-1214 and camptothecin are insoluble in water. Another limitation is that the TTM was installed onto the small-molecule splitter module at the first step. This limits the type of TTMs that can be incorporated into the drug conjugate, as purification becomes problematic for TTMs such as folic acid or macromolecules. In addition, the selective functionalization of 1-aminobenzene-3,5-dicarboxylic acid derivatives were difficult, leading to the generation of undesired products.

Accordingly, the drug conjugate bearing dual-warheads was modified to include a wider array of tumor-targeting modules, which can be coupled via “click chemistry” (Figure 7.1). Furthermore, the water solubility and efficacy may be increased by the incorporation of topotecan, a more potent water-soluble camptothecin derivative which has been approved by the FDA to treat various types of cancer. Lastly, a trisubstituted 1,3,5-triazine core derived from cyanuric chloride was chosen as the small-molecule splitter module. Cyanuric chloride can be easily and selectively functionalized with different amines and the resulting 1,3,5-triazine core may have increased water solubility given the presence of the amine moieties.

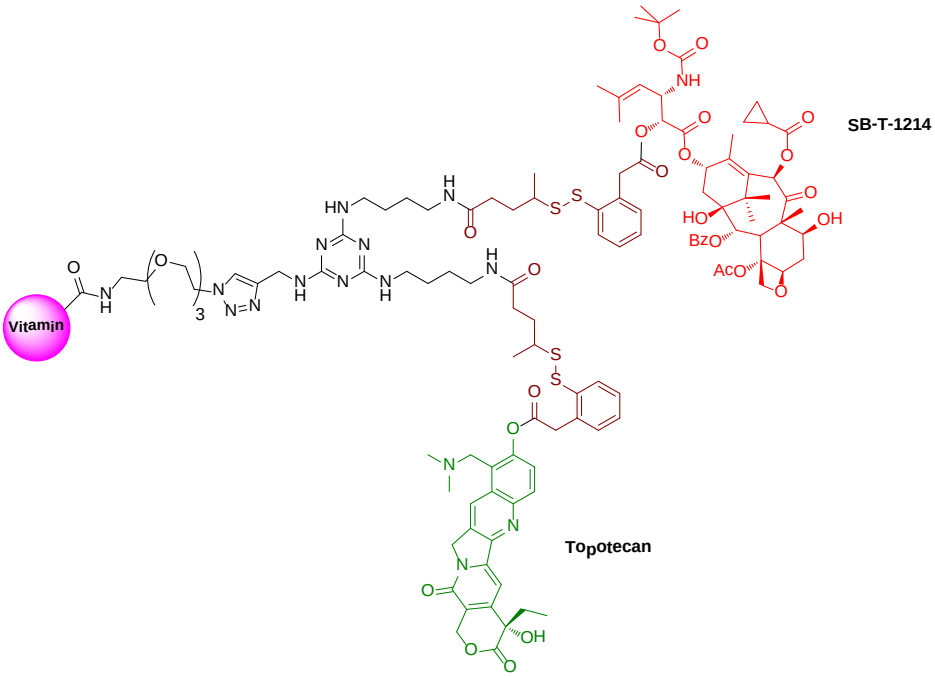

Figure 7.1: 2nd tumor-targeting drug conjugate bearing dual-warheads

Through the use of "click chemistry" a variety of TTMs, such as vitamins (i.e. biotin and folic acid), PUFAs (i.e. DHA and LNA), hylauronic acids, monoclonal antibodies, as well as drug delivery systems modified with a terminal azide, can be coupled to the 1,3,5-triazine splitter module bearing dual-warheads. These TTMs will guide the drug conjugate to the tumor site and internalize into cancer cells. Both SB-T-1214 and topotecan will be released from the carrier after intracellular thiol-mediated cleavage of the disulfide linkers.

§ 7.1.2 Topotecan

Topotecan (Figure 7.2), a semisynthetic water-soluble analog of camptothecin, is a potent DNA topoisomerase I inhibitor that has shown promising antitumor activity against a wide variety of tumors, such as ovarian cancer and small cell lung cancer.[1-7] Topotecan (Hycamtin, GlaxoSmithKline) was approved by the FDA for the treatment of ovarian cancer (1996), cervical cancer (2006) and small cell lung cancer (2007), making it the first topoisomerase inhibitor for oral use.[8, 9]

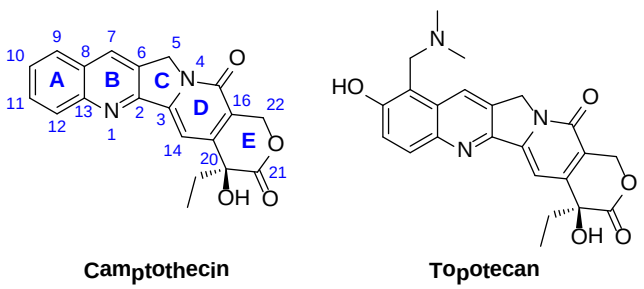

Figure 7.2: Camptothecin and topotecan

The mechanism of action of topotecan is similar to that of camptothecin. Using the x-ray crystal structure of human topoisomerase I covalently joined to DNA and bound to topotecan, Stewart et al. elucidated that the drug acts as an uncompetitive inhibitor (Figure 7.3).[10] Topotecan mimics a DNA base pair and intercalates between the upstream (-1) and downstream (+1) base pairs at the site of DNA cleavage, thereby displacing the downstream DNA, preventing religation of the cleaved DNA strand.[10]

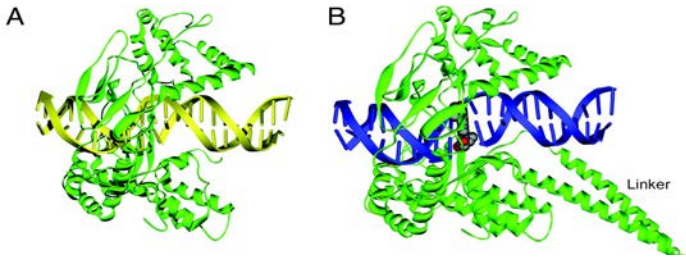

Figure 7.3: Structure of topoisomerase I-DNA complex with (A) and without (B) bound topotecan (adapted from [10])

§ 7.1.3 Clinical Applications of Topotecan in Combination Chemotherapy

As mentioned in the previous chapter, the use of a taxoid in combination with a camptothecin demonstrated promising results in patients being treated for non-small cell lung cancer (NSCLC), esophageal cancer, as well as various types of solid tumors.[11-15] In a phase I study, patients with ovarian cancer (OC) or small cell lung cancer (SCLC) were treated with cisplatin (40 mg/m^2), paclitaxel (85 mg/m^2), both in one-hour infusion, and escalating doses of topotecan (starting from 0.75 mg/m^2), in a 30-minute infusion, on a weekly basis.[16] This treatment program proved to be a well-tolerated and active approach for the treatment of both cancers, as an overall 58% OC and 44% SCLC patients obtained complete responses.

In another study, 45 OC patients, previously treated with carboplatin or cisplatin with paclitaxel, were treated with topotecan (1.75 mg/m^2) and paclitaxel (70 mg/m^2) on a weekly basis for 3 consecutive weeks.[17] This treatment program demonstrated complete and partial responses in 39% of the patients and stable disease in 43%, with a median survival time of 9 months. Accordingly, the combination of topotecan and paclitaxel was deemed a well-tolerated and active chemotherapy regimen. A similar treatment program was administered to pretreated patients with SCLC.[18] In this phase II study, an overall response rate of 26.8% was observed. The combination of topotecan and docetaxel is currently being evaluated in a phase II study for the treatment of SCLC.[19]

§ 7.1.4 Topotecan as Fluorescence Probe

In addition to its water-soluble and clastogenic properties, topotecan also has fluorescence properties, which are relevant for a variety of biomedical and clinical applications, such as studying drug interaction with biomolecules, and evaluating cytotoxicity and noninvasive detection *in vivo*.[20] Topotecan displays fluorescence when exited by one-photon between 350 and 420 nm.[21, 22] Burke et al. were able to detect micromolar concentrations of topotecan (0.05 and 1 μM) in human plasma and whole blood using two-photon excitation at 730 or 820 nm.[23]

Skin, blood and tissues are translucent at these wavelengths, making noninvasive clinical sensing of topotecan a possibility.[23]

To study the mechanism of resistance to the camptothecins in MXR-overexpressing S1-M1-80 (human colon) and MCF-7 AdVp3000 (human breast) cancer cell lines, Bates et al. used confocal microscopy (CFM) to determine the localization and energy-dependent accumulation of topotecan, as well as other camptothecins, in the cancer cell lines. For the localization experiments, cells were incubated with 5 μM topotecan at 37 °C for 1 hour and then analyzed using CFM (Figure 7.4).

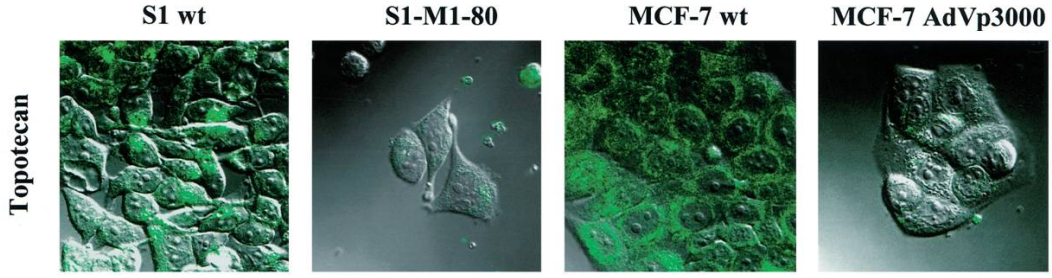

Figure 7.4: CFM image demonstrating the localization of 5 μM topotecan in S1 and MCF-7 parent and drug resistant cancer cell lines (adapted from [24])

As seen from the CFM images, parent cell lines (S1 and MCF-7) had higher intracellular drug levels, as depicted by the green color, compared to the drug resistant cell lines (S1-M1-80 and MCF-7 AdVp3000) which have low or no fluorescence staining.[24] From the CFM images, it was concluded that topotecan fluorescence was more cytoplasmic rather than nuclear and that a perinuclear staining pattern was observed in all cell lines, suggesting the accumulation of drug in a vascular compartment.[24]

Bates et al. determined that the lower fluorescence levels present in the drug-resistant cell lines could be increased by incubating the cells in energy-depleted conditions (i.e. pretreating the cells with sodium azide and deoxyglucose). In this experiment, cells were incubated in PBS containing 50 mM deoxyglucose and 15 mM sodium azide at 37 °C for 20 minutes and then incubated with 20 μM topotecan for an additional 30 minutes. The results of this experiment are illustrated in Figure 7.5.

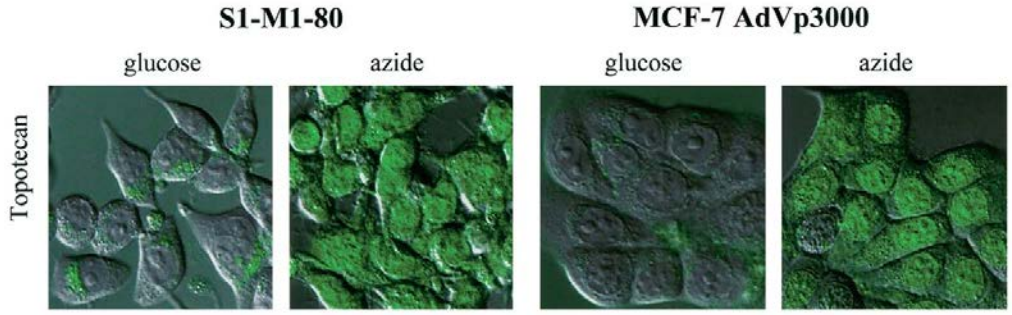

Figure 7.5: CFM images demonstrating the energy-dependent accumulation of 20 μM topotecan in drug-resistant cell lines, S1-M1-80 and MCF-7 AdVp3000 (adapted from [24])

As depicted in Figure 7.5, the intensity of fluorescence greatly increased compared to the drug-resistant cells not pretreated with deoxyglucose and sodium azide (Figure 7.4), as a result of the increased accumulation of the drug.[24] It was observed that both cytoplasmic and nuclear

accumulation of topotecan increased under these energy-depleted conditions, implying that the reduced total accumulation observed in these cells is due to an energy-dependent transport mechanism, such as MXR.[24] The fluorescence experiments reported by Burke and Bates show that topotecan has fluorescence activity that can be exploited *in vitro* and *in vivo*. Accordingly, the use of topotecan as a warhead in a drug conjugate serves two purposes (1) as a cytotoxic warhead and (2) a fluorescence marker, thus making the drug conjugate detectable in cancer cells and tumor tissue *in vitro* and *in vivo*.

§ 7.2.0 Results and Discussion

§ 7.2.1 Biological Evaluation of the Synergistic Activity of SB-T-1214 and Topotecan

As mentioned in the previous chapter, the drug interaction between paclitaxel and a camptothecin was evaluated in different cancer cell lines and in those experiments it was found that the combination of paclitaxel with a camptothecin has additive or synergistic effects.[12, 25, 26] Furthermore, in the previous chapter, it was shown that the equimolar combination of SB-T-1214 with camptothecin possesses one order of magnitude greater potency against human ovarian cancer cell lines A2780 and ID-8 compared to camptothecin as a single drug and that a sequential administration of SB-T-1214 followed by camptothecin showed excellent activity against different breast cancer cell lines. In a similar experiment, the activity of SB-T-1214 and topotecan combined was also evaluated. For this experiment, an equimolar combination of SB-T-1214 and topotecan was administered to various cancer cell lines. The cells were incubated with the drug combination for 48 hours at 37 °C. The IC_{50} values obtained from these experiments are listed in Table 7.1. As seen from the data in Table 7.1, the combination of SB-T-1214 with topotecan showed subnanomolar activity against MCF-7 (human breast) cancer cell line; similar results were obtained for the combination of SB-T-1214 and camptothecin. Again, greater potency was observed against A2780, CFPac-1, HT-29 and ID-8 cancer cells treated with the drug combination, as IC_{50} values are 3 to 4 times more potent than topotecan as a single drug. The combination showed substantial activity in ID-8 (human ovarian) cancer cell line (IC_{50} of 4.49 nM) compared to that of topotecan (IC_{50} of 54.3 nM). With these preliminary results, the activity of SB-T-1214 with topotecan was screened in various breast cancer cell lines. These results are listed in Table 7.2.

Table 7.1: Biological Evaluation of Equimolar Combination of SB-T-1214 and Topotecan against Various Cancer Cell Lines

	IC_{50} (nM)						
Drug	**A2780 (ovarian cancer)**	**CFPac-1 (pancreatic cancer)**	**DLD-1 (colon cancer)**	**HT-29 (colon cancer)**	**ID8 (ovarian cancer)**	**MCF-7 (breast cancer)**	**Panc-1 (pancreatic cancer)**
Paclitaxel	16.2 ± 8.28	68.0 ± 22.9	29.5 ± 10.8	11.6 ± 3.57	14.5 ± 5.88	6.25 ± 0.76	1.97 ± 0.76
SB-T-1214	0.36 ± 0.03	0.38 ± 0.14	0.38 ± 0.21	0.73 ± 0.30	2.51 ± 1.24	0.35 ± 0.11	0.35 ± 0.14
Topotecan	46.3 ± 8.1	40.8 ± 5.22	>5000	518 ± 26.0	54.3 ± 8.7	28.1 ± 7.3	>5000
SB-T-1214:Topotecan	15.1 ± 4.6	13.1 ± 3.2	>5000	196 ± 21	4.49 ± 1.17	0.21 ± 0.16	>5000

Table 7.2: Biological Evaluation of Equimolar Combination of SB-T-1214 and Topotecan against Various Breast Cancer Cell Lines

	IC_{50} (nM)					
Taxane	**BT20**	**LCC6 wt**	**LCC6 MDR**	**MCF-7**	**MDA MB 231**	**SkBr3**
SB-T-1214	0.20 ± 0.06	0.68 ± 0.33	0.86 ± 0.15	0.35 ± 0.11	18.9 ± 9.7	0.48 ± 0.03
Topotecan	490 ± 2	421 ± 224	489 ± 317	28.1 ± 7.3	386 ± 106	353 ± 120
SB-T-1214:Topotecan	537 ± 34	533 ± 243	470 ± 178	0.21 ± 0.16	0.51 ± 0.02	0.47 ± 0.01

- Cells were suspended in RPMI with L-glutamine (Lonza BioWhittaker, BW12-702F), with 5% FBS (Thermo Scientific, HyClone, SH3007003), 5% Nu Serum (BD Biosciences, 355100) and 1% Penn Strip before administration of drug
- Cells were incubated for 48 hours at 37 °C with 5% CO_2 after administration of drug
- The optical density was determined using Acsent Multiskan optical density reader
- The reported values are a calculated averages of IC_{50} values determined from three individual experiments
- IC_{50} values were calculated using SigmaPlot v 10.0
- All IC_{50} values are report in nM scale unless otherwise noted

As seen from Table 7.2, selectivity is observed amongst the breast cancer cell lines, as the combination of SB-T-1214 with topotecan showed excellent activity against MCF-7, MDA MB 231 and SkBr3 breast cancer cell lines, yielding IC_{50} values 2 to 3 orders of magnitude greater than that of topotecan as a single agent. Interestingly, there is no change in activity in the combination of drugs against BT20, LCC6 wt and LCC6 MDR compared to the IC_{50} values of topotecan against the same cancer cell lines.

To evaluate the effects of sequential drug treatment, cancer cells were treated with SB-T-1214 and incubated for 24 hours at 37 °C followed by the treatment with topotecan and an additional incubation period of 24 hours at 37 °C. Furthermore, the order of addition was switched, treating with topotecan first followed by SB-T-1214. Also, the activities of SB-T-1214 and topotecan alone were evaluated for 24 and 48 hour incubation periods. For these experiments MCF-7, MDA MB 231 and SkBr3 human breast cancer cell lines were used. These results are listed in Table 7.3.

Table 7.3: Biological Evaluation of Single Drug Administration and Sequential-Treatment of Drug Combination against Various Breast Cancer Cell Lines

Taxane	Time of Incubation (h)	IC_{50} (nM) MCF-7	MDA MB 231	SkBr3
SB-T-1214	**24**	26.8 ± 9.61	23.2 ± 12.5	33.2 ± 19.2
SB-T-1214	**48**	0.56 ± 0.34	18.9 ± 9.7	0.48 ± 0.03
Topotecan	**24**	>5000	>5000	>5000
Topotecan	**48**	338 ± 59.9	386 ± 106	353 ± 120
SB-T-1214:Topotecan*	**-**	0.53 ± 0.28	45.3 ± 35.2	0.46 ± 0.04
Topotecan:SB-T-1214‡	**-**	69.0 ± 13.4	>5000	263 ± 127

* Cells were treated with SB-T-1214 for 24 hours at 37 °C with 5% CO_2 then treated with topotecan for an additional 24 hours at 37 °C with 5% CO_2: total incubation time with drug is 48 hours

‡ Cells were treated with topotecan for 24 hours at 37 °C with 5% CO_2 then treated with SB-T-1214 for an additional 24 hours at 37 °C with 5% CO_2: total incubation time with drug is 48 hours

- Cells were suspended in RPMI with L-glutamine (Lonza BioWhittaker, BW12-702F), with 5% FBS (Thermo Scientific, HyClone, SH3007003), 5% Nu Serum (BD Biosciences, 355100) and 1% Penn Strip before administration of drug
- Cells were incubated for 24 or 48 hours at 37 °C with 5% CO_2 after administration of drug
- The optical density was determined using Acsent Multiskan optical density reader
- The reported values are a calculated averages of IC_{50} values determined from three individual experiments
- IC_{50} values were calculated using SigmaPlot v 10.0
- All IC_{50} values are report in nM scale unless otherwise noted

As seen from Table 7.3, in general, a longer incubation period with single drugs leads to lower IC_{50} values. Topotecan had no observed activity within a 24 hour period. When the cancer cells are treated with SB-T-1214 followed by topotecan, there is a slight increase in activity observed against MCF-7 and SkBr3 cancer cell lines compared to treatment with SB-T-1214 as a single agent. The IC_{50} value of the sequentially administered drug combination against MCF-7 is 0.53 nM compared to an IC_{50} value of 0.56 nM for SB-T-1214 alone (48 h incubation). The drug combination shows one order of magnitude greater potency against MDA MB 231 cancer cell line (IC_{50} 45.3 nM) compared to topotecan as a single drug. Lastly, the treatment of topotecan followed by SB-T-1214 quenched the activity of the combination in all three of the breast cancer cell lines evaluated; a result similar to that observed when cells were treated with camptothecin then with SB-T-1214. Overall, these results demonstrate that the SB-T-1214 and topotecan

provide an effective combination with increased cell kill potential in different cancer cell lines. Thus, a drug conjugate with both SB-T-1214 and topotecan may have higher efficacy than the single agents.

§ 7.2.2 Internalization of PEGylated Vitamin-FITC Conjugates

As previously discussed, biotin and folate receptors are overexpressed on the surface of cancer cells. The internalization of fluorescence-labeled biotin and folate probes has been evaluated in several cell lines using various labeling agents.[27-38] To confirm the internalization of both biotin and folate for use as TTM in our redesigned tumor-targeting drug conjugate bearing dual-warheads, biotin-PEG_3- and folate-PEG_3-FITC probes were synthesized. Vitamin-PEG_3-azide can be achieved in two steps; activation in the presence of HOSu and DCC, followed by the addition of azido-PEG_3-amine. However, this route is troublesome when preparing folate-PEG_3-azide, as purification of folate derivatives is extremely difficult. Accordingly, the preparation of both vitamin-PEG_3-FITC probes was achieved by treating vitamin-PEG_3-amine with FITC in the presence of base. Vitamin-PEG_3-amine was prepared by subjecting vitamin and azido-PEG_3-amine to standard peptide coupling conditions using EDC, followed by Staudinger reduction (Scheme 7.1).[39]

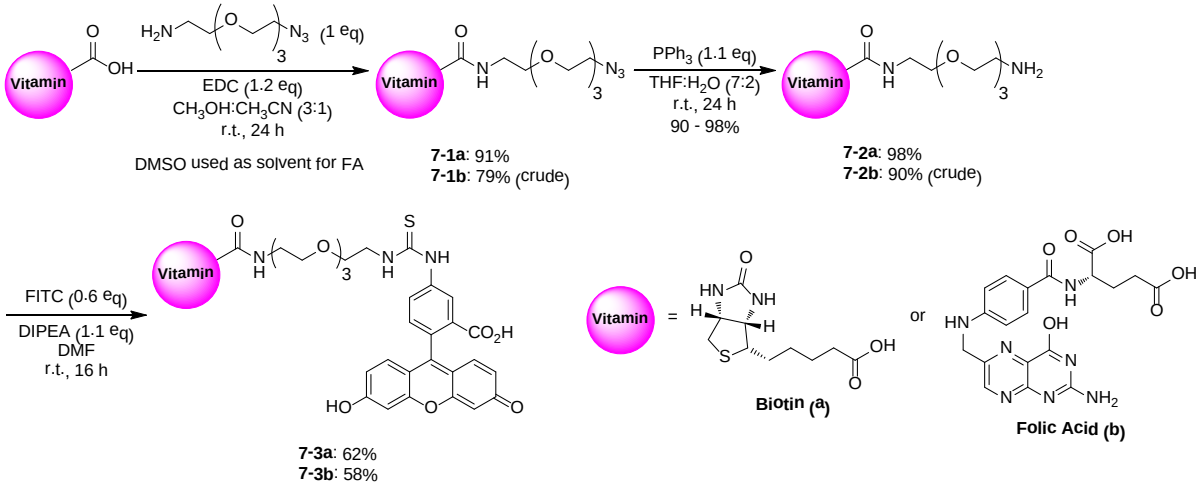

Scheme 7.1: Synthesis of vitamin-PEG_3-FITC probes

The synthesis of **7-1a** and **7-1b** was achieved following the protocol described by Famulok et al.[39] The treatment of biotin and folic acid with azido-PEG_3-amine (11-azido-3,6,9-trioxaundecan-1-amine) in the presence of EDC gave **7-1a** and **7-1b** in good yields, 91% and 79%, respectively. The use of EDC simplifies the purification of the product, as the urea byproduct generated by EDC is water-soluble. Thus, the byproduct can be removed with aqueous washing. Staudinger reduction of the resulting azides **7-1a** and **7-1b** using triphenylphosphine in THF and water afforded the corresponding amines **7-2a** and **7-2b** in excellent yields, 98% and 90%, respectively. The addition of the free amine **7-2a** or **7-2b** to FITC in the presence of base gave the corresponding fluorescence-labeled vitamins **7-3a** and **7-3b** in moderate yields, 62% and 58%, respectively.

The internalization of both fluorescence-labeled vitamin probes was evaluated in ID-8 (ovarian) cancer cells and MCF-7 (breast) cancer cells. The overexpression of biotin and folate

receptors in ID-8 was previously reported.[27] However, the overexpression of these receptors has not been reported for MCF-7 cells. MCF-7 cells were chosen due to previously reported cytotoxicity data of taxoid-topotecan mixtures. The internalization of the FITC-probes was monitored using FACS and CFM. Cells were treated with 10 μM vitamin-PEG-FITC probe and incubated for 1 h or 3 h at 37 °C and then the cells were washed with PBS (3 times), resuspended in PBS containing 2% formulin and analyzed by FACS and CFM (Figures 7.6 and 7.7).

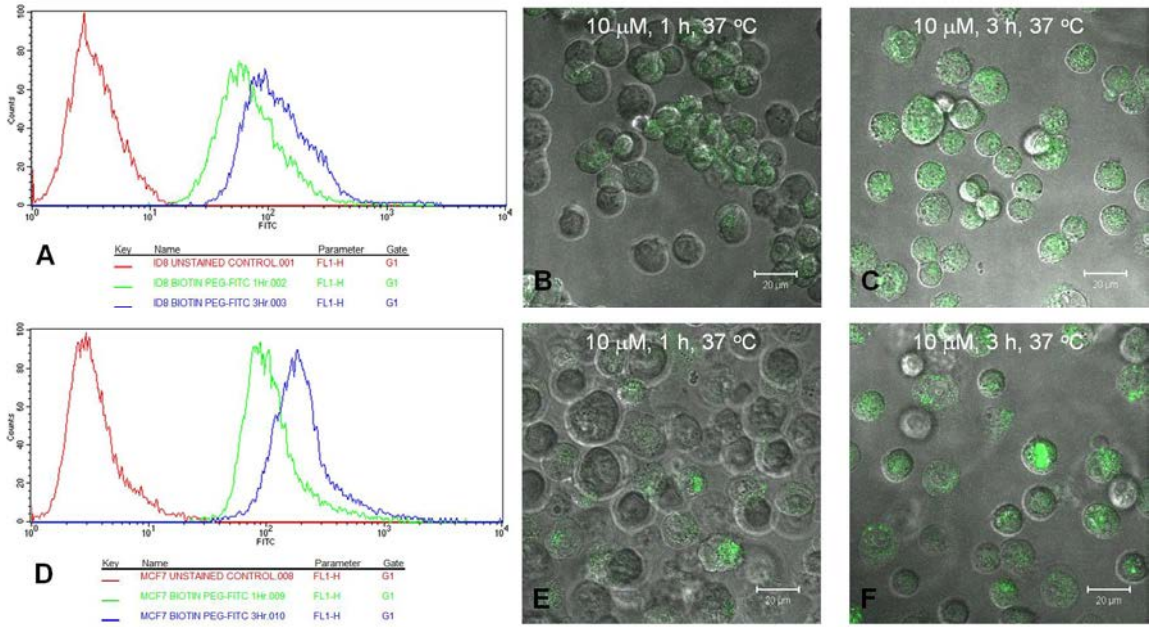

Figure 7.6: FACS analysis and CFM images evaluating the internalization of 10 μM biotin-PEG-FITC into ID-8 and MCF-7 cancer cell lines incubated for 1 h and 3 h at 37 °C. (A) FACS histogram of ID-8 cells incubated with 10 μM biotin-PEG-FITC; (B) CFM image of ID-8 cells incubated with 10 μM biotin-PEG-FITC for 1 h; (C) CFM image of ID-8 cells incubated with 10 μM biotin-PEG-FITC for 3 h; (D) FACS histogram of MCF-7cells incubated with 10 μM biotin-PEG-FITC; (E) CFM image of MCF-7 cells incubated with 10 μM biotin-PEG-FITC for 1 h; (F) CFM image of MCF-7 cells incubated with 10 μM biotin-PEG-FITC for 3 h

As you can see from the FACS and CFM data, internalization into both ID-8 and MCF-7 cells occurred within 1 hour after the administration of 10 μM biotin-PEG-FITC. As both FACS and CFM data show, internalization of the FITC-probe increases as time increases. Thus, the PEG chain does not interfere with the internalization of biotin, thus making biotin-PEG a possible TTM.

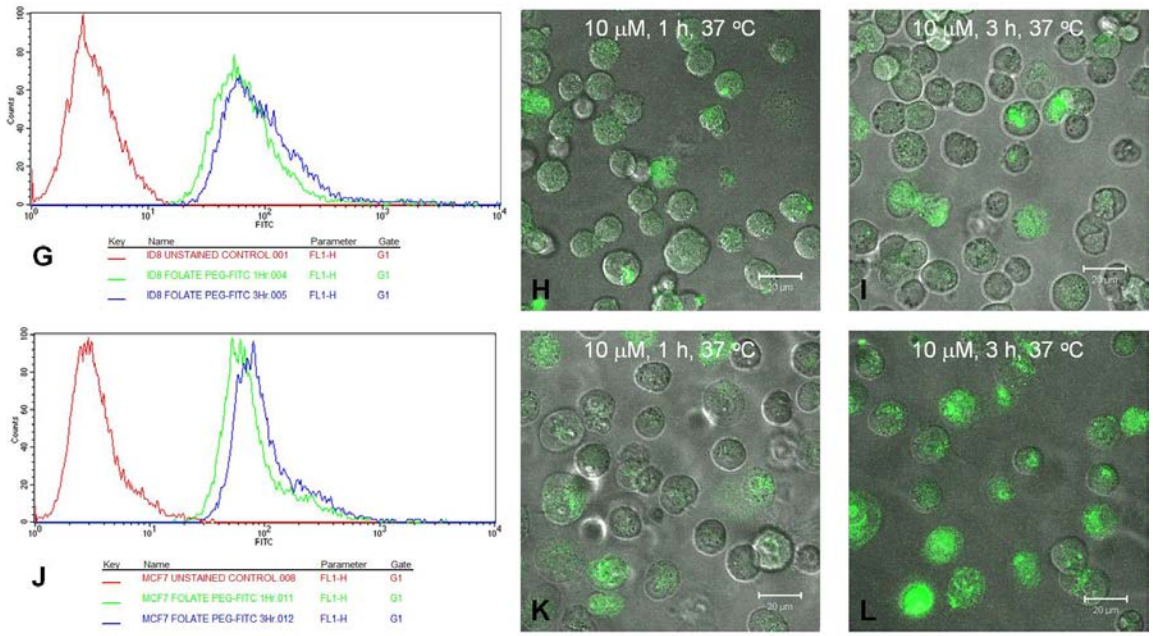

Figure 7.7: FACS analysis and CFM images evaluating the internalization of 10 µM folate-PEG-FITC into ID-8 and MCF-7 cancer cell lines incubated for 1 h and 3 h at 37 °C. (G) FACS histogram of ID-8 cells incubated with 10 µM folate-PEG-FITC; (H) CFM image of ID-8 cells incubated with 10 µM folate-PEG-FITC for 1 h; (I) CFM image of ID-8 cells incubated with 10 µM folate-PEG-FITC for 3 h; (J) FACS histogram of MCF-7cells incubated with 10 µM folate-PEG-FITC; (K) CFM image of MCF-7 cells incubated with 10 µM folate-PEG-FITC for 1 h; (L) CFM image of MCF-7 cells incubated with 10 µM folate-PEG-FITC for 3 h

The internalization of folate-PEG-FITC was also observed in ID-8 and MCF-7 cells. Again, as the incubation period with FITC-probe increases, internalization increases. In addition, the PEG moiety does not significantly influence the internalization of folate. Furthermore, this experiment also shows that biotin and folate receptors are overexpressed in MCF-7 cells. With these preliminary results, the internalization of both vitamin-PEG-FITC probes was evaluated in all of the breast cancer cell lines which were used for cytotoxicity determination. For this experiment, BT-20, LCC6 wt, LCC6 MDR, MDA MB 231 and SkBr3 breast cancer cell lines were treated with 10 µM vitamin-PEG-FITC probe and incubated for 1 h at 37 °C and internalization was monitored using FACS (Figure 7.8).

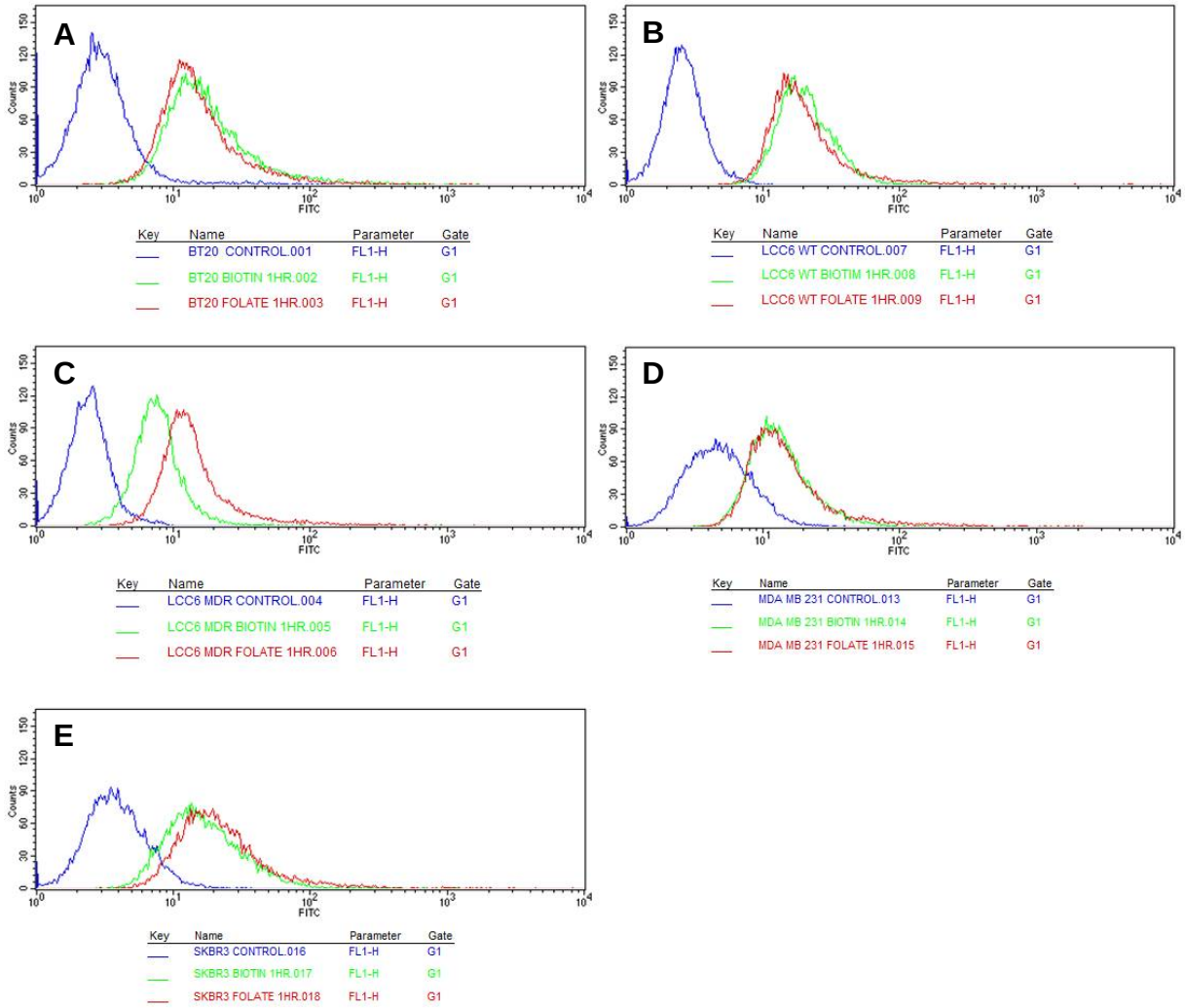

Figure 7.8: FACS analysis and histogram overlays evaluating internalization of 10 µM vitamin-PEG-FITC incubated in different breast cancer cell lines for 1 hour at 37 °C. (A) BT-20; (B) LCC6 wt; (C) LCC6 MDR; (D) MDA MB 231; (E) SkBr3.

As observed from the FACS data, both biotin- and folate-PEG-FITC probes internalize into the 5 different breast cancer cell lines. The most vitamin internalization was observed in the BT-20, LCC6 wt and SkBr3 cell lines. Furthermore, more folate internalization was observed in LCC6 MDR cells, which implies that folate receptors are overexpressed in this cell line. The internalization of both biotin and folate are equal in the other breast cancer cell lines. Of the three cell lines, there was greater internalization of both biotin- and folate-PEG-FITC in MCF-7 compared to MDA MB 231 and SkBr3; MDA MB 231 showing the least internalization. This internalization data suggests that both biotin and folate can be used to as TTMs to target some breast cancer cell lines.

§ 7.2.3 Synthesis of Topotecan

The synthesis of topotecan starting from camptothecin was reported by a number of groups.[40-45] Most synthetic routes require the modification of 10-hydroxycamptothecin. The

conversion of camptothecin to 10-hydroxycamptothecin is achieved by a series of reduction and oxidation reactions. [40-44] The synthesis of 10-hydroxycamptothecin begins with the *in situ* generation of Pt(0) by reducing platinum oxide in the presence of H_2. Camptothecin is added to *in situ* generated Pt(0), forming air sensitive 1,2,6,7-tetrahydrocamptothecin which is immediately oxidized in the presence of lead(IV) tetraacetate to yield a mixture of 10-hydroxycamptothecin, 10-acetoxycamptothecin and camptothecin. Treating this mixture with acetic acid under reflux yields a mixture of 10-hydroxycamptothecin and camptothecin, which was used for the synthesis of topotecan (Scheme 7.2).[40-42, 45]

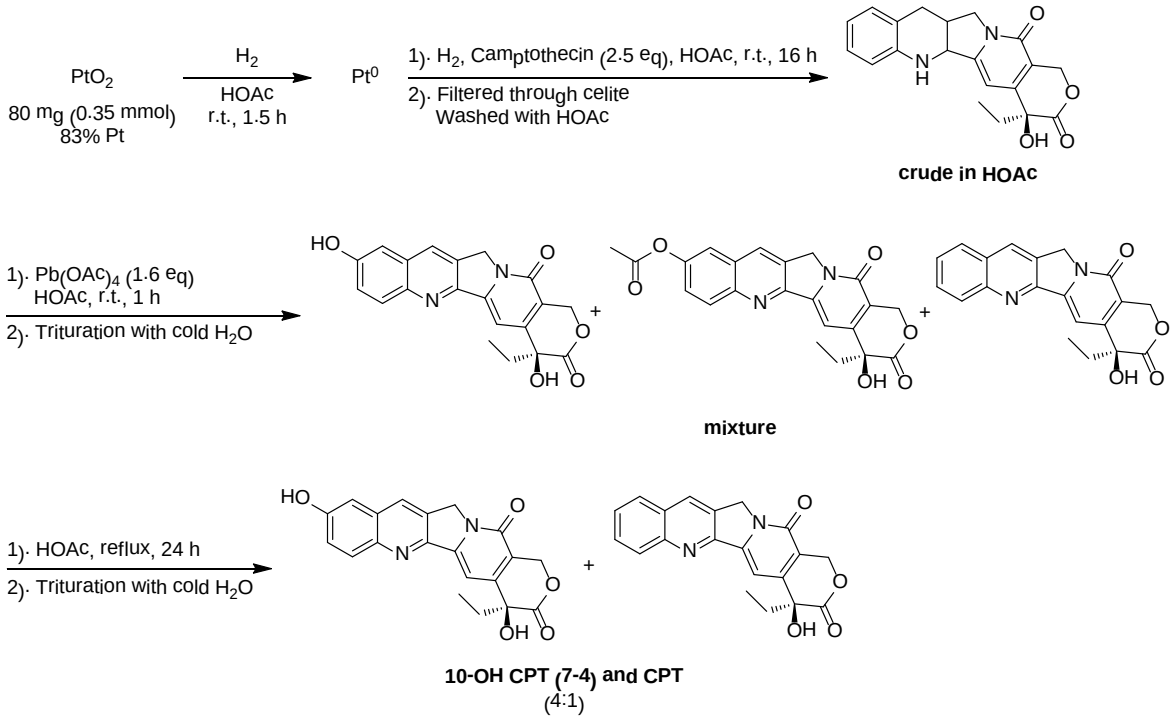

Scheme 7.2: Synthesis of 10-hydroxycamptothecin

It is worthy of note that Acharyulu et al. reported that the hydrogenation of camptothecin affords 1,2,6,7-tetrahydrocamptothecin with inconsistent yield and quality on a large scale but proceeds with reasonable yield on small scales.[45] Subjecting camptothecin to the hydrogenation conditions afforded crude containing the intermediate 1,2,6,7-tetrahydrocamptothecin. The intermediate was not isolated because it is unstable and readily converts back to camptothecin when exposed to air for long periods.[46] The crude was immediately treated with lead (IV) acetate to yield crude containing 10-hydroxycamptothecin (**7-4**), 10-acetoxycamptothecin and camptothecin. The resulting crude was refluxed in acetic acid to convert 10-acetoxycamptothecin to 10-hydroxycamptothecin (**7-4**). The crude mixture was analyzed via HPLC to determine the ratio of **7-4** to camptothecin (4:1), which was then used without further purification for the synthesis of topotecan.[41, 42] The conversion of **7-4** was attempted using two methods (Scheme 7.3).

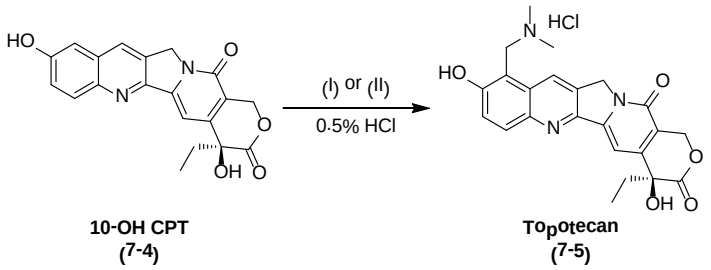

10-OH CPT (7-4) **Topotecan (7-5)**

(I) 37% aq. CH_2O (0.08 mL), 40% aq. $HN(CH_3)_2$ (0.08 mL), HOAc, r.t., 72 h
(II) 40% aq. $HN(CH_3)_2$ (0.66 mL), CH_2Cl_2 (3 mL), K_2CO_3 (120 mg), r.t., 5 h

Scheme 7.3: Conversion of 10-hydroxycamptothecin to topotecan

In the first method, reported by Kingsbury et al., the imine formed from dimethylamine and formaldehyde, is nucleophilically attacked by **7-4** to afford topotecan (**7-5**).[42] The reaction using this method was messy but afforded a crude mixture containing **7-5**. The second method, reported by Acharyulu et al. uses dichloromethane as both solvent and reactant to generate an imine.[45] This method afforded topotecan hydrochloride in moderate yield (60%) after extraction with ethyl acetate and trituration with 0.5% HCl. Topotecan hydrochloride is light-sensitive and can be stored in the dark at -20 °C. The compound is completely soluble in water or DMSO.

§ 7.2.4 Synthesis of Topotecan-Linker "Coupling-Ready Construct"

The synthesis of topotecan-linker coupling-ready constructs was prepared using the same protocols employed for the synthesis of SB-T-1214-Me-linker-CO_2H and SB-T-1214-Me-linker-OSu constructs, discussed in an earlier chapter. Topotecan-Me-linker-CO_2H was obtained using standard DIC coupling conditions in the presence of disulfide linker **4-13** (Scheme 7.4).

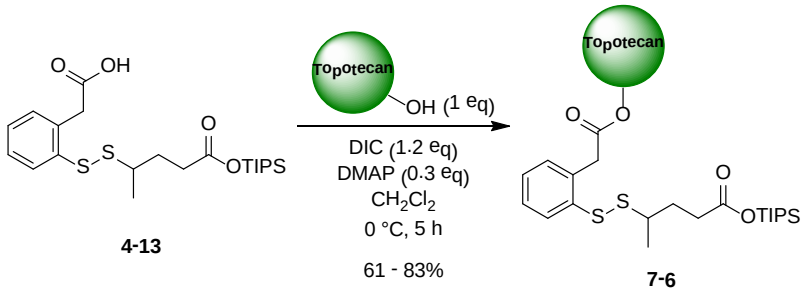

4-13 **7-6**

Scheme 7.4: Synthesis of topotecan-linker

All topotecan reactions should be done in the dark and at 0 °C to prevent decomposition of the drug. The coupling of **4-13** to topotecan afforded **7-6** in good yields (61 – 83%). It is assumed that coupling occurred at the C-10 hydroxyl moiety of topotecan, based on literature precedence of conjugation reactions using with C-10 hydroxyl bearing camptothecin derivatives.[47, 48] In these studies it was found that the C-10 hydroxyl is more reactive than the sterically blocked C-20 hydroxyl.[47, 48] However, to determine which hydroxyl is involved in the coupling of topotecan to the disulfide linker, COSY experiments with **7-6** and 10-hydroxylcamptothecin-linker will be examined. The silyl-deprotection of **7-6** was attempted using three methods (Scheme 7.5).

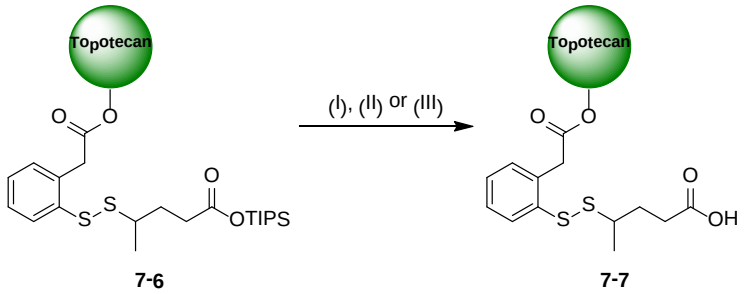

7-6 7-7

(I) HF/py (excess, 0.01 mL/mg), CH_3CN:py (1:1), r.t., 16 h
(II) CsF (2 eq), CH_3OH:PhH (1:1), r.t., 15 min
(III) 0.1% HCl, EtOH, r.t., 2 h

Scheme 7.5: Deprotection of topotecan-Me-linker-TIPS using CsF

The use of HF in pyridine (method I) successfully removed the silyl group based on thin layer chromatography (TLC). However, removal of pyridine required multiple washings of the organic layer with aqueous copper sulfate. The desilylated product **7-7** can easy be trapped in this aqueous wash resulting in little to no product isolation. Deprotection using cesium fluoride (method II) afforded the desired deprotected product in moderate yield (57%). Lastly, the use of 1% HCl as silyl-deprotecting agent also generated **7-7**, however, isolation was difficult after purification. Accordingly, TIPS-deprotection using CsF gave the best results. Activation of the resulting carboxylic acid, **7-7**, to the corresponding OSu-activated ester was accomplished in the presence of HOSu and DIC (Scheme 7.6).

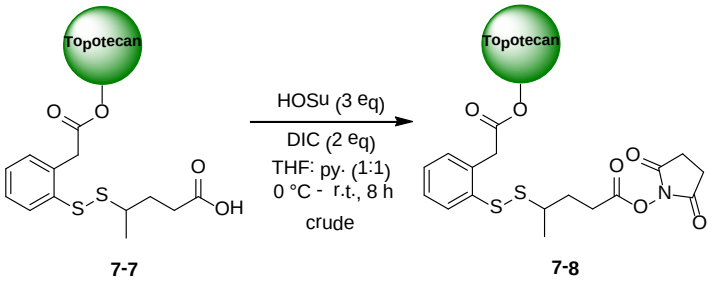

7-7 7-8

Scheme 7.6: Activation of topotecan-linker

Similar to the activation of camptothecin-linker-OSu, purification of **7-8** was not done, as the resulting crude was used in the next step. It is worthy of note that topotecan and topotecan derivatives interact well with both silica and alumina gels, making purification by column chromatography very difficult. An alternative would be to avoid the activation step and couple topotecan-linker, **7-7**, directly to TTMs with free amines in the presence of a coupling reagent, such as DCC, DIC or EDC, among others.

§ 7.2.5 Selective Cyanuric Chloride Functionalization

For the synthesis of the drug conjugate bearing dual-warheads, a trisubstituted 1,3,5-triazine core derived from cyanuric chloride was chosen as the small-molecule splitter module. Modifications of the triazine core entail the selective functionalization of the three chlorine

moieties. As such, Boc-protected and phthalamide-protected handles were prepared. Boc-protection of 1,4-diaminobutane was achieved by treating the diamine with Boc-anhydride (Scheme 7.7).

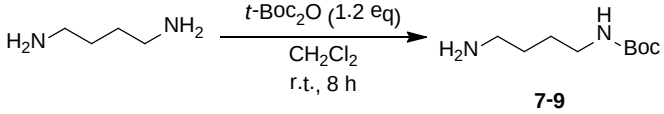

Scheme 7.7: Boc-protection of 1,4-diaminobutane

Selective Boc-protection of 1,4-diaminobutane gave **7-9** in excellent yield (92%). The reaction is fairly clean; however, di-Boc-protected product was isolated. Furthermore, unreacted 1,4-diaminobutane was removed during aqueous extraction.

The phthalamide-protected handle was prepared from the nucleophilic substitution of 2-(4-bromobutyl)phthalamide with sodium azide to afford **7-10**. The resulting azide can be converted to the corresponding amine via H_2/Pd catalyzed reduction or by Staudinger reduction using triphenylphosphine (Scheme 7.8).[49]

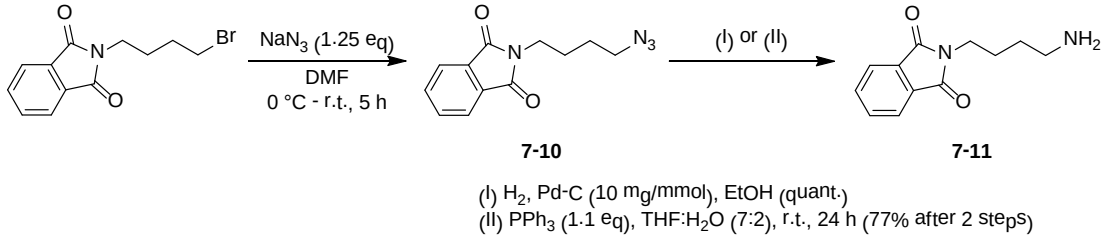

Scheme 7.8: Synthesis of 2-(4-aminobutyl)phthalamide

The treatment of 2-(4-bromobutyl)phthalamide with sodium azide gave **7-10** in good yield (82%). Reduction of azide **7-10** using H_2 over Pd-C affords **7-11** in excellent yield (100%) after simple filtration. Whereas, reduction using triphenylphosphine in THF and water is a messier reaction, as excess PPh_3, as well as the generated triphenylphosphine oxide (TPPO) have to be removed. Excess PPh_3 can be removed by washing the resulting crude with ethyl acetate. TPPO can be removed by washing with benzene. It is worthy of note that the solubility of **7-11** is poor in most organic solvents.

Selective functionalization of cyanuric chloride was achieved by using a modified procedure developed by Campbell and Hatton.[50] Campbell and Hatton found that each chloride atom can be selectively substituted with different amines based on the temperature of the reaction. Accordingly, cyanuric chloride was treated with propargyl amine in the presence of base at 0 °C for 1 hour, and then to the same pot **7-9** was added and allowed to react at room temperature (Scheme 7.9).

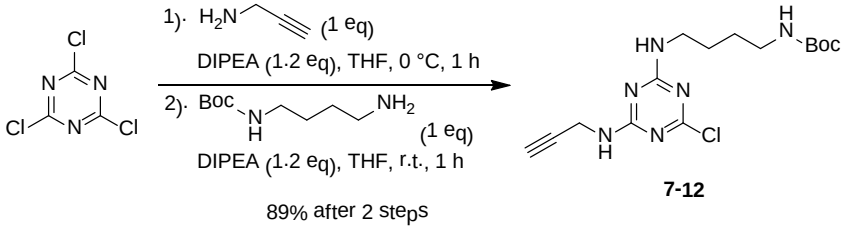

Scheme 7.9: Modifications of cyanuric chloride

Cyanuric chloride dissolves completely in THF. As propargyl amine with DIPEA is slowly added, white precipitate forms. After one hour at 0 °C, the next amine is added to afford **7-12** in good yield (89% after 2 steps) after filtration and evaporation of the reaction solvent. The mono-chloro triazine **7-12** was then treated with **7-11** in the presence of DIPEA under reflux conditions (Scheme 7.10).

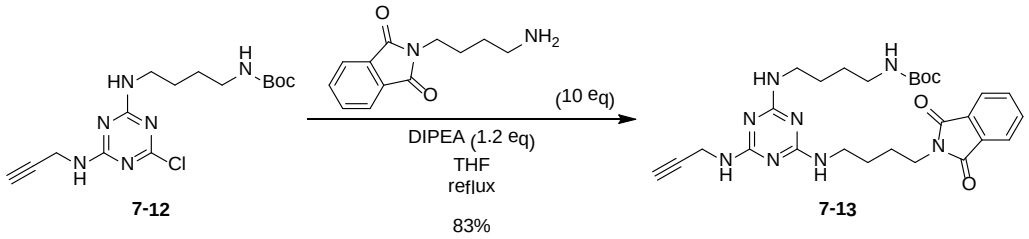

Scheme 7.10: 1,3,5-Trisubstituted triazine

The aromatic substitution reaction afforded **7-13** in good yield (83%). However, purification was difficult, as excess **7-11** co-eluted with the product, resulting in an additional purification process. Decreasing the amount of **7-11** used will ease purification. Furthermore, **7-11** is not soluble in THF, but it is soluble in hot isopropanol. Thus, THF can be replaced with isopropanol. With the selective functionalization steps, a 1,3,5-trisubstituted triazine was prepared bearing two protected amines and one terminal alkyne. Drug-linker compounds can be coupled to the resulting free-amines after sequential deprotection of the protecting groups (i.e. phthalamide and Boc), and any TTM with a terminal alkyne can be coupled to the 1,3,5-trisubstituted triazine using "click chemistry."

§ 7.2.6 2nd Tumor-Targeting Drug Conjugate Bearing Dual-Warheads

Trisubstituted 1,3,5-triazine **7-13** was chosen as the small-molecule splitter module as it was easily prepared in 3 steps starting from commercially available cyanuric chloride. Removal of the phthalamide protected group was achieved using hydrazine monohydrate followed by the addition of acid. The resulting free amine was coupled to **7-7** using EDC and DMAP (Scheme 7.11).

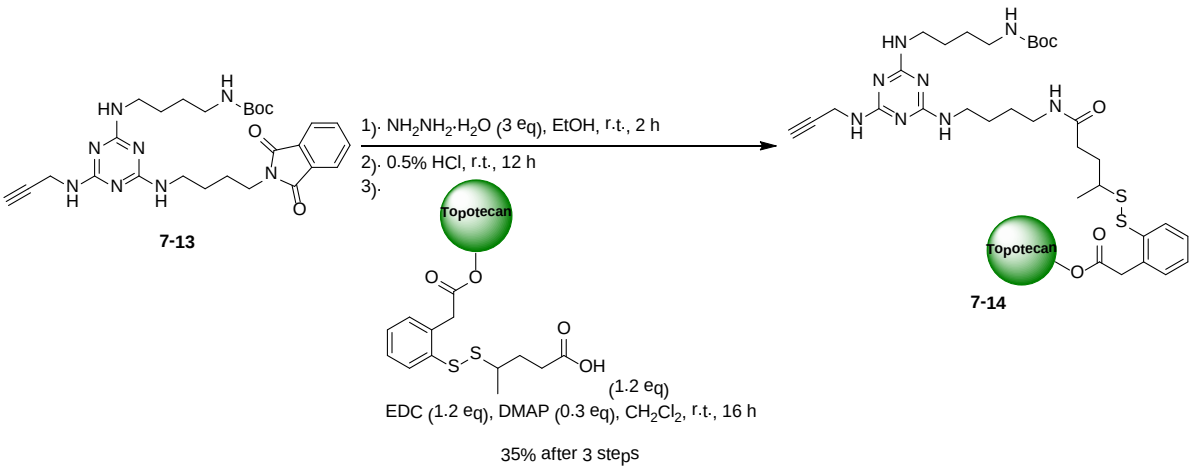

Scheme 7.11: Coupling of topotecan-Me-linker coupling to triazine splitter

Phthalamide deprotection proceeded smoothly and the corresponding free amine was isolated after filtration and passing through silica gel plug. It is worthy of note that the resulting phthalazide byproduct has a similar R_f value to that of the free-amine. For optimal yields in the subsequent coupling reactions, the phthalazide should be removed. Furthermore, Boc-deprotection was a concern during the phthalamide removal but it was not observed. Adding the corresponding amine to **7-7** pretreated with EDC and DMAP afforded **7-14** in fair yield (35% after 3 steps). Boc-deprotection was achieved using TFA, and the corresponding amine was coupled to SB-T-1214-Me-linker-CO_2H (**4-19**) in the presence of EDC and DMAP (Scheme 7.12).

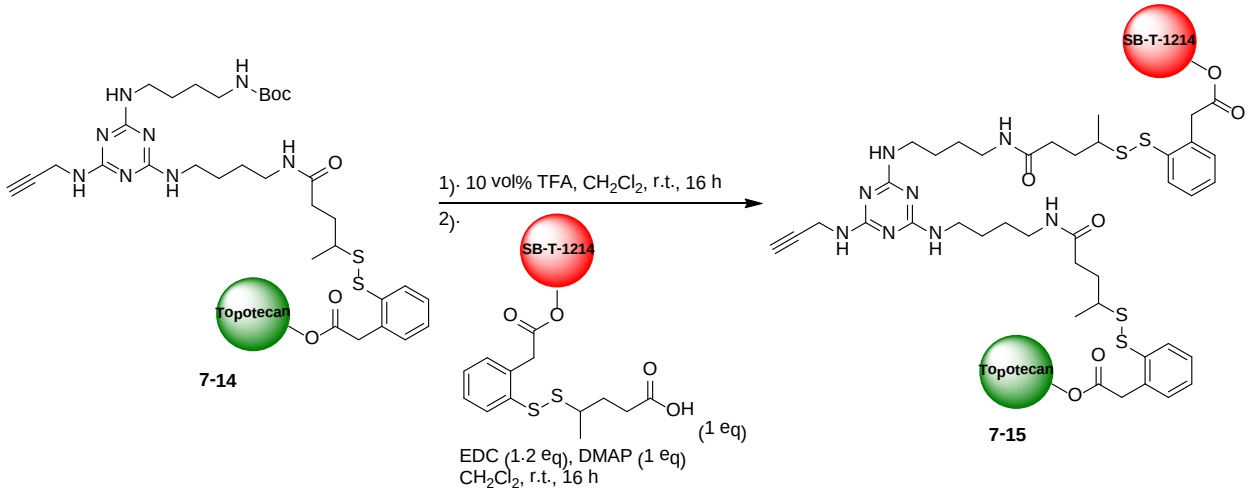

Scheme 7.12: Coupling of SB-T-1214-Me-linker to triazine splitter

Boc removal using TFA afforded the corresponding free amine after quenching with solid sodium bicarbonate and filtrating over Celite. Adding the free amine to **4-19** pretreated with EDC and DMAP afforded **7-15** in fair yield (47% after 2 steps). Purification of this compound via flash column chromatography was problematic, as the compound interacted well with silica

gel. Biotin-PEG_3-azide was installed onto **7-15** via "click" reaction using CuCl and ascorbic acid (Scheme 7.13).

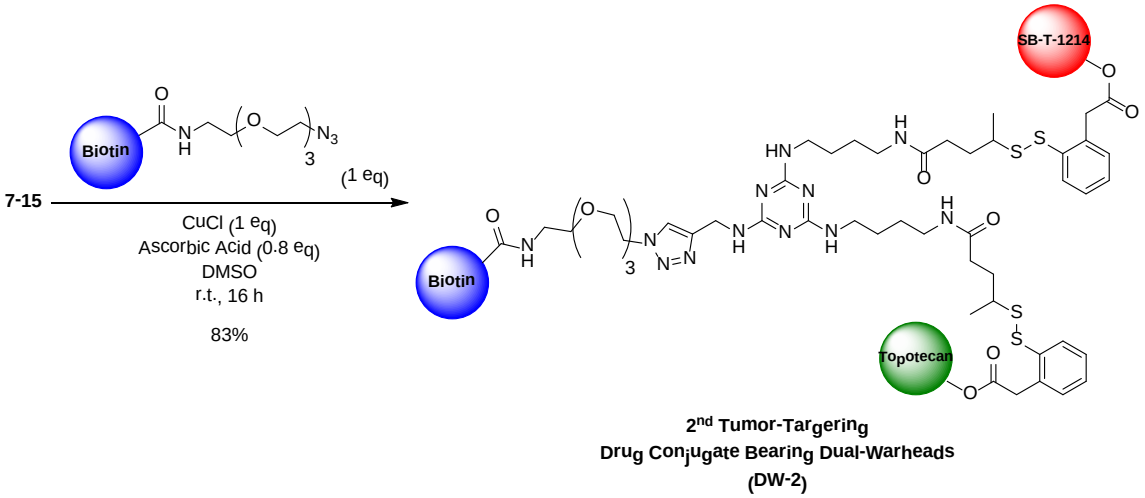

Scheme 7.13: Synthesis of 2nd tumor-targeting drug conjugate bearing dual warheads via "click" reaction

The "click" reaction was done in a glove-box, which entailed an incubation period of 8 hours before the addition of the CuCl to **7-15** and biotin-PEG_3-azide mixture. The reaction was left in the glove-box after the addition of CuCl. After 8 hours, water was added to the reaction mixture. The resulting precipitate was purified using column chromatography to afford **DW-2** in good yield (83%). The biological evaluation of **DW-2** will be discussed later in this chapter.

§ 7.2.7 Synthesis of Drug-Conjugates Bearing One Warhead and One Dummy Molecule

To further examine the possible synergistic activity between SB-T-1214 and a camptothecin (via a single molecule), a tumor-targeting drug conjugate bearing one warhead and one "dummy" molecule was designed. The "dummy" molecule will be conjugated via a disulfide linker. After cleavage of the linker, the "dummy" should not have any beneficial nor toxic effects. As such, isopropanol was chosen as the "dummy" molecule. The incorporation of isopropanol into the disulfide linker was attempted in two ways, (1) coupling to methyl-branched disulfide linker in the presence of DIC, and (2) the ring-opening, nucleophilic attack of thiolactone in the presence of sodium isopropyl alkoxide.

The coupling of isopropanol to the methyl-branched disulfide linker was attempted by treating **4-13** with neat DIC, forming the anhydride followed by the addition of isopropanol and DMAP (Scheme 7.14).

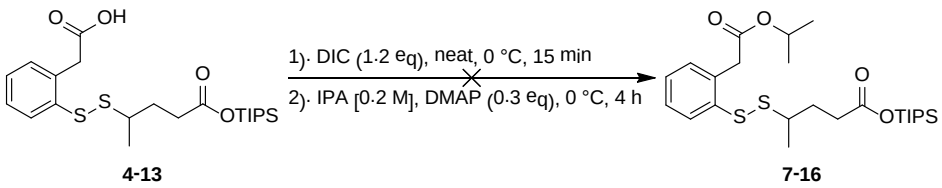

4-13 **7-16**

Scheme 7.14: Attempted synthesis of isopropyl-ester methyl-branched disulfide linker

The linker-anhydride was formed based on the formation of urea (a white solid) in the reaction flask. However, after the addition of isopropanol, no further reaction was observed. This may be caused by the steric hindrance from isopropyl moiety, blocking the nucleophilic activity of the hydroxyl. Accordingly, the generation of an isopropyl alkoxide to be used in the nucleophilic ring-opening of benzo[*b*]thiophen-2(3*H*)-one (**4-1**) was examined (Scheme 7.15).

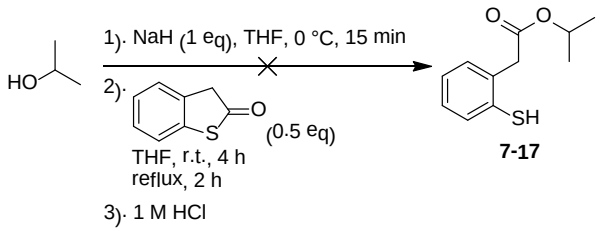

Scheme 7.15: Attempted synthesis of isopropyl-ester phenylacetic acid

This ring-opening nucleophilic attack did not produce the desired product, as only starting material was obtained. Thus, it was concluded that isopropanol was not a good candidate for the dummy molecule. As such, phenol was chosen as its replacement. The incorporation of phenol into the methyl-branched linker was achieved by treating **4-13** with phenol in the presence of DIC and DMAP, followed by silyl-moiety deprotection using HF/py and activation of the resulting carboxylic acid with HOSu in the presence of DIC (Scheme 7.16).

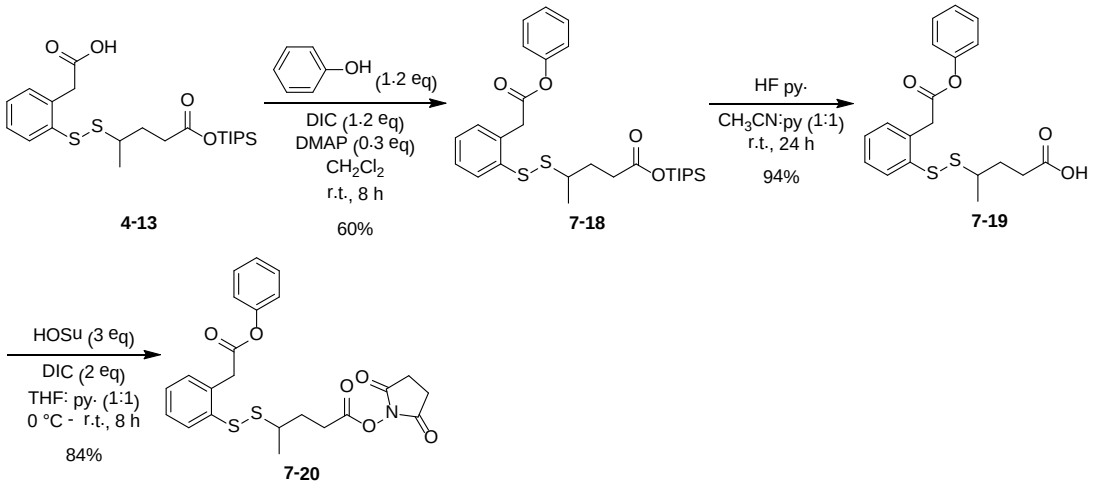

Scheme 7.16: Synthesis of phenol-ester methyl-branched disulfide linker

The addition of phenol to **4-13** pretreated with DIC and DMAP afforded **7-18** in moderate yield (60%). Deprotection of the TIPS moiety using HF in pyridine proceeded smoothly giving **7-19** in excellent yield (94%). Lastly, activation of the carboxylic acid to the corresponding OSu-activated ester in the presence of HOSu and DIC gave **7-20** in good yield (84%). This linker moiety bearing a "dummy" phenol will be installed onto a 1,3,5-trisubstituted triazine.

As mentioned above, the deprotection of the phthalamide moiety was messy, as the removal of the resulting phthalazide byproduct was difficult to remove from the desired product. As such, a different protecting group was employed. The synthesis of Fmoc-protected 1,4-

diaminobutane begins with the Fmoc-protection of N^1-Boc-1,4-diaminobutane in the presence of Fmoc-OSu followed by Boc-deprotection using TFA (Scheme 7.17).

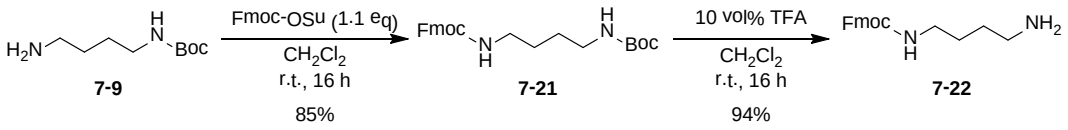

Scheme 7.17: Fmoc-protection of 1,4-diaminobutane

Fmoc-protection of **7-9** in the presence of Fmoc-OSu afforded **7-21** in high yield (85%). Boc-deprotection also proceeded smoothly giving **7-22** in excellent yield (94%). It is worthy of note that this protocol for Fmoc-protection of 1,4-diaminobutane is not atom economically efficient. Unfortunately, no high atom economical routes have been reported. Using the same protocol as mentioned above, the modifications to the triazine core can be accomplished so that a terminal alkyne is present and the terminal amines are protected with Boc and Fmoc moieties (Scheme 7.18).

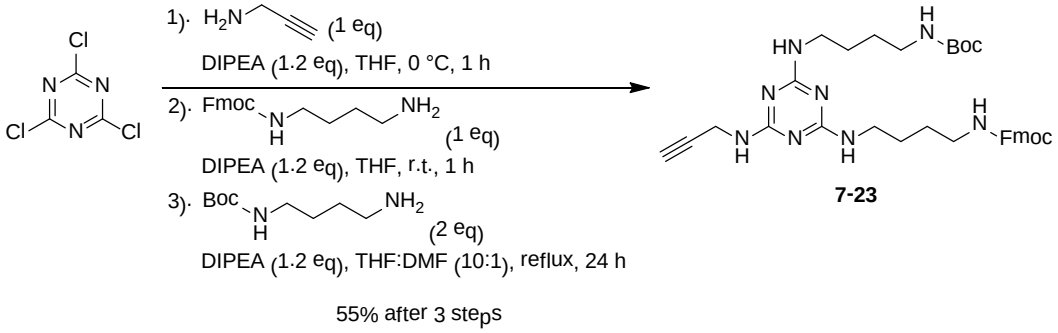

Scheme 7.18: Modifications of cyanuric chloride to bear terminal Boc- and Fmoc-protected amines and terminal alkyne

The selective functionalization of cyanuric chloride with propargyl amine, **7-22** and **7-9** afforded the 1,3,5-trisubstituted triazine **7-23** in moderate yield (55% after 3 steps). **7-23** was used for "click" reaction with bioin-PEG_3-azide. Several byproducts were observed when ascorbic acid was used as a catalyst in the previous "click" reaction. To decrease byproduct formation, bathophenanthroline sulfate was used as a catalyst (Scheme 7.19).

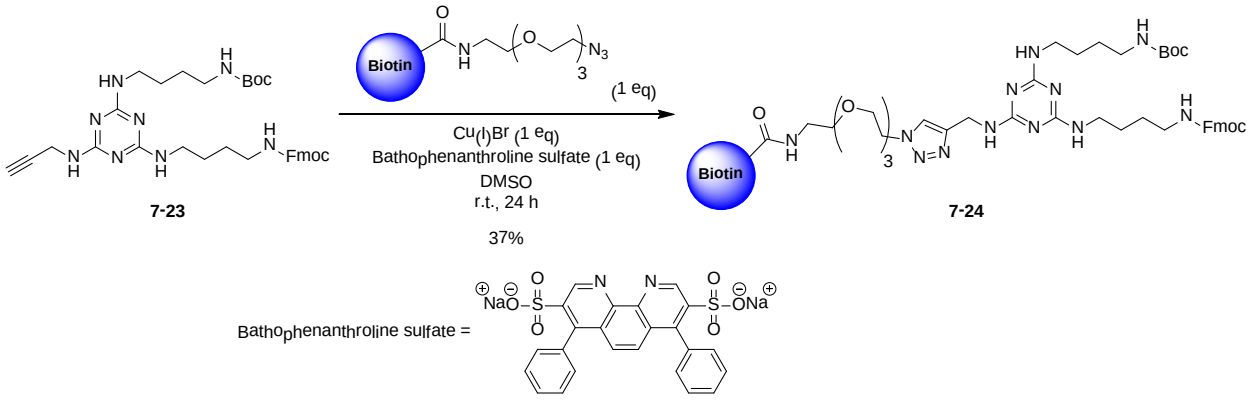

Scheme 7.19: Attempted optimization of biotinylation via "click" reaction

The use of bathophenanthroline sulfate as the catalyst limited byproduct formation, thus leading to a cleaner reaction. However, **7-24** was obtained in low yield (37%). Other catalysts should be explored in future reactions. The Fmoc moiety was deprotected in the presence of piperidine and the corresponding free-amine was added to **7-20** (Scheme 7.20).

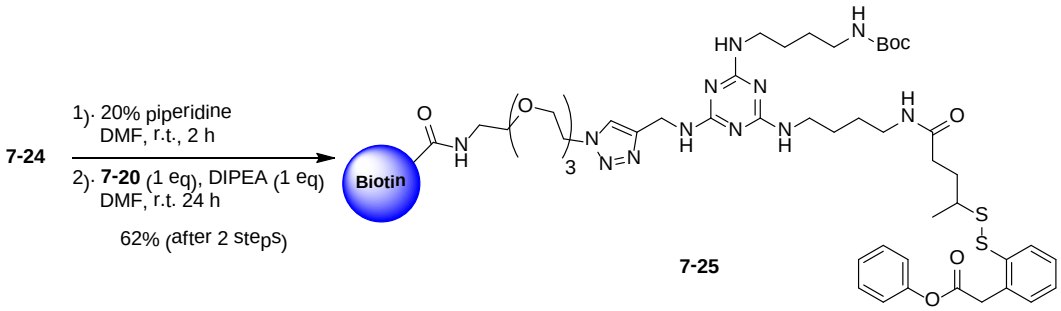

Scheme 7.20: Coupling of dummy-linker molecule to triazine splitter

Fmoc-deprotection using piperidine was fast and clean giving the corresponding amine after extraction and filtration. The corresponding amine with DIPEA was then added to **7-20** to afford **7-25** in moderate yield (62% after 2 steps). The Boc moiety was deprotected using TFA and the corresponding amine was coupled to **4-20** (Scheme 7.21).

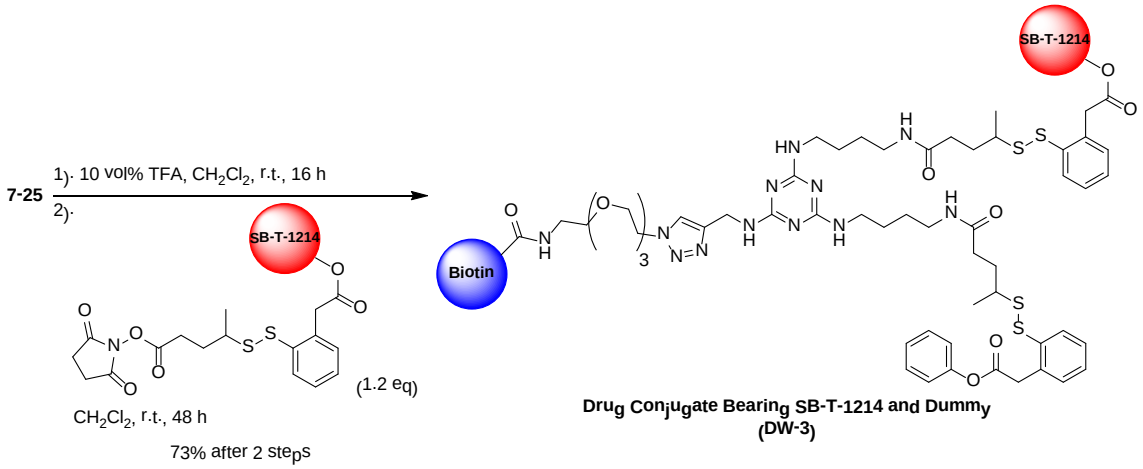

Scheme 7.21: Synthesis of drug conjugate bearing SB-T-1214 and one dummy molecule

The coupling of **4-20** to **7-25** afforded **DW-3** in good yield (73%). The biological evaluation of this drug conjugate will be discussed in the next section. Topotecan-linker compound and **7-25** coupling reactions were also attempted (Scheme 7.22).

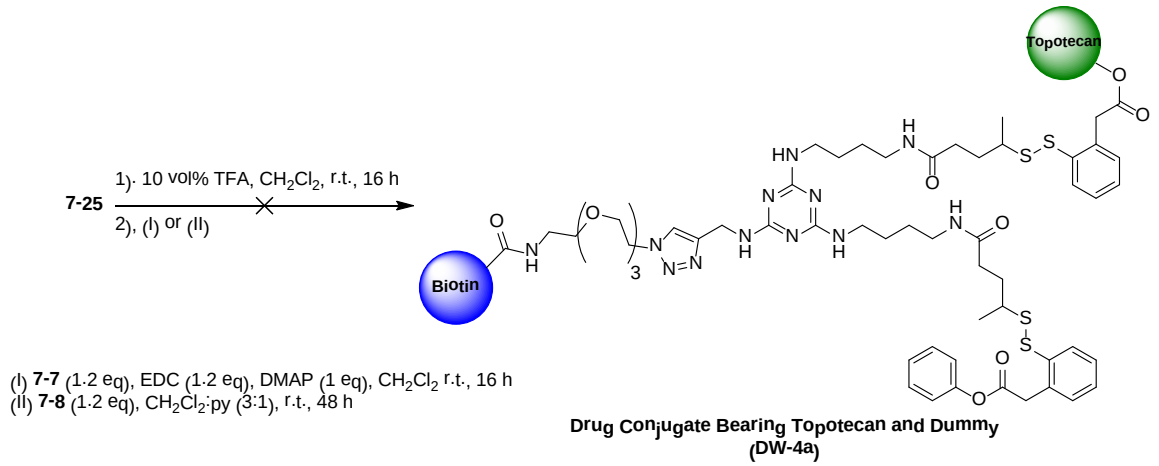

Scheme 7.22: Topotecan-linker coupling attempts

Whereas, the coupling of **4-20** and **7-25** yielded the desired drug conjugate, coupling reactions involving topotecan-linker compounds **7-7** and **7-8** did not generate the corresponding drug conjugate. Similar to the synthesis of **7-14**, topotecan-linker **7-7** was pretreated with EDC and DMAP, followed by the addition of **7-25**. Based on TLC, new spots were generated. However after column chromatography, no desired product was obtained. Accordingly, direct coupling of **7-25** with the activated ester **7-8** was attempted. Based on TLC, no reaction occurred after 24 h. It was observed that the reaction mixture was getting darker over time. After 48 h, no reaction was observed, and the starting materials were not recovered. An alternative coupling was attempted as topotecan-linker starting materials were scarce. The coupling of **7-25** to camptothecin-Me-linker-OSu (**4-23b**) was attempted (Scheme 7.23)

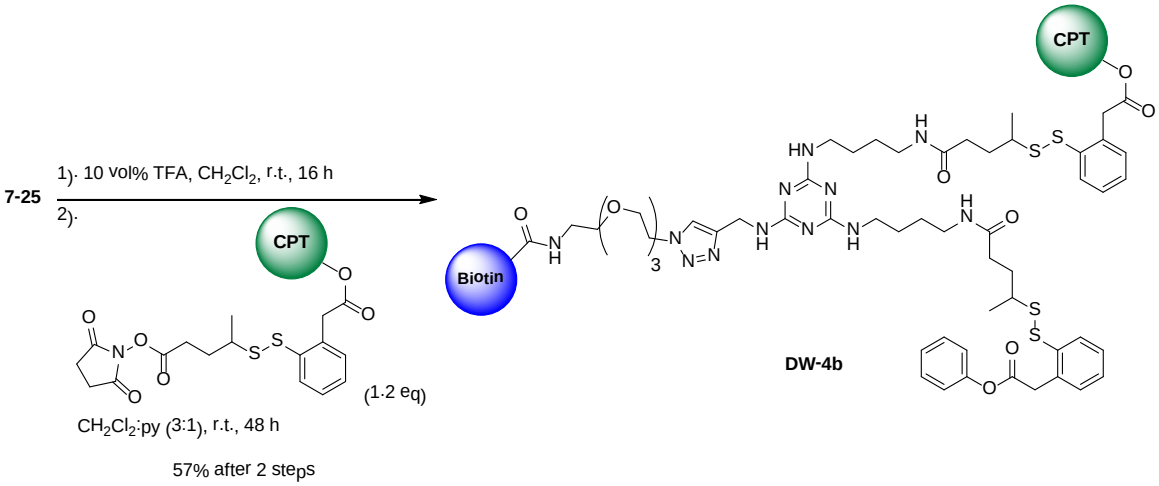

Scheme 7.23: Synthesis of drug conjugate bearing camptothecin and one dummy molecule

The addition of **7-25** to **4-23b** afforded **DW-4b** in moderate yield (57% after 2 steps). The success of CPT-linker coupling warrants a closer investigation to determine the reasons for topotecan-linker coupling failures. The topotecan-linker coupling may have failed due to the relative instability of topotecan at room temperature. Or the topotecan-linker derivatives may not be stable under basic conditions, as both coupling reactions were done in the presence of base,

whereas in the synthesis of **7-14** a catalytic amount of DMAP was used. Optimal coupling conditions with topotecan-linker derivatives will be examined.

§ 7.2.8 Biological Evaluation of Drug Conjugate Bearing Dual-Warheads and Investigation of Synergistic Activity of One Warhead and One Dummy Drug Conjugates

The biological activities of **DW-2**, **DW-3** and **DW-4b** were evaluated against a series of human breast cancer cell lines. The results from this experiment are listed in Table 7.4 (data of free drug and free drug combinations were shown previously). These cancer cell lines were previously shown to express the biotin receptor as determined by FACS analysis of cells incubated with biotin-PEG_3-FITC. Furthermore, the combination of SB-T-1214 and topotecan gave promising results against MCF-7, MDA MB 231 and SkBr3 in MTT assays. Surprisingly, as seen from Table 7.4, drug conjugate **DW-3** (SB-T-1214 with phenol) showed the best *in vitro* activity providing the lowest IC_{50} values against the cancer cell lines tested, whereas, both **DW-2** (SB-T-1214 and topotecan) and **DW-4b** (camptothecin and phenol) did not show any significant activity compared to the combination of free drugs. Accordingly, glutathione ethyl ester (GSH-OEt) was added to the cells, to assure cleavage of the drug-linker disulfide bond, after incubation with the drug conjugates. These results are listed in Table 7.5.

Table 7.4: Biological Evaluation of Drug Conjugates DW-2, DW-3 and DW-4b against Various Breast Cancer Cell Lines

	IC_{50} (nM)					
Taxane	**BT20**	**LCC6 wt**	**LCC6 MDR**	**MCF-7**	**MDA MB 231**	**SkBr3**
SB-T-1214	0.20 ± 0.06	0.68 ± 0.33	0.86 ± 0.15	0.35 ± 0.11	18.9 ± 9.7	0.48 ± 0.03
Camptothecin	230 ± 25	2.43 ± 1.48 μM	381 ± 98	159 ± 63	503 ± 8	705 ± 277
SB-T-1214:CPT	475 ± 8	324 ± 78	492 ± 5	0.34 ± 0.14	406 ± 140	3.74 ± 1.15
Topotecan	490 ± 2	421 ± 224	489 ± 317	28.1 ± 7.3	386 ± 106	353 ± 120
SB-T-1214:Topotecan	537 ± 34	533 ± 243	470 ± 178	0.21 ± 0.16	0.51 ± 0.02	0.48 ± 0.01
DW-2	390 ± 136	127 ± 20	591 ± 379	88.3 ± 22.0	39.4 ± 34	227 ± 106
DW-3	4.13 ± 1.25	53.5 ± 1.3	4.69 ± 2.82	38.7 ± 20.9	32.9 ± 13.1	5.46 ± 0.45
DW-4b	45.6 ± 30.4	448 ± 73	309 ± 115	242 ± 42	419 ± 327	250 ± 21

- Cells were suspended in RPMI-1640 Medium 10 x (Sigma Aldrich, R1145) supplemented with tissue culture grade water, 0.3 g/L L-glutamine, 2.0 g/L sodium bicarbonate, 10% FBS, and 1% Penn Strep before administration of drug conjugate
- Cells were incubated for 48 hours at 37 °C with 5% CO_2 after administration of drug conjugate

Table 7.5: Biological Evaluation of Drug Conjugates DW-2, DW-3 and DW-4b against Various Breast Cancer Cell Lines with Addition of GSH-OEt

	IC_{50} (nM)				
Taxane	**LCC6 wt**	**LCC6 MDR**	**MCF-7**	**MDA MB 231**	**SkBr3**
SB-T-1214	0.68 ± 0.33	0.86 ± 0.15	0.35 ± 0.11	2.89 ± 1.67	0.48 ± 0.03
Topotecan	421 ± 224	489 ± 317	28.1 ± 7.3	386 ± 106	353 ± 120
SB-T-1214:Topotecan	533 ± 243	470 ± 178	0.21 ± 0.16	0.51 ± 0.02	0.49 ± 0.01
DW-2	4.30 ± 1.45	35.2 ± 4.8	7.42 ± 1.32	4.11 ± 0.76	2.66 ± 1.51
DW-3	5.33 ± 0.43	44.4 ± 7.52	3.04 ± 1.89	8.26 ± 3.27	4.72 ± 0.10
DW-4b	104 ± 17.8	247 ± 17.6	252 ± 20.2	469 ± 318	292 ± 107

- Cells were suspended in RPMI-1640 Medium 10 x (Sigma Aldrich, R1145) supplemented with tissue culture grade water, 0.3 g/L L-glutamine, 2.0 g/L sodium bicarbonate, 10% FBS, and 1% Penn Strep
- Cells were incubated for 24 hours at 37 °C with 5% CO_2 after administration of drug conjugate washed with DPBS, resuspended in RPMI with 6 eq. GSH-OEt and incubated for 48 hours at 37 °C with 5% CO_2

- The optical density was determined using Acsent Multiskan optical density reader
- The reported values are a calculated averages of IC_{50} values determined from three individual experiments
- IC_{50} values were calculated using SigmaPlot v 10.0
- All IC_{50} values are report in nM scale unless otherwise noted

As seen from Table 7.5, the addition of 6 equivalents GSH-OEt greatly increased the observed potency of **DW-2** in all of the breast cancer cell lines evaluated. In this experiment, cancer cells were incubated with the drug conjugate for 24 h, and then the cells were washed thoroughly with PBS and resuspended in cell culture media containing 6 molar equivalents of GSH-OEt. In general, **DW-2** demonstrated greater potency in the breast cancer cell lines tested compared to **DW-3** and **DW-4b** after the addition of GSH-OEt. This result confirms that excess GSH-OEt internalized into the cancer cells and cleaved the disulfide bonds of the drug conjugate releasing both taxoid and topotecan inside the cell. **DW-2** demonstrated 2 orders of magnitude greater potency against LCC6 wt and 1 order of magnitude greater potency against LCC6 MDR compared to the free drug combination of SB-T-1214 (24 h) followed by topotecan (24 h). The activity of **DW-2** against MCF-7, MDA MB 231 and SkBr3 is less potent than the free drug combination. These results suggest that the disulfide linkers are being cleaved so that topotecan is being released before SB-T-1214, resulting in lower activity. Thus, it is reasonable to assume that by changing the disulfide linker used to conjugate SB-T-1214 (to the drug conjugate) to a different disulfide linker that cleaves faster than the methyl-branched linker would increase the potency of the drug conjugate. The change in linker-cleavage would assure the release of taxoid before topotecan, resulting in their synergistic activity. A tumor-targeting drug conjugate with two different disulfide linkers used to conjugate SB-T-1214 and a camptothecin, such as topotecan or SN-38, is currently being explored in the Ojima laboratory.

§ 7.3.0 Summary

Two novel tumor-targeting drug conjugates have been synthesized; (1) a drug conjugate bearing dual-warheads (SB-T-1214 and topotecan), and (2) a drug conjugate bearing one warhead (SB-T-1214 or camptothecin) and one dummy molecule (phenol). Both drug conjugates utilize biotin as a tumor-targeting module. The presence of biotin increases tumor-specificity of the drug conjugates, as cancer cells overexpress vitamin receptors. The internalization of biotin-PEG_3-FITC probes was observed using CFM and FACs against different breast cancer cell lines. The warheads chosen were SB-T-1214, a 2^{nd}-generation taxoid that inhibits microtubule depolymerization, and topotecan, a camptothecin analog that inhibits DNA topoisomerase I. The combination of SB-T-1214 and topotecan gave promising results in MTT assays against different cancer cell lines, especially in breast cancer cell lines that may overexpress vitamin receptors. It is reasonable to assume that the dual mechanism of action makes the drug conjugate bearing dual-warheads highly efficacious. Furthermore, 1,3,5-trisubstituted triazine, derived from the facile selective functionalization of cyanuric chloride, was chosen as a small-molecule splitter module.

The drug conjugate bearing one warhead and phenol as a dummy molecule was synthesized to evaluate possible synergistic activity present in the drug conjugate bearing both SB-T-1214 and topotecan. Phenol was chosen as a dummy molecule to mimic a warhead but will not introduce any beneficial or adverse effects after release. The biological activity of the tumor-targeting drug conjugate bearing multiple branches was discussed. From these results, it can be concluded that through the use of a 1,3,5-trisubstituted triazine as a small-molecule splitter module different combinations of cytotoxic agents can be installed into a single drug conjugate that can specifically deliver cytotoxic drugs to cancer cells. Along that line, a variety of warhead, TTM and imaging agent combinations can be achieved in a single drug conjugate through the use of a small-molecule splitter module, such as 1,3,5-trisubstituted triazine.

§ 7.4.0 Experimental

Caution

Taxoids and topotecan have been established as a potent cytotoxic agent. Thus, they and all structurally related compounds and derivatives must be considered as mutagens and potential reproductive hazards for both males and females. Appropriate precautions (i.e. use of gloves, goggles, lab coat and fume hood) must be taken while handling these compounds.

General information

All chemical were obtained from Sigma-Aldrich, Fisher Scientific or VWR International, and used as is unless otherwise noted. All reactions were carried out under nitrogen in oven dried glassware using standard Schlenk techniques unless otherwise noted. Reactions were monitored by thin layer chromatography (TLC) using E. Merck 60F254 precoated silica gel plates and alumina plate depending on the compounds. Dry solvents were degassed under nitrogen and were dried using the PURESOLV system (Inovatative Technologies, Newport, MA). Tetrahydrofuran was freshly distilled from sodium metal and benzophenone. Dichloromethane was also distilled immediately prior to use under nitrogen from calcium hydride. Toluene was also distilled immediately prior to use under nitrogen from calcium hydride. Yields refer to chromatographically and spectroscopically pure compounds. Flash chromatography was performed with the indicated solvents using Fisher silica gel (particle size 170-400 Mesh).^{1}H, ^{13}C and ^{9}F data were obtained using either 300 MHz Varian Gemni 2300 (75 MHz ^{13}C, 121 MHz ^{19}F) spectrometer, the 400 MHz Varian INOVA 400 (100 MHz ^{13}C) spectrometer or the 500 MHz Varian INOVA 500 (125 MHz ^{13}C) in $CDCl_3$ as solvent unless otherwise stated. Chemical shifts (δ) are reported in ppm and standardized with solvent as internal standard based on literature reported values.[51] Melting points were measured on Thomas Hoover Capillary melting point apparatus and are uncorrected. Optical rotations were measured on Perkin-Elmer Model 241 polarimeter.

Vitamin-PEG_3-N_3 (7-1)[39]

Method 1:

7-1a: A mixture of biotin (250 mg, 1 mmol), DCC (250 mg, 1.2 mmol) and HOSu (240 mg, 2 mmol) was dissolved in DMF [0.5 M]. The mixture was stirred at 50 °C and the reaction was monitored via TLC. After 24 h, the reaction solvent was diluted with ether and the resulting crude was washed with IPA and CH_3CN to yield biotin-OSu (294 mg, 83% yield) which was used in the subsequent step without further purification; m.p. 193-196 °C; ^{1}H NMR (300 MHz, DMSO-d_6, ppm) δ 1 1.485-1.715 (m, 8H), 2.547 (s, 2 H), 2.695 (t, *J* = 9.2 Hz, 3 H), 2.855 (s, 4 H), 4.193 (m, 1 H), 4.346 (m, 1 H), 6.419 (d, *J* = 24 Hz, 2 H).

To a solution of biotin-OSu (100 mg, 0.04 mmol) dissolved in DMF [0.1 M] was added 11-azido-3,6,9-trioxaundecan-1-amine (200 mg, 0.04 mmol). The mixture was stirred at room temperature and the reaction was monitored via TLC. After 48 h, the reaction mixture was diluted with water. The aqueous layer was washed with $CHCl_3$ (3 x 50 mL), collected and lyophilized. The resulting crude was dissolved in acetone:hexanes (4:1) and purified using flash column chromatography on silica gel (acetone:hexanes = 4:1) to yield **7-1a** (145, 92% yield) as an orange oil:

7-1b: Folic acid (250 mg, 0.6 mmol), EDC (119 mg, 0.8 mmol) and HOSu (72 mg, 0.8 mmol) was dissolved in DMSO [0.1 M]. The mixture was stirred at room temperature for 30 minutes. After 30 minutes, to the mixture was added 11-azido-3,6,9-trioxaundecan-1-amine (0.112 mL, 0.6 mmol). The mixture was stirred at room temperature and the reaction was monitored via reverse-phase TLC. After 24 h, the reaction was diluted with water. The aqueous layer was washed with $CHCl_3$ (3 x 20 mL) and the aqueous layer was lyophilized to yield crude containing **7-1b** (343 mg) with an additional unknown product. The crude material was used without further purification.

Method 2:

To a solution of vitamin and EDC (1.2 eq.) dissolved in a 3:1 mixture of CH_3CN:CH_3OH [0.1 M] was added 11-azido-3,6,9-trioxaundecan-1-amine (1 eq.). The mixture was stirred at room temperature and monitored via TLC. After 24 h, the solvent was evaporated and the resulting crude was purified using flash column chromatography on silica gel (10% CH_3OH in CH_2Cl_2) to yield **7-1**:

7-1a (365 mg, 91% yield), an oily yellow solid: biotin (220 mg, 0.8 mmol), EDC (200 mg, 1 mmol), 9 mL CH_3CN:CH_3OH (3:1), 11-azido-3,6,9-trioxaundecan-1-amine (0.17 mL, 0.8 mmol); ^{1}H NMR (300 MHz, CD_3OD, ppm) δ 1.407-1.456 (m, 2 H), 1.598-1.698 (m, 4 H), 2.190-2.239 (t, J = 7.5 Hz, 2 H), 2.677-2.720 (d, J = 12.9 Hz, 1 H), 2.893-2.951 (dd, J_1 = 4.8 Hz, J_2 = 7.8 Hz, 1 H), 3.201 (m, 1 H), 3.346-3.389 (m, 4 H), 3.518-3.554 (t, J = 5.4 Hz, 2 H), 3.597-3.682 (m, 6 H), 4.279-4.320 (m, 1 H), 4.467-4.508 (m, 1 H), 8.023 (br s, 1 H). All data are consistent with literature values.[39]

7-1b (310 mg crude, 79% crude yield), a sticky red solid: folate (250 mg, 0.6 mmol), EDC (119 mg, 0.8 mmol), DMSO [0.2 M], 11-azido-3,6,9-trioxaundecan-1-amine (0.13 mL, 0.6 mmol). After 24 h, the reaction was diluted with water. The aqueous layer was washed with $CHCl_3$ (3 x 20 mL) and the aqueous layer was lyophilized. The resulting crude was washed with cold water to yield crude containing **7-1b** with an additional unknown product. The crude material was used without further purification.

Vitamin-PEG$_3$-NH$_2$ (7-2)[39]

A mixture of **7-1** and Ph_3P (1.1 eq.) dissolved in a 7:2 mixture of THF:water [0.1 M]. The mixture was stirred at room temperature and the reaction was monitored via TLC. After 16 h, the reaction solvent was evaporated and the resulting crude was washed with ether, dichloromethane and then washed with benzene to yield **7-2**

7-1a (120 mg, 0.2 mmol), Ph_3P (84 mg, 0.22 mmol) to yield **7-2a** (110 mg, 97% yield), as a sticky yellow solid: ^{1}H NMR (300 MHz, DMSO-d_6, ppm) δ 1.407-1.456 (m, 2 H), 1.598-1.698 (m, 4 H), 2.190-2.239 (t, J = 7.5 Hz, 2 H), 2.677-2.720 (d, J = 12.9 Hz, 1 H), 2.893-2.951 (dd, J_1 = 4.8 Hz, J_2 = 7.8 Hz, 1 H), 3.201 (m, 1 H), 3.346-3.389 (m, 4 H), 3.518-3.554 (t, J = 5.4 Hz, 2 H), 3.597-3.682 (m, 6 H), 4.279-4.320 (m, 1 H), 4.467-4.508 (m, 1 H). All data are consistent with literature values.[39]

7-1b (100 mg crude), Ph_3P (44 mg, 0.1 mmol) to yield crude **7-2b** (100 mg, 90% crude yield), as a red-orange solid, which was used without further purification.

Vitamin-PEG-FITC (7-3)

A mixture of **7-2** and FITC (0.6 eq.) was dissolved in DMF [0.1 M]. To the mixture was added DIPEA (1.1 eq.). The mixture was stirred at room temperature and the reaction was monitored

via TLC. After 24 h, to the mixture was added ethyl ether forming precipitate. The precipitate was filtered, washed with ethyl ether and then with CH_2Cl_2 to yield **7-3**:
7-3a (30 mg, 62% yield), as a waxy orange solid: **7-2a** (25 mg, 0.06 mmol), FITC (16 mg, 0.036 mmol); ^{1}H NMR (400 MHz, CD_3OD, ppm) δ 1.307-1.462 (m, 10 H), 1.560-1.737 (m, 3 H), 2.213 (t, *J* = 7.2 Hz, 1 H), 2.712 (m, 1 H), 2.877 (s, 3 H), 3.014 (s, 3 H), 3.172-3.317 (m, 3 H), 3.502-3.772 (m, 10 H), 3.845 (br s, 1 H), 4.273-4.304 (m, 1 H), 4.462-4.494 (m, 1 H), 6.551-6.585 (m, 1 H), 6.683-6.703 (m, 3 H), 7.167 (d, *J* = 8.4 Hz, 1 H), 7.557-7.588 (m, 2 H), 7.633-7.688 (m, 3 H), 7.793 (d, *J* = 7.6 Hz, 1 H), 7.997 (s, 1 H), 8.191 (s, 1 H); HRMS TOF MS ES+ *m/z* calcd for $C_{39}H_{45}N_5O_{10}S_2$ $(M+H)^+$ 808.2608, found 808.2682 (Δ 7.4 ppm).
7-3b (30 mg, 58% yield), as a red solid: **7-2b** (40 mg, 0.06 mmol), FITC (16 mg, 0.036 mmol); ^{1}H NMR (400 MHz, DMSO-d_6, ppm) δ 1.148 (s, 7 H), 2.256 (m, 3 H), 2.686 (s, 2 H), 2.846 (s, 3 H), 4.432 (s, 3 H), 6.525-6.623 (m, 11 H), 6.848-6.883 (m, 4 H), 7.139 (m, 3 H), 7.514-7.906 (m, 11 H), 8.597 (s, 1 H), 8.979-9.186 (m, 1 H), 10.080 (br s, 1 H); FIA-MS MS (ESI) *m/z* found 1020.3 $(M+16)^+$ ($C_{48}H_{48}N_{10}O_{13}S$ requires 1004.3).

10-Hydroxycamptothecin (7-4)[42]
This compound was prepared using the exact procedure described by Kingsbury, et. al.[42] Pt^0 was prepared by vigorously stirring Pt_2O in HOAc under H_2 at room temperature. After 1 h, the reaction vessel was purged with N_2. To the mixture was added CPT (320 mg, 0.9 mmol) dissolved in HOAc. The reaction vessel was purged with H_2 and stirred at room temperature. After the absorption of H_2 reached completion (16 h), the H_2 was evacuated by purging with N_2. The reaction mixture was filtered over celite and washed with HOAc to yield 4,5,6,7-tetrahydroxyCPT in HOAc. To the mixture was added 1 equivalent $Pb(OAc)_4$. The reaction was stirred at room temperature for 1 h. The reaction mixture was filtered over celite to yield a mixture of 10-hydroxyCPT, 10-acetoxyCPT and CPT. The mixture was dissolved in 50% HOAc and the reaction was stirred under reflux conditions for 1 h. The reaction solvent was evaporated to yield 190 mg of 10-hydroxyCPT (**7-4**) with CPT in a 4:1 ratio.

Topotecan (7-5)[42, 45]
Method 1
To crude **7-4** (60 mg, 1.5 mmol) dissolved in 1.86 mL HOAc was added 0.04 mL CH_2O, dropwise, followed by the dropwise addition of 0.04 mL 40% aqueous $HN(CH_3)_2$. The mixture was stirred vigorously at room temperature and monitored via TLC. After 48 h, the starting material was consumed based on TLC. The reaction solvent was evaporated. The resulting crude was dissolved in CH_3OH filtered through celite and purified using Yamazen Prep chromatography to yield crude containing topotecan (20 mg, 37% crude yield) as yellow/brown solid, which was used without further purification.
Method 2
To crude **7-4** (40 mg, 1 mmol) and K_2CO_3 (238 mg, 1.6 mmol) suspended in CH_2Cl_2 (5.5 mL) was added 1.3 mL 40% aqueous $HN(CH_3)_2$. The mixture was stirred in the dark at room temperature. After 5 hours, the reaction mixture was filtered, the solid was washed with ethyl acetate and the combined filtrate was extracted with ethyl acetate (3 x 10 mL). The organic layers were combined, dried over $MgSO_4$ and concentrated *in vacuo*. The resulting crude was triturated with 0.5% aq. HCl (5.5 mL) to dissolve the water-soluble adduct. Water-soluble fraction was washed with ethyl ether (3 x 10 mL) and ethyl acetate (3 x 10 mL). The aqueous layer was lyophilized to yield **7-5** (24 mg, 60% yield), as a bright yellow solid:

All data are consistent for each method: ^{1}H NMR (300 MHz, DMSO-d_6, ppm) δ 1.077 (t, *J* = 7.5 Hz, 6 H), 1.993-2.081 (m, 4 H), 2.913 (s, 12 H), 3.083 (s, 16 H), 4.586 (s, 3 H), 5.432-5.443 (m, 4 H), 5.486 (br s, 1 H), 5.562 (s, 1 H), 5.606 (s, 1 H), 5.661 (s, 1 H), 7.734 (s, 1 H), 7.761 (s, 3 H), 8.289 (d, *J* = 3.3 Hz, 4 H), 9.246 (br s, 2 H). All values are consistent with literature values.[42, 45]

Topotecan-Me-linker-TIPS (7-6)

To **7-5** (20 mg, 0.04 mmol) and **4-13** (20 mg, 0.04 mmol) with DMAP (2 mg, 0.012 mmol) dissolved in CH_2Cl_2 [0.1] and cooled to 0 °C was added DIC (0.01 mL, 0.08 mmol), dropwise. The mixture was stirred at 0 °C and the reaction was monitored via TLC. After 5 hours, the reaction solvent was evaporated and the resulting crude was purified using flash column chromatography on silica gel (hexanes:ethyl acetate = 1:1 followed by 5% CH_3OH in CH_2Cl_2) to yield **7-6** (33 mg, 83% yield), as a bright yellow solid; ^{1}H NMR (300 MHz, $CDCl_3$, ppm) δ 0.975-1.045 (m, 3 H), 1.080 (m, 21 H), 1.179-1.310 (m, 4 H), 2.907-2.928 (m, 2 H), 3.197 (s, 2 H), 3.244 (s, 6 H), 3.730-3.827 (m 2 H), 4.774 (m, 1 H), 5.325 (m, 1 H), 5.850 (m, 1 H), 6.923-6.995 (m, 3 H), 7.558-7.616 (m, 1 H), 8.080 (d, *J* = 7.8 Hz, 2 H), 8.177-8.258 (m, 1 H), 8.831-8.862 (m, 1 H); ^{13}C NMR (400 MHz, $CDCl_3$, ppm) δ 10.472, 22.762, 32.355, 33.427, 34.298, 48.383, 52.195, 52.366, 52.758, 69.022, 75.364, 100.846, 121.365, 130.141, 130.689, 130.820, 131.187, 132.474, 133.299, 133.605, 133.745, 151.632, 152.864, 155.119, 160.366, 176.574, 200.298.

Topotecan-Me-linker-CO_2H (7-7)

Method 1:

7-6 (33 mg, 0.03 mmol) was dissolved in a 1:1 mixture of CH_3CN:py [0.01 M] and cooled to 0 °C. To the mixture was added HF pyridine (0.33 mL). The mixture was stirred at room temperature and the reaction was monitored via TLC. After 16 h, the reaction was quenched with 0.2 M citric acid (5 x amount of HF pyridine used) and extracted with CH_2Cl_2 (2 x). The organic layers were washed with $CuSO_4$ (3 x), then washed with brine (3 x), collected, dried over $MgSO_4$ and concentrated *in vacuo*. Trace **7-7** was obtained:

Method 2:

To a solution of **7-6** (40 mg, 0.05 mmol) dissolved in benzene [0.01 M] was added a solution of CsF (15 mg, 0.1 mmol) dissolved in CH_3CN [0.01 M] producing a yellow slurry. The mixture was stirred at room temperature. After 15 min, the reaction was diluted with CH_2Cl_2 and quenched with aqueous KH_2PO_4. The aqueous layer was extracted with CH_2Cl_2 (3 x 20 mL). The organic layer was combined, washed with brine (1 x 10 mL), dried over Na_2SO_4 and concentrated *in vacuo* to yield **7-7** (17 mg, 57% yield) as a bright-yellow solid:

Method 3:

To **7-6** (15 mg, 0.019 mmol) was added 0.2 mL of 0.1% in EtOH. The mixture was stirred at room temperature and the reaction was monitored via TLC. After 2 h, the reaction was quenched with H_2O and the aqueous layer was lyophilized. The resulting crude was passed through a short alumina gel plug (10% CH_3OH in CH_2Cl_2 as eluent) to yield no desired product.

^{1}H NMR (400 MHz, $CDCl_3$, ppm) δ 0.821-0.884 (m, 4 H), 0.932-0.999 (m, 3 H), 1.060 (d, *J* = 6.4 Hz, 2 H), 1.253 (m, 8 H), 1.909 (s, 1 H), 2.773-2.901 (m, 12 H), 3.412 (s, 1 H), 5.222 (s, 1 H), 5.318 (d, *J* = 16.4 Hz, 1 H), 5.518 (d, *J* = 16.4 Hz, 1 H), 6.942-7.204 (m, 1 H), 7.411 (d, *J* = 9.2 Hz, 1 H), 7.572 (s, 1 H), 7.942 (d, *J* = 9.6 Hz, 1 H), 8.667 (br s, 1 H); MS ES+ *m/z* calcd for $C_{36}H_{37}N_3O_8S_2$ $(M+H)^+$ 704.2, found 704.2.

Topotecan-Me-linker-OSu (7-8)
To a mixture of **7-7** (15 mg, 0.01 mmol) and HOSu (32 mg, 0.01 mmol) dissolved in pyridine was added DIC (0.01 mL, 0.02 mmol). The mixture was stirred at room temperature and the reaction was monitored via TLC and LC/MS. After 5 h, the reaction solvent was evaporated and the resulting crude was extracted with $CHCl_3$ (3 x 50 mL). The organic layers were collected, washed with brine (1 x 50 mL), dried over $MgSO_4$ and concentrated *in vacuo* to yield crude containing **7-8** (30 mg, 75% crude yield) as a bright yellow/green solid, which was used without further purification.

***N*^{1}-Boc-1,4-diaminobutane (7-9)[52]**
To 1,4-diaminobutane (5 g, 56 mmol) dissolved in CH_2Cl_2 [0.1 M] was added *t*-Boc_2O (1.5 g, 5.6 mmol), dropwise via an additional funnel. Upon addition, white precipitate formed. After 8 h, the reaction solvent was evaporated, diluted with water and extracted with $CHCl_3$ (3 x 50 mL). The organic layers were collected, dried over $MgSO_4$ and concentrated *in vacuo* to yield **7-9** (1 g, 92% yield) without further purification: ^{1}H NMR (300 MHz, $CDCl_3$, ppm) δ 1.417 (s, 9 H), 2.552 (t, *J* = 1.8 Hz, 8 H), 2.998 (m, 3 H), 3.208 (d, *J* = 5.1 Hz, 1 H), 3.387 (s, 3 H), 4.226-4.251 (m, 1 H), 4.273-4.394 (m, 1 H), 6.846 (br s, 1 H). All data are consistent with literature values.[52]

***N*-(4-Aminobutyl)phthalimide (7-11)[49]**
Method 1
To *N*-(4-bromobutyl)phthalimide (1 g, 35 mmol) dissolved in EtOH [0.1 M] was added 10% Pd-C (350 mg). After 18 h of stirring under H_2 atmosphere at room temperature, the solution was filtered over celite and the solvent was concentrated in vacuo to yield **7-11** (894 mg, quantitative yield), as an off-white foam:
Method 2
A mixture of *N*-(4-bromobutyl)phthalimide (1 g, 35 mmol) and NaN_3 (290 mg, 44 mmol) was dissolved in DMF [3 M] and cooled to 0 °C in an ice-bath. The ice-bath was removed and the mixture was stirred at room temperature. After 5 h, the reaction was quenched with 10 mL 10% aqueous LiCl, extracted with ethyl acetate (3 x 20 mL), dried over $MgSO_4$ and concentrated to yield a crude mixture containing **7-10** and DMF (1.09 g). To the resulting crude was added 1.03 g PPh_3 dissolved in 45 mL of a 7:2 mixture of THF:water. The mixture was stirred at room temperature and the reaction was monitored via TLC. After 24 h, the reaction solvent was evaporated. The resulting crude was washed with CH_2Cl_2, ethyl acetate and then with benzene to yield **7-11** (419 mg, 77% after 2 steps) as an off-white solid containing trace amounts of TPPO:
^{1}H NMR (300 MHz, $CDCl_3$, ppm) δ 1.387 (s, 4 H), 1.477-1.493 (m, 2 H), 1.648-1.721 (m, 2 H), 3.092-3.158 (m, 1 H), 3.641-3.714 (m, 2 H), 4.634 (br s, 1 H), 7.659-7.695 (m, 2 H), 7.774-7.815 (m, 2 H). All data are consistent with literature values.[49]

2-[4-Boc-aminobutylamino]-4-aminopropargyl-6-chloro-*s*-triazine (7-12)
To cyanuric chloride (270 mg, 1.4 mmol) dissolved in THF [0.01 M] was added propargyl amine (0.99 mL, 1.4 mmol) and DIPEA (1 mL, 1.6 mmol) dissolved in THF [0.2 M]. The mixture was stirred at room temperature. As the reaction proceeded the mixture became cloudy. After 1 h, to the mixture was added *N*^{1}-Boc-butylamine (272 mg, 1.4 mmol) and DIPEA (1 mL, 1.7 mmol) dissolved in THF [0.5 M]. The mixture was stirred at room temperature and the reaction was monitored via TLC. After 1 h, the reaction solvent was evaporated. The resulting crude was

diluted with $CHCl_3$ and the resulting precipitate was collected via vacuum filtration. The filtrate was washed with $CHCl_3$ to yield **7-12** (464 mg, 89% yield after 2 steps), as an off-white solid: ^{1}H NMR (300 MHz, $CDCl_3$, ppm) δ 1.412 (s, 9 H), 2.037 (s, 2 H), 2.219 (t, *J* = 2.7 Hz, 1 H), 3.302 (m, 2 H), 3.479 (m, 2 H),4.158 (br s, 3 H), 6.452 (br s, 1 H), 9.984 (br s, 1 H).

2-[4-Boc-aminobutylamino]-4- aminopropargyl-6-(4-phthalimidobutylamino)-*s*-triazine (7-13)

To **7-12** (150 mg, 0.4 mmol) dissolved in THF [0.01 M] was added DIPEA (0.5 mL, 0.5 mmol) followed by **7-11** (80 mg, 0.8 mmol) dissolved in 1 mL THF. The mixture was stirred under reflux conditions and the reaction was monitored via TLC. After 24 h, the mixture was cooled to room temperature, the solvent was evaporated and the resulting crude was purified using flash column chromatography on silica gel (10% CH_3OH in CH_2Cl_2) to yield **7-13** (52 mg, 50 % yield) as a yellow solid: IR (υ_{max} [cm^{-1}]) 1633.52, 2054.49, 2929.15, 3287.42; ^{1}H NMR (300 MHz, DMSO-d_6, ppm) δ 1.421 (s, 9 H), 1.540-1.563 (m, 2 H), 2.766-2.815 (t, *J* = 7.8 Hz, 2 H), 2.927-2.991 (q, J_1 = 6.3 Hz, J_2 = 6.6 Hz, 2 H), 3.637 (s, 2 H), 3.755 (s, 2 H), 4.040-4.054 (d, *J* = 4.2 Hz, 2 H), 4.116-4.144 (dd, J_1 = 2.7 Hz, J_2 = 2.4 Hz, 3 H), 6.913 (m, 1 H), 8.150-8.392 (m, 4 H); FIA-MS MS (ESI) *m/z* calcd for $C_{27}H_{36}N_8O_4$ $(M+H)^+$ 537.3, found 537.1.

2-[4-Boc-aminobutylamino]-4-PEG-biotinylamino-6-Topotecan-Me-linker-4-aminobutylamino-*s*-triazine (7-14)

To **7-13** (40 mg, 0.07 mmol) dissolved in EtOH [0.1 M] was added anhydrous hydrazine (0.07 mL, 0.2 mmol). The mixture was stirred under reflux conditions and the reaction was monitored via TLC. After 16 h, the reaction was quenched with solid $NaHCO_3$. The solids were filtered and the mother liquor was evaporated. The resulting crude was purified using flash column chromatography on silica gel (10% CH_3OH in CH_2Cl_2) to yield the corresponding free-amine (20 mg, 0.05 mmol) as a yellow oil which was used in the next step without further purification. The resulting free-amine, EDC (7 mg, 0.06 mmol) and DMAP (2 mg, 0.02 mmol) was dissolved in CH_2Cl_2 [0.1 M]. To the mixture was added **7-7** (50 mg, 0.06 mmol) dissolved in CH_2Cl_2 [0.1 M]. The mixture was stirred at room temperature and the reaction was monitored via TLC. After 24 h, the mixture was purified directly using flash column chromatography on silica gel to yield **7-14** (15 mg, 35% yield), as orange-yellow oil: ^{1}H NMR (400 MHz, CD_3OD, ppm) δ 0.876-0.971 (m, 3 H), 1.179-1.418 (m, 16 H), 1.487 (d, *J* = 5.6 Hz, 2 H), 2.002 (s, 1 H), 2.146 (s, 1 H), 2.576 (t, *J* = 5.2 Hz), 2.786 (s, 4 H), 2.929 (s, 1 h), 3.052 (s, 1 H), 3.426-3.453 (m, 2H), 3.608-3.682 (m, 2 H), 3.847-3.966 (m, 2 H), 4.107-4.282 (m, 3 H), 5.576 (m, 2 H), faint peaks in aromatic region.

"Click-Ready" splitter bearing dual-warheads (7-15)

7-14 (10 mg, 0.008 mmol) was dissolved in 2 mL of a mixture of 10% TFA in CH_2Cl_2. The mixture was stirred at room temperature. After 24 h, the reaction was quenched with solid $NaHCO_3$. The solids were filtered and the mother liquor was evaporated to yield crude containing the corresponding free-amine.

4-19 (9 mg, 0.008 mmol), EDC (1.5 mg, 0.01 mmol), DMAP (1 mg, 0.008 mmol) were dissolved in CH_2Cl_2 [0.05 M]. To the mixture was added free-amine dissolved in CH_2Cl_2 [0.5 M]. The mixture was stirred at room temperature and the reaction was monitored via TLC. After 16 h, the mixture was purified directly using flash column chromatography on silica gel (10% CH_3OH in CH_2Cl_2) to yield **7-15** (10 mg, 47% after 2 steps), as a yellow/off-white solid: ^{1}H

NMR (300 MHz, CD_3OD, ppm) δ 0.890 (m, 2 H), 1.003 (t, *J* = 4.5 Hz, 3 H), 1.079 (d, *J* = 6.3 Hz, 2 H), 1.167 (m, 3 H), 1.223-1.411 (m, 62 H), 1.561-1.757 (m, 6 H), 1.911-1.974 (m, 3 H), 2.148 (s, 3 H), 2.354-2.378 (m, 3 H), 2.461-2.487 (m, 2 H), 2.541 (m, 2 H), 2.650-2.684 (m, 5 H), 2.916-2.985 (m, 6 H), 3.176-3.251 (m, 12 H), 3.403 (t, *J* = 5.1 Hz, 2 H), 3.885 (t, *J* = 5.4 Hz, 2 H), 4.024-4.203 (m, 1 H), 5.327 (m, 2 H), 5.549-5.674 (m, 1 H), 6.093-6.137 (m, 1 H), 6.442 (br s, 1 H), 6.964 (d, *J* = 7.5 Hz, 1 H), 7.251-7.321 (m, 1 H), 7.504 (t, *J* = 7.5 Hz, 1 H), 7.579-7.659 (m, 2 H), 7.785-7.810 (m, 1 H), 8.049-8.204 (m, 2 H), 8.845 (br s, 1 H).

Tumor-targeting drug-conjugate bearing dual-warheads SB-T-1214 and topotecan (DW-2)
Two 1 M solutions of; (1) **7-15** (10 mg, 0.006 mmol) with **7-1a** (3.5 mg, 0.006 mmol) and ascorbic acid (1 mg, 0.005 mmol); and (2) CuCl (0.6 mg, 0.006 mmol) in DMSO were deoxygenated and incubated in a glovebox at room temperature for 8 h. After 8 h, to the solution containing **7-15**, **7-1a** and ascorbic acid was added the solution containing CuCl. The mixture was left in the glovebox for an additional 8 h. After that period, the mixture was removed from the glovebox, the reaction mixture was diluted with water and the resulting precipitate was collected. The resulting crude was purified via flash column chromatography over silica gel (hexanes:ethyl acetate = 1:1 followed by 10% CH_3OH in CH_2Cl_2) to yield **DW-2** (8 mg, 83% yield) as a yellow/off-white solid: ^{1}H NMR (500 MHz, $CDCl_3$, ppm) δ 0.845-0.904 (m, 3 H), 0.945-1.008 (m, 5 H), 1.131 (s, 2 H), 1.162 (s, 6 H), 1.254-1.403 (m, 24 H), 1.540 (m, 6 H), 1.635-1.672 (m, 6 H), 1.723-1.775 (m, 8 H), 1.841-1.865 (m, 2 H), 1.912 (s, 4 H), 2.053 (s, 3 H), 2.079 (s, 1 H), 2.181 (s, 1 H), 2.360-2.406 (m, 8 H), 2.525-2.560 (m, 3 H), 2.654-2.700 (m, 9 H), 2.837 (s, 2 H), 2.973-3.031 (m, 12 H), 3.188 (m, 1 H), 3.307 (t, *J* = 5 Hz, 2 H), 3.362 (s, 2 H), 3.383-3.405 (m, 1 H), 3.507-3.553 (m, 3 H), 3.801 (br s, 2 H), 3.928-4.004 (m, 3 H), 4.096-4.152 (m, 4 H), 4.185-4.317 (q, J_1 = 16.5 Hz, J_2 = 49.5 Hz, 6 H), 4.423 (m, 3 H), 4.932-4.989 (m, 6 H), 5.125 (s, 4 H), 5.310 (s, 1 H), 5.678 (d, *J* = 7.5 Hz, 2 H), 6.200 (m, 3 H), 6.296 (s, 2 H), 7.298-7.312 (m, 2 H), 7.384 (t, *J* = 5 Hz, 2 H), 7.476 (t, *J* = 7.5 Hz, 2 H), 7.604 (t, *J* = 7 Hz, 2 H), 7.768-7.814 (m, 4 H), 8.023 (s, 4 H), 8.111 (m, 3 H); ^{13}C NMR (400 MHz, $CDCl_3$, ppm) δ 9.203, 9.386, 9.569, 13.035, 14.816, 18.504, 20.161, 20.334, 22.132, 22.394, 23.285, 24.341, 24.477, 25.352, 25.547, 25.802, 26.278, 26.506, 26.722, 27.820, 28.221, 28.607, 29.711, 30.565, 31.834, 35.026, 35.481, 35.594, 36.828, 38.693, 38.739, 42.602, 43.163, 44.919, 45.804, 46.697, 50.108, 58.436, 67.108, 71.631, 72.059, 74.882, 75.185, 75.554, 76.381, 79.127, 80.973, 81.183, 84.454, 113.932, 126.931, 127.684, 128.045, 128.145, 128.265, 128.344, 128.426, 128.592, 129.319, 129.609, 130.171, 131.076, 131.293, 132.523, 133.092, 133.197, 133.537, 143.287.

Attempted synthesis of IPA-Me-linker-OTIPS (7-16)
To **4-13** (100 mg, 0.2 mmol) was added DIC (0.04 mL, 0.3 mmol). The mixture was stirred at 0 °C, neat for 15 min. To the mixture was added DMAP (3 mg, 0.2 mmol) dissolved in 1 mL IPA. The mixture was stirred at 0 °C. After 4 h, the starting material was consumed. The mixture was purified directly using flash column chromatography on silica gel (hexanes:ethyl acetate = 1:1) to yield 60 mg white unknown solid. No desired product was obtained.

Attempted synthesis of isopropyl 2-(2-sulfhydrlphenyl)acetate (7-17)
To IPA (0.075 mL, 1 mmol) was added a suspension of NaH (40 mg, 0.1 mmol) in THF [0.3 M]. The mixture was stirred at 0 °C for 10 min. To the mixture was added **4-1** (75 mg, 0.5 mmol) dissolved in THF [0.3 M]. After the addition, the solution turned yellow. The mixture was stirred at room temperature and the reaction was monitored via TLC. After 4 h, no reaction was

observed on TLC. The mixture was then stirred under reflux conditions. After 2 h, no reaction was observed on TLC. The reaction was quenched with water, the pH was adjusted to 2 with 1M HCl and extracted with ethyl ether (3 x 50 mL) to yield 70 mg **4-1**. No desired product was formed.

Phenol-Me-linker-TIPS (7-18)

To **4-13** (260 mg, 0.5 mmol), phenol (54 mg, 0.6 mmol) and DMAP (21 mg, 0.1 mmol) dissolved in CH_2Cl_2 [0.1 M] was added DIC (0.1 mL, 0.6 mmol). The mixture was stirred at room temperature and the reaction was monitored via TLC. After 8 h, the reaction was quenched with aqueous NH_4Cl, extracted with CH_2Cl_2 (3 x 20 mL). The organic layers were dried over $MgSO_4$ and concentrated in vacuo. The resulting crude was purified using Yamazen automotive column chromatography to yield **7-18** (184 mg, 60% yield), as a white solid: ^{1}H NMR (300 MHz, $CDCl_3$, ppm) δ 1.132-1.181 (m, 18 H), 1.277-1.389 (m, 4 H), 1.868 (m, 1 H), 2.041 (s, 2 H), 2.329-2.383 (m, 2 H), 2.998 (m, 2 H), 3.567-3.654 (m, 3 H), 4.101 (s, 2 H), 7.041-7.118 (m, 2 H), 7.160-7.237 (m, 1 H), 7.279-7.416 (m, 4 H), 7.850 (d, J = 4.8 Hz, 1 H); ^{13}C NMR (400 MHz, $CDCl_3$, ppm) δ 12.095, 17.976, 20.753, 31.225, 33.229, 39.596, 46.327, 121.606, 121.712, 125.999, 127.859, 128.473, 129.513, 129.581, 130.431, 130.492, 131.031, 133.618, 137.883, 151.027, 169.535, 173.140; HRMS MS ES+ *m/z* calcd for $C_{28}H_{40}O_4S_2Si$ $(M+H)^+$ 533.2137, found 533.2222 (Δ 8.5 ppm).

Phenol-Me-linker-CO_2H (7-19)

To **7-18** (200 mg, 0.4 mmol) dissolved in a 1:1 mixture of CH_3CN:py [0.05 M] was added 2 mL HF:py. The mixture was stirred at room temperature and the reaction was monitored via TLC. After 24 h, the reaction was quenched with 0.2 M citric acid and extracted with CH_2Cl_2 (2 x 20 mL). The organic layer was washed with aqueous $CuSO_4$ (3 x 20 mL), then washed with brine (3 x 20 mL), dried over $MgSO_4$ and concentrated *in vacuo*. The resulting crude was purified using flash column chromatography on silica gel (hexanes:ethyl acetate = 1:1) to yield **7-19** (133 mg, 94% yield), as a white solid: ^{1}H NMR (400 MHz, $CDCl_3$, ppm) δ 1.070-1.148 (m, 4 H), 1.241-1.301 (m, 3 H), 1.848-1.991 (m, 1 H), 2.046 (s, 1 H), 2.394-2.439 (m, 1 H), 2.936-2.969 (m, 1 H), 4.067-4.150 (m, 2 H), 7.094-7.116 (m, 1 H), 7.208-7.376 (m, 4 H), 7.801 (m, 1 H); HRMS MS ES+ *m/z* calcd for $C_{19}H_{20}O_4S_2$ $(M+H)^+$ 377.0803, found 377.0883 (Δ 8.0 ppm).

Phenol-Me-linker-OSu (7-20)

To **7-19** (133 mg, 0.4 mmol) and HOSu (122 mg, 1.2 mmol) dissolved in a 4:3 solution of THF:py [0.1 M] was added DIC (0.07 mL, 0.5 mmol). The mixture was stirred at room temperature and the reaction was monitored via TLC. After 48 h, the solvent was evaporated and the resulting crude was purified using flash column chromatography on silica gel (hexanes:ethyl acetate = 1:1) to yield **7-20** (140 mg, 84% yield), as a white solid: ^{1}H NMR (400 MHz, $CDCl_3$, ppm) δ 1.070-1.148 (m, 4 H), 1.241-1.301 (m, 3 H), 1.848-1.991 (m, 1 H), 2.046 (s, 1 H), 2.394-2.439 (m, 1 H), 2.936-2.969 (m, 1 H), 4.067-4.150 (m, 2 H), 7.094-7.116 (m, 1 H), 7.208-7.376 (m, 4 H), 7.801 (m, 1 H).

***N^1*-Boc-*N^4*-Fmoc-1,4-diaminobutane (7-21)[53]**

To **7-9** (2.6 g, 14 mmol) dissolved in CH_2Cl_2 [1.0 M] was added Fmoc-OSu (5.1 g, 15 mmol) dissolved in CH_2Cl_2 [1.0 M] over a period of 4 h. After the addition, the mixture was stirred at room temperature and the reaction was monitored via TLC. After 16 h, the reaction solvent was evaporated. The resulting crude was washed with ethyl acetate to yield **7-21** (4.8 g, 85% yield),

as a white solid: ^{1}H NMR (300 MHz, DMSO-d_6, ppm) δ 1.417 (s, 9 H), 2.552 (t, *J* = 1.8 Hz, 8 H), 2.998 (m, 3 H), 3.208 (d, *J* = 5.1 Hz, 1 H), 3.387 (s, 3 H), 4.226-4.251 (m, 1 H), 4.273-4.394 (m, 1 H), 6.846 (br s, 1 H), 7.313-7.487 (m, 4 H), 7.728 (d, *J* = 5.1 Hz, 2 H), 7.927 (d, *J* = 7.5 Hz, 2 H). All data are consistent with literature values.[53]

N^1-Fmoc-1,4-diaminobutane (7-22)

7-21 (3.8 g, 9 mmol) was dissolved in a solution containing 10% TFA in CH_2Cl_2 [0.2 M]. The mixture was stirred at room temperature and the reaction was monitored via TLC using ninhydrin as a stain. After 16 h, the reaction was quenched with aqueous $NaHCO_3$ and extracted with CH_2Cl_2 (3 x 50 mL). The organic layers were combined, dried over MgSO4 and concentrated in vacuo to yield **7-22** (2.7 g, 94% yield), as a yellow solid: ^{1}H NMR (300 MHz, DMSO-d_6, ppm) δ 1.467 (s, 4 H), 2.699 (s, 1 H), 3.016 (br s, 2 H), 4.252 (d, *J* = 6.3 Hz, 1 H), 4.324 (s, 2 H), 7.352-7.489 (m, 6 H), 7.719 (d, *J* = 7.5 Hz, 2 H), 7.880-7.953 (m, 3 H).

2-[4-Boc-aminobutylamino]-4-[4-Fmoc-aminobutylamino]-6-aminopropargyl-*s*-triazine (7-23)

To a solution of cyanuric chloride (1.19 g, 6.4 mmol) dissolved in THF [0.05 M] and cooled to 0 °C was added propargyl amine (4.4 mL, 6.4 mmol) dissolved in THF [0.5 M] with DIPEA (1.5 mL, 7.6 mmol). The mixture was stirred at 0 °C for 1 h. To the mixture was then added **7-22** (2 g, 6.4 mmol) dissolved in THF [0.5 M] with DIPEA (1.5 mL, 7.6 mmol), dropwise. The mixture was stirred at room temperature. As the reaction proceeded the mixture became cloudy. After 1 h, the solvent was evaporated. The resulting crude was triturated with IPA. The resulting precipitate was washed with IPA and vacuum dried to give 1.76 g of the mono-Cl triazine, as a light-brown solid. To mono-Cl triazine (1.55 g, 3.3 mmol) dissolved in THF [0.05 M] was added **7-9** (2 g, 15 mmol) dissolved in THF [0.05 M] with DIPEA (3 mL, 3.6 mmol). The mixture was stirred under reflux conditions and monitored via TLC. After 3 h, the reaction mixture was cloudy. To the mixture was added 5 mL DMF. After the addition, the reaction mixture was cloudy. The mixture was stirred under reflux conditions. After 16 h, the reaction vessel was allowed to cool to room temperature, the reaction solvent was evaporated. The resulting crude was triturated with water and the resulting precipitate was washed with water, and then lyophilized. The resulting crude was purified using flash column chromatography (10% CH_3OH in CH_2Cl_2) to yield **7-23** (2.22 g, 55% yield after 3 steps), as a sticky dark-orange solid: ^{1}H NMR (300 MHz, $CDCl_3$, ppm) δ 1.416-1.563 (m, 32 H), 1.946-1.955 (m, 3 H), 2.217 (d, *J* = 13.2 Hz, 1 H), 2.656 (s, 3 H), 3.005-3.081 (m, 5 H), 3.322 (m, 3 H), 3.410-3.481 (m, 1 H), 4.127 (br s, 1 H), 5.100 (s, 1 H), 5.406 (m, 1 H), 7.535 (d, *J* = 6 Hz, 1 H), 7.644-7.741 (m, 2 H).

2-[4-Boc-aminobutylamino]-4-[4-Fmoc-aminobutylamino]-6-biotinylamino-PEG-*s*-triazine (7-24)

Two 1 M solutions of: (1) **7-23** (182 mg, 0.3 mmol) with **7-1a** (136 mg, 0.3 mmol) in DMSO; (2) and CuBr (53 mg, 0.3 mmol) in DMSO were deoxygenated and incubated in a glovebox at room temperature for 8 h. After 8 h, to the solution containing **7-23** and **7-1a** was added deoxygenated bathophenanthroline sulfate (387 mg, 0.9 mmol), followed by the addition of the solution containing CuBr. The mixture was left in the glovebox for an additional 8 h. After that period, the mixture was removed from the glovebox, the reaction mixture was diluted with water. The resulting precipitate was collected and washed with water, then with CH_2Cl_2 and ethyl acetate. The organic layers were combined and evaporated to yield **7-24** (114 mg, 37% yield), as a waxy

orange solid: ^{1}H NMR (400 MHz, CD_3OD, ppm) δ 2.106-2.372 (m, 38 H), 2.844-2.901 (m, 3 H), 3.566-3.602 (m, 2 H), 3.694 (s, 1 H), 3.731 (m, 3 H), 3.831-3.861 (m, 2 H), 4.189-4.246 (m, 12 H), 4.342 (s, 1 H), 4.540 (br s, 2 H), 4.945-4.976 (m, 1 H), 5.146 (m, 1 H), 5.218-5.263 (m, 6 H), 8.004-8.043 (m, 4 H), 8.237 (t, *J* = 7.2 Hz, 1 H), 8.284 (d, *J* = 7.2 Hz, 1 H), 8.340 (d, *J* = 7.2 Hz, 1 H), 8.590 (br s, 1 H); ^{13}C NMR (400 MHz, CD_3OD, ppm) δ 25.641, 27.037, 27.637, 28.289, 28.578, 35.552, 39.255, 39.240, 39.854, 50.198, 55.798, 60.404, 62.172, 69.207, 69.397, 70.049, 70.262, 78.647, 94.629, 119.610, 120.566, 123.814, 129.149, 133.960, 135.121, 144.630, 157.310, 164.846, 166.022, 174.847, 194.297.

2-[4-Boc-aminobutylamino]-4-Phenol-Me-linker-6-biotinylamino-PEG-*s*-triazine (7-25)

7-24 (50 mg, 0.04 mmol) was dissolved in a solution containing 20% piperidine in DMF [0.02 M]. The mixture was stirred at room temperature and the reaction was monitored via TLC using ninhydrin as a stain. After 2 h, the reaction mixture was quenched with aqueous $NaHCO_3$ and extracted with CH_2Cl_2 (3 x 10 mL). The organic layers were combined, dried over $MgSO_4$ and concentrated *in vacuo*. The resulting crude dissolved in CH_2Cl_2 and filtered through cotton. The organic solvent was evaporated to yield crude containing the corresponding free-amine of **7-24**. To the resulting free-amine was added **7-20** (25 mg, 0.04 mmol) dissolved in DMF [0.2 M], followed by the addition of DIPEA (0.05 mL, 0.04 mmol). The mixture was stirred at room temperature and the reaction was monitored via TLC. After 36 h, the reaction solvent was evaporated and the resulting crude was purified using flash column chromatography on silica gel (hexanes:ethyl acetate = 1:1) to yield **7-25** (35 mg, 62% yield), as an orange oil: ^{1}H NMR (500 MHz, CD_3OD, ppm) δ 0.847-0.978 (m, 2 H), 1.109 (d, *J* = 6.5 Hz, 1 H), 1.250-1.340 (m, 6 H), 1.445-1.590 (m, 8 H), 1.639-1.687 (m, 8 H), 1.786-1.892 (m, 3 H), 2.322-2.438 (m, 3 H), 2.913-2.969 (m, 2 H), 3.063 (m, 1 H), 3.136 (t, *J* = 6 Hz, 1 H), 3.321-3.381 (m, 3 H), 3.477-3.526 (m, 4 H), 3.590 (t, *J* = 6 Hz, 1 H), 3.638 (m, 1 H), 3.787 (m, 1 H), 3.902 (s, 1 H), 3.966 (s, 1 H), 4.145-4.187 (q, J_1 = 7 Hz, J_2 = 7.5 Hz, 2 H), 6.682 (t, *J* = 9 Hz, 1 H), 6.957-6.999 (q, J_1 = 3 Hz, J_2 = 9 Hz, 1 H), 7.025-7.065 (q, J_1 = 3 Hz, J_2 = 9 Hz, 1 H), 7.110-7.331 (m, 5 H), 7.355-7.444 (m, 1 H), 7.782 (d, *J* = 8.5 Hz, 2 H).

Drug conjugate bearing one warhead and one dummy molecule general procedure (DW-3, DW-4a and DW-4b)

7-25 was dissolved in a solution containing 10% TFA in CH_2Cl_2. The mixture was stirred at room temperature and the reaction was monitored via TLC using ninhydrin as a stain. After 8 to 16 h, to the reaction was added solid $NaHCO_3$. The organic solvent was filtered through cotton, collected and concentrated *in vacuo* to yield crude containing corresponding free-amine of **7-25**. To the resulting free-amine was added 1.2 equivalents of Drug-Me-linker-OSu dissolved in a 2:1 solution of CH_2Cl_2:py. The mixture was stirred at room temperature and the reaction was monitored via TLC. After 24 to 48 h, the reaction solvent was evaporated and the resulting crude was purified using flash column chromatography on silica gel (hexanes:ethyl acetate = 1:1, followed by 10% CH_3OH in CH_2Cl_2) to yield **DW-3 and DW-4b**:

7-25 (15 mg, 0.01 mmol), **4-20** (15 mg, 0.01 mmol) to yield **DW-3** (21 mg, 73% yield after 2 steps), as an off-white solid: ^{1}H NMR (400 MHz, $CDCl_3$, ppm) δ 0.830-0.864 (m, 3 H), 0.950 (m, 4 H), 1.090-1.106 (m, 9 H), 1.217-1.329 (m, 30 H), 1.377-1.419 (m, 3 H), 1.471-1.527 (m, 9 H), 1.571-1.609 (m, 8 H), 1.628 (s, 4 H), 1.678 (m, 9 H), 1.797-2.041 (m, 20 H), 2.294-2.349 (m, 10 H), 2.380 (br s, 1 H), 2.496 (m, 1 H), 2.619-2.647 (m, 2 H), 2.796 (s, 2 H), 2.891-2.962 (m, 2 H), 3.272 (t, *J* = 5.6 Hz, 3 H), 3.319-3.349 (m, 3 H), 3.449 (s, 2 H), 3.471 (t, *J* = 5.2 Hz, 3 H),

3.559 (t, *J* = 4.8 Hz, 2 H), 3.612 (d, *J* = 4 Hz, 1 H), 3.758 (d, *J* = 6.4 Hz, 1 H), 3.870 (s, 2 H), 3.911-3969 (m, 1 H), 4.053 (m, 1 H), 4.141 (dd, J_1 = 10.2 Hz, J_2 = 8 Hz, 2 H), 4.380 (m, 1 H), 4.820 (m, 1 H), 4.887-4.949 (m, 3 H), 5.083 (m, 1 H), 5.630 (d, *J* = 7.2 Hz, 1 H), 6.147 (m, 1 H), 6.251 (s, 1 H), 7.155-7.196 (m, 6 H), 7.245 (m, 1 H), 7.439 (t, *J* = 8 Hz, 2 H), 7.571 (t, *J* = 5.6 Hz, 1 H), 7.711-7.774 (m, 2 H), 8.071 (d, *J* = 7.2 Hz, 2 H); ^{13}C NMR (400 MHz, $CDCl_3$, ppm) δ 9.499, 9.757, 13.203, 14.978, 18.674, 20.556, 21.171, 22.590, 24.677, 24.730, 25.739, 25.891, 26.483, 26.703, 26.870, 28.418, 29.495, 30.497, 30.861, 31.286, 35.718, 38.602, 38.943, 42.942, 43.231, 43.382, 45.849, 46.759, 46.881, 47.397, 58.658, 72.272, 75.186, 79.428, 81.189, 84.710, 86.911, 94.628, 120.156, 127.623, 127.828, 128.815, 129.217, 129.551, 129.801, 130.006, 130.310, 130.370, 132.685, 133.770, 135.713, 136.737, 137.390, 143.605, 155.170, 167.145, 168.336, 169.049, 169.262, 169.421, 169.839, 170.142, 170.636, 171.592, 175.257, 204.306, 210.976.

7-25 (10 mg, 0.01 mmol), **7-7** (10 mg, 0.01 mmol), EDC (2 mg, 0.012 mmol), DMAP (1 mg, 0.01 mmol), CH_2Cl_2 [0.05 M], r.t., 16 h; **DW-4a** was not observed.

7-25 (10 mg, 0.01 mmol), **7-8** (10 mg, 0.01 mmol); **DW-4a** was not observed.

7-25 (10 mg, 0.01 mmol), **4-23b** (10 mg, 0.01 mmol) to yield **DW-4b** (10 mg, 53% yield after 2 steps), as an off-white/yellow solid: ^{1}H NMR (400 MHz, $CDCl_3$, ppm) δ 0.888-0.914 (m, 2 H), 0.969-1.024 (m, 4 H), 1.070 (t, J = 6 Hz, 1 H), 1.170-1.215 (m, 10 H), 1.264-1.367 (m, 21 H), 1.420-1.643 (m, 22 H), 1.890-1.978 (m, 5 H), 2.183-2.251 (m, 2 H), 2.320-2.396 (m, 4 H), 2.516-2.594 (m, 3 H), 2.716 (s, 12 H), 2.839-2.983 (m, 15 H), 3.315-3.336 (m, 4 H), 3.371 (s, 8 H), 3.525 (m, 4 H), 3.613 (m, 4 H), 3.666-3.808 (m, 5 H), 3.925 (s, 3 H), 4.120-4.175 (m, 4 H), 5.136 (s, 2 H), 5.303-5.423 (m, 3 H), 5.635 (d, *J* = 14 Hz, 1 H), 5.758 (d, *J* = 14 Hz, 1 H), 7.236 (s, 5 H), 7.686-7.778 (m, 3 H), 7.842-7.901 (m, 1 H), 7.959-7.976 (m, 1 H), 8.265-8.300 (m, 1 H), 8.411-8.428 (m, 1 H), 8.637 (br s, 1 H).

Cell culture system for MTT assay

Cell lines (obtained from ATCC unless otherwise noted and maintained at SBU Cell Culture/Hybridoma Facility) were cultured in RPMI-1640 with L-glutamine (Lonza BioWhittaker, BW12-702F: A2780, DLD-1, ID-8, LCC6 MDR, LCC6 wt, MCF-7), DMEM (Lonza BioWhittaker, BW12-604F: BT-20, CFPac-1, MDA MB 231, Panc-1) or McCoy's 5A (Gibco #16600: HT-29, SkBr3) supplemented with 5% FBS (Thermo Scientific, HyClone, SH3007003), 5% Nu Serum (BD Biosciences, 355100) and 1% Penn Strip, at 37 °C in a humidified incubator with 5% CO_2. Cell lines treated with drug conjugate **DW-1** were cultured in RPMI-1640 Medium 10 x (Sigma Aldrich, R1145) supplemented with tissue culture grade water, 0.3 g/L L-glutamine, 2.0 g/L sodium bicarbonate, 10% FBS, and 1% Penn Strep. The cells were washed with DPBS and dissociated using TrypLE. The cells were incubated at 37 °C until the cells were detached from the plate, transferred to a centrifuge vial and pelleted via centrifugation at 1500 rpm for 5 min. The cells were counted per 1 mL media. The desired amount of cell media was added to the cell solution so that 8,000 cells can added to each well of a 96-well plate in 200 μL aliquots. After the addition, the cells were incubated at 37 °C with 5% CO_2.

Single drug MTT assay

A serial dilution of the drug compound (SB-T-1214 or topotecan) dissolved in sterile DMSO was added using fully-supplemented RPMI. The residual medium in each well was aspirated and 100 μL of the different drug-concentration solutions were added to each well of every column of the

96-well plate. After the addition of the drug solution, the cells were incubated at 37 °C for 48 hours. After the incubation period, the media was aspirated and the cells were washed with DPBS. To the washed cells 0.5 μL of a solution of 5 mg MTT (3-(4,5-dimethylthiazol-2-yl)-2,5-diphenyltetrazolium bromide) per 10 mL color-less media or DPBS were added. The cells were then incubated at 37 °C for 3 hours. After the incubation period, the MTT solution was aspirated and the remaining crystals were washed with DPBS. The crystals were dissolved using a 0.5 μL of 0.4 M HCl in isopropanol. The plates were shaken for 10 minutes to assure that all of the crystals are dissolved. The optical density was determined from the resulting solutions using the Acsent Multiskan optical density reader.

Simultaneous drug treatment MTT assay

Cells were resuspended in 200 μL medium with approximately 8000 to 10,000 cells per well of a 96-well plate and incubated at 37 °C with 5% CO_2 for 24 hours before drug treatment. A serial dilution of a 1-to-1 mixture of SB-T-1214 and topotecan dissolved in sterile DMSO was added using media. The residual media in each well were aspirated and the different drug solutions were added to each well of every column of the 96-well plate. After the addition of the drug solution, the cells were incubated at 37 °C for 48 hours. After the incubation period, the media was aspirated and the cells were washed with DPBS. To the washed cells 0.5 μL of a solution of 5 mg MTT per 10 mL color-less media or DPBS were added. The cells were then incubated at 37 °C for 3 hours. After the incubation period, the MTT solution was aspirated and the remaining crystals were washed with DPBS. The crystals were dissolved using a 0.5 μL of 0.4 M HCl in isopropanol. The plates were shaken for 10 minutes to assure that all of the crystals are dissolved. The optical density was determined from the resulting solutions using the Acsent Multiskan optical density reader.

Sequential drug treatment MTT assay

Cells were resuspended in 200 μL medium with approximately 8000 to 10,000 cells per well of a 96-well plate and incubated at 37 °C with 5% CO_2 for 24 hours before drug treatment. Two sets of serial dilutions of SB-T-1214 and topotecan dissolved in sterile DMSO were added using media. The residual media in each well were aspirated and the different drug solutions were added to each well of every column of the 96-well plate. After the addition of the first drug solution, the cells were incubated at 37 °C for 24 hours. After the incubation period, the second drug solution was added followed by an additional 24 hour incubation period at 37 °C. After the second incubation period, the media was aspirated and the cells were washed with DPBS. To the washed cells 0.5 μL of a solution of 5 mg MTT per 10 mL color-less media or DPBS were added. The cells were then incubated at 37 °C for 3 hours. After the incubation period, the MTT solution was aspirated and the remaining crystals were washed with DPBS. The crystals were dissolved using a 0.5 μL of 0.4 M HCl in isopropanol. The plates were shaken for 10 minutes to assure that all of the crystals are dissolved. The optical density was determined from the resulting solutions using the Acsent Multiskan optical density reader. Each experiment was run in triplicate.

Drug conjugate MTT assay

A serial dilution of **DW-2, DW-3** and **DW-4b** dissolved in sterile DMSO was prepared by the addition of fully-supplemented RPMI-1640 Medium 10 x. The residual medium in each well was aspirated and the different drug-concentration solutions were added to each well of every column

of the 96-well plate in 100 μL aliquots. After the addition of the drug solution, the cells were incubated at 37 °C for 48 or 72 hour periods. After the incubation period, the medium was aspirated and the cells were washed with DPBS and then 40 μL of 0.5 mg/mL MTT in DPBS was added to each well. The cells were then incubated at 37 °C for 3 hours. After the incubation period, the MTT solution was aspirated and the remaining crystals were dissolved using a 40 μL of 0.4 M HCl in isopropanol. The plates were shaken for 10 minutes to assure that all of the crystals are dissolved. The optical density was determined from the resulting solutions using the Acsent Multiskan optical density reader. Each experiment was run in triplicate.

For cells treated with GSH-OEt: After the addition of the drug solution, the cells were incubated at 37 °C for 24 hours. The washed cells were resuspended in 100 μL fully-supplemented RPMI-1640 Medium 10 x containing 6 equivalents of GSH-OEt dissolved in RPMI-1640 Medium 10 x. After the addition of GSH-OEt, the cells were incubated at 37 °C for 48 hours. After the incubation period, the medium was aspirated and the cells were washed with DPBS and then 40 μL of 0.5 mg/mL MTT in DPBS was added to each well. The cells were then incubated at 37 °C for 3 hours. After the incubation period, the MTT solution was aspirated and the remaining crystals were dissolved using a 40 μL of 0.4 M HCl in isopropanol. The plates were shaken for 10 minutes to assure that all of the crystals are dissolved. The optical density was determined from the resulting solutions using the Acsent Multiskan optical density reader. Each experiment was run in triplicate.

Data analysis for MTT assay

The optical density data was used to calculate IC_{50} values for each drug on a given cell line using the Hill slope equation. The optical density values obtained from each concentration of drug solution were divided by the optical density value obtained from the cells with zero drug concentration. Using SigmaPlot v.10, the ratios were plotted versus the drug concentration and the IC_{50} values were calculated from the plot using the pre-programmed calculation within the SigmaPlot program.

Cell culture system for PEGylated vitamin-FITC conjugate internalization

Cells were resuspended in RPMI-1640 Medium 10 x (Sigma Aldrich, R1145) supplemented with tissue culture grade water, 0.3 g/L L-glutamine, 2.0 g/L sodium bicarbonate, 10% FBS, and 1% Penn Strep., and incubated at 37 °C in a humidified 5% CO_2 incubator for 2 to 3 days. The cells were washed with DPBS and dissociated using TrypLE. The cells were allowed to sit at room temperature until the cells were detached from the plate, transferred to a centrifuge vial and pelleted via centrifugation at 1500 rpm for 5 min. Media was added to the pellet and the pellet was disrupted. The cells were counted per 1 mL. The desired amount of media was added so that 50,000 cells could be added to each well of a 6-well plate. After the addition, the cells were resuspended fully-supplemented RPMI-1640 Medium 10 x and incubated at 37 °C for 1 day. After the incubation period, the cells will be treated with 10 μM **7-3a** or **7-3b** and incubated for 1 and 3 hour time periods. After this incubation period, the media was aspirated, the cells were washed with DPBS (2 times) and then dissociated using Hank's Enzyme Free Dissociation Solution. The dissociated cells were transferred to a centrifuge tube and pelleted via centrifugation at 1500 rpm for 5 min. The resulting pellet was washed twice with DPBS (10 mL then 1 mL). After the final wash, internalization was monitored using FACS and CFM. For CFM analysis, cells resuspended onto uncoated glass-bottomed culture dishes (MatTek Corp.).

Flow cytometry analysis of treated cells was performed with a FACSCalibur flow cytometer (SBU Medical Center Core facility laboratory), operating at a 488 nm excitation wavelength and detecting emission wavelengths with a 530/30 nm bandpass filter. Cell samples suspended in 2% formulin in DPBS were count with a minimal 10,000 cells per sample using CellQuest 3.3 software (Becton Dickinson) and the distribution of FITC fluorescence was analyzed using WinMDI 2.9 freeware (Joseph Trotter, Scripps Research Institute).
Confocal fluorescence microscopy (CFM) experiments were performed using a Zeiss LSM 510 META NLO two-photon laser scanning confocal microscope system, operating at a 488 nm excitation wavelength using a 505-550 nm bandpass filter. Images were captured using a C-Apochromat 63x/1.2 water (corr.) objective or a Plan-Apochromat 100x/1.45 oil objective. Acquired data were analyzed using LSM 510 META software.

§ 7.5.0 References

1. Creemers, G. J.; Bolis, G.; Gore, M.; Scarfone, G.; Lacave, A. J.; Guastalla, J. P.; Despax, R.; Kreinberg, R.; Van Belle, S.; Hudson, I.; Verweij, J.; ten Bokkel Huinink, W. W. Topotecan, an active drug in the second-line treatment of epithelial ovarian cancer: results of a large European phase II study. *J. Clin. Oncol.* **1996,** 12, 3056-3061.
2. ten Bokkel Huinink, W. W.; Gore, M.; Carmichael, J.; Gordon, A.; Malfetano, J.; Hudson, I.; Broom, C.; Scarabelli, C.; Davidson, N.; Spanczynski, M.; Bolis, G.; Malmström, H.; Coleman, R.; Fields, S. C.; Heron, J. F. Topotecan versus paclitaxel for the treatment of recurrent epithelial ovarian cancer. *J. Clin. Oncol.* **1997,** 15, 2183-2193.
3. Kudelka, A. P.; Tresukosol, D.; Edwards, C. L.; Freedman, R. S.; Levenback, C.; Chantarawiroj, P.; De Leon, C. G.; Kim, E. E.; Madden, T.; Wallin, B.; Hord, M.; Verschraegen, C.; Raber, M.; Kavanagh, J. J. Pase II study of intravenous topotecan as a 5-day infusion for refractory epithelial ovarian carcinoma. *J. Clin. Oncol.* **1996,** 14, 1552-1557.
4. Swisher, E. M.; Mutch, D. G.; Rader, J. S.; Elbendary, A.; Herzog, T. J. Topotecan in platinum-and paclitaxel resistant ovarian cancer. *Gynecol. Oncol.* **1997,** 66, 480-486.
5. Hoskins, P.; Eisenhauer, E.; Beare, S.; Roy, M.; Drouin, P.; Stuart, G.; Bryson, P.; Grimshaw, R.; Capstick, V.; Zee, B. Randomized phase II study of two schedules of topotecan in previously treated patients with ovarian cancer: a National Cancer Institute of Canada Clinical Trials Group Study. *J. Clin. Oncol.* **1998,** 16, 2233-2237.
6. Bookman, M. A.; Malmström, H.; Bolis, G.; Gordon, A.; Lissoni, A.; Krebs, J. B.; Fields, S. Z. Topotecan for the treatment of advanced epithelial ovarian cancer: an open label phase II study in patients treated after prior chemotherapy that contained cisplatin or carboplatin and paclitaxel. *J. Clin. Oncol.* **1998,** 16, 3345-3352.
7. McGuire, W. P.; Blessing, J. A.; Bookman, M. A.; Lentz, S. S.; Dunton, C. J. Topotecan has substantial antitumor activity as first-line salvage therapy in platinum-sensitive epithelial ovarian carcinoma: a Gynecologic Oncology Group Study. *J. Clin. Oncol.* **2000,** 18, 1062-1067.
8. Levy, T.; Inbar, M.; Menczer, J.; Grisaru, D.; Glezerman, M.; Safra, T. Phase II study of weekly topotecan in patients with recurrent or persistent epithelial ovarian cancer. *Gynecol. Oncol.* **2004,** 95, 686-690.
9. O'Brien, M.; Eckardt, J.; Ramlau, R. Recent Advances with Topotecan in the Treatment of Lung Cancer. *The Oncologist* **2007,** 12, 1194-1204.

10. Staker, B. L.; Hjerrild, K.; Feese, M. D.; Behnke, C. A.; Burgin Jr., A. B.; Stewart, L. The mechanism of topoisomerase I poisoning by a camptothecin analog. *Proc. Natl. Acad. Sci. U.S.A.* **2002,** 99, 15387-15392.
11. Murren, J. R.; Peccerillo, K.; DiStasio, S. A.; Li, X.; Leffert, J. J.; Pizzorno, G.; Burtness, B. A.; McKeon, A.; Cheng, Y.-c. Dose escalation and pharamacokinetic study of irinotecan in combination with paclitaxel in patients with advanced cancer. *Cancer Chemother. Pharmacol.* **2000,** 45, 43-50.
12. Madden, T.; Newman, R. A.; Antoun, G.; Johansen, M. J.; Ali-Osman, F. Low-level taxane exposure increases the activity of topoisomerase I targeted agents. *Proc. Am. Assoc. Cancer Res.* **1998,** 39, 527.
13. Adjei, A. A.; Argiris, A.; Murren, J. R. Docetaxel and irinotecan, alone and in combination, in the treatment of non-small cell lung cancer. *Semin. Oncol.* **1999,** 26 (5 Suppl 16), discussion 41-42.
14. Govindan, R.; Read, W.; Faust, J.; Trinkaus, K.; Ma, M. K.; Baker, S. D.; McLeod, H. L.; Perry, M. C. Phase II study of docetaxel and irinotecan in metastatic or recurrent esophageal cancer: a preliminary report. *Oncology (Williston Park)* **2003,** 17 (9 Suppl 8), 27-31.
15. Hecht, J. R.; Blanke, C. D.; Benson III, A.; Lenz, H. J. Irinotecan and paclitaxel in metastatic adenocarcinoma of the esophagus and gastric cardia. *Oncology (Williston Park)* **2003,** 17 (9 Suppl 8), 13-15.
16. Frasci, G.; Panza, N.; Comella, P.; Carteni, G.; Guida, T.; Nicolella, G. P.; Natale, M.; Lombardi, R.; Apicella, A.; Pacilio, C.; Gravina, A.; Lapenta, L.; Comelia, G. Cisplatin-topotecan-paclitaxel weekly administration with G-CSF support for ovarian and small-cell lung cancer patients: A dose-finding study *Ann. Oncol.* **1999,** 10, 355-358.
17. Stathopoulos, G. P.; Malamos, N. A.; Aravantinos, G.; Rigatos, S.; Christodoulou, C.; Stathopoulos, J.; Skarlos, D. Weekly administration of topotecan–paclitaxel as second-line treatment in ovarian cancer *Cancer Chemother. Pharmacol.* **2007,** 60, 123-128.
18. Stathopoulos, G. P.; Christodoulou, C.; Stathopoulos, J.; Skarlos, D.; Rigatos, S.; Giannakakis, T.; Armenaki, O.; Antoniou, D.; Athanasiadis, A.; Giamboudakis, P.; Dimitroulis, J.; Georgatou, N.; Katis, K. Second-line chemotherapy in small cell lung cancer in a modified administration of topotecan combined with paclitaxel: a phase II study *Cancer Chemother. Pharmacol.* **2006,** 57, 796-800.
19. Morgensztern, D.; Perry, M. C.; Govindan, R. A phase II study of topotecan and docetaxel in patients with sensitive relapse small cell lung cancer. *Acta Oncologica* **2008,** 47, 152-153.
20. Aaron, J. J.; Trajkovska, S. Fluorescence Studies of Anti-Cancer Drugs - Analytical and Biomedical Applications. *Curr. Drug Targets* **2006,** 7, 1067-1081.
21. Burke, T. G.; Mishra, A. K.; Wani, M. C.; Wall, M. E. Lipid bilayer partitioning and stability of camptothecin drugs. *Biochemistry* **1993,** 32, 5352-5364.
22. Mi, Z.; Malak, H.; Burke, T. G. Reduced Albumin Binding Promotes the Stability and Activity of Topotecan in Human Blood. *Biochemistry* **1995,** 34, 13722-13728.
23. Burke, T. G.; Malak, H.; Gryczynski, I.; Mi, Z.; Lakowicz, J. R. Fluorescence Detection of the Anticancer Drug Topotecan in Plasma and Whole Blood by Two-Photon Excitation. *Anal. Biochem.* **1996,** 242, 266-270.
24. Brangi, M.; Litman, T.; Ciotti, M.; Nishiyama, K.; Kohlhagen, G.; Takimoto, C.; Robey, R.; Pommier, Y.; Fojo, T.; Bates, S. E. Camptothecin resistance: Role of the ATP-binding

cassetter (ABC), mitoxantrone-resistance half-transporter (MXR), and potential for glucuronidation in MXR-expressing cells. *Cancer Res.* **1999,** 59, 5938-5946.
25. Kaufmann, S. H.; Peereboom, D.; Buckwalter, C. A.; Svingen, P. A.; Grochow, L. B.; Donehower, R. C.; Rowinsky, E. K. Cytotoxic effects of topotecan combined with various anticancer agents in human cancer cell lines. *J. Natl. Cancer Inst.* **1996,** 88, 734-741.
26. Kano, Y.; Akutsu, M.; Tsunoda, S.; Mori, K.; Suzuki, K.; Adachi, K. I. *In vitro* schedule-dependent interaction between paclitaxel and SN-38 (the active metabolite or irinotecan) in human carcinoma cell lines. *Cancer Chemother. Pharmacol.* **1998,** 42, 91-98.
27. Russell-Jones, G., McTavish, Kirsten, McEwan, John, Rice, John, Nowotnik, David. Vitamin-mediated targeting as a potential mechanism to increase drug uptake by tumours. *J. of Inorg. Biochem.* **2004,** 98, 1625-1633.
28. Chen, S.; Zhao, X.; Chen, J.; Chen, J.; Kuznetsova, L.; Wong, S. S.; Ojima, I. Mechanism-based tumor-targeting drug delivery system. Validation of efficient vitamin receptor-mediated endocytosis and drug release. *Bioconjugate Chem.* **2010,** 21, 979-987.
29. Ojima, I. Guided Molecular Missiles for Tumor-Targeting Chemotherapy-Case Studies Using the Second-Generation Taxoid as Warheads. *Acc. Chem. Res.* **2008,** 41, 108-119.
30. Chen, J., Chen, S., Zhao, X., Kuznetsova, L., Wong, S.S., Ojima, I. Functionalized Single-walled Carbon Nanotubes as Rationally Designed Vehicles for Tumor-Targeted Drug Delivery. *J. Am. Chem. Soc.* **2008,** 130, 16778-16785.
31. Ojima, I. Tumor-targeting drug delivery of chemotherapeutic agents. *Pure Appl. Chem.* **2011,** 83, 1685-1698.
32. Ojima, I.; Zuniga, E. S.; Berger, W. T.; Seitz, J. D. Tumor-targeting drug delivery of new-genreation taxoids. *Future Med. Chem.* **2012,** 4, 33-50.
33. Chen, S., Zhao, X., Chen, J., Chen, J., Kuznetsova, L., Wong, S.S., Ojima, I. Mechanism-based tumor-targeting drug delivery system. Validation of efficient vitamin receptor-mediated endocytosis and drug release. *Bioconjugate Chem.* **2010,** 21, 979-987.
34. Leamon, C. P.; Reddy, J. A. Folate-targeted chemotherapy. *Adv. Drug Delivery Rev.* **2004,** 56, 1127-1141.
35. Y., L.; Low, P. S. Folate-mediated delivery of macromolecular anticancer therapeutic agents. *Adv. Drug Delivery Rev.* **2002,** 54, 675-693.
36. Lee, J. W.; Lu, J. Y.; Low, P. S.; Fuchs, P. L. Synthesis and evaluation of taxol-folic acid conjugates as targeted antineoplastics. *Bioorg. & Med. Chem.* **2002,** 10, 2397-2414.
37. Xia, W.; Low, P. S. Folate-targeted therapies for cancer. *J. Med. Chem.* **2010,** 53, 6811-6824.
38. Reddy, J. A.; Leamon, C. P. Folate receptor targeted cancer chemotherapy. In *Targeted Drug Strategies for Cancer and Inflammation*, Jackman, A. L.; Leamon, C. P., Eds. Springer Science+Buisness Media, LLC: 2011; pp 135-150.
39. Fusz, S.; Srivatsan, S. G.; Ackermann, D. A.; Famulok, M. Photocleavable initiator nucleotide substrates for an aldolase ribozyme. *J. Org. Chem.* **2008,** 73, 5069-5077.
40. Wani, M. C.; Nicholas, A. W.; Wall, M. E. Plant antitumor agents. 23. Synthesis and antileukemic activity of camptothecin analogs. *J. Med. Chem.* **1986,** 29, 2358-2363.
41. Li, Q.-Y.; Zu, Y.-G.; Shi, R.-Z.; Yao, L.-P. Review Camptothecin: Current Perspectives. *Curr. Med. Chem.* **2006,** 13, 1-19.
42. Kingsbury, W. D.; Boehm, J. C.; Jakas, D. R.; Holden, K. G.; Hecht, S. M.; Gallagher, G.; Caranfa, M. J.; McCabe, F. L.; Faucette, L. F.; Johnson, R. K.; Hertzberg, R. P. Synthesis of

Water-Soluble (Aminoalkyl)camptothecin Analogues: Inhibition of Topoisomerase I and Antitumor Activity. *J. Med. Chem.* **1991,** 34, 98-107.
43. Curran, D. P. Towards new anticancer drugs: a decade of advances in synthesis of camptothecins and related alkaloids. *Tetrahedron* **2003,** 59, 8649-8687.
44. Puri, S. C.; Handa, G.; Dhar, K. L.; Suri, O. P.; Qazi, G. N. Process for preparing topotecan from 10-hydroxy-4-(*S*) camptothecin. 2003.
45. Sekhar, N. M.; Anjaneyulu, Y.; Acharyulu, P. V. R. Synthesis of 10-Hydroxycamptothecin: Evaluation of New Moderators for the Chemoselective Reduction of Camptothecin. *Synth. Comm.* **2011,** 41, 2828-2834.
46. Wood, J. L.; Fortunak, J. M.; Mastrocola, A. R.; Mellinger, M.; Burk, P. L. An efficient conversion of camptothecin to 10-hydroxycamptothecin. *J. Org. Chem.* **1995,** 60, 5739-5740.
47. Sawada, S.; Yokokura, T.; Miyasaka, T. Synthesis of CPT-11 (irinotecan hydrochloride trihydrate). *Ann. N. Y. Acad. Sci.* **1996,** 803, 13-28.
48. Okuno, S.; Harada, M.; Yano, T.; Yano, S.; Kiuchi, S.; Tsuda, N.; Sakamura, Y.; Imai, J.; Kawaguchi, T.; Tsujihara, K. Complete Regression of Xenografted Human Carcinomas by Camptothecin Analogue-Carboxymethyl Dextran Conjugate (T-0128). *Cancer Res.* **2000,** 60, 2988-2995.
49. Varghese, S.; Gupta, D.; Baran, T.; Jimjit, A.; Gore, S. D.; Casero Jr., R. A.; Woster, P. M. Alkyl-substituted polyaminohydroxamic acids: a novel class of histone deacetylase inhibitors. *J. Med. Chem.* **2005,** 48, 6350-6365.
50. Campbell, J. R.; Hatton, R. E. Unsymmetrically Substituted Melamines. *J. Org. Chem.* **1961,** 26, 2786-2789.
51. Gottlieb, H. E.; Kotlyar, V.; Nudelman, A. NMR Chemical Shifts of Common Laboratory Solvents as Trace Impurities. *J. Org. Chem.* **1997,** 62, 7512-7515.
52. Callahan, J. F.; Ashton-Shue, D.; Bryan, H. G.; Bryan, W. M.; Heckman, G. D.; Kinter, L. B.; McDonald, J. E.; Moore, M. L.; Schmidt, D. B. Structure-activity relationships of novel vasopressin antagonists containing C-terminal diaminoalkanes and (aminoalkyl)guanidines. *J. Med. Chem.* **1989,** 32, 391-396.
53. Dong, Y.; Le Quesne, P. W. Total synthesis of magnolamide. *Heterocycles* **2002,** 56, 221-225.

Chapter 8

Design, Synthesis and Biological Evaluation of Novel Tumor-Targeting Drug Conjugates with Dual-Guiding Modules and Dual-Warheads. 3. Drug Conjugate with Biotin and Folic Acid and Other Applications.

Chapter Contents

§ 8.1.0 Introduction

§ 8.1.1 Other Small-Molecule Splitter Module Applications

As discussed in chapters 6 and 7, it was shown that multiple warheads can be conjugated to a single tumor-targeting module (TTM) via a small-molecular splitter module. These drug conjugates were designed to deliver multiple cytotoxic warheads specifically to tumor cells through a single molecule. Derivatives of 1-aminobenzene-3,5-dicarboxylic acid and cyanuric chloride allow selective functionalization to bear multiple branches. For example, cyanuric chloride has been used in the development of dendrimeric drug delivery vehicles with a large number of cytotoxic, solubilizing and imaging agents.[1-4] These drug delivery systems solubilize a payload of paclitaxel and have been shown to deliver acute toxicity *in vivo*. A promising approach along these lines is to develop drug conjugates with any combination of TTMs, warheads and imaging agents.

§ 8.1.2 Taxoid-Based Drug Conjugate Bearing Dual-Vitamins

Tumors are heterogeneous masses of cells where each tumor cell is substantially different from another. As such, individual tumor cells require different levels of vitamins and nutrients to maintain their growth. Therefore, the relative level of vitamin receptor overexpression differs from cell to cell in the tumor, i.e. the number of biotin receptors on one cell is different from the number of biotin receptors on a neighboring cell. Accordingly, it is reasonable to hypothesize that the tumor-targeting efficacy would be enhanced if a drug conjugate possessed different types of TTMs, such as two different vitamins. This drug conjugate was designed to target the different TTM receptors of the heterogeneous tumor cell population, assuring tumor-specific delivery of the drug conjugate to the majority of the cells. After the drug conjugate has been internalized, the drug can be cleaved from its carrier in its active form. For this purpose, we have designed a novel taxoid-based tumor-targeting drug conjugate which bears dual-TTM (Figure 8.1).[5, 6]

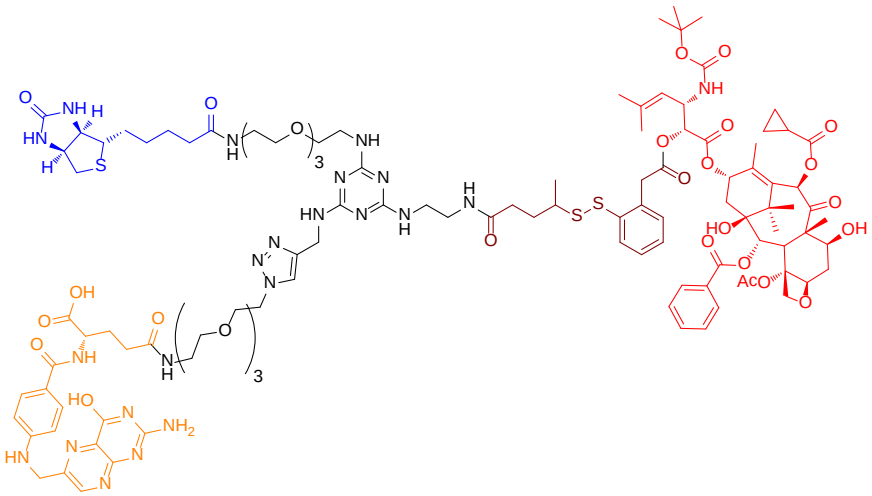

Figure 8.1: Tumor-targeting drug conjugate bearing dual-TTM

Biotin and folic acid were chosen as TTMs. Through the use of fluorescence-labeled vitamins, it was shown that biotin and folate receptors are overexpressed on cancer cell

surfaces.[5-16] Thus, drug conjugates with vitamins as TTM are guided to the tumor site and internalized via receptor mediated endocytosis (RME). After the drug conjugate is internalized, the disulfide linker is cleaved releasing the warhead, SB-T-1214, in its active form.

§ 8.1.3 Taxoid-Based Drug Conjugate Bearing Dual-PUFA

The omega-3 fatty acid, alpha-linolenic acid (α-LNA) is the most common omega-3 fatty acid in the Western diet and is found in a number of seed oils. LNA can only be obtained by humans through dietary sources and it has been shown that the intake of LNA has antitumor properties.[17, 18] As discussed in chapter 3, PUFAs, such as linolenic acid, are readily taken up by cancer cells.[19] From FACS analysis of LNA-FITC, it was shown that LNA is internalized into a variety of cancer cells within 1 hour of incubation and that LNA-FITC internalized into normal cells (HS-27) at a slower rate compared to that of cancer cells. Thus, drug conjugates with LNA as TTM may target tumors selectively. However, the mechanism or proteins responsible for PUFA internalization remain unknown. Accordingly, a novel taxoid-based tumor-targeting drug conjugate with two LNA moieties has been designed to evaluate the efficacy of internalization into cancer cells (Figure 8.2).

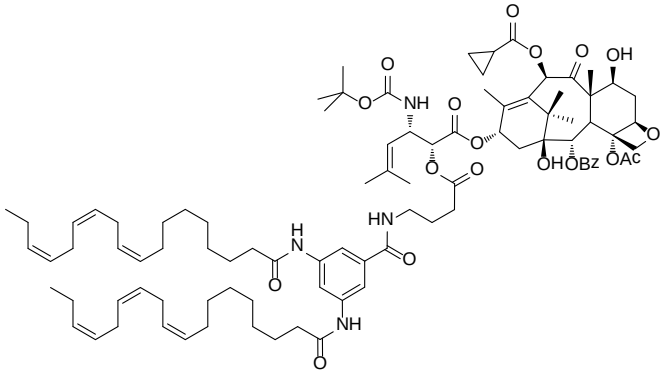

Figure 8.2: Tumor-targeting drug conjugate bearing dual-LNA

It is reasonable to assume that the ester bond linking the PUFA and the taxoid in the PUFA-taxoid drug conjugates, such as DHA-paclitaxel, is cleaved by an intracellular esterase. Along these lines, γ-aminobutyric acid (GABA) was chosen as a spacer module to conjugate the taxoid to the small-molecule splitter module in order to release the taxoid in a similar manner as the taxoid is released from the PUFA-taxoid drug conjugate.[20, 21]

§ 8.1.4 Taxoid-Based Drug Conjugate with One TTM and One Imaging Agent

Imaging is crucial for drug development as it provides relevant physiological information that can be used by clinicians and scientists to treat cancer patients. Single-photon emission computed tomography (SPECT) and positron emission tomography (PET) allow for the immediate noninvasive evaluation of metabolic activity, tumor perfusion and tumor response.[20, 22, 23] For example, using 2-^{18}F-fluoro-2-deoxyglucose (FDG), glucose metabolism was detected via PET to assess tumor response to adjuvant and neoadjuvant chemotherapy from multiple organs.[21, 24] Furthermore, a number of radiolabeled probes were used to assess biochemical

processes via SPECT, such as ^{99m}Tc-labeled Annexin V was used to measure apoptosis in solid tumors after treatment, and ^{67}Ga has been used to diagnose lymphoma, breast cancer, lung cancer, as well as other cancers.[25, 26]

SPECT imaging uses γ-rays to evaluate biochemical processes. This technique requires the use of γ-emitting radioisotopes. A variety of radioisotopes have been developed and used for SPECT imaging. These radiotracers include ^{99m}Tc, ^{123}I, ^{111}In, ^{201}Tl, ^{67}Ga and ^{131}I. The radiotracers are high-energy γ-emitters, ranging from 100 to 300 keV, with half-lives ranging from 6 hours to several days.[25] SPECT imaging has been used to locate tumors, assess angiogenesis and evaluate tumor vasculature.

PET imaging uses positron-emitting radioisotopes for localization of the radiotracer. ^{11}C, ^{13}N, ^{15}O and ^{19}F are commonly used radioisotopes.[25] These isotopes emit a positron from the nucleus that is captured by an electron from the same or neighboring atom, resulting in an inherent resolution limit on millimeter scale.[27] This decay process generates two 511-keV photons that traverse in opposite directions.[25] The two photons are detected by a ring detector consisting of scintillation detectors whose signals are amplified by photomultiplier tubes.[25] Images are reconstructed by collecting each volume over several minutes.

To monitor drug circulation, accumulation, metabolism and overall fate, novel taxoid-based tumor-targeting drug conjugates were designed with a radioisotope as the labeling agent, and a vitamin as the TTM (Figure 8.3). These drug conjugates were designed to specifically deliver the cytotoxic warhead to cancer cells, where it is internalized via RME.

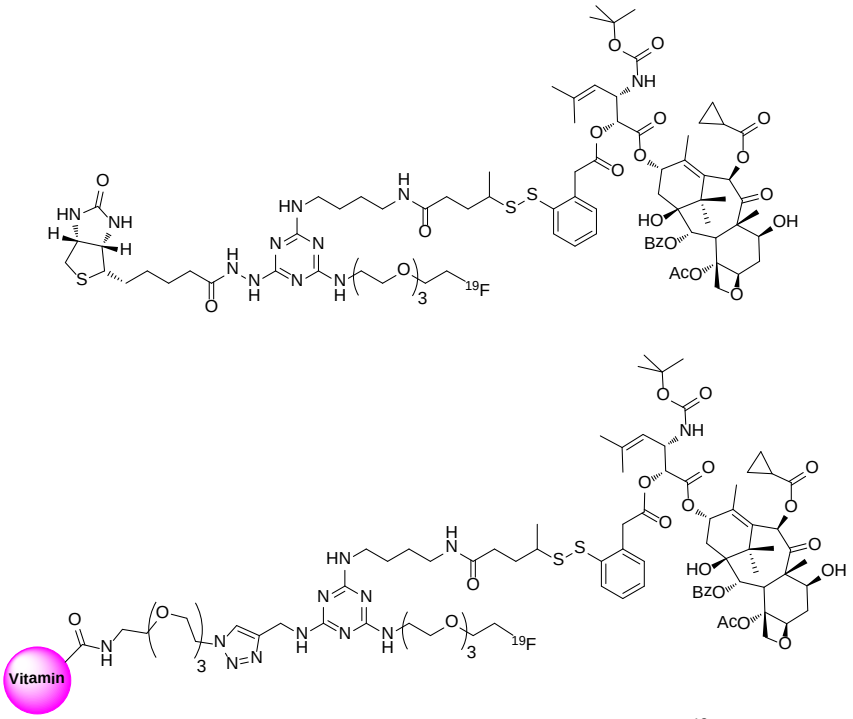

Figure 8.3: Tumor-targeting drug conjugate with ^{19}F

The presence of ^{19}F allows for the detection of the drug conjugates *in vivo* using SPECT or PET imaging. Thus, the location and accumulation of the drug conjugate can be monitored over time. After the drug conjugate has been internalized into cancer cells and the taxoid has been cleaved, the fate of the residual splitter module can also be monitored.

§ 8.2.0 Results and Discussion

§ 8.2.1 Internalization of Dual-Vitamin-FITC Probe

The tumor-targeting drug conjugate bearing dual-TTMs was designed with the hypothesis that a drug conjugate with biotin and folate as TTMs would increase the efficacy of drug conjugate internalization into heterogeneous tumor cells. To test this hypothesis, a dual-vitamin-FITC probe was prepared and the internalization of the probe was evaluated using FACS. A 1,3,5-trisubstituted triazine was chosen as the small-molecule splitter module that was selectively functionalized with *N*-Boc-ethylenediamine (**5-13**) and biotin-PEG$_3$-amine (**7-2a**) (Scheme 8.1).

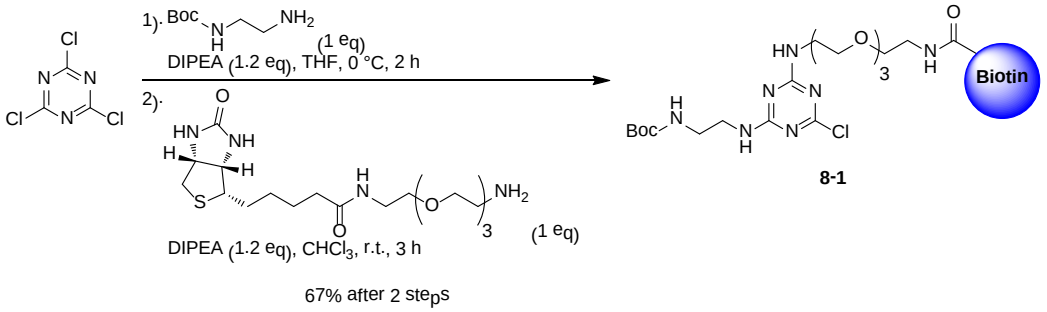

Scheme 8.1: Modifications to cyanuric chloride

Cyanuric chloride was selectively modified using a procedure similar to one reported by Campbell and Hatton.[28] The addition of *N*-Boc-ethylenediamine with base to cyanuric chloride at 0 °C, followed by the addition of biotin-PEG$_3$-amine with base at room temperature gave **8-1** in good yield (67% after 2 steps). Chloroform was used to dissolve biotin-PEG$_3$-amine. In addition, longer reaction times (compared to reaction times reported in chapter 7) were allotted in both steps to assure reaction completion. After isolation from column chromatography, **8-1** was treated with folate-PEG$_3$-amine (**7-2b**) in the presence of base under reflux conditions (Scheme 8.2).

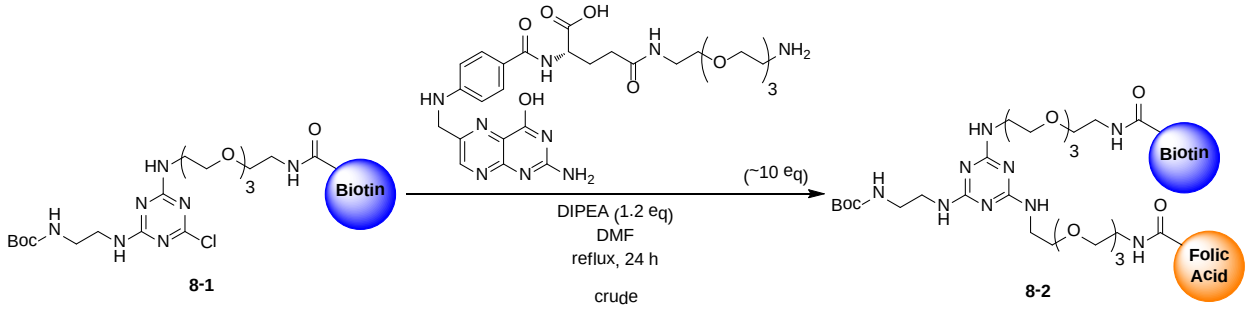

Scheme 8.2: 1,3,5-Trisubstituted triazine with dual-vitamin

The coupling of folate-PEG$_3$-amine and **8-1**was originally attempted using THF as solvent. However, after 24 h, no product was observed via mass spectroscopy. Accordingly, the reaction solvent was evaporated and DMF was added. Stirring under reflux conditions afforded a

crude mixture containing **8-2** after washing with different organic solvents. As with other folate derivatives, purification of **8-2** was difficult. The resulting crude **8-2** was treated with TFA in dichloromethane to remove the Boc moiety and then treated with FITC (Scheme 8.3).

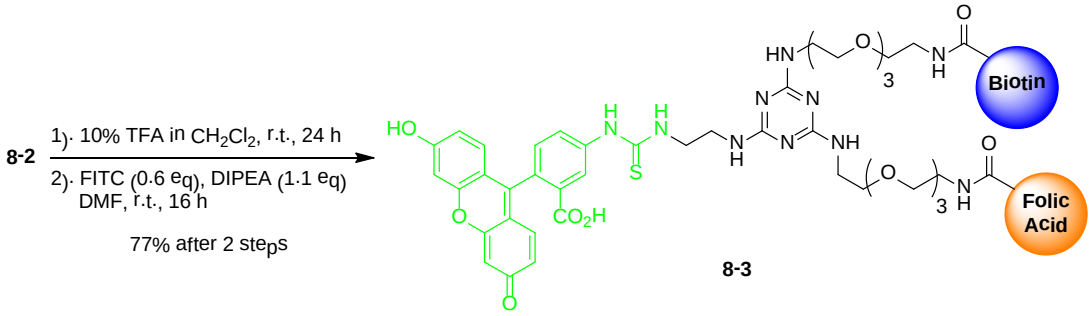

Scheme 8.3: Dual-vitamin-FITC probe

The standard Boc-deprotection procedure gave the corresponding free amine, which was obtained after quenching with sodium bicarbonate and filtration. The resulting amine was added to FITC in the presence of base to afford **8-3** (77% after 2 steps) after passing through a short silica gel plug. As previously discussed, ID-8 (ovarian) cancer cells overexpress the biotin and folate receptors. Using ID-8 (ovarian) cancer cell line as a control, the internalization of the FITC-labeled **8-3** was evaluated in MCF-7 (breast) cancer cell using FACS.

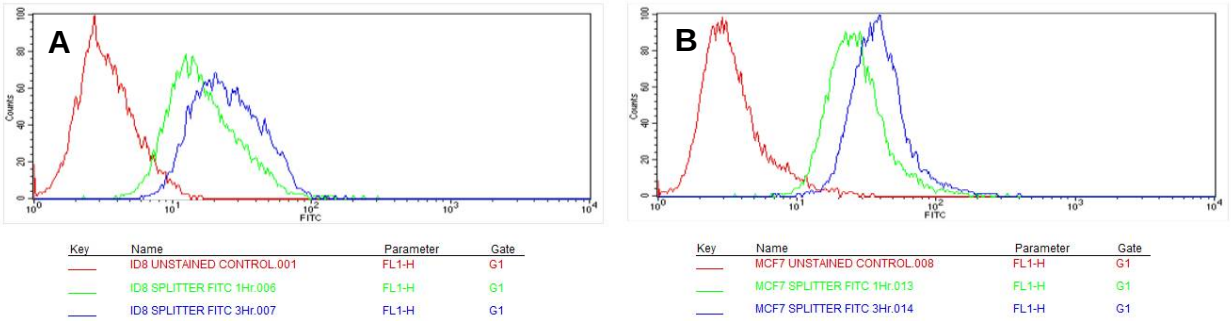

Figure 8.4: FACS analysis and histogram overlays evaluating internalization of 10 µM dual-vitamin-FITC incubated in ID-8 and MCF-7 cancer cell lines for 1 h and 3 h at 37 °C. (A) ID-8; (B) MCF-7.

The cells were cultured in fully-supplemented RPMI-1640 Medium 10 x and incubated at 37 °C with 5% CO_2. Then the cells were treated with10 µM **8-3** for 1 hour and 3 hour incubation periods. After the incubation period, the cells were washed with PBS (3 times), resuspended in PBS containing 2% formulin and analyzed using FACS. As seen from the histograms, **8-3** internalization was observed in both cancer cell lines within 1 hour (green line) and internalization increased with a longer incubation time (blue line). These results confirm the reported overexpression of biotin- and folate-receptors in ID-8 cells. Furthermore, MCF-7 cells also overexpress the vitamin receptors. However, whether or not the efficacy of internalization increased has not been determined. Comparing the internalization rates of biotin-PEG_3-FITC and folate-PEG_3-FITC (chapter 7, Figures 7.6A-F and 7.7G-I) with that of **8-3** in the same two cancer cell lines, the rate at which **8-3** internalizes appears to be slower than the single vitamin-FITC probes, as the **8-3** peaks (green and blue lines) are slightly overlapping with the autofluorescence

of the cells (red line). This overlap was not seen with the single vitamin probes with the same incubation time (chapter 7: fig. 7.7). It is reasonable to assume that the size of **8-3** slowed the rate of internalization and if the incubation time were prolonged, more probe internalization would be observed. This, however, would suggest a decrease of internalization efficacy. The efficacy of internalization of a drug conjugate with two TTMs is still being examined.

§ 8.2.2 Synthesis of Taxoid-Based Tumor-Targeting Drug Conjugate Bearing Dual-Vitamin

The use of 1,3,5-trisubstituted triazine as a small-molecule splitter module was successful in the synthesis of a tumor-targeting drug conjugate with SB-T-1214 and topotecan as warheads. Accordingly, the same type of splitter module was used for the preparation of taxoid-based drug-conjugate bearing dual-vitamins. For this purpose, cyanuric chloride will be selectively functionalized with propargyl amine, *N*-biotinyl-1,4-butanediamine and hydrazine. *N*-Biotinyl-1,4-butanediamine (**8-4**) was prepared by treating 1,4-butanediamine with excess biotin methyl ester (**5-1**) (Scheme 8.4).

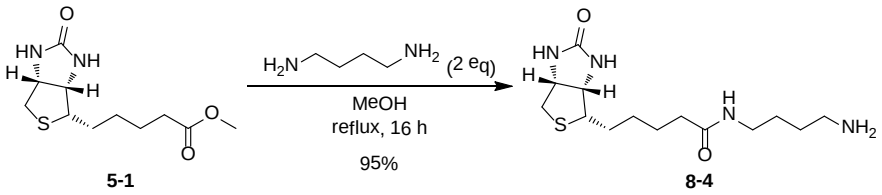

Scheme 8.4: Synthesis of N^1-butylbiotin-1,4-diamine

The addition of biotin methyl ester to 1,4-butanediamine afforded **8-4** in excellent yield (95%). 1,4-Butanediamine was chosen as a spacer to extended the bulky fused-ring biotin away from the splitter module. Employing the exact reaction conditions as Campbell and Hatton, cyanuric chloride was treated with **8-4**, then with aqueous NaOH, followed by the addition of propargyl amine and a second basification at a higher temperature (Scheme 8.5).[28]

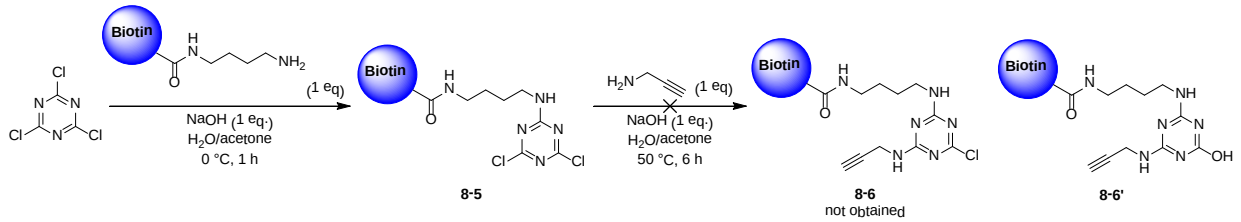

Scheme 8.5: Modification of cyanuric chloride

The dichloro-triazine **8-5** was not isolated after basification; instead it was subjected to the addition of propargyl amine and base. However, this sequence of addition did not afford **8-6**. Based on IR, the compound obtained was the hydrolyzed form of **8-6**, i.e. the chlorine moiety has replaced with a hydroxyl moiety. It was hypothesized that the second treatment basification step using aqueous NaOH resulted in the formation of the hydrolyzed product. Accordingly, the dichloro-triazine **8-5** was treated with propargyl amine and not treated with NaOH. Then the resulting mono-chloro triazine **8-6** was treated with hydrazine (Scheme 8.6)

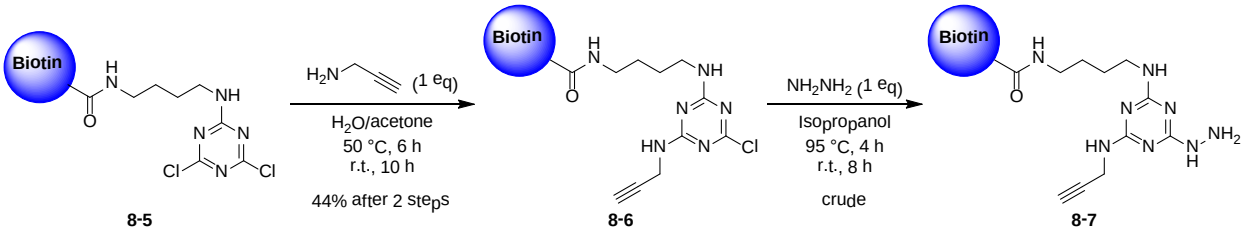

Scheme 8.6: Hydrazine formation or triazine splitter

The addition of propargyl amine to **8-5** without the addition of NaOH afforded **8-6** in moderate yield (44% after 2 steps). Thus, confirming that the hydrolysis was caused by the addition of NaOH. Treating **8-6** with hydrazine gave crude containing **8-7**, which was immediately treated with SB-T-1214-Me-linker-OSu (**4-20**) (Scheme 8.7).

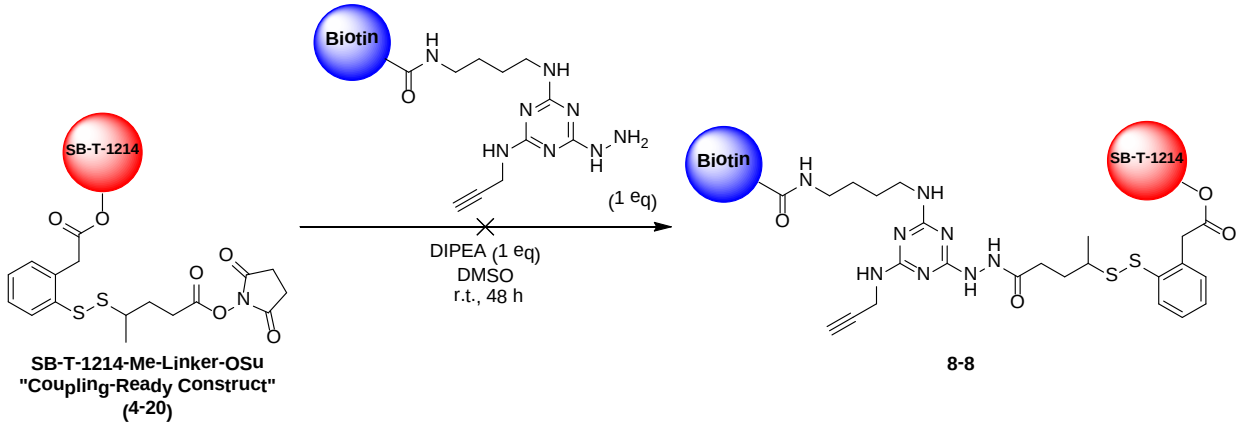

Scheme 8.7: Attempted drug-linker splitter module coupling

As was discussed in chapter 6, the use of hydrazine as a spacer for splitter module coupling did not afford the desired coupled compound. It is reasonable to assume that sterics was the cause for no reaction being observed. A similar outcome was observed in the coupling between **8-7** and **4-20**, as **8-8** was not produced. Thus, **8-6** was treated with *N*-Boc-ethylenediamine to extend the free amine away from the splitter module (Scheme 8.8).

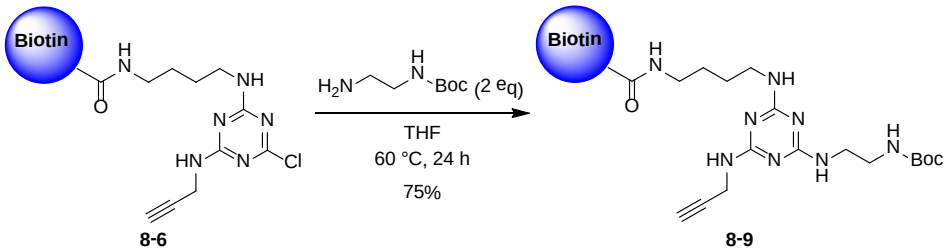

Scheme 8.8: Splitter module amine extension

Installation of *N*-Boc-ethylenediamine to **8-6** was achieved in good yield (75%) after column chromatography. The two additional carbons should separate the reactive free amine from the splitter enabling coupling to a variety of activated esters or carboxylic acids via peptide coupling. Accordingly, the resulting **8-9** was treated with TFA to remove and Boc moiety, and the corresponding amine was added to **4-20** (Scheme 8.9).

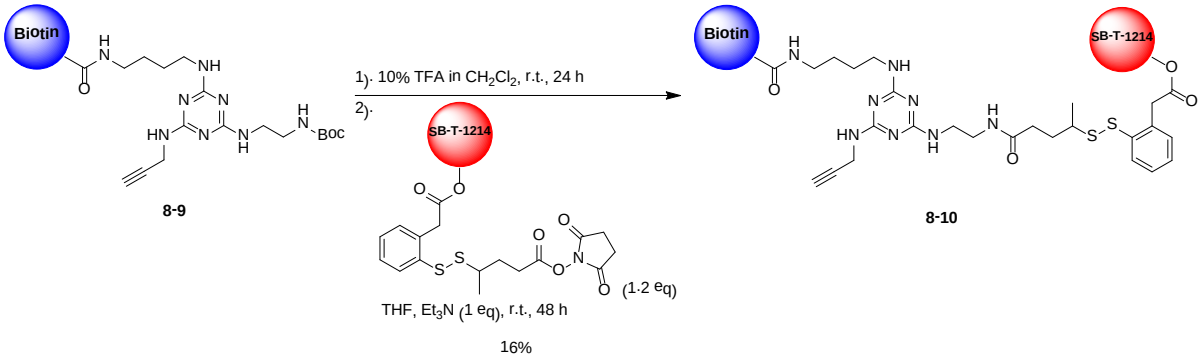

Scheme 8.9: Drug-linker splitter module coupling

The two carbons introduced by the installation of *N*-Boc-ethylenediamine proved sufficient to extend the amine away from the splitter module. However, sterics may still be an issue for coupling, as **8-10** was obtained in low yield (16%). As such, it was hypothesized that coupling via "click chemistry" would be difficult at the terminal alkyne. For this purpose, model "click" reactions were attempted.

§ 8.2.3 Model "Click" Reactions of Splitter Module

To evaluate the reactivity of the 1,3,5-trisubstitution triazine with a terminal alkyne introduced by propargyl amine, a model splitter module was prepared. Compound **8-9** was subjected to CuI-catalyzed "click" conditions in the presence of 11-azido-3,6,9-trioxaundecan-1-amine (Scheme 8.10).

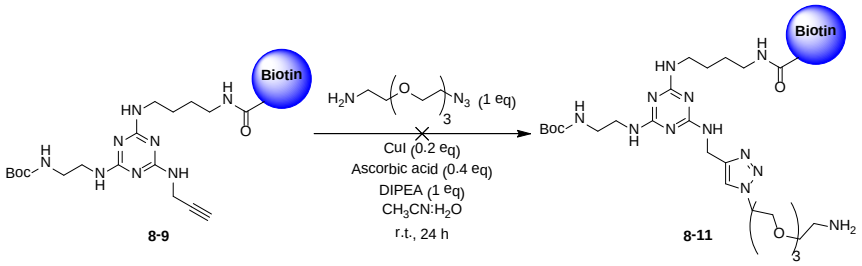

Scheme 8.10: 1st attempted model "click" reaction

Although the proposed "click" conditions were mimicked for the synthesis of drug conjugate bearing dual-vitamin, the CuI-catalyzed "click" reaction between **8-19** and 11-azido-3,6,9-trioxaundecan-1-amine did not afford **8-11**. This result suggests that the terminal alkyne may be too sterically blocked to react. To further examine the reactivity of the terminal alkyne, a second model splitter module was prepared that bears two terminal alkynes. This splitter module was obtained from treating cyanuric chloride with propargyl amine and *N*-Boc-ethylenediamine under basic conditions and at different temperatures (Scheme 8.11).

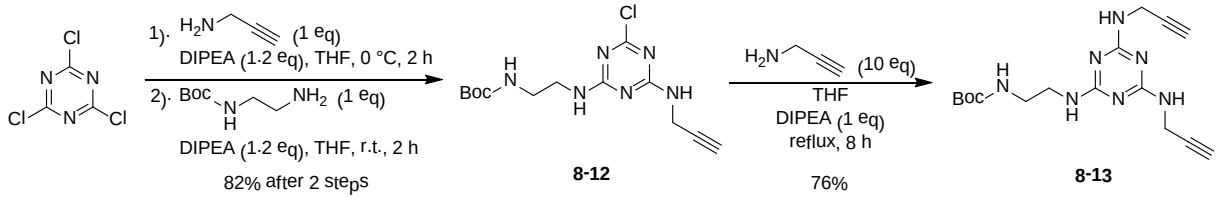

Scheme 8.11: Synthesis of splitter module with two terminal alkynes

The sequential addition of propargyl amine and *N*-Boc-ethylenediamine to cyanuric chloride at 0 °C and room temperature, respectively, gave **8-12** in good yield (82% after 2 steps). **8-12** was then treated with propargyl amine in the presence of base in refluxing THF to afford **8-13** in good yield (76%). Splitter module **8-13** was then subjected to CuI-catalyzed "click" conditions in the presence of two different azido-PEG-amine moieties (Scheme 8.12).

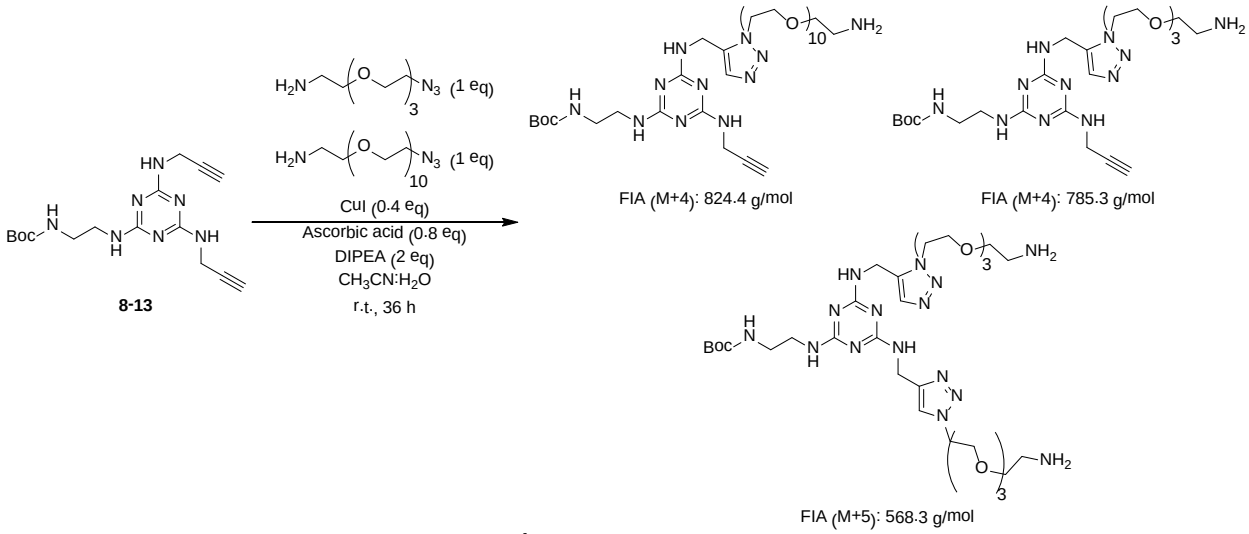

Scheme 8.12: 2nd attempted model "click" reaction

Although the products of the model "click" reactions were not isolated due to scale, analysis of the crude mixture via mass spectroscopy showed the presence of the three products listed above with no starting material. The presence of the three products suggests that sterics could play a role in the rate in which the "click" reaction proceeds. However, the presence of "bis-PEG" product suggests that the terminal alkyne is still reactive towards "click" conditions after one alkyne has reacted. As such, the taxoid-based drug conjugate bearing dual-vitamin was redesigned such that both vitamins are installed on the 1,3,5-trisubstituted triazine splitter module via PEG chains as spacers.

§ 8.2.4 Synthesis of Redesigned Taxoid-Based Drug Conjugate Bearing Dual-Vitamins

The synthesis of biotin-PEG_3-amine (**7-2a**) and folate-PEG_3-azide (**7-3b**) were discussed in the previous chapter. Both of these vitamin derivatives will be incorporated onto the splitter module. Accordingly, cyanuric chloride was sequentially treated with *N*-Boc-ethylenediamine and **7-2a** in the presence of base and at different temperatures. The resulting mono-chloro

triazine was then treated with propargyl amine in the presence of base in refluxing THF (Scheme 8.13).

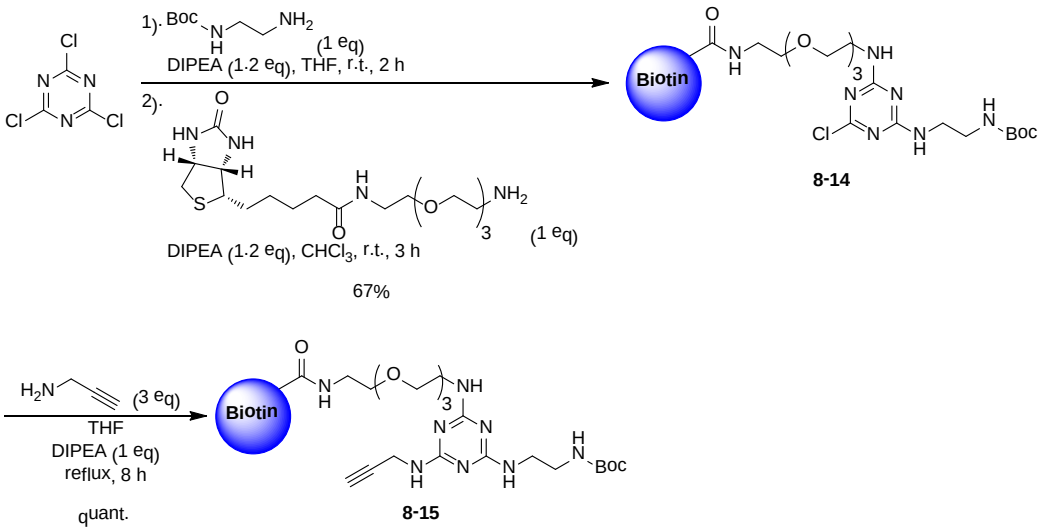

Scheme 8.13: Modifications of splitter module

The selective functionalization of cyanuric chloride with *N*-Boc-ethylenediamine and then with **7-2a** gave **8-14** in moderate yield (67%). After isolation from column chromatography, **8-14** was treated with propargyl amine to generate a "click-ready" 1,3,5-trisubstituted triazine, **8-15**, in quantitative yield. **8-15** was treated with TFA and the corresponding amine was treated with **4-20** (Scheme 8.14).

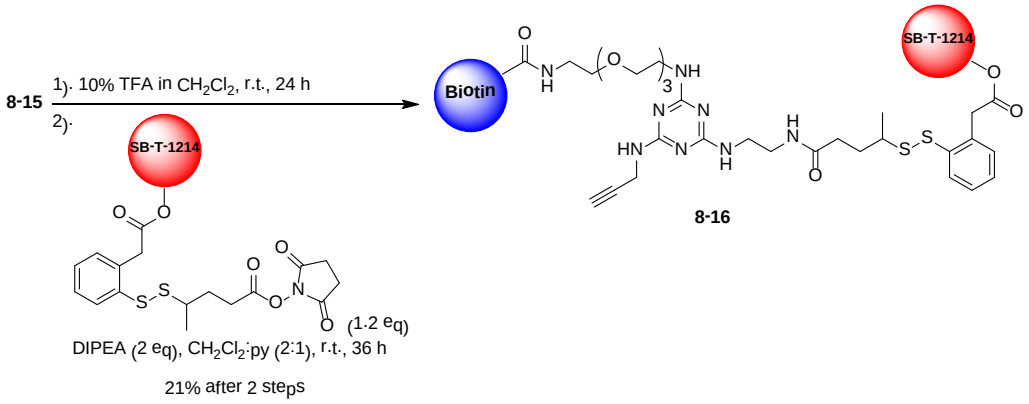

Scheme 8.14: Drug-linker to "click-ready" splitter coupling

Boc-deprotection in the presence of TFA generated the corresponding amine after quenching with sodium bicarbonate and extraction. Coupling of SB-T-1214-Me-linker-OSu coupling-ready construct with the splitter module gave **8-16** in fair yield (21% after 2 steps). Containing a terminal alkyne, **8-16** is "click-ready" and can be coupled to any TTM with a terminal azide. As such, **8-16** was subjected to CuI-catalyzed "click" conditions in the presence of **7-1b** (Scheme 8.15).

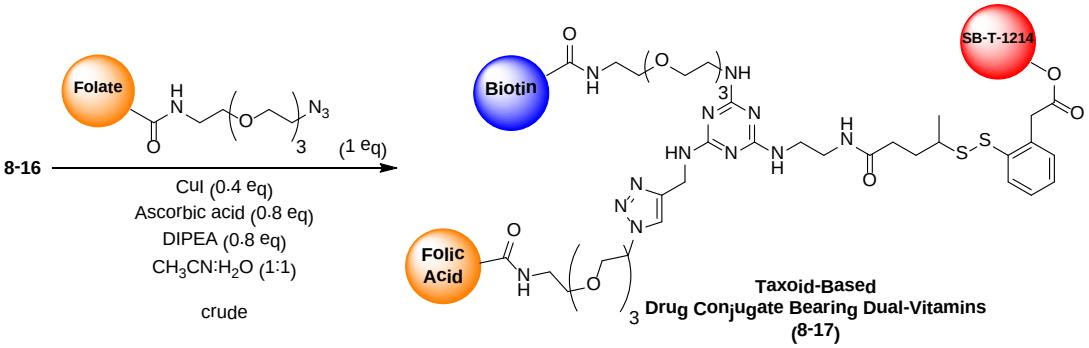

Scheme 8.15: Synthesis of taxoid-based drug conjugate bearing dual-vitamins via "click chemistry"

The "click" reaction was conducted in a glove box. The splitter module, folate-PEG-azide and additives dissolved in a 1-to-1 mixture of acetonitrile and water were incubated in the glove box for 8 hours prior to the addition of the CuI in 1-to-1 acetonitrile and water. The mixture was left in the glove box for 16 h after the addition of CuI. The resulting crude was washed with water. However, further purification of the crude was not done as the crude only dissolves in DMSO. Purification and biological evaluation of the taxoid-based drug conjugate bearing dual-vitamins are currently being examined.

§ 8.2.5 Synthesis of Taxoid-Based Drug Conjugate Bearing Dual-PUFA

Based on results obtained from biological assays of PUFA-taxoid and PUFA-linker-taxoid drug conjugates, as previously discussed in chapter 3 and 4, respectively, a novel drug conjugate that contains two PUFA moieties as TTMs has been designed to evaluate the efficacy of drug conjugate internalization and potency. 3,5-Diamino-1-benzoic acid has been chosen as the small-molecule splitter module and GABA has been chosen as a spacer to conjugate the taxoid to the splitter module. 3,5-Diamino-1-benzoic acid was treated with linolenic acid methyl ester in the presence of base at an elevated temperature, followed by peptide coupling of GABA (Scheme 8.16).

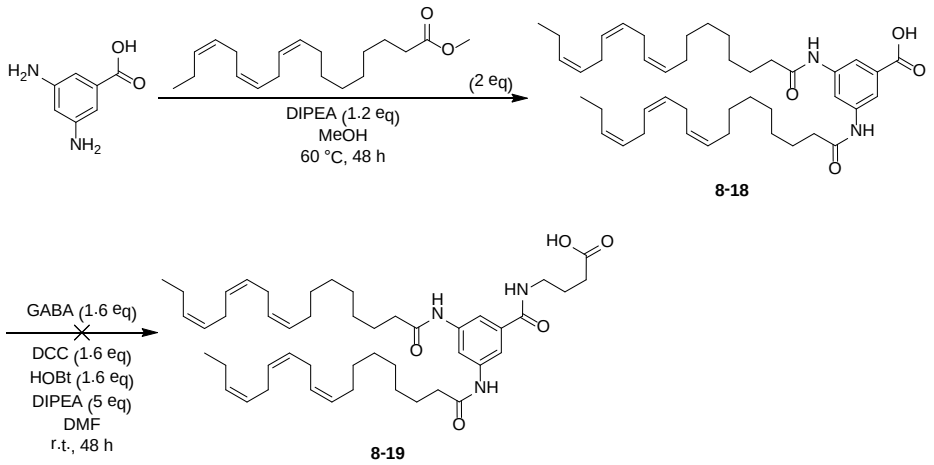

Scheme 8.16: Preparation of splitter module with GABA and dual-LNA

The addition of linolenic acid methyl ester to 3,5-diamino-1-benzoic acid resulted in crude containing **8-18**, based on mass spectroscopy analysis. However, the addition of GABA to the resulting crude containing **8-18** in standard peptide coupling conditions did not yield **8-19**. Immediately after the addition of DIPEA, the reaction mixture became dark red. After 48 h, the reaction was quenched with water and extracted. The organic layer did not contain the product and the aqueous layer was lyophilized to yield a dark red/black solid. The synthesis of taxoid-based drug conjugate bearing dual-LNA is still being examined. An alternative route towards **8-19** is to use γ-aminobutyric acid benzyl ester in the coupling reaction followed by benzyl-deprotection. The corresponding carboxylic acid can be coupled to the C-2' position of SB-T-1214 using EDC (Scheme 8.17).

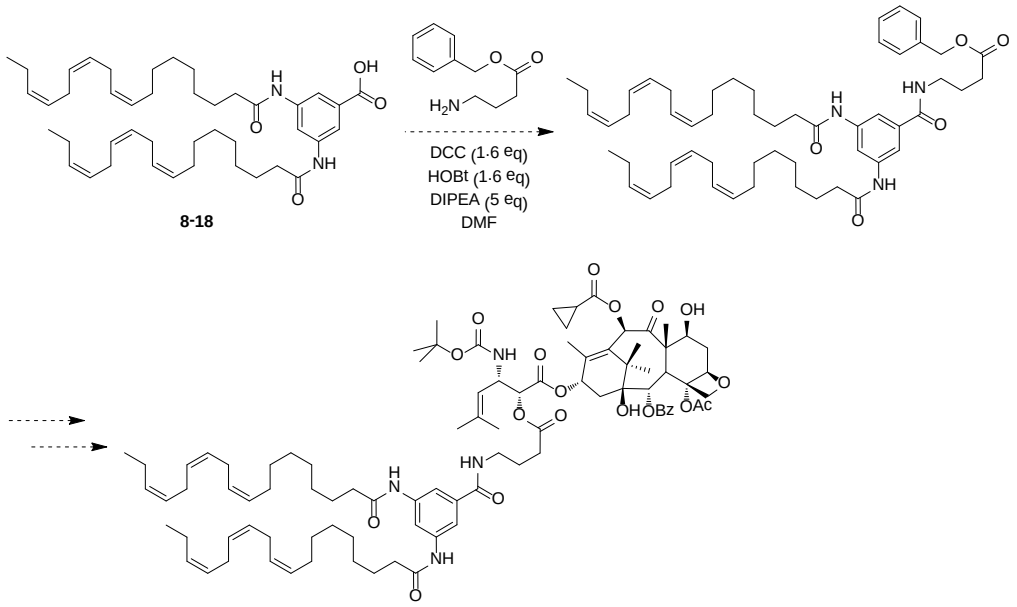

Scheme 8.17: Proposed alternative route towards taxoid-based drug conjugate bearing dual-LNA

§ 8.2.6 Synthesis of Taxoid-Based Drug Conjugate with One TTM and One Imaging Agent

The benefits of imaging were briefly discussed earlier in this chapter. To exploit those benefits, a novel taxoid-based drug conjugate with one TTM and one imaging agent was designed. Biotin was chosen as the TTM and ^{19}F was chosen as the imaging agent. ^{19}F can be detected using PET, thus the drug conjugate can be detected *in vivo* after the radioisotope is installed. 11-Azido-3,6,9-trioxaundecan-1-amine was chosen as the spacer to install the radioisotope onto a 1,3,5-trisubstituted triazine splitter module. To examine the fluorination of the PEG spacer, asymmetric modifications of 11-azido-3,6,9-trioxaundecan-1-amine were performed. These modifications entail selective mesylation of tetraethylene glycol in the presence of MsCl and base, followed by mesyl-substitution with an azido moiety (8.18).[29, 30]

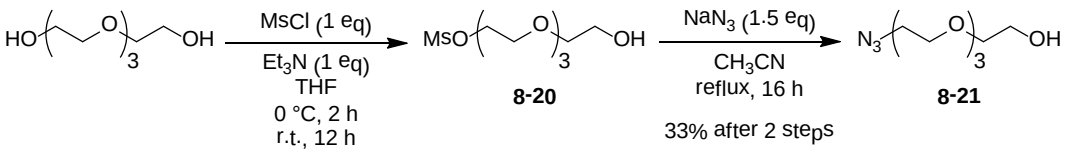

Scheme 8.18: Preparation of azido-PEG$_3$

Mesylation of tetraethylene glycol afforded a crude mixture containing the mono-mesylated-PEG$_3$ **8-20**. Literature precedence calls for purification via column chromatography of **8-20** but the reaction was clean based on TLC using cerium ammonium molybdate (CAM) as staining agent.[29, 30] As such, the reaction mixture was passed through Celite and used without further purification. The resulting crude was treated with sodium azide to afford **8-21** in fair yield (33% after 2 steps). **8-21** was treated with MsCl in the presence of base and the resulting mesylate was used in a model fluorination reaction (Scheme 8.19).[29-31]

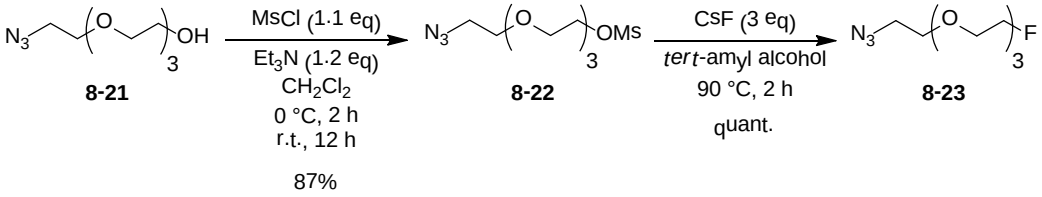

Scheme 8.19: Model fluorination reaction

The addition of MsCl with **8-21** in the presence of base gave **8-22** in good yield (87%). Chi et al. reported a novel method of fluorination using alkali metal fluorides in *tert*-alcohol media.[31] Chi concluded that nonpolar protic solvents enhance the reactivity of alkali metal fluorides, resulting in high yielding S_N2 substitution.[31] The protocol developed by Chi et al. was employed on **8-22** using CsF as the fluorine source affording **8-23** in quantitative yield. This result suggests that the PEG spacer can be used as a functionalizable branch for fluorination. For this purpose, **8-21** was treated with TIPSCl, followed by Staudinger reduction (Scheme 8.20).

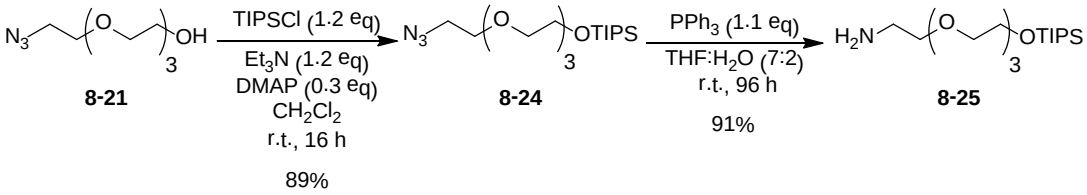

Scheme 8.20: Preparation of TIPSO-PEG$_3$-amine

The sequential treatment of **8-21** with TIPSCl in the presence of base followed by triphenylphosphine in THF and water afforded **8-24** and **8-25** in 89% and 91% yield, respectively. It is worthy of note that the conversion of **8-24** to **8-25** did not complete after 48 h, and the recovered **8-24** was again subjected to the reducing conditions for another 48 h. **8-25** is a key intermediate used to functionalize cyanuric chloride. Cyanuric chloride was selectively functionalized with biotin hydrazide, *N*-Fmoc-1,4-butanediamine and **8-25** in the presence of base and at different temperatures (Scheme 8.21).

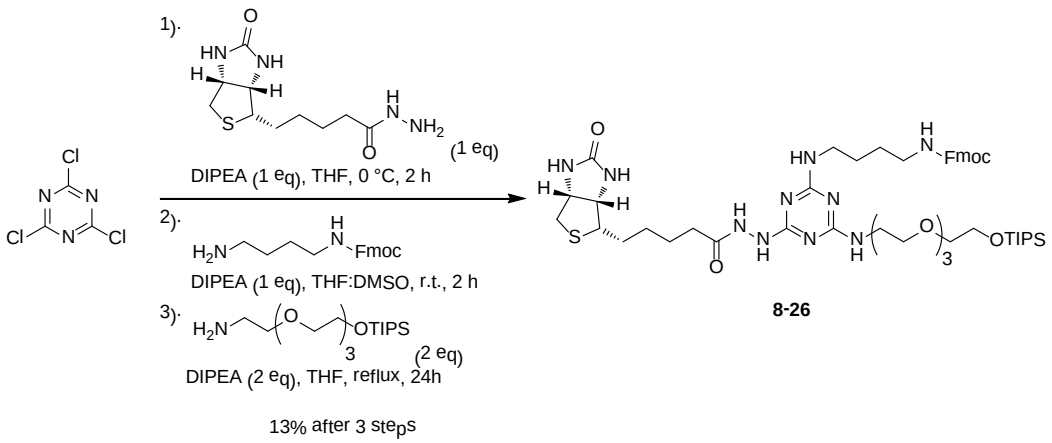

Scheme 8.21: 1,3,5-Trisubstituted triazine modification

The selective modification of cyanuric chloride with the three different amines afforded **8-26** in low yield (13% after 3 steps). The low yield may have been a result of low solubility of biotin hydrazide and *N*-Fmoc-1,4-butanediamine in THF. Reaction yields would be improved if DMSO were used as solvent for the first two steps. Lyophilization of the reaction solvent, followed by the addition of **8-25** in THF under reflux conditions should provide better results. The synthesis of taxoid-based drug conjugates with one TTM and one imaging agent is currently being explored using cold-materials. Once the synthetic route has been optimized, synthesis using radioisotopes will commence. From **8-26**, four additional steps are required to prepare the desired drug conjugate.

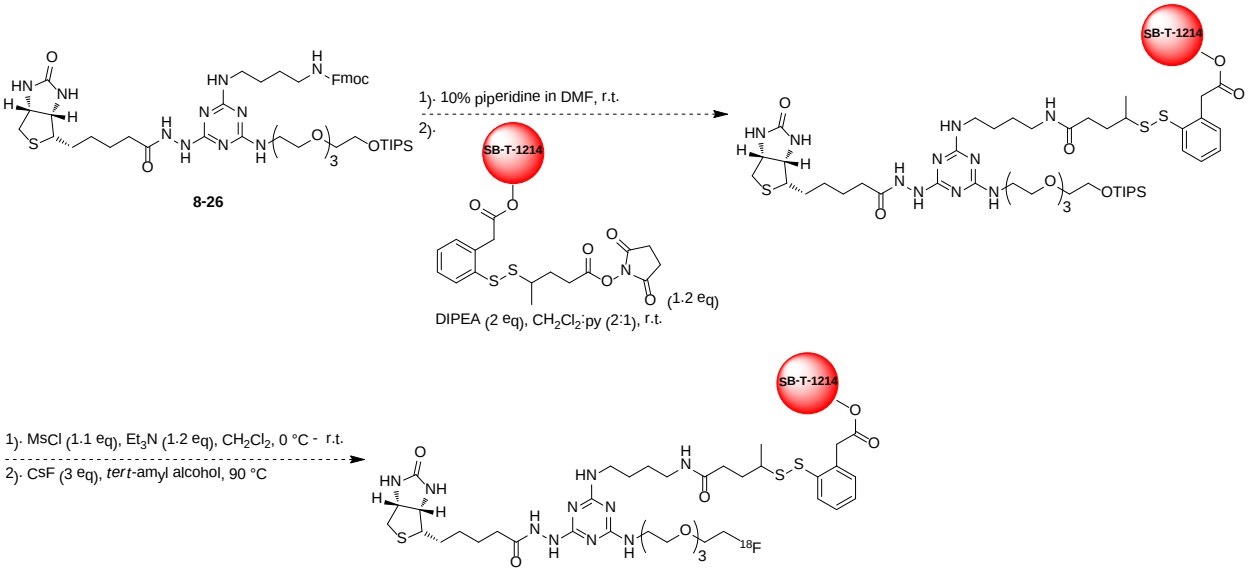

Scheme 8.22: Steps towards taxoid-based drug conjugate with one TTM and one imaging agent

§ 8.3.0 Summary

Small-molecule splitter modules were employed in the synthesis of a number of taxoid-based drug conjugates and molecular probes that can be used for *in vitro* and *in vivo* imaging. In

the previous two chapters, drug conjugates bearing dual-warheads were developed that show significant activity in a number of cancer cell lines. This chapter focused on other applications of small-molecule splitter modules. These applications include; (1) the development of a fluorescence-labeled probe bearing dual-vitamins, which was used to assess the efficacy of internalization into cancer cells, (2) the synthesis of a drug conjugate with dual-vitamins, and (3) the preparation of a drug conjugate with one TTM and one imaging agent. The syntheses discussed highlight the benefits of using splitter modules in drug development, as a wide variety of warheads, TTMs and imaging agents can be combined into a single molecule, thus having significant ramifications in the development of new chemotherapeutic agents and drug delivery systems. Through the use of splitter modules, drug delivery systems can be developed that specifically deliver synergistic drug pairs to tumors, guided by different TTMs, thus increasing the efficacy of internalization. Furthermore, the internalization, accumulation and metabolism can be assessed *in vitro* and *in vivo* with the addition of a fluorescence probe and radioisotope.

§ 8.4.0 Experimental

Caution

Taxoids has been established as a potent cytotoxic agent. Thus, they and all structurally related compounds and derivatives must be considered as mutagens and potential reproductive hazards for both males and females. Appropriate precautions (i.e. use of gloves, goggles, lab coat and fume hood) must be taken while handling these compounds.

General information

All chemical were obtained from Sigma-Aldrich, Fisher Scientific or VWR International, and used as is unless otherwise noted. All reactions were carried out under nitrogen in oven dried glassware using standard Schlenk techniques unless otherwise noted. Reactions were monitored by thin layer chromatography (TLC) using E. Merck 60F254 precoated silica gel plates and alumina plate depending on the compounds. Dry solvents were degassed under nitrogen and were dried using the PURESOLV system (Inovatative Technologies, Newport, MA). Tetrahydrofuran was freshly distilled from sodium metal and benzophenone. Dichloromethane was also distilled immediately prior to use under nitrogen from calcium hydride. Toluene was also distilled immediately prior to use under nitrogen from calcium hydride. Yields refer to chromatographically and spectroscopically pure compounds. Flash chromatography was performed with the indicated solvents using Fisher silica gel (particle size 170-400 Mesh).^{1}H, ^{13}C and ^{9}F data were obtained using either 300 MHz Varian Gemni 2300 (75 MHz ^{13}C, 121 MHz ^{19}F) spectrometer, the 400 MHz Varian INOVA 400 (100 MHz ^{13}C) spectrometer or the 500 MHz Varian INOVA 500 (125 MHz ^{13}C) in $CDCl_3$ as solvent unless otherwise stated. Chemical shifts (δ) are reported in ppm and standardized with solvent as internal standard based on literature reported values.[32] Melting points were measured on Thomas Hoover Capillary melting point apparatus and are uncorrected. Optical rotations were measured on Perkin-Elmer Model 241 polarimeter.

2-[2-Boc-amino-ethylamino]-4-biotinylamino-PEG-amino-6-chloro-*s*-triazine (8-1)

To a solution of cyanuric chloride (40 mg, 0.2 mmol) dissolved in THF [0.01 M] was added *N*-Boc-ethylenediamine (35 mg, 0.2 mmol) dissolved in 1 mL THF with DIPEA (0.08 mL, 0.4

mmol). The reaction was stirred at room temperature. As the reaction proceeded the mixture became cloudy. After 1 h at room temperature, to the mixture was added biotin-PEG_3-amine (90 mg, 0.2 mmol) dissolved in THF [0.2 M] with DIPEA (0.08 mL, 0.4 mmol). The mixture was stirred at room temperature and the reaction was monitored via TLC. After 1 h, the reaction solvent was evaporated and the resulting crude was purified using flash column chromatography (5% CH_3OH in CH_2Cl_2) to yield **8-1** (100 mg, 67% yield after 2 steps), as an off-white solid: ^{1}H NMR (300 MHz, $CDCl_3$, ppm) δ 0.874 (m, 3 H), 1.149-1.196 (t, *J* = 6.9 Hz, 6 H,), 1.364-1.514 (m, 36 H), 2.170-2.219 (t, *J* = 7.2 Hz, 2 H), 2.512-2.527 (t, *J* = 2.4 Hz, 2 H), 2.764 (m, 1 H), 2.894 (m, 1 H), 3.016-3.091 (q, J_1 = 7.5 Hz, J_2 = 7.2 Hz, J_3 = 7.5 Hz, 9 H), 3.399 (s, 4 H), 3.567-3.660 (m, 22 H), 4.270 (m, 1 H), 4.473 (m, 1 H), 5.564 (m, 1 H), 6.215 (s, 1 H), 6.884 (m, 1 H), 7.918 (br s, 1 H), 10.943 (br s, 4 H); ^{13}C NMR (500 MHz, $CDCl_3$, ppm) δ 14.713, 19.989, 21.251, 28.170, 30.718, 30.749, 31.035, 38.431, 41.704, 41.738, 43.107, 43.821, 44.683, 56.835, 58.167, 62.889, 64.445, 71.463, 72.467, 72.642, 72.894, 73.004, 73.046, 166.636, 167.990, 168.352, 172.159, 173.189, 176.057, 176.953, 186.787.

2-[2-Boc-amino-ethylamino]-4-biotinylamino-PEG-amino-6-folate-PEG-amino-*s*-triazine (8-2)

To a slurry of folate-PEG_3-amine (10 mg, 0.01 mmol) in THF [0.01 M] was added DIPEA (0.01 mL, 0.01 mmol) followed by **8-1** (95 mg, 1 mmol) dissolved in 1 mL THF. The mixture was stirred under reflux conditions and monitored via FIA. After 24 h, FIA analysis showed no product formation. The reaction solvent was evaporated, and the resulting crude was dissolved in 5 mL DMF. The mixture was stirred at room temperature and monitored via FIA. After 24 hours, the mixture was diluted with ethyl acetate. The resulting precipitate was collected and washed with ethyl acetate and then with dichloromethane to yield **8-2** (15 mg, 76 % crude yield) as a yellow solid, which was used without further purification.

2-[2-FITC-amino-ethylamino]-4-biotinylamino-PEG-amino-6-folate-PEG-amino-*s*-triazine (8-3)

8-2 (10 mg, 0.01 mmol) was dissolved in a solution containing 10% TFA in CH_2Cl_2. The mixture was stirred at room temperature and the reaction was monitored via TLC using ninhydrin as a stain. After 24 h, the reaction mixture was quenched with aqueous $NaHCO_3$ and extracted with CH_2Cl_2 (3 x 20 mL). The organic layers were combined, dried over $MgSO_4$ and concentrated *in vacuo* to yield crude containing free amine (10 mg, quantitative yield), as a brown oil. To the crude and FITC (10 mg, 0.006 mmol) dissolved in CH_2Cl_2 [0.05 M] was added DIPEA (0.01 mL, 0.011 mmol). The mixture was stirred at room temperature and the reaction was monitored via TLC. After 16 h, the reaction solvent was evaporated and the resulting crude was purified using flash column chromatography on silica gel (10% CH_3OH in CH_2Cl_2) to yield **8-3** (10 mg, 77% yield after 2 steps), as a waxy orange-yellow solid: ^{1}H NMR (500 MHz, $CDCl_3$, ppm) δ 1.089 (t, *J* = 7.5 Hz, 4 H), 1.258 (m, 2 H), 1.480 (m, 11 H), 1.548 (t, *J* = 7.5 Hz, 3 H), 1.964-1989 (m, 4 H), 2.660 (s, 1 H), 2.829 (s, 10 H), 2.956 (s, 1 H), 3.080-3.135 (m, 2 H), 3.151-3.180 (m, 8 H), 3.262-3.689 (m, 22 H), 5.905 (s, 1 H), 6.681 (m, 2 H), 7.464 (m, 1 H), 7.562-7.833 (m, 12 H), 8.012 (m, 1 H); ^{13}C NMR (500 MHz, $CDCl_3$, ppm) δ 14.702, 17.269, 20.851, 21.594, 23.910, 28.136, 28.228, 30.676, 31.092, 32.336, 35.662, 37.626, 39.160, 39.968, 41.013, 41.936, 44.656, 45.556, 45.682, 45.819, 49.802, 51.194, 56.164, 56.393, 58.464, 72.219, 72.493, 72.581, 72.802, 72.863, 72.955, 73.332, 116.526, 124.117, 124.807, 124.941, 131.135,

131.231, 131.677, 131.864, 131.982, 132.230, 132.398, 132.467, 132.501, 134.629, 134.652, 134.694, 134.774, 135.743, 135.835, 136.315, 136.403, 137.406, 162.398, 175.660.

4-Biotinyl-1,4-diamine (8-4)

To 1,4-diaminobutane (102 mg, 1.1 mmol) dissolved in CH_3OH [0.3 M] was added biotin methyl ester (100 mg, 0.4 mmol) dissolved in CH_3OH [0.1 M]. The reaction vessel was fixed with a condenser and the mixture was stirred under reflux conditions. After 16 h, the reaction mixture was allowed to cool to room temperature and the reaction solvent was evaporated. The resulting crude was washed with cold CH_3OH to yield **8-4** (116 mg, 95% yield), as an off-white solid: ^{1}H NMR (300 MHz, DMSO-d_6, ppm) δ 1.276-1.611 (m, 12 *H*), 2.085 (t, *J* = 8.4 Hz, 2 H), 2.345 (t, *J* = 7.8 Hz, 2 H), 2.594 (s, 2 H), 2.637 (s, 2 H), 2.836-2.893 (dd, J_1 = 4.8 Hz, J_2 = 7.5, J_3 = 4.8, Hz, 1 H), 3.062 (m, 1 H), 3.149 (m, 1 H), 3.472 (br s, 4 H), 4.174 (m, 1 H), 4.343 (m, 1 H), 6.413-6.485 (d, *J* = 21.6 Hz, 2 H).

2-[4-Biotinylbutylamino]-4-aminoproparagyl-6-chloro-*s*-triazine (8-6)

Method 1

This compound was prepared following the procedure developed by Campbell and Hatton.[28] A slurry of cyanuric chloride (80 mg, 0.4 mmol) in 0.25 mL of hot acetone was prepared by adding 0.75 mL of cold water. The slurry was cooled to 0 °C in an ice-bath. To the slurry was added **8-4** (130 mg, 0.4 mmol) followed by 1.2 mmol of NaOH dissolved in water. After the additions, the temperature was maintained and the mixture was stirred for 1 hour to yield **8-5**, which was not isolated. After 1 h, proparagyl amine (0.01 mL, 1.2 mmol) was added followed by 1.2 mmol of NaOH dissolved in water. Following the additions, the reaction temperature was raised to 50 °C and stirred for 6 h. After 6 h, the mixture was cooled to room temperature and the resulting precipitate was collected and washed with acetone to yield **8-6'**, the hydrolyzed form of **8-6** as a white solid.

Method 2

A slurry of cyanuric chloride (230 mg, 1.2 mmol) in 0.5 mL of hot acetone was prepared by adding 1 mL of cold water. The slurry was cooled to 0 °C in an ice-bath. To the slurry was added **8-4** (375 mg, 1.2 mmol) followed by 1.2 mmol of NaOH dissolved in water. After the additions, the temperature was maintained and the mixture was stirred for 1 hour to yield **8-5**, which was not isolated. After 1 h, proparagyl amine (0.01 mL, 1.2 mmol) was added. Following the addition, the reaction temperature was raised to 50 °C and stirred for 6 h. After 6 h, the mixture was cooled to room temperature and the resulting precipitate was collected and washed with acetone to yield **8-6** (244 mg, 44% yield after 2 steps), as an off-white solid:

IR (υ_{max} [cm^{-1}]) 1632.9, 20.35.80, 2933.84, 2035.80; ^{1}H NMR (300 MHz, $CDCl_3$, ppm) δ 1.000-1.044 (m, 7 H), 3.062 (s, 2 H), 3.117-3.435 (m, 5 H), 3.959 (s, 1 H), 4.301-4.326 (m, 2 H), 8.000 (m, 2 H).

2-[4-Biotinylbutylamino]-4-aminoproparagyl-6-hydrazide-*s*-triazine (8-7)

A mixture of **8-6** (100 mg, 0.2 mmol) and 10 mL of 2-propanol was heated to 90 °C in an oil-bath. As the temperature of the oil-bath reached 55 °C, NH_2NH_2 (0.01 mL, 0.1 mmol) was added rapidly. At 90 °C, 0.1 mmol of NaOH dissolved in water was added. After the addition, the temperature was maintained and the mixture was stirred for 4 h. Then the mixture was cooled to room temperature and the resulting precipitate was collected and washed with water to yield crude containing **8-7** (101 mg, quant. crude yield) which was used without further purification.

Attempted synthesis of 2-[4-biotinylbutylamino]-4-aminoproparagyl-6-[4-SB-T-1214-Me-linker-hydrazide]-*s*-triazine (8-8)

To **4-20** (10 mg, 0.01 mmol) dissolved in DMSO [0.01 M] cooled at 0 °C was added **8-7** (6 mg, 0.008 mmol) dissolved in DMSO [0.01 M] followed by the addition of DIPEA (0.008 mmol), dropwise. The mixture was stirred at room temperature and the reaction was monitored via TLC. After 24 h, no product formation was observed.

2-[4-Biotinylbutylamino]-4-aminopropargyl-6-(2-Boc-amino-ethylamino)-*s*-triazine (8-9)

To a solution of **8-6** (50 mg, 0.09 mmol) dissolved in THF [0.01 M] was added DIPEA (0.01 mL, 0.18 mmol) followed by N^1-Boc-ethylamine (144 mg, 0.9 mmol) dissolved in THF [0.1 M]. The mixture was stirred under reflux conditions and the reaction was monitored via TLC. After 8 h, the mixture was cooled to room temperature, the solvent was evaporated and the resulting crude was purified using flash column chromatography on silica gel (20% CH_3OH in CH_2Cl_2) to yield **8-9** (43 mg, 76 % yield) as a yellow solid: ^{1}H NMR (300 MHz, DMSO-d_6, ppm) δ 1.421 (s, 9 H), 1.540-1.563 (m, 2 H), 2.766-2.815 (t, J = 7.8 Hz, 2 H), 2.927-2.991 (q, 2 H, J_1 = 6.3 Hz, J_2 = 6.3 Hz, J_3 = 6.6 Hz), 3.637 (s, 2 H), 3.755 (s, 2 H), 4.040-4.054 (d, 2 H, J = 4.2 Hz), 4.116-4.144 (dd, 3 H, J_1 = 2.4 Hz, J_2 = 2.7 Hz), 6.913 (m, 1 H), 8.150-8.392 (m, 8 H).

2-[4-Biotinylamino]-4-aminoproparagyl-6-[(2-SB-T-1214-Me-linker-amino)ethanylamino]-*s*-triazine (8-10)

8-9 (40 mg, 0.07 mmol) was dissolved in a solution containing 10% TFA in CH_2Cl_2. The mixture was stirred at room temperature and the reaction was monitored via TLC using ninhydrin as a stain. After 24 h, the reaction mixture was quenched with aqueous $NaHCO_3$ and extracted with CH_2Cl_2 (3 x 20 mL). The organic layers were combined, dried over MgSO4 and concentrated *in vacuo* to yield crude containing the free amine of **8-9** (30 mg, quantitative yield), as a red oil. To **4-20** (10 mg, 0.03 mmol) dissolved in THF [0.2 M] was added the crude containing the free amine of **8-9** (10 mg, 0.02 mmol) dissolved in THF [0.2 M] followed by the addition of DIPEA (0.02 mmol), dropwise. The mixture was stirred at room temperature and the reaction was monitored via TLC. After 24 h, the reaction solvent was evaporated and the resulting crude was purified using flash column chromatography on silica gel (20% CH_3OH in CH_2Cl_2) to yield **8-10** (6 mg, 16% yield) as a yellow solid: ^{1}H NMR (400 MHz, $CDCl_3$, ppm) δ 0.953-1.003 (m, 10 H), 1.144 (s, 3 H), 1.251 (m, 9 H), 1.659 (s, 3 H), 1.708-1.726 (d, J = 7.2 Hz, 3 H), 1.854 (m, 1 H), 1.903 (s, 3 H), 1.936-2.133 (m, 2 H), 2.352 (m, 4 H), 2.490-2.566 (m, 1 H), 2.640-2.677 (t, J = 7.2 Hz, 1 H), 2.998 (m, 1 H), 3.062 (s, 2 H), 3.117-3.435 (m, 5 H), 3.790-3.808 (d, J = 4 Hz), 3.959 (s, 1 H), 4.167-4.189 (d, J = 8.8 Hz), 4.291-4.312 (d, J = 8.4 Hz), 4.301-4.326 (m, 2 H), 4.400-4.444 (q, J_1 = 6.8 Hz, J_2 = 4 Hz, J_3 = 6.8 Hz, 1 H), 4.785-4.806 (m, 1 H), 4.926-4.976 (m, 2 H), 5.085-5.106 (m, 1 H), 5.660-5.677 (d, J = 6.8 Hz, 1 H), 6.165-6.210 (m, 1 H), 6.279 (s, 1 H), 7.276-7.341 (m, 1 H), 7.454-7.493 (t, J = 7.6 Hz, 2 H), 7.581-7.618 (t, J = 7.6 Hz, 1 H), 7.783-7.805 (m, 1 H), 8.000 (m, 2 H), 8.101-8.122 (m, 2 H).

Attempted 2-[4-Biotinylbutylamino]-4-PEG-amino-6-(2-Boc-amino-ethylamino)-*s*-triazine (8-11)

To **8-11** (20 mg, 0.04 mmol), CuI (2 mg, 0.008 mmol) and ascorbic acid (3 mg, 0.016 mmol) dissolved in a 1:1 mixture of CH_3CN:water [0.2 M] was added DIPEA (0.01 mL, 0.04 mmol) followed by the addition of azido-PEG-amine (0.006 mL, 0.005 mmol). The mixture was stirred

at room temperature and the reaction was monitored via FIA. After 24 h, FIA analysis showed the presence of starting material and no product formation.

2-[2-Boc-aminoethylamino]-4-aminopropargyl-6-chloro-*s*-triazine (8-12)
To a solution of cyanuric chloride (100 mg, 0.6 mmol) dissolved in THF [0.01 M] was added propargyl amine (0.4 mL, 0.6 mmol) dissolved in 8.3 mL THF with DIPEA (1.65 mL, 0.8 mmol). The reaction was stirred at room temperature. As the reaction proceeded the mixture became cloudy. After 1 h at room temperature, to the mixture was added N^1-Boc-ethylenediamine (140 mg, 0.6 mmol) dissolved in 2 mL THF with DIPEA (1.65 mL, 0.8 mmol). The mixture was stirred at room temperature and monitored via TLC. After 1 h, the reaction solvent was evaporated. The resulting crude was diluted with $CHCl_3$ and the resulting precipitate was collected via vacuum filtration. The filtrate was washed with $CHCl_3$ to yield **8-12** (110 mg, 82% yield after 2 steps), as an off-white solid: ^{1}H NMR (300 MHz, $CDCl_3$, ppm) δ 1.412 (s, 9 H), 2.037 (s, 2 H), 2.219 (t, 1 H, *J* = 2.4, Hz), 3.302 (m, 2 H), 3.479 (m, 2 H),4.158 (br s, 3 H), 6.452 (br s, 1 H), 9.984 (br s, 1 H).

2-[2-Boc-amino-ethylamino]-4,6-aminodipropargyl-*s*-triazine (8-13)
To a solution of **8-12** (50 mg, 0.1 mmol) dissolved in THF [0.01 M] was added DIPEA (0.02 mL, 0.1 mmol) followed by propargyl amine (0.8 mL, mmol) dissolved in 1 mL THF. The mixture was stirred under reflux conditions and the reaction was monitored via TLC. After 8 h, the mixture was cooled to room temperature, the solvent was evaporated and the resulting crude was purified using flash column chromatography on silica gel (20% CH_3OH in CH_2Cl_2) to yield **8-13** (40 mg, 76 % yield) as a yellow solid: ^{1}H NMR (300 MHz, $CDCl_3$, ppm) δ 1.412 (s, 9 H), 2.037 (s, 2 H), 2.219 (m, 2 H), 3.308-3.490 (m, 4 H) 4.162 (br s, 4 H), 5.338 (br s, 1 H) 6.479 (br s, 1 H), 9.220 (br s, 1 H).

Attempted "Click" reaction with 8-13
To **8-13** (10 mg, 0.03 mmol), CuI (2 mg, 0.012 mmol) and ascorbic acid (3 mg, 0.024 mmol) dissolved in a 1:1 mxiture of CH_3CN:water [0.2 M] was added 0.01 mL (0.03 mmol) DIPEA followed by the addition of 11-azido-3,6,9-trioxaundecan-1-amine (0.006 mL, 0.03 mmol) and *O*-(2-aminoethyl)-*O′*-(2-azidoethyl)nonaethylene glycol (15 mg, 0.03 mmol). The mixture was stirred at room temperature and the reaction was monitored via FIA. After 36 h, the reaction mixture was diluted with water. The resulting precipitate was filtered via vacuum filtration and the mother liquor was analyzed using FIA. FIA analysis showed the presence of three "click" products. No material isolated.

2-[2-Boc-amino-ethylamino]-4-biotinylamino-PEG-amino-6-chloro-*s*-triazine (8-14)
To a solution of cyanuric chloride (40 mg, 0.2 mmol) dissolved in THF [0.01 M] was added *N*-Boc-ethylenediamine (35 mg, 0.2 mmol) dissolved in 1 mL THF with DIPEA (0.08 mL, 0.4 mmol). The reaction was stirred at room temperature. As the reaction proceeded the mixture became cloudy. After 1 h at room temperature, to the mixture was added biotin-PEG_3-amine (90 mg, 0.2 mmol) dissolved in THF [0.2 M] with DIPEA (0.08 mL, 0.4 mmol). The mixture was stirred at room temperature and the reaction was monitored via TLC. After 1 h, the reaction solvent was evaporated and the resulting crude was purified using flash column chromatography (5% CH_3OH in CH_2Cl_2) to yield **8-14** (100 mg, 67% yield after 2 steps), as an off-white solid: ^{1}H NMR (300 MHz, $CDCl_3$, ppm) δ 0.874 (m, 3 H), 1.149-1.196 (t, *J* = 6.9 Hz, 6 H,), 1.364-1.514

(m, 36 H), 2.170-2.219 (t, J = 7.2 Hz, 2 H), 2.512-2.527 (t, J = 2.4 Hz, 2 H), 2.764 (m, 1 H), 2.894 (m, 1 H), 3.016-3.091 (q, J_1 = 7.5 Hz, J_2 = 7.2 Hz, J_3 = 7.5 Hz, 9 H), 3.399 (s, 4 H), 3.567-3.660 (m, 22 H), 4.270 (m, 1 H), 4.473 (m, 1 H), 5.564 (m, 1 H), 6.215 (s, 1 H), 6.884 (m, 1 H), 7.918 (br s, 1 H), 10.943 (br s, 4 H); ^{13}C NMR (500 MHz, $CDCl_3$, ppm) δ 14.713, 19.989, 21.251, 28.170, 30.718, 30.749, 31.035, 38.431, 41.704, 41.738, 43.107, 43.821, 44.683, 56.835, 58.167, 62.889, 64.445, 71.463, 72.467, 72.642, 72.894, 73.004, 73.046, 166.636, 167.990, 168.352, 172.159, 173.189, 176.057, 176.953, 186.787.

2-[2-Boc-amino-ethylamino]-4-biotinylamino-PEG-amino-6-aminopropargyl-*s*-triazine (8-15)

To a solution of **8-14** (60 mg, 0.01 mmol) dissolved in THF [0.01 M] was added DIPEA (0.01 mL, 0.01 mmol) followed by the addition of propargyl amine (0.6 mL, 0.1 mmol) dissolved in THF [0.03 M]. The mixture was stirred under reflux conditions and the reaction was monitored via TLC. After 24 h, the reaction solvent was evaporated to yield **8-15** (60 mg, quant. yield), as an orange solid: ^{1}H NMR (500 MHz, $CDCl_3$, ppm) δ 1.459-1.499 (m, 36 H), 1.598 (m, 4 H), 2160-2.190 (t, J = 7.5 Hz, 2 H), 2.709-2.734 (m, 1 H), 2.827 (m, 1 H),3.027-3.080 (m, 9 H), 3.374 (s, 2 H), 3.517 (t, J = 4.5 Hz, 2 H), 3.576-3.629 (m, 20 H), 4.266 (m, 1 H), 4.464 (m, 1 H), 5.881 (m, 1 H), 6.269 (s, 1 H), 6.869 (m, 1 H), 7.281 (s, 1 H), 7.870 (s, 1 H), 10.906 (br s, 4 H); MS ES+ *m/z* calcd for $C_{34}H_{55}N_7O_7S$ $(M+H)^+$ 706.4, found 709.4.

2-[2-SB-T-1214-Me-linker-ethylamino]-4-biotinylamino-PEG-amino-6-aminoprogarpyl-*s*-triazine (8-16)

8-15 (50 mg, 0.07 mmol) was dissolved in a solution containing 10% TFA in CH_2Cl_2. The mixture was stirred at room temperature and the reaction was monitored via TLC using ninhydrin as a stain. After 24 h, the reaction mixture was quenched with aqueous $NaHCO_3$ and extracted with CH_2Cl_2 (3 x 20 mL). The organic layers were combined, dried over MgSO4 and concentrated *in vacuo* to yield crude containing the free amine (60 mg, quantitative yield), as a yellow oil. To the crude (25 mg, ~0.04 mmol) and DIPEA (0.14 mL, 0.08 mmol) dissolved in a 3:1 mixture of CH_2Cl_2:pyridine [0.1 M] was added SB-T-1214-Me-linker-OSu (50 mg, 0.05 mmol) dissolved in CH_2Cl_2 [0.5 M]. The mixture was stirred at room temperature and the reaction was monitored via TLC. After 36 h, the reaction solvent was evaporated and the resulting crude was purified using flash column chromatography on silica gel (10% CH_3OH in CH_2Cl_2) to yield **8-16** (15 mg, 21% yield after 2 steps), as a yellow solid: m.p. 185-186 °C; ^{1}H NMR (500 MHz, $CDCl_3$, ppm) δ 0.876-0.904 (m, 1 H), 0.952-1.027 (m, 2 H), 1.066 (m, 1 H), 1.121-1.136 (m, 2 H), 1.172 (s, 2 H), 1.232-1.286 (m, 8 H), 1.367 (s, 8 H), 1.422-1.433 (m, 11 H), 1.467-1.496 (m, 4 H), 1.616 (m, 4 H), 1.681 (s, 2 H), 1.722-1.737 (m, 4 H), 1.876 (m, 2 H), 1.923 (s, 2 H), 2.113 (m, 2 H), 2.215 (br s, 4 H), 2.368 (s, 3 H), 2.496-2.558 (m, 2H), 2.688-2.741 (m, 1 H), 2.875-2.930 (m, 2 H), 3.005-3.051 (m, 2 H), 3.090-3.127 (m, 1 H), 3.488 (s, 2 H), 3.600-3.709 (m, 15 H), 3.810 (d, J = 3.82 Hz, 1 H), 3.977-4.031 (m, 1 H), 4.084-4.118 (m, 1 H), 4.161-4.199 (m, 3 H), 4.300 (d, J = 4.31 Hz, 2 H), 4.401-4.422 (dd, J_1 = 5 Hz, J_2 = 10 Hz, 1 H), 4.476-4.510 (m, 1 H), 4.965 (br s, 2 H), 5.136 (m, 2 H), 5.680 (d, J = 7 Hz, 1 H), 6.168-6.205 (m, 1 H), 6.431 (s, 1 H), 7.287-7.313 (m, 3 H), 7.483 (t, J = 8 Hz, 2 H), 7.611 (t, J = 7.5 Hz, 1 H), 7.692 (t, J = 7.5 Hz, 1 H), 7.733-7.804 (m, 1 H), 8.112 (d, J = 7 Hz, 2 H), 8.622 (s, 2 H); ^{13}C NMR (500 MHz, $CDCl_3$, ppm) δ 9.302, 9.446, 9.841, 13.248, 14.956, 18.689, 20.882, 22.666, 25.929, 26.801, 28.448, 29.875, 30.542, 31.552, 33.699, 35.938, 38.905, 39.414, 40.757, 41.789, 43.405, 46.107, 53.248, 58.560, 62.210, 70.390, 72.037, 75.330, 75.642, 76.575, 79.292, 81.257,

84.672, 120.111, 123.935, 128.003, 128.542, 128.822, 129.513, 130.332, 132.844, 133.558, 133.793, 136.168, 137.686, 140.418, 149.987, 155.246, 167.122, 168.503, 169.907, 170.727, 170.810, 173.519, 174.991, 189.706, 204.162; MS ES+ *m/z* calcd for $C_{87}H_{118}N_8O_{22}S_3$ $(M+H)^+$ 1723.7, found 1726.7.

Drug conjugate bearing dual-TTM (8-17)
To **8-16** (10 mg, 0.01 mmol), folate-PEG_3-azide (4 mg, 0.01 mmol) and ascorbic acid (0.01 mg, 0.008 mmol) dissolved in a 1:1 mixture of CH_3CN:water [0.2 M] was added DIPEA (0.01 mL, 0.03 mmol) followed by the addition of CuI (0.5 mg, 0.004 mmol) suspended in CH_3CN:water [1 M]. Upon the addition of base and CuI the solution became dark red. The mixture was stirred at room temperature and the reaction was monitored via TLC. After 36 h, the reaction mixture was diluted with water. The resulting precipitate was filtered via vacuum filtration. Characterization in progress. Furthermore purification is required.

3,5-Bis-linolenyl-1-benzoic acid (8-18)
To 3,5-diaminobenzoic acid (116 mg, 0.8 mmol) dissolved in CH_3OH [0.1 M] was added DIPEA (0.14 mL, 0.8 mmol), followed by LNA-methyl ester (0.5 mL, 1.6 mmol), dropwise. The mixture was stirred under reflux conditions and the reaction was monitored via TLC. After 24 h, the mixture was cooled to room temperature and diluted with water. The aqueous layer was washed with CH_2Cl_2 (3 x 25 mL), $CHCl_3$ (3 x 25 mL) and then with ethyl acetate (3 x 25 mL). The aqueous layer was collected and lyophilized. The residual was washed with methanol to yield 782 mg crude material containing **8-18** which was used without further purification.

Attempted synthesis of 4-amino-*N*-3,5-bis(linoleniccarbonyl)phenylbutanamide (8-19)
To crude **8-18** (282 mg, ~ 0.4 mmol), DCC (138 mg, 0.67 mmol), HOBt (91 mg, 0.67 mmol) and GABA (69 mg, 0.67 mmol) was dissolved in DMF [0.1 M]. The mixture was stirred at room temperature for 10 minutes. To the mixture was added DIPEA (0.4 mL, 2 mmol). After the addition of base, the solution became cloudy and orange in color. The mixture was stirred at room temperature and monitored via TLC. As the reaction proceeded, the reaction solvent became dark-red. After 48 h, the mixture was diluted with hexanes. The resulting precipitate was washed with methanol. The residual was purified using flash column chromatography. No desired product was obtained.

2-{2-[2-(2-hydroxyethoxy)ethoxy]ethoxy}ethyl methanesulfonate (8-20)
The synthesis of compound **8-20** was attempted using the protocol described by Frisch.[33] To a solution of tetraethylene glycol (10 g, 5 mmol) and Et_3N (7.16 mL, 5 mmol) dissolved in THF [0.06 M] at 0 °C was added methanesulfonyl chloride (4 mL, 5 mmol), dropwise. The mixture was stirred at 0 °C for 2 h and then stirred at room temperature for 12 h. After 12 h, the reaction mixture was filtered through Celite and the filtrate was concentrated *in vacuo* to give crude **8-20**, as yellow oil, which was used in the subsequent step without further purification.

2-{2-[2-(2-Azidoethoxy)ethoxy]ethoxy}ethanol (8-21)[33]
To the resulting crude containing **8-20** dissolved in CH_3CN [0.17 M] was added NaN_3 (2.8 g, 7.5 mmol) producing an orange reaction mixture. The mixture was stirred under reflux conditions. After 16 h, the mixture was cooled to room temperature, quenched with H_2O and the mixture was extracted with CH_2Cl_2 (3 x 50 mL). The organic layers were combined, dried over $MgSO_4$

and concentrated *in vacuo*. The resulting crude was purified using flash column chromatography on silica gel (pure ethyl acetate) to give **8-21** (3.71 g, 33% yield after 2 steps), as a yellow oil: ^{1}H NMR (300 MHz, $CDCl_3$, ppm) δ 2.531 (t, *J* = 6.3 Hz, 2 H), 3.387 (t, *J* = 5.1 Hz, 2 H), 3.588-3.745 (m, 14 H). These values are consistent with literature values.[33]

2-{2-[2-(2-Azidoethoxy)ethoxy]ethoxy}ethyl methanesulfonate (8-22)
To **8-21** (500 mg, 2.3 mmol) dissolved in CH_2Cl_2 [0.6 M] was added Et_3N (0.38 mL, 2.7 mmol), followed by the methansulfonyl chloride (0.195 mL, 2.5 mmol), dropwise at 0 °C. The mixture was stirred at 0 °C for 2 h and then at room temperature. After 12 h at room temperature, the reaction mixture was filtered through Celite. The filtrate was evaporated. The resulting crude was purified by flash column chromatography on silica gel (hexanes:ethyl acetate = 1:9) to give **8-22** (589 mg, 87% yield), as a colorless oil: ^{1}H NMR (300 MHz, $CDCl_3$, ppm) δ 3.060 (s, 3 H), 3.378 (t, *J* = 4.5 Hz, 2 H), 3.641-3.678 (m, 10 H), 3.745-3.775 (m, 2 H), 4.351-4.384 (m, 2 H); IR (υ_{max} [cm^{-1}]): 1107.49, 2101.34, 2870.97.

2-{2-[2-(2-Azidoethoxy)ethoxy]ethoxy}ethyl fluoride (8-23)
8-22 (50 mg, 0.2 mmol) and CsF (77 mg, 0.6 mmol) dissolved in *tert*-amyl alcohol [0.4 M] were heated at 90 °C for 2 h. After 2 h, the reaction mixture was allowed to cool to room temperature. The crude material was purified using flash column chromatography on silica gel (hexanes:ethyl acetate = 1:9) to give **8-23** (36 mg, 100% yield), as a white solid: ^{1}H NMR (300 MHz, $CDCl_3$, ppm) δ 3.071 (s, 1 H), 3.387 (t, *J* = 5.1 Hz, 2 H), 3.654-3.711 (m, 14 H), 3.796 (t, *J* = 4.2 Hz, 2 H), 4.484 (t, *J* = 3.9 Hz, 1 H), 4.644 (t, *J* = 4.5 Hz, 1 H); ^{19}F NMR (300 MHz, $CDCl_3$, ppm) δ -10.282 (m); IR (υ_{max} [cm^{-1}]): 1110.07, 2099.67, 2869.38; HRMS MS ES+ *m/z* calcd for $C_8H_{16}FN_3O_3$ $(M+H)^+$ 222.1176, found 222.1254 (Δ 7.8 ppm).

2-{2-[2-(2-Azidoethoxy)ethoxy]ethoxy}ethoxy triisopropylsilyl ester (8-24)
To **8-23** (1 g, 4 mmol) and DMAP (167 mg, 0.12 mmol) dissolved in CH_2Cl_2 [0.4 M] was added Et_3N (1.3 mL, 5.2 mmol), followed by the dropwise addition of TIPSCl (1.1 mL, 4.8 mmol) at 0 °C. The mixture was stirred at room temperature. After 16 h, the reaction was quenched with aq. NH_4Cl and extracted with CH_2Cl_2 (3 x 50 mL). The organic layers were collected, dried over $MgSO_4$ and concentrated *in vacuo*. The resulting crude was purified using flash column chromatography on silica gel (hexanes:ethyl acetate = 3:1) to give **8-24** (1.53 g, 89% yield), as a colorless oil: ^{1}H NMR (300 MHz, $CDCl_3$, ppm) δ 1.055 (s, 21 H), 3.383 (t, *J* = 4.2 Hz, 1 H), 3.387 (t, *J* = 5.7 Hz, 2 H), 3.584 (t, *J* = 5.1 Hz, 2 H), 3.664 (s, 10 H), 3.834 (t, *J* = 5.4 Hz, 2 H); HRMS MS ES+ *m/z* calcd for $C_{17}H_{37}N_3O_4Si$ $(M+H)^+$ 376.2553, found 376.2640 (Δ 8.7 ppm).

2-{2-[2-(2-Aminoethoxy)ethoxy]ethoxy}ethoxy triisopropylsilyl ester (8-25)
8-24 (1 g, 0.3 mmol) and Ph_3P (838 mg, 0.36 mmol) dissolved in THF:H_2O (7:2) [0.02 M] was stirred at room temperature. After 48 h, the mixture was extracted with ethyl ether (3 x 50 mL). The organic layers were combined, dried over $MgSO_4$ and concentrated *in vacuo*. The resulting crude was purified using column chromatography on silica gel (hexanes followed by 1:1 hexanes: ethyl acetate followed by 10% CH_3OH in CH_2Cl_2) to give **8-25** (642 mg, 69% yield) and **8-24** (300 mg). The recovered **8-24** was again subjected to the reduction conditions to give **8-25** (200 mg, 72% yield overall 91% yield), as a colorless oil: ^{1}H NMR (300 MHz, $CDCl_3$, ppm) δ 1.055 (s, 21 H), 1.491 (br s, 2 H), 2.858 (m, 1 H), 3.503 (t, *J* = 3.9 Hz, 2 H), 3.584 (t, *J* =

6.0 Hz, 2 H), 3.602-3.673 (m, 6 H), 3.883 (t, *J* = 5.7 Hz, 2 H); HRMS MS ES+ *m/z* calcd for $C_{17}H_{39}NO_4Si$ $(M+H)^+$ 350.2648, found 350.2726 (Δ 7.8 ppm).

2-[4-Fmoc-aminobutylamino]-4-TIPSO-PEG-amino-6-biotinylhydrazidyl-*s*-triazine (8-26)
To a solution of cyanuric chloride (150 mg, 0.8 mmol) dissolved in THF [0.05 M] and cooled to 0 °C was added biotin-hydrazide (130 mg, 0.8 mmol) dissolved in THF [0.5 M] with DIPEA (0.3 mL, 0.8 mmol), dropwise. The mixture was stirred at 0 °C for 2 h. To the mixture was then added *N'*-Fmoc-1,4-diaminobutane (256 mg, 0.8 mmol) dissolved in THF [0.5 M] with DIPEA (0.3 mL, 0.8 mmol). The mixture was stirred at room temperature. As the reaction proceeded the mixture became cloudy. After 2 h, the solvent was evaporated. The resulting crude was triturated with hexanes. The resulting precipitate was washed with ethyl acetated and vacuum dried to give crude containing mono-Cl triazine, as a light-green solid. To the crude (180 mg, ~0.3 mmol) dissolved in THF [0.05 M] was added **8-25** (200 mg, 0.6 mmol) dissolved in THF [0.05 M] with DIPEA (0.06 mL, 0.3 mmol). The mixture was stirred under reflux conditions and monitored via TLC. After 24 h, the reaction vessel was allowed to cool to room temperature, the reaction solvent was evaporated. To the resulting crude was added aq. NH_4Cl and organic material was extracted with $CHCl_3$ (4 x 25 mL). The organic layers were combined, dried over $MgSO_4$ and concentrated *in vacuo* to give **8-26** (66 mg, 13% yield after 3 steps), as a red oil: ^{1}H NMR (300 MHz, $CDCl_3$, ppm) δ 0.847-0.978 (m, 2 H), 1.055-1.340 (m, 27 H), 1.445-1.590 (m, 8 H), 1.639-1.687 (m, 8 H), 1.786-1.892 (m, 3 H), 2.322-2.438 (m, 3 H), 2.913-2.969 (m, 2 H), 3.063 (m, 1 H), 3.136 (t, *J* = 6 Hz, 1 H), 3.321-3.381 (m, 3 H), 3.477-3.526 (m, 4 H), 3.590 (t, *J* = 6 Hz, 1 H), 3.638 (m, 1 H), 3.787 (m, 1 H), 3.902 (s, 1 H), 3.966 (s, 1 H), 4.145-4.187 (q, J_1 = 7 Hz, J_2 = 7.5 Hz, 2 H), 6.682 (t, *J* = 9 Hz, 1 H), 6.957-6.999 (q, J_1 = 3 Hz, J_2 = 9 Hz, 1 H), 7.025-7.065 (q, J_1 = 3 Hz, J_2 = 9 Hz, 1 H), 7.110-7.331 (m, 5 H), 7.355-7.444 (m, 1 H), 7.782 (d, *J* = 8.5 Hz, 2 H).

Cell culture system for MTT assay
Cell lines (obtained from ATCC unless otherwise noted and maintained at SBU Cell Culture/Hybridoma Facility) were cultured in RPMI-1640 Medium 10 x (Sigma Aldrich, R1145: ID-8, MCF-7) supplemented with 5% FBS (Thermo Scientific, HyClone, SH3007003), 5% Nu Serum (BD Biosciences, 355100) and 1% Penn Strip, at 37 °C in a humidified incubator with 5% CO_2. The cells were washed with DPBS and dissociated using TrypLE. The cells were incubated at 37 °C until the cells were detached from the plate, transferred to a centrifuge vial and pelleted via centrifugation at 1500 rpm for 5 min. The cells were counted per 1 mL media. The desired amount of cell media was added to the cell solution so that 8,000 cells can added to each well of a 96-well plate in 200 μL aliquots. After the addition, the cells were incubated at 37 °C with 5% CO_2.

Cell culture system for PEGylated vitamin-FITC conjugate internalization
Cells were resuspended in RPMI-1640 Medium 10 x (Sigma Aldrich, R1145) supplemented with tissue culture grade water, 0.3 g/L L-glutamine, 2.0 g/L sodium bicarbonate, 10% FBS, and 1% Penn Strep., and incubated at 37 °C in a humidified 5% CO_2 incubator for 2 to 3 days. The cells were washed with DPBS and dissociated using TrypLE. The cells were allowed to sit at room temperature until the cells were detached from the plate, transferred to a centrifuge vial and pelleted via centrifugation at 1500 rpm for 5 min. Media was added to the pellet and the pellet was disrupted. The cells were counted per 1 mL. The desired amount of media was added so that 50,000 cells could be added to each well of a 6-well plate. After the addition, the cells were

resuspended fully-supplemented RPMI-1640 Medium 10 x and incubated at 37 °C for 1 day. After the incubation period, the cells were treated with 10 μM **8-3** and incubated for 1 and 3 hour time periods. After this incubation period, the media was aspirated, the cells were washed with DPBS (2 times) and then dissociated using Hank's Enzyme Free Dissociation Solution. The dissociated cells were transferred to a centrifuge tube and pelleted via centrifugation at 1500 rpm for 5 min. The resulting pellet was washed twice with DPBS (10 mL then 1 mL). After the final wash, internalization was monitored using FACS and CFM. For CFM analysis, cells resuspended onto uncoated glass-bottomed culture dishes (MatTek Corp.).
Flow cytometry analysis of treated cells was performed with a FACSCalibur flow cytometer (SBU Medical Center Core facility laboratory), operating at a 488 nm excitation wavelength and detecting emission wavelengths with a 530/30 nm bandpass filter. Cell samples suspended in 2% formulin in DPBS were count with a minimal 10,000 cells per sample using CellQuest 3.3 software (Becton Dickinson) and the distribution of FITC fluorescence was analyzed using WinMDI 2.9 freeware (Joseph Trotter, Scripps Research Institute).

§ 8.5.0 References

1. Chen, H.-T.; Neerman, M. F.; Parrish, A. R.; Simanek, E. E. Cytotoxicity, Hemolysis, and Acute in Vivo Toxicity of Dendrimers Based on Melamine, Candidate Vehicles for Drug Delivery. *J. Amer. Chem. Soc.* **2004,** 126, 10044-10048.
2. Neerman, M. F.; Zhang, W.; Parrish, A. R.; Simanek, E. E. *In vitro* and *in vivo* evaluation of a melamine dendrimer as a vehicle for drugdelivery. *Int. J. Pharm.* **2004,** 281, 129-132.
3. Lim, J.; Simanek, E. E. Toward the Next-Generation Drug Delivery Vehicle: Synthesis of a Dendrimer with Four Orthogonally Reactive Groups. *Mol. Pharm.* **2005,** 2, 273-277.
4. Lim, J.; Simanek, E. E. Synthesis of Water-Soluble Dendrimers Based on Melamine Bearing 16 Paclitaxel Groups. *Org. Lett.* **2008,** 10, 201-204.
5. Ojima, I. Tumor-targeting drug delivery of chemotherapeutic agents. *Pure Appl. Chem.* **2011,** 83, 1685-1698.
6. Ojima, I.; Zuniga, E. S.; Berger, W. T.; Seitz, J. D. Tumor-targeting drug delivery of new-genreation taxoids. *Future Med. Chem.* **2012,** 4, 33-50.
7. Russell-Jones, G., McTavish, Kirsten, McEwan, John, Rice, John, Nowotnik, David. Vitamin-mediated targeting as a potential mechanism to increase drug uptake by tumours. *J. of Inorg. Biochem.* **2004,** 98, 1625-1633.
8. Chen, S.; Zhao, X.; Chen, J.; Chen, J.; Kuznetsova, L.; Wong, S. S.; Ojima, I. Mechanism-based tumor-targeting drug delivery system. Validation of efficient vitamin receptor-mediated endocytosis and drug release. *Bioconjugate Chem.* **2010,** 21, 979-987.
9. Ojima, I. Guided Molecular Missiles for Tumor-Targeting Chemotherapy-Case Studies Using the Second-Generation Taxoid as Warheads. *Acc. Chem. Res.* **2008,** 41, 108-119.
10. Chen, J., Chen, S., Zhao, X., Kuznetsova, L., Wong, S.S., Ojima, I. Functionalized Single-walled Carbon Nanotubes as Rationally Designed Vehicles for Tumor-Targeted Drug Delivery. *J. Am. Chem. Soc.* **2008,** 130, 16778-16785.
11. Chen, S., Zhao, X., Chen, J., Chen, J., Kuznetsova, L., Wong, S.S., Ojima, I. Mechanism-based tumor-targeting drug delivery system. Validation of efficient vitamin receptor-mediated endocytosis and drug release. *Bioconjugate Chem.* **2010,** 21, 979-987.

12. Leamon, C. P.; Reddy, J. A. Folate-targeted chemotherapy. *Adv. Drug Delivery Rev.* **2004,** 56, 1127-1141.
13. Y., L.; Low, P. S. Folate-mediated delivery of macromolecular anticancer therapeutic agents. *Adv. Drug Delivery Rev.* **2002,** 54, 675-693.
14. Lee, J. W.; Lu, J. Y.; Low, P. S.; Fuchs, P. L. Synthesis and evaluation of taxol-folic acid conjugates as targeted antineoplastics. *Bioorg. & Med. Chem.* **2002,** 10, 2397-2414.
15. Xia, W.; Low, P. S. Folate-targeted therapies for cancer. *J. Med. Chem.* **2010,** 53, 6811-6824.
16. Reddy, J. A.; Leamon, C. P. Folate receptor targeted cancer chemotherapy. In *Targeted Drug Strategies for Cancer and Inflammation*, Jackman, A. L.; Leamon, C. P., Eds. Springer Science+Buisness Media, LLC: 2011; pp 135-150.
17. Narisawa, T.; Fukaura, Y.; Yazawa, K.; Ishikawa, C.; Isoda, Y.; Nishizawa, Y. Colon cancer prevention with a small amount of dietary perilla oil high in alpha-linolenic acid in an animal model. *Cancer* **1994,** 73, 2069-2075.
18. Fritsche, K. L.; Johnston, P. V. Effect of dietary alpha-linolenic acid on growth, metastasis, fatty acid profile and prostaglandin production of two murine mammary adenocarcinomas. . *J. Nutri.* **1990,** 120, 1601-1609.
19. Sauer, L. A., Dauchy, R.T., Blask, D.E. Mechanism for the antitumor and anticachectic effects of n-3 fatty acids. *Cancer Res.* **2000,** 60, 5289-5295.
20. Willmann, J. K.; van Bruggen, N.; Dinkelborg, L. M.; Gambhir, S. S. Molecular imaging in drug development. *Nat. Rev. Drug Discov.* **2008,** 7, 591-607.
21. Harry, V. N.; Semple, S. I.; Parkin, D. E.; Gilbert, F. J. Use of new imaging techniques to predict tumour response to therapy. *Lancet Oncol.* **2010,** 11, 92-102.
22. Josephs, D.; Spicer, J.; O'Doherty, M. Molecular imaging in clinical trials. *Target. Oncol.* **2009,** 4, 151-168.
23. Padhani, A. R.; Miles, K. A. Multiparametric imaging of tumor response to therapy. *Radiology* **2010,** 256, 348-364.
24. Kostakoglu, L. FDG-PET evaluation of reponse to treatment. *PET Clinics* **2008,** 3, 37-75.
25. Mettler, F. A.; Guiberteau Jr., M. J. *Essentials of Nuclear Medicine Imaging*. 5th ed.; Saunders: Philadelphia, PA, 2006.
26. Blankenberg, F. G.; Katsikis, P. D.; Tait, J. F.; Davis, R. E.; Naumovski, L.; Ohtsuki, K.; Kopiwoda, S.; Abrams, M. J.; Strauss, H. W. Imaging of apoptosis (programmed cell death) with 99mTc annexin V. . *J. Nucl. Med.* **1999,** 40, 184-191.
27. Chang, J. C.; Gambhir, S. S.; Willmann, J. K. Imaging Techniques in Drug Development and Clinical Practice. In *Drug Delivery in Oncology*, Kratz, F.; Senter, P.; Steinhagen, H., Eds. Wiley-VCH Verlag GmbH & Co. KGaA: Weinheim, Germany, 2012; Vol. 1, pp 189-224.
28. Campbell, J. R.; Hatton, R. E. Unsymmetrically Substituted Melamines. *J. Org. Chem.* **1961,** 26, 2786-2789.
29. Drew, M. E.; Chworost, A.; Oroudjev, E.; Hansma, H.; Yamakoshi, Y. A tripod molecular tip for single molecule ligand-receptor force spectroscopy by AFM. *Langmuir* **2010,** 26, 7117-7125.
30. Schwabacher, A. W.; Lane, J. W.; Schiesher, M. W.; Leigh, K. M.; Johnson, C. W. Desymmetrization reactions: efficient preparation of unsymmetrically substituted linker molecules. *J. Org. Chem.* **1998,** 63, 1727-1729.
31. Kim, D. W.; Ahn, D.-S.; Oh, Y.-H.; Lee, S.; Kil, H. S.; Oh, S. J.; Lee, S. J.; Kim, J. S.; J.S., R.; Moon, D. H.; Chi, D. Y. A New Class of S_N2 Reactions Catalyzed by Protic Solvents:

Facile Fluorination for Isotopic Labeling of Diagnostic Molecules. *J. Amer. Chem. Soc.* **2006,** 128, 16394-16397.
32. Gottlieb, H. E.; Kotlyar, V.; Nudelman, A. NMR Chemical Shifts of Common Laboratory Solvents as Trace Impurities. *J. Org. Chem.* **1997,** 62, 7512-7515.
33. Frisch, B.; Boeckler, C.; Schuber, F. Synthesis of Short Polyoxyethylene-Based Heterobifunctional Cross-Linking Reagents. Application to the Coupling of Peptides to Liposomes. *Bioconjugate Chem.* **1996,** 7, 180-186.

Chapter 9

Macromolecular Drug Delivery Systems

Chapter Contents

§ 9.1.0 Introduction

§ 9.1.1 Macromolecular Drug Delivery Systems

Considerable effort has been made to find cancer-specific markers that can be exploited for tumor-specific delivery of traditional chemotherapeutic drugs and their analogs. As discussed in the previous chapters, a promising approach along this line is the development of tumor-targeting drug conjugates. The drugs conjugates previously mentioned are single compounds that consist of one or two cytotoxic drugs (warheads) connected to a tumor-targeting module (TTM) via cleavable covalent bonds or cleavable linkers. These drug conjugates are prodrugs that have been designed to remain inactive until they are specifically delivered to the tumor site, guided by the TTM and internalized, where the warhead is released from the carrier. Macromolecules, such as monoclonal antibodies (mAbs) and oncolytic adenoviruses (Ads), are excellent drug delivery systems (DDSs) for prodrug development. With multiple reactive sites, it is possible to functionalize mAbs and Ads with a large number of warheads and TTMs. Antibody and adenovirus-drug conjugates specifically target cancer cells and have the capability to deliver a cytotoxic payload. Furthermore, the carrier also possesses anticancer activity. Thus, conjugating cytotoxic agents to mAbs or Ads increases the tumor-specificity of the cytotoxic agents while increasing the efficacy of the macromolecular carrier.

§ 9.1.2 Monoclonal Antibodies

Recent advances in hybridoma and antibody engineering have provided the development of chimeric, humanized and fully human monoclonal antibodies that can be engineered to target specific antigens expressed by cancer cells. Antibodies are grouped into five classes based on the sequence of their heavy chain constant regions: IgM, IgD, IgG, IgE and IgA.[1] The IgG class is the most commonly used for cancer immunotherapy. Each of the five classes can then be subdivided into two functional units: the fragment of antigen binding (Fab) and the constant fragment (Fc) (Figure 6.1). The Fab contains the variable region, which consists of the complementarity-determining regions (CDRs) that form the antigen binding site and confer antigen specificity. The Fc is capable of initiating complement-dependent cytotoxicity (CDC).

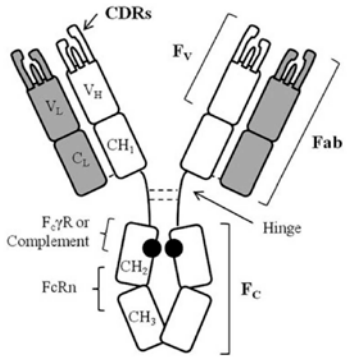

Figure 9.1: Structure of IgG (adapted from [2])

Monoclonal antibodies target epidermal growth factor receptors (EGFRs), such as EGFR, HER2, HER3 and HER4, which are overexpressed during tumorigenesis. For example, cetuximab (Erbitux; Bristol-Myers Squibb) and panitumumab (Vectibix; Amgen) function by preventing growth receptor dimerization, a vital step for initiating EGFR-mediated signal transduction.[3] Whereas trastuzumab (Herceptin, Genentech), a humanized monoclonal antibody, is specific to and inhibits the function of HER2, a gene that is overexpressed in early-stage breast cancers.

By blocking ligand binding and signaling through these growth receptors, mAbs serve to inhibit growth rates and angiogenesis and induce apoptosis. Furthermore, several mAbs have the ability to sensitize tumors to chemotherapeutic agents; as such mAbs have been used in combination with small molecule chemotherapeutic agents.[2] For example, cetuximab treatment has been combined with 5-fluorouracil (a thymidylate synthase inhibitor), folinic acid (an antimetabolite) and irinotecan (a topoisomerase I inhibitor) to prolong progression-free survival in metastatic colon cancer patients, and trastuzumab has been combined with cisplatin (DNA alkylating agent) and paclitaxel (a microtubule stabilizer) for the treatment of metastatic breast cancer.

In many cases, the combination of mAb with a chemotherapeutic agent has shown to increase survival and response rate, in comparison to the mAb alone. Thus, it is highly advantageous to combine a mAb to a cytotoxic compound through antibody-drug conjugates (ADCs). Antibody-drug conjugates combine tumor-specificity and antitumor activity of mAbs with the potent anticancer activity of cytotoxic agents.[4-6] Conjugation of a mAb to a cytotoxic agent increases the tumor-specificity of the cytotoxic agent, allowing the cytotoxic agent to be specifically delivered to tumor cells without affecting normal, healthy cells, while increasing the cancer cell-killing potential of mAbs.[6]

§ 9.1.3 Mesothelin as a Target for Immunoconjugate

Mesothelin is an antigen to mAb K1, which specifically recognizes several ovarian cancer cells.[7] Mesothelin is attached to the cell surface through glycosyl-phoshatidyl inositol link to the carboxyl terminus. Though its function is unknown, mesothelin was reported to interact with CA124, an ovarian cancer antigen, and this interaction may play a role in ovarian cancer metastasis. Furthermore, mesothelin in human bodies contains a unique distribution pattern, as its expression is limited to mesothelial cells lining the pleura, peritoneum and pericardium. However, mesothelin is overexpressed in ovarian, pancreatic and non-small lung cancers, as well as in mesothelioma.[8-10] Thus, mesothelin is a potential target for anticancer treatment.

Clone m912 was found to have a high affinity to mesothelin after a screening of 300 clones.[11] Fab m912 was converted to single chain and IgG1 formats. Fab m912 bound to mesothelin with an EC_{50} of 20 nmol/L. The IgG1 format of Fab m912 showed an effective binding affinity of ~1.5 nmol/L. This antibody is fully human and in Fab, scFv and IgG formats were able to specifically target and bind to human mesothelin. Furthermore, m912 is the first reported fully human monoclonal antibody which binds to mesothelin (Figure 9.2). As such, the use of the scFv format of m912 as a drug delivery system is currently being examined.

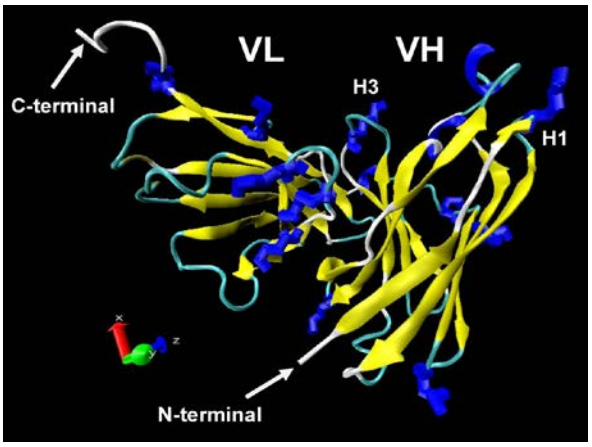

Figure 9.2: Protein structure of scFv917

§ 9.1.4 Oncolytic Adenoviruses

Oncolytic adenoviruses are viruses which have been designed and developed to selectively target and kill cancer cells by infecting, replicating and killing these cells. Adenoviruses (Ads) have linear, non-enveloped, double-stranded DNA genomes. Approximately 50 different serotypes of human Ad have been discovered and these serotypes are divided into 6 distinct subgroups (A through F) with different pathophysiologies. The Ad serotypes 2 and 5 have been widely studied as gene therapy vectors.[12]

Adenoviruses internalize through endocytosis and have the ability to transfer genes to both dividing and undividing cells.[13, 14] The virus capsid, which is the protein outer-coat that is comprised of structural proteins hexon, fibers and penton, is the key for efficient viral infection.[15] The capsid outer shell has icosahedron geometry. Each vertex of the capsid is capped with a penton base, which is comprised of a homopentameric ring of proteins. From these penton bases protrude homotrimeric fiber protein that form penton fiber capsomers (Figure9.3).[12]

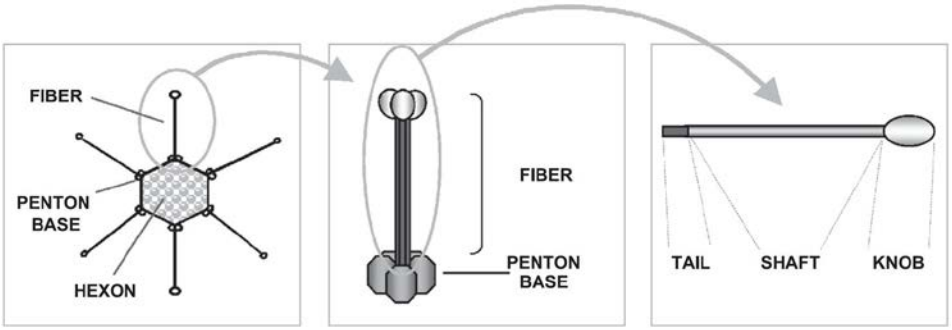

Figure 9.3: Structure of adenovirus (adapted from [12])

Infection is mediated by the penton and fiber capsid proteins, which interact with cellular factors to permit the passage of viral particles into the cell. The fiber is responsible for cell attachment. The fiber of subgroup C Ad binds to the coxsackievirus-adenovirus receptor (CAR) cell surface protein.[16] The CAR bears structural similarity to immunoglobin (Ig) gene superfamily proteins. CAR contains two Ig-like regions, D1 and D2, which interact with the Ad2 and Ad12 fiber knob. These regions are sufficient for binding.

After the fiber binds to CAR, the penton proteins bind to $\alpha_v\beta_3$ or $\alpha_v\beta_5$ integrins through a conserved Arg-Gly-Asp (RGD) motif.[12, 17] The RGD sites lie at the ends of flexible loops, allowing access to integrins. When the fiber is bound, IgG recognition of RGD motifs is sterically hindered, thus preventing antibody neutralization of RGD.[18] Upon fiber release, the penton undergoes structural changes. These structural changes initiate the subsequent steps of virus cell entry (Figure 9.4).

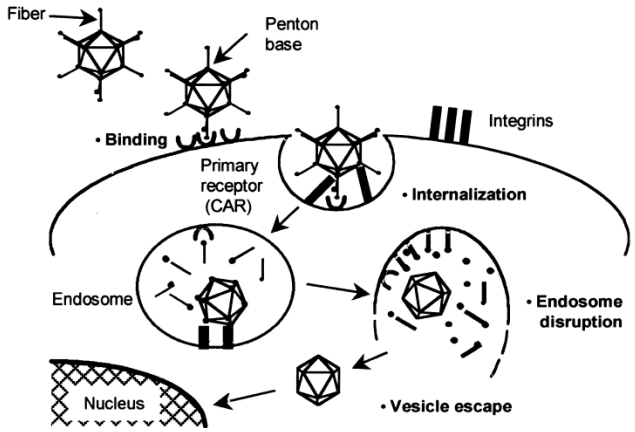

Figure 9.4: Pathway of adenoviral infection (adapted from [19])

The Ad is internalized via endocytosis and transferred into an endosome after binding (Figure 9.4). While in the endosome, the capsid sheds excess fiber proteins, thus exposing more penton proteins.[19, 20] When the pH drops to 6, the virus penetrates the endosomal membrane and escapes to the cytosol.[19] While in the cytosol, Ad capsids translocate toward the nucleus and accumulate at the nuclear periphery. The caspids then dock at the nuclear pore complex (NPC) and import nuclear material to the nucleus of the cell.[21]

Conditionally replicative oncolytic adenoviruses are designed to preferentially replicate in cancer cell, leading to selective tumor toxicity. Some of these viruses carry a toxic transgene designed to amplify the inherent cytotoxic nature. However, in clinical trials these viruses have shown limited efficacy. As such, Ads have been combined with cytotoxic agents, such as paclitaxel and cisplatin, to increase the efficacy of the virus and tumor-specificity of the cytotoxic agent. Thus, the use of Ads as a drug delivery system in prodrug development shows promise.

§ 9.1.5 Tumor-Targeting Adenovirus

The TRAIL (TNF related apoptosis inducing ligand) transgene is one of the most promising oncolytic Ads in clinical trials, which induces apoptosis in the infected cell and mediates substantial bystander cytotoxicity. It has been hypothesized that the conjugation of taxoid to AdTRAIL would promote synergistic anticancer activity, increased efficacy and tumor-specificity. This conjugation has been achieved through selective chemical modification routes for adenovirus. Carrico, et al. reported the incorporation and modification of a non-canonical sugar residue, *O*-GlcNAz on serine 109 of the fiber protein, as a means of chemoselectively tailoring Ad particles.[22] The azide modification provides a means to couple folate as the TTM and a taxoid as the warhead (Figure 9.4).

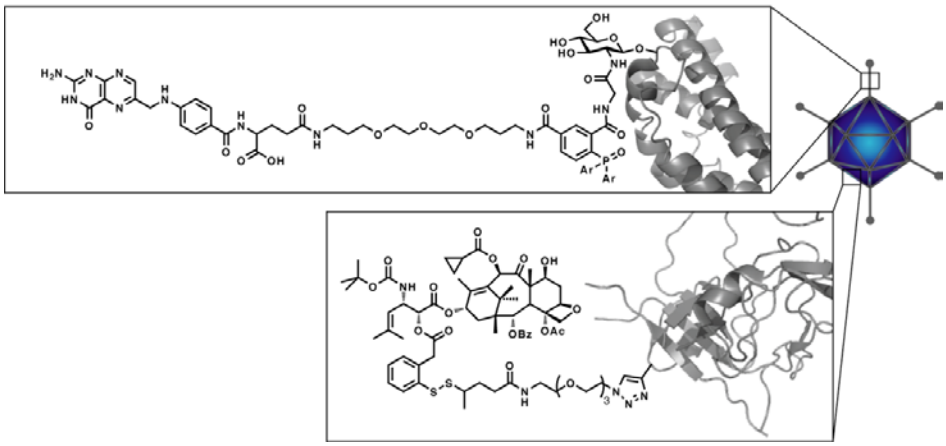

Figure 9.5: Folate-Adenovirus-SB-T-1214 drug conjugate

§ 9.2.0 Results and Discussion

§ 9.2.1 scFv917-Me-Linker-SB-T-1214 Drug Conjugate

In collaboration with the National Cancer Institute (NCI), the synthesis of scFv917-linker-taxoid drug conjugate is currently in progress. The scFv917 antibody is one-sixth the size of a normal monoclonal antibody and bears 17 free lysines which are accessible to coupling. The drug conjugate synthesis was attempt using SB-T-1214-Me-linker-OSu coupling-ready construct (**4-20**) (Scheme 9.1).

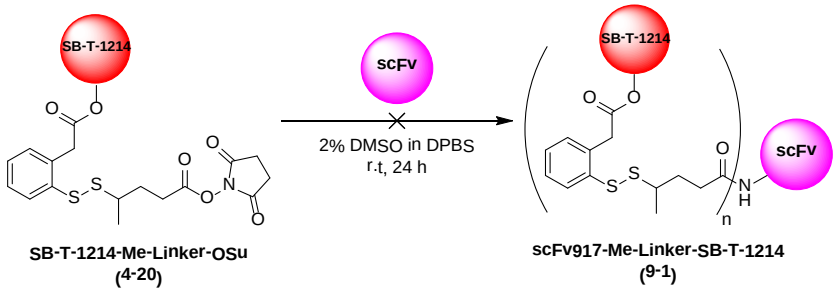

Scheme 9.1: 1st attempted synthesis of scFv917-Me-linker-SB-T-1214

The antibody was shipped as a 5.2 μM stock solution in DPBS. The synthesis was done at a microscale level. A 100 μM stock solution of **4-20** in DMSO was prepared. To this stock solution was added the antibody in DPBS. However, after 24 h no reaction was observed. MALDI analysis of the starting material suggested that the antibody was impure. NCI prepared more of the antibody and sent a purer batch. The coupling of **4-20** to pure scFv917 was examined (Scheme 9.2).

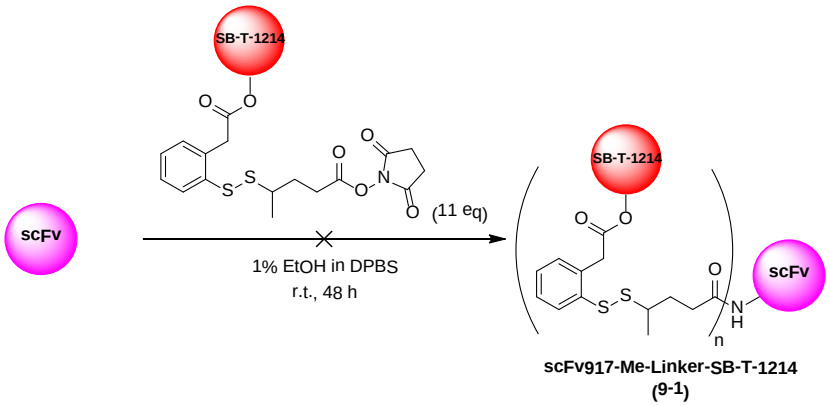

Scheme 9.2: 2nd attempted synthesis of scFv917-Me-linker-SB-T-1214

For this reaction a large excess of **4-20** (11 equivalents) was used. Ethanol was used as co-solvent as other coupling reactions involving macromolecules performed in the Ojima laboratory were successful. However, similar to the initial coupling attempts, the addition of antibody to **4-20** resulted in the formation of precipitate and no reaction. The precipitate was determined to be **4-20** which crashed out of solution with the addition of DPBS. To assist the coupling reaction, the synthesis of water-soluble taxoid was attempted.

§ 9.2.2 Water-Soluble Taxoid for Coupling in Aqueous Media Using PEG

It was hypothesized that the hydrophobicity of the SB-T-1214-Me-linker-OSu "coupling-ready construct" may prevent the mAb from fully interacting with the reactive site of the construct. As such, water-soluble taxoid-linker "coupling-ready constructs" were designed. The use of PEG-moieties to increase water solubility of taxoids has been discussed in several articles.[23-27] Accordingly, it was proposed that the incorporation of a PEG moiety to the C-7 position of SB-T-1214 would increase the water-solubility of the "coupling-ready" construct. For this purpose, 11-azido-3,6,9-trioxaundecan-1-amine was prepared starting from dimesylation of tetraethylene glycol, followed by selective substitution in the presence of sodium azide (Scheme 9.3).[28, 29]

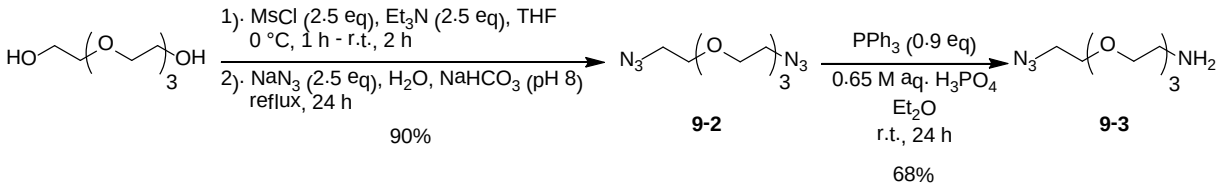

Scheme 9.3: Synthesis of 11-azido-3,6,9-trioxaundecan-1-amine

Dimesylation of tetraethylene glycol was accomplished using excess mesylchloride. The dimesylate was not isolated and immediately treated with sodium azide in aqueous buffer to afford **9-2** in excellent yield (90%). Subjecting **9-2** to selective reduction in the presence of triphenylphosphine and phosphoric acid gave **9-3** in moderate yield (68%). Lee, et al. reported that the incorporation of carboxylic acid and ether moieties help increase the water-soluble of taxoid-PEG compounds.[27] For this purpose, **9-3** was treated with diglycolic anhydride (DGA) to

give **9-4**. The free carboxylic acid was protected with allyl alcohol and the azide was reduced using Staudinger reduction conditions (Scheme 9.4).

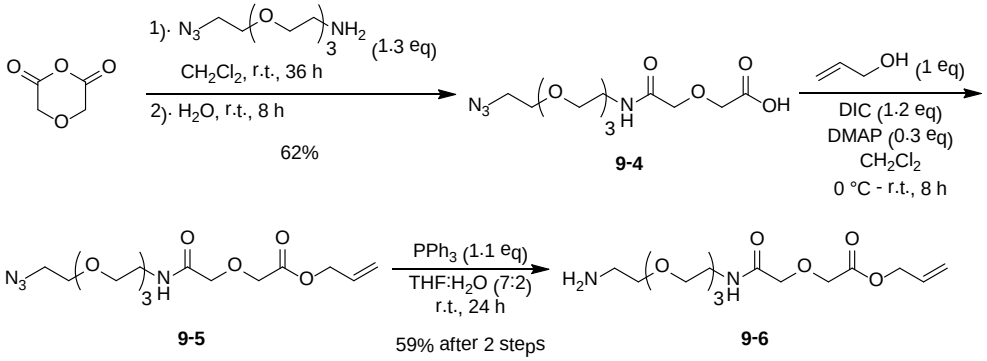

Scheme 9.4: Synthesis of modified PEG chain

Ring-opening substitution of **9-3** to DGA gave **9-4** in moderate yield (62%). The resulting free acid was protected with an Alloc moiety in the presence of allyl alcohol, DIC and DMAP to give **9-5**. Reduction of **9-5** in the presence of triphenylphosphine in THF and water affords **9-6** in moderate yield (59% after 2 steps). It was reported that the solubility of paclitaxel increases in water when the C-7 position is modified with a PEG moiety.[27] Furthermore, this PEG-modification does not substantially affect the activity of the drug.[27] For this purpose, **9-6** was treated with diglycolic anhydride giving **9-7**. The coupling of **9-7** to 2'-OTBS-SB-T-1214 (previously prepared by Dr. Xianrui Zhao) was attempted using DIC and DMAP (Scheme 9.5).

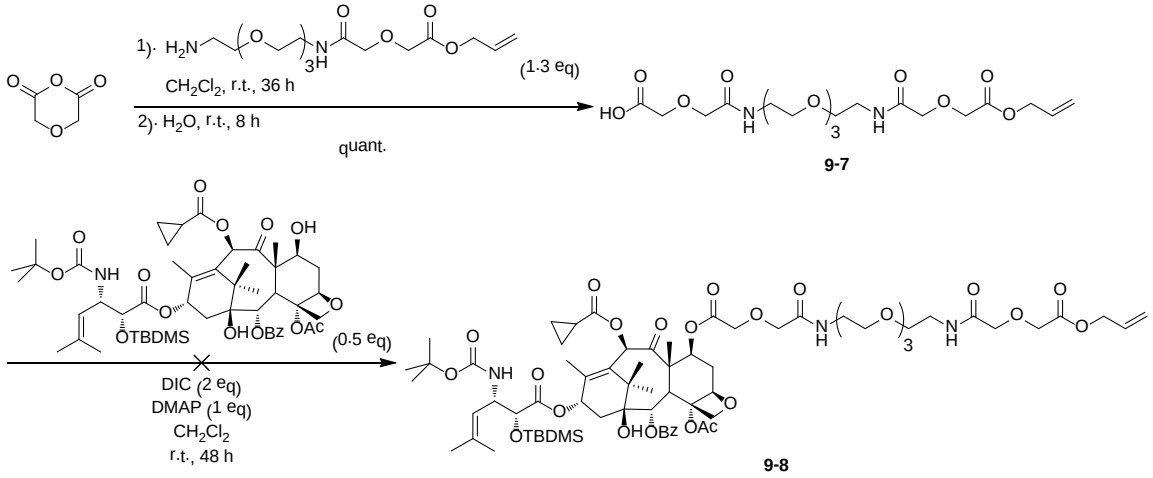

Scheme 9.5: 1st attempted synthesis of SB-T-1214 bearing PEG moiety at C-7 position

The ring-opening substitution reaction between **9-6** and DGA afforded **9-7** in quantitative yield. However, the attempted coupling of **9-7** to the C-7 position of the taxoid did not generate **9-8**. It was hypothesized that DIC was not the optimal choice of coupling reagent and that DCC or EDC may give better results when coupling to the C-7 position of the taxoid. Accordingly, coupling of **9-4** to 2'-OTBS-SB-T-1214 was attempted using both DCC and EDC as a model reaction (Scheme 9.6).

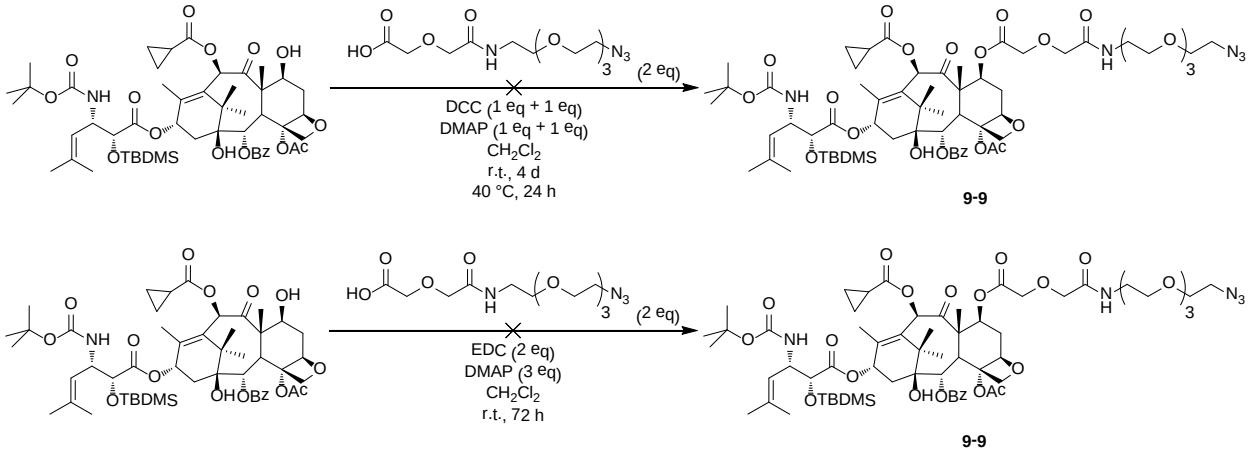

Scheme 9.6: Attempted coupling of PEG to C-7 position of taxoid

Unfortunately, **9-9** was not obtained when either DCC or EDC was used as a coupling reagent. It is reasonable to assume that the C-7 hydroxyl moiety of the taxoid is too sterically hindered to react. Also, the freely rotating bonds of the PEG moiety may also block the carboxylic acid moiety from reacting. Furthermore, it is unknown whether or not the PEG chain would affect the cytotoxic activity of the taxoid. Accordingly, C-7 position modification with a cleavable amino acid was examined.

§ 9.2.3 Water-Soluble Taxoid for Coupling in Aqueous Media Using Amino Acids

The amine and carboxylic acid moieties of amino acids are zwitterionic, making amino acids amphiprotic and easily water soluble. Thus, amino acids have been used as spacers in taxoid-based prodrugs and taxoid derivatives to increase the water solubility of these compounds.[30, 31] These amino acids are attached to the C-2` hydroxyl of the taxoid. The amino acid residue is cleaved while in circulation, thus the cytotoxicity of the taxoid is not affected. It was hypothesized that the incorporation of amino acid residues to the C-7 position would also increase the water solubility of the taxoid. Furthermore, the amino acid residue can be cleaved from the taxoid under basic or acidic conditions after coupling to the mAb or protein. For this purpose, a Glu-Lys dipeptide was designed (Figure 9.6).

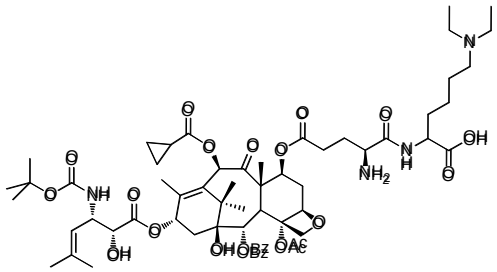

Figure 9.6: SB-T-1214 bearing Glu-Lys dipeptide at C-7 position

Glutamic acid has a γ-carboxylic acid which can intramolecularly cyclize with the α-amine to form pyroglutamic acid or pyroglutamate. This cyclization can occur spontaneously and is found in many proteins. Exploiting this cyclization, a C-7 γ-Glu-Lys-taxoid has been designed.

This dipeptide spacer has been designed to have the cyclization of the α-amine and γ-ester release the drug, as well as generate pyroglutamic acid (Figure 9.7).

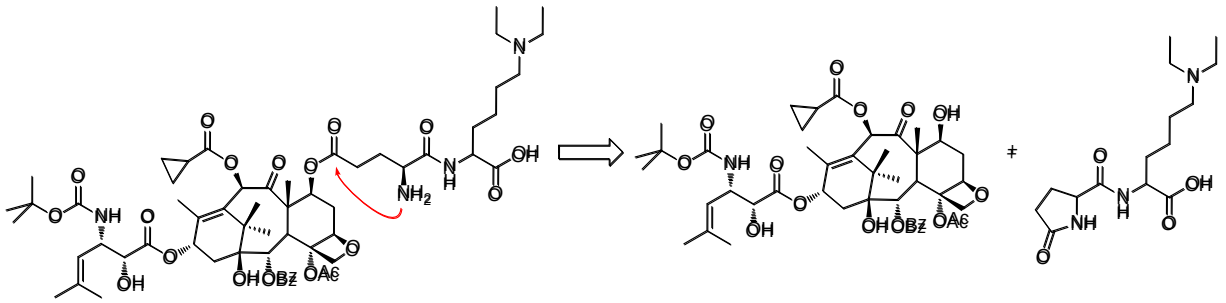

Figure 9.7: Proposed dipeptide cleavage from SB-T-1214

The synthesis of the Glu-Lys dipeptide begins with functional group modifications of both Glu and Lys. The modifications of Glu entail the selective protection of the γ-carboxylic acid, leaving the α-carboxylic acid free to react with Lys. Selective protection was attempted via benzyl-protection the α-carboxylic acid using DCC (Scheme 9.7).

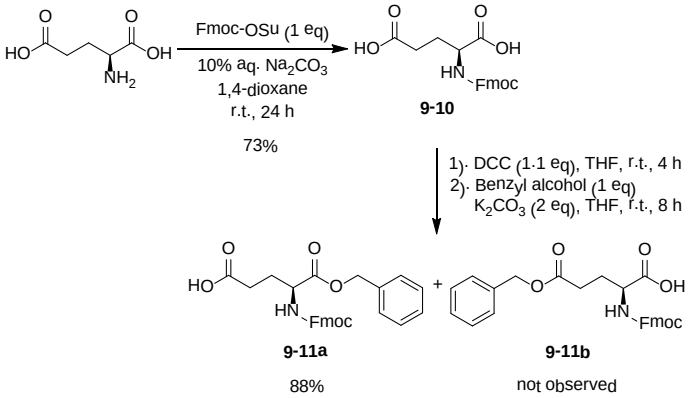

Scheme 9.7: Attempted selective benzyl-protection of Glu

Fmoc-protection of Glu in the presence of Fmoc-OSu gave **9-10** in moderate yield (73%). The Fmoc moiety was installed assuming that it will sterically block the α-carboxylic acid, thus hinder the reactivity. Unfortunately, treatment of **9-10** with DCC and then with benzyl alcohol gave α-benzyl-Glu, **9-11a**, as the major product. The desired γ-benzyl-Glu, **9-11b**, was not observed. However, *N*-Fmoc-γ-Cbz-Glu is commercially available. Accordingly, *N*-Fmoc-γ-Cbz-Glu was added to N_{ε}-Boc-α-Alloc-Lys in the presence of DCC. Boc-deprotection, two reductive alkylations of lysine ε-amine, Cbz-deprotection and esterification was attempted to generate a model compound to examine pyroglutamic acid formation (Scheme 9.8).

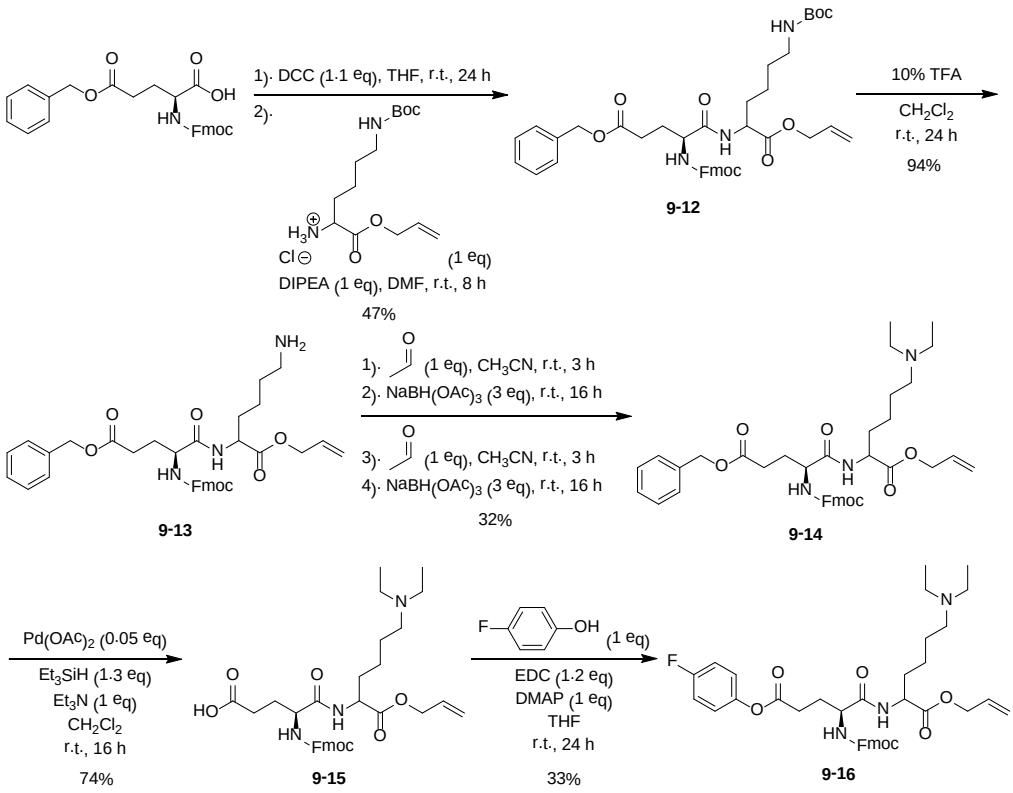

Scheme 9.8: Synthesis of Glu-Lys dipeptide

The dipeptide **9-12** was obtained in fair yield (47%). Boc deprotection was achieved using TFA to afford **9-13** (94%), which was immediately subjected to reductive alkylation to give **9-14** in fair yield (32%). The reductive alkylation steps were messy, leading to the formation of several byproducts or reaction intermediates. Cbz-deprotection was achieved using lead (II) acetate and triethylsilane to give **9-15** in moderate yield (74%). Esterification of **9-15** with *p*-fluorophenol in the presence of EDC gave **9-16** in fair yield (33%). It should be noted that the purification of each intermediate is very difficult using column chromatography. To test intramolecular ring-closure and pyroglutamic acid formation, dipeptide **9-17** was dissolved in water and heated (Scheme 9.9).[32]

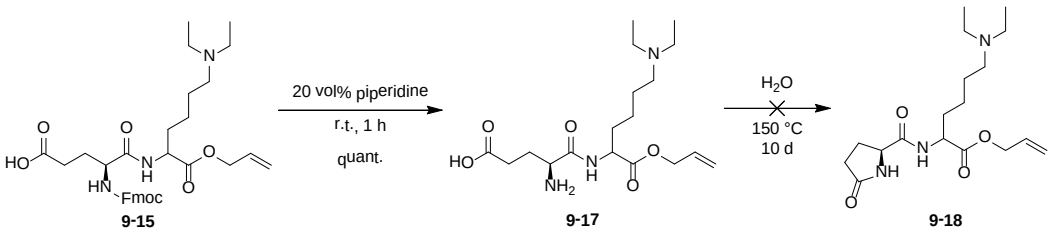

Scheme 9.9: Pyroglutamic acid formation

Fmoc-deprotection was achieved using 20% piperidine in DMF to give **9-17** in quantitative yield. Unfortunately, the formation of the pyroglumatic lactam was not observed after 10 days at elevated temperatures, as described by Martin et al.[32] The cyclization of Glu is currently being examined using higher temperatures and by changing the pH of the reaction

media. To increase the overall yield of the isolated dipeptide and to limit formation of impurities, the synthesis of the Glu-Lys dipeptide was attempted via solid-phase synthesis (Scheme 9.10).

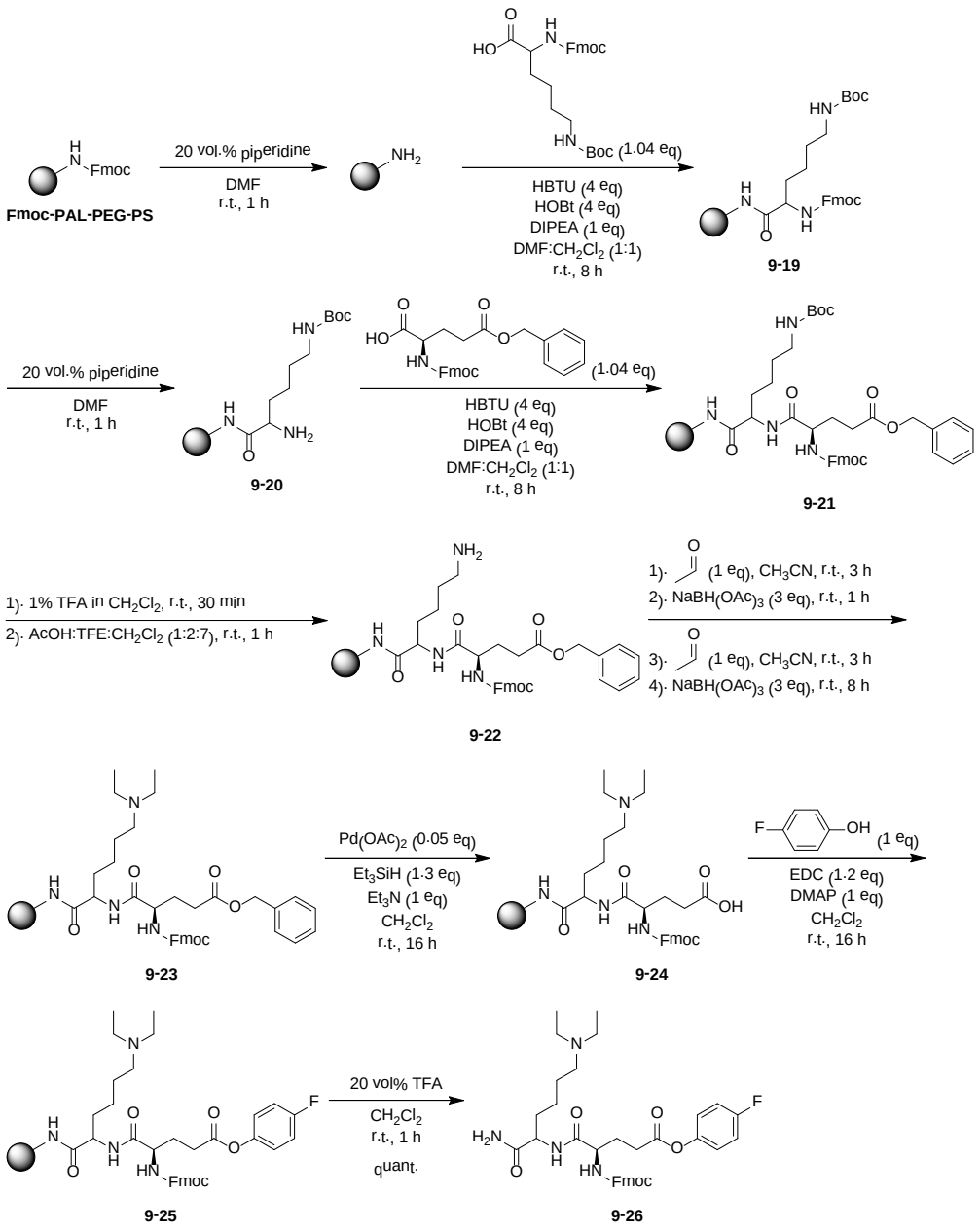

Scheme 9.10: Synthesis of Glu-Lys dipeptide using solid phase synthesis

Through solid-phase synthesis the desired dipeptide, **9-26**, was obtained in excellent overall yield. It should be noted that to incorporate SB-T-1214 to the taxoid, the resin will have to be cleaved prior to drug coupling. Cleaving the resin early will result in a dipeptide bearing a terminal carboxylic acid and a terminal amide. The resulting amide may interfere with the drug coupling. This coupling is currently being examined.

§ 9.2.4 Tumor-Targeting Oncolytic Adenovirus-Linker-SB-T-1214 Drug Conjugate

In collaboration with the Carrico research group (Stony Brook University), a novel taxoid-based drug conjugate that employs a surface-modified oncolytic adenovirus as both DDS and cytotoxic agent has been designed. The surfaces of two Ads have been modified to bear an alkyne or azide, respectively. Thus drug moieties can be "clicked" to the virus using modified drug compounds. For this purpose, SB-T-1214-Me-linker-OSu "coupling-ready" construct was modified to bear a terminal alkyne or azide moiety (Scheme 9.11 and 9.12).

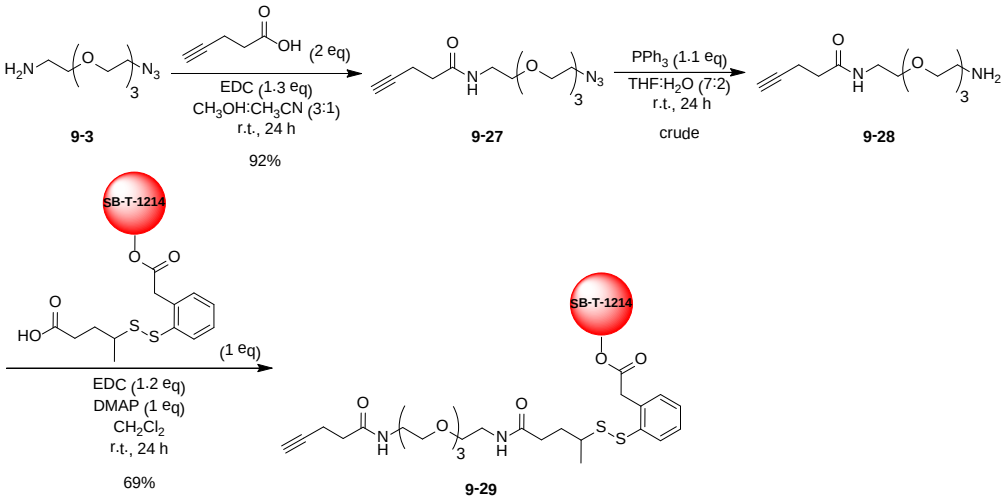

Scheme 9.11: Synthesis of SB-T-1214-Me-linker-PEG-spacer-alkyne

The coupling of **9-3** to 4-pentynoic acid in the presence of EDC afforded **9-27** in excellent yield (92%). Staudinger reduction of **9-27** gave the corresponding amine (**9-28**), which was then added to **4-19** in the presence of EDC to give **9-29** in moderate yield (69%). **9-29** has a terminal alkyne that can be coupled to the azide-Ads using CuCl-catalyzed "click" conditions. It is worthy of note that **9-29** was not soluble in a mixture of DMSO and water, as the addition of water to **9-29** dissolved in DMSO lead to the compound crashing out of solution. Thus, **9-29** was not used in coupling to azide-Ads. To prepare the terminal azide bearing taxoid-linker compound, **4-19** was treated with EDC and DMAP, followed by the addition of **9-3** (Scheme 9.12).

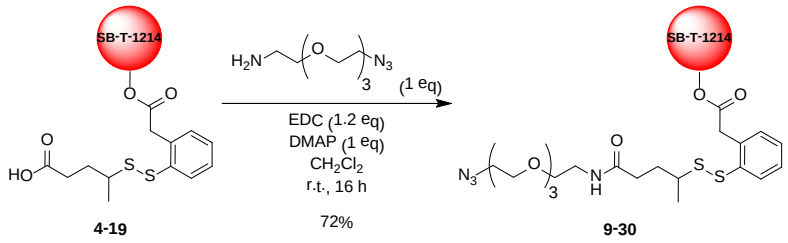

Scheme 9.12: Synthesis of SB-T-1214-Me-linker-PEG-azide

The resulting treatment of **4-19** with **9-3** in the presence of EDC and DMAP gave **9-32** in moderate yield (72%). **9-30** contains a terminal azide which can be used for coupling to alkyne-Ads using CuCl-catalyzed "click" conditions. Furthermore, **9-30** remained soluble in a mixture of DMSO and water. The coupling of **9-30** to alkyne-Ads was examined in collaboration with

Partha Banerjee (Carrico research group). AdTRAIL is a modified Ad developed in the Carrico laboratory which bears folate on the virion surface, coupled via PEG moieties.[22, 33] Further modifications include an alkyne moiety on the viron surface which can be utilized for coupling. The coupling of AdTRAIL with **9-30** was done using copper assisted 'click' reaction conditions under de-oxygenating conditions in the presence of 3 mM bathophenanthroline disodium salt and 1 mM CuBr for 12 h at room temperature. AdTRAIL-PEG-linker-SB-T-1214 was purified by size exclusion and used to infect ID-8 cancer cells at multiplicities of infection (MOIs) that were expected to be subtoxic for AdTRAIL alone.[33]

Levels of free SB-T-1214 equivalent to that loaded on virion, as well as unmodified AdTRAIL were used for comparison. Importantly, the only difference between the processing of AdTRAIL and AdTRAIL-PEG-linker-SB-T-1214 was the addition of HPG during production of the latter. Specifically, AdTRAIL was exposed to identical 'click' conditions as AdTRAIL-PEG-linker-SB-T-1214, however due to the absence of homopropargylglycine, AdTRAIL was presumably unmodified. Five days post infection, cytotoxicity was assessed via MTT assay (Roche, KitI) (Figure 9.8).

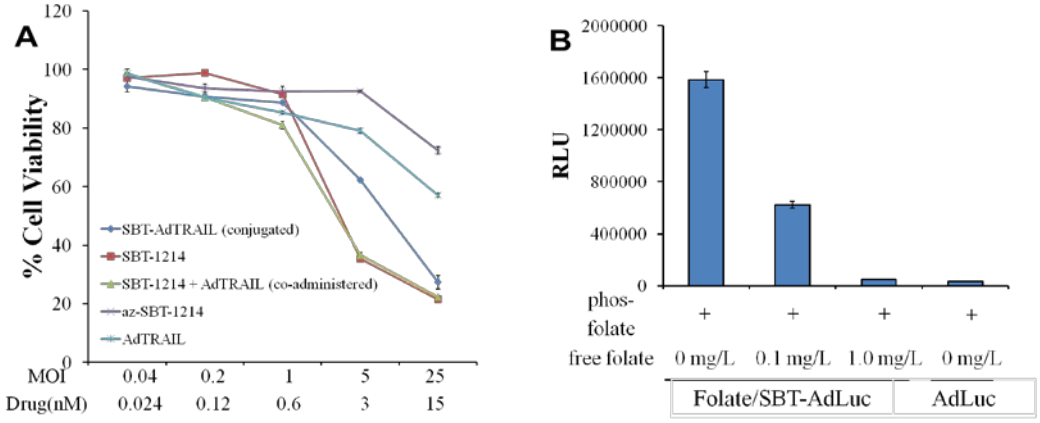

Figure 9.8: Biological evaluation of SBT-AdTRAIL: (A) MTT assay to determine cytotoxicity of HPG and GalNAz incorporated TRAIL-Ad5 – chemically labeled with SBT-1214. Comparison of cytoxicity profiles of metabolically unlabeled TRAIL-Ad5(AdTRAIL), free drug (SBT-1214), free azide-drug conjugate (az-SBT-1214), and co-administered AdTRAIL and SBT-1214 (SBT-1214 + AdTRAIL) with drug labeled TRAIL expressing adenovirus (SBT-AdTRAIL) on ovarian carcinoma cells (ID8); (B) Targeting analysis of SB-T-1214 and folate modified AdLuc. Luciferase analysis of 4T1 cells 24 hours post infection with modified virions both in the presence and absence of external folic acid showing dose dependent gene expression.

TRAIL expressing viruses that were covalently linked with az-SB-T-1214 demonstrated an increase in cytotoxicity compared to free azSB-T-1214 and AdTRAIL alone, consistent with the proposed synergistic effect (Figure 9.8A). Unmodified SB-T-1214, both alone and co-administered with AdTRAIL demonstrated higher levels of cell cytotoxicity. Presumably, this effect is due to a difference in the kinetics of cellular penetration of the free drug versus covalently linked SB-T-1214 and AdTRAIL.

Furthermore, the addition of az-SB-T-1214 to Ad may alter the uptake profiles of the Ad-drug conjugate compared to folate-Ad (Figure 9.8B). In order to explore these effects, dually modified Ad bearing a luciferase transgene (AdLuc) were screened against 4T1 (murine breast) cancer cell line. Cells grown under folate free media for 2 weeks were seeded on 96 well plates at concentrations of 10,000 cells per well. Infection was accomplished at a MOI of 50 and cells were examined for luciferase activity 24 h post infection (Luc-Bright-Glow). Folate targeted SB-

T-1214 AdTRAIL demonstrated a 30 fold increase in transgene expression on breast cancer cell type (4T1) compared to virion lacking O-GlcNAz. In addition, treatment of cells with free folate prior to infection led to a dose dependent loss in virus infection (Figure 9.8B).

§ 9.3.0 Summary

Macromolecules are currently being developed and used as carriers for a large number of cytotoxic agents, TTMs and imaging agents. A number of mAb-based immunoconjugates have been developed and are currently in human clinical trials. However, only a few immunoconjugates have been given FDA-approval. There are several benefits that macromolecules, such as mAbs and Ads, have as drug delivery systems. Monoclonal antibody- and adenovirus-based DDSs can specifically target cancer cells. Thus, DDSs functionalized with multiple cytotoxic drugs can deliver a payload to cancer cells, increasing the efficacy of the drugs released. Cytotoxic agents can be installed onto these DDSs at specific reactive sites, i.e. the free amine of accessible lysines or terminal alkynes or azides. However, coupling of hydrophobic drug to these water-soluble DDSs can be difficult. Thus, novel water-soluble drugs need to be developed. Water-solubility can be obtained through the incorporation of water-soluble moieties to the drug. Macromolecules will play a crucial role in the future of drug development. These macromolecular-based drug conjugates will possess excellent tumor-specificity and substantial anticancer efficacy, thus enabling the treatment of challenging tumors.

§ 9.4.0 Experimental

Caution

Taxoids have been established as a potent cytotoxic agent. Thus, they and all structurally related compounds and derivatives must be considered as mutagens and potential reproductive hazards for both males and females. Appropriate precautions (i.e. use of gloves, goggles, lab coat and fume hood) must be taken while handling these compounds.

General information

All chemical were obtained from Sigma-Aldrich, Fisher Scientific or VWR International, and used as is unless otherwise noted. All reactions were carried out under nitrogen in oven dried glassware using standard Schlenk techniques unless otherwise noted. Reactions were monitored by thin layer chromatography (TLC) using E. Merck 60F254 precoated silica gel plates and alumina plate depending on the compounds. Dry solvents were degassed under nitrogen and were dried using the PURESOLV system (Inovatative Technologies, Newport, MA). Tetrahydrofuran was freshly distilled from sodium metal and benzophenone. Dichloromethane was also distilled immediately prior to use under nitrogen from calcium hydride. Toluene was also distilled immediately prior to use under nitrogen from calcium hydride. Yields refer to chromatographically and spectroscopically pure compounds. Flash chromatography was performed with the indicated solvents using Fisher silica gel (particle size 170-400 Mesh).^{1}H, ^{13}C and ^{9}F data were obtained using either 300 MHz Varian Gemni 2300 (75 MHz ^{13}C, 121 MHz ^{19}F) spectrometer, the 400 MHz Varian INOVA 400 (100 MHz ^{13}C) spectrometer or the 500 MHz Varian INOVA 500 (125 MHz ^{13}C) in $CDCl_3$ as solvent unless otherwise stated. Chemical shifts (δ) are reported in ppm and standardized with solvent as internal standard based on

literature reported values.[34] Melting points were measured on Thomas Hoover Capillary melting point apparatus and are uncorrected. Optical rotations were measured on Perkin-Elmer Model 241 polarimeter.

Experimental procedure

scFv917-Me-linker-SB-T-1214 drug conjugate (9-1)

Attempt 1

A 4 μL solution containing a final concentration of 100 μM SB-T-1214-linker-OSu coupling-ready construct (**4-20**) in DMSO was prepared. To this solution was added 200 μL of 5.2 μM solution of scFv in DPBS. Following the addition, the reaction mixture became cloudy and precipitate formed after 10 minutes. The heterogeneous mixture was mixed for 24 h at room temperature. MALDI analysis of the mixture determined that no reaction occurred.

Attempt 2

A 465.3 μM solution of SB-T-1214-linker-OSu coupling-ready construct (**4-20**) in 2.4 μL ethanol was prepared. To this solution was added 200 μL of 42.3 μM scFv in DPBS. Precipitate formed upon addition of the antibody to the construct. The mixture was vortexed, and then a 91 μL aliquot was removed and transferred to a centrifuge tube. To this aliquot was added an additional 9 μL ethanol. Both scFv and construct mixtures were stirred at room temperature for 48 h. MALDI analysis of both mixtures determined that no reaction occurred.

Azido-PEG$_3$-azide (9-2)[28, 29]

To tetraethylene glycol (10 g, 52 mmol) and MsCl (10 mL, 130 mmol) dissolved in THF [2 M] cooled to 0 °C was slowly added Et_3N (18 mL, 130 mmol) over 20 min. During the addition, off-white precipitate formed. The mixture was stirred at 0 °C for 30 min. After 30 min, the ice-bath was removed and the mixture was stirred at room temperature. After 2 h, water was added to dissolve precipitate. The reaction vessel was placed back into ice-bath and the reaction solution pH was adjusted to 8 with solid $NaHCO_3$. To the mixture was added NaN_3 (8.5 g, 130 mmol). The organic solvent was evaporated *in vacuo* and the remaining aqueous layer was retained. The aqueous layer was stirred under reflux conditions. After 24 h, the mixture was cooled to room temperature. The aqueous layer was extracted with ethyl ether (5 x 50 mL). The organic layers were collected, washed with brine (3 x 50 mL), dried over $MgSO_4$ and concentrated *in vacuo* to yield **9-2** (11 g, 90% yield); ^{1}H NMR (300 MHz, $CDCl_3$, ppm) δ 3.26-3.29 (m, 3 H), 3.47-3.50 (m, 1 H), 3.55-3.58 (m, 11 H). All data are consistent with literature values.[28, 29]

Azido-PEG$_3$-amine (9-3)[28, 29]

To **9-2** (9 g, 37 mmol) dissolved in 0.65 M aqueous H_3PO_4 (84 mL) was slowly added PPh_3 (8.7 g, 33 mmol) dissolved in ethyl ether [2 M]. After the addition, the reaction solution became cloudy and pink. The mixture was stirred at room temperature. After 24 h, the mixture was diluted with water and extracted with ethyl ether (3 x 50 mL). The aqueous layer was collected. To the aqueous layer was added KOH (6.75 g). The mixture was stored in the freezer. After 16 h, TPPO precipitate formed. Solids were filtered over a Büchner funnel and washed with water. The mixture was extracted with CH_2Cl_2 (5 x 100 mL). The organic layers were combined, dried over $MgSO_4$ and concentrated *in vacuo* to yield **9-3** (5.5 g, 68% yield): ^{1}H NMR (300 MHz, $CDCl_3$, ppm) δ 1.820 (s, 2 H), 2.715 (br s, 2 H), 3.246 (t, J = 4.8 Hz, 2 H), 3.369 (t, J = 5.4 Hz, 2 H), 3.510 (s, 11 H). All data are consistent with literature values.[28, 29]

DGA-PEG$_3$-azide (9-4)[35]

To DGA (90 mg, 0.8 mmol) was added **9-3** (0.2 mL, 1 mmol) dissolved in CH_2Cl_2 [0.01 M]. The mixture was stirred at room temperature and the reaction was monitored via TLC. After 36 h, 1 mL water was added and the mixture was stirred at room temperature. After 8 h, $MgSO_4$ was added and the organic layer was filtered through celite to yield **9-4** (160 mg, 62% yield) as orange oil: ^{1}H NMR (300 MHz, $CDCl_3$, ppm) δ 1.820 (s, 3 H), 2.715 (br s, 2 H), 3.246 (t, *J* = 4.8 Hz, 2 H), 3.369 (t, *J* = 5.4 Hz, 2 H), 3.510 (s, 11 H), 5.188 (s, 1 H). All data are consistent with literature values.[35]

Allyloxycarbonylmethoxyacetyl-PEG-amine (9-6)[35]

To **9-4** (100 mg, 0.3 mmol) dissolved in CH_2Cl_2 [0.2 M] cooled to 0 °C was added a solution containing allyl alcohol (0.02 mL, 0.3 mmol) and DMAP (11 mg, 0.09 mmol) in CH_2Cl_2 [0.2 M], followed by the addition of DIC (0.05 mL, 0.36 mmol). The mixture was stirred at room temperature and the reaction was monitored via TLC. After 8 h, the reaction solution was filtered through celite and the mother liquor was evaporated to yield a crude mixture containing **9-5**. To the crude mixture containing **9-5** was added PPh_3 (110 mg, 0.33 mmol). The solids were dissolved in 2 mL 7[35]:2 THF:water [0.01 M]. The mixture was stirred at room temperature and the reaction was monitored via TLC, staining with ninhydrin. After 24 h, the reaction solvent was evaporated. The residue was triturated with ethyl ether forming a precipitate. The organic layer was filtered through cotton, evaporated and the resulting crude was purified using flash column chromatography on silica gel (10% toluene in $CHCl_3$) to yield TPPO and (10% CH_3OH in $CHCl_3$) to yield **9-6** (62 mg, 59% yield after 2 steps), as orange oil: ^{1}H NMR (300 MHz, $CDCl_3$, ppm) δ 1.102-1.457 (m, 3 H), 1.514-1.946 (m, 2 H), 3.110 (s, 1 H), 3.333-3.374 (m, 2 H), 3.440 (s,2 H), 3.457-3.725 (m, 14 H), 4.028 (br s, 1 H). All values are consistent with literature values.

***N*-Allyloxycarbonylmethoxyacetyl-*N'*-hydroxycarbonylmethoxyacetyl-PEG-diamine (9-7)**

To DGA (10 mg, 0.08 mmol) was added **9-6** (40 mg, 0.1 mmol) dissolved in CH_2Cl_2 [0.01 M]. The mixture was stirred at room temperature and the reaction was monitored via TLC. After 36 h, water (0.1 mL) was added and the mixture was stirred at room temperature. After 8 h, $MgSO_4$ was added and the organic layer was filtered through celite to yield **9-7** (42 mg, quant. yield) as orange oil: ^{1}H NMR (300 MHz, $CDCl_3$, ppm) δ 1.232 (t, *J* = 7.2 Hz, 4 H), 1.376 (m, 4 H), 1.573 (m, 1 H), 1.705 (m, 1 H), 1.940 (m, 1 H), 2.019 (s, 2 H), 3.230 (m, 1 H), 3.351 (br s, 3 H), 3.518-3.744 (m, 26 H), 4.202 (br s, 1 H),

Attempted synthesis of 2`-TBS-(*N*-allyloxycarbonylmethoxyacetylamino-PEG)carbamoylmethoxyacetyl-SB-T-1214 (9-8)

A mixture of 2`-OTBS-SB-T-1214 (40 mg, 0.04 mol), **9-7** (20 mg, 0.08 mmol), DIC (0.01 mL, 0.08 mmol) and DMAP (2 mg, 0.04 mmol) was dissolved in CH_2Cl_2 [0.05 M]. The mixture was stirred at room temperature and the reaction was monitored via TLC. After 48 h, no reaction was observed, the reaction solvent was evaporated and the resulting crude was purified using flash column chromatography on silica gel to yield 48 mg crude mixture containing 2`-OTBDMS-SB-T-1214 and diisopropylurea.

Attempted synthesis of 2`-TBS-(N-azidoethyl-PEG)carbamoylmethoxyacetyl-SB-T-1214 (9-9)

Method 1

To 2`-OTBS-SB-T-1214 (45 mg, 0.04 mmol), **9-5** (20 mg, 0.08 mmol), and DMAP (2 mg, 0.04 mmol) dissolved in CH_2Cl_2 [0.05 M] and cooled to 0 °C was added DCC (12 mg, 0.04 mmol). The mixture was stirred at room temperature and the reaction was monitored via TLC. After 24 h, no reaction was observed on TLC. To the mixture was added another 1 equivalent DMAP and 1 equivalent of DCC. The mixture was stirred at room temperature for an additional 72 h. No reaction was observed on TLC. The mixture was then stirred at 40 °C. After 24 h, no reaction was observed, the reaction solvent was evaporated and the resulting crude was purified using flash column chromatography on silica gel to yield 2`-OTBDMS-SB-T-1214 (30 mg, 67% recovered starting material).

Method 2

A mixture of 2`-OTBS-SB-T-1214 (50 mg, 0.05 mmol), **9-5** (22 mg, 0.1 mmol), EDC (20 mg, 0.1 mmol) and DMAP (24 mg, 0.15 mmol) was dissolved in CH_2Cl_2 [0.05 M]. The mixture was stirred at room temperature and the reaction was monitored via TLC. After 72 h, no reaction was observed, the reaction solvent was evaporated and the resulting crude was purified using flash column chromatography on silica gel to yield 2`-OTBDMS-SB-T-1214 (38 mg, 76% recovered starting material).

***N*-Fmoc-Glu-OH (9-10)[36]**

To Glu (500 mg, 4 mmol) and Fmoc-OSu (963 mg, 4 mmol) dissolved in 1,4-dioxane [0.2 M] was added 10% aqueous Na_2CO_3 (45 mL) over a period of 10 min. During the addition, the reaction solution became cloudy; 30 min after the addition, the solution cloudy and slightly yellow; 45 min after the addition, the solution became clear. The mixture was stirred at room temperature and the reaction was monitored via TLC. After 8 h, the reaction solution became cloudy. Upon which, the pH was adjusted to 8 with 1 M Na_2CO_3. The alkali layer was extracted with ether (3 x 50 mL). The aqueous layer was collected, the pH was adjusted to 2 with 1 M HCl and extracted with ethyl acetate (5 x 20 mL). The organic layers were collected, dried over $MgSO_4$ and concentrated *in vacuo* to yield **9-10** (911 mg, 73% yield): m.p. 182-184 °C; ^{1}H NMR (300 MHz, CD_3OD, ppm) δ 1.984-2.015 (m, 2 H), 2.228-2.292 (m, 1 H), 2.485 (t, *J* = 7.8 Hz, 2 H), 3.699 (s, 1 H), 4.227-4.303 (m, 2 H), 4.353-4.401 (m, 2 H), 5.113 (br s, 3 H), 7.324-7.449 (m, 4 H), 7.693-7.731 (m, 2 H), 7.809 (d, *J* = 7.5 Hz, 2 H). All data are consistent with literature values.[36]

Attempted synthesis of (*S*)-*N*-Fmoc-γ-benzyl-Glu-OH (9-11b)

A mixture of **9-10** (200 mg, 0.5 mmol) and DCC (124 mg, 0.55 mmol) was dissolved in THF [1 M]. The mixture was stirred at room temperature for 4 h. To the mixture was added a suspension containing benzyl alcohol (0.06 mL, 0.5 mmol) and K_2CO_3 (150 mg, 1 mmol) in THF [1 M]. After the addition, the reaction mixture became cloudy. The mixture was stirred at room temperature. After 8 h, the reaction mixture was filtered over a Büchner funnel, the solids were washed with CH_2Cl_2, the mother liquor was extracted with CH_2Cl_2, was washed with 1 M HCl (1 x 50 mL), then washed with brine (2 x 50 mL). The organic layer was collected, dried over $MgSO_4$ and concentrated *in vacuo*. The resulting crude was purified using flash column chromatography (36% ethyl acetate in hexanes with 1% AcOH) to yield **9-11a** (220 mg, 88% yield): ^{1}H NMR (300 MHz, CD_3OD, ppm) δ 1.956-2.057 (m, 2 H), 2.195-2.268 (m, 2 H), 2.423-

2.523 (m, 2 H), 2.838 (br s, 2 H), 4.192-4.238 (m, 2 H), 4.304-4.437 (m, 5 H), 4.997 (br s, 4 H), 5.154 (s, 1 H), 5.201 (d, *J* = 2.4 Hz, 2 H), 7.679 (m, 4 H), 7.818 (m, 4 H); formation of **9-11b** was not observed.

(*S*)-*N*-Fmoc-γ-benzyl-Glu-(*S*)-δ-*N*-Boc-Lys-allyl ester (9-12)
To N_{α}-Fmoc-Glu-γ-Cbz (356 mg, 0.77 mmol), N_{ε}-Boc-Lys-α-Alloc (250 mg, 0.77 mmol) and EDC (150 mg, 0.9 mmol) dissolved in THF [1 M] was added DIPEA (0.1 mL, 1.5 mmol). After the addition of DIPEA, the solution became clear. The mixture was stirred at room temperature and the reaction was monitored via TLC. After 16 h, the reaction solvent was evaporated and the resulting crude was purified via Yamazen automotive column chromatography to yield **9-12** (266 mg, 47% yield), as an off-white solid: m.p. 104-107 °C; ^{1}H NMR (300 MHz, $CDCl_3$, ppm) δ 1.259 (t, *J* = 7.2 Hz, 2 H), 1.416 (s, 9 H), 1.638 (m, 1 H), 1.751 (m, 1 H), 2.433 (m, 1 H), 2.548-2.572 (m, 2 H), 3.058-3.079 (m, 2 H), 4.205 (t, *J* = 7.5 Hz, 1 H), 4.574-4.629 (m, 3 H), 5.140 (s, 1 H), 5.231 (d, *J* = 10.2 Hz, 1 H), 5.721 (m, 1 H), 5.881 (m, 1 H), 6.789 (m, 1 H), 7.263-7.352 (m, 7 H), 7.575 (d, *J* = 7.5 Hz, 1 H), 7.746 (d, *J* = 7.5 Hz, 1 H).

(*S*)-*N*-Fmoc-γ-benzyl-Glu-(*S*)-Lys-allyl ester (9-13)
To **9-12** (350 mg, 0.48 mmol) was added a mixture of 10% TFA in CH_2Cl_2. The mixture was stirred at room temperature and the reaction was monitored via TLC. After the addition of TFA solution, the reaction mixture became cloudy. After 24 h, solid $NaHCO_3$ was added. The mixture was then diluted with water and extracted with CH_2Cl_2 (3 x 50 mL). The organic layer was collected, dried over $MgSO_4$ and concentrated *in vacuo* to yield **9-13** (284 mg, 94% yield), as a yellow solid, which was used without further purification.

(*S*)-*N*-Fmoc-γ-benzyl-Glu-(*S*)-δ-*N,N*-diethyl-Lys-allyl ester (9-14)
To **9-13** (245 mg, 0.4 mmol) dissolved in CH_3CN [0.1 M] was added acetaldehyde (0.02 mL, 0.4 mmol). The mixture was stirred at room temperature for 3 h. To the mixture was added $NaBH(OAc)_3$ (67 mg, 1.2 mmol) slowly over a period of 10 minutes. The mixture was stirred at room temperature for 16 h. To the mixture was added acetaldehyde (0.02 mL, 0.4 mmol). The mixture was stirred at room temperature for 3 h. To the mixture was added $NaBH(OAc)_3$ (67 mg, 1.2 mmol) slowly over a period of 10 minutes. The mixture was stirred at room temperature. After 16 h, the reaction solvents were evaporated. The resulting crude was dissolved in ethyl acetate (10 mL). The organic layer was washed with water (3 x 10 mL) and then with brine (3 x 10 mL). The organic layer was filtered through Norit, celite and silica gel to yield **9-14** (85 mg, 32% yield) as a white solid: ^{1}H NMR (300 MHz, $CDCl_3$, ppm) δ 0.831-0.878 (m, 4 H), 1.321 (s, 9 H), 1.345-1.412 (dd, J_1 = 3.9 Hz, J_2 = 9.9 Hz, 2 H), 1.998-2.068 (m, 1 H), 2.166-2.251 (m, 1 H), 2.489 (t, *J* = 7.2 Hz, 1 H), 3.772-3.815 (m, 1 H), 3.995 (m, 1 H), 4.272-4.342 (m, 1 H), 4.605 (br s, 1 H), 4.706 (s, 1 H), 5.119 (d, J = 2.1 Hz, 1 H), 5.832-5.922 (m, 1 H), 6.075 (s, 1 H), 7.297-7.339 (m, 11 H), 7.560-7.584 (m, 1 H), 7.704-7.760 (m, 1 H).

(*S*)-*N*-Fmoc-Glu-(*S*)-δ-*N,N*-diethyl-Lys-allyl ester (9-15)
To a mixture of **9-14** (40 mg, 0.07 mmol) and $Pd(OAc)_2$ (0.6 mg, 0.003 mmol) dissolved in CH_2Cl_2 [0.03 M] was added Et_3SiH (0.012 mL, 0.09 mmol), followed by the addition of Et_3N (0.008 mL, 0.07 mmol). The mixture was stirred at room temperature and the reaction was monitored via TLC. After 16 h, the reaction mixture was quenched with aqueous $NaHCO_3$, extracted with CH_2Cl_2 (5 x 20 mL), dried over $MgSO_4$ and concentration *in vacuo*. The resulting

crude was purified using flash column chromatography on silica gel (hexanes:ethyl acetate = 1:1) to yield **9-15** (26 mg, 74% yield) as a white solid: ^{1}H NMR (300 MHz, $CDCl_3$, ppm) δ 1.241-1.327 (m, 10 H), 1.630-1.786 (m, 10 H), 1.916-2.218 (m, 8 H), 2.480 (t, J = 6.9 Hz, 2 H), 3.422-3.519 (m, 1 H), 3.652 (br s, 1 H), 3.817-3.924 (m, 1 H), 3.980-4.017 (dt, J_1 = 3.9 Hz, J_2 = 4.8 Hz, 1 H), 4.062-4.220 (m, 1 H), 5.074-5.161 (m, 2 H), 5.693 (s, 1 H), 7.268-7.377 (m, 10 H), 7.558-7.635 (m, 1 H), 7.743 (d, J = 7.8 Hz, 1 H).

(*S*)-*N*-Fmoc-γ-p-fluorophenyl-Glu-(*S*)-δ-*N*,*N*-diethyl-Lys-allyl ester (9-16)

A mixture of **9-15** (25 mg, 0.04 mmol), EDC (7 mg, 0.048 mmol), DMAP (5 mg, 0.04 mmol) and p-fluorophenol (5 mg, 0.04 mmol) dissolved in THF [0.01 M] was stirred at room temperature. The reaction was monitored via TLC. After 48 h, the reaction mixture was quenched with aqueous $NaHCO_3$, extracted with CH_2Cl_2 (3 x 25 mL), dried over $MgSO_4$ and concentrated *in vacuo*. The resulting crude was purified using flash column chromatography on silica gel (hexanes:ethyl acetate = 1:1) to yield **9-16** (10 mg, 33% yield) as a white solid: ^{1}H NMR (300 MHz, $CDCl_3$, ppm) δ 0.825-0.898 (m, 3 H), 1.189-1.396 (m, 16 H), 1.908 (s, 5 H), 2.067 (s, 2 H), 2.481-2.587 (m, 2 H), 4.163-4.236 (m, 1 H), 4.329-4.358 (m, 2 H), 4598 (br s, 2 H), 5.120-5.132 (m, 2 H), 5.227-5.340 (m, 3 H), 5.803-5.941 (m, 1 H), 7.297-7-401 (m, 8 H), 7.560-7.628 (m, 2 H), 7.680-7.760 (m, 2 H).

Attempted synthesis of pyroglutamyl-Lys dipeptide (9-18)

To **9-16** (20 mg, 0.04 mmol) was added a mixture of 20% piperidine in DMF. The mixture was stirred at room temperature and the reaction was monitored via TLC. After 2 h, the reaction solvent was evaporated, diluted with H_2O, quenched with aq. $NaHCO_3$ and extracted with ethyl acetate (3 x 30 mL). The organic layers were collected, dried over $MgSO_4$ and concentrated *in vacuo* to yield **9-17** (15 mg, quantitative yield). The resulting **9-17** (15 mg, 0.04 mmol) was dissolved in 2 mL water. The solution was stirred at 150 °C. The reaction was monitored via TLC. After 10 days, formation of **9-18** was not observed.

(*S*)-*N*-Fmoc-γ-p-fluorophenyl-Glu-(*S*)-δ-*N*,*N*-diethyl-Lys-amide(9-26)

Fmoc-PAL-PEG-PS resin (1 g, 0.19 mmol/g) was treated with 3 ml of 20% piperidine in DMF for 1 h. The obtained resin was washed with DMF (3 x 2 mL), then with CH_2Cl_2 (3 x 2 mL) and dried under vacuum. Deprotected resin (1 g, 0.19 mmol) was placed in a 10 mL round-bottemed flask capped with septum. Then 2 ml of a solution of HOBt (116 mg, 0.76 mmol) in a 1:1 mixture of DMF:CH_2Cl_2 was added and the resin was allowed to swell for 10 min. To the resin was added 6 ml of a 1:1 mixture of DMF:CH_2Cl_2, containing HBTU (288 mg, 0.76 mmol), N_ε-Boc-N_α-Fmoc-Lys (93 mg, 0.27 mmol) and DIPEA (0.13 mL, 0.76 mmol). The mixture was stirred at room temperature for 8 hours. The resulting resin was washed with DMF (3 × 10 ml), CH_2Cl_2 (2 × 10 ml), CH_3OH (2 × 10 ml) and dried in vacuum to yield **9-19** (1.116 g, 0.19 mmol). The resulting resin **9-19** was treated with 6 ml of 20% piperidine in DMF for 1 h at room temperature, then washed with DMF (2 x 3 mL) and CH_2Cl_2 (2 x 3 mL) and vacuum dried to yield **9-20** (955 mg, 0.19 mmol) which gave a positive ninhydrin stain on TLC. To the resulting **9-20** was added 2 ml of a solution of HOBt (116 mg, 0.76 mmol) in a 1:1 mixture of DMF:CH_2Cl_2. The resin was allowed to swell for 10 min. To the resin was added 6 ml of a 1:1 mixture of DMF:CH_2Cl_2, containing HBTU (288 mg, 0.76 mmol), N_α-Fmoc-Glu-γ-benzyl ester (91 mg, 0.2 mmol) and DIPEA (0.13 mL, 0.76 mmol). The mixture was stirred at room temperature for 8 hours. The obtained resin was washed consecutively with DMF (10 mL), 1:1

DMF:CH_2Cl_2 (10 mL), CH_2Cl_2 (2 × 10 mL), CH_3OH (2 × 10 mL) and vacuum dried to yield **9-21** (830 mg, 0.16 mmol). The resin **9-21** (200 mg, 0.04 mmol) was treated with 3 mL of 1% TFA in CH_2Cl_2. The mixture was stirred at room temperature over 30 min. To the mixture was added a 1:2:7 mixture of AcOH:TFE:CH_2Cl_2. The mixture was stirred at room temperature for 1 h. The obtained resin was washed with CH_2Cl_2 (5 x 5 mL) and vacuum dried to yield **9-22** (200 mg, 0.04 mmol) which gave a positive ninhydrin stain on TLC. The resulting resin **9-22** in 5 mL CH_3CN was treated with acetaldehyde (0.03 mL, 0.4 mmol) at room temperature for 3 h followed by the addition of $NaBH(OAc)_3$ (60 mg, 1.2 mmol) for 1 h. The resin was then treated again with acetaldehyde (0.03 mL, 0.4 mmol) at room temperature for 3 h followed by the addition of $NaBH(OAc)_3$ (60 mg, 1.2 mmol) for 8 h. The obtained resin was washed with water (5 x 10 mL) and vacuum dried overnight to yield **9-23** (157 mg, 0.03 mmol). To the resulting resin **9-23** in 2 mL CH_2Cl_2 was added $Pd(OAc)_2$ (0.57 mg, 0.0015 mmol), Et_3SiH (0.01 mL, 0.036 mmol) and Et_3N (0.01 mL, 0.03 mmol). The mixture was stirred at room temperature for 16 h. The obtained resin was washed with CH_2Cl_2 (5 x 10 mL) and vacuum dried to yield **9-24** (155 mg, 0.03 mmol). To the resulting resin **9-24** in 2 mL CH_2Cl_2 was added p-fluorophenol (13 mg, 0.12 mmol), EDC (19 mg, 0.036 mmol) and DMAP (4 mg, 0.03 mmol). The mixture was stirred at room temperature for 16 h. The obtained resin was washed with CH_2Cl_2 (3 x 10 mL), CH_3OH (3 x 10 mL) and vacuum dried to yield **9-25** (153 mg, 0.03 mmol). The cleavage step for resin **9-25** was carried out in 2 ml of 20% TFA in CH_2Cl_2 for 1 hour. The resin was separated, washed with CH_3OH (15 ml), CH_2Cl_2 (10 ml) and CH_3OH (10 ml). Filtrates were combined and evaporated. The oily residue was purified using Yamazen automotive column chromatography to yield **9-26** (27 mg, quantitative yield), as a waxy orange-yellow solid: ^{1}H NMR (300 MHz, CD_3OD, ppm) δ 1.079-1.101 (m, 16 H), 1.264 (m, 1 H), 1.332-1.365 (q, J_1 = 3 Hz, J_2 = 3.9 Hz, 4 H), 1.872-1.990 (m, 1 H), 2.060-2.177 (m, 1 H), 2.451 (t, J = 7.5 Hz, 2 H), 3.289-3.311 (m, 1 H), 3.712-3.842 (m, 2 H), 4.015-4.054 (m, 1 H), 4.175-4.267 (m, 1 H), 4.585-4.625 (m, 1 H), 5.096 (s, 1 H), 5.208-5.347 (m, 1 H), 7.285-7.384 (m, 8 H), 7.498-7.644 (m, 4H).

***N*-Pent-4-ynolylamino-PEG-azide (9-27)**

To **9-3** (0.1 mL, 0.5 mmol) was added 4-pentynoic acid (100 mg, 1 mmol) and EDC (195 mg, 0.65 mmol) dissolved in a 3:1 mixture of CH_3CN:CH_3OH. The mixture was stirred at room temperature and the reaction was monitored via TLC. After 16 h, the reaction solvent was evaporated *in vacuo*. The resulting crude was purified using flash column chromatography (hexanes:ethyl actate = 2:1) to yield **9-27** (130 mg, 92% yield), as orange-brown oil: ^{1}H NMR (400 MHz, $CDCl_3$, ppm) δ 1.969 (t, J = 2.4 H, 1 H), 2.333-2.369 (m, 2 H), 2.437-2.479 (m, 3 H), 3.340 (t, J = 4.4 Hz, 3 H), 3.377-3.415 (q, J_1 = 4.8 Hz, J_2 = 5.2 Hz, 4 H), 3.500 (t, J = 5.2 Hz, 3 H), 3.574-3.628 (m, 13 H); ^{13}C NMR (500 MHz, $CDCl_3$, ppm) δ 16.968, 17.486, 35.784, 37.825, 41.925, 53.303, 64.262, 71.563, 71.913, 72.451, 72.615, 72.848, 72.936, 72.997, 73.142, 73.172, 73.222, 73.252, 73.283,75.156, 85.702, 173.780, 176.397.

***N*-Pent-4-ynolylamino-PEG-amine (9-28)**

A mixture of **9-27** (100 mg, 0.33 mmol) and PPh_3 (45 mg, 0.36 mmol) was dissolved in a 7:2 mixture of THF:water [0.1 M]. The mixture was stirred at room temperature and the reaction was monitored via TLC. After a positive ninhydrin stain, the mixture solvent was evaporated. The resulting crude was triturated with toluene to yield crude containing TPPO and **9-28** (109 mg), as yellow oil: ^{1}H NMR (400 MHz, $CDCl_3$, ppm) δ 1.952 (t, J = 2.4 Hz, 1 H), 2.341-2.379 (m, 2 H), 2.434-2.475 (m, 2 H), 2.834 (t, J = 5.2 Hz, 3 H), 3.001 (br s, 6 H), 3.362 (s, 1 H), 3.391 (t, J =

5.2 Hz, 2 H), 3.465-3.502 (q, J_1 = 4.8 Hz, J_2 = 5.2 Hz, 4 H), 3.536-3.594 (m, 12 H), 3.654 (t, J = 4.4 Hz, 1 H).

SB-T-1214-Me-linker-PEG-pent-4-ynamide (9-29)

To a solution of **4-19** (55 mg, 0.05 mmol) and DMAP (0.05 mmol) dissolved in CH_2Cl_2 [0.1 M], cooled to 0 °C, was added EDC (0.06 mmol) dissolved in CH_2Cl_2 [0.1 M]. To this mixture was added crude containing **9-28** (14 mg, 0.05 mmol) dissolved in CH_2Cl_2 [0.1 M]. The mixture was stirred at room temperature and monitored via TLC. After 16 h, the reaction solvent was evaporated, and the resulting crude was purified using flash column chromatography on silica gel (hexanes:ethyl acetate = 1:1) to yield **9-29** (47 mg, 69% yield), as a white solid: ^{1}H NMR (400 MHz, $CDCl_3$, ppm) δ 0.821-0.848 (m, 1 H), 0.939-0.968 (m, 2 H), 1.093-1.123 (m, 12 H), 1.223 (s, 5 H), 1.318 (s, 12 H), 1.725 (s, 8 H), 1.868 (d, J = 4.4 Hz, 6 H), 2.337 (s, 5 H), 2.600-2.633 (m, 2 H), 2.697 (br s, 1 H), 3.035 (m, 1 H), 3.772-3.825 (m, 2 H), 4.028 (br s, 1 H), 4.142 (d, J = 8.4 Hz, 1 H), 4.267 (d, J = 8.4 Hz, 1 H), 4.417 (m, 1 H), 4.793 (m, 1 H), 4.887-4.955 (m, 3 H), 5.150 (br s, 1 H), 5.637 (d, J = 6.8 Hz, 1 H), 6.142 (m, 1 H), 6.273 (s, 1 H), 7.029-7.059 (t, J_1 = J_2 = 6.8 Hz, 1 H), 7.420-7.458 (t, J_1 = J_2 = 7.6 Hz, 2 H), 7.550-7.619 (m, 2 H), 7.677 (d, J = 8 Hz, 1 H), 8.068 (d, J = 7.6 Hz, 2 H), 8.400 (br s, 1 H)

SB-T-1214-Me-linker-PEG-azide (9-30)

To a solution of **4-19** (15 mg, 0.01 mmol) and DMAP (1 mg, 0.01 mmol) dissolved in CH_2Cl_2 [0.01 M] was added EDC (2 mg, 0.012 mmol) dissolved in CH_2Cl_2 (0.5 mL). To this mixture was added **9-3** (0.02 mL, 0.01 mmol). The mixture was stirred at room temperature and monitored via TLC. After 16 h, the reaction solvent was evaporated, and the resulting crude was dissolved in 5 mL ethyl acetate. The organic layer was washed with aqueous NH_4Cl (2 x 5 mL), then with water (2 x 5 mL) and with brine (1 x 5 mL). The organic layer was collected, and concentrated *in vacuo*. The resulting crude was purified using flash column chromatography on silica gel (hexanes:ethyl acetate = 2:1) to yield **9-30** (13 mg, 72% yield), as a white solid: ^{1}H NMR (400 MHz, $CDCl_3$, ppm) δ 0.821-0.848 (m, 1 H), 0.939-0.968 (m, 2 H), 1.093-1.123 (m, 12 H), 1.223 (s, 5 H), 1.318 (s, 12 H), 1.725 (s, 8 H), 1.868 (d, J = 4.4 Hz, 6 H), 2.337 (s, 5 H), 2.600-2.633 (m, 2 H), 2.697 (br s, 1 H), 3.035 (m, 1 H), 3.772-3.825 (m, 2 H), 4.028 (br s, 1 H), 4.142 (d, J = 8.4 Hz, 1 H), 4.267 (d, J = 8.4 Hz, 1 H), 4.417 (m, 1 H), 4.793 (m, 1 H), 4.887-4.955 (m, 3 H), 5.150 (br s, 1 H), 5.637 (d, J = 6.8 Hz, 1 H), 6.142 (m, 1 H), 6.273 (s, 1 H), 7.029-7.059 (t, J_1 = J_2 = 6.8 Hz, 1 H), 7.420-7.458 (t, J_1 = J_2 = 7.6 Hz, 2 H), 7.550-7.619 (m, 2 H), 7.677 (d, J = 8 Hz, 1 H), 8.068 (d, J = 7.6 Hz, 2 H), 8.400 (br s, 1 H).

Reaction of HPG and GalNAz-AdTRAIL with phosphine-folate and SB-T-1214-PEG-azide

AdTRAIL was obtained from Prof. Andre Lieber, University of Washington, Seattle. The virions were metabolically labeled with HPG and GalNAz as described above. 50 µL of 1 x 10^{12} metabolically labeled viral particles/mL in a 100 mM tris buffer at pH 8.0 was treated with phosphine–Folate at a final concentration of 300 µM in room temperature for 3 hours. After which time, bathophenanthroline disulphonic acid disodium salt (3 mM) and SBT-1214-PEG-azide (500 µM), was added and the resultant mixture kept in an argon-filled glove bag for 6 hours to deoxygenate. Next copper bromide at a final concentration of 1 mM was added to the mixture and the reaction allowed to proceed for 12 hours [37] inside the glove bag. The samples were then removed from the glove bag and quenched by addition of 10 mM EDTA. The particles were purified using Centri-Sep spin columns and quantified with QuantIT Picogreen

Dye labeling[38]. Subsequently, MTT and Targeting assays were performed using these modified virions.

Cell culture system for MTT assay

Adenovirus bearing TRAIL were metabolically labeled with HPG and GalNAz as described. Chemical labeling of these viruses with SBT-1214-PEG-azide was carried via the copper catalyzed "click" reaction in deoxygenating conditions (as for azido-TAMRA). The viruses were purified over centriSep spin columns and quantified using QuantiT Picogreen assay. Human ovarian cancer cells, ID8 were seeded in 96 well plates at concentrations of 10,000 cells/mL. 24 hours after seeding, these cells were infected with different MOI of SBT-1214 labeled AdTRAIL. Control experiments were run by infecting cells with metabolically unlabeled AdTRAIL (these were chemically treated exactly as the azide, alkyne enabled virions). Cells were also treated with increasing concentrations of SBT-1214-PEG-azide – to account for the increasing MOI of infection. The cells were incubated at 37°C incubator for 5 days. After this they were treated with MTT reagent obtained from Cell Proliferation KitI (Roche, Eugene,OR). After a 4 hour incubation at 37°C the cells were again treated with solubilization buffer and left overnight. Absorbance was measured at 580 nm using a PerkinElmer Victor X plate reader.

Cell culture system for targeting assay

Luciferase transgene bearing Ad5 were metabolically labeled with HPG and GalNAz as described. The viruses were chemically labeled with folate bearing phosphine-probe (phosphine-PEG-folate) and SBT-1214-PEG-azide using Staudinger ligation and Cu catalyzed "click" chemistry in a deoxygenated glove under same conditions (as for FLAG/ TAMRA labeling) and the reaction quenched with 10 mM EDTA. Viruses were purified on Centri Sep spin columns and quantified using QuantIT Picogreen assay (Molecular Probes, Eugene, OR) and stored in a 0.9 mM $CaCl_2$ and 0.5 mM $MgCl_2$ buffer in PBS containing 10% glycerol. Mouse breast cancer cell line 4T1 was cultivated in minus folate media for 2 weeks after which they were seeded in 96 well plates at a density of 10,000 cells per well and cultivated for a day in minus folate media containing 2% FCS. After 24 hours the cells were infected with labeled virus at an MOI of 50. 24 hours post infection the cells were treated with 100 µL of reconstituted luciferase substrate from Bright Glo™ Luciferase assay Kit (Promega, Madison,WI); luciferase expression was evaluated using a PerkinElmer Victor X luminescence plate reader (emission 528 ± 10 nm).

§ 9.5.0 References

1. Weiner, L. M.; Surana, R.; Wang, S. Monoclonal antibodies: versatile platforms for cancer immunotherapy. *Nature Rev. Immunology* **2010,** 10, 317-327.
2. Goldsmith, L. E.; Robinson, M. K. Engineering Antibodies for Cancer Therapy. In *Antibody Expression and Production*, Al-Rubeai, M., Ed. Springer Science & Business Media: 2011; Vol. Cell Engineering 7, pp 197-233.
3. Li, S.; Schmitz, K. R.; Jeffrey, P. D.; Wiltzius, J. J. W.; Kussie, P.; Ferguson, K. M. Structural basis for inhibition of the epidermal growth factor receptor by cetuximab. *Cancer Cell* **2005,** 7, 301-311.
4. Trail, P. A.; Bianchi, A. B. Monoclonal antibody drug conjugates in the treatment of cancer. *Curr. Opin. Immunol.* **1999,** 11, 584-588.

5. Wu, A. M.; Senter, P. D. Arming antibodies: prospects and challenges for immunoconjugates. *Nat. Biotechnol.* **2005,** 23, 1137-1146.
6. Chari, R. V. J. Targeted cancer therapy: conferring specificity to cytotoxic drugs. *Acc. Chem. Res.* **2008,** 41, 98-107.
7. Chang, K.; Pastan, I.; Willingham, M. C. Isolation and characterization of a monoclonal antibody, K1, reactive with ovarian cancers and normal mesothelium. *Int. J. Cancer* **1992,** 50, 373-381.
8. Argani, P.; Iacobuzio-Donahue, C.; Ryu, B.; Rosty, C.; Goggins, M.; Wilentz, R. E.; Murugesan, S. R.; Leach, S. D.; Jaffee, E.; Yeo, C. J.; Cameron, J. L.; Kern, S. E.; Hruban, R. H. Mesothelin Is Overexpressed in the Vast Majority of Ductal Adenocarcinomas of the Pancreas: Identification of a New Pancreatic Cancer Marker by Serial Analysis of Gene Expression (SAGE). *Clin. Cancer Res.* **2001,** 7, 3862-3868.
9. R., H.; Kreitman, R. J.; Pastan, I.; Willingham, M. C. Localization of mesothelin in epithelial ovarian cancer. *Appl. Immunohistochem. Mol. Morphol.* **2005,** 13.
10. Li, M.; Bharadwaj, U.; Zhang, R.; Zhang, S.; Mu, H.; Fisher, W. E.; Brunicardi, F. C.; Chen, C.; Yao, Q. Mesothelin is a maglinent factor and theraoeutic vaccines target for pancreatic cancer. *Mol. Cancer. Ther.* **2008,** 7, 286-296.
11. Feng, Y.; Xiao, X.; Zhu, Z.; Streaker, E.; Ho, M.; Pastan, I.; Dimitrov, D. S. A novel human monoclonal antibody that binds with high affinity to mesothelin-expressing cells and kills them by antibody-dependent cell-mediated cytotoxicity. *Mol. Cancer. Ther.* **2009,** 8, 1113-1118.
12. Medina-Kauwe, L. K. Endocytosis of adenovirus and adenovirus capsid proteins *Adv. Drug. Del. Rev.* **2003,** 55, 1486-1496.
13. Kozarsky, K. F.; Wilson, J. M. Gene therapy: adenovirus vectors. *Curr. Opin. in Genetics and Devel.* **1993,** 3, 499-503.
14. Greber, U. F.; Willetts, M.; Webster, P.; Helenius, A. Stepwise dismantling of adenovirus 2 during entry into cells. *Cells* **1993,** 75, 477-486.
15. Michael, S. I.; Curiel, D. T. Strategies to achieve targeted gene delivery via the receptor-mediated endocytosis pathway. *Gene Therapy* **1994,** 1, 223-232.
16. Bergelson, J. M.; Cunningham, J. A.; Droguett, G.; Kurt-Jones, E. A.; Krithivas, A.; Hong, J. S.; Horwitz, M. S.; Crowell, R. L.; Finberg, R. W. Isolation of a common receptor for Coxsakie B viruses and adenoviruses 2 and 5. *Science* **1997,** 275, 1320-1323.
17. Wickham, T. J.; Mathias, P.; Cheresh, D. A.; Nemerow, G. R. Integrins $\alpha_v\beta_3$ and $\alpha_v\beta_3$ promote adenovirus internalization but no virus attachment. *Cell* **1993,** 73, 309-319.
18. Stewart, P. L.; Chiu, C. Y.; Huang, S.; Muir, T.; Zhao, Y.; Chait, B.; Mathias, P.; Nemerow, G. R. Cryo-EM visualization of an exposed RGD epitope on adenovirus that escapes antibody neutralization. *EMBO Journal* **1997,** 16, 1189-1198.
19. Reynolds, P. N.; Curiel, D. T. New generation adenoviral vectors improve gene transfer by coxsackie and adenoviral receptor-independent cell entry. *Kidney Int.* **2002,** 61, S24-S31.
20. Greber, U. F.; Webster, P.; Weber, J.; Helenius, A. The role of the adenovirus protease on virus entry into cells. *EMBO Journal* **1996,** 15, 1766-1777.
21. Greber, U. F.; Souomalainen, M.; Stidwill, R. P.; Boucke, K.; Ebersold, M. W.; Helenius, A. The role of the nuclear pore complex in adenovirus DNA entry. *EMBO J.* **1997,** 16, 5998-6007.
22. Banerjee, P. S.; Ostapchuk, P.; Hearing, P.; Carrico, I. S. Chemoselective Attachment of Small Molecule Effector Functionality to Human Adenoviruses Facilitates Gene Delivery to Cancer Cells. *J. Am. Chem. Soc.* **2010,** 132, 13615-13617.

23. Greenwald, R. B.; Pendri, A.; Bolikal, D. Highly Water Soluble Taxol Derivatives: 7-Polyethylene Glycol Carbamates and Carbonates. *J. Org. Chem.* **1995,** 60, 331-336.
24. Miller, M. L.; Roller, E. E.; Zhao, R. Y.; Leece, B. A.; Ab, O.; Baloglu, E.; Goldmacher, V. S.; Chari, R. V. Synthesis of Taxoids with Improved Cytotoxicity and Solubility for Use in Tumor-Specific Delivery. *J. Med. Chem.* **2004,** 47, 4802-4805.
25. Li, C.; Inoue, T.; Yang, D. J.; Milas, L.; Hunter, N. R.; Kim, E. E.; Wallace, S. Synthesis and evaluation of water-soluble polyethylene glycol-paclitaxel conjugate as a paclitaxel prodrug. . *Anti-cancer Drugs* **1996,** 7, 642-648.
26. Greenwald, R. B.; Gilbert, C. W.; Pendri, A.; Conover, C. D.; Xia, J.; Martinez, A. Drug Delivery Systems: Water Soluble Taxol 2‘-Poly(ethylene glycol) Ester Prodrugs - Design and in Vivo Effectiveness. *J. Med. Chem.* **1996,** 39, 424-431.
27. Lee, J. W.; Lu, J. Y.; Low, P. S.; Fuchs, P. L. Synthesis and evaluation of taxol-folic acid conjugates as targeted antineoplastics. *Bioorg. & Med. Chem.* **2002,** 10, 2397-2414.
28. Drew, M. E.; Chworost, A.; Oroudjev, E.; Hansma, H.; Yamakoshi, Y. A tripod molecular tip for single molecule ligand-receptor force spectroscopy by AFM. *Langmuir* **2010,** 26, 7117-7125.
29. Schwabacher, A. W.; Lane, J. W.; Schiesher, M. W.; Leigh, K. M.; Johnson, C. W. Desymmetrization reactions: efficient preparation of unsymmetrically substituted linker molecules. *J. Org. Chem.* **1998,** 63, 1727-1729.
30. Paradis, R.; Page, M. New active paclitaxel amino acids derivatives with improved water solubility. *Anticancer Res.* **1998,** 18, 2711-2716.
31. Yamaguchi, T.; Harada, N.; Ozaki, K.; Arakawa, H.; Oda, K.; Nakanishi, N.; Tsujihara, K.; Hashiyama, T. Synthesis of taxoids 5. Synthesis and evaluation of novel water-soluble prodrugs of a 3`-desphenyl-3`-cyclopropyl analogue of docetaxel. *Bioorg. & Med. Chem. Lett.* **1999,** 9, 1639-1644.
32. Martin, L. L.; Scott, S. J.; Agnew, M. N.; Stescak, L. J. A novel synthesis of 1,4-dihydrobenzo[*c*]-1,5-naphthyridin-2(3*H*)-ones from pyrrolo[1,2-*b*]isoquiolines. *J. Org. Chem.* **1986,** 51, 3697-3700.
33. Banerjee, P. S.; Zuniga, E. S.; Ojima, I.; Carrico, I. S. Targeted and armed oncolytic adenovirus via chemoselective modification. *Bioorg. & Med. Chem. Lett.* **2011,** 21, 4985-4988.
34. Gottlieb, H. E.; Kotlyar, V.; Nudelman, A. NMR Chemical Shifts of Common Laboratory Solvents as Trace Impurities. *J. Org. Chem.* **1997,** 62, 7512-7515.
35. Lee, J. W.; Lu, J. Y.; Low, P. S.; Fuchs, P. L. Synthesis and evaluation of taxol-folic acid conjugates as targeted antineoplastics. *Bioorg. Med. Chem.* **2002,** 10, 2397-2414.
36. Ibrahim, T. S.; Tala, S. R.; El-Feky, S. A.; Abdel-Samii, Z. K.; Katritzky, A. R. Benzotriazole Reagents for the Syntheses of Fmoc-, Boc-, and Alloc-Protected Amino Acids. *Synlett* **2011**, 2013-2016.
37. Gupta, S. S.; Kuzelka, J.; Singh, P.; Lewis, W. G.; Manchester, M.; Finn, M. G. Accelerated Bioorthogonal Conjugation: A Practical Method for the Ligation of Diverse Functional Molecules to a Polyvalent Virus Scaffold. *Bioconj. Chem.* **2005,** 16, 1572-1579.
38. Murakami, P.; McCaman, M. T. Quantitation of Adenovirus DNA and Virus Particles with the PicoGreen Fluorescent Dye. *Anal. Biochem.* **1999,** 274, 283-288.

Bibliography

Chapter 1 References

1. Hanahan, D.; Weinberg, R. A. Hallmarks of Cancer: The Next Generation. *Cell* **2011,** 144, 646-674.
2. Jemal, A., Bray, F., Center, M.M., Ferlay, J., Ward, E., Forman, D. Global Cancer Statistics. *CA Cancer J. Clin.* **2011,** 61, 69-90.
3. Siegel, R., Ward, E., Brawley, O., Jemal, A. Cancer Statistics, 2011. *CA Cancer J. Clin.* **2011,** 61, 212-236.
4. Jernal, A.; Siegel, R.; Ward, E.; Murray, T.; Xu, J.; Smigal, C.; Thun, M. J. Cancer Statistics, 2006. *CA Cancer J Clin* **2006,** 56, 106-130.
5. Adams, D. J.; Wahl, M. L.; Flowers, J. L.; Sen, B.; Colvin, M.; Dewhirst, M. W.; Manikumar, G.; Wani, M. C. Camptothecin analogs with enhanced activity against human breast cancer cells. II. Impact of the tumor pH gradient. *Cancer Chemo. and Pharm.* **2005,** 57, 145-154.
6. Ulukan, H.; Swaan, P. W. Camptothecins, a review of their chemotherapeutical potential. *Drugs* **2002,** 62, 2039-2057.
7. Wall, M. E.; Wani, M. C.; Cook, C. E.; Palmer, K. H.; McPhail, A. T.; Sim, G. A. Plant antitumor agents. I. The isolation and structure of camptothecin, a novel alkaloidal leukemia and tumor inhibitor from camptotheca acuminate. *J. Am. Chem. Soc.* **1966,** 88, 3888-3890.
8. Li, Q.-Y.; Zu, Y.-G.; Shi, R.-Z.; Yao, L.-P. Review Camptothecin: Current Perspectives. *Curr. Med. Chem.* **2006,** 13, 1-19.
9. Wall, M. E.; Wani, M. C. Camptothecin and Taxol: Discovery to Clinic-Thirteenth Bruce F. Cain Memorial Award LEcture. *Cancer Res.* **1995,** 55, 753-760.
10. Wani, M. C.; Taylor, H. L.; Wall, M. E.; Coggon, P.; McPhail, A. T. Plant antitumor agents. VI. Isolation and structure of taxol, a novel antileukemic and antitumor agent from Taxus brevifolia. *J. Am. Chem. Soc.* **1971,** 93, 2325-2327.
11. Schiff, P. B.; Fant, J.; Horwitz, S. B. Promotion of microtubule assembly in vitro by taxol. *Nature* **1979,** 277, 665-667.
12. Schiff, P. B.; Horwitz, S. B. Taxol Stabilizes Microtubules in Mouse Fibroblast Cells. *Proc. Natl. Acad. Sci. U.S.A.* **1980,** 77, 1561-1565.
13. Downing, K. H.; Nogales, E. Tubulin and microtubule structure. *Curr. Opin. Cell Biol.* **1998,** 10, 16-22.
14. Jordan, M. A.; Wilson, L. Microtubules as a target for anticancer drugs. *Nat. Rev. Cancer* **2004,** 4, 253-265.
15. Jordan, M. A. Mechanism of action of antitumor drugs that interact with microtubules and tubulin. *Curr. Med. Chem.: Anti-Cancer Agents* **2002,** 2, 1-17.
16. Margolis, R. L.; Rauch, C. T.; Wilson, L. Mechanism of colchicine-dimer addition to microtubule ends: implications for the microtubule polymerization mechanism. *Biochemistry* **1980,** 19, 5550-5557.
17. Hadfield, J. A.; Ducki, S.; Hirst, N.; McGown, A. T. Tubulin and microtubules as targets for anticancer drugs. *Prog. Cell Cycle Res.* **2003,** 5, 309-325.
18. Ojima, I., Chen, J., Sun, L., Borella, C. P., Wang, T., Miller, M. L., Lin, S., Geng, X., Kuznetsova, L., Qu, C., Gallagher, G., Zhao, X., Zanardi, I., Xia, S., Horwitz, S.B., St. Clair, J.

M., Guerriero, J.L., Bar-Sagi, D., Veith, J. M., Pera, P., Bernacki, R. J. Design, Synthesis, and Biological Evaluation of New-Generation Taxoids. *J. Med. Chem.* **2008,** 51, 3203-3221.
19. Nicolaou, K. C.; Dai, W.-M.; Guy, R. K. Chemistry and Biology of Taxol. *Angew. Chem., Int. Ed. Engl.* **1994,** 33, 15-44.
20. Holton, R. A.; Somoza, C.; Kim, H. B.; Liang, F.; Biediger, R. J.; Boatman, P. D.; Shindo, M.; Smith, C. C.; Kim, S.; Nadizadeh, H.; Suzuki, Y.; Tao, C.; Vu, P.; Tang, S.; Zhang, P.; Murthi, K. K.; Gentile, L. N.; Liu, J. H. First total synthesis of taxol. 1. Functionalization of the B ring. *J. Am. Chem. Soc.* **1994,** 116, 1597-1598.
21. Holton, R. A.; Somoza, C.; Kim, H. B.; Liang, F.; Biediger, R. J.; Boatman, P. D.; Shindo, M.; Smith, C. C.; Kim, S.; Nadizadeh, H.; Suzuki, Y.; Tao, C.; Vu, P.; Tang, S.; Zhang, P.; Murthi, K. K.; Gentile, L. N.; Liu, J. H. First total synthesis of taxol. 2. Completion of the C and D rings. *J. Am. Chem. Soc.* **1994,** 116, 1599-1600.
22. Nicolaou, K. C.; Nantermet, P. G.; Ueno, H.; Guy, R. K.; Couladouros, E. A.; Sorensen, E. J. Total Synthesis of Taxol. 1. Retrosynthesis, Degradation, and Reconstitution. *J. Am. Chem. Soc.* **1995,** 117, 624-633.
23. Nicolaou, K. C.; Liu, J. J.; Yang, Z.; Ueno, H.; Sorensen, E. J.; Claiborne, C. F.; Guy, R. K.; Hwang, C. K.; Nakada, M.; Nantermet, P. G. Total Synthesis of taxol. 2. Construction of A and C ring intermediates and initial attempts to construct the ABC ring system. *J. Am. Chem. Soc.* **1995,** 117, 634-644.
24. Nicolaou, K. C.; Yang, Z.; Liu, J. J.; Nantermet, P. G.; Claiborne, C. F.; Renaud, J.; Guy, R. K.; Shibayama, K. Total Synthesis of Taxol. 3. Formation of Taxol's ABC Ring Skeleton. *J. Am. Chem. Soc.* **1995,** 117, 645-652.
25. Nicolaou, K. C.; Ueno, H.; Liu, J. J.; Nantermet, P. G.; Yang, Z.; Renaud, J.; Paulvannan, K.; Chadha, R. Total Synthesis of Taxol. 4. The Final Stages and Completion of the Synthesis. *J. Am. Chem. Soc.* **1995,** 117, 653-659.
26. Danishefsky, S. J.; Masters, J. J.; Young, W. B.; Link, J. T.; Snyder, L. B.; Magee, T. V.; Jung, D. K.; Isaacs, R. C. A.; Bornmann, W. G.; Alaimo, C. A.; Coburn, C. A.; Di Grandi, M. J. Total Synthesis of Baccatin III and Taxol. *J. Am. Chem. Soc.* **1996,** 12, 2843-2859.
27. Wender, P. A.; Badham, N. F.; Conway, S. P.; Floreancig, P. E.; Glass, T. E.; Granicher, C.; Houze, J. B.; Janichen, J.; Lee, D.; Marquess, D. G.; McGrane, P. L.; Meng, W.; Mucciaro, T. P.; Muhlebach, M.; Natchus, M. G.; Paulsen, H.; Rawlins, D. B.; Satkofsky, J.; Shuker, A. J.; Sutton, J. C.; Taylor, R. E.; Tomooka, K. The Pinene Path to Taxanes. 5. Stereocontrolled Synthesis of a Versatile Taxane Precursor. *J. Am. Chem. Soc.* **1997,** 119, 2755-2756.
28. Morihira, K.; Hara, R.; Kawahara, S.; Nishimori, T.; Nakamura, N.; Kusama, H.; Kuwajima, I. Enantioselective Total Synthesis of Taxol. *J. Am. Chem. Soc.* **1998,** 120, 12980-12981.
29. Mukaiyama, T.; Shiina, I.; Iwadare, H.; Saitoh, M.; Nishimura, T.; Ohkawa, N.; Sakoh, H.; Nishimura, K.; Tani, Y.-i.; Hasegawa, M.; Yamada, K.; Saitoh, K. Asymmetric Total Synthesis of Taxol. *Chem. Eur. J.* **1999,** 5, 121-161.
30. Doi, T.; Fuse, S.; Miyamoto, S.; Nakai, K.; Sasuga, D.; Takahashi, T. A Formal Total Synthesis of Taxol Aided by an Automated Synthesizer. *Chem. Asian. J.* **2006,** 1, 370-383.
31. Denis, J. N.; Greene, A. E.; Guenard, D.; Gueritte-Voegelein, F.; Mangatal, L.; Potier, P. Highly efficient, practical approach to natural taxol. *J. Am. Chem. Soc.* **1988,** 110, 5917-5919.
32. Guénard, D.; Guéritte-Voegelein, F.; Potier, P. Taxol and taxotére: discovery, chemistry, and structure-activity relationships. *Acc. Chem. Res.* **1993,** 26, 160-167.

33. Colin, M.; Guénard, D.; Guéritte-Voegelein, F.; Potier, P. Taxotére, European Patent Application. Eur. Pat. Appl. 1988.
34. Guéritte-Voegelein, F.; Mangatal, L.; Guénard, D.; Potier, P.; Guilhem, J.; Cesario, M.; Pascard, C. Structure of a Synthetic Taxol Precursor: *N-tert*-Butoxycarbonyl-10-deacetyl-*N*-debenzoyltaxol. *Acta Crystallogr.* **1990,** C46, 781-784.
35. Bissery, M.; Guéritte-Voegelein, F.; Guénard, D.; Lavelle, F. Experimental Antitumor Activity of Taxotére (RP 56976, NSC 628503), a Taxol Analog. *Cancer Res.* **1991,** 51, 4845-4852.
36. Ojima, I. Recent Advances in the β-Lactam Synthon Method. *Acc. Chem. Res.* **1995,** 28, 383-389.
37. Ojima, I.; Sun, C. M.; Zucco, M.; Park, Y. H.; Duclos, O.; Kuduk, S. D. A Highly Efficient Route to Taxotère by The β-Lactam Synthon Method. *Tetrahedron Lett.* **1993,** 34, 4149-4152.
38. Ojima, I.; Habus, I.; Zhao, M. Efficient and Practical Asymmetric Synthesis of the Taxol C-13 Side Chain, N-Benzoyl-(2R,3S)-3-phenylisoserine, and Its Analogues via Chiral 3-Hydroxy-4-aryl-β-lactams through Chiral Ester Enolate-Imine Cyclocondensation. *J. Org. Chem.* **1991,** 56, 1681-1683.
39. Ojima, I.; Habus, I.; Zhao, M.; Zucco, M.; Park, Y. H.; Sun, C. M.; Brigaud, T. New and Efficient Approaches to the Semisynthesis of Taxol and Its C-13 Side Chain Analogs by Means of β-Lactam Synthon Method. *Tetrahedron* **1992,** 48, 6985-7012.
40. Ojima, I., Slater, J. C., Michaud, E., Kuduk, S. D., Bounaud, P. Y., Vrignaud, P., Bissery, M. C., Veith, J. M., Pera, P., Bernacki, R. J. Syntheses and Structure-Activity Relationships of the Second-Generation Antitumor Taxoids: Exceptional Activity against Drug-Resistant Cancer Cells. *J. Med. Chem.* **1996,** 39, 3889-3896.
41. Ojima, I.; Kuznetsova, L.; Ungureanu, I. M.; Pepe, A.; Zanardi, I.; Chen, J. Fluoro-β-lactams as Useful Building Blocks for the Synthesis of Fluorinated Amino Acids, Dipeptides, and Taxoids. In *Fluorine-containing Synthons*, Soloshonok, V. A., Ed. American Chemical Society/Oxford University Press: Washington, D.C., 2005; pp 544-561.
42. Ojima, I.; Slater, J. C. Synthesis of Novel 3`-Trifluoromethyl Taxoids Through Effective Kinetic Resolution of Racemic 4-CF_3-β-Lactams With Baccatins. *Chirality* **1997,** 9, 487-494.
43. Ojima, I.; Kuduk, S. D.; Slater, J. C.; Gimi, R. H.; Sun, C. M. Syntheses of New Fluorine-Containing Taxoids by Means of β-Lactam Synthon Method. *Tetrahedron* **1996,** 52, 209-224.
44. Kingston, D. G. I. Recent Advances in the Chemistry of Taxol1,2. *J. Nat. Prod.* **2000,** 63, 726-734.
45. Ojima, I. Tumor-targeting drug delivery of chemotherapeutic agents. *Pure Appl. Chem.* **2011,** 83, 1685-1698.
46. Ojima, I.; Zuniga, E. S.; Berger, W. T.; Seitz, J. D. Tumor-targeting drug delivery of new-genreation taxoids. *Future Med. Chem.* **2012,** 4, 33-50.
47. Georg, G. I. *The Organic Chemistry of b-Lactams and refereces cited therein*. VCH: New York, 1992.
48. Ojima, I. β-Lactam Synthon Method – Enantiomerically Pure β-Lactams as Synthetic Intermediates. In *The Organic Chemistry of β-Lactams and β-Lactam Antibiotics*, Georg, G. I., Ed. VCH Publishers: New York, 1992; pp 197-255.
49. Hatanaka, N.; Abe, R.; Ojima, I. β-Lactam as Synthetic Intermediate: Synthesis of Leucine-Enkephalin. *Chem. Lett.* **1981**, 1297-1298.

50. Hatanaka, N.; Ojima, I. Effective Method for the Asymmetric Synthesis of Bis-β-lactams by the Cycloaddition of Azidoketen to Benzylideneamines Bearing a Chiral β-Lactam Backbone. *J. Chem. Soc., Chem. Commun.* **1981**, 344-346.
51. Ojima, I.; Yamato, T.; Nakahashi, K. Synthesis of Novel and Chiral Bisazetidines by the Hydroalane Reduction of Bis-β-lactams. *Tetrahedron Lett.* **1985,** 26, 2035-2038.
52. Ojima, I.; Qiu, X. Asymmetric Alkylation of Chiral β-Lactam Ester Enolates. A New Approach to the Synthesis of α-Alkylated α-Amino Acids. *J. Am. Chem. Soc.* **1987,** 109, 6537-6538.
53. Ojima, I.; Shimizu, N.; Qiu, X.; Chen, H.-J. C.; Nakahashi, K. New Aspects of β-Lactam Chemistry: β-Lactams as Chiral Building Blocks. *Bull. Soc. Chim. France* **1987**, 649-658.
54. Cossio, F. P.; Lopez, C.; Oiarbide, M.; Palomo, C.; Aparicio, D.; Rubiales, G. Synthetic utility of azetidin-2,3-diones: a new approach to 3-hydroxyethyl-β-lactams and α-amino acid derivatives. *Tetrahedron Lett.* **1988,** 29, 3133-3136.
55. Ojima, I.; Park, Y. H.; Sun, C. M.; Zhao, M.; Brigaud, T. New and Efficient Routes to Norstatine and Its Analogs with High Enantiomeric Purity by β-Lactam Synthon Method. *Tetrahedron Lett.* **1992,** 33, 5739-5742.
56. Staudinger, H. Zur Kenntniss der Ketene. Diphenylketen. *Justus Liebigs Ann. Chem.* **1907,** 356, 51-123.
57. Cossio, F. P.; Arrieta, A.; Sierra, M. A. The Mechanism of the Ketene-Imine (Staudinger) Reaction in its Centennial: Still an Unsolved Problem? *Acc. Chem. Res.* **2008,** 41, 925-936.
58. Venturini, A.; Gonzalez, J. Mechanistic Aspects of the Ketene-Imine Cycloaddition Reactions. *Mini Rev. Med. Chem.* **2006,** 3, 185-194.
59. Dumas, S.; Hegedus, L. S. Electronic Effects on the Stereochemical Outcome of the Photochemical Reaction of Chromium Carbene Compleses with Imines to Form β-Lactams. *J. Org. Chem.* **1994,** 59, 4967-4971.
60. Georg, G. I.; Ravikumar, V. T. Stereocontrolled ketene-imine cycloaddition reactions. In *Organic Chemistry β-lactams*, G.I., G., Ed. VCH Publishing: New York, NY, 1993; pp 295-368.
61. Hegedus, L. S.; Montgomery, J.; Narukawa, Y.; Snustad, D. C. A contribution to the confusion surrounding the reaction of ketenes with imines to produce β-lactams. A comparison of stereoselectivity dependence on the method of ketene generation: acid chloride/triethylamine s photolysis of chromium carbene complexes. *J. Am. Chem. Soc.* **1991,** 113, 5784-5791.
62. Cossio, F. P.; Ugalde, J. M.; Lopez, X.; Lecea, B.; Palomo, C. A semiempirical theoretical study on hte formation of 5784-5791-lactams from ketenes and imine. *J. Am. Chem. Soc.* **1993,** 115, 995-1004.
63. Lopez, R.; Sordo, T. L.; Sordo, J. A.; Gonzalez, J. Torquoelectronic effect in the control of the stereoselectivity of ketene-imine cycloaddition reactions. *J. Org. Chem.* **1993,** 58, 7036-7037.
64. Cossio, F. P.; Arrieta, A.; Lecea, B.; Ugalde, J. M. Chiral Control in the Staudinger Reaction between Ketenes and Imines. A Theoretical SCF-MO Study on Asymmetric Torquoselectivity. *J. Am. Chem. Soc.* **1994,** 116, 2085-2093.
65. Wang, Y.; Liang, Y.; Jiao, L.; Du, D.-M.; Xu, J. Do Reaction Conditions Affect the Stereoselectivity in the Staudinger Reaction? *J. Org. Chem.* **2006,** 71, 6983-6990.
66. Brieva, R.; Crich, J. Z.; Sih, C. J. Chemoenzymic synthesis of the C-13 side chain of taxol: optically active 3-hydroxy-4-phenyl β-lactam derivatives. *J. Org. Chem.* **1993,** 58, 1068-1075.

67. Banik, B. K.; Manhas, M. S.; Bose, A. K. Stereospecific Glycosylation via Ferrier Rearrangement for Optical Resolution. *J. Org. Chem.* **1994,** 59, 4714-4716.
68. Patel, R. N. Enzymic processes for the resolution of enantiomeric mixtures of compounds useful as intermediates in the preparation of taxanes. 1995.
69. Holton, R. A.; Vu, P. Enzymatic process for the resolution of enantiomeric mixtures of b-lactams. 2001029245, 2001.
70. Kuznetsova, L.; Ungureanu, I.; Pepe, A.; Zanardi, I.; Wu, X.; Ojima, I. Trifluoromethyl- and difluoromethyl-β-lactams as useful building blocks for the synthesis of fluorinated amino acids, dipeptides, and fluoro-taxoids. *J Fluor. Chem* **2004,** 125, 487-500.
71. Chen, J.; Kuznetsova, L.; Ungureanu, I.; Ojima, I. Recent Advances in the Synthesis of α-Hydroxy-β-amino Acids and Their Use in the SAR Studies of Taxane Anticancer Agents. In *Enantioselective Synthesis of Amino Acids, Second Edition*, Juaristi, E.; Soloshonok, V., Eds. John Wiley: New York, 2005; pp 447-476.
72. Kuznetsova, L. V.; Pepe, A.; Ungureanu, I. M.; Pera, P.; Bernacki, R. J.; Ojima, I. Syntheses and structure-activity relationships of novel 3'-difluoromethyl and 3'-trifluoromethyl-taxoids. *J. Fluor. Chem.* **2008,** 129, 817-828.
73. Lin, S.; Geng, X.; Qu, C.; Tynebor, R.; Gallagher, D.; Pollina, E.; Rutter, J.; Ojima, I. Synthesis of Highly Potent Second-Generation Taxoids Through Effective Kinetic Resolution Coupling of Racemic β-Lactams with Baccatins. *Chirality* **2000,** 12, 431-441.
74. Geney, R.; Sun, L.; Pera, P.; Bernacki, R. J.; Xia, S.; Horwitz, S. B.; Simmerling, C. L.; Ojima, I. Use of the Tubulin Bound Paclitaxel Conformation for Structure-Based Rational Drug Design. *Chem. & Bio.* **2005,** 12, 339-348.
75. Ojima, I.; Slater, J. C.; Kuduk, S. D.; Takeuchi, C. S.; Gimi, R. H.; Sun, C. M.; Park, Y. H.; Pera, P.; Veith, J. M.; Bernacki, R. J. Syntheses and Structure-Activity Relationships of Taxoids Derived from 14-beta-Hydroxy-10-deacetylbaccatin III. *J. Med. Chem.* **1997,** 40, 267-278.
76. Ojima, I.; Wang, T.; Miller, M. L.; Lin, S.; Borella, C. P.; Geng, X.; Pera, P.; Bernancki, R. J. Synthesis and structure-activity relationships of new second-generation taxoids. *Bioorg. Med. Chem. Lett.* **1999,** 9, 3423-3428.
77. Ojima, I.; Songnian, L.; Wang, T. Recent Advances in the Medicinal Chemistry of Taxoids with Novel -Amino Acid Side Chains. *Curr. Med. Chem.* **1999,** 6, 927-954.
78. Ferlini, C., Distefano, M., Pignatelli, F., Lin, S., Riva, A., Bombardelli, E., Mancuso, S., Ojima, I., Scambia, G. Antitumor activity of novel taxanes that act as the same time as cytotoxic agents and P-glycoprotein inhibitors. *Brit. J. Cancer* **2000,** 83, 1762-1768.
79. Geney, R.; Chen, J.; Ojima, I. Recent Advances in the New Generation Taxane Anticancer Agents *Med. Chem.* **2005,** 1, 125-139.
80. Ehrlichova, M., Vaclavikova, R., Ojima, I., Pepe, A., Kuznetsova, L.V., Chen, J., Truksa, J., Kovar, J., Gut, I. Transport and cytotoxicity of paclitaxel, docetaxel, and novel taxanes in human breast cancer cells. *Arch Pharmacol* **2005,** 372, 95-105.
81. Kovar, J., Ehrlichova, M., Smejkalova, B., Zanardi, I., Ojima, I., Gut, I. Comparison of cell death-inducing effect of novel taxane SB-T-1216 and paclitaxel in breast cancer cells. *Anticancer Res.* **2009,** 29, 2951-2960.
82. Gottlieb, H. E.; Kotlyar, V.; Nudelman, A. NMR Chemical Shifts of Common Laboratory Solvents as Trace Impurities. *J. Org. Chem.* **1997,** 62, 7512-7515.

83. Brieva, R.; Crich, J. Z.; Sih, C. J. Chemoenzymic synthesis of the C-13 side chain of taxol: optically active 3-hydroxy-4-phenyl .beta.-lactam derivatives. *J. Org. Chem.* **1993,** 58, 1068-1075.
84. Ojima, I.; Habus, I.; Zhao, M.; Zucco, M.; Park, Y. H.; Sun, C. M.; Brigaud, T. New and efficient approaches to the semisynthesis of taxol and its C-13 side chain analogs by means of [beta]-lactam synthon method. *Tetrahedron* **1992,** 48, 6985-7012.
85. Cree, I. A. Principles of Cancer Cell Culture. In *Methods in Molecular Biology*, Cree, I. A., Ed. Springer Science + Business Media, LLC: 2011; Vol. 731, pp 13-26.
86. Mosmann, T. Rapid colorimetric assay for cellular growth and survival: Application to proliferation and cytotoxicity assays. *J. Immunological Methods* **1983,** 65, 55-63.

Chapter 2 References

1. Pierce, G. B.; Speers, W. C. Tumors as Caricatures of the Process of Tissue Renewal: Prospects for Therapy by Directing Differentiation. *Cancer Res.* **1988,** 48, 1996-2004.
2. Beere, H. M.; Hickman, J. A. Differentiation: a suitable strategy for cancer chemotherapy? *Anti-cancer Drug Design* **1993,** 8, 299-322.
3. Leszczyniecka, M.; Roberts, T.; Dent, P.; Grant, S.; Fisher, P. B. Differentiation therapy of human cancer: basic science and clinical applications. *Pharmacol. Ther.* **2001,** 90, 105-156.
4. Li, L.; Neaves, W. B. Normal Stem Cells and Cancer Stem Cells: The Niche Matters. *Cancer Res.* **2006,** 66, 4553-4557.
5. Botchkina, G. I., Zuniga, E.S., Das, M.,, Wang, Y., Wang, H., Zhu, S., Savitt, A.G., Rowehl, R.A., Leyfman, Y., Ju, J., Shroyer, K., Ojima, I. New-generation taxoid SB-T-1214 inhibits stem cell-related gene expression in 3D cancer spheriods induced by purified colon tumor-initiating cells. *Mol. Cancer* **2010,** 9, 192-204.
6. Becker, A. J.; McCulloch, E. A.; Till, J. E. Cytological Demonstration of the Clonal Nature of Spleen Colonies Derived from Transplanted Mouse Marrow Cells. *Nature* **1963,** 197, 452-454.
7. Siminovitch, L.; McCulloch, E. A.; Till, J. E. The distribution of colony-forming cells among spleen colonies. *J. Cell. Comp. Physiol.* **1963,** 62, 327-336.
8. Clarke, M. F.; Dick, J. E.; Dirks, P. B.; Eaves, C. J.; Jamieson, C. H. M.; Jones, D. L.; Visvader, J.; Weissman, I. L.; Wahl, G. M. Cancer Stem Cells—Perspectives on Current Status and Future Directions: AACR Workshop on Cancer Stem Cells. *Cancer Res.* **2006,** 66, 9339-9344.
9. Al-Hajj, M.; Wicha, M. S.; Benito-Hernandez, A.; Morrison, S. J.; Clarke, M. F. Prospective identification of tumorigenic breast cancer cells. *Pcot Natl Acad Sci USA* **2003,** 100, 3983-3988.
10. Al-Hajj, M.; Clarke, M. F. Self-renewal and solid tumor stem cells. *Oncogene* **2004,** 23, 7274-7282.
11. Schatton, T.; Frank, N. Y.; Frank, M. H. Identification and targeting of cancer stem cells. *BioEssays* **2009,** 32, 1037-1049.
12. Bonnet, D.; Dick, J. E. Human acute myeloid leukemia is organized as a hierarchy that originates from a primitive hematopoietic cell. *Nature Med.* **1997,** 3, 730-737.
13. Miyamoto, T.; Weissman, I. L.; Akashi, K. AML1/ETO-expressing nonleukemic stem cells in acute myelogenous leukemia with 8;21 chromosomal translocation. *Proc. Natl. Acad. Sci. U.S.A.* **2000,** 97, 7521-7526.

14. George, A. A.; Franklin, J.; Kerkof, K.; Shah, A. J.; Price, M.; Tsark, E.; Bockstoce, D.; Yao, D.; Hart, N.; Carcich, S.; Parkman, R.; Crooks, G. M.; Weinberg, K. Detection of leukemic cells in the CD34+ CD38− bone marrow progenitor population in children with acute lymphoblastic leukemia. *Blood* **2001,** 97, 3925-3930.
15. Mauro, M. J.; Drucker, B. J. Chronic myelogenous leukemia. *Curr. Opin. Oncol.* **2001,** 13, 3-7.
16. Li, L.; Xie, T. Stem cell niche: structure and function. *Annu. Rev. Cell. Dev. Biol.* **2005,** 21, 605-631.
17. Spradling, A.; Drummond-Barbosa, D.; Kai, T. Stem cells find their niche. *Nature* **2001,** 414, 98-104.
18. Kirchner, T.; Müller, S.; Hattori, T.; Mukaisyo, K.; Papadopulos, T.; Brabletz, T.; Jung, A. Metaplasia, intraepithelial neoplasia and early cancer of the stomach are related to dedifferentiated epithelial cells defined by cytokeratin-7 expression in gastritis *Virchows Archiv.* **2001,** 439, 512-522.
19. Shmelkov, S. V.; Clair, R.; Lyden, D.; Rafii, S. AC133/CD133/Prominin-1. *Int. J. Biochem. Cell Biol.* **2005,** 37, 715-719.
20. Collin, A. T.; Berry, P. A.; Hyde, C.; Stower, M. J.; Maitland, N. J. Prospective identification of tumorigenic prostate cancer stem cells. *Cancer Res.* **2005,** 65, 10946-10951.
21. Jin, L.; Hope, K. J.; Zhai, Q.; Smadja-Joffe, F.; Dick, J. E. Targeting of CD44 eradicates human acute myeloid leukemic stem cells. *Nat. Med.* **2006,** 10, 167-174.
22. Krause, D. S.; Lazarides, K.; von Andrian, U. H.; Van Etten, R. A. Requirement for CD44 in homing and engraftment of BCR-ABL-expressing leukemic stem cells. *Nat. Met.* **2006,** 10, 1175-1180.
23. Patrawala, L.; Calhoun, T.; Schneider-Broussard, R.; Li, H.; Bhatia, B.; Tang, S.; Reilly, J. G.; Chandra, D.; Zhou, J.; Claypool, K.; Coghlan, L.; Tang, D. G. Highly purified CD44+ prostate cancer cells from xenograft human tumors are enriched in tumorigenic and metastatic progenitor cells. *Oncogene* **2006,** 25, 1696-1708.
24. Dalerba, P.; Dylla, S. J.; Park, I. K.; Liu, R.; Wang, X.; Cho, R. W.; Hoey, T.; Gurney, A.; Huang, E. H.; Simeone, D. M.; Shelton, A. A.; Parmiani, G.; Castelli, C.; Clarke, M. F. Phenotypic characterization of human colorectal cancer stem cells. *PNAS* **2007,** 104, 10158-10163.
25. Haraguch, M.; Ohkuma, M.; Sakashita, H.; Matsuzaki, S.; Tanaka, F.; Mimori, K.; Kamohara, Y.; Inoue, H.; Mori, M. CD133+CD44+ Population Efficiently Enriches Colon Cancer Initiating Cells. *Ann. Surgical Oncol.* **2008,** 15, 2927-2933.
26. Rowehl, R. H.; Crawford, H.; Dufour, A.; Leyfman, Y.; Ju, J.; Botchkina, G. I. Genomic Analysis of Prostate Cancer Stem Cells Isolated from Highly Metastatic Cell Line. *Cancer Genomics and Proteomics* **2008,** 5, 301-309.
27. Botchkina, I. L.; Rowehl, R. A.; Rivadeneira, D. E.; Karpeh, M. S. J.; Crawford, H.; Dufour, A.; Ju, J.; Weng, Y.; Leyfman, Y.; Botchkina, G. I. Phenotypic Subpopulations of Metastatic Colon Cancer Stem Cells. *Cancer Geno. Proteo.* **2009,** 6, 19-30.
28. Hong, S. P.; Wen, J.; Bang, S.; Park, S.; Song, S. Y. CD44-positive cells are responsible for gercitabine resistance in pancreatic cancer cells. *Int. J. Cancer* **2009,** 125, 2323-2331.
29. Ponta, H.; Sherman, L.; Herrlich, P. A. CD44: From adhesion molecules to signalling regulators. *Nat. Rev. Mol. Cell Biol.* **2003,** 4, 33-45.
30. Marhaba, R.; Zoller, M. CD44 in cancer progression: adhesion, migration and growth regulation. *J. Mol. Histol.* **2004,** 35, 211-231.

31. Gotley, D. C.; Fawcett, J.; Walsh, M. D.; Reeder, J. A.; Simmons, D. L.; Antalis, T. M. Alternatively spliced variants of the cell adhesion molecule CD44 and tumour progression in colorectal cancer. *Brit. J. Cancer* **1996,** 74, 342-351.
32. Frank, N. Y.; Pendse, S. S.; Lapchak, P. H.; Margaryan, A.; Shlain, D.; Doeing, C.; Sayegh, M. N.; Frank, M. H. Regulation of progenitor cell fusion of ABCB5 P-glycoprotein, a novel human ATP-binding cassette transporter. *J. Biol. Chem.* **2005,** 278, 47156-47165.
33. Frank, N. Y.; Margaryan, A.; Huang, Y.; Schatton, T.; Waaga-Gasser, A. M.; Gasser, M.; Sayegh, M. H.; Sadee, W.; Frank, M. H. ABCB5-meditated doxorubicin transport and chemoresistance in human malignant melanoma. *Cancer Res.* **2005,** 65, 4320-4333.
34. Bao, S.; Wu, Q.; McLendon, R. E.; Hao, Y.; Shi, Q.; Hjelmelad, A. B.; Dewhirst, M. W.; Bigner, D. D.; Rich, J. N. Glioma stem cells promote radioresistance by preferential activation of the DNA damage response. *Nature* **2006,** 444, 756-760.
35. Liu, G.; Yuan, X.; Zeng, Z.; Tunici, P.; Ng, H.; Abdulkadir, I. R.; Lu, L.; Irvin, D.; Black, K. L.; Yu, J. S. Analysis of gene expression and chemoresistance of CD133+ cancer stem cells in glioblastoma. *Mol. Cancer* **2006,** 5, 67-79.
36. Bertolini, G.; Roz, L.; Perego, P.; Tortoreto, M.; Fontanella, E.; Gatti, L.; Pratesi, G.; Fabbri, A.; Andriani, F.; Tinelli, S.; Roz, E.; Caserini, R.; Lo Vullo, S.; Camerini, T.; Mariani, L.; Delia, D.; Calabro, E.; Pastorino, U.; Sozzi, G. Highly tumorigenic lung cancer CD133+ cells display stem-like features and are spared by cisplatin treatment. *Proc. Natl. Acad. Sci. U.S.A.* **2009,** 106, 16281-16286.
37. Dallas, N. A.; Xia, L.; Fan, F.; Gray, M. J.; Gaur, P.; van Buren, G.; Samuel, S.; Kim, M. P.; Lim, S. J.; Ellis, L. M. Chemoresistant colorectal cancer cells, the cancer stem cell phenotype, and increased sensitivity to insulin-like growth factor-1 receptor inhibition. *Cancer Res.* **2009,** 69, 1951-1957.
38. Vlashi, E.; McBride, W. H.; Pajonk, F. Radiation responses of cancer stem cells. *J. Cell. Biochem.* **2009,** 108, 339-342.
39. Liu, Q.; Nguyen, D. H.; Dong, Q.; Shitaku, P.; Chung, K.; Liu, O. Y.; Tso, J. L.; Liu, J. Y.; Konkankit, V.; Cloughesy, T. F.; Mischel, P. S.; Lane, T. F.; Liau, L. M.; Nelson, S. F.; Tso, C. L. Molecular properties of CD133+ glioblastoma stem cells derived from treatment-refractory recurrent brain tumors. *J. Neurooncol.* **2009,** 94, 1-19.
40. Dirks, P. B. Cancer: Stem cells and brain tumours. *Nature* **2006,** 444, 687-688.
41. Eramo, A.; Ricci-Vitiani, L.; Zeuner, A.; Pallini, R.; Lotti, F.; Sette, G.; Pilozzi, E.; Larocca, L. M.; Peschle, C.; De Maria, R. Chemotherapy resistance of glioblastoma stem cells. *Cell Death Differ.* **2006,** 13, 1238-1241.
42. Woodward, W. A.; Chen, M. S.; Behbod, F.; Alfaro, M. P.; Buchholz, T. A.; Rosen, J. M. WNT/β-catenin mediates radiation resistance of mouse mammary progenitor cells. *Proc. Natl. Acad. Sci. U.S.A.* **2007,** 104, 618-623.
43. Todaro, M.; Alea, M. P.; Stefano, A. B.; Cammareri, P.; Vermeulen, L.; Lovino, F.; Tripodo, C.; Russo, A.; Gulotta, G.; Medema, J. P.; Stassi, G. Colon cancer stem cells dictate tumor growth and resist cell death by production of interleukin-4. *Cell Stem Cell* **2007,** 1, 389-402.
44. Bleau, A. M.; Hambardzumyan, D.; Ozawa, T.; Fomchenko, E. I.; Huse, J. T.; Brennan, C. W.; Holland, E. C. PTEN/PI3K/Akt pathway regulates the side population phenotype and ABCG2 activity in glimoa tumor stem-like cells. *Cell Stem Cell* **2009,** 4, 226-235.
45. Al-Hajj, M.; Wicha, M. S.; Benito-Hernandez, A.; Morrison, S. J.; Clarke, M. F. Prospective identification of tumorigenic breast cancer cells. *PNAS USA* **2003,** 100, 3983-3988.

46. Zeppernick, F.; Ahmadi, R.; Campos, B.; Dictus, C.; Helmke, B. M.; Becker, N.; Lichter, P.; Unterberg, A.; Radlwimmer, B.; Herold-Mende, C. C. Stem Cell Marker CD133 Affects Clinical Outcome in Glioma Patients. *Clin. Cancer Res.* **2008,** 14, 123-129.
47. Maeda, S.; Shinchi, H. H.; Kurahara, H. Y.; Mataki, Y.; Maemura, K.; Sato, M.; Natsugoe, S.; Aikou, T.; Takao, S. S. CD133 expression is correlated with lymph node metastasis and vascular endothelial growth factor-C expression in pancreatic cancer. *Brit. J. Cancer* **2008,** 98, 1389-1397.
48. Horst, D.; Kriegl, L.; Engel, J.; Kirchner, T.; Jung, A. CD13 expression is an independent prognostic marker for low survival in colorectal cancer. *Brit. J. Cancer* **2008,** 99, 1285-1289.
49. Lapidot, T.; Sirard, C.; Vormoor, J.; Murdoch, B.; Hoang, T.; Caceres-Cortes, J.; Minden, M.; Paterson, B.; Caligiuri, M. A.; Dick, J. E. A cell initiating human acute myeloid leukaemia after transplanation into SCID mice. *Nature* **1994,** 367, 645-648.
50. Singh, S. K.; Clarke, I. D.; Terasaki, M.; Bonn, V. E.; Hawkins, C.; Squire, J.; Dirks, P. B. Identification of a cancer stem cell in human brain tumors. *Cancer Res.* **2003,** 63, 5821-5828.
51. Bussolati, B.; Bruno, S.; Grange, C.; Buttiglieri, S.; Deregibus, M. C.; Cantino, D.; Camussi, G. Isolation of renal progenitor cells from adult human kidney. *Am. J. Pathol.* **2005,** 166, 545-555.
52. Suetsugu, A.; Nagaki, M.; Aoki, H.; Motohashi, T.; Kunisada, T.; Moriwaki, H. Characterization of CD133+ hepatocellular carcinoma cells as cancer stem/progenitor cells. *Biochem. and Biophys. Res. Comm.* **2006,** 351, 820-824.
53. Yin, S.; Li, J.; Hu, C.; Chen, X.; Yao, M. CD133 positive hepatocellular carcinoma cells possess high capacity for tumorigenicity. *Int. J. Cancer* **2007,** 120, 1444-1450.
54. O'Brien, C. A.; Pollett, A.; Gallinger, S.; Dick, J. A human colon cancer cell capable of initiating tumor growth in immunodeficient mice. *Nature* **2007,** 445, 106-110.
55. Ricci-Vitiani, L.; Lombardi, D. G.; Pilozzi, E.; Biffoni, M.; Todaro, M.; Peschle, C.; De Maria, R. Identification and expansion of human colon-cancer-initiating cells. *Nature* **2007,** 445, 111-115.
56. Hermann, P. C.; Huber, S. L.; Herrler, T.; Aicher, A.; Ellwart, J. W.; Guba, M.; Bruns, C. J.; Heeschen, C. Distinct populations of cancer stem cells determine tumor growth and metastatic activity in human pancreatic cancer. *Cell Stem Cell* **2007,** 1, 313-323.
57. Southam, C. M.; Brunschwig, A. Quantitative studies of autotransplantation of human cancer. *Cancer* **1961,** 14, 971-978.
58. Salsbury, A. J. The significance of the circulating cancer cell. *Cancer Treat. Rev.* **1975,** 2, 55-72.
59. Reya, T.; Morrison, S. J.; Clarke, M. F.; Weissman, I. L. Stem cells, cancer, and cancer stem cells. *Nature* **2001,** 414, 105-111.
60. Stockler, M.; Wilcken, N. R. C.; Chersi, D.; Simes, R. J. Systematic reviews of chemotherapy and endocrine therapy in metastatic breast cancer. *Cancer Treat. Rev.* **2000,** 26, 151-168.
61. Park, C. H.; Bergsagal, D. E.; McCulloch, E. A. Mouse myeloma tumor stem cells: a primary cell culture assay. *J. Natl. Cancer Inst.* **1971,** 46, 411-422.
62. Harrison, D. E.; Lerner, C. P. Most primitive hematopoietic stem cells are stimulated to cycle rapidly after treatment with 5-fluorouracil. *Blood* **1991,** 78, 1237-1240.
63. Dean, M.; Fojo, T.; Bates, S. Tumor stem cell and drug resistance. *Nat. Rev. Cancer* **2005,** 5, 275-284.

64. Donnenberg, V. S.; Donnenberg, A. D. Multiple drug resistance in cancer revisited: the cancer stem cell hypothesis. *J. Clin. Pharmacol.* **2005,** 45, 872-877.
65. Mimeault, M.; Hauke, R.; Mehra, P. P.; Batra, S. K. Recent advances in cancer stem/progenitor cell research: therapeutic implications for overcoming resistance to the most aggressive cancers. *J. Cell. Mol. Med.* **2007,** 11, 981-1011.
66. Kirkland, S. C. Type I collagen inhibits differentiation and promotes a stem cell-like phenotype in human colorectal carcinoma cells. *Brit. J. Cancer* **2009,** 101, 320-326.

Chapter 3 References

1. Gottesman, M. M., Pastan, I. Biochemistry of multidrug resistance mediated by the multidrug transporter. *Annu. Rev. Biochem.* **1993,** 62, 385-427.
2. Jack, D. L.; Yang, N. M.; Saier, M. H. J. The drug/metabolite transporter superfamily. *Eur. J. Biochem.* **2001,** 268, 3620-3639.
3. Ferlini, C., Distefano, M., Pignatelli, F., Lin, S., Riva, A., Bombardelli, E., Mancuso, S., Ojima, I., Scambia, G. Antitumor activity of novel taxanes that act as the same time as cytotoxic agents and P-glycoprotein inhibitors. *Brit. J. Cancer* **2000,** 83, 1762-1768.
4. Allen, H. K.; Donao, J.; Wang, H. H.; Cloud-Hansen, K. A.; Davies, J.; Handelsman, J. Call of the wild: antibiotic resistance genes in natural environments. *Nature Rev. Microbio.* **2010,** 8, 251-259.
5. Devita Jr., V. T.; Chu, E. A History of Cancer Chemotherapy. *Cancer Res.* **2008,** 68, 8643-8653.
6. Druker, B. J.; Lydon, N. B. Lessons learned from the development of an Abl tyrosine kinase inhibitor for chronic myelogenous leukemia. *J. Clin. Invest.* **2000,** 105, 3-7.
7. Drucker, B. J.; Tamura, S.; Buchdunger, E.; Ohno, S.; Segal, G. M.; Fanning, S.; Zimmerman, J.; Lydon, N. B. Effects of a selective inhibitor of the Abl tyrosine kinase on the growth of Bcr-Abl positive cells. *Nat. Med.* **1996,** 2, 561-566.
8. Krause, D. S.; Van Etten, R. A. Tyrosine kinases as targets for cancer therapy. *N. Engl. J. Med.* **2005,** 2, 172-187.
9. Doronina, S. O., Mendelsohn, B.A., Bovee, T.D., Cerveny, C.G., Alley, S.C., Meyer, D.L., Oflazoghu, E., Toki, B.E., Sanderson, R.J., Zabinski, R.F., Wahl, A.F., Senter, P.D. Enhanced Activity of Monomethylauristatin F through Monoclonal Antibody Delivery: Effects of Linker Technology on Efficacy and Toxicity. *Bioconjugate Chem.* **2006,** 17, 114-124.
10. Beck, A., Haeuw, J.F., Wurch, T., Goetsch, L., Bailly, C., Corvaia, N. The next generation of antibody-drug conjugates comes of age. *Discov. Med.* **2010,** 10, 329-339.
11. Bradley, M. O., Webb, N.L., Anthony, F.H., Devanesan, P., Wittman, P.A., Hemamalini, S., Chander, M.C., Baker, S.D., He, L., Horowitz, S.B., Swindell, C.S. Tumor targeting by covalent conjugation of a natural fatty acid to taxol. *Clin. Cancer Res.* **2001,** 7, 3229-3238.
12. Whelan, J. Targeted taxane therapy for cancer. *Drug Discovery Today* **2002,** 7, 90-92.
13. Wahl, A. F.; Donaldson, K. L.; Mixan, B. J.; Trail, P. A.; Siegall, C. B. Selective tumor sensitization to taxanes with the mAb-drug conjugate cBR96-doxorubicin. *Int. J. Cancer* **2001,** 4, 590-600.
14. Hamann, P. R.; Hinman, L. M.; Beyer, C. F.; Lindh, D.; Upeslacis, J.; Flowers, D. A.; Bernstein, I. An Anti-CD33 Antibody−Calicheamicin Conjugate for Treatment of Acute Myeloid Leukemia. Choice of Linker. *Bioconjugate Chem.* **2002,** 13, 40-46.

15. Sauer, L. A., Dauchy, R.T., Blask, D.E. Mechanism for the antitumor and anticachectic effects of n-3 fatty acids. *Cancer Res.* **2000,** 60, 5289-5295.
16. Wigmore, S. J., Ross, J.A., Falconer, J.S., Plester, C.E., Tisdale, M.J., Carter, D.C., Fearon, K.C.H. The effect of polyunsaturated fatty acids on the progress of cachexia in patients with pancreatic cancer. *Nutrition* **1996,** 12, S27-S30.
17. Hawkins, R. A.; Sangster, K.; Arends, M. J. Apoptotic death of pancreatic cancer cells induced by polyunsaturated fatty acids varies with double bond number an involves an oxidative mechanism. *J. Pathol.* **1998,** 185, 61-70.
18. Grammatikos, S. I., Subbaiah, P.V., Victor, T.A., Miller, W.M. n-3 and n-6 fatty acid processing and growth effects in neoplastic and non-cancerous human mammary epithelial cell lines. *Brit. J. Cancer* **1994,** 70, 219-227.
19. Diomede, L., Colotta, F., Piovani, B., Re, F., Modest, E.J., Salmona, M. Induction of apoptosis in human leukemic cells by the ether lipid 1-octadecyl-2-methyl-racglycero-3-phosphocholine. A possible basis for its selective action. *Int. J. Cancer Res.* **1993,** 53, 124-130.
20. Seitz, J. D.; Ojima, I. Drug Conjugates with Polyunsaturated Fatty Acids. In *Drug Delivery in Oncology: From Basic Research to Cancer Therapy*, 1st ed.; Kratz, F.; Senter, P.; Steinhagen, H., Eds. Wiley-VCH Verlag GmbH & co. KGaA.: 2010; Vol. 3, pp 1323-1360.
21. Ibrahim, N. K., Desai, N., Legha, S., Soon-Shiong, P., Theriault, R.L., Rivera, E., Esmaeli, B., Ring, S.E., Bedikian, A., Hortobagyi, G.N., Ellerhorst, J.A. Phase I and pharmacokinetic study ABI-007, a cremophor-free, protein-stabilized nanoparticle formulation of paclitaxel. *Clin. Cancer Res.* **2002,** 8, 1038-1044.
22. Desai, N., Trieu, V., Yao, Z., Louie, L., Ci, S., Yang, A., Tao, C., De, T., Beals, B., Dykes, D., Noker, P., Yao, R., Labao, E., Hawkins, M., Soon-Shiong, P. Increased antitumor activity, intratumor paclitaxel concentrations, and endothelial cell transport of cremophor-free, albumin-bound paclitaxel, ABI-007, compared with cremophor-based paclitaxel. *Clin. Cancer Res.* **2006,** 12, 1317-1324.
23. Rose, D. P.; Connolly, J. M. Omega-3 fatty acids as cancer chemopreventive agents. *Pharmacol. Ther.* **1999,** 83, 217-244.
24. Tuller, E. R.; Brock, A. L.; Yu, H.; Lou, J. R.; Benbrook, D. M.; Ding, W.-Q. PPARα signaling mediates the synergistic cytotoxicity of clioquinol and docosahexaenoic acid in human cancer cells. *Biochem. Pharmacol.* **2009,** 77, 1480-1486.
25. Zhuo, Z.; Zhang, L.; Mu, Q.; Lou, Y.; Gong, Z.; Shi, Y.; Quyang, G.; Zhang, Y. The effect of combination treatment with docosahexaenoic acid and 5-fluorouracil on the mRNA expression of apoptosis-related genes, including the novel gene BCL2L12, in gastric cancer cells. *In Vitro Cell. Dev. Biol. Anim.* **2009,** 45, 69-74.
26. Yamamoto, D.; Kiyozuka, Y.; Adachi, Y.; Takada, H.; Hioki, K.; Tsubura, A. Synergistic action of apoptosis induced by eicosapentaenoic acid and TNP-470 on human breast cancer cells. *Breast Cancer Res. Treat.* **1999,** 55, 149-160.
27. Nakagawa, H.; Yamamoto, D.; Kiyozuka, Y.; Tsuta, K.; Uemura, Y.; Hioki, K.; Tsutsui, Y.; Tsubura, A. Effects of genistein and synergistic action in combination with eicosapentaenoic acid on the growth of breast cancer cell lines. *J. Cancer Res. Clin. Oncol.* **2000,** 126, 448-454.
28. Menendez, J. A.; Ropero, S.; del Mar Barbacid, M.; Montero, S.; Solanas, M.; Escrich, E.; Cortes-Funes, H.; Colmer, R. Synergistic interaction between vinorelbine and gamma-linolenic acid in breast cancer cells. *Eur. J. Cancer* **2001,** 37, 402-413.
29. Ojima, I.; Zuniga, E. S.; Berger, W. T.; Seitz, J. D. Tumor-targeting drug delivery of new-genreation taxoids. *Future Med. Chem.* **2012,** 4, 33-50.

30. Ojima, I.; Slater, J. C.; Michaud, E.; Kuduk, S. D.; Bounaud, P.-Y.; Vrignaud, P.; Bissery, M.-C.; Veith, J.; Pera, P.; Bernacki, R. J. Syntheses and structure–activity relationships of the second generation antitumor taxoids. Exceptional activity against drug-resistant cancer cells. *J. Med. Chem.* **1996,** 39, 3889-3896.
31. Ojima, I.; Slater, J. C.; Kuduk, S. D.; Takeuchi, C. S.; Gimi, R. H.; Sun, C. M.; Park, Y. H.; Pera, P.; Veith, J. M.; Bernacki, R. J. Syntheses and Structure-Activity Relationships of Taxoids Derived from 14-beta-Hydroxy-10-deacetylbaccatin III. *J. Med. Chem.* **1997,** 40, 267-278.
32. Ojima, I., Slater, J. C., Michaud, E., Kuduk, S. D., Bounaud, P. Y., Vrignaud, P., Bissery, M. C., Veith, J. M., Pera, P., Bernacki, R. J. Syntheses and Structure-Activity Relationships of the Second-Generation Antitumor Taxoids: Exceptional Activity against Drug-Resistant Cancer Cells. *J. Med. Chem.* **1996,** 39, 3889-3896.
33. Ojima, I. Guided Molecular Missiles for Tumor-Targeting Chemotherapy-Case Studies Using the Second-Generation Taxoid as Warheads. *Acc. Chem. Res.* **2008,** 41, 108-119.
34. Cushman, M.; Jayaraman, M.; Vroman, J. A.; Fukunaga, A. K.; Fox, B. M.; Kohlhagen, G.; Strumberg, D.; Pommier, Y. Synthesis of new indeno[1,2-c]isoquinolines: cytotoxic non-camptothecin topoisomerase I inhibitors. *J. Med. Chem.* **2000,** 43, 3688-3698.
35. Anthony, S.; Jayaraman, M.; Laco, G.; Kohlhagen, G.; Kohn, K. W.; Cushman, M.; Pommier, Y. Differential Induction of Topoisomerase I-DNA Cleavage Complexes by the Indenoisoquinoline MJ-III-65 (NSC 706744) and Camptothecin: Base Sequence Analysis and Activity against Camptothecin-Resistant Topoisomerases I. *Cancer Res* **2003,** 63, 7428-7435.
36. Xiao, X.; Antony, S.; Kohlhagen, G.; Pommier, Y.; Cushman, M. Design, synthesis, and biological evaluation of cytotoxic 11-aminoalkenylindenoisoquinoline and 11-diaminoalkenylindeoisoquinoline topoisomerase I inhibitors. *Bioorg. & Med. Chem.* **2004,** 12, 5147-5160.
37. Hertzberg, R. P.; Caranfa, M. J.; Holden, K. G.; Jakas, D. R.; Gallagher, D.; Mattern, M. R.; Mong, S.-M.; Bartus, J.-O.; Johnson, R. K.; Kingsbury, W. D. Modification of the hydroxylactone ring of camptothecin: inhibition of mammalian topoisomerase I and biological activity. *J. Med. Chem.* **1989,** 32, 715-720.
38. Hsiang, Y. H.; Lihou, M. G.; Liu, F. Arrest of replication forks by drug-stabilized topoisomerase I-DNA cleavable complexes as a mechanism of cell killing by camptothecin. *Cancer Res.* **1989,** 49, 5077-5082.
39. Giovanella, B. C.; Hinz, H. R.; Kozielski, A. J.; Stehlin Jr., J. S.; Silber, R.; Potmesil, M. Complete growth inhibition of human cancer xenografts in nude mice by treatment with 20-(S)-Camptothecin. *Cancer Res.* **1991,** 51, 3052-3055.
40. Wani, M. C.; Ronman, P. E.; Lindley, J. T.; Wall, M. E. Plant antitumor agents. 18. Synthesis and biological activity of camptothecin analogs. *J. Med. Chem.* **1980,** 23, 554-560.
41. Gottlieb, H. E.; Kotlyar, V.; Nudelman, A. NMR Chemical Shifts of Common Laboratory Solvents as Trace Impurities. *J. Org. Chem.* **1997,** 62, 7512-7515.

Chapter 4 References

1. Devita Jr., V. T.; Chu, E. A History of Cancer Chemotherapy. *Cancer Res.* **2008,** 68, 8643-8653.

2. Mauger, A. B.; Burke, P. J.; Somani, H. H.; Friedlos, F.; Knox, R. J. Self-Immolative Prodrugs: Candidates for Antibody-Directed Enzyme Prodrug Therapy in Conjunction with a Nitroreductase Enzyme. *J. Med. Chem.* **1994,** 37, 3452-3458.
3. Schmidt, F.; Florent, J. C.; Monneret, C.; Straub, R.; Czech, J.; Gerken, M.; Bosslet, K. Glucuronide prodrugs of hydroxy compounds for antibody directed enzyme prodrug therapy (ADEPT) : A phenol nitrogen mustard carbamate. *Bioorg. Med. Chem. Lett.* **1997,** 7, 1071-1076.
4. Ojima, I., Geng, X., Wu, X., Qu, C., Borella, C. P., Xie, H., Wilhelm, S. D., Leece, B. A., Bartle, L. M., Goldmacher, V. S., Chari, R. V. J. Tumor-Specific Novel Taxoid-Monoclonal Antibody Conjugates. *J. Med. Chem.* **2002,** 45, 5620-5623.
5. Chen, J., Chen, S., Zhao, X., Kuznetsova, L., Wong, S.S., Ojima, I. Functionalized Single-walled Carbon Nanotubes as Rationally Designed Vehicles for Tumor-Targeted Drug Delivery. *J. Am. Chem. Soc.* **2008,** 130, 16778-16785.
6. Burke, P. J.; Senter, P. D.; Meyer, D. W.; Miyamoto, J. B.; Anderson, M.; Toki, B. E.; Manikumar, G.; Wani, M. C.; Kroll, D. J.; Jeffery, S. C. Design, Synthesis, and Biological Evaluation of Antibody−Drug Conjugates Comprised of Potent Camptothecin Analogues. *Bioconjugate Chem.* **2009,** 20, 1242-1250.
7. Vlahov, I. R.; Vite, G. D.; Kleindi, P. J.; Wang, Y.; Santhapuram, H. K. R.; You, F.; Howard, S. J.; Kim, S.-H.; Lee, F. F. Y.; Leamon, C. P. Regioselective synthesis of folate receptor-targeted agents derived from epothilone analogs and folic acid. *Bioorg. Med. Chem. Lett.* **2010,** 20, 4578-4581.
8. Chen, S., Zhao, X., Chen, J., Chen, J., Kuznetsova, L., Wong, S.S., Ojima, I. Mechanism-based tumor-targeting drug delivery system. Validation of efficient vitamin receptor-mediated endocytosis and drug release. *Bioconjugate Chem.* **2010,** 21, 979-987.
9. Meyer, Y.; Richard, J.-A.; Massonneau, M.; Renard, P.-Y.; Romieu, A. Development of a New Nonpeptidic Self-Immolative Spacer. Application to the Design of Protease Sensing Fluorogenic Probes. *Org. Lett.* **2008,** 10, 1517-1520.
10. Zhang, X.-B.; Waibel, M.; Hasserodt, J. An Autoimmolative Spacer Allows First-Time Incorporation of a Unique Solid-State Fluorophore into a Detection Probe for Acyl Hydrolases. *Chem. Eur. J.* **2010,** 16, 792-795.
11. Antunes, I. F.; Haisma, H. J.; Elsinga, P. H.; Dierckx, R. A.; de Vries, E. F. J. Synthesis and Evaluation of [18F]-FEAnGA as a PET Tracer for β-Glucuronidase Activity. *Bioconjugate Chem.* **2010,** 21, 911-920.
12. Amir, R. J.; Pessah, N.; Shamis, M.; Shabat, D. Self-Immolative Dendrimers. *Angew. Chem., Int. Ed.* **2003,** 42, 4494-4499.
13. Avital-Shmilovici, M.; Shabat, D. Self-immolative dendrimers: A distinctive approach to molecular amplification. *Soft Matter* **2010,** 6, 1073-1080.
14. Ducry, L.; Stump, B. Antibody-drug conjugates: linking cytotoxic payloads to monoclonal antibodies. *Bioconjugate Chem.* **2010,** 21, 5-13.
15. Hamann, P. R.; Hinman, L. M.; Beyer, C. F.; Lindh, D.; Upeslacis, J.; Flowers, D. A.; Bernstein, I. An Anti-CD33 Antibody−Calicheamicin Conjugate for Treatment of Acute Myeloid Leukemia. Choice of Linker. *Bioconjugate Chem.* **2002,** 13, 40-46.
16. Trail, P. A.; Willner, D.; Lasch, S. J.; Henderson, A. J.; Hofstead, S.; Casazza, A. M.; Firestone, R. A.; Hellström, I.; Hellström, K. E. Cure of xenografted human carcinomas by BR96-doxorubicin immunoconjugates. *Science* **1993,** 261, 212-215.

17. Kaneko, T.; Willner, D.; Monkovic, I.; Knipe, J. O.; Braslawsky, G. R.; Greenfield, R. S.; Vyas, D. M. New hydrazone derivatives of Adriamycin and their immunoconjugates - a correlation between acid stability and cytotoxicity. *Bioconjugate Chem.* **1991,** 2, 133-141.
18. Rejmanová, P.; Kopeček, J.; Duncan, R.; Lloyd, J. B. Stability in rat plasma and serum of lysosomally degradable oligopeptide sequences in N-(2-hydroxypropyl) methacrylamide copolymers. *Biomaterials* **1985,** 6, 45-48.
19. Dalton King, H.; Dubowchik, G. M.; Mastalerz, H.; Willner, D.; Hofstead, S. J.; Firestone, R. A.; Lasch, S. J.; Trail, P. A. Monoclonal Antibody Conjugates of Doxorubicin Prepared with Branched Peptide Linkers: Inhibition of Aggregation by Methoxytriethyleneglycol Chains. *J. Med. Chem.* **2002,** 45, 4336-4343.
20. Dubowchik, G. M.; Firestone, R. A.; Padilla, L.; Willner, D.; Hofstead, S.; Mosure, K.; Knipe, J. O.; Lasch, S. J.; Trail, P. A. Cathepsin B-Labile Dipeptide Linkers for Lysosomal Release of Doxorubicin from Internalizing Immunoconjugates: Model Studies of Enzymatic Drug Release and Antigen-Specific In Vitro Anticancer Activity. *Bioconjugate Chem.* **2002,** 13, 855-869.
21. Doronina, S. O., Mendelsohn, B.A., Bovee, T.D., Cerveny, C.G., Alley, S.C., Meyer, D.L., Oflazoghu, E., Toki, B.E., Sanderson, R.J., Zabinski, R.F., Wahl, A.F., Senter, P.D. Enhanced Activity of Monomethylauristatin F through Monoclonal Antibody Delivery: Effects of Linker Technology on Efficacy and Toxicity. *Bioconjugate Chem.* **2006,** 17, 114-124.
22. Beck, A., Haeuw, J.F., Wurch, T., Goetsch, L., Bailly, C., Corvaia, N. The next generation of antibody-drug conjugates comes of age. *Discov. Med.* **2010,** 10, 329-339.
23. Liu, C.; Tadayoni, B. M.; Bourret, L. A.; Mattocks, K. M.; Derr, S. M.; Widdison, W. C.; Kedersha, N. L.; Ariniello, P. D.; Goldmacher, V. S.; Lambert, J. M.; Blätter, W. A.; Chari, R. V. Eradication of large colon tumor xenografts by targeted delivery of maytansinoids. *Proc. Natl. Acad. Sci. U.S.A.* **1996,** 93, 8618-8623.
24. Chari, R. V. J. Targeted Delivery of chemotherapeuitcs: tumor-activated prodrug therapy. *Adv. Drug Deliv. Rev.* **1998,** 31, 89-104.
25. Chari, R. V. J. Targeted cancer therapy: conferring specificity to cytotoxic drugs. *Acc. Chem. Res.* **2008,** 41, 98-107.
26. Tolcher, A. W.; Ochoa, L.; Hammond, L. A.; Patnaik, A.; Edwards, T.; Takimoto, C.; Smith, L.; de Bono, J.; Schwartz, G.; Mays, T.; Jonak, Z. L.; Johnson, R.; DeWitte, M.; Martino, H.; Audette, C.; Maes, K.; Chari, R. V.; Lambert, J. M.; Rowinsky, E. K. Cantuzumab Mertansine, a Maytansinoid Immunoconjugate Directed to the CanAg Antigen: A Phase I, Pharmacokinetic, and Biologic Correlative Study *J. Clin. Oncol.* **2003,** 21, 211-222.
27. Widdison, W. C.; Wilhelm, S. D.; Cavanagh, E. E.; Whiteman, K. R.; Leece, B. A.; Kovtun, Y.; Goldmacher, V. S.; Xie, H.; Steeves, R. M.; Lutz, R. J.; Zhao, R.; Wang, L.; Blattler, W. A.; Chari, R. V. J. Semisynthetic Maytansine Analogues for the Targeted Treament of Cancer. *J. Med. Chem.* **2006,** 49, 4392-4408.
28. Erickson, H. K.; Park, P. U.; Widdison, W. C.; Kovtun, Y. V.; Garrett, L. M.; Hoffman, K.; Lutz, R. J.; Goldmacher, V. S.; Blätter, W. A. Antibody-Maytansinoid conjugates are activated in targeted cancer cells by lysosomal degradation and linker-dependent intracellular processing. *Cancer Res.* **2006,** 66, 4426-4433.
29. Ranson, M.; Sliwkowski, M. X. Perspectives on anti-HER monoclonal antibodies. *Oncology* **2002,** 63, 17-24.
30. Polson, A. G.; Calemine-Fenaux, J.; Chan, P.; Chang, W.; Christensen, E.; Clark, S.; de Sauvage, F. J.; Eaton, D.; Elkins, K.; Elliott, J. M.; Frantz, G.; Fuji, R. N.; Gray, A.; Harden, K.;

Ingle, G. S.; Kljavin, N. M.; Koeppen, H.; Nelson, C.; Prabhu, S.; Raab, H.; Ross, S.; Stephan, J.-P.; Scales, S. J.; Spencer, S. D.; Vandlen, R.; Wranik, B.; Yu, S.-F.; Zheng, B.; Ebens, A. Antibody-drug conjugates for the treatment of non-Hodgkin's lymphoma: Target and linker-drug selection. *Cancer Res.* **2009,** 69, 2358-2364.
31. Kovtun, Y. V.; Audette, C. A.; Ye, Y.; Xie, H.; Ruberti, M. F.; Phinney, S. J.; Leece, B. A.; Chittenden, T.; Blätter, W. A.; Goldmacher, V. S. Antibody-drug conjugates designed to eradicate tumors with homogenous and heterogeneous expression of the target antigen. *Cancer Res.* **2006,** 66, 3214-3221.
32. Lewis Phillips, G. D.; Li, G.; Dugger, D. L.; Crocker, L. M.; Parsons, K. L.; Mai, E.; Blätter, W. A.; Lambert, J. M.; Chari, R. V.; Lutz, R. J.; Wong, W. L. T.; Jacobson, F. S.; Koeppen, H.; Schwall, R. H.; Kenkare-Mitra, S. R.; Spencer, S. D.; Sliwkowski, M. X. Targeting HER2-Positive Breast Cancer with Trastuzumab-DM1, an Antibody–Cytotoxic Drug Conjugate. *Cancer Res.* **2008,** 68, 9280-9290.
33. Fishkin, N.; Maloney, E. K.; Chari, R. V. J.; Singh, R. A novel pathway for maytansinoid release from thioether linked antibody-drug conjugates (ADCs) under oxidative conditions. *Chem. Commun.* **2011,** 47, 10752-10754.
34. Ojima, I. Use of Fluorine in the Medicinal Chemistry and Chemical Biology of Bioactive Compounds-A Case Study on Fluorinated Taxane Anticancer Agents. *ChemBioChem* **2004,** 5, 628-635.
35. Ojima, I. Guided Molecular Missiles for Tumor-Targeting Chemotherapy-Case Studies Using the Second-Generation Taxoid as Warheads. *Acc. Chem. Res.* **2008,** 41, 108-119.
36. Kigawa, J., Minagawa, Y., Kanamori, Y., Itamochi, H., Cheng, X., Okada, M., Oisho, T., Terakawa, N. Glutathione concentration may be a useful predictor of response to second-line chemotherapy in patients with ovarian cancer. *Cancer* **1998,** 82, 697-702.
37. Ojima, I. Tumor-targeting drug delivery of chemotherapeutic agents. *Pure Appl. Chem.* **2011,** 83, 1685-1698.
38. Ojima, I.; Zuniga, E. S.; Berger, W. T.; Seitz, J. D. Tumor-targeting drug delivery of new-genreation taxoids. *Future Med. Chem.* **2012,** 4, 33-50.
39. Banerjee, P. S.; Zuniga, E. S.; Ojima, I.; Carrico, I. S. Targeted and armed oncolytic adenovirus via chemoselective modification. *Bioorg. & Med. Chem. Lett.* **2011,** 21, 4985-4988.
40. Bordwell, F. G., Fried, H.E. Heterocyclic aromatic anions with 4n + 2 pi-electrons. *J. Org. Chem.* **1991,** 56, 4218-4223.
41. Shaabani, A.; Tavasoli-Rad, F.; Lee, D. G. Potassium Permanganate Oxidation of Organic Compounds. *Syn. Comm.* **2005,** 35, 571 - 580.
42. Samukov, V. V. A Simple Preparation of 3-(2-Pyridyldithio)-Propionic Acid. *Syn. Comm.* **1998,** 28, 3213 - 3217.
43. Olah, G.; Karpeles, R.; Narang, S. Synthetic methods and reactions: 107. Preparation of omega-haloalkylcarboxylic acids and esters or related compounds from lactones and boron trihalides. *Synthesis* **1982,** 11, 963-965.
44. Crabb, T.; Trethewey, A. Compounds with bridgehead nitrogen. Part 54. The stereochemistry of some derivatives of perhydrothiazolo[3,4-a]pyridine and the synthesis of 9-methylperhydro-3,8,methano-1,3-thiazocines. *J. Chem. Soc., Perkin Trans I* **1988,** 5, 1173-1178.
45. Sobik, P.; Grunenberg, J.; Brczky, K.; Laatsch, H.; Wagner-Dbler, I.; Schulz, S. Identification, synthesis, and conformation of tri- and tetrathiacycloalkanes from Marine Bacteria. *J. Org. Chem.* **2007,** 72, 3776-3782.

46. Pereira, D.; Hai, T. T.; Nelson, D. A Convenient Large Scale Synthesis of N,N'-Disuccinimidyl Carbonate. *Syn. Comm.* **1998,** 28, 4019-4024.
47. Sauer, L. A., Dauchy, R.T., Blask, D.E. Mechanism for the antitumor and anticachectic effects of n-3 fatty acids. *Cancer Res.* **2000,** 60, 5289-5295.
48. Grammatikos, S. I., Subbaiah, P.V., Victor, T.A., Miller, W.M. n-3 and n-6 fatty acid processing and growth effects in neoplastic and non-cancerous human mammary epithelial cell lines. *Brit. J. Cancer* **1994,** 70, 219-227.
49. Diomede, L., Colotta, F., Piovani, B., Re, F., Modest, E.J., Salmona, M. Induction of apoptosis in human leukemic cells by the ether lipid 1-octadecyl-2-methyl-racglycero-3-phosphocholine. A possible basis for its selective action. *Int. J. Cancer Res.* **1993,** 53, 124-130.
50. Gottlieb, H. E.; Kotlyar, V.; Nudelman, A. NMR Chemical Shifts of Common Laboratory Solvents as Trace Impurities. *J. Org. Chem.* **1997,** 62, 7512-7515.
51. Dickinson, R. P., Iddon, B. Condensed Thiophen Ring Systems. Part III. A New Synthesis of Benzo[b]thiophen-2(3H)- and - 3(2H)-ones and Some Reactions of Benzo[b]thiophen-2(3H)-one with Dimethyl Sulphate in the Presence of Base. *J. Chem. Soc.* **1970,** 14, 1926-1928.
52. Charles, M. Überführung des Oxindols in das 2-Keto-dihydro-1-thionaphthen (»Thio-oxindol«). *Chem. Ber.* **1912,** 45, 1481-1485.
53. Chari, R. V. J.; Widdison, W. C. Methods for preparation of cytotoxic conjugates of maytansinoids and cell binding agents. 2003.

Chapter 5 References

1. Chari, R. V. J. Targeted Delivery of chemotherapeuitcs: tumor-activated prodrug therapy. *Adv. Drug Deliv. Rev.* **1998,** 31, 89-104.
2. Ojima, I., Geng, X., Wu, X., Qu, C., Borella, C. P., Xie, H., Wilhelm, S. D., Leece, B. A., Bartle, L. M., Goldmacher, V. S., Chari, R. V. J. Tumor-Specific Novel Taxoid-Monoclonal Antibody Conjugates. *J. Med. Chem.* **2002,** 45, 5620-5623.
3. Wu, X.; Ojima, I. Tumor specific novel taxoid-monoclonal antibody conjugates. *Curr. Med. Chem.* **2004,** 11, 429-438.
4. Doronina, S. O., Mendelsohn, B.A., Bovee, T.D., Cerveny, C.G., Alley, S.C., Meyer, D.L., Oflazoghu, E., Toki, B.E., Sanderson, R.J., Zabinski, R.F., Wahl, A.F., Senter, P.D. Enhanced Activity of Monomethylauristatin F through Monoclonal Antibody Delivery: Effects of Linker Technology on Efficacy and Toxicity. *Bioconjugate Chem.* **2006,** 17, 114-124.
5. Beck, A., Haeuw, J.F., Wurch, T., Goetsch, L., Bailly, C., Corvaia, N. The next generation of antibody-drug conjugates comes of age. *Discov. Med.* **2010,** 10, 329-339.
6. Wagner, E.; Curiel, D.; Cotten, M. Delivery of drugs, proteins and genes into cells using transferrin as a ligand for receptor-mediated endocytosis. *Adv. Drug Delivery Rev.* **1994,** 14, 113-135.
7. Oh, S.; Kim, B. S.; Singh, N. P.; Lai, H.; Sasaki, T. Synthesis and Anti-cancer Activity of Covalent Conjugates of Artemisinin and a Transferrin-receptor Targeting Peptide. *Cancer Lett.* **2008,** 272, 110-121.
8. Nakase, I.; Gallis, B.; Takatani-Nakase, T.; Oh, S.; Lacoste, E.; Singh, N. P.; Goodlet, D. R.; Tanaka, S.; Futaki, S.; Lai, H.; Sasaki, T. Transferrin receptor-dependent cytotoxicity of artemisinin-transferrin conjugates on prostate cancer cells and induction of apoptosis. *Cancer Lett.* **2009,** 274, 290-298.

9. Russell-Jones, G., McTavish, Kirsten, McEwan, John, Rice, John, Nowotnik, David. Vitamin-mediated targeting as a potential mechanism to increase drug uptake by tumours. *J. of Inorg. Biochem.* **2004,** 98, 1625-1633.
10. Chen, S.; Zhao, X.; Chen, J.; Chen, J.; Kuznetsova, L.; Wong, S. S.; Ojima, I. Mechanism-based tumor-targeting drug delivery system. Validation of efficient vitamin receptor-mediated endocytosis and drug release. *Bioconjugate Chem.* **2010,** 21, 979-987.
11. Ojima, I. Guided Molecular Missiles for Tumor-Targeting Chemotherapy-Case Studies Using the Second-Generation Taxoid as Warheads. *Acc. Chem. Res.* **2008,** 41, 108-119.
12. Chen, J., Chen, S., Zhao, X., Kuznetsova, L., Wong, S.S., Ojima, I. Functionalized Single-walled Carbon Nanotubes as Rationally Designed Vehicles for Tumor-Targeted Drug Delivery. *J. Am. Chem. Soc.* **2008,** 130, 16778-16785.
13. Ojima, I. Tumor-targeting drug delivery of chemotherapeutic agents. *Pure Appl. Chem.* **2011,** 83, 1685-1698.
14. Ojima, I.; Zuniga, E. S.; Berger, W. T.; Seitz, J. D. Tumor-targeting drug delivery of new-genreation taxoids. *Future Med. Chem.* **2012,** 4, 33-50.
15. Chen, S., Zhao, X., Chen, J., Chen, J., Kuznetsova, L., Wong, S.S., Ojima, I. Mechanism-based tumor-targeting drug delivery system. Validation of efficient vitamin receptor-mediated endocytosis and drug release. *Bioconjugate Chem.* **2010,** 21, 979-987.
16. Leamon, C. P.; Reddy, J. A. Folate-targeted chemotherapy. *Adv. Drug Delivery Rev.* **2004,** 56, 1127-1141.
17. Y., L.; Low, P. S. Folate-mediated delivery of macromolecular anticancer therapeutic agents. *Adv. Drug Delivery Rev.* **2002,** 54, 675-693.
18. Lee, J. W.; Lu, J. Y.; Low, P. S.; Fuchs, P. L. Synthesis and evaluation of taxol-folic acid conjugates as targeted antineoplastics. *Bioorg. & Med. Chem.* **2002,** 10, 2397-2414.
19. Xia, W.; Low, P. S. Folate-targeted therapies for cancer. *J. Med. Chem.* **2010,** 53, 6811-6824.
20. Reddy, J. A.; Leamon, C. P. Folate receptor targeted cancer chemotherapy. In *Targeted Drug Strategies for Cancer and Inflammation*, Jackman, A. L.; Leamon, C. P., Eds. Springer Science+Buisness Media, LLC: 2011; pp 135-150.
21. Weinstein, S. J.; Hartman, T. J.; Stolzenberg-Solomon, R.; Pietinen, P.; Barrett, M. J.; Taylor, P. R.; Virtamo, J.; Albanes, D. Null Association between Prostate Cancer and Serum Folate, Vitamin B6, Vitamin B12, and Homocysteine. *Cancer Epidemiol., Biomarkers & Prevention* **2003,** 12, 1271-1272.
22. Sabharanjak, S.; Mayor, S. Folate receptor endocytosis and trafficking. *Adv. Drug Deliv. Rev.* **2004,** 56, 1099-1109.
23. Lu, Y.; Low, P. S. Folate-mediated delivery of macromolecular anticancer therapeutic agents. *Adv. Drug Deliv. Rev.* **2002,** 54, 675-693.
24. Lu, Y.; Sega, E.; Leamon, C. P.; Low, P. S. Folate receptor-targeted immunotherapy of cancer: Mechanism and therapeutic potential. *Adv. Drug Deliv. Rev.* **2004,** 56, 1161-1176.
25. Reddy, J. A.; Westrick, E.; Vlahov, I.; Howard, S. J.; Santhapuram, H. K.; Leamon, C. P. Folate receptor specific anti-tumor activity of folate-mitomycin conjugates. *Cancer Chemother. Pharmacol.* **2006,** 58, 229-236.
26. Satyam, A. Design and synthesis of releasable folate–drug conjugates using a novel heterobifunctional disulfide-containing linker. *Bioorg. Med. Chem. Lett.* **2008,** 18, 3196-3199.
27. Ladino, C. A.; Chari, R. V. J.; Bourret, L. A.; Kedersha, N. L.; Goldmacher, V. S. Folate-maytansinoids: target-selective drugs of low molecular weight. *Int. J. Cancer* **1997,** 73, 859-864.

28. Lee, J. W.; Lu, J. Y.; Low, P. S.; Fuchs, P. L. Synthesis and evaluation of taxol-folic acid conjugates as targeted antineoplastics. *Bioorg. Med. Chem.* **2002,** 10, 2397-2414.
29. Steinberg, G.; Borch, R. F. Synthesis and evaluation of pteroic acid-conjugated nitroheterocyclic phosphoramigates as folate receptor-targeted alkylating agents. *J. Med. Chem.* **2001,** 44, 69-73.
30. Aronov, O.; Horowitz, A. T.; Gabizon, A.; Gibson, D. Folate-targeted PEG as a potential carrier for Carboplatin analogs. Synthesis and *in vitro* studies. *Bioconjugate Chem.* **2003,** 14, 563-574.
31. Liu, J.; Kolar, C.; Lawson, T. A.; Gmeiner, W. H. Targeted drug delivery to chemoresistant cells: folic acid derivatization of FdIMP[10] enhances cytotoxicity toward 5-FU-resistant human colorectal tumor cells. *J. Org. Chem.* **2001,** 66, 5655-5663.
32. Zempleni, J.; Wijeratne, S. S.; Hassan, Y. I. Biotin. *Biofactors* **2009,** 35, 36-46.
33. Minko, T.; Paranjpe, P. V.; Qiu, B.; Lalloo, A.; Won, R.; Stein, S.; Sinko, P. J. Enhancing the anticancer efficacy of camptothecin using biotinylated poly(ethylene glycol) conjugates in sensitive and multidrug-resistant human ovarian carcinoma cells. *Cancer Chemother. Pharmacol.* **2002,** 50, 143-150.
34. Su, J.; Chen, F.; Cryns, V. L. Catechol Polymers for pH-Responsive, Targeted Drug Delivery to Cancer Cells. *J. Amer. Chem. Soc.* **2011,** 133, 11850-11853.
35. Kim, S. Y.; Cho, S. H.; Lee, Y. M.; Chu, L.-Y. Biotin-Conjugated Block Copolymeric Nanoparticles as Tumor-Targeted Drug Delivery Systems. *Macromolecular Res.* **2007,** 15, 646-655.
36. Yellepeddi, V. K.; Kuman, A.; Palakurthi, S. Biotinylated Poly(amido)amine (PAMAM) Dendrimers as Carriers for Drug Delivery to Ovarian Cancer Cells *In Vitro*. *Anticancer Res.* **2009,** 29, 2933-2944.
37. Heo, D. N.; Yang, D. H.; Moon, H.-J.; Lee, J. B.; Bae, M. S.; Lee, S. C.; Lee, W. J.; Sun, I.-C.; Kwon, I. K. Gold nanoparticles surface-functionalized with paclitaxel drug and biotin receptor as theranostic agents for cancer therapy. *Biomaterials* **2012,** 33, 856-866.
38. Cushman, M.; Jayaraman, M.; Vroman, J. A.; Fukunaga, A. K.; Fox, B. M.; Kohlhagen, G.; Strumberg, D.; Pommier, Y. Synthesis of new indeno[1,2-c]isoquinolines: cytotoxic non-camptothecin topoisomerase I inhibitors. *J. Med. Chem.* **2000,** 43, 3688-3698.
39. Anthony, S.; Jayaraman, M.; Laco, G.; Kohlhagen, G.; Kohn, K. W.; Cushman, M.; Pommier, Y. Differential Induction of Topoisomerase I-DNA Cleavage Complexes by the Indenoisoquinoline MJ-III-65 (NSC 706744) and Camptothecin: Base Sequence Analysis and Activity against Camptothecin-Resistant Topoisomerases I. *Cancer Res* **2003,** 63, 7428-7435.
40. Xiao, X.; Antony, S.; Kohlhagen, G.; Pommier, Y.; Cushman, M. Design, synthesis, and biological evaluation of cytotoxic 11-aminoalkenylindenoisoquinoline and 11-diaminoalkenylindeoisoquinoline topoisomerase I inhibitors. *Bioorg. & Med. Chem.* **2004,** 12, 5147-5160.
41. Gottlieb, H. E.; Kotlyar, V.; Nudelman, A. NMR Chemical Shifts of Common Laboratory Solvents as Trace Impurities. *J. Org. Chem.* **1997,** 62, 7512-7515.
42. Corey, E. J.; Mehrotra, M. M. A simple and enantioselective synthesis of (+)-biotin. *Tetrahedron Lett.* **1988,** 29, 57-60.
43. Pasut, G.; Canal, F.; Dalla Via, L.; Arpicco, S.; Veronese, F. M.; Schiavon, O. Antitumoral activity of PEG-gemcitabine prodrugs targeted by folic acid. *J. Control. Release* **2008,** 127, 239-248.

44. Anbharasi, V.; Cao, N.; Feng, S.-S. Doxorubicin conjugated to D-α-tocopheryl polyethylene glycol succinate and folic acid as a prodrug for targeted chemotherapy. *J. Biomed. Mater. Res. A* **2010,** 94A, 730-743.

Chapter 6 References

1. Conti, J. A.; Kemeny, N. E.; Saltz, L. B.; Huang, Y.; Tong, W. P.; Chou, T. C.; Sun, M.; Pulliam, S.; Gonzalez, C. Irinotecan is an active agent in untreated patients with metastatic colorectal cancer. *J. Clin. Oncol.* **1996,** 14, 709-715.
2. Twelves, C.; Scheithauer, W.; McKendrick, J.; Seitz, J.-F.; Van Hazel, G.; Wong, A.; Diaz-Rubio, E.; Gilberg, F.; Cassidy, J. Capecitabine versus 5-fluorouracil/folinic acid as adjuvant therapy for stage III colon cancer: final results from the X-ACT trial with analysis by age and preliminary evidence of a pharmacodynamic marker of efficacy *Ann Oncol* **2011,** Sept. 6, 1-9.
3. Grothey, A.; Sargent, D.; Goldberg, R. M.; Schmoll, H.-J. Survival of Patients With Advanced Colorectal Cancer Improves With the Availability of Fluorouracil-Leucovorin, Irinotecan, and Oxaliplatin in the Course of Treatment *J. Clin. Oncol.* **2004,** 22, 1209-1214.
4. Mross, K.; Kratz, F. Limits of Conventional Cancer Chemotherapy. In *Drug Delivery in Oncology*, Kratz, F.; Senter, P.; Steinhagen, H., Eds. Wiley-VCH Verlag GmbH & co. KGaA: Weinheim, Germany, 2012; Vol. 1, pp 3-31.
5. Frei III, E.; Holland, J. F.; Schneiderman, M. A.; Pinkel, D.; Selkirk, G.; Freireich, E. J.; Silver, R. T.; Gold, G. L.; Regelson, W. A Comparative Study of Two Regimens of Combination Chemotherapy in Acute Leukemia. *Blood* **1958,** 13, 1126-1148.
6. Frei III, E.; Freireich, E. J.; Gehan, E.; Pinkel, D.; Holland, J. F.; Selawry, O.; Haurani, F.; Spurr, C.; Hayes, D. M.; James, G. W.; Rothberg, H.; Sodee, B.; Rundles, R. W.; Schroeder, L. R.; Hoogstraten, B.; Wolman, I. J.; Traggis, D. G.; Cooper, T.; Ebaugh, F.; Taylor, R. Studies of Sequential and Combination Antimetabolite Therapy in Acute Leukemia: 6-Mercaptopurine and Methotrexate. *Blood* **1961,** 18, 431-454.
7. Frei III, E.; Karon, M.; Levin, R. H.; Freireich, E. J.; Taylor, R. J.; Hananian, J.; Selawry, O.; Holland, J. F.; Hoogstraten, B.; Wolman, I. J.; Abir, E.; Sawitsky, A.; Lee, S.; Mills, S. D.; Burgert Jr., E. O.; Spurr, C. L.; Patterson, R. B.; Ebaugh, F. G.; James III, G. W.; Moon, J. H. The Effectiveness of Combinations of Antileukemic Agents in Inducing and Maintaining Remission in Children with Acute Leukemia. *Blood* **1965,** 26, 642-656.
8. Scott, J. L. The effect of nitrogen mustard and maintenance chlorambucil in the treatment of advanced Hodgkin's disease. *Cancer Chemother. Rep.* **1963,** 27, 27-32.
9. DeVita Jr., V. T.; Serpick, A. A.; Carbone, P. P. Combination chemotherapy in the treatment of advanced Hodgkin's disease. *Ann. Intern. Med.* **1970,** 73, 881-895.
10. Devita, V. T.; Lewis, B. J.; Rozencweig, M.; Muggia, F. M. The chemotherapy of Hodgkin's diesease: past experiences and future directions. *Cancer* **1978,** 42(2 suppl), 979-990.
11. Devita Jr., V. T.; Chu, E. A History of Cancer Chemotherapy. *Cancer Res.* **2008,** 68, 8643-8653.
12. Greenspan, E. M.; Fieber, M.; Lesnick, G.; Edelman, S. Response of advanced breast cancer to the combination of the anti-metabolite methotrexate and the alkylating agent thiotepa. *J. Mt Sinai Hosp.* **1963,** 30, 246-267.

13. Canellos, G. P.; Pocock, S. J.; Taylor III, S. G.; Sears, M. E.; Klassen, D. J.; Band, P. R. Combination chemotherapy for metastatic breast carcinoma. Prospective comparison of multiple drug therapy with L-phenylalanine mustard. *Cancer* **1976,** 38, 1882-1886.
14. Bonadonna, G.; Brusamolino, E.; Valagussa, P.; Rossi, A.; Brugnatelli, L.; Brambilla, C.; De Lena, M.; Tancini, G.; Bajetta, E.; Musumeci, R.; Veronesi, U. Combination chemotherapy as an adjuvant treatment in operable brease cancer. *N. Engl. J. Med.* **1976,** 294, 405-410.
15. Gradishar, W. J.; Meza, L. A.; Amin, B.; Samid, D.; Hill, T.; Chen, Y.-M.; Lower, E. E.; Marcom, P. K. Capecitabine plus paclitaxel as front-line combination therapy for metastatic breast cancer: a multicenter phase II study. *J. Clin. Oncol.* **2004,** 22, 2321-2327.
16. Blum, J. L.; Dees, E. C.; Chacko, A.; Doane, L.; Ethirajan, S.; Hopkins, J.; McMahon, R.; Merten, S.; Negron, A.; Neubauer, M.; Ilegbodu, D.; Boehm, K. A.; Asmar, L.; O.Shaughnessy, J. A. Phase II trial of capecitabine and weekly paclitaxel as first-line therapy for metastatic breast cancer. *J. Clin. Oncol.* **2006,** 24, 4384-4390.
17. Murren, J. R.; Peccerillo, K.; DiStasio, S. A.; Li, X.; Leffert, J. J.; Pizzorno, G.; Burtness, B. A.; McKeon, A.; Cheng, Y.-c. Dose escalation and pharamacokinetic study of irinotecan in combination with paclitaxel in patients with advanced cancer. *Cancer Chemother. Pharmacol.* **2000,** 45, 43-50.
18. Lilenbaum, R. C.; Ratain, M. J.; Miller, A. A.; Hargis, J. B.; Hollis, D. R.; Rosner, G. L.; O'Brien, S. M.; Brewster, L.; Green, M. R.; Schilsky, R. L. Phase I study of paclitaxel and topotecan in patients with advanced tumors: a Cancer and Leukemia Group B study. *J. Clin. Oncol.* **1995,** 13, 2230-2237.
19. Bissery, M. C.; Vrignaud, P.; Lavelle, F. In vivo evaluation of the docetaxel-irinotecan combination. *Proc. Am. Assoc. Cancer Res.* **1996,** 37, 378.
20. Langer, C. J. Irinotecan/Taxane combinations in advanced non-small-cell lung cancer. *Clin. Lung Cancer* **2002,** 4, S10-S14.
21. Wall, M. E.; Wani, M. C. Camptothecin and Taxol: Discovery to Clinic-Thirteenth Bruce F. Cain Memorial Award Lecture. *Cancer Research* **1995,** 55, 753-760.
22. Ulukan, H.; Swaan, P. W. Camptothecins, a review of their chemotherapeutical potential. *Drugs* **2002,** 62, 2039-2057.
23. Lu, A. J.; Zheng, Z. S.; Zou, H. J.; Luo, X. M.; Jiang, H. L. 3D-QSAR study of 20 (S)-camptothecin analogs. *Euro. J. Med. Chem.* **2007,** 42, 307-314.
24. Rivory, L. P. New drugs for the colorectal cancer-mechanisms of action. *Australian Prescriber* **2002,** 25, 108-110.
25. Redinbo, M. R.; Stewart, L.; Kuhn, P.; Champoux, J. J.; Hol, W. G. J. Crystal structure of human topoisomerase I in covalent and noncovalent complexes with DNA. *Science* **1998,** 279, 1504-1513.
26. Fraser, T. R. The antagonism between the actions of active substances. *Br. Med. J.* **1872,** 2, 485-487.
27. Zhao, L.; Wientjes, M. G.; Au, J. L.-S. Evaluation of Combination Chemotherapy Integration of Nonlinear Regression, Curve Shift, Isobologram, and Combination Index Analyses. *Clin. Cancer Res.* **2004,** 10, 7994-8004.
28. Steel, G. G.; Peckham, M. J. Exploitable mechanisms in combined radiotherapy-chemotherapy. The concept of additivity. *Int. J. Radiat. Oncol. Biol. Phys.* **1979,** 5, 85-93.
29. Chou, T.-C.; Talalay, P. Quantitative analysis of dose-effect relationships: the combined effects of multiple drugs or enzyme inhibitors. *Adv. Enzyme Regul.* **1984,** 22, 27-55.

30. Kaufmann, S. H.; Peereboom, D.; Buckwalter, C. A.; Svingen, P. A.; Grochow, L. B.; Donehower, R. C.; Rowinsky, E. K. Cytotoxic effects of topotecan combined with various anticancer agents in human cancer cell lines. *J. Natl. Cancer Inst.* **1996,** 88, 734-741.
31. Kano, Y.; Akutsu, M.; Tsunoda, S.; Mori, K.; Suzuki, K.; Adachi, K. I. *In vitro* schedule-dependent interaction between paclitaxel and SN-38 (the active metabolite or irinotecan) in human carcinoma cell lines. *Cancer Chemother. Pharmacol.* **1998,** 42, 91-98.
32. Madden, T.; Newman, R. A.; Antoun, G.; Johansen, M. J.; Ali-Osman, F. Low-level taxane exposure increases the activity of topoisomerase I targeted agents. *Proc. Am. Assoc. Cancer Res.* **1998,** 39, 527.
33. Adjei, A. A.; Argiris, A.; Murren, J. R. Docetaxel and irinotecan, alone and in combination, in the treatment of non-small cell lung cancer. *Semin. Oncol.* **1999,** 26 (5 Suppl 16), discussion 41-42.
34. Govindan, R.; Read, W.; Faust, J.; Trinkaus, K.; Ma, M. K.; Baker, S. D.; McLeod, H. L.; Perry, M. C. Phase II study of docetaxel and irinotecan in metastatic or recurrent esophageal cancer: a preliminary report. *Oncology (Williston Park)* **2003,** 17 (9 Suppl 8), 27-31.
35. Hecht, J. R.; Blanke, C. D.; Benson III, A.; Lenz, H. J. Irinotecan and paclitaxel in metastatic adenocarcinoma of the esophagus and gastric cardia. *Oncology (Williston Park)* **2003,** 17 (9 Suppl 8), 13-15.
36. Ohtsu, H.; Nakanishi, Y.; Bastow, K. F.; Lee, F.-Y.; Lee, K.-H. Antitumor agents 216. Synthesis and evaluation of paclitaxel–camptothecin conjugates as novel cytotoxic agents. *Bioorg. & Med. Chem.* **2003,** 11, 1851-1857.
37. Ojima, I. Guided Molecular Missiles for Tumor-Targeting Chemotherapy-Case Studies Using the Second-Generation Taxoid as Warheads. *Acc. Chem. Res.* **2008,** 41, 108-119.
38. Ojima, I. Tumor-targeting drug delivery of chemotherapeutic agents. *Pure Appl. Chem.* **2011,** 83, 1685-1698.
39. Ojima, I.; Zuniga, E. S.; Berger, W. T.; Seitz, J. D. Tumor-targeting drug delivery of new-genreation taxoids. *Future Med. Chem.* **2012,** 4, 33-50.
40. Chen, S., Zhao, X., Chen, J., Chen, J., Kuznetsova, L., Wong, S.S., Ojima, I. Mechanism-based tumor-targeting drug delivery system. Validation of efficient vitamin receptor-mediated endocytosis and drug release. *Bioconjugate Chem.* **2010,** 21, 979-987.
41. Jensen, P. B.; Holm, B.; Sorensen, M.; Christensen, I. J.; Sehested, M. *In vitro* cross-resistance and collateral sensitivity in seven resistant small-cell lung cancer cell lines: preclinical identification of suitable drug partners to taxotere, taxol, topotecan and gemcitabin. *Br. J. Cancer* **1997,** 75, 869-877.
42. Shah, M. A.; Schwartz, G. K. The relevance of drug sequence in combination chemotherapy. *Drug Resist. Update* **2000,** 3, 335-356.
43. Ishida, H.; Qi, Z.; Sokabe, M.; Donowaki, K.; Inoue, Y. Molecular Design and Synthesis of Artificial Ion Channels Based on Cyclic Peptides Containing Unnatural Amino Acids. *J. Org. Chem.* **2001,** 66, 2978-2989.
44. Toda, F.; Hyoda, S.; Okada, K.; Hirotsu, K. Isolation of Anhydrous Hydrazine as Stable Inclusion Complexes with Hydroquinone and p-Methoxyphenol, and their Solid State Reaction with Esters which gives Pure Hydrazides. *J. Chem. Soc., Chem. Commun.* **1995**, 1531-1532.
45. Crapatureanu, S.; Serbanescu, R.; Brevitt, S. B.; Kluger, R. Molecular Necklaces. Cross-Linking Hemoglobin with Reagents Containing Covalently Attached Ligands. *Bioconjugate Chem.* **1999,** 10, 1058-1067.

46. Ravikumar, V. T. A Convenient Large Scale Synthesis of *N*-BOC-Ethylenediamine. *Synth. Comm.* **1994,** 24, 1767-1772.
47. Stachel, S. J.; Coburn, C. A.; Steele, T. G.; Jones, K. G.; Loutzenhiser, E. F.; Gregro, A. R.; Rajapakse, H. A.; Lai, M.-T.; Crouthamel, M.-C.; Xu, M.; Tugusheva, K.; Lineberger, J. E.; Pietrak, B. L.; Espeseth, A. S.; Shi, X.-P.; Chen-Dodson, E.; Holloway, M. K.; Munshi, S.; Simon, A. J.; Kuo, L.; Vacca, J. P. Structure-Based Design of Potent and Selective Cell-Permeable Inhibitors of Human β-Secretase (BACE-1). *J. Med. Chem.* **2004,** 47, 6447-6450.
48. Gottlieb, H. E.; Kotlyar, V.; Nudelman, A. NMR Chemical Shifts of Common Laboratory Solvents as Trace Impurities. *J. Org. Chem.* **1997,** 62, 7512-7515.
49. Kubik, S.; Bitta, J. Cyclic Hexapeptides with Free Carboxylate Groups as New Receptors for Monosaccharides. *Org. Lett.* **2001,** 3, 2637-2640.
50. Yoshiizumi, K.; Nakajima, F.; Dobashi, R.; Nishimura, N.; Ikeda, S. 2,4-Bis(octadecanoylamino)benzenesulfonic acid sodium salt as a novel scavenger receptor inhibitor with low molecular weight. *Bioorg. Med. Chem. Lett.* **2004,** 14, 2791-2795.

Chapter 7 References

1. Creemers, G. J.; Bolis, G.; Gore, M.; Scarfone, G.; Lacave, A. J.; Guastalla, J. P.; Despax, R.; Kreinberg, R.; Van Belle, S.; Hudson, I.; Verweij, J.; ten Bokkel Huinink, W. W. Topotecan, an active drug in the second-line treatment of epithelial ovarian cancer: results of a large European phase II study. *J. Clin. Oncol.* **1996,** 12, 3056-3061.
2. ten Bokkel Huinink, W. W.; Gore, M.; Carmichael, J.; Gordon, A.; Malfetano, J.; Hudson, I.; Broom, C.; Scarabelli, C.; Davidson, N.; Spanczynski, M.; Bolis, G.; Malmström, H.; Coleman, R.; Fields, S. C.; Heron, J. F. Topotecan versus paclitaxel for the treatment of recurrent epithelial ovarian cancer. *J. Clin. Oncol.* **1997,** 15, 2183-2193.
3. Kudelka, A. P.; Tresukosol, D.; Edwards, C. L.; Freedman, R. S.; Levenback, C.; Chantarawiroj, P.; De Leon, C. G.; Kim, E. E.; Madden, T.; Wallin, B.; Hord, M.; Verschraegen, C.; Raber, M.; Kavanagh, J. J. Pase II study of intravenous topotecan as a 5-day infusion for refractory epithelial ovarian carcinoma. *J. Clin. Oncol.* **1996,** 14, 1552-1557.
4. Swisher, E. M.; Mutch, D. G.; Rader, J. S.; Elbendary, A.; Herzog, T. J. Topotecan in platinum-and paclitaxel resistant ovarian cancer. *Gynecol. Oncol.* **1997,** 66, 480-486.
5. Hoskins, P.; Eisenhauer, E.; Beare, S.; Roy, M.; Drouin, P.; Stuart, G.; Bryson, P.; Grimshaw, R.; Capstick, V.; Zee, B. Randomized phase II study of two schedules of topotecan in previously treated patients with ovarian cancer: a National Cancer Institute of Canada Clinical Trials Group Study. *J. Clin. Oncol.* **1998,** 16, 2233-2237.
6. Bookman, M. A.; Malmström, H.; Bolis, G.; Gordon, A.; Lissoni, A.; Krebs, J. B.; Fields, S. Z. Topotecan for the treatment of advanced epithelial ovarian cancer: an open label phase II study in patients treated after prior chemotherapy that contained cisplatin or carboplatin and paclitaxel. *J. Clin. Oncol.* **1998,** 16, 3345-3352.
7. McGuire, W. P.; Blessing, J. A.; Bookman, M. A.; Lentz, S. S.; Dunton, C. J. Topotecan has substantial antitumor activity as first-line salvage therapy in platinum-sensitive epithelial ovarian carcinoma: a Gynecologic Oncology Group Study. *J. Clin. Oncol.* **2000,** 18, 1062-1067.
8. Levy, T.; Inbar, M.; Menczer, J.; Grisaru, D.; Glezerman, M.; Safra, T. Phase II study of weekly topotecan in patients with recurrent or persistent epithelial ovarian cancer. *Gynecol. Oncol.* **2004,** 95, 686-690.

9. O'Brien, M.; Eckardt, J.; Ramlau, R. Recent Advances with Topotecan in the Treatment of Lung Cancer. *The Oncologist* **2007,** 12, 1194-1204.
10. Staker, B. L.; Hjerrild, K.; Feese, M. D.; Behnke, C. A.; Burgin Jr., A. B.; Stewart, L. The mechanism of topoisomerase I poisoning by a camptothecin analog. *Proc. Natl. Acad. Sci. U.S.A.* **2002,** 99, 15387-15392.
11. Murren, J. R.; Peccerillo, K.; DiStasio, S. A.; Li, X.; Leffert, J. J.; Pizzorno, G.; Burtness, B. A.; McKeon, A.; Cheng, Y.-c. Dose escalation and pharamacokinetic study of irinotecan in combination with paclitaxel in patients with advanced cancer. *Cancer Chemother. Pharmacol.* **2000,** 45, 43-50.
12. Madden, T.; Newman, R. A.; Antoun, G.; Johansen, M. J.; Ali-Osman, F. Low-level taxane exposure increases the activity of topoisomerase I targeted agents. *Proc. Am. Assoc. Cancer Res.* **1998,** 39, 527.
13. Adjei, A. A.; Argiris, A.; Murren, J. R. Docetaxel and irinotecan, alone and in combination, in the treatment of non-small cell lung cancer. *Semin. Oncol.* **1999,** 26 (5 Suppl 16), discussion 41-42.
14. Govindan, R.; Read, W.; Faust, J.; Trinkaus, K.; Ma, M. K.; Baker, S. D.; McLeod, H. L.; Perry, M. C. Phase II study of docetaxel and irinotecan in metastatic or recurrent esophageal cancer: a preliminary report. *Oncology (Williston Park)* **2003,** 17 (9 Suppl 8), 27-31.
15. Hecht, J. R.; Blanke, C. D.; Benson III, A.; Lenz, H. J. Irinotecan and paclitaxel in metastatic adenocarcinoma of the esophagus and gastric cardia. *Oncology (Williston Park)* **2003,** 17 (9 Suppl 8), 13-15.
16. Frasci, G.; Panza, N.; Comella, P.; Carteni, G.; Guida, T.; Nicolella, G. P.; Natale, M.; Lombardi, R.; Apicella, A.; Pacilio, C.; Gravina, A.; Lapenta, L.; Comelia, G. Cisplatin-topotecan-paclitaxel weekly administration with G-CSF support for ovarian and small-cell lung cancer patients: A dose-finding study *Ann. Oncol.* **1999,** 10, 355-358.
17. Stathopoulos, G. P.; Malamos, N. A.; Aravantinos, G.; Rigatos, S.; Christodoulou, C.; Stathopoulos, J.; Skarlos, D. Weekly administration of topotecan–paclitaxel as second-line treatment in ovarian cancer *Cancer Chemother. Pharmacol.* **2007,** 60, 123-128.
18. Stathopoulos, G. P.; Christodoulou, C.; Stathopoulos, J.; Skarlos, D.; Rigatos, S.; Giannakakis, T.; Armenaki, O.; Antoniou, D.; Athanasiadis, A.; Giamboudakis, P.; Dimitroulis, J.; Georgatou, N.; Katis, K. Second-line chemotherapy in small cell lung cancer in a modified administration of topotecan combined with paclitaxel: a phase II study *Cancer Chemother. Pharmacol.* **2006,** 57, 796-800.
19. Morgensztern, D.; Perry, M. C.; Govindan, R. A phase II study of topotecan and docetaxel in patients with sensitive relapse small cell lung cancer. *Acta Oncologica* **2008,** 47, 152-153.
20. Aaron, J. J.; Trajkovska, S. Fluorescence Studies of Anti-Cancer Drugs - Analytical and Biomedical Applications. *Curr. Drug Targets* **2006,** 7, 1067-1081.
21. Burke, T. G.; Mishra, A. K.; Wani, M. C.; Wall, M. E. Lipid bilayer partitioning and stability of camptothecin drugs. *Biochemistry* **1993,** 32, 5352-5364.
22. Mi, Z.; Malak, H.; Burke, T. G. Reduced Albumin Binding Promotes the Stability and Activity of Topotecan in Human Blood. *Biochemistry* **1995,** 34, 13722-13728.
23. Burke, T. G.; Malak, H.; Gryczynski, I.; Mi, Z.; Lakowicz, J. R. Fluorescence Detection of the Anticancer Drug Topotecan in Plasma and Whole Blood by Two-Photon Excitation. *Anal. Biochem.* **1996,** 242, 266-270.

24. Brangi, M.; Litman, T.; Ciotti, M.; Nishiyama, K.; Kohlhagen, G.; Takimoto, C.; Robey, R.; Pommier, Y.; Fojo, T.; Bates, S. E. Camptothecin resistance: Role of the ATP-binding cassetter (ABC), mitoxantrone-resistance half-transporter (MXR), and potential for glucuronidation in MXR-expressing cells. *Cancer Res.* **1999,** 59, 5938-5946.
25. Kaufmann, S. H.; Peereboom, D.; Buckwalter, C. A.; Svingen, P. A.; Grochow, L. B.; Donehower, R. C.; Rowinsky, E. K. Cytotoxic effects of topotecan combined with various anticancer agents in human cancer cell lines. *J. Natl. Cancer Inst.* **1996,** 88, 734-741.
26. Kano, Y.; Akutsu, M.; Tsunoda, S.; Mori, K.; Suzuki, K.; Adachi, K. I. *In vitro* schedule-dependent interaction between paclitaxel and SN-38 (the active metabolite or irinotecan) in human carcinoma cell lines. *Cancer Chemother. Pharmacol.* **1998,** 42, 91-98.
27. Russell-Jones, G., McTavish, Kirsten, McEwan, John, Rice, John, Nowotnik, David. Vitamin-mediated targeting as a potential mechanism to increase drug uptake by tumours. *J. of Inorg. Biochem.* **2004,** 98, 1625-1633.
28. Chen, S.; Zhao, X.; Chen, J.; Chen, J.; Kuznetsova, L.; Wong, S. S.; Ojima, I. Mechanism-based tumor-targeting drug delivery system. Validation of efficient vitamin receptor-mediated endocytosis and drug release. *Bioconjugate Chem.* **2010,** 21, 979-987.
29. Ojima, I. Guided Molecular Missiles for Tumor-Targeting Chemotherapy-Case Studies Using the Second-Generation Taxoid as Warheads. *Acc. Chem. Res.* **2008,** 41, 108-119.
30. Chen, J., Chen, S., Zhao, X., Kuznetsova, L., Wong, S.S., Ojima, I. Functionalized Single-walled Carbon Nanotubes as Rationally Designed Vehicles for Tumor-Targeted Drug Delivery. *J. Am. Chem. Soc.* **2008,** 130, 16778-16785.
31. Ojima, I. Tumor-targeting drug delivery of chemotherapeutic agents. *Pure Appl. Chem.* **2011,** 83, 1685-1698.
32. Ojima, I.; Zuniga, E. S.; Berger, W. T.; Seitz, J. D. Tumor-targeting drug delivery of new-genreation taxoids. *Future Med. Chem.* **2012,** 4, 33-50.
33. Chen, S., Zhao, X., Chen, J., Chen, J., Kuznetsova, L., Wong, S.S., Ojima, I. Mechanism-based tumor-targeting drug delivery system. Validation of efficient vitamin receptor-mediated endocytosis and drug release. *Bioconjugate Chem.* **2010,** 21, 979-987.
34. Leamon, C. P.; Reddy, J. A. Folate-targeted chemotherapy. *Adv. Drug Delivery Rev.* **2004,** 56, 1127-1141.
35. Y., L.; Low, P. S. Folate-mediated delivery of macromolecular anticancer therapeutic agents. *Adv. Drug Delivery Rev.* **2002,** 54, 675-693.
36. Lee, J. W.; Lu, J. Y.; Low, P. S.; Fuchs, P. L. Synthesis and evaluation of taxol-folic acid conjugates as targeted antineoplastics. *Bioorg. & Med. Chem.* **2002,** 10, 2397-2414.
37. Xia, W.; Low, P. S. Folate-targeted therapies for cancer. *J. Med. Chem.* **2010,** 53, 6811-6824.
38. Reddy, J. A.; Leamon, C. P. Folate receptor targeted cancer chemotherapy. In *Targeted Drug Strategies for Cancer and Inflammation*, Jackman, A. L.; Leamon, C. P., Eds. Springer Science+Buisness Media, LLC: 2011; pp 135-150.
39. Fusz, S.; Srivatsan, S. G.; Ackermann, D. A.; Famulok, M. Photocleavable initiator nucleotide substrates for an aldolase ribozyme. *J. Org. Chem.* **2008,** 73, 5069-5077.
40. Wani, M. C.; Nicholas, A. W.; Wall, M. E. Plant antitumor agents. 23. Synthesis and antileukemic activity of camptothecin analogs. *J. Med. Chem.* **1986,** 29, 2358-2363.
41. Li, Q.-Y.; Zu, Y.-G.; Shi, R.-Z.; Yao, L.-P. Review Camptothecin: Current Perspectives. *Curr. Med. Chem.* **2006,** 13, 1-19.

42. Kingsbury, W. D.; Boehm, J. C.; Jakas, D. R.; Holden, K. G.; Hecht, S. M.; Gallagher, G.; Caranfa, M. J.; McCabe, F. L.; Faucette, L. F.; Johnson, R. K.; Hertzberg, R. P. Synthesis of Water-Soluble (Aminoalkyl)camptothecin Analogues: Inhibition of Topoisomerase I and Antitumor Activity. *J. Med. Chem.* **1991,** 34, 98-107.
43. Curran, D. P. Towards new anticancer drugs: a decade of advances in synthesis of camptothecins and related alkaloids. *Tetrahedron* **2003,** 59, 8649-8687.
44. Puri, S. C.; Handa, G.; Dhar, K. L.; Suri, O. P.; Qazi, G. N. Process for preparing topotecan from 10-hydroxy-4-(*S*) camptothecin. 2003.
45. Sekhar, N. M.; Anjaneyulu, Y.; Acharyulu, P. V. R. Synthesis of 10-Hydroxycamptothecin: Evaluation of New Moderators for the Chemoselective Reduction of Camptothecin. *Synth. Comm.* **2011,** 41, 2828-2834.
46. Wood, J. L.; Fortunak, J. M.; Mastrocola, A. R.; Mellinger, M.; Burk, P. L. An efficient conversion of camptothecin to 10-hydroxycamptothecin. *J. Org. Chem.* **1995,** 60, 5739-5740.
47. Sawada, S.; Yokokura, T.; Miyasaka, T. Synthesis of CPT-11 (irinotecan hydrochloride trihydrate). *Ann. N. Y. Acad. Sci.* **1996,** 803, 13-28.
48. Okuno, S.; Harada, M.; Yano, T.; Yano, S.; Kiuchi, S.; Tsuda, N.; Sakamura, Y.; Imai, J.; Kawaguchi, T.; Tsujihara, K. Complete Regression of Xenografted Human Carcinomas by Camptothecin Analogue-Carboxymethyl Dextran Conjugate (T-0128). *Cancer Res.* **2000,** 60, 2988-2995.
49. Varghese, S.; Gupta, D.; Baran, T.; Jimjit, A.; Gore, S. D.; Casero Jr., R. A.; Woster, P. M. Alkyl-substituted polyaminohydroxamic acids: a novel class of histone deacetylase inhibitors. *J. Med. Chem.* **2005,** 48, 6350-6365.
50. Campbell, J. R.; Hatton, R. E. Unsymmetrically Substituted Melamines. *J. Org. Chem.* **1961,** 26, 2786-2789.
51. Gottlieb, H. E.; Kotlyar, V.; Nudelman, A. NMR Chemical Shifts of Common Laboratory Solvents as Trace Impurities. *J. Org. Chem.* **1997,** 62, 7512-7515.
52. Callahan, J. F.; Ashton-Shue, D.; Bryan, H. G.; Bryan, W. M.; Heckman, G. D.; Kinter, L. B.; McDonald, J. E.; Moore, M. L.; Schmidt, D. B. Structure-activity relationships of novel vasopressin antagonists containing C-terminal diaminoalkanes and (aminoalkyl)guanidines. *J. Med. Chem.* **1989,** 32, 391-396.
53. Dong, Y.; Le Quesne, P. W. Total synthesis of magnolamide. *Heterocycles* **2002,** 56, 221-225.

Chapter 8 References

1. Chen, H.-T.; Neerman, M. F.; Parrish, A. R.; Simanek, E. E. Cytotoxicity, Hemolysis, and Acute in Vivo Toxicity of Dendrimers Based on Melamine, Candidate Vehicles for Drug Delivery. *J. Amer. Chem. Soc.* **2004,** 126, 10044-10048.
2. Neerman, M. F.; Zhang, W.; Parrish, A. R.; Simanek, E. E. In vitro and in vivo evaluation of a melamine dendrimer as a vehicle for drugdelivery. *Int. J. Pharm.* **2004,** 281, 129-132.
3. Lim, J.; Simanek, E. E. Toward the Next-Generation Drug Delivery Vehicle: Synthesis of a Dendrimer with Four Orthogonally Reactive Groups. *Mol. Pharm.* **2005,** 2, 273-277.
4. Lim, J.; Simanek, E. E. Synthesis of Water-Soluble Dendrimers Based on Melamine Bearing 16 Paclitaxel Groups. *Org. Lett.* **2008,** 10, 201-204.

5. Ojima, I. Tumor-targeting drug delivery of chemotherapeutic agents. *Pure Appl. Chem.* **2011,** 83, 1685-1698.
6. Ojima, I.; Zuniga, E. S.; Berger, W. T.; Seitz, J. D. Tumor-targeting drug delivery of new-genreation taxoids. *Future Med. Chem.* **2012,** 4, 33-50.
7. Russell-Jones, G., McTavish, Kirsten, McEwan, John, Rice, John, Nowotnik, David. Vitamin-mediated targeting as a potential mechanism to increase drug uptake by tumours. *J. of Inorg. Biochem.* **2004,** 98, 1625-1633.
8. Chen, S.; Zhao, X.; Chen, J.; Chen, J.; Kuznetsova, L.; Wong, S. S.; Ojima, I. Mechanism-based tumor-targeting drug delivery system. Validation of efficient vitamin receptor-mediated endocytosis and drug release. *Bioconjugate Chem.* **2010,** 21, 979-987.
9. Ojima, I. Guided Molecular Missiles for Tumor-Targeting Chemotherapy-Case Studies Using the Second-Generation Taxoid as Warheads. *Acc. Chem. Res.* **2008,** 41, 108-119.
10. Chen, J., Chen, S., Zhao, X., Kuznetsova, L., Wong, S.S., Ojima, I. Functionalized Single-walled Carbon Nanotubes as Rationally Designed Vehicles for Tumor-Targeted Drug Delivery. *J. Am. Chem. Soc.* **2008,** 130, 16778-16785.
11. Chen, S., Zhao, X., Chen, J., Chen, J., Kuznetsova, L., Wong, S.S., Ojima, I. Mechanism-based tumor-targeting drug delivery system. Validation of efficient vitamin receptor-mediated endocytosis and drug release. *Bioconjugate Chem.* **2010,** 21, 979-987.
12. Leamon, C. P.; Reddy, J. A. Folate-targeted chemotherapy. *Adv. Drug Delivery Rev.* **2004,** 56, 1127-1141.
13. Y., L.; Low, P. S. Folate-mediated delivery of macromolecular anticancer therapeutic agents. *Adv. Drug Delivery Rev.* **2002,** 54, 675-693.
14. Lee, J. W.; Lu, J. Y.; Low, P. S.; Fuchs, P. L. Synthesis and evaluation of taxol-folic acid conjugates as targeted antineoplastics. *Bioorg. & Med. Chem.* **2002,** 10, 2397-2414.
15. Xia, W.; Low, P. S. Folate-targeted therapies for cancer. *J. Med. Chem.* **2010,** 53, 6811-6824.
16. Reddy, J. A.; Leamon, C. P. Folate receptor targeted cancer chemotherapy. In *Targeted Drug Strategies for Cancer and Inflammation*, Jackman, A. L.; Leamon, C. P., Eds. Springer Science+Buisness Media, LLC: 2011; pp 135-150.
17. Narisawa, T.; Fukaura, Y.; Yazawa, K.; Ishikawa, C.; Isoda, Y.; Nishizawa, Y. Colon cancer prevention with a small amount of dietary perilla oil high in alpha-linolenic acid in an animal model. *Cancer* **1994,** 73, 2069-2075.
18. Fritsche, K. L.; Johnston, P. V. Effect of dietary alpha-linolenic acid on growth, metastasis, fatty acid profile and prostaglandin production of two murine mammary adenocarcinomas. . *J. Nutri.* **1990,** 120, 1601-1609.
19. Sauer, L. A., Dauchy, R.T., Blask, D.E. Mechanism for the antitumor and anticachectic effects of n-3 fatty acids. *Cancer Res.* **2000,** 60, 5289-5295.
20. Willmann, J. K.; van Bruggen, N.; Dinkelborg, L. M.; Gambhir, S. S. Molecular imaging in drug development. *Nat. Rev. Drug Discov.* **2008,** 7, 591-607.
21. Harry, V. N.; Semple, S. I.; Parkin, D. E.; Gilbert, F. J. Use of new imaging techniques to predict tumour response to therapy. *Lancet Oncol.* **2010,** 11, 92-102.
22. Josephs, D.; Spicer, J.; O'Doherty, M. Molecular imaging in clinical trials. *Target. Oncol.* **2009,** 4, 151-168.
23. Padhani, A. R.; Miles, K. A. Multiparametric imaging of tumor response to therapy. *Radiology* **2010,** 256, 348-364.
24. Kostakoglu, L. FDG-PET evaluation of reponse to treatment. *PET Clinics* **2008,** 3, 37-75.

25. Mettler, F. A.; Guiberteau Jr., M. J. *Essentials of Nuclear Medicine Imaging*. 5th ed.; Saunders: Philadelphia, PA, 2006.
26. Blankenberg, F. G.; Katsikis, P. D.; Tait, J. F.; Davis, R. E.; Naumovski, L.; Ohtsuki, K.; Kopiwoda, S.; Abrams, M. J.; Strauss, H. W. Imaging of apoptosis (programmed cell death) with 99mTc annexin V. . *J. Nucl. Med.* **1999,** 40, 184-191.
27. Chang, J. C.; Gambhir, S. S.; Willmann, J. K. Imaging Techniques in Drug Development and Clinical Practice. In *Drug Delivery in Oncology*, Kratz, F.; Senter, P.; Steinhagen, H., Eds. Wiley-VCH Verlag GmbH & Co. KGaA: Weinheim, Germany, 2012; Vol. 1, pp 189-224.
28. Campbell, J. R.; Hatton, R. E. Unsymmetrically Substituted Melamines. *J. Org. Chem.* **1961,** 26, 2786-2789.
29. Drew, M. E.; Chworost, A.; Oroudjev, E.; Hansma, H.; Yamakoshi, Y. A tripod molecular tip for single molecule ligand-receptor force spectroscopy by AFM. *Langmuir* **2010,** 26, 7117-7125.
30. Schwabacher, A. W.; Lane, J. W.; Schiesher, M. W.; Leigh, K. M.; Johnson, C. W. Desymmetrization reactions: efficient preparation of unsymmetrically substituted linker molecules. *J. Org. Chem.* **1998,** 63, 1727-1729.
31. Kim, D. W.; Ahn, D.-S.; Oh, Y.-H.; Lee, S.; Kil, H. S.; Oh, S. J.; Lee, S. J.; Kim, J. S.; J.S., R.; Moon, D. H.; Chi, D. Y. A New Class of S_N2 Reactions Catalyzed by Protic Solvents: Facile Fluorination for Isotopic Labeling of Diagnostic Molecules. *J. Amer. Chem. Soc.* **2006,** 128, 16394-16397.
32. Gottlieb, H. E.; Kotlyar, V.; Nudelman, A. NMR Chemical Shifts of Common Laboratory Solvents as Trace Impurities. *J. Org. Chem.* **1997,** 62, 7512-7515.
33. Frisch, B.; Boeckler, C.; Schuber, F. Synthesis of Short Polyoxyethylene-Based Heterobifunctional Cross-Linking Reagents. Application to the Coupling of Peptides to Liposomes. *Bioconjugate Chem.* **1996,** 7, 180-186.

Chapter 9 References

1. Weiner, L. M.; Surana, R.; Wang, S. Monoclonal antibodies: versatile platforms for cancer immunotherapy. *Nature Rev. Immunology* **2010,** 10, 317-327.
2. Goldsmith, L. E.; Robinson, M. K. Engineering Antibodies for Cancer Therapy. In *Antibody Expression and Production*, Al-Rubeai, M., Ed. Springer Science & Business Media: 2011; Vol. Cell Engineering 7, pp 197-233.
3. Li, S.; Schmitz, K. R.; Jeffrey, P. D.; Wiltzius, J. J. W.; Kussie, P.; Ferguson, K. M. Structural basis for inhibition of the epidermal growth factor receptor by cetuximab. *Cancer Cell* **2005,** 7, 301-311.
4. Trail, P. A.; Bianchi, A. B. Monoclonal antibody drug conjugates in the treatment of cancer. *Curr. Opin. Immunol.* **1999,** 11, 584-588.
5. Wu, A. M.; Senter, P. D. Arming antibodies: prospects and challenges for immunoconjugates. *Nat. Biotechnol.* **2005,** 23, 1137-1146.
6. Chari, R. V. J. Targeted cancer therapy: conferring specificity to cytotoxic drugs. *Acc. Chem. Res.* **2008,** 41, 98-107.
7. Chang, K.; Pastan, I.; Willingham, M. C. Isolation and characterization of a monoclonal antibody, K1, reactive with ovarian cancers and normal mesothelium. *Int. J. Cancer* **1992,** 50, 373-381.

8. Argani, P.; Iacobuzio-Donahue, C.; Ryu, B.; Rosty, C.; Goggins, M.; Wilentz, R. E.; Murugesan, S. R.; Leach, S. D.; Jaffee, E.; Yeo, C. J.; Cameron, J. L.; Kern, S. E.; Hruban, R. H. Mesothelin Is Overexpressed in the Vast Majority of Ductal Adenocarcinomas of the Pancreas: Identification of a New Pancreatic Cancer Marker by Serial Analysis of Gene Expression (SAGE). *Clin. Cancer Res.* **2001,** 7, 3862-3868.
9. R., H.; Kreitman, R. J.; Pastan, I.; Willingham, M. C. Localization of mesothelin in epithelial ovarian cancer. *Appl. Immunohistochem. Mol. Morphol.* **2005,** 13.
10. Li, M.; Bharadwaj, U.; Zhang, R.; Zhang, S.; Mu, H.; Fisher, W. E.; Brunicardi, F. C.; Chen, C.; Yao, Q. Mesothelin is a maglinent factor and theraoeutic vaccines target for pancreatic cancer. *Mol. Cancer. Ther.* **2008,** 7, 286-296.
11. Feng, Y.; Xiao, X.; Zhu, Z.; Streaker, E.; Ho, M.; Pastan, I.; Dimitrov, D. S. A novel human monoclonal antibody that binds with high affinity to mesothelin-expressing cells and kills them by antibody-dependent cell-mediated cytotoxicity. *Mol. Cancer. Ther.* **2009,** 8, 1113-1118.
12. Medina-Kauwe, L. K. Endocytosis of adenovirus and adenovirus capsid proteins *Adv. Drug. Del. Rev.* **2003,** 55, 1486-1496.
13. Kozarsky, K. F.; Wilson, J. M. Gene therapy: adenovirus vectors. *Curr. Opin. in Genetics and Devel.* **1993,** 3, 499-503.
14. Greber, U. F.; Willetts, M.; Webster, P.; Helenius, A. Stepwise dismantling of adenovirus 2 during entry into cells. *Cells* **1993,** 75, 477-486.
15. Michael, S. I.; Curiel, D. T. Strategies to achieve targeted gene delivery via the receptor-mediated endocytosis pathway. *Gene Therapy* **1994,** 1, 223-232.
16. Bergelson, J. M.; Cunningham, J. A.; Droguett, G.; Kurt-Jones, E. A.; Krithivas, A.; Hong, J. S.; Horwitz, M. S.; Crowell, R. L.; Finberg, R. W. Isolation of a common receptor for Coxsakie B viruses and adenoviruses 2 and 5. *Science* **1997,** 275, 1320-1323.
17. Wickham, T. J.; Mathias, P.; Cheresh, D. A.; Nemerow, G. R. Integrins $\alpha_v\beta_3$ and $\alpha_v\beta_3$ promote adenovirus internalization but no virus attachment. *Cell* **1993,** 73, 309-319.
18. Stewart, P. L.; Chiu, C. Y.; Huang, S.; Muir, T.; Zhao, Y.; Chait, B.; Mathias, P.; Nemerow, G. R. Cryo-EM visualization of an exposed RGD epitope on adenovirus that escapes antibody neutralization. *EMBO Journal* **1997,** 16, 1189-1198.
19. Reynolds, P. N.; Curiel, D. T. New generation adenoviral vectors improve gene transfer by coxsackie and adenoviral receptor-independent cell entry. *Kidney Int.* **2002,** 61, S24-S31.
20. Greber, U. F.; Webster, P.; Weber, J.; Helenius, A. The role of the adenovirus protease on virus entry into cells. *EMBO Journal* **1996,** 15, 1766-1777.
21. Greber, U. F.; Souomalainen, M.; Stidwill, R. P.; Boucke, K.; Ebersold, M. W.; Helenius, A. The role of the nuclear pore complex in adenovirus DNA entry. *EMBO J.* **1997,** 16, 5998-6007.
22. Banerjee, P. S.; Ostapchuk, P.; Hearing, P.; Carrico, I. S. Chemoselective Attachment of Small Molecule Effector Functionality to Human Adenoviruses Facilitates Gene Delivery to Cancer Cells. *J. Am. Chem. Soc.* **2010,** 132, 13615-13617.
23. Greenwald, R. B.; Pendri, A.; Bolikal, D. Highly Water Soluble Taxol Derivatives: 7-Polyethylene Glycol Carbamates and Carbonates. *J. Org. Chem.* **1995,** 60, 331-336.
24. Miller, M. L.; Roller, E. E.; Zhao, R. Y.; Leece, B. A.; Ab, O.; Baloglu, E.; Goldmacher, V. S.; Chari, R. V. Synthesis of Taxoids with Improved Cytotoxicity and Solubility for Use in Tumor-Specific Delivery. *J. Med. Chem.* **2004,** 47, 4802-4805.

25. Li, C.; Inoue, T.; Yang, D. J.; Milas, L.; Hunter, N. R.; Kim, E. E.; Wallace, S. Synthesis and evaluation of water-soluble polyethylene glycol-paclitaxel conjugate as a paclitaxel prodrug. . *Anti-cancer Drugs* **1996,** 7, 642-648.
26. Greenwald, R. B.; Gilbert, C. W.; Pendri, A.; Conover, C. D.; Xia, J.; Martinez, A. Drug Delivery Systems: Water Soluble Taxol 2‘-Poly(ethylene glycol) Ester Prodrugs - Design and in Vivo Effectiveness. *J. Med. Chem.* **1996,** 39, 424-431.
27. Lee, J. W.; Lu, J. Y.; Low, P. S.; Fuchs, P. L. Synthesis and evaluation of taxol-folic acid conjugates as targeted antineoplastics. *Bioorg. & Med. Chem.* **2002,** 10, 2397-2414.
28. Drew, M. E.; Chworost, A.; Oroudjev, E.; Hansma, H.; Yamakoshi, Y. A tripod molecular tip for single molecule ligand-receptor force spectroscopy by AFM. *Langmuir* **2010,** 26, 7117-7125.
29. Schwabacher, A. W.; Lane, J. W.; Schiesher, M. W.; Leigh, K. M.; Johnson, C. W. Desymmetrization reactions: efficient preparation of unsymmetrically substituted linker molecules. *J. Org. Chem.* **1998,** 63, 1727-1729.
30. Paradis, R.; Page, M. New active paclitaxel amino acids derivatives with improved water solubility. *Anticancer Res.* **1998,** 18, 2711-2716.
31. Yamaguchi, T.; Harada, N.; Ozaki, K.; Arakawa, H.; Oda, K.; Nakanishi, N.; Tsujihara, K.; Hashiyama, T. Synthesis of taxoids 5. Synthesis and evaluation of novel water-soluble prodrugs of a 3`-desphenyl-3`-cyclopropyl analogue of docetaxel. *Bioorg. & Med. Chem. Lett.* **1999,** 9, 1639-1644.
32. Martin, L. L.; Scott, S. J.; Agnew, M. N.; Stescak, L. J. A novel synthesis of 1,4-dihydrobenzo[*c*]-1,5-naphthyridin-2(3*H*)-ones from pyrrolo[1,2-*b*]isoquiolines. *J. Org. Chem.* **1986,** 51, 3697-3700.
33. Banerjee, P. S.; Zuniga, E. S.; Ojima, I.; Carrico, I. S. Targeted and armed oncolytic adenovirus via chemoselective modification. *Bioorg. & Med. Chem. Lett.* **2011,** 21, 4985-4988.
34. Gottlieb, H. E.; Kotlyar, V.; Nudelman, A. NMR Chemical Shifts of Common Laboratory Solvents as Trace Impurities. *J. Org. Chem.* **1997,** 62, 7512-7515.
35. Lee, J. W.; Lu, J. Y.; Low, P. S.; Fuchs, P. L. Synthesis and evaluation of taxol-folic acid conjugates as targeted antineoplastics. *Bioorg. Med. Chem.* **2002,** 10, 2397-2414.
36. Ibrahim, T. S.; Tala, S. R.; El-Feky, S. A.; Abdel-Samii, Z. K.; Katritzky, A. R. Benzotriazole Reagents for the Syntheses of Fmoc-, Boc-, and Alloc-Protected Amino Acids. *Synlett* **2011**, 2013-2016.
37. Gupta, S. S.; Kuzelka, J.; Singh, P.; Lewis, W. G.; Manchester, M.; Finn, M. G. Accelerated Bioorthogonal Conjugation: A Practical Method for the Ligation of Diverse Functional Molecules to a Polyvalent Virus Scaffold. *Bioconj. Chem.* **2005,** 16, 1572-1579.
38. Murakami, P.; McCaman, M. T. Quantitation of Adenovirus DNA and Virus Particles with the PicoGreen Fluorescent Dye. *Anal. Biochem.* **1999,** 274, 283-288.

Appendices

Appendix 1
Chapter 1 NMR Spectra

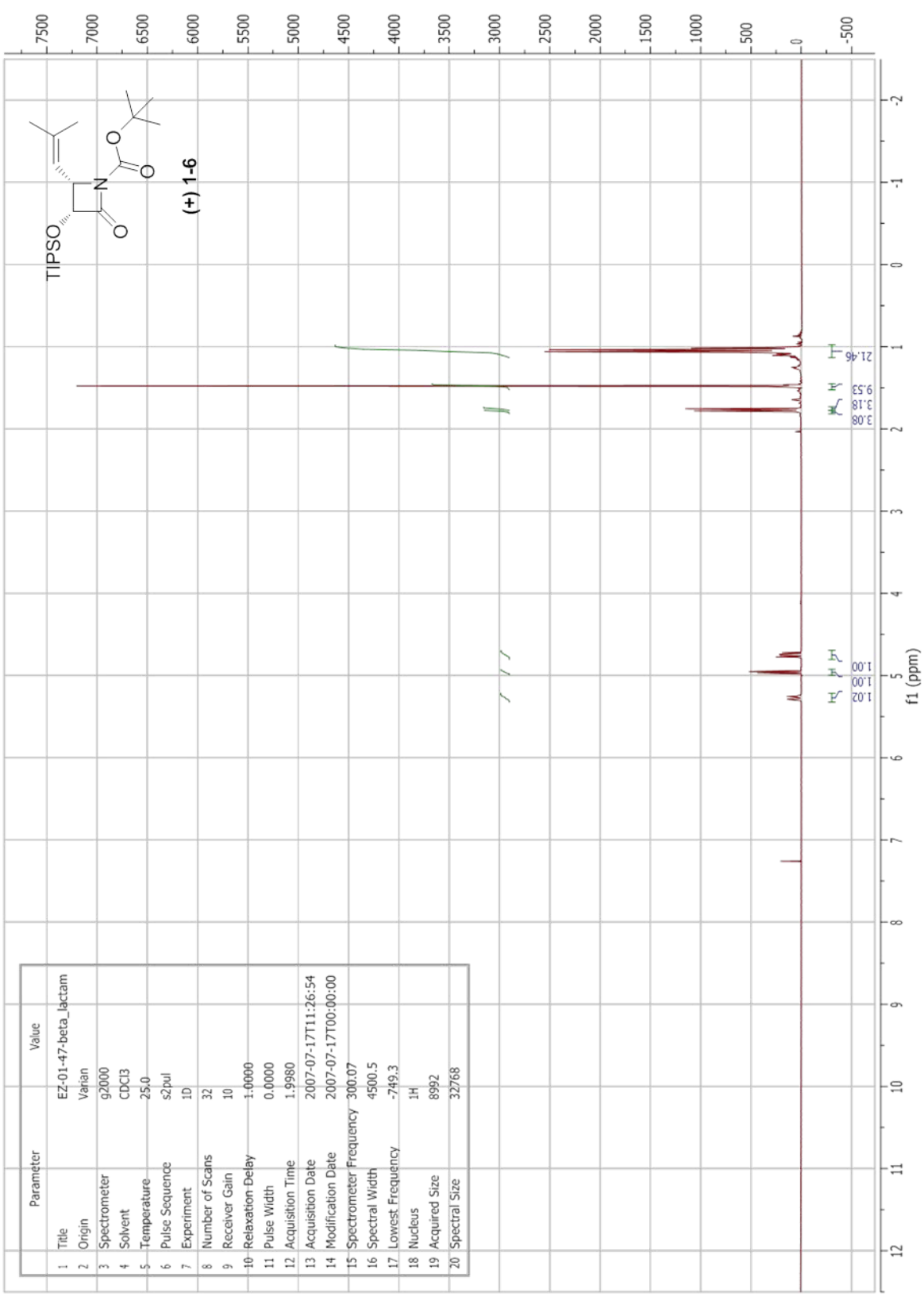

	Parameter	Value
1	Title	EZ-01-47-beta_lactam
2	Origin	Varian
3	Spectrometer	g2000
4	Solvent	CDCl3
5	Temperature	25.0
6	Pulse Sequence	s2pul
7	Experiment	1D
8	Number of Scans	32
9	Receiver Gain	10
10	Relaxation Delay	1.0000
11	Pulse Width	0.0000
12	Acquisition Time	1.9980
13	Acquisition Date	2007-07-17T11:26:54
14	Modification Date	2007-07-17T00:00:00
15	Spectrometer Frequency	300.07
16	Spectral Width	4500.5
17	Lowest Frequency	-749.3
18	Nucleus	1H
19	Acquired Size	8992
20	Spectral Size	32768

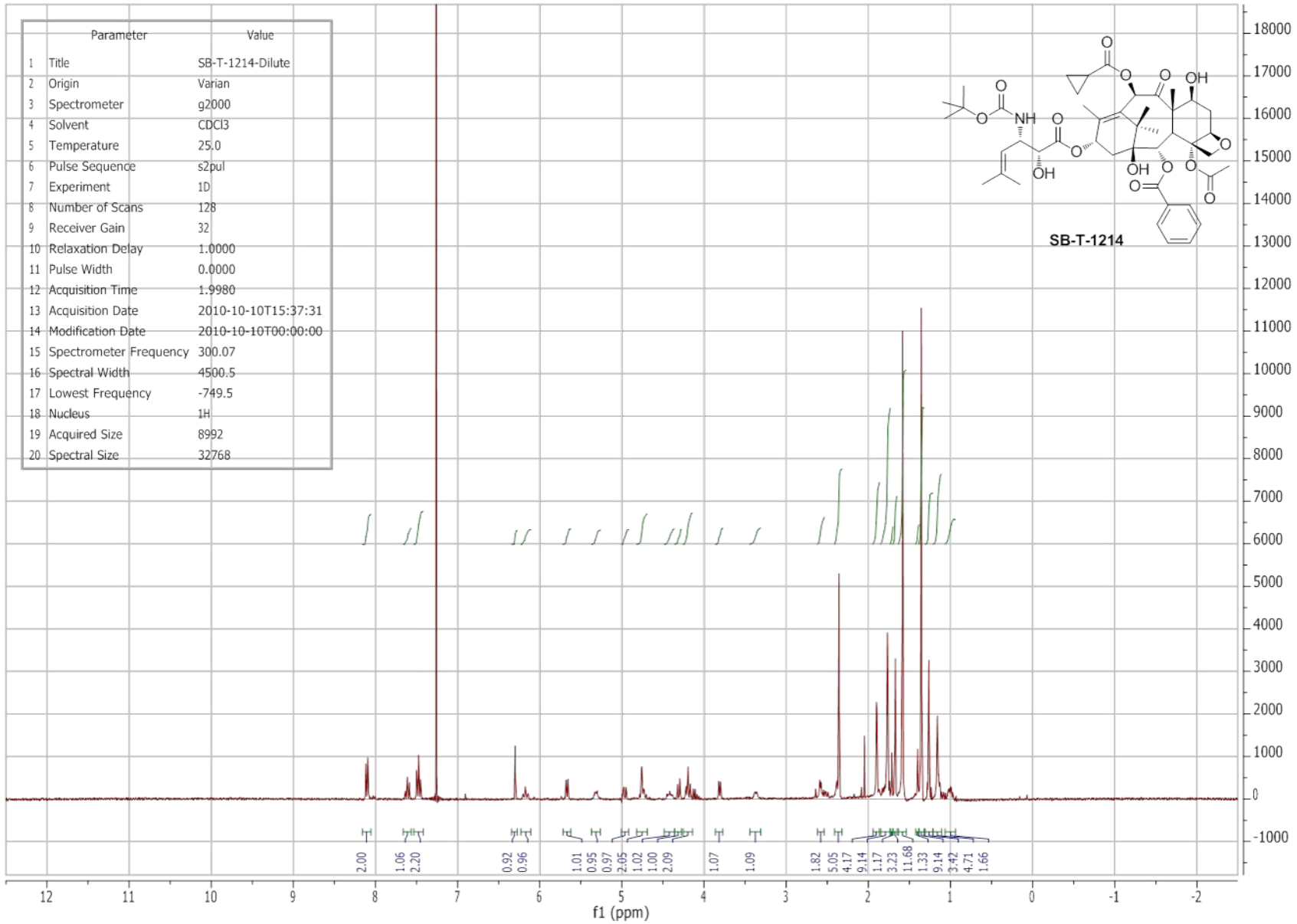
Parameter Value
1 Title SB-T-1214-Dilute
2 Origin Varian
3 Spectrometer g2000
4 Solvent CDCl3
5 Temperature 25.0
6 Pulse Sequence s2pul
7 Experiment 1D
8 Number of Scans 128
9 Receiver Gain 32
10 Relaxation Delay 1.0000
11 Pulse Width 0.0000
12 Acquisition Time 1.9980
13 Acquisition Date 2010-10-10T15:37:31
14 Modification Date 2010-10-10T00:00:00
15 Spectrometer Frequency 300.07
16 Spectral Width 4500.5
17 Lowest Frequency -749.5
18 Nucleus 1H
19 Acquired Size 8992
20 Spectral Size 32768
SB-T-1214
f1 (ppm)

Appendix 2
Chapter 3 NMR Spectra

	Parameter	Value
1	Title	EZ-06-74-LNA-SBT1214
2	Origin	Varian
3	Spectrometer	inova
4	Solvent	CDCl3
5	Temperature	25.0
6	Pulse Sequence	s2pul
7	Experiment	1D
8	Number of Scans	120
9	Receiver Gain	46
10	Relaxation Delay	1.0000
11	Pulse Width	0.0000
12	Acquisition Time	3.2725
13	Acquisition Date	2011-07-10T17:32:07
14	Modification Date	2011-07-09T23:00:00
15	Spectrometer Frequency	399.83
16	Spectral Width	6000.6
17	Lowest Frequency	-990.3
18	Nucleus	1H
19	Acquired Size	19637
20	Spectral Size	65536

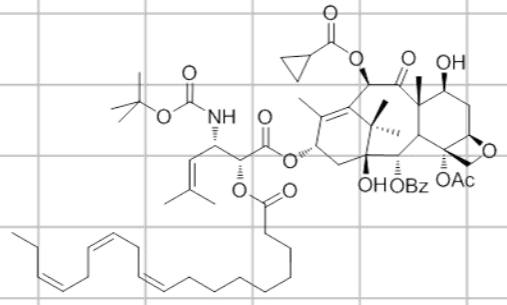

LNA-SB-T-1214
(3-1)

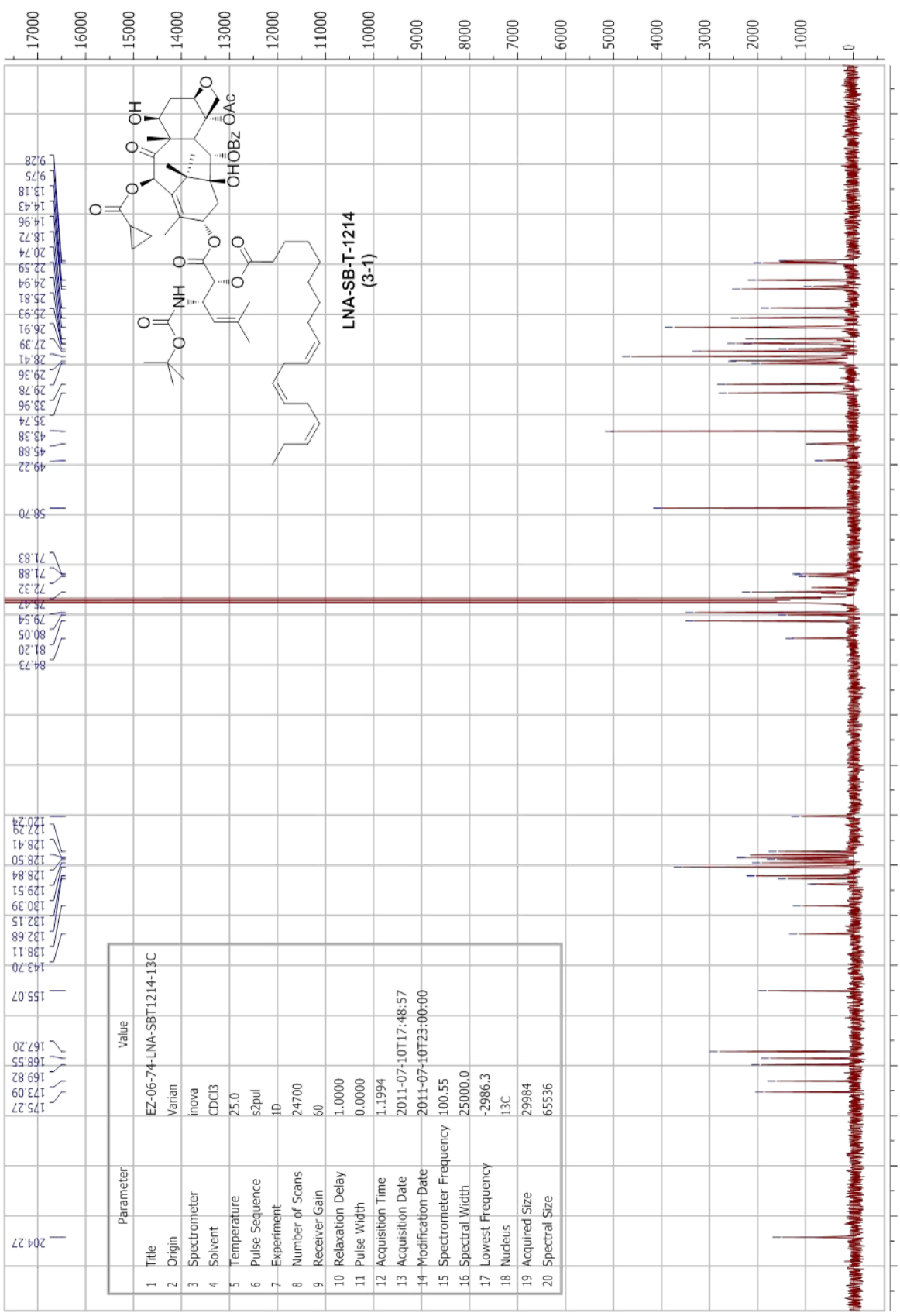
LNA-SB-T-1214
(3-1)
f1 (ppm)
Parameter
Value
1 Title
EZ-06-74-LNA-SBT1214-13C
2 Origin
Varian
3 Spectrometer
inova
4 Solvent
CDCl3
5 Temperature
25.0
6 Pulse Sequence
s2pul
7 Experiment
1D
8 Number of Scans
24700
9 Receiver Gain
60
10 Relaxation Delay
1.0000
11 Pulse Width
0.0000
12 Acquisition Time
1.1994
13 Acquisition Date
2011-07-10T17:48:57
14 Modification Date
2011-07-10T23:00:00
15 Spectrometer Frequency
100.55
16 Spectral Width
25000.0
17 Lowest Frequency
-2986.3
18 Nucleus
13C
19 Acquired Size
29984
20 Spectral Size
65536

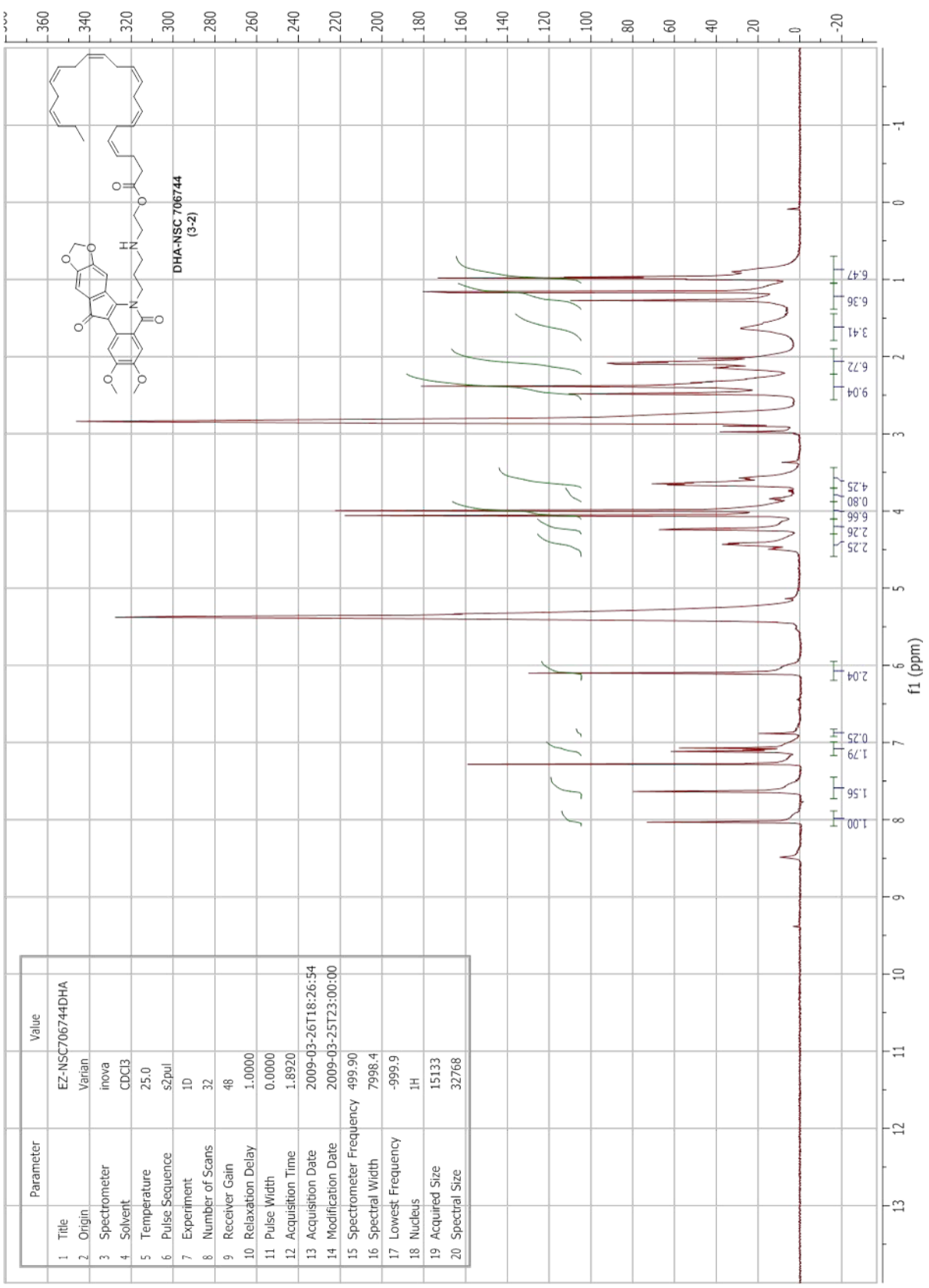

	Parameter	Value
1	Title	EZ-NSC706744DHA
2	Origin	Varian
3	Spectrometer	inova
4	Solvent	CDCl3
5	Temperature	25.0
6	Pulse Sequence	s2pul
7	Experiment	1D
8	Number of Scans	32
9	Receiver Gain	48
10	Relaxation Delay	1.0000
11	Pulse Width	0.0000
12	Acquisition Time	1.8920
13	Acquisition Date	2009-03-26T18:26:54
14	Modification Date	2009-03-25T23:00:00
15	Spectrometer Frequency	499.90
16	Spectral Width	7998.4
17	Lowest Frequency	-999.9
18	Nucleus	1H
19	Acquired Size	15133
20	Spectral Size	32768

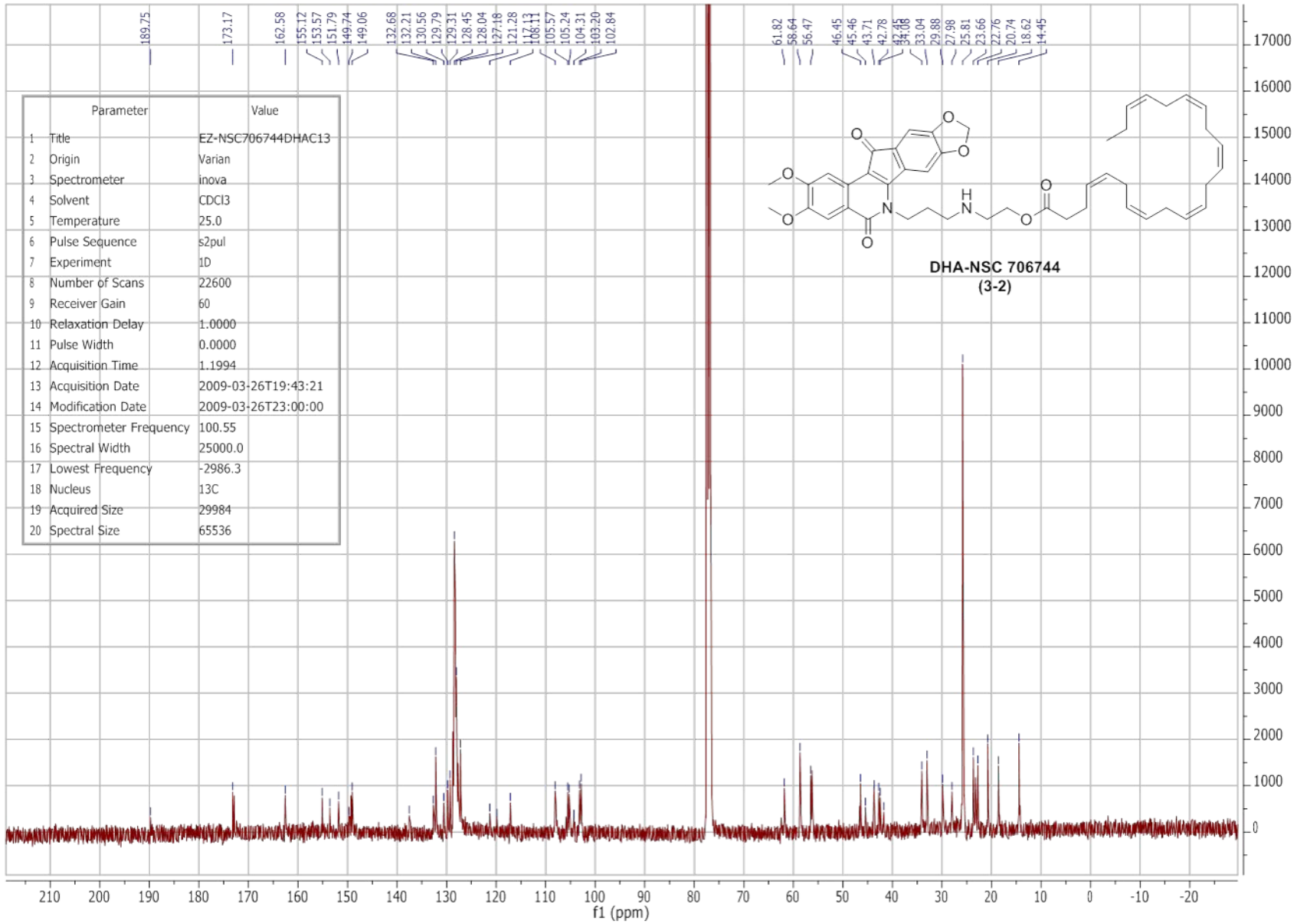
189.75
173.17
162.58
155.12
153.57
151.79
149.74
149.06
132.68
132.21
130.56
129.79
129.31
128.45
128.04
127.18
121.28
117.13
108.11
105.57
105.24
104.31
103.20
102.84
61.82
58.64
56.47
46.45
45.46
43.71
42.78
42.45
34.08
33.04
29.88
27.98
25.81
23.66
22.76
20.74
18.62
14.45
Parameter Value
1 Title EZ-NSC706744DHAC13
2 Origin Varian
3 Spectrometer inova
4 Solvent CDCl3
5 Temperature 25.0
6 Pulse Sequence s2pul
7 Experiment 1D
8 Number of Scans 22600
9 Receiver Gain 60
10 Relaxation Delay 1.0000
11 Pulse Width 0.0000
12 Acquisition Time 1.1994
13 Acquisition Date 2009-03-26T19:43:21
14 Modification Date 2009-03-26T23:00:00
15 Spectrometer Frequency 100.55
16 Spectral Width 25000.0
17 Lowest Frequency -2986.3
18 Nucleus 13C
19 Acquired Size 29984
20 Spectral Size 65536
DHA-NSC 706744
(3-2)
17000
16000
15000
14000
13000
12000
11000
10000
9000
8000
7000
6000
5000
4000
3000
2000
1000
0
210 200 190 180 170 160 150 140 130 120 110 100 90 80 70 60 50 40 30 20 10 0 -10 -20
f1 (ppm)

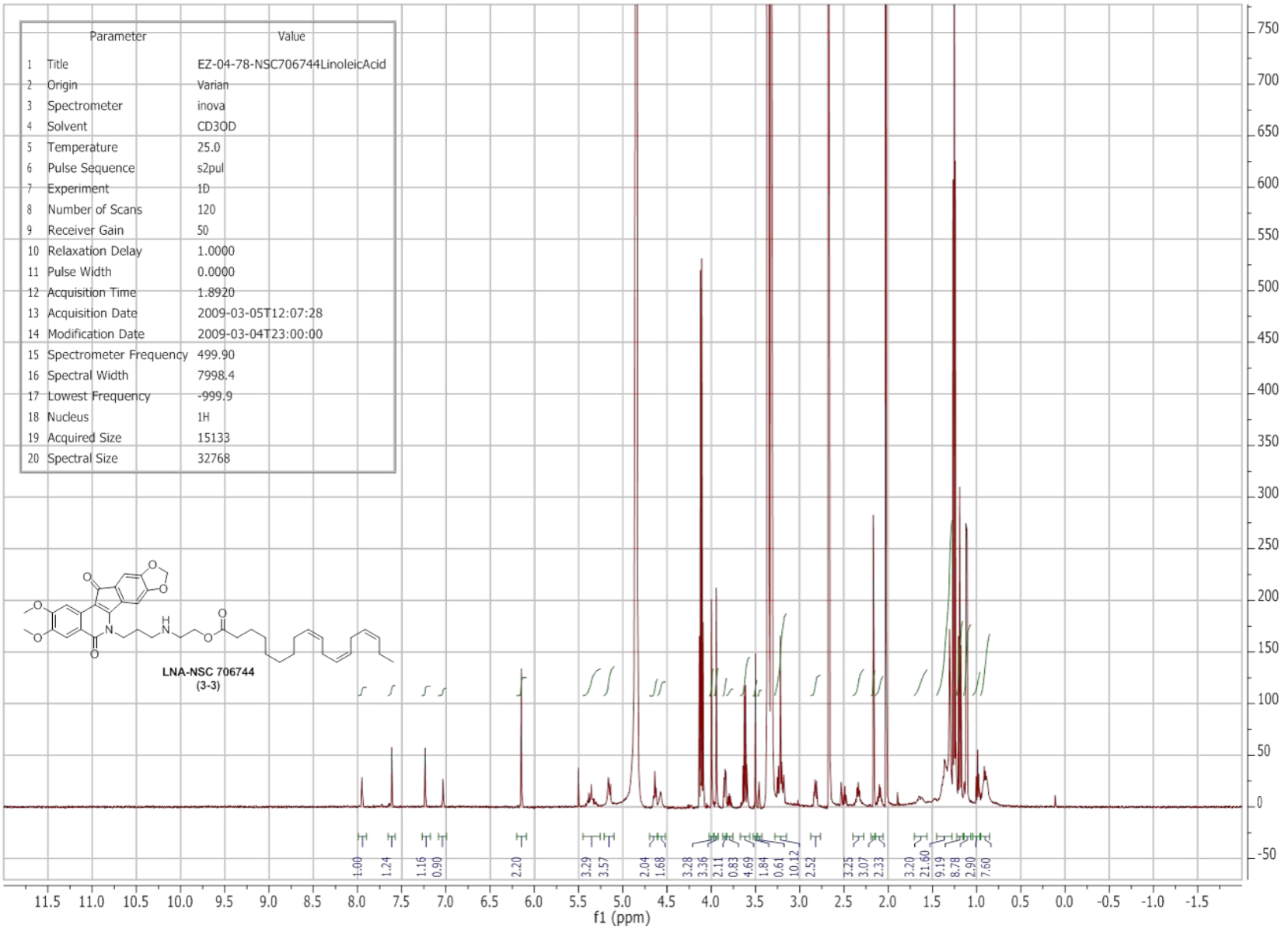
Parameter Value
1 Title EZ-04-78-NSC706744LinoleicAcid
2 Origin Varian
3 Spectrometer inova
4 Solvent CD3OD
5 Temperature 25.0
6 Pulse Sequence s2pul
7 Experiment 1D
8 Number of Scans 120
9 Receiver Gain 50
10 Relaxation Delay 1.0000
11 Pulse Width 0.0000
12 Acquisition Time 1.8920
13 Acquisition Date 2009-03-05T12:07:28
14 Modification Date 2009-03-04T23:00:00
15 Spectrometer Frequency 499.90
16 Spectral Width 7998.4
17 Lowest Frequency -999.9
18 Nucleus 1H
19 Acquired Size 15133
20 Spectral Size 32768
LNA-NSC 706744
(3-3)
f1 (ppm)

Appendix 3
Chapter 4 NMR Spectra

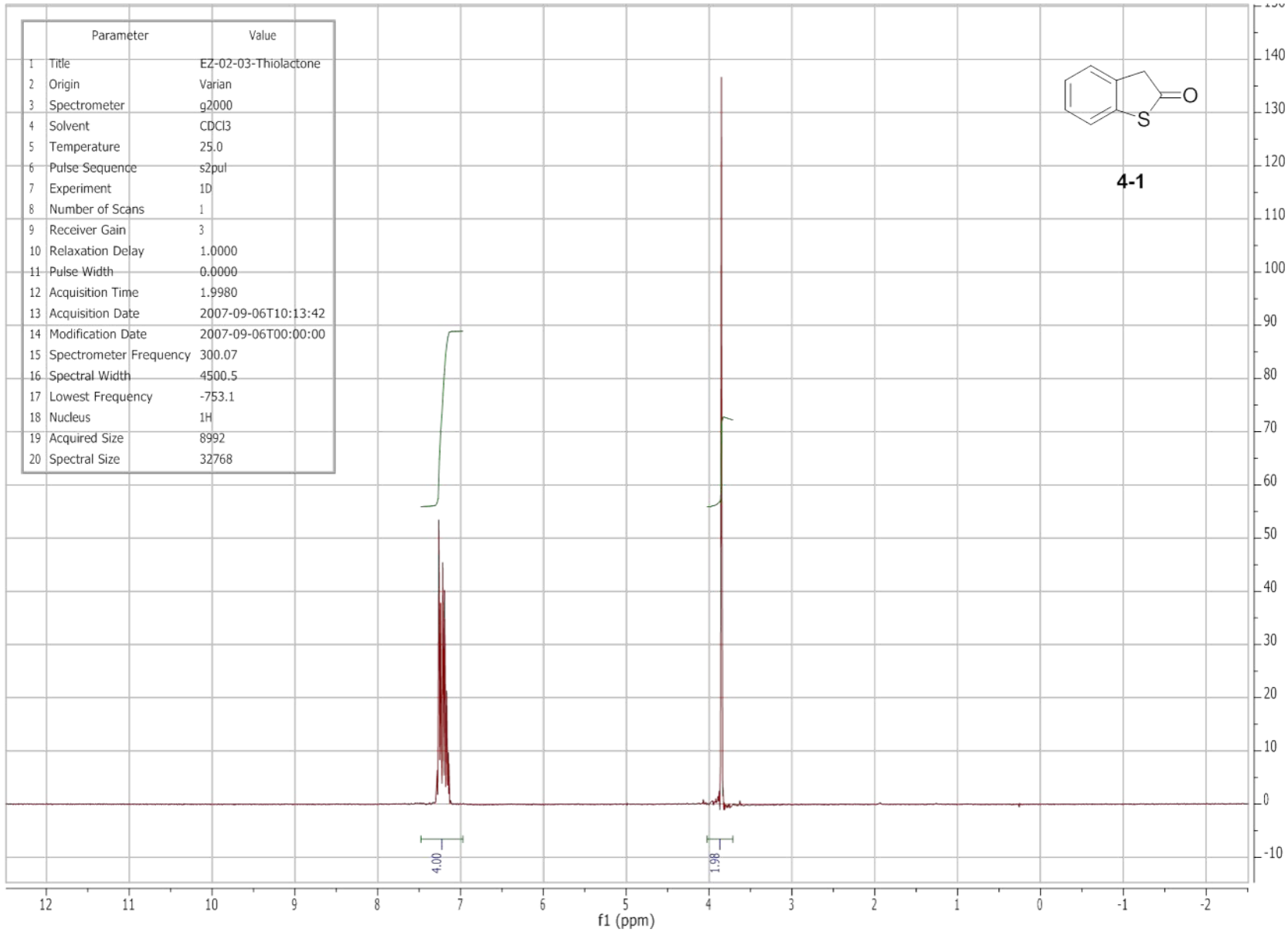
Parameter Value
1 Title EZ-02-03-Thiolactone
2 Origin Varian
3 Spectrometer g2000
4 Solvent CDCl3
5 Temperature 25.0
6 Pulse Sequence s2pul
7 Experiment 1D
8 Number of Scans 1
9 Receiver Gain 3
10 Relaxation Delay 1.0000
11 Pulse Width 0.0000
12 Acquisition Time 1.9980
13 Acquisition Date 2007-09-06T10:13:42
14 Modification Date 2007-09-06T00:00:00
15 Spectrometer Frequency 300.07
16 Spectral Width 4500.5
17 Lowest Frequency -753.1
18 Nucleus 1H
19 Acquired Size 8992
20 Spectral Size 32768
O
S
4-1
4.00
1.98
f1 (ppm)

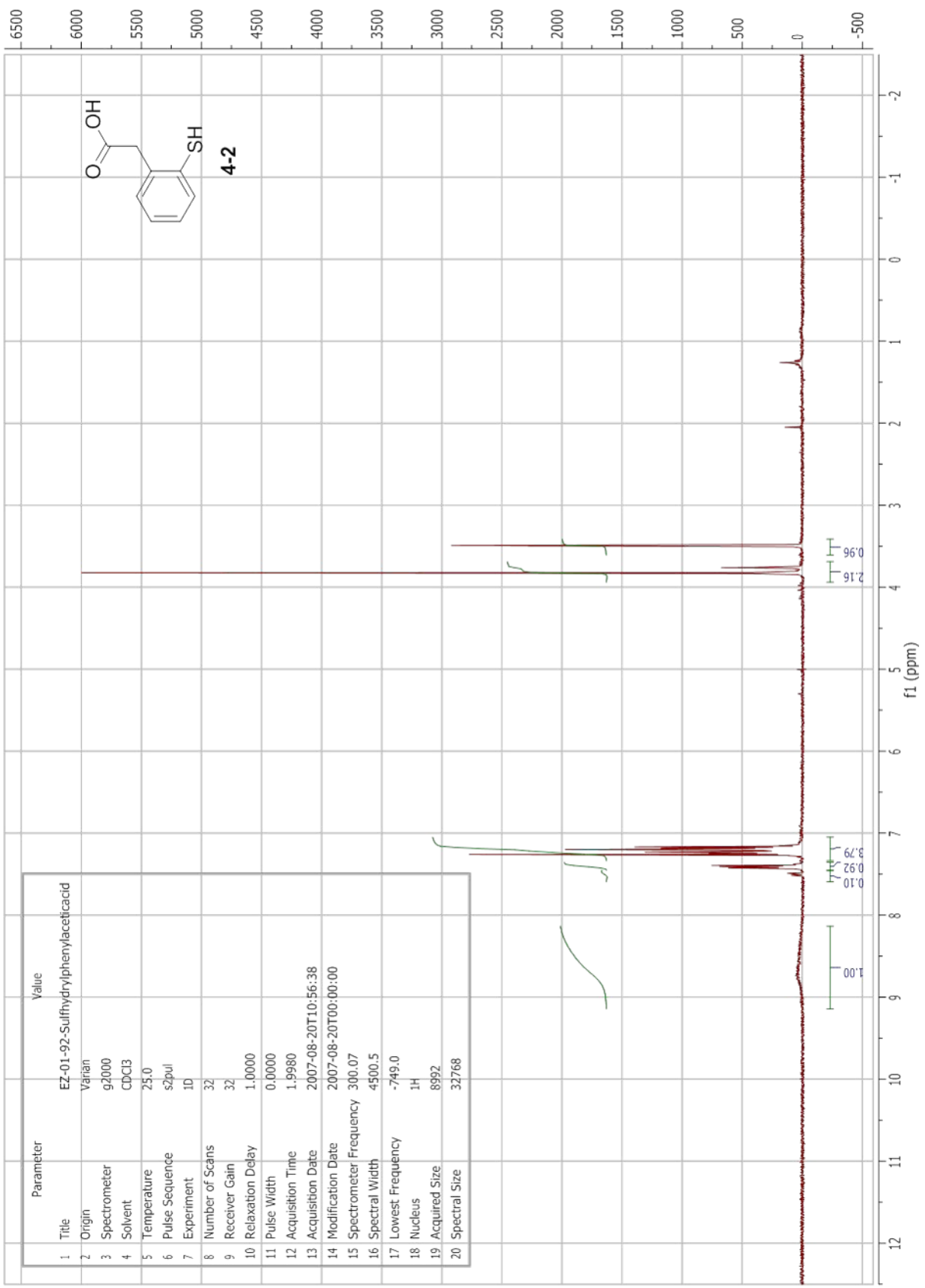
Parameter Value
1 Title EZ-01-92-Sulfhydrylphenylaceticacid
2 Origin Varian
3 Spectrometer g2000
4 Solvent CDCl3
5 Temperature 25.0
6 Pulse Sequence s2pul
7 Experiment 1D
8 Number of Scans 32
9 Receiver Gain 32
10 Relaxation Delay 1.0000
11 Pulse Width 0.0000
12 Acquisition Time 1.9980
13 Acquisition Date 2007-08-20T10:56:38
14 Modification Date 2007-08-20T00:00:00
15 Spectrometer Frequency 300.07
16 Spectral Width 4500.5
17 Lowest Frequency -749.0
18 Nucleus 1H
19 Acquired Size 8992
20 Spectral Size 32768
OH
O
SH
4-2
1.00
0.10
0.92
3.79
2.16
0.96
f1 (ppm)

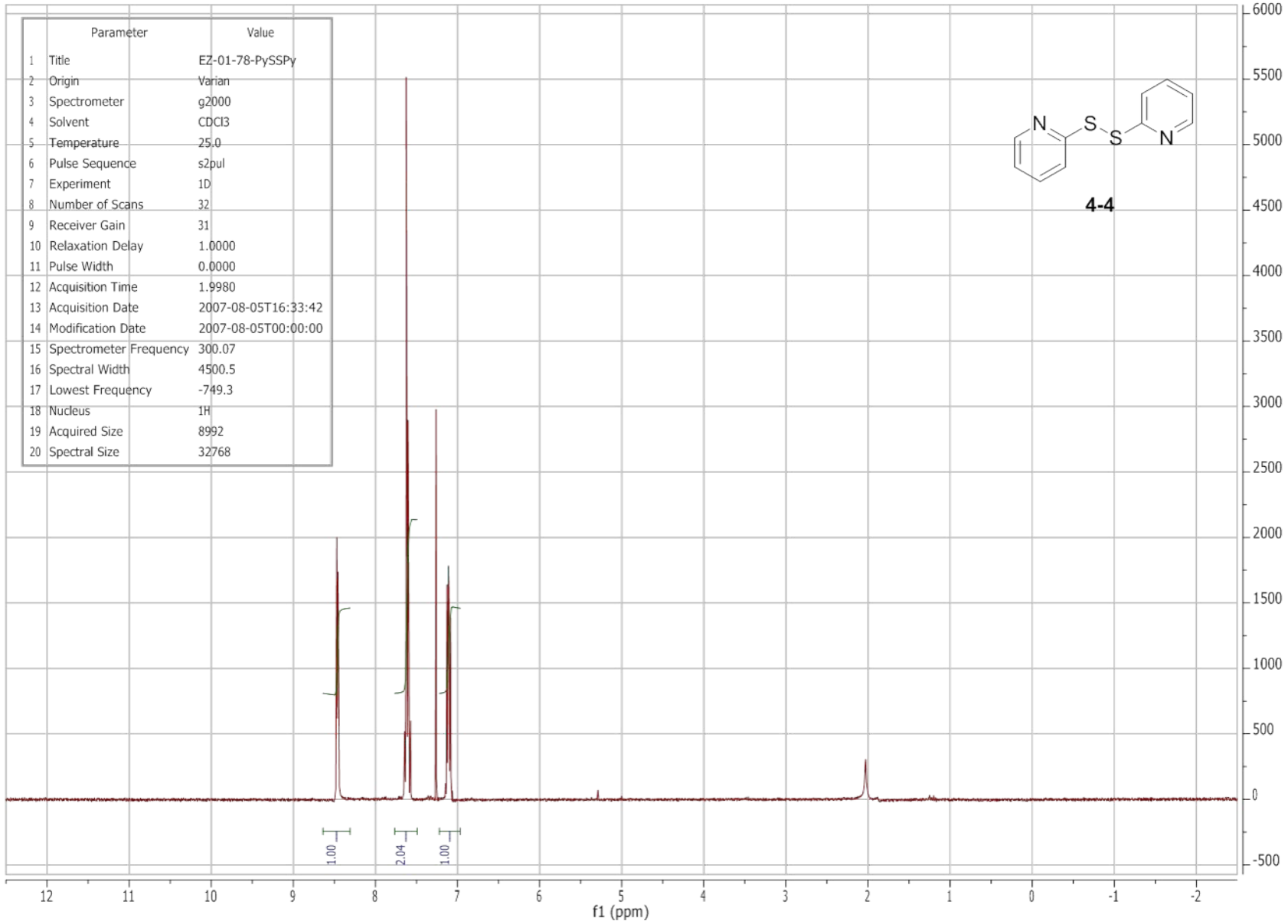
Parameter Value
1 Title EZ-01-78-PySSPy
2 Origin Varian
3 Spectrometer g2000
4 Solvent CDCl3
5 Temperature 25.0
6 Pulse Sequence s2pul
7 Experiment 1D
8 Number of Scans 32
9 Receiver Gain 31
10 Relaxation Delay 1.0000
11 Pulse Width 0.0000
12 Acquisition Time 1.9980
13 Acquisition Date 2007-08-05T16:33:42
14 Modification Date 2007-08-05T00:00:00
15 Spectrometer Frequency 300.07
16 Spectral Width 4500.5
17 Lowest Frequency -749.3
18 Nucleus 1H
19 Acquired Size 8992
20 Spectral Size 32768
N
S
S
N
4-4
1.00
2.04
1.00
f1 (ppm)

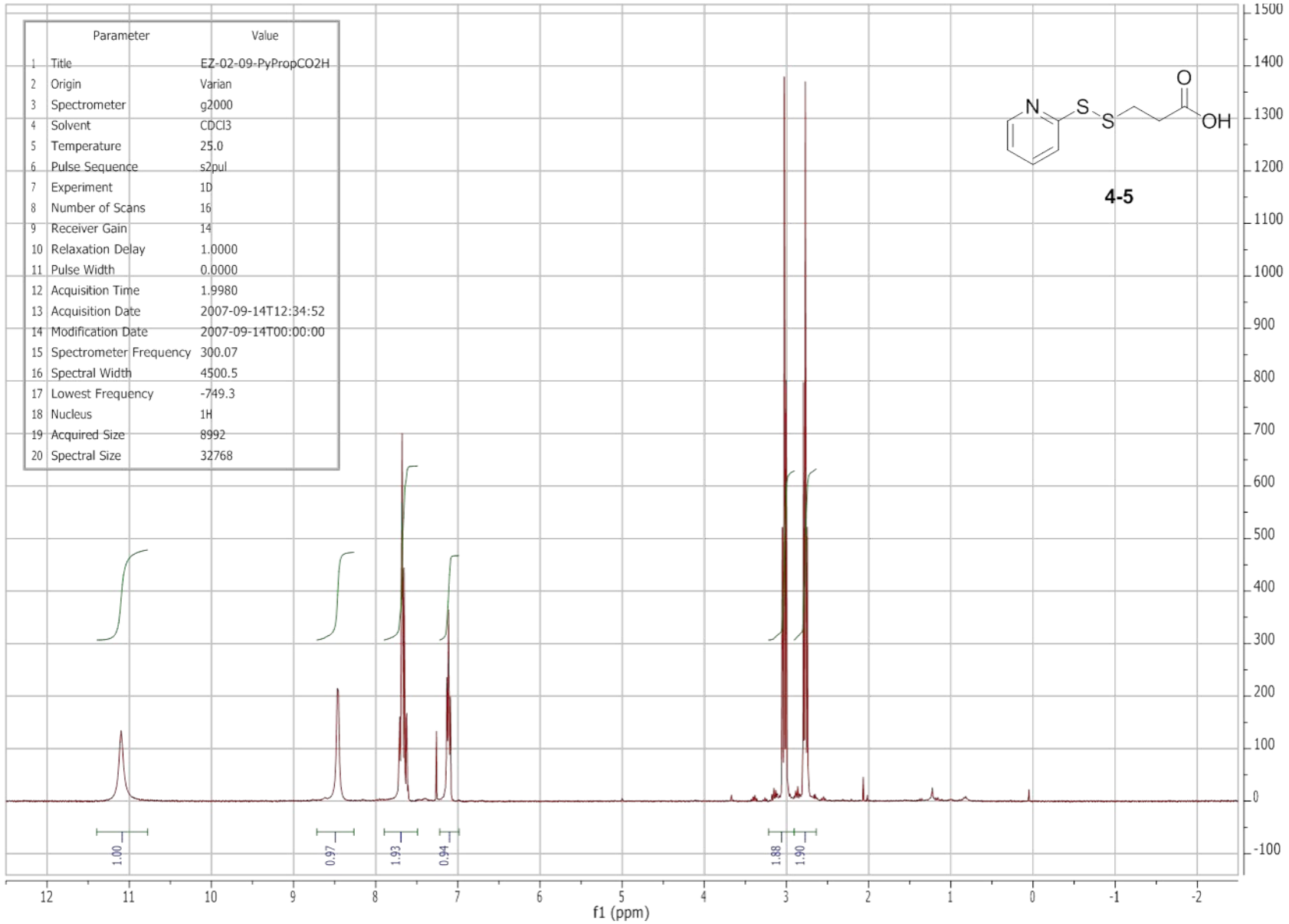
Parameter Value
1 Title EZ-02-09-PyPropCO2H
2 Origin Varian
3 Spectrometer g2000
4 Solvent CDCl3
5 Temperature 25.0
6 Pulse Sequence s2pul
7 Experiment 1D
8 Number of Scans 16
9 Receiver Gain 14
10 Relaxation Delay 1.0000
11 Pulse Width 0.0000
12 Acquisition Time 1.9980
13 Acquisition Date 2007-09-14T12:34:52
14 Modification Date 2007-09-14T00:00:00
15 Spectrometer Frequency 300.07
16 Spectral Width 4500.5
17 Lowest Frequency -749.3
18 Nucleus 1H
19 Acquired Size 8992
20 Spectral Size 32768
N
S
S
O
OH
4-5
1.00
0.97
1.93
0.94
1.88
1.90
f1 (ppm)

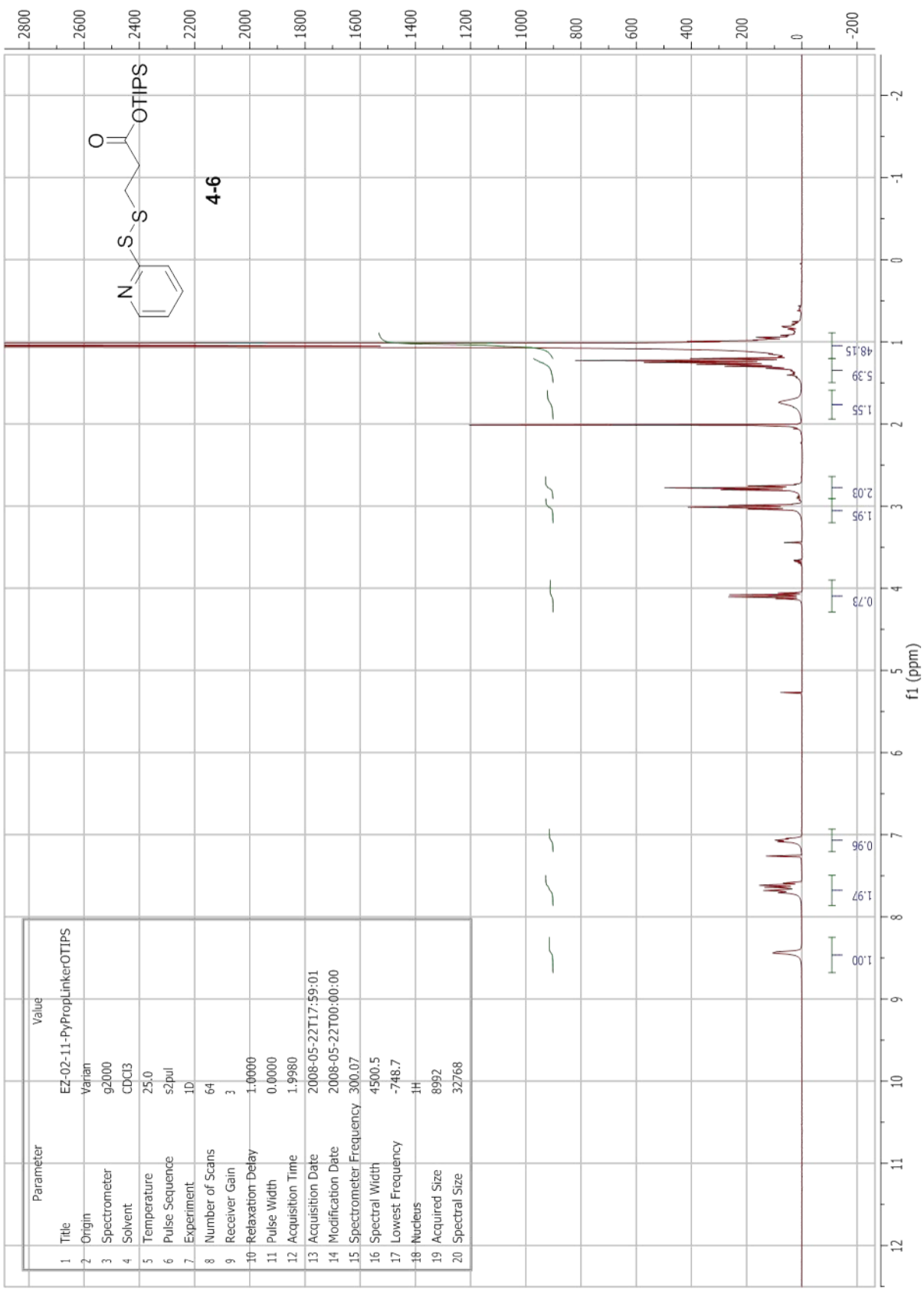

	Parameter	Value
1	Title	EZ-02-11-PyPropLinkerOTIPS
2	Origin	Varian
3	Spectrometer	g2000
4	Solvent	CDCl3
5	Temperature	25.0
6	Pulse Sequence	s2pul
7	Experiment	1D
8	Number of Scans	64
9	Receiver Gain	3
10	Relaxation Delay	1.0000
11	Pulse Width	0.0000
12	Acquisition Time	1.9980
13	Acquisition Date	2008-05-22T17:59:01
14	Modification Date	2008-05-22T00:00:00
15	Spectrometer Frequency	300.07
16	Spectral Width	4500.5
17	Lowest Frequency	-748.7
18	Nucleus	1H
19	Acquired Size	8992
20	Spectral Size	32768

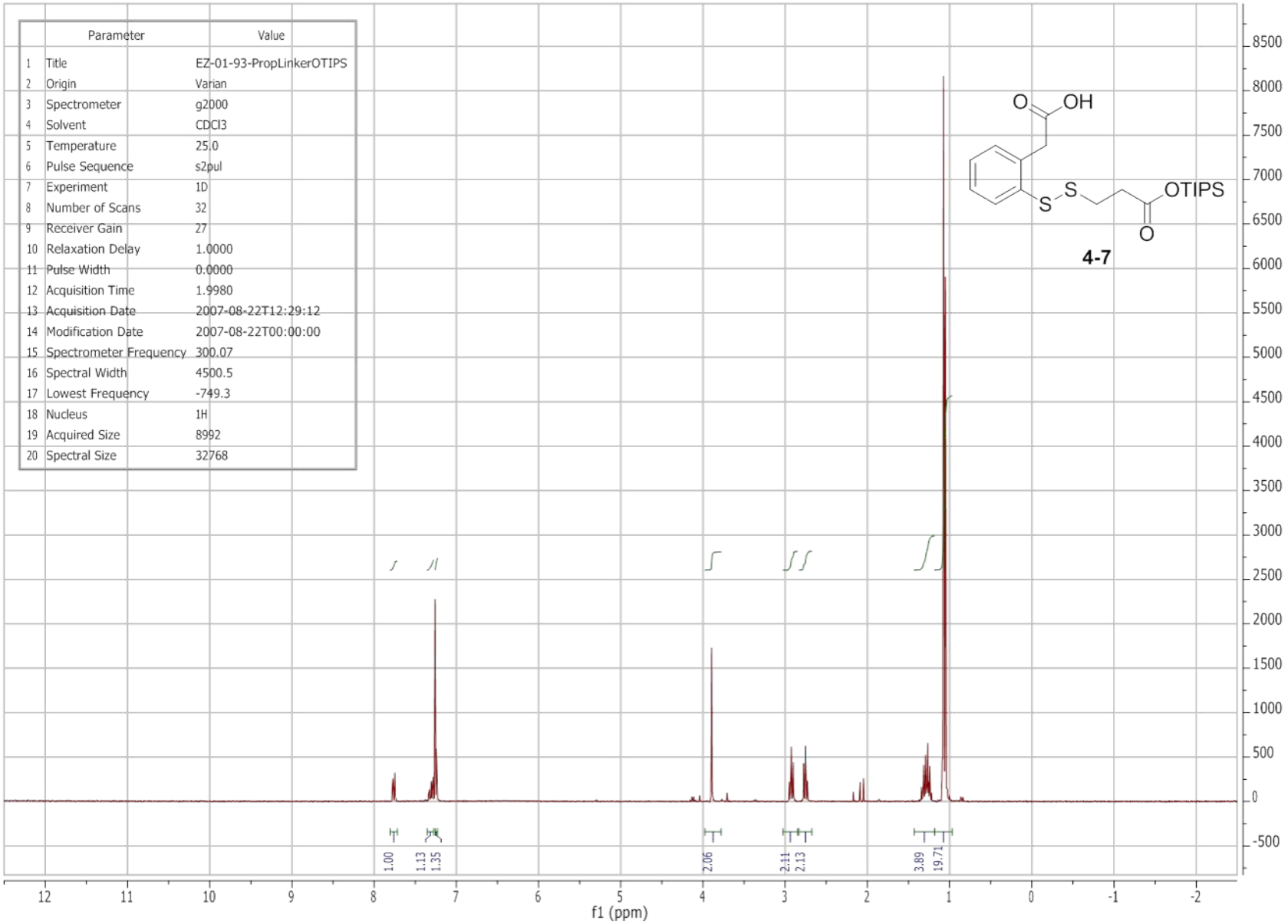
Parameter Value
1 Title EZ-01-93-PropLinkerOTIPS
2 Origin Varian
3 Spectrometer g2000
4 Solvent CDCl3
5 Temperature 25.0
6 Pulse Sequence s2pul
7 Experiment 1D
8 Number of Scans 32
9 Receiver Gain 27
10 Relaxation Delay 1.0000
11 Pulse Width 0.0000
12 Acquisition Time 1.9980
13 Acquisition Date 2007-08-22T12:29:12
14 Modification Date 2007-08-22T00:00:00
15 Spectrometer Frequency 300.07
16 Spectral Width 4500.5
17 Lowest Frequency -749.3
18 Nucleus 1H
19 Acquired Size 8992
20 Spectral Size 32768
O
OH
S
S
OTIPS
O
4-7
1.00
1.13
1.35
2.06
2.11
2.13
3.89
19.71
f1 (ppm)

	Parameter	Value
1	Title	EZ-03-31-crude
2	Origin	Varian
3	Spectrometer	g2000
4	Solvent	CDCl3
5	Temperature	25.0
6	Pulse Sequence	s2pul
7	Experiment	1D
8	Number of Scans	64
9	Receiver Gain	3
10	Relaxation Delay	1.0000
11	Pulse Width	0.0000
12	Acquisition Time	1.9980
13	Acquisition Date	2008-02-28T09:42:54
14	Modification Date	2008-02-27T23:00:00
15	Spectrometer Frequency	300.07
16	Spectral Width	4500.5
17	Lowest Frequency	-749.0
18	Nucleus	1H
19	Acquired Size	8992
20	Spectral Size	32768

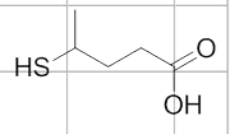

4-10

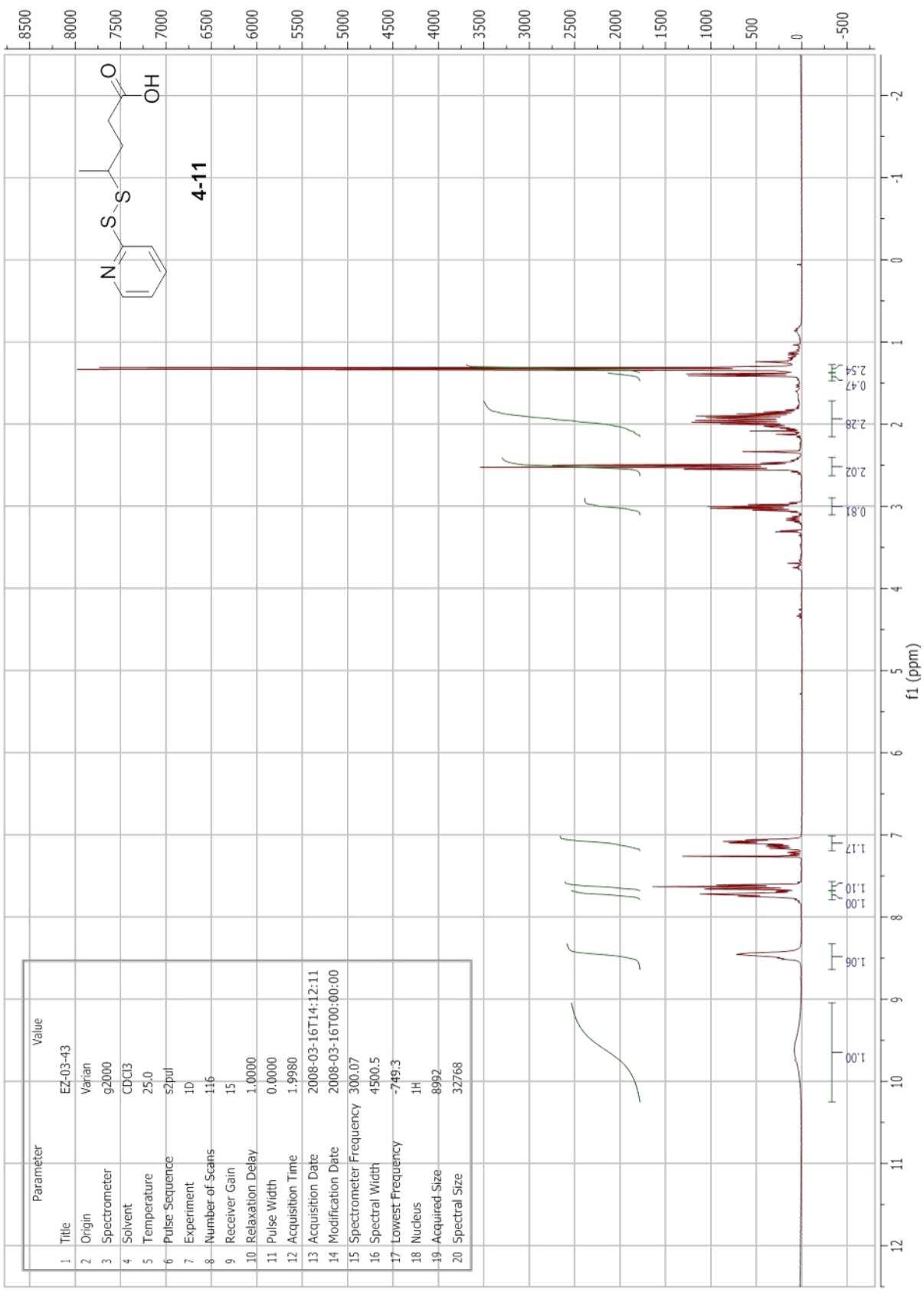

	Parameter	Value
1	Title	EZ-03-43
2	Origin	Varian
3	Spectrometer	g2000
4	Solvent	CDCl3
5	Temperature	25.0
6	Pulse Sequence	s2pul
7	Experiment	1D
8	Number of Scans	116
9	Receiver Gain	15
10	Relaxation Delay	1.0000
11	Pulse Width	0.0000
12	Acquisition Time	1.9980
13	Acquisition Date	2008-03-16T14:12:11
14	Modification Date	2008-03-16T00:00:00
15	Spectrometer Frequency	300.07
16	Spectral Width	4500.5
17	Lowest Frequency	-749.3
18	Nucleus	1H
19	Acquired Size	8992
20	Spectral Size	32768

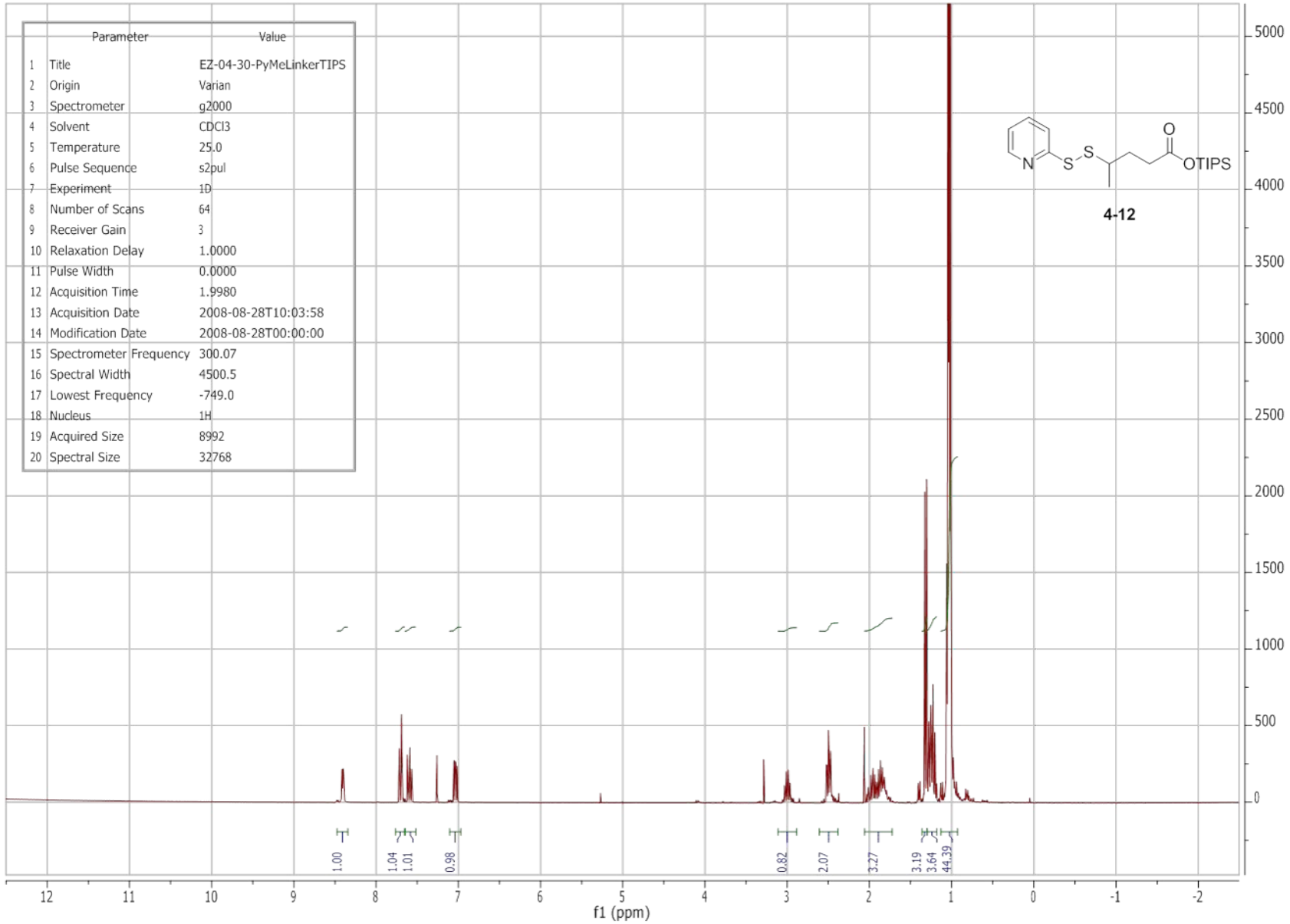
Parameter Value
1 Title EZ-04-30-PyMeLinkerTIPS
2 Origin Varian
3 Spectrometer g2000
4 Solvent CDCl3
5 Temperature 25.0
6 Pulse Sequence s2pul
7 Experiment 1D
8 Number of Scans 64
9 Receiver Gain 3
10 Relaxation Delay 1.0000
11 Pulse Width 0.0000
12 Acquisition Time 1.9980
13 Acquisition Date 2008-08-28T10:03:58
14 Modification Date 2008-08-28T00:00:00
15 Spectrometer Frequency 300.07
16 Spectral Width 4500.5
17 Lowest Frequency -749.0
18 Nucleus 1H
19 Acquired Size 8992
20 Spectral Size 32768
N
S
S
O
OTIPS
4-12
1.00
1.04
1.01
0.98
0.82
2.07
3.27
3.19
3.64
44.39
f1 (ppm)

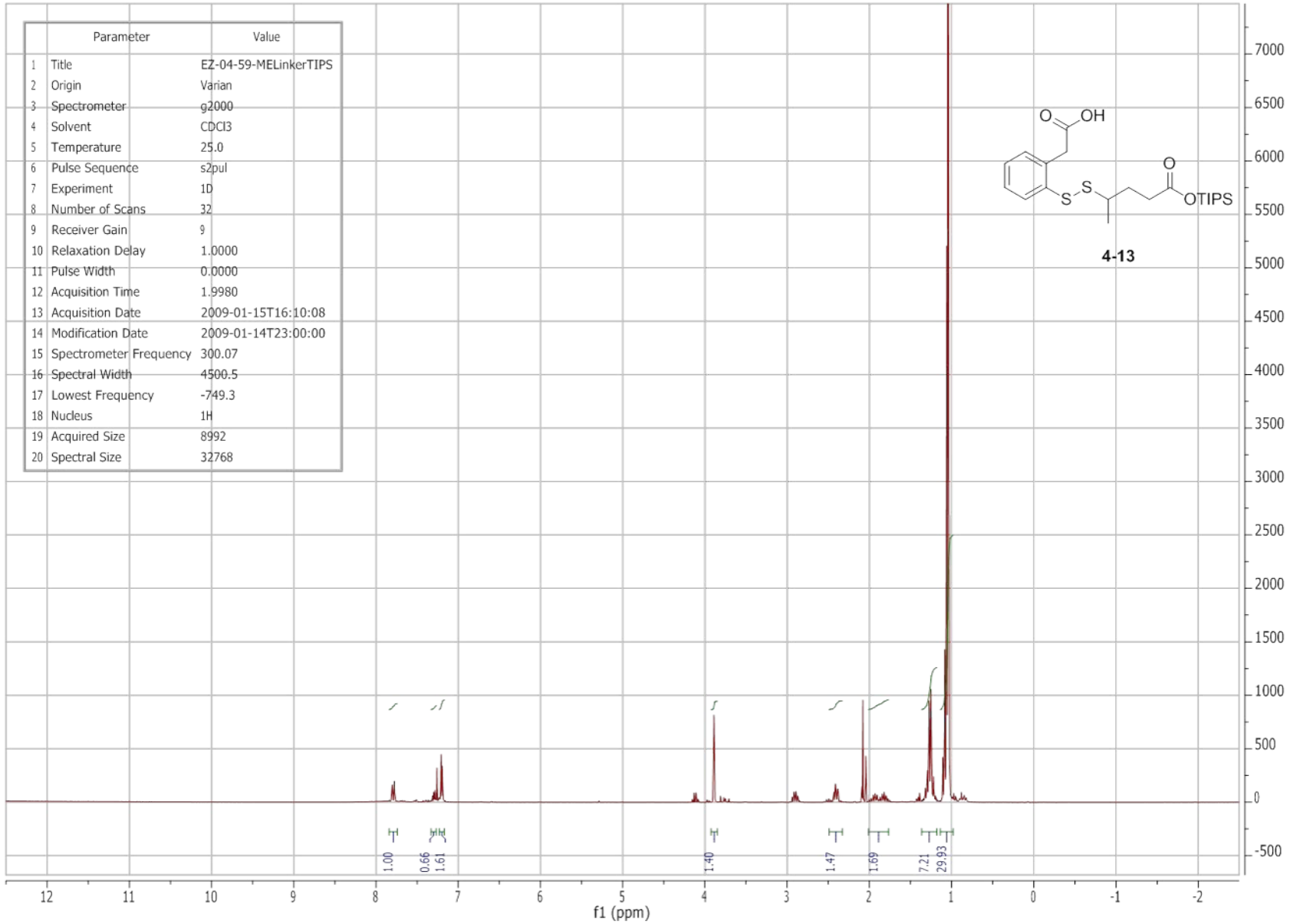
Parameter Value
1 Title EZ-04-59-MELinkerTIPS
2 Origin Varian
3 Spectrometer g2000
4 Solvent CDCl3
5 Temperature 25.0
6 Pulse Sequence s2pul
7 Experiment 1D
8 Number of Scans 32
9 Receiver Gain 9
10 Relaxation Delay 1.0000
11 Pulse Width 0.0000
12 Acquisition Time 1.9980
13 Acquisition Date 2009-01-15T16:10:08
14 Modification Date 2009-01-14T23:00:00
15 Spectrometer Frequency 300.07
16 Spectral Width 4500.5
17 Lowest Frequency -749.3
18 Nucleus 1H
19 Acquired Size 8992
20 Spectral Size 32768
O
OH
S
S
O
OTIPS
4-13
1.00
0.66
1.61
1.40
1.47
1.69
7.21
29.93
f1 (ppm)

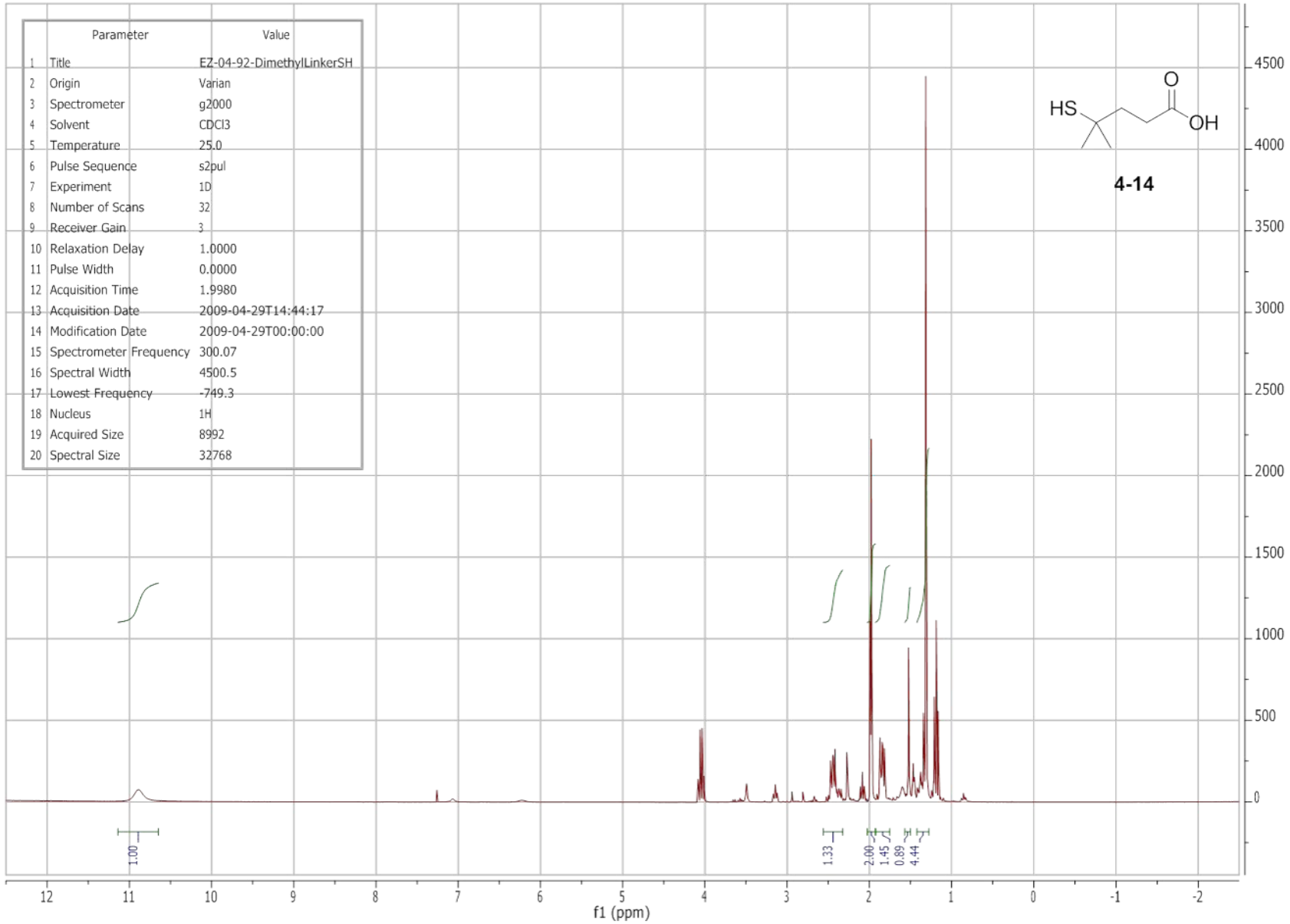
Parameter Value
1 Title EZ-04-92-DimethylLinkerSH
2 Origin Varian
3 Spectrometer g2000
4 Solvent CDCl3
5 Temperature 25.0
6 Pulse Sequence s2pul
7 Experiment 1D
8 Number of Scans 32
9 Receiver Gain 3
10 Relaxation Delay 1.0000
11 Pulse Width 0.0000
12 Acquisition Time 1.9980
13 Acquisition Date 2009-04-29T14:44:17
14 Modification Date 2009-04-29T00:00:00
15 Spectrometer Frequency 300.07
16 Spectral Width 4500.5
17 Lowest Frequency -749.3
18 Nucleus 1H
19 Acquired Size 8992
20 Spectral Size 32768
HS
O
OH
4-14
1.00
1.33
2.00
1.45
0.89
4.44
f1 (ppm)

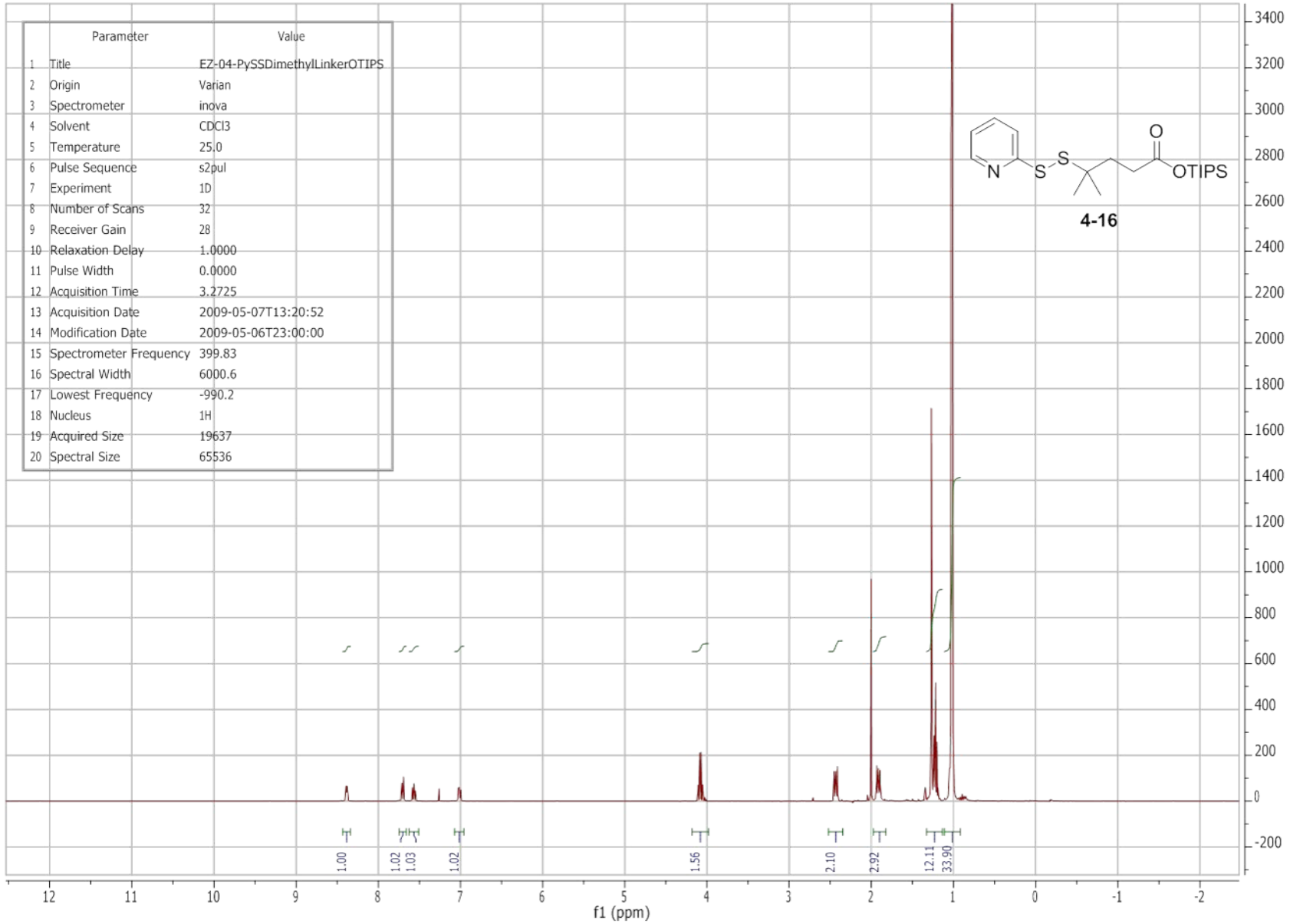
Parameter Value
1 Title EZ-04-PySSDimethylLinkerOTIPS
2 Origin Varian
3 Spectrometer inova
4 Solvent CDCl3
5 Temperature 25.0
6 Pulse Sequence s2pul
7 Experiment 1D
8 Number of Scans 32
9 Receiver Gain 28
10 Relaxation Delay 1.0000
11 Pulse Width 0.0000
12 Acquisition Time 3.2725
13 Acquisition Date 2009-05-07T13:20:52
14 Modification Date 2009-05-06T23:00:00
15 Spectrometer Frequency 399.83
16 Spectral Width 6000.6
17 Lowest Frequency -990.2
18 Nucleus 1H
19 Acquired Size 19637
20 Spectral Size 65536
N
S
S
O
OTIPS
4-16
1.00
1.02
1.03
1.02
1.56
2.10
2.92
12.11
33.90
f1 (ppm)

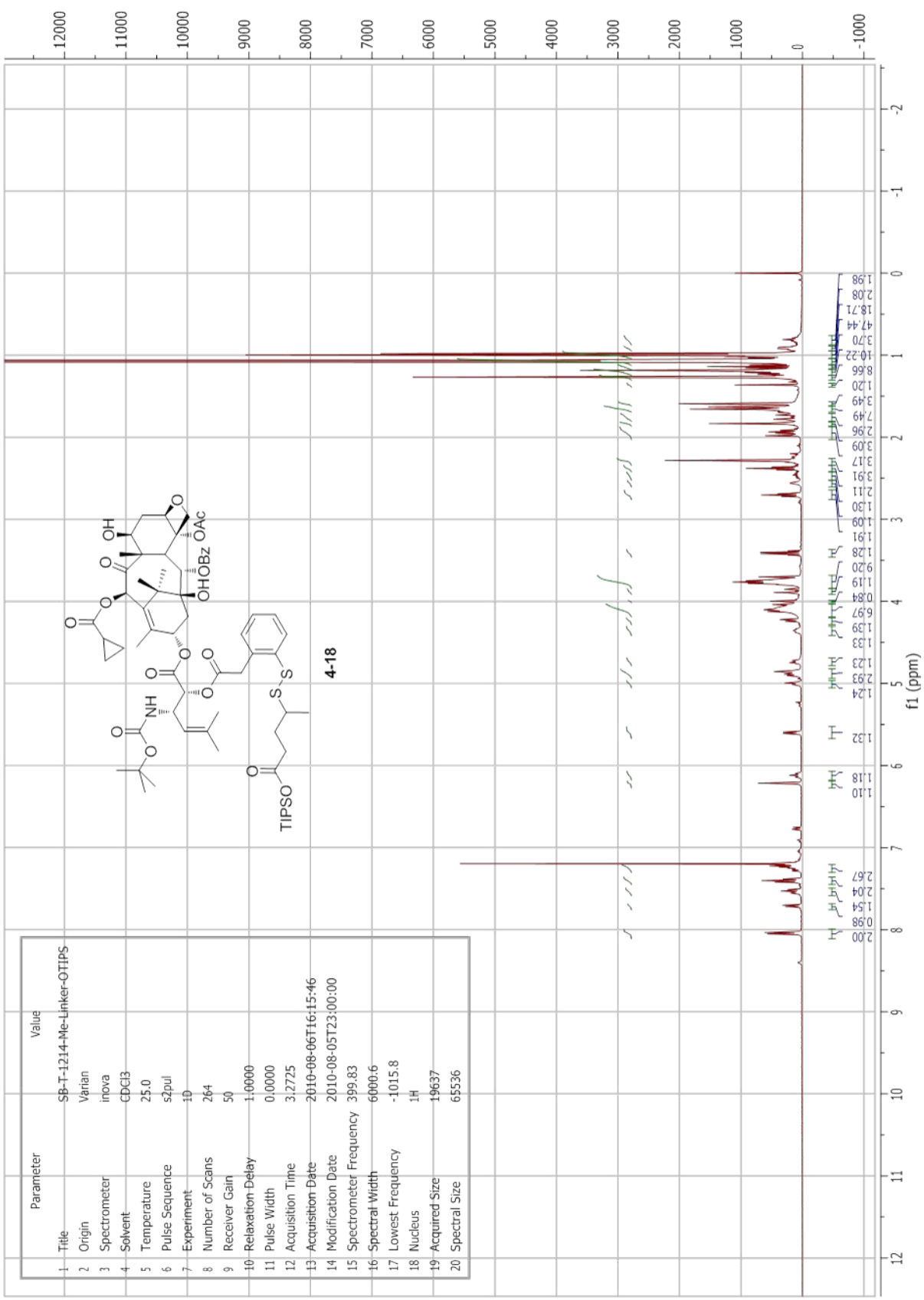
Parameter Value
1 Title SB-T-1214-Me-Linker-OTIPS
2 Origin Varian
3 Spectrometer inova
4 Solvent CDCl3
5 Temperature 25.0
6 Pulse Sequence s2pul
7 Experiment 1D
8 Number of Scans 264
9 Receiver Gain 50
10 Relaxation Delay 1.0000
11 Pulse Width 0.0000
12 Acquisition Time 3.2725
13 Acquisition Date 2010-08-06T16:15:46
14 Modification Date 2010-08-05T23:00:00
15 Spectrometer Frequency 399.83
16 Spectral Width 6000.6
17 Lowest Frequency -1015.8
18 Nucleus 1H
19 Acquired Size 19637
20 Spectral Size 65536
4-18
TIPSO
OHOBz
OAc
OH
NH
f1 (ppm)

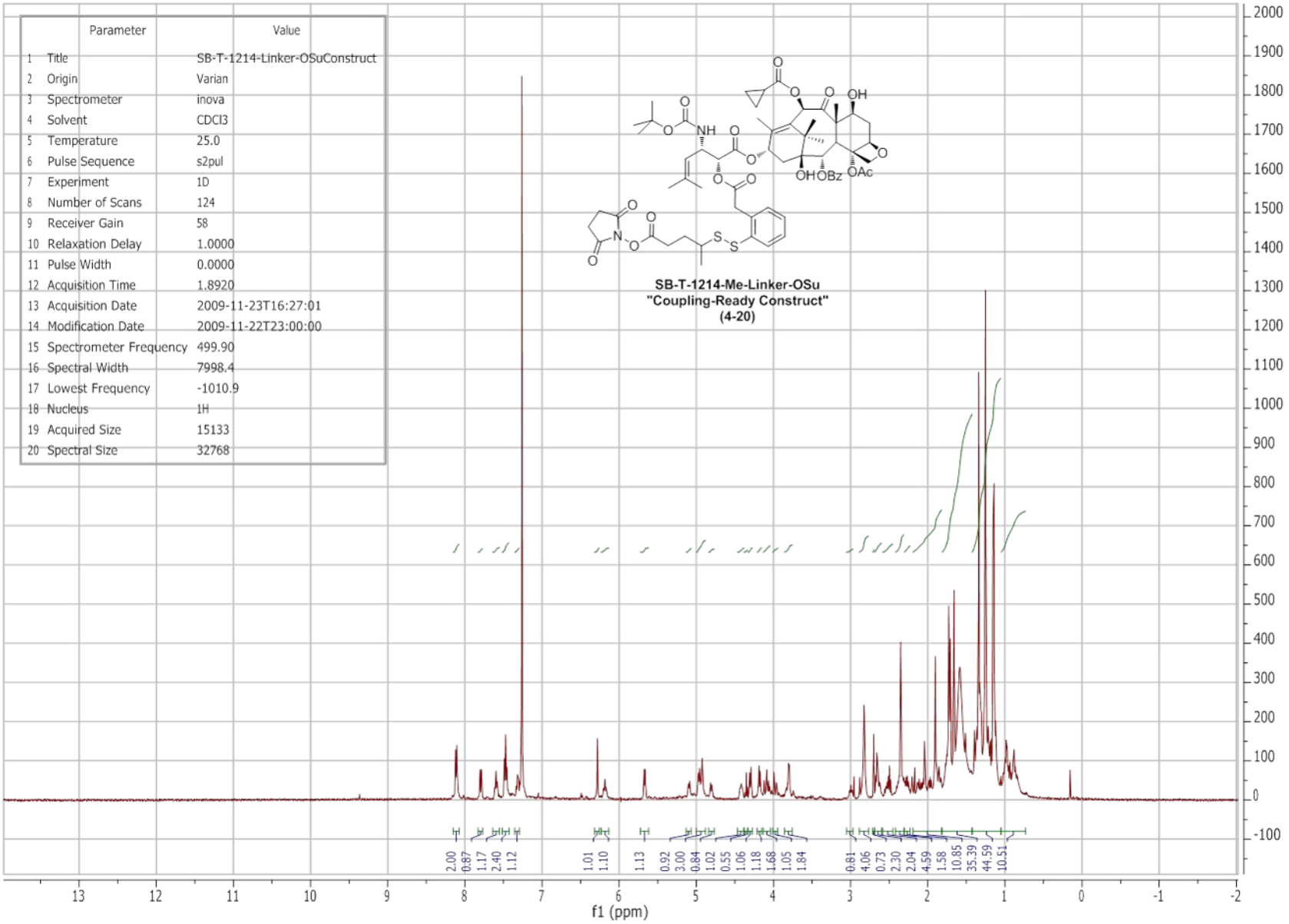
Parameter Value
1 Title SB-T-1214-Linker-OSuConstruct
2 Origin Varian
3 Spectrometer inova
4 Solvent CDCl3
5 Temperature 25.0
6 Pulse Sequence s2pul
7 Experiment 1D
8 Number of Scans 124
9 Receiver Gain 58
10 Relaxation Delay 1.0000
11 Pulse Width 0.0000
12 Acquisition Time 1.8920
13 Acquisition Date 2009-11-23T16:27:01
14 Modification Date 2009-11-22T23:00:00
15 Spectrometer Frequency 499.90
16 Spectral Width 7998.4
17 Lowest Frequency -1010.9
18 Nucleus 1H
19 Acquired Size 15133
20 Spectral Size 32768
SB-T-1214-Me-Linker-OSu
"Coupling-Ready Construct"
(4-20)
f1 (ppm)

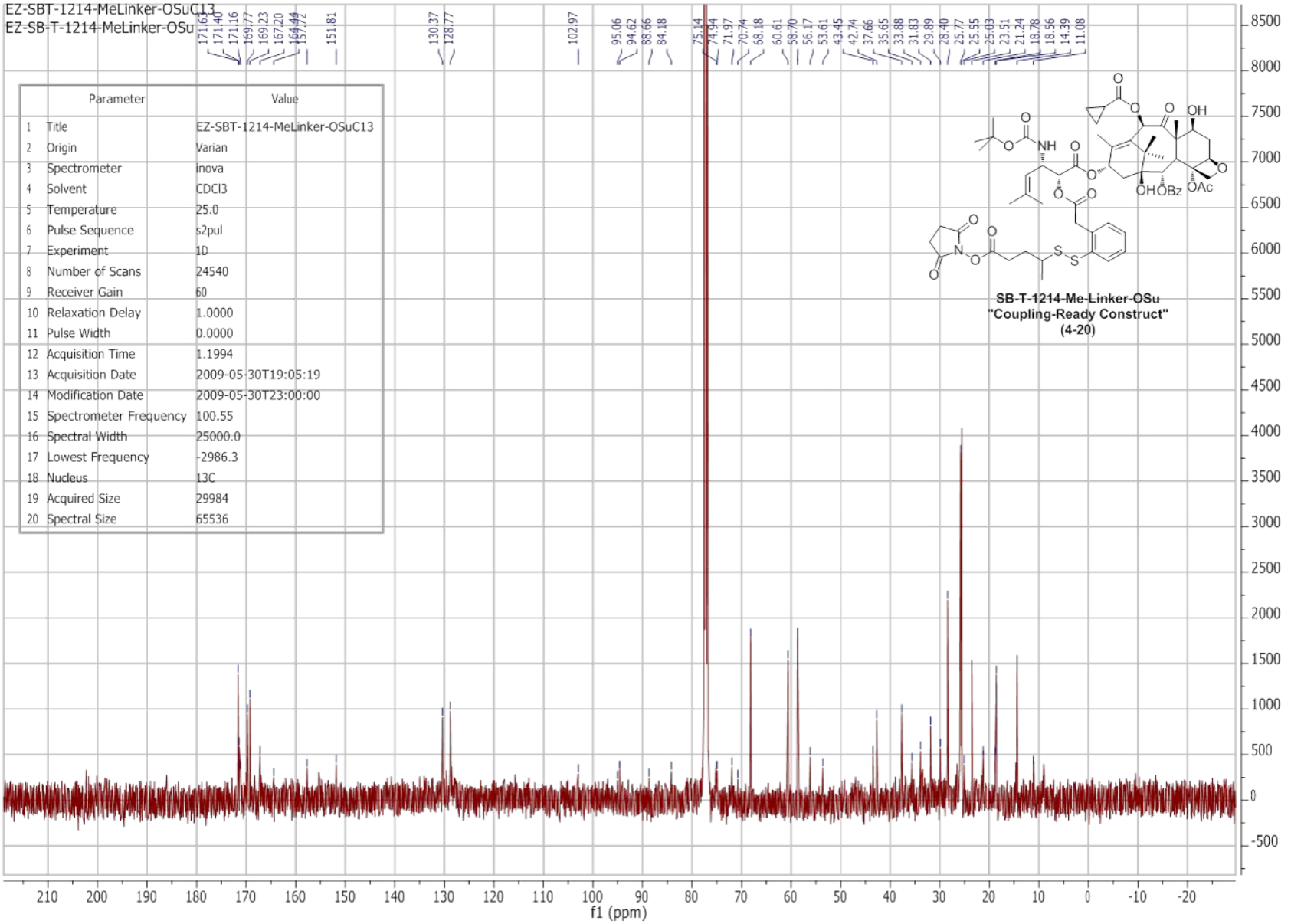
EZ-SBT-1214-MeLinker-OSuC13
EZ-SB-T-1214-MeLinker-OSu
171.63
171.40
171.16
169.77
169.23
167.20
164.44
157.72
151.81
130.37
128.77
102.97
95.06
94.62
88.66
84.18
75.14
74.94
71.97
70.74
68.18
60.61
58.70
56.17
53.61
43.45
42.74
37.66
35.65
33.88
31.83
29.89
28.40
25.77
25.55
25.03
23.51
21.24
18.78
18.56
14.39
11.08
Parameter Value
1 Title EZ-SBT-1214-MeLinker-OSuC13
2 Origin Varian
3 Spectrometer inova
4 Solvent CDCl3
5 Temperature 25.0
6 Pulse Sequence s2pul
7 Experiment 1D
8 Number of Scans 24540
9 Receiver Gain 60
10 Relaxation Delay 1.0000
11 Pulse Width 0.0000
12 Acquisition Time 1.1994
13 Acquisition Date 2009-05-30T19:05:19
14 Modification Date 2009-05-30T23:00:00
15 Spectrometer Frequency 100.55
16 Spectral Width 25000.0
17 Lowest Frequency -2986.3
18 Nucleus 13C
19 Acquired Size 29984
20 Spectral Size 65536
SB-T-1214-Me-Linker-OSu
"Coupling-Ready Construct"
(4-20)
f1 (ppm)

	Parameter	Value
1	Title	EZ-CPTPropanoicLinker
2	Origin	Varian
3	Spectrometer	inova
4	Solvent	CDCl3
5	Temperature	25.0
6	Pulse Sequence	s2pul
7	Experiment	1D
8	Number of Scans	64
9	Receiver Gain	38
10	Relaxation Delay	1.0000
11	Pulse Width	0.0000
12	Acquisition Time	3.2725
13	Acquisition Date	2008-07-13T19:34:50
14	Modification Date	2008-07-12T23:00:00
15	Spectrometer Frequency	399.83
16	Spectral Width	6000.6
17	Lowest Frequency	-989.7
18	Nucleus	1H
19	Acquired Size	19637
20	Spectral Size	65536

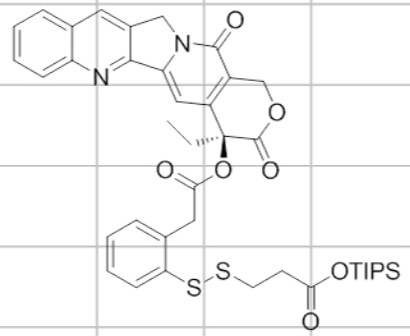

4-21a

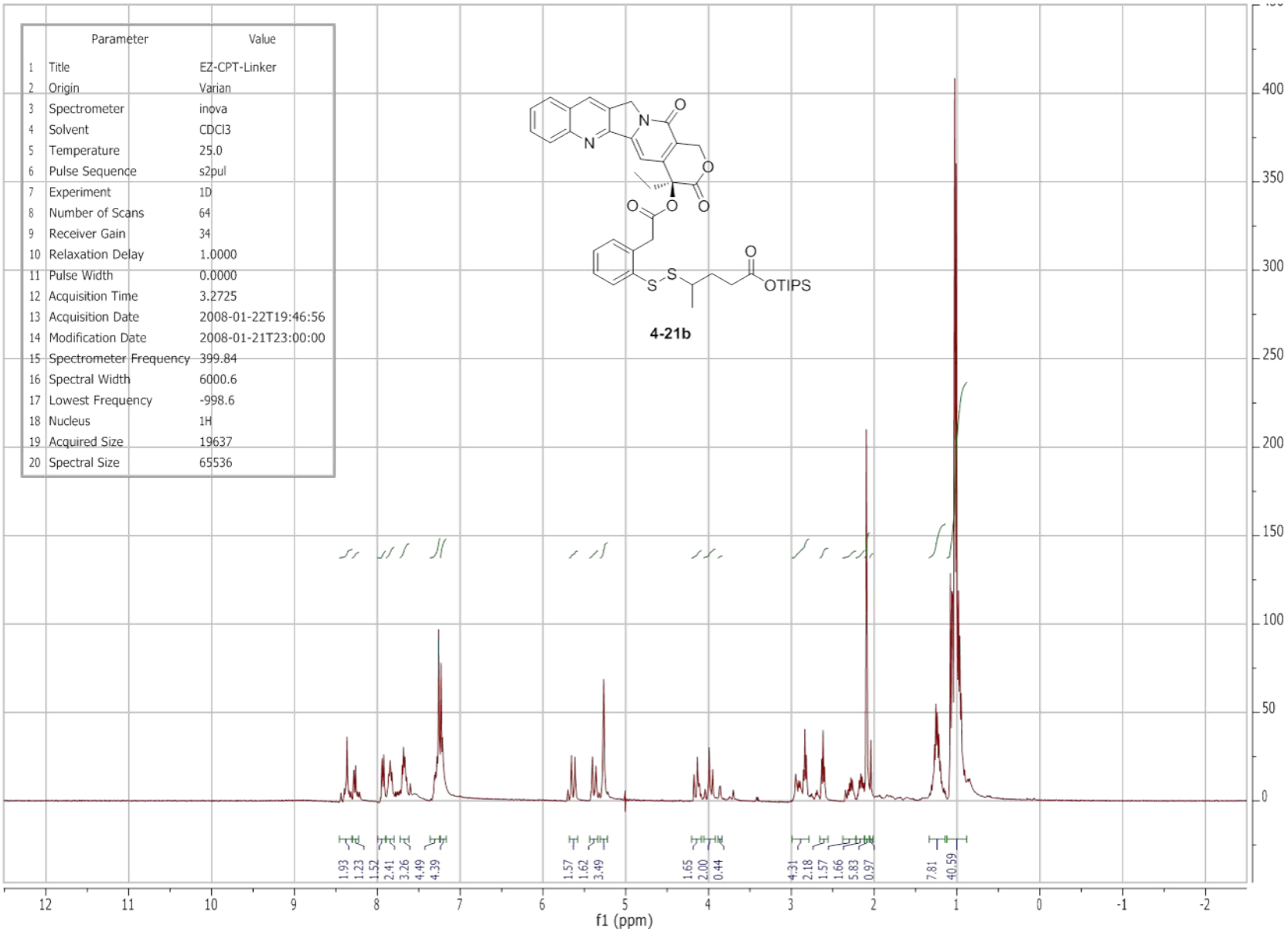
Parameter Value
1 Title EZ-CPT-Linker
2 Origin Varian
3 Spectrometer inova
4 Solvent CDCl3
5 Temperature 25.0
6 Pulse Sequence s2pul
7 Experiment 1D
8 Number of Scans 64
9 Receiver Gain 34
10 Relaxation Delay 1.0000
11 Pulse Width 0.0000
12 Acquisition Time 3.2725
13 Acquisition Date 2008-01-22T19:46:56
14 Modification Date 2008-01-21T23:00:00
15 Spectrometer Frequency 399.84
16 Spectral Width 6000.6
17 Lowest Frequency -998.6
18 Nucleus 1H
19 Acquired Size 19637
20 Spectral Size 65536
OTIPS
4-21b
f1 (ppm)

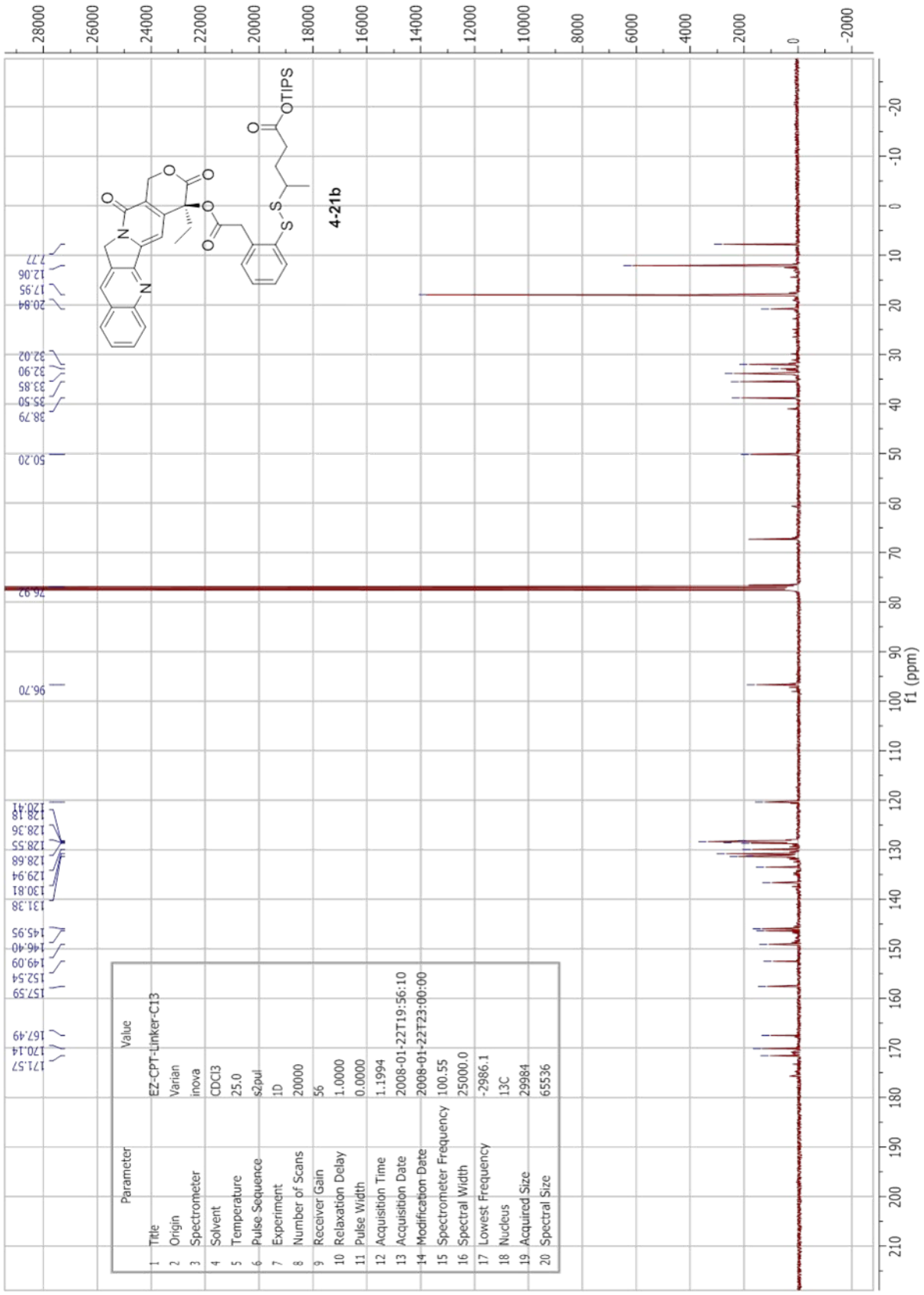
4-21b
OTIPS
f1 (ppm)
Parameter Value
1 Title EZ-CPT-Linker-C13
2 Origin Varian
3 Spectrometer inova
4 Solvent CDCl3
5 Temperature 25.0
6 Pulse Sequence s2pul
7 Experiment 1D
8 Number of Scans 20000
9 Receiver Gain 56
10 Relaxation Delay 1.0000
11 Pulse Width 0.0000
12 Acquisition Time 1.1994
13 Acquisition Date 2008-01-22T19:56:10
14 Modification Date 2008-01-22T23:00:00
15 Spectrometer Frequency 100.55
16 Spectral Width 25000.0
17 Lowest Frequency -2986.1
18 Nucleus 13C
19 Acquired Size 29984
20 Spectral Size 65536

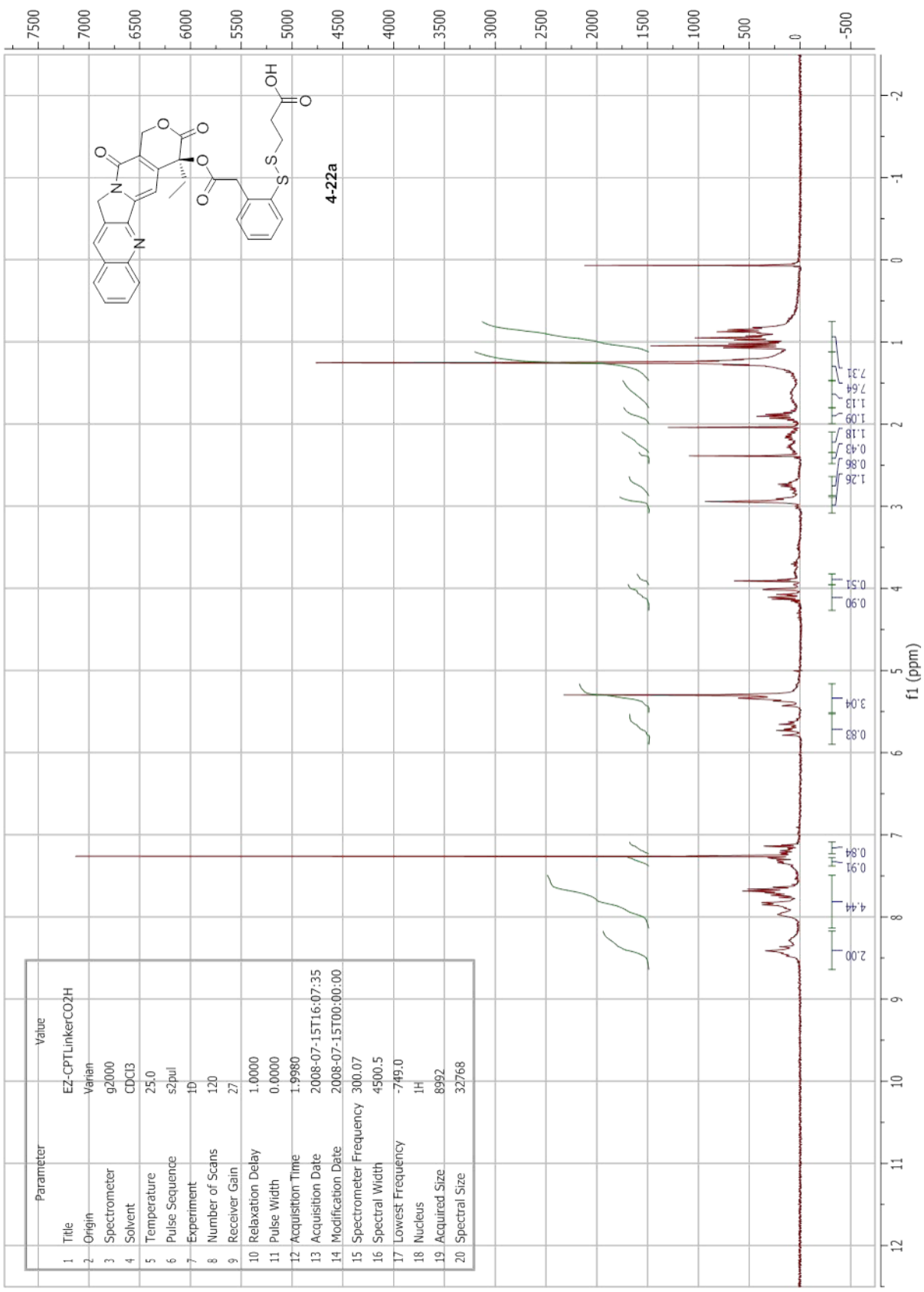

	Parameter	Value
1	Title	EZ-CPTLinkerCO2H
2	Origin	Varian
3	Spectrometer	g2000
4	Solvent	CDCl3
5	Temperature	25.0
6	Pulse Sequence	s2pul
7	Experiment	1D
8	Number of Scans	120
9	Receiver Gain	27
10	Relaxation Delay	1.0000
11	Pulse Width	0.0000
12	Acquisition Time	1.9980
13	Acquisition Date	2008-07-15T16:07:35
14	Modification Date	2008-07-15T00:00:00
15	Spectrometer Frequency	300.07
16	Spectral Width	4500.5
17	Lowest Frequency	-749.0
18	Nucleus	1H
19	Acquired Size	8992
20	Spectral Size	32768

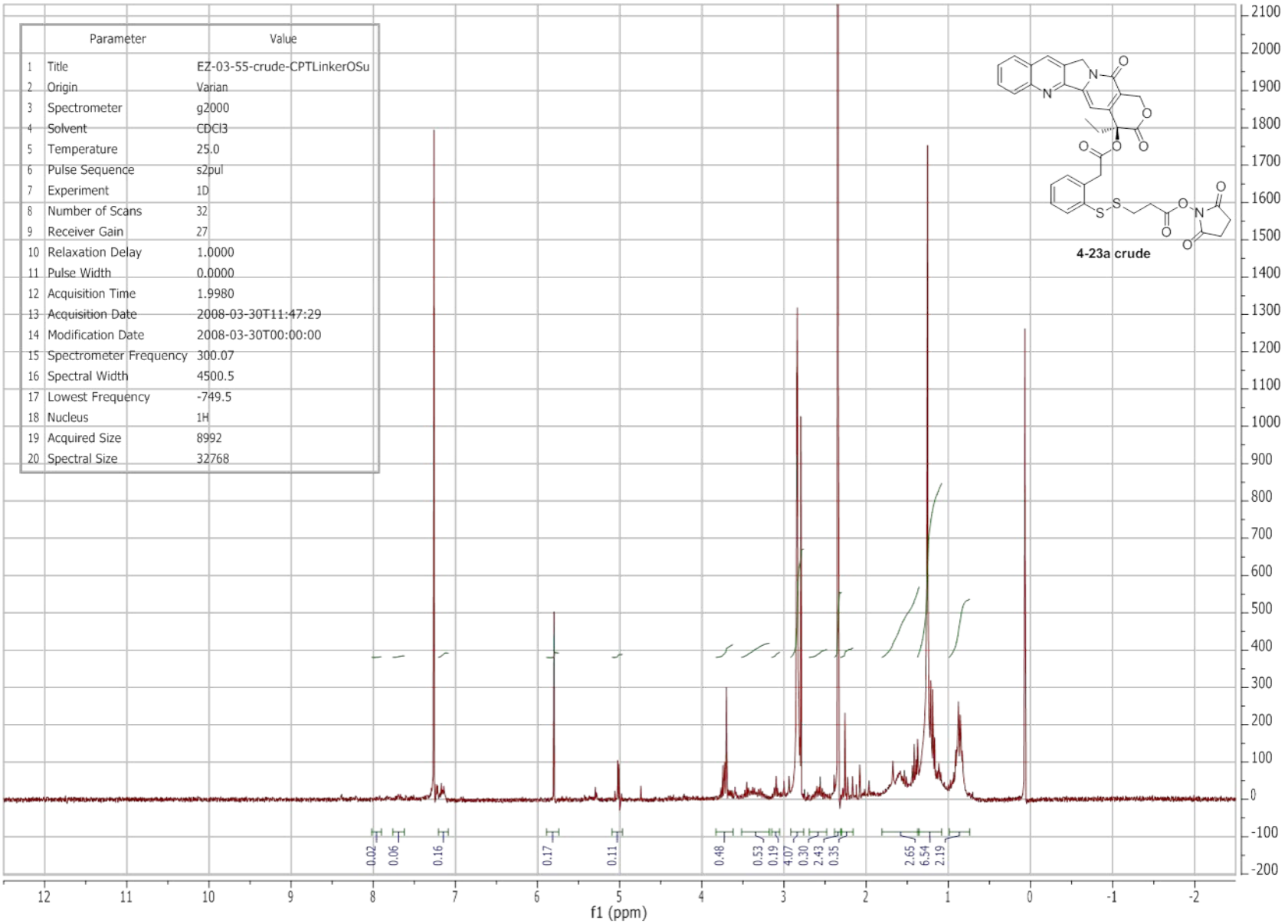
Parameter Value
1 Title EZ-03-55-crude-CPTLinkerOSu
2 Origin Varian
3 Spectrometer g2000
4 Solvent CDCl3
5 Temperature 25.0
6 Pulse Sequence s2pul
7 Experiment 1D
8 Number of Scans 32
9 Receiver Gain 27
10 Relaxation Delay 1.0000
11 Pulse Width 0.0000
12 Acquisition Time 1.9980
13 Acquisition Date 2008-03-30T11:47:29
14 Modification Date 2008-03-30T00:00:00
15 Spectrometer Frequency 300.07
16 Spectral Width 4500.5
17 Lowest Frequency -749.5
18 Nucleus 1H
19 Acquired Size 8992
20 Spectral Size 32768
4-23a crude
0.02 0.06 0.16 0.17 0.11 0.48 0.53 0.19 4.07 0.30 2.43 0.35 2.65 6.54 2.19
f1 (ppm)

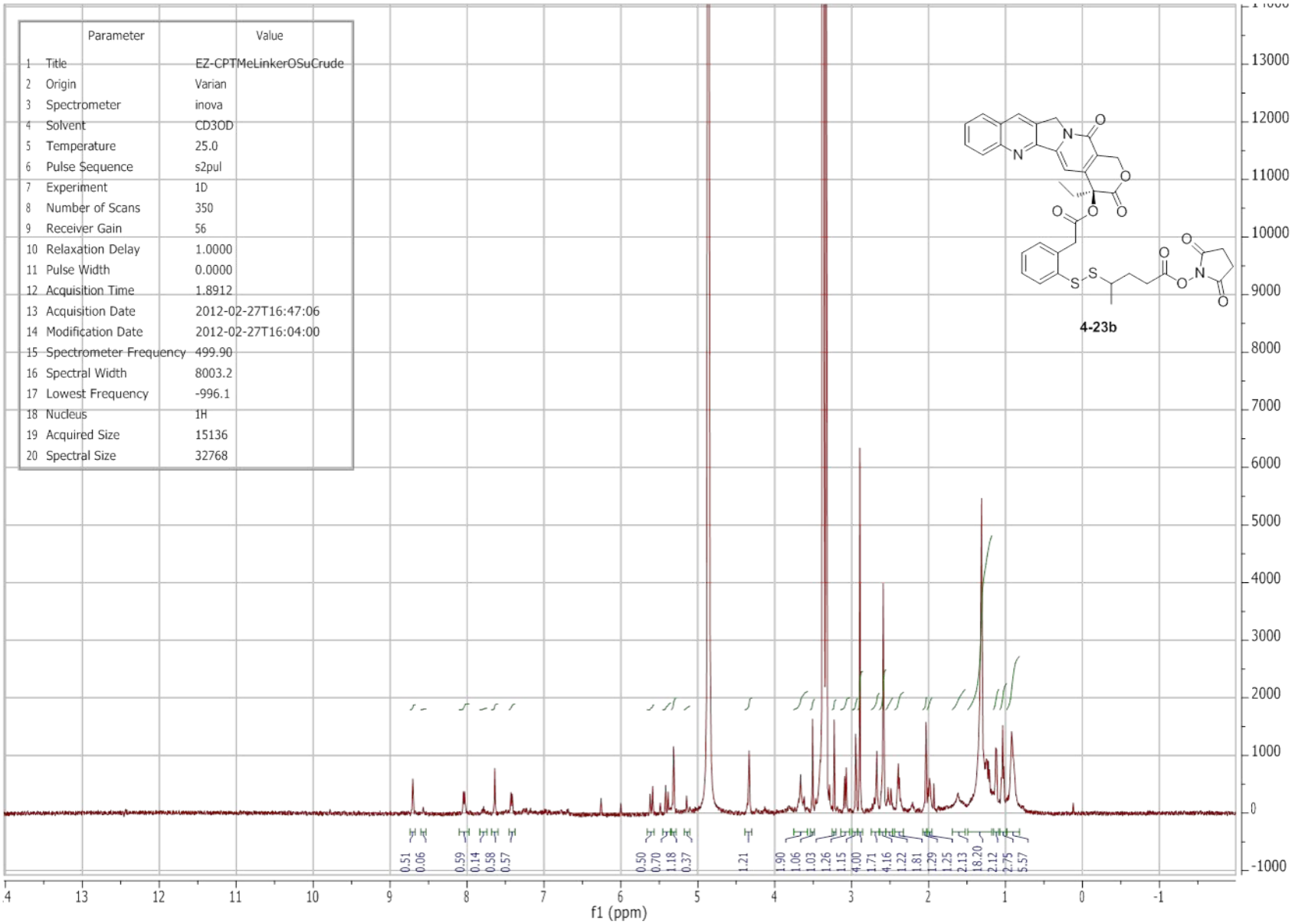
Parameter Value
1 Title EZ-CPTMeLinkerOSuCrude
2 Origin Varian
3 Spectrometer inova
4 Solvent CD3OD
5 Temperature 25.0
6 Pulse Sequence s2pul
7 Experiment 1D
8 Number of Scans 350
9 Receiver Gain 56
10 Relaxation Delay 1.0000
11 Pulse Width 0.0000
12 Acquisition Time 1.8912
13 Acquisition Date 2012-02-27T16:47:06
14 Modification Date 2012-02-27T16:04:00
15 Spectrometer Frequency 499.90
16 Spectral Width 8003.2
17 Lowest Frequency -996.1
18 Nucleus 1H
19 Acquired Size 15136
20 Spectral Size 32768
4-23b
f1 (ppm)

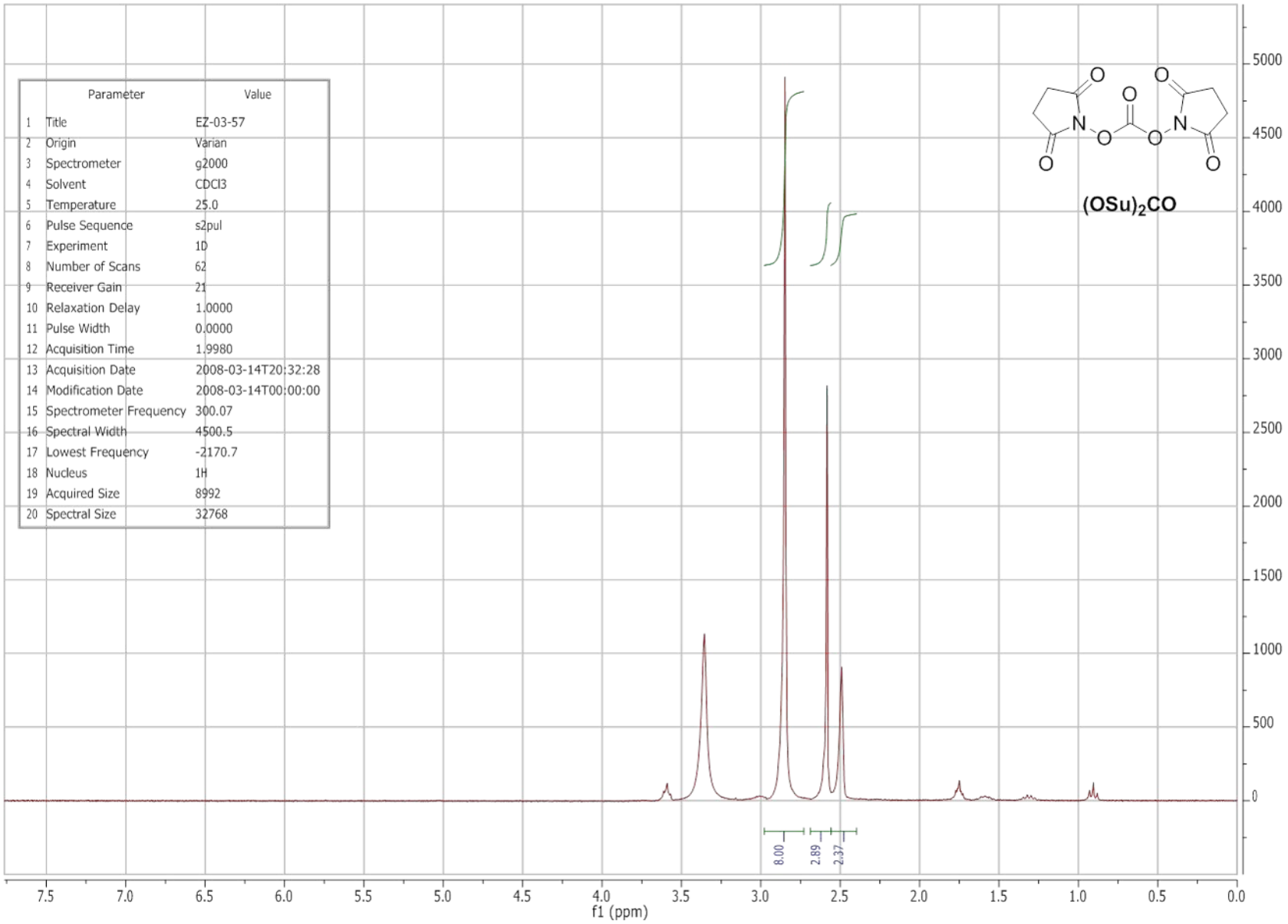
Parameter Value
1 Title EZ-03-57
2 Origin Varian
3 Spectrometer g2000
4 Solvent CDCl3
5 Temperature 25.0
6 Pulse Sequence s2pul
7 Experiment 1D
8 Number of Scans 62
9 Receiver Gain 21
10 Relaxation Delay 1.0000
11 Pulse Width 0.0000
12 Acquisition Time 1.9980
13 Acquisition Date 2008-03-14T20:32:28
14 Modification Date 2008-03-14T00:00:00
15 Spectrometer Frequency 300.07
16 Spectral Width 4500.5
17 Lowest Frequency -2170.7
18 Nucleus 1H
19 Acquired Size 8992
20 Spectral Size 32768
(OSu)2CO
8.00
2.89
2.37
f1 (ppm)

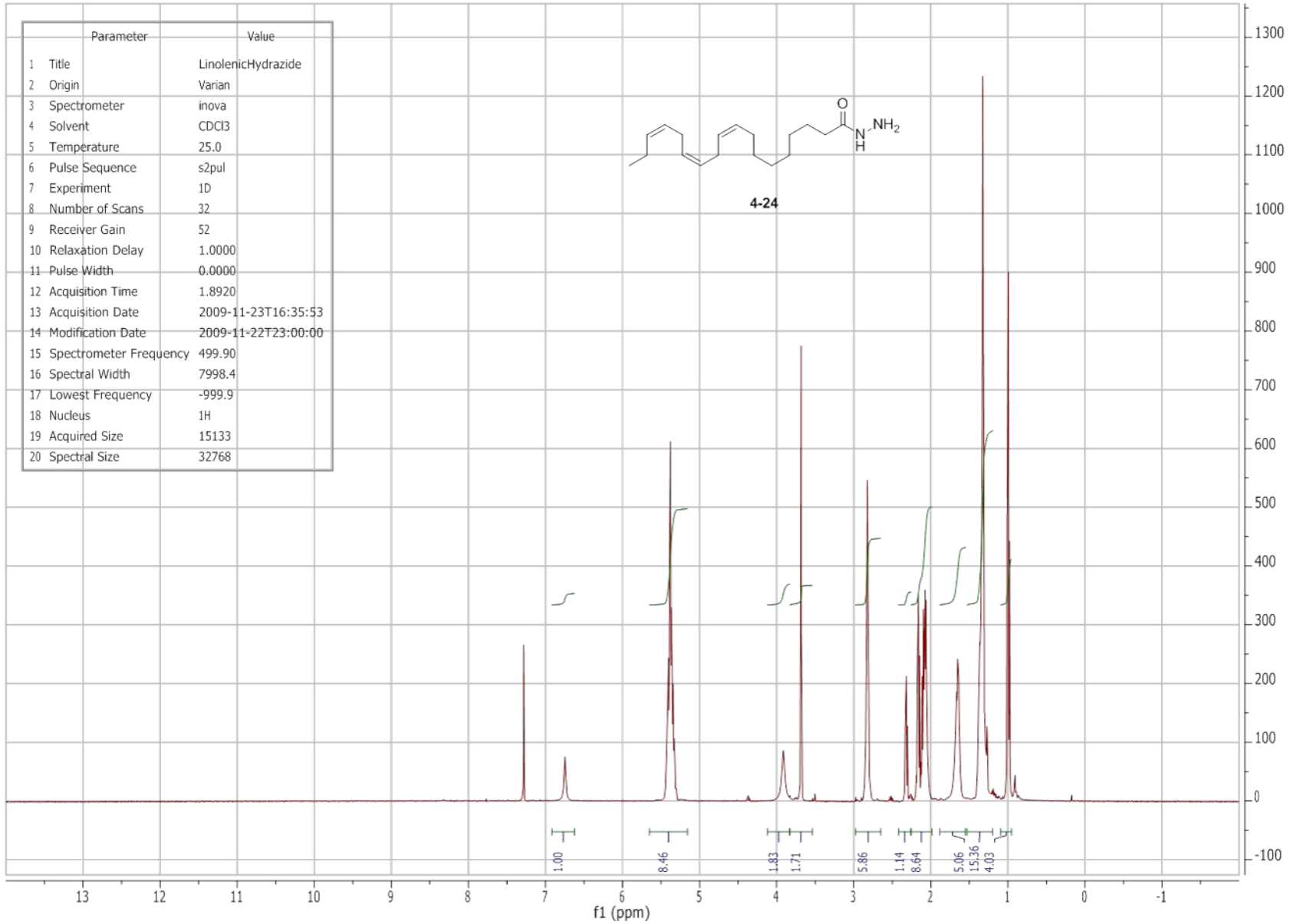
Parameter Value
1 Title LinolenicHydrazide
2 Origin Varian
3 Spectrometer inova
4 Solvent CDCl3
5 Temperature 25.0
6 Pulse Sequence s2pul
7 Experiment 1D
8 Number of Scans 32
9 Receiver Gain 52
10 Relaxation Delay 1.0000
11 Pulse Width 0.0000
12 Acquisition Time 1.8920
13 Acquisition Date 2009-11-23T16:35:53
14 Modification Date 2009-11-22T23:00:00
15 Spectrometer Frequency 499.90
16 Spectral Width 7998.4
17 Lowest Frequency -999.9
18 Nucleus 1H
19 Acquired Size 15133
20 Spectral Size 32768
O
N
H
NH2
4-24
1.00
8.46
1.83
1.71
5.86
1.14
8.64
5.06
15.36
4.03
f1 (ppm)

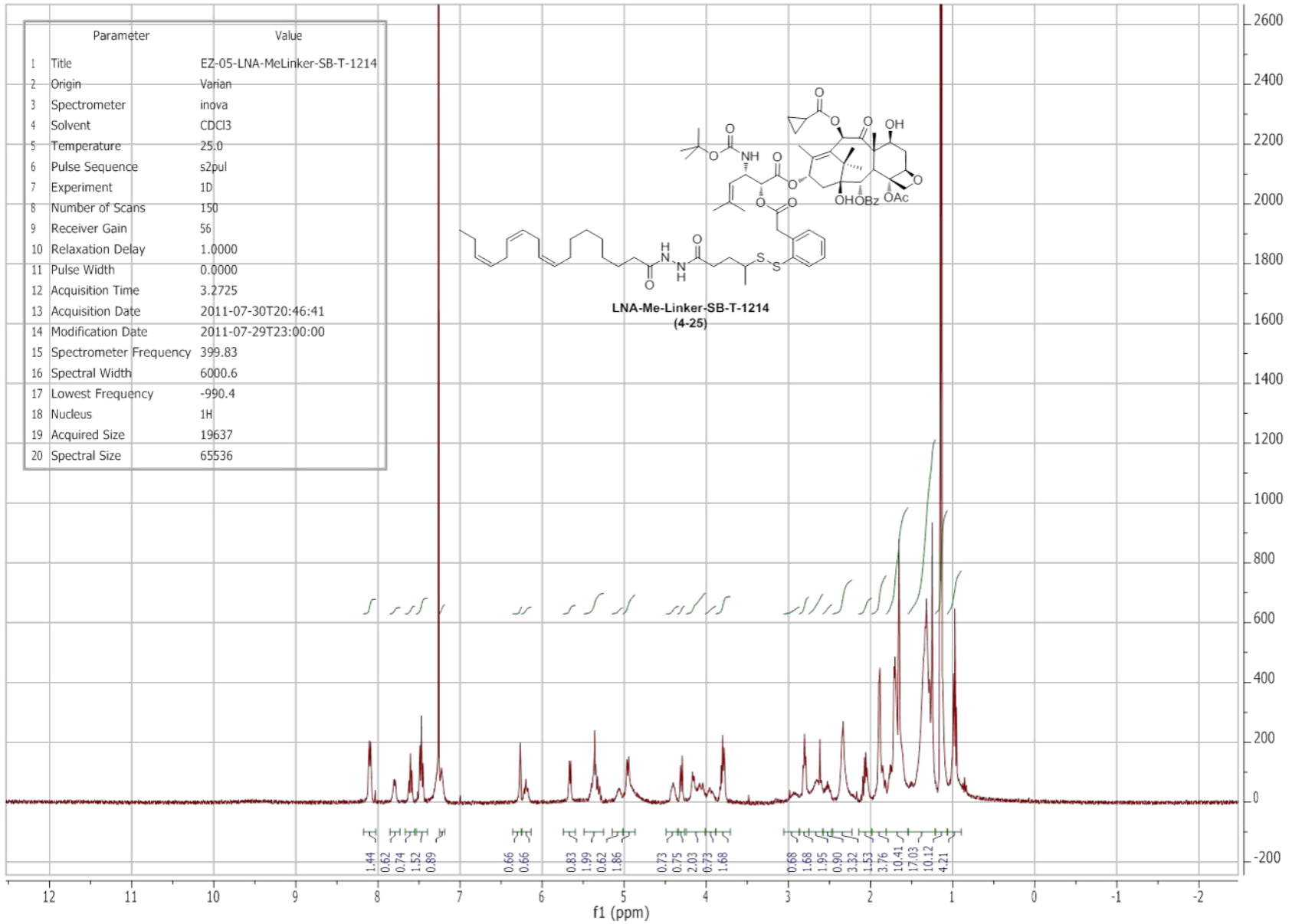
Parameter Value
1 Title EZ-05-LNA-MeLinker-SB-T-1214
2 Origin Varian
3 Spectrometer inova
4 Solvent CDCl3
5 Temperature 25.0
6 Pulse Sequence s2pul
7 Experiment 1D
8 Number of Scans 150
9 Receiver Gain 56
10 Relaxation Delay 1.0000
11 Pulse Width 0.0000
12 Acquisition Time 3.2725
13 Acquisition Date 2011-07-30T20:46:41
14 Modification Date 2011-07-29T23:00:00
15 Spectrometer Frequency 399.83
16 Spectral Width 6000.6
17 Lowest Frequency -990.4
18 Nucleus 1H
19 Acquired Size 19637
20 Spectral Size 65536
LNA-Me-Linker-SB-T-1214
(4-25)
f1 (ppm)

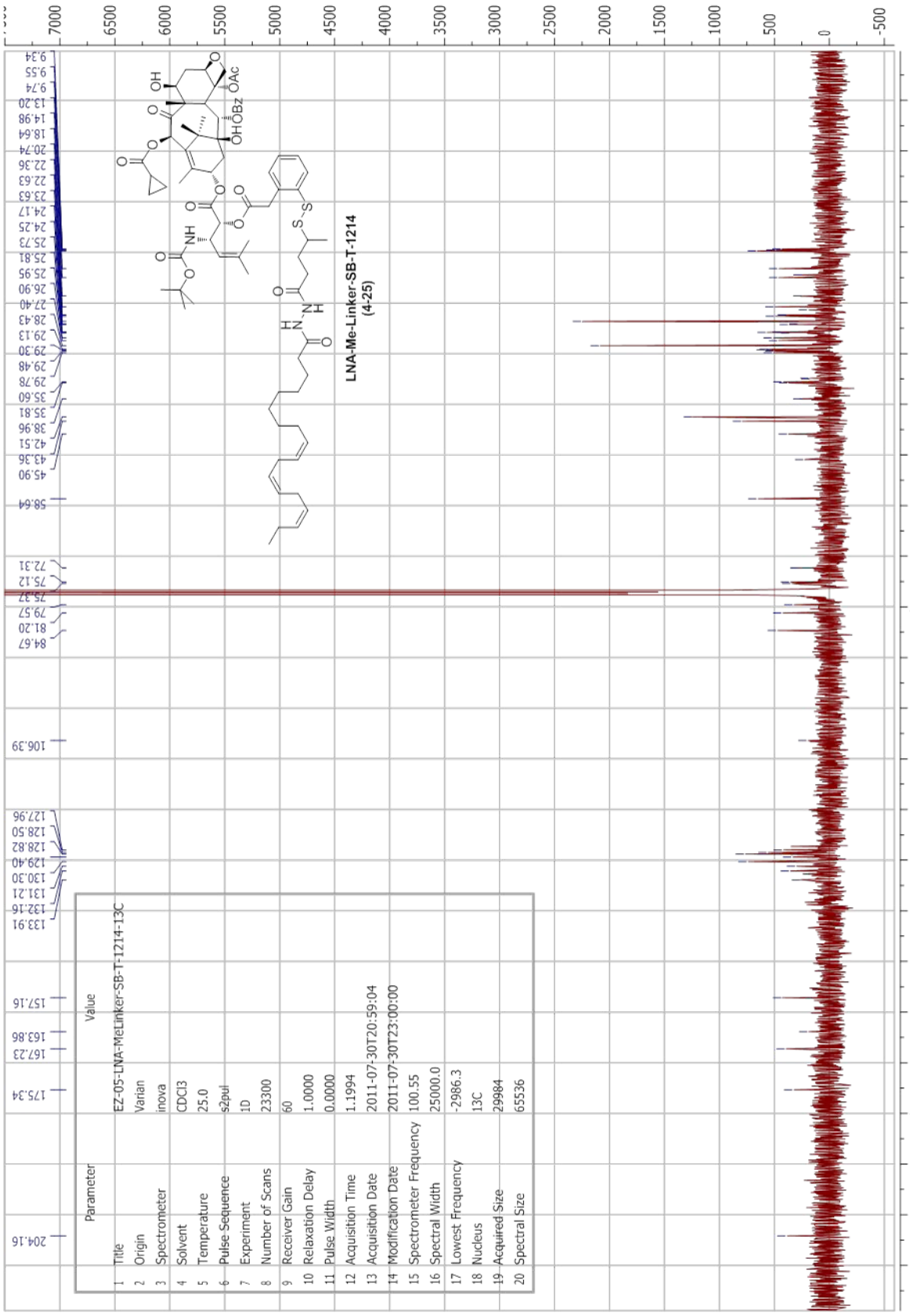

	Parameter	Value
1	Title	EZ-05-LNA-MeLinker-SB-T-1214-13C
2	Origin	Varian
3	Spectrometer	inova
4	Solvent	CDCl3
5	Temperature	25.0
6	Pulse Sequence	s2pul
7	Experiment	1D
8	Number of Scans	23300
9	Receiver Gain	60
10	Relaxation Delay	1.0000
11	Pulse Width	0.0000
12	Acquisition Time	1.1994
13	Acquisition Date	2011-07-30T20:59:04
14	Modification Date	2011-07-30T23:00:00
15	Spectrometer Frequency	100.55
16	Spectral Width	25000.0
17	Lowest Frequency	-2986.3
18	Nucleus	13C
19	Acquired Size	29984
20	Spectral Size	65536

Appendix 4
Chapter 5 NMR Spectra

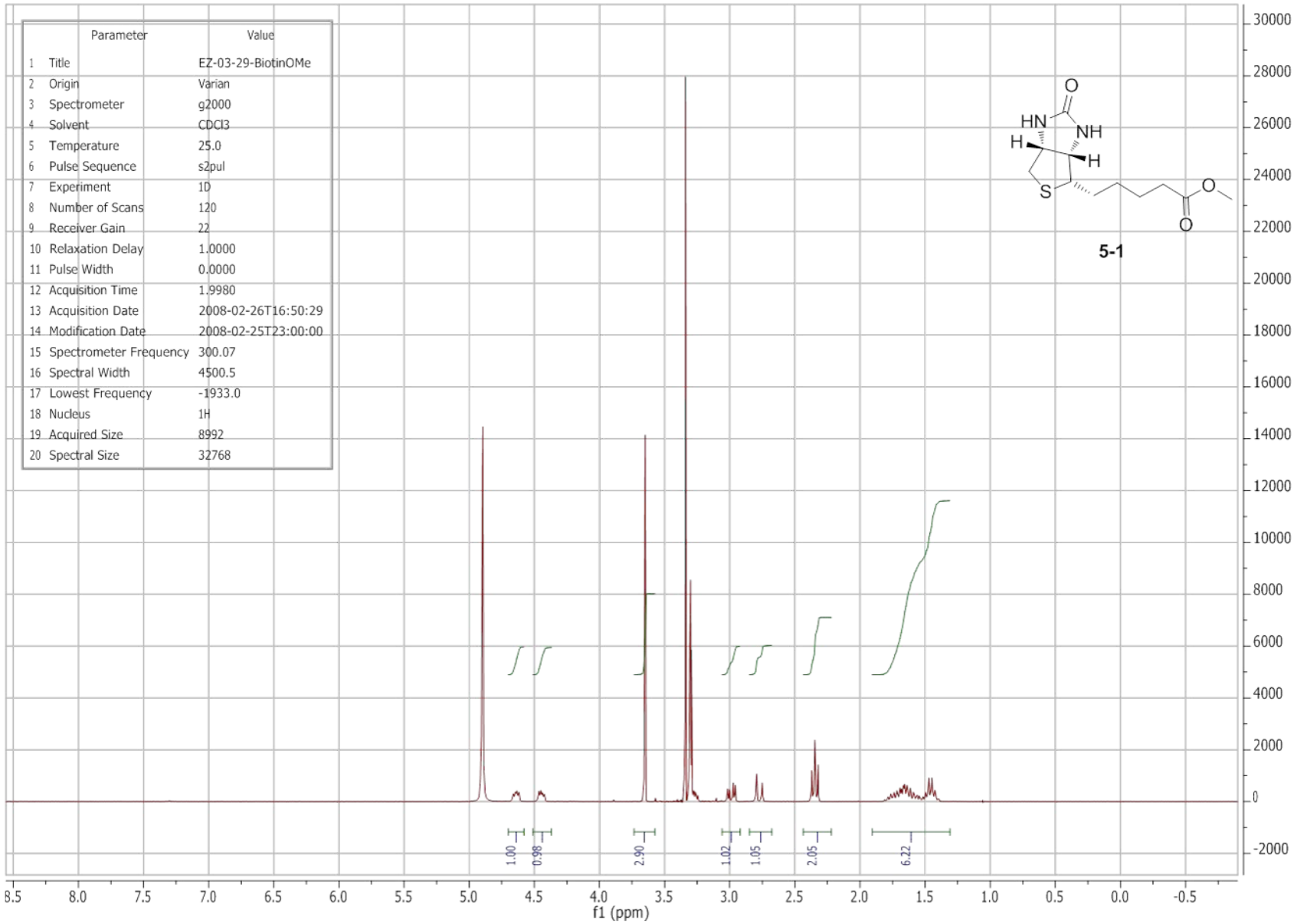
Parameter Value
1 Title EZ-03-29-BiotinOMe
2 Origin Varian
3 Spectrometer g2000
4 Solvent CDCl3
5 Temperature 25.0
6 Pulse Sequence s2pul
7 Experiment 1D
8 Number of Scans 120
9 Receiver Gain 22
10 Relaxation Delay 1.0000
11 Pulse Width 0.0000
12 Acquisition Time 1.9980
13 Acquisition Date 2008-02-26T16:50:29
14 Modification Date 2008-02-25T23:00:00
15 Spectrometer Frequency 300.07
16 Spectral Width 4500.5
17 Lowest Frequency -1933.0
18 Nucleus 1H
19 Acquired Size 8992
20 Spectral Size 32768
HN
NH
H
H
S
O
O
O
5-1
1.00
0.98
2.90
1.02
1.05
2.05
6.22
f1 (ppm)

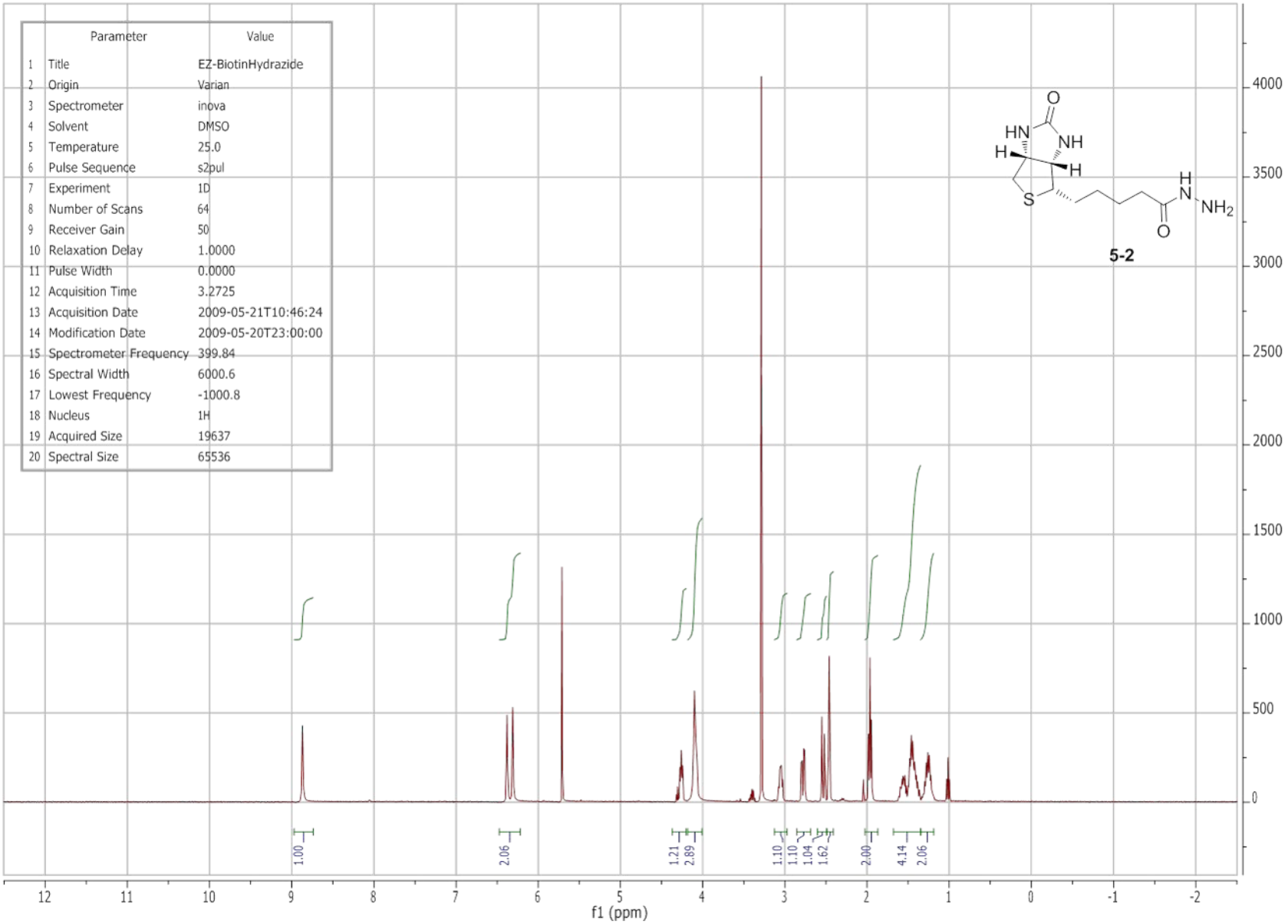
Parameter Value
1 Title EZ-BiotinHydrazide
2 Origin Varian
3 Spectrometer inova
4 Solvent DMSO
5 Temperature 25.0
6 Pulse Sequence s2pul
7 Experiment 1D
8 Number of Scans 64
9 Receiver Gain 50
10 Relaxation Delay 1.0000
11 Pulse Width 0.0000
12 Acquisition Time 3.2725
13 Acquisition Date 2009-05-21T10:46:24
14 Modification Date 2009-05-20T23:00:00
15 Spectrometer Frequency 399.84
16 Spectral Width 6000.6
17 Lowest Frequency -1000.8
18 Nucleus 1H
19 Acquired Size 19637
20 Spectral Size 65536
5-2
f1 (ppm)

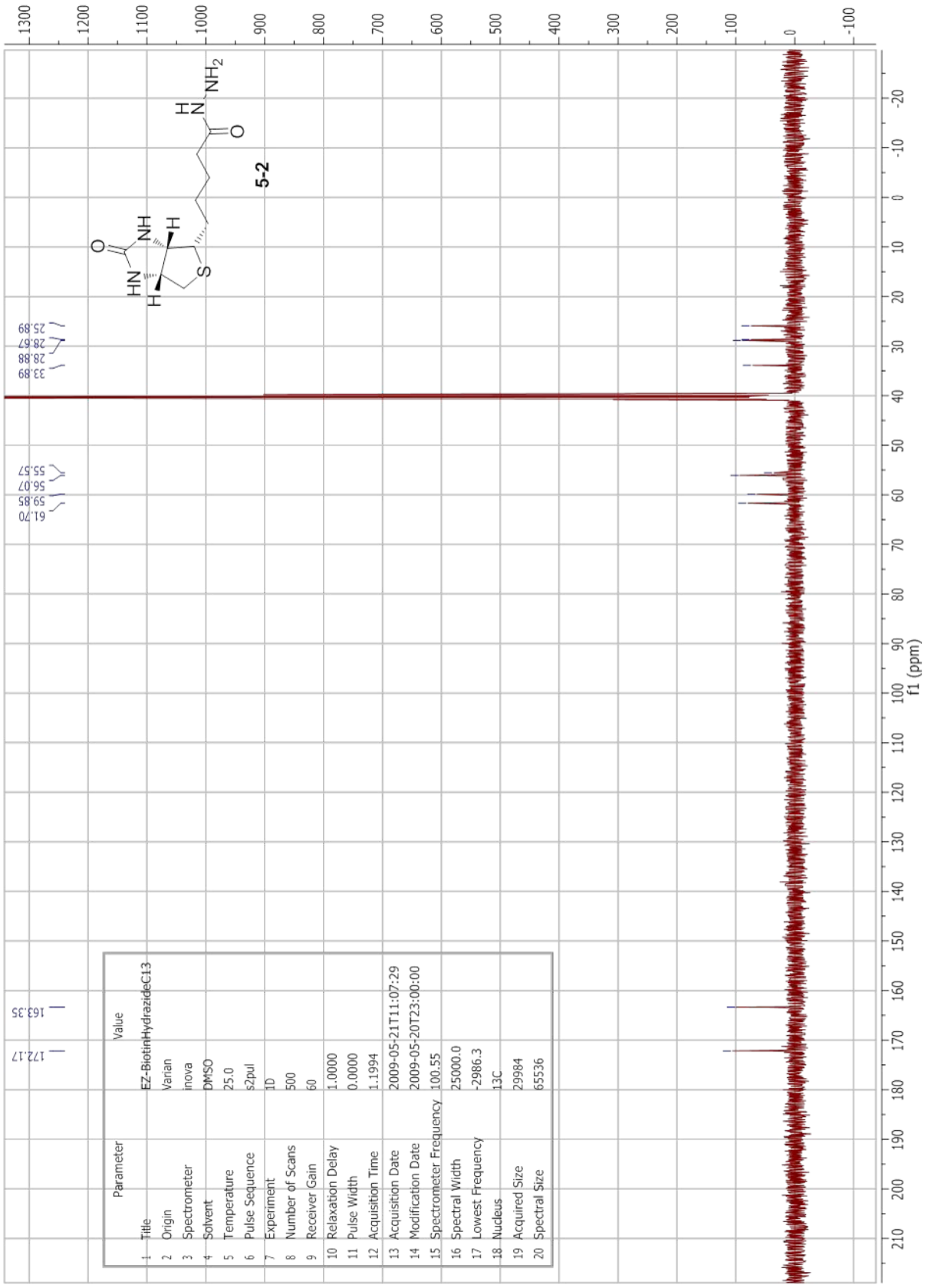
5-2
f1 (ppm)
Parameter
Value
1 Title EZ-BiotinHydrazideC13
2 Origin Varian
3 Spectrometer inova
4 Solvent DMSO
5 Temperature 25.0
6 Pulse Sequence s2pul
7 Experiment 1D
8 Number of Scans 500
9 Receiver Gain 60
10 Relaxation Delay 1.0000
11 Pulse Width 0.0000
12 Acquisition Time 1.1994
13 Acquisition Date 2009-05-21T11:07:29
14 Modification Date 2009-05-20T23:00:00
15 Spectrometer Frequency 100.55
16 Spectral Width 25000.0
17 Lowest Frequency -2986.3
18 Nucleus 13C
19 Acquired Size 29984
20 Spectral Size 65536

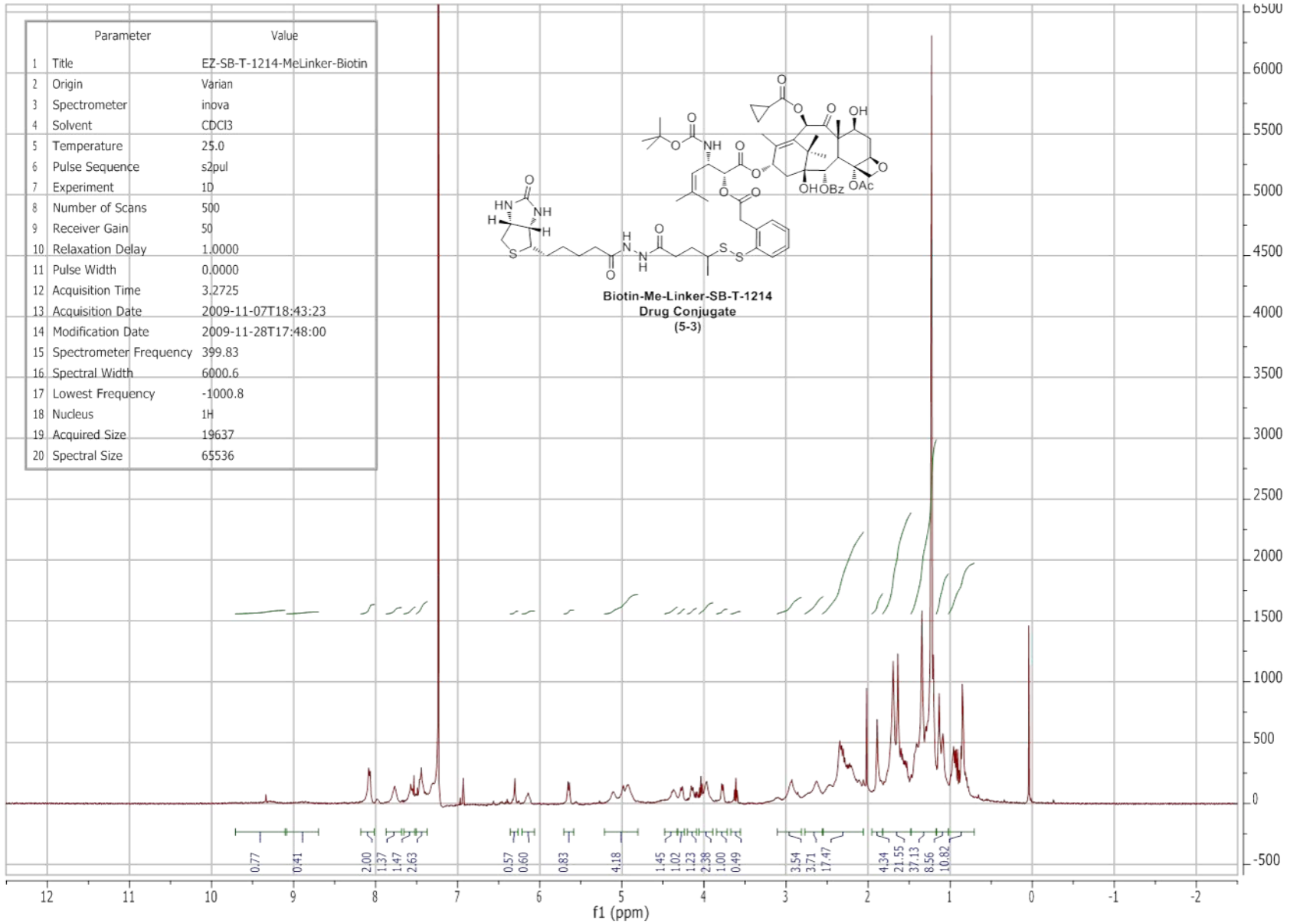
Parameter Value
1 Title EZ-SB-T-1214-MeLinker-Biotin
2 Origin Varian
3 Spectrometer inova
4 Solvent CDCl3
5 Temperature 25.0
6 Pulse Sequence s2pul
7 Experiment 1D
8 Number of Scans 500
9 Receiver Gain 50
10 Relaxation Delay 1.0000
11 Pulse Width 0.0000
12 Acquisition Time 3.2725
13 Acquisition Date 2009-11-07T18:43:23
14 Modification Date 2009-11-28T17:48:00
15 Spectrometer Frequency 399.83
16 Spectral Width 6000.6
17 Lowest Frequency -1000.8
18 Nucleus 1H
19 Acquired Size 19637
20 Spectral Size 65536
Biotin-Me-Linker-SB-T-1214
Drug Conjugate
(5-3)
0.77 0.41 2.00 1.37 1.47 2.63 0.57 0.60 0.83 4.18 1.45 1.02 1.23 2.38 1.00 0.49 3.54 3.71 17.47 4.34 21.55 37.13 8.56 10.82
f1 (ppm)

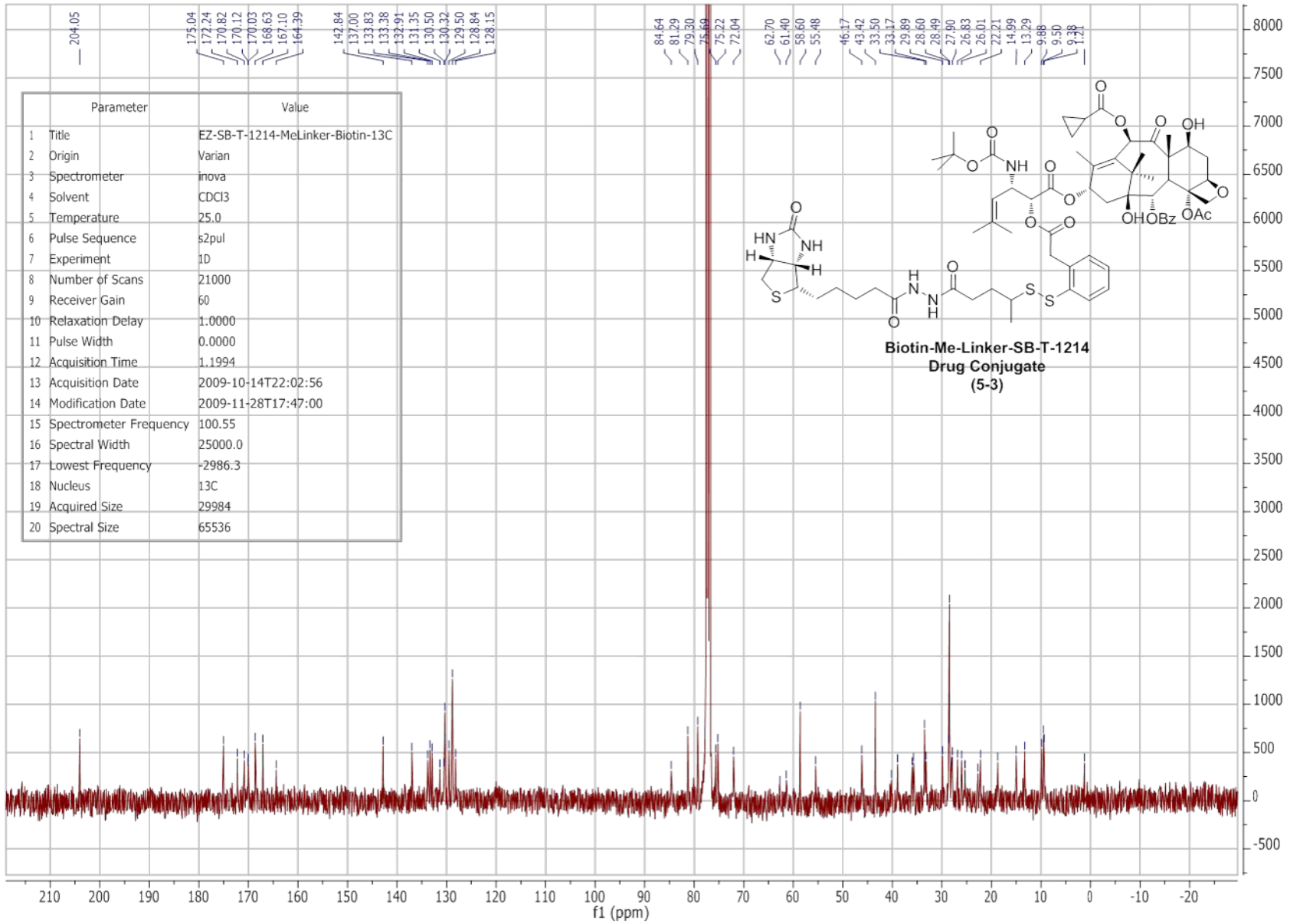
204.05
175.04
172.24
170.82
170.12
170.03
168.63
167.10
164.39
142.84
137.00
133.83
133.38
132.91
131.35
130.50
130.32
129.50
128.84
128.15
84.64
81.29
79.30
75.69
75.22
72.04
62.70
61.40
58.60
55.48
46.17
43.42
33.50
33.17
29.89
28.60
28.49
27.90
26.83
26.01
22.21
14.99
13.29
9.88
9.50
9.38
1.21
Parameter Value
1 Title EZ-SB-T-1214-MeLinker-Biotin-13C
2 Origin Varian
3 Spectrometer inova
4 Solvent CDCl3
5 Temperature 25.0
6 Pulse Sequence s2pul
7 Experiment 1D
8 Number of Scans 21000
9 Receiver Gain 60
10 Relaxation Delay 1.0000
11 Pulse Width 0.0000
12 Acquisition Time 1.1994
13 Acquisition Date 2009-10-14T22:02:56
14 Modification Date 2009-11-28T17:47:00
15 Spectrometer Frequency 100.55
16 Spectral Width 25000.0
17 Lowest Frequency -2986.3
18 Nucleus 13C
19 Acquired Size 29984
20 Spectral Size 65536
Biotin-Me-Linker-SB-T-1214
Drug Conjugate
(5-3)
f1 (ppm)

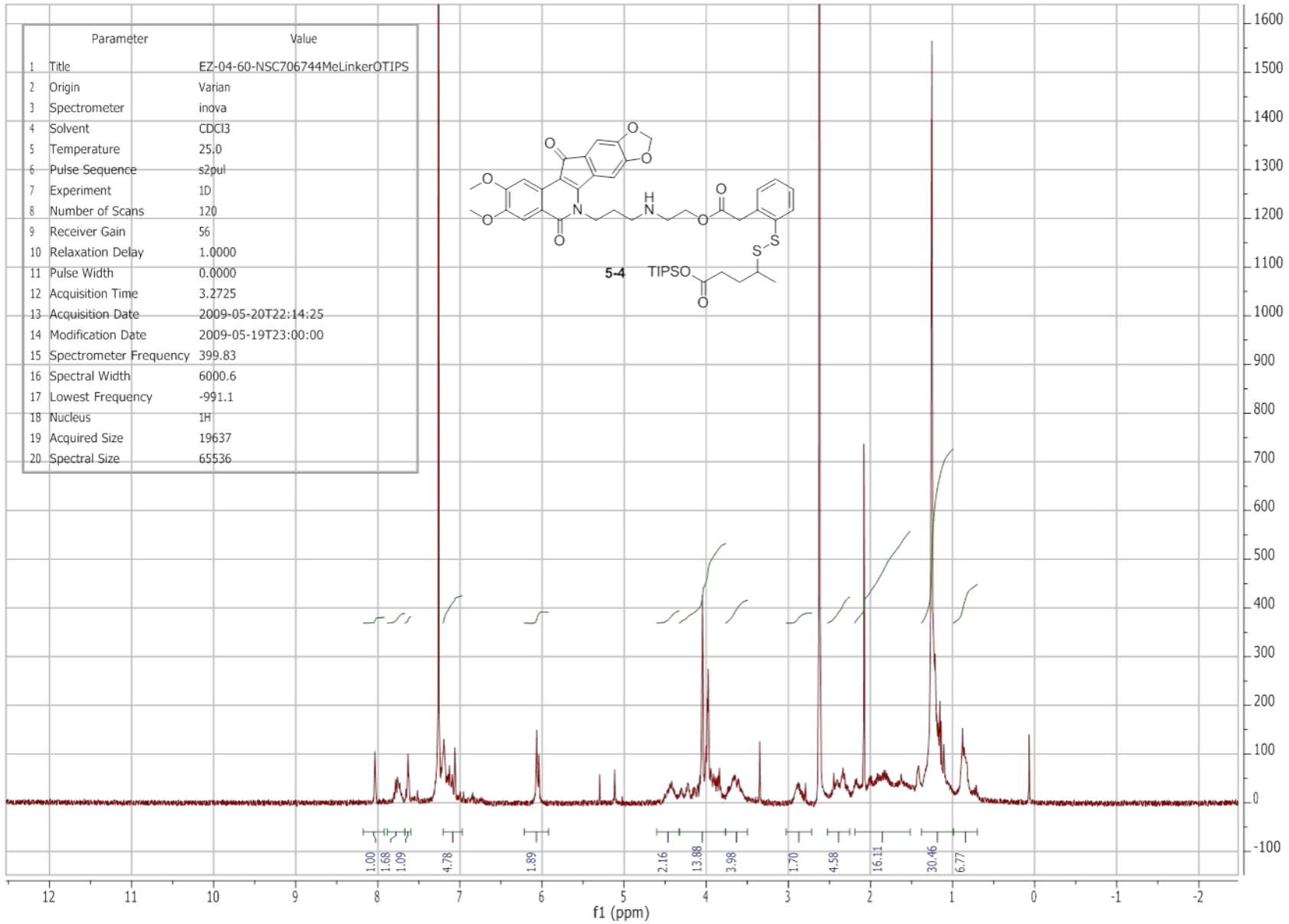
Parameter Value
1 Title EZ-04-60-NSC706744MeLinkerOTIPS
2 Origin Varian
3 Spectrometer inova
4 Solvent CDCl3
5 Temperature 25.0
6 Pulse Sequence s2pul
7 Experiment 1D
8 Number of Scans 120
9 Receiver Gain 56
10 Relaxation Delay 1.0000
11 Pulse Width 0.0000
12 Acquisition Time 3.2725
13 Acquisition Date 2009-05-20T22:14:25
14 Modification Date 2009-05-19T23:00:00
15 Spectrometer Frequency 399.83
16 Spectral Width 6000.6
17 Lowest Frequency -991.1
18 Nucleus 1H
19 Acquired Size 19637
20 Spectral Size 65536
5-4
TIPSO
1.00
1.68
1.09
4.78
1.89
2.16
13.88
3.98
1.70
4.58
16.11
30.46
6.77
f1 (ppm)

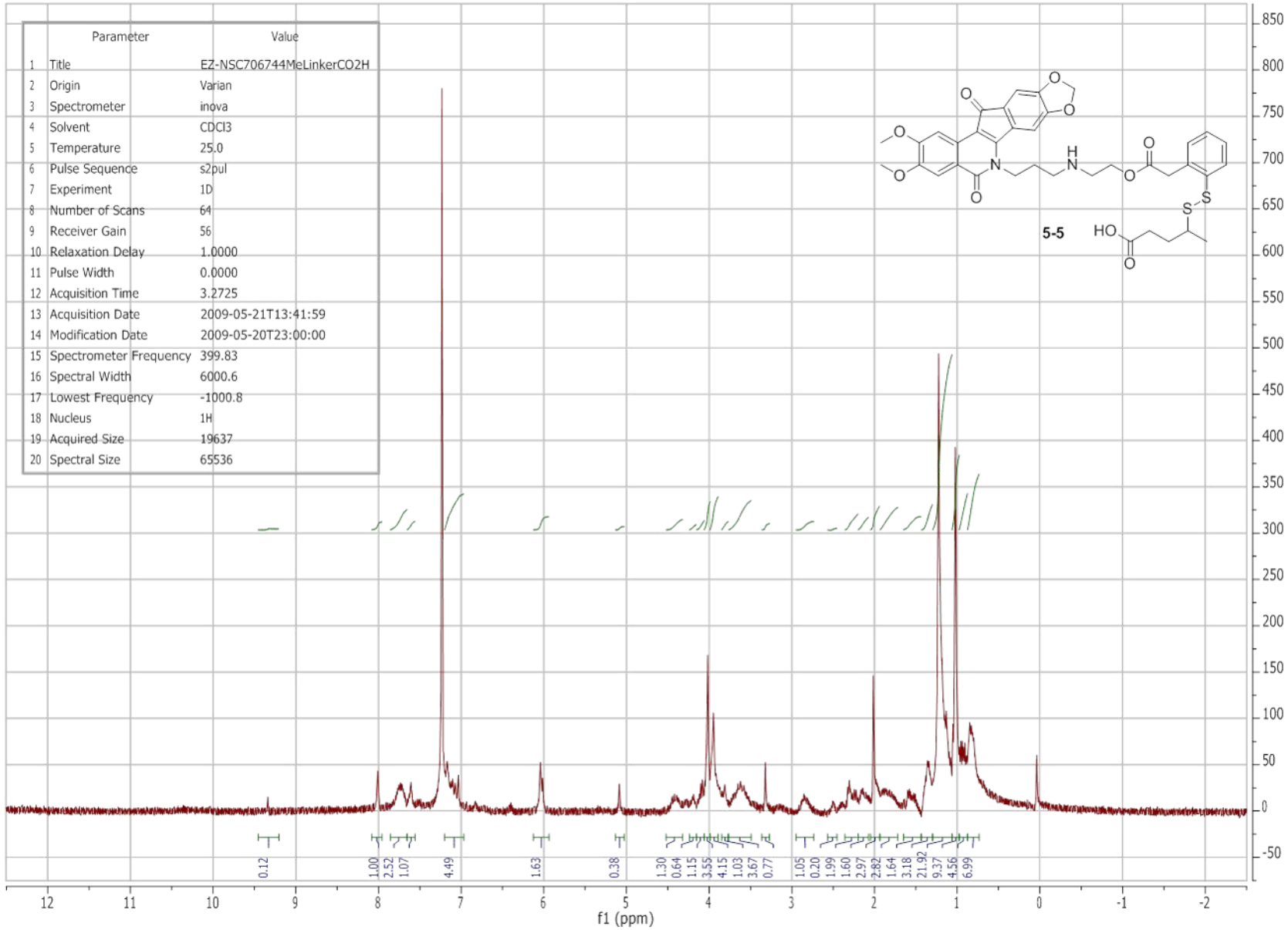
Parameter Value
1 Title EZ-NSC706744MeLinkerCO2H
2 Origin Varian
3 Spectrometer inova
4 Solvent CDCl3
5 Temperature 25.0
6 Pulse Sequence s2pul
7 Experiment 1D
8 Number of Scans 64
9 Receiver Gain 56
10 Relaxation Delay 1.0000
11 Pulse Width 0.0000
12 Acquisition Time 3.2725
13 Acquisition Date 2009-05-21T13:41:59
14 Modification Date 2009-05-20T23:00:00
15 Spectrometer Frequency 399.83
16 Spectral Width 6000.6
17 Lowest Frequency -1000.8
18 Nucleus 1H
19 Acquired Size 19637
20 Spectral Size 65536
5-5
0.12
1.00
2.52
1.07
4.49
1.63
0.38
1.30
0.64
1.15
3.55
4.15
1.03
3.67
0.77
1.05
0.20
1.99
1.60
2.97
2.82
1.64
3.18
21.92
9.37
4.56
6.99
f1 (ppm)

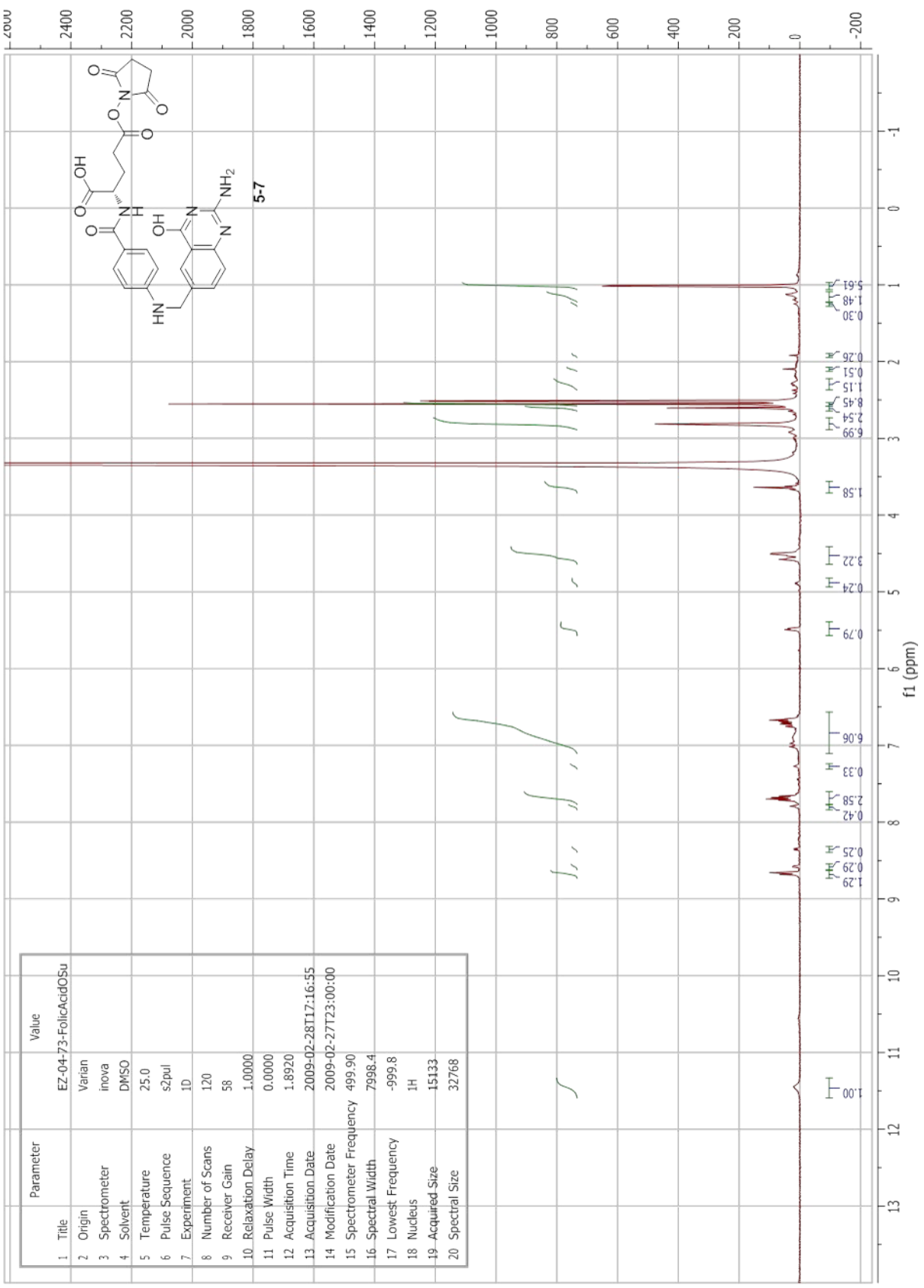

	Parameter	Value
1	Title	EZ-04-73-FolicAcidOSu
2	Origin	Varian
3	Spectrometer	inova
4	Solvent	DMSO
5	Temperature	25.0
6	Pulse Sequence	s2pul
7	Experiment	1D
8	Number of Scans	120
9	Receiver Gain	58
10	Relaxation Delay	1.0000
11	Pulse Width	0.0000
12	Acquisition Time	1.8920
13	Acquisition Date	2009-02-28T17:16:55
14	Modification Date	2009-02-27T23:00:00
15	Spectrometer Frequency	499.90
16	Spectral Width	7998.4
17	Lowest Frequency	-999.8
18	Nucleus	1H
19	Acquired Size	15133
20	Spectral Size	32768

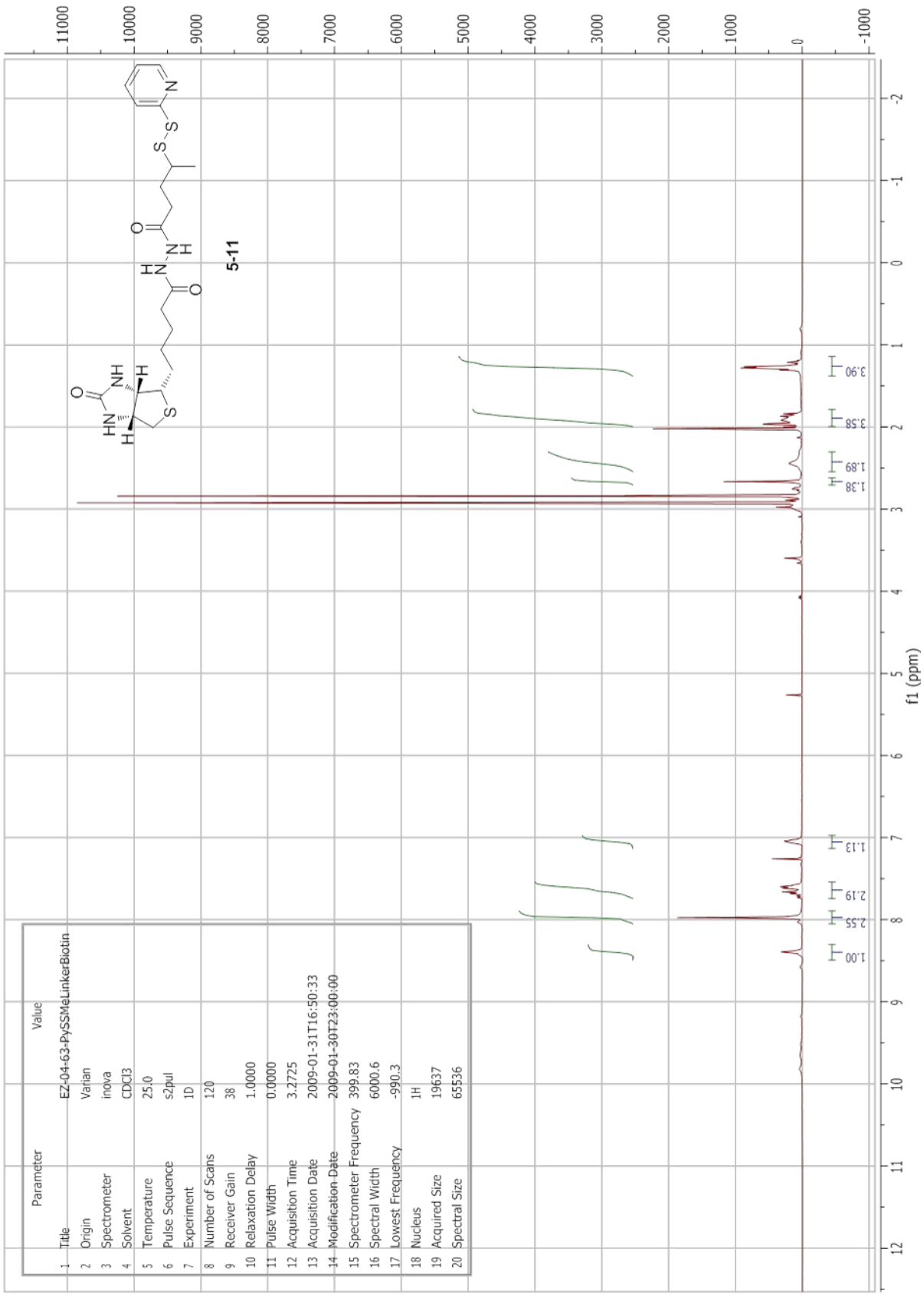

	Parameter	Value
1	Title	EZ-04-63-PySSMeLinkerBiotin
2	Origin	Varian
3	Spectrometer	inova
4	Solvent	CDCl3
5	Temperature	25.0
6	Pulse Sequence	s2pul
7	Experiment	1D
8	Number of Scans	120
9	Receiver Gain	38
10	Relaxation Delay	1.0000
11	Pulse Width	0.0000
12	Acquisition Time	3.2725
13	Acquisition Date	2009-01-31T16:50:33
14	Modification Date	2009-01-30T23:00:00
15	Spectrometer Frequency	399.83
16	Spectral Width	6000.6
17	Lowest Frequency	-990.3
18	Nucleus	1H
19	Acquired Size	19637
20	Spectral Size	65536

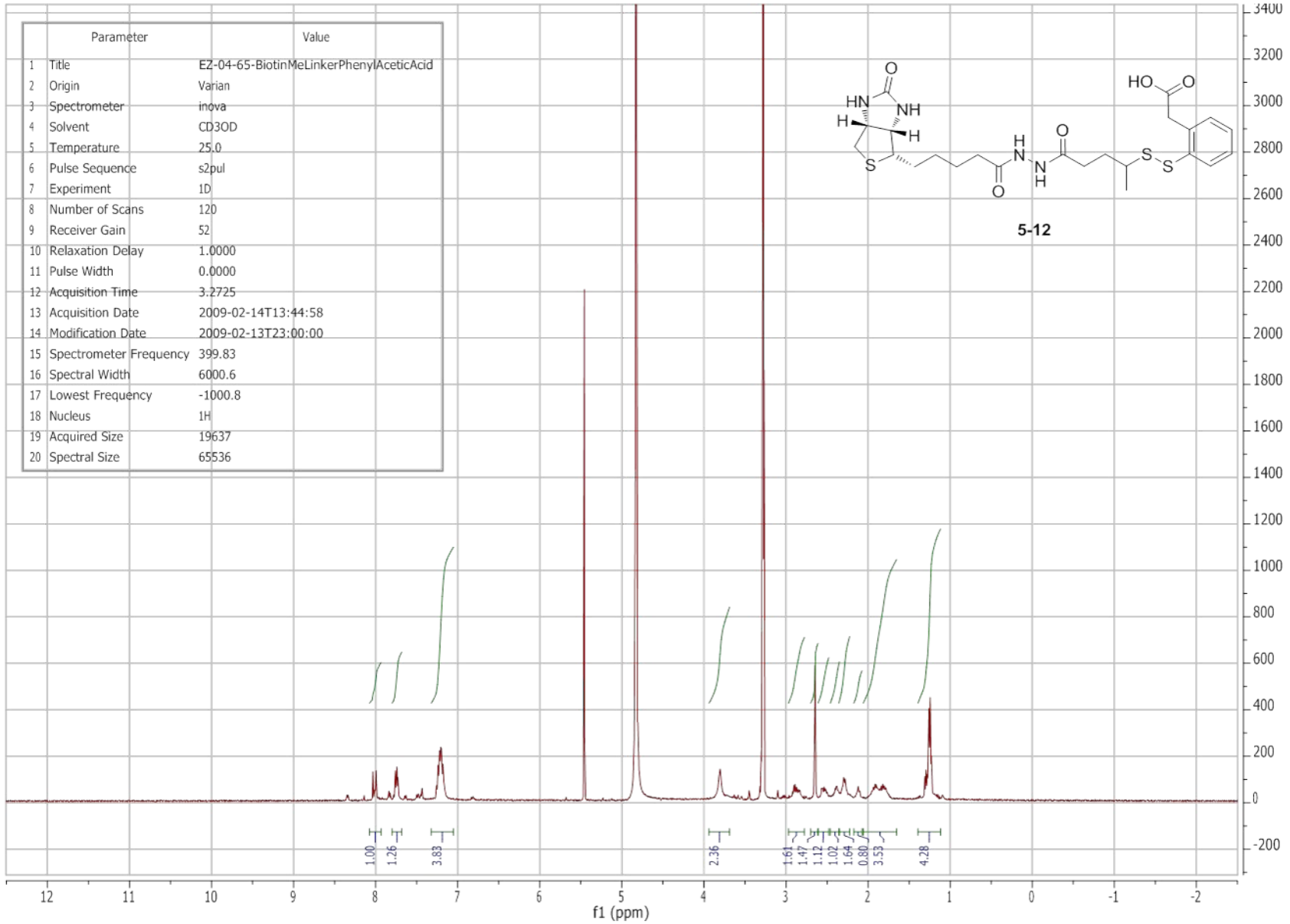
Parameter Value
1 Title EZ-04-65-BiotinMeLinkerPhenylAceticAcid
2 Origin Varian
3 Spectrometer inova
4 Solvent CD3OD
5 Temperature 25.0
6 Pulse Sequence s2pul
7 Experiment 1D
8 Number of Scans 120
9 Receiver Gain 52
10 Relaxation Delay 1.0000
11 Pulse Width 0.0000
12 Acquisition Time 3.2725
13 Acquisition Date 2009-02-14T13:44:58
14 Modification Date 2009-02-13T23:00:00
15 Spectrometer Frequency 399.83
16 Spectral Width 6000.6
17 Lowest Frequency -1000.8
18 Nucleus 1H
19 Acquired Size 19637
20 Spectral Size 65536
5-12
f1 (ppm)

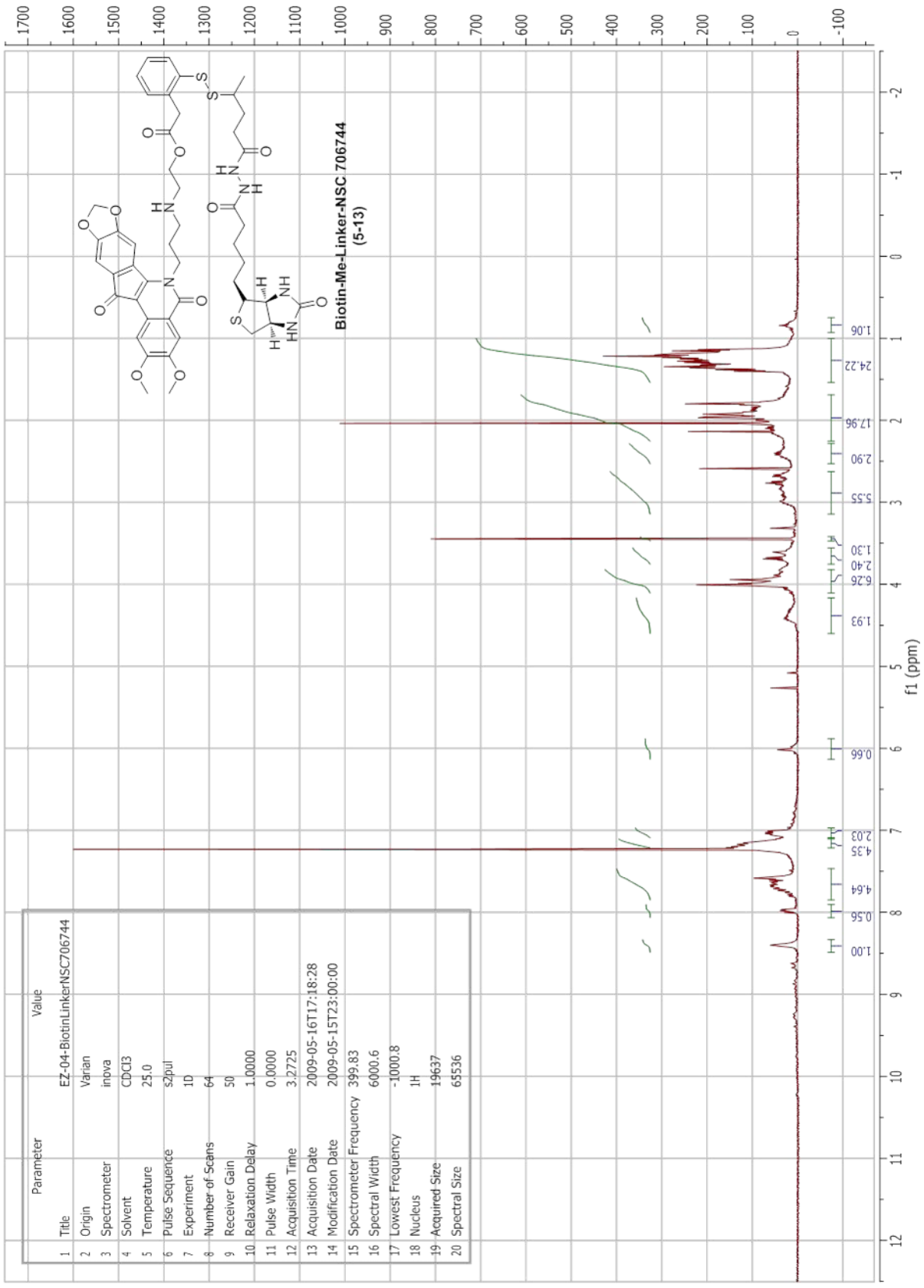

	Parameter	Value
1	Title	EZ-04-BiotinLinkerNSC706744
2	Origin	Varian
3	Spectrometer	inova
4	Solvent	CDCl3
5	Temperature	25.0
6	Pulse Sequence	s2pul
7	Experiment	1D
8	Number of Scans	64
9	Receiver Gain	50
10	Relaxation Delay	1.0000
11	Pulse Width	0.0000
12	Acquisition Time	3.2725
13	Acquisition Date	2009-05-16T17:18:28
14	Modification Date	2009-05-15T23:00:00
15	Spectrometer Frequency	399.83
16	Spectral Width	6000.6
17	Lowest Frequency	-1000.8
18	Nucleus	1H
19	Acquired Size	19637
20	Spectral Size	65536

Appendix 5
Chapter 6 NMR Spectra

	Parameter	Value
1	Title	EZ-02-57-DiCO2MeBocSplitter
2	Origin	Varian
3	Spectrometer	inova
4	Solvent	CDCl3
5	Temperature	25.0
6	Pulse Sequence	s2pul
7	Experiment	1D
8	Number of Scans	16
9	Receiver Gain	46
10	Relaxation Delay	1.0000
11	Pulse Width	0.0000
12	Acquisition Time	3.2725
13	Acquisition Date	2007-11-09T19:06:18
14	Modification Date	2007-11-08T23:00:00
15	Spectrometer Frequency	399.84
16	Spectral Width	6000.6
17	Lowest Frequency	-1000.8
18	Nucleus	1H
19	Acquired Size	19637
20	Spectral Size	65536

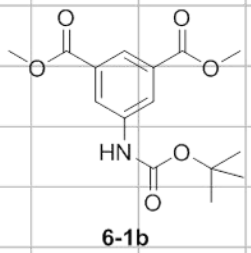

6-1b

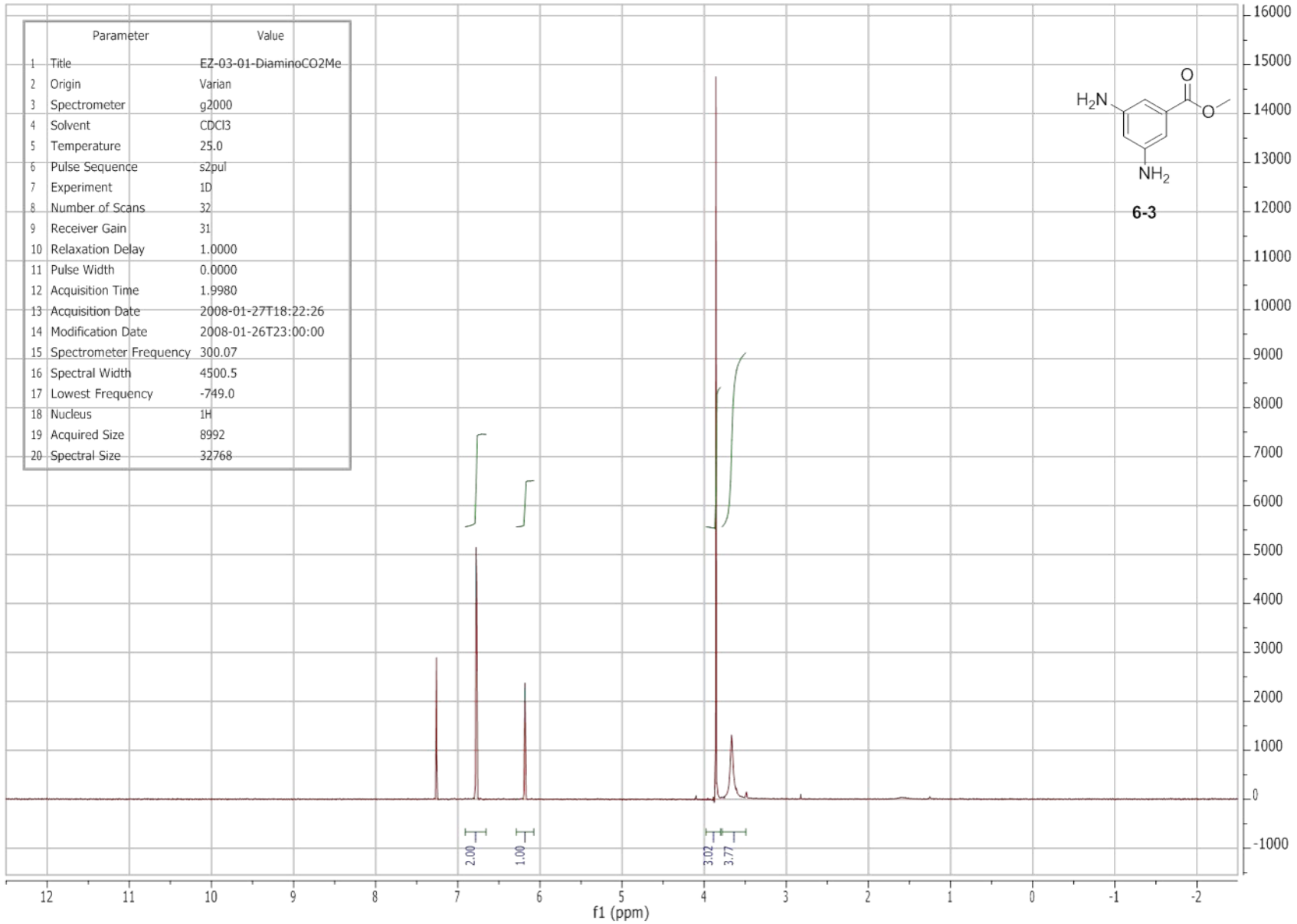
Parameter Value
1 Title EZ-03-01-DiaminoCO2Me
2 Origin Varian
3 Spectrometer g2000
4 Solvent CDCl3
5 Temperature 25.0
6 Pulse Sequence s2pul
7 Experiment 1D
8 Number of Scans 32
9 Receiver Gain 31
10 Relaxation Delay 1.0000
11 Pulse Width 0.0000
12 Acquisition Time 1.9980
13 Acquisition Date 2008-01-27T18:22:26
14 Modification Date 2008-01-26T23:00:00
15 Spectrometer Frequency 300.07
16 Spectral Width 4500.5
17 Lowest Frequency -749.0
18 Nucleus 1H
19 Acquired Size 8992
20 Spectral Size 32768
H2N
O
O
NH2
6-3
2.00
1.00
3.02
3.77
f1 (ppm)

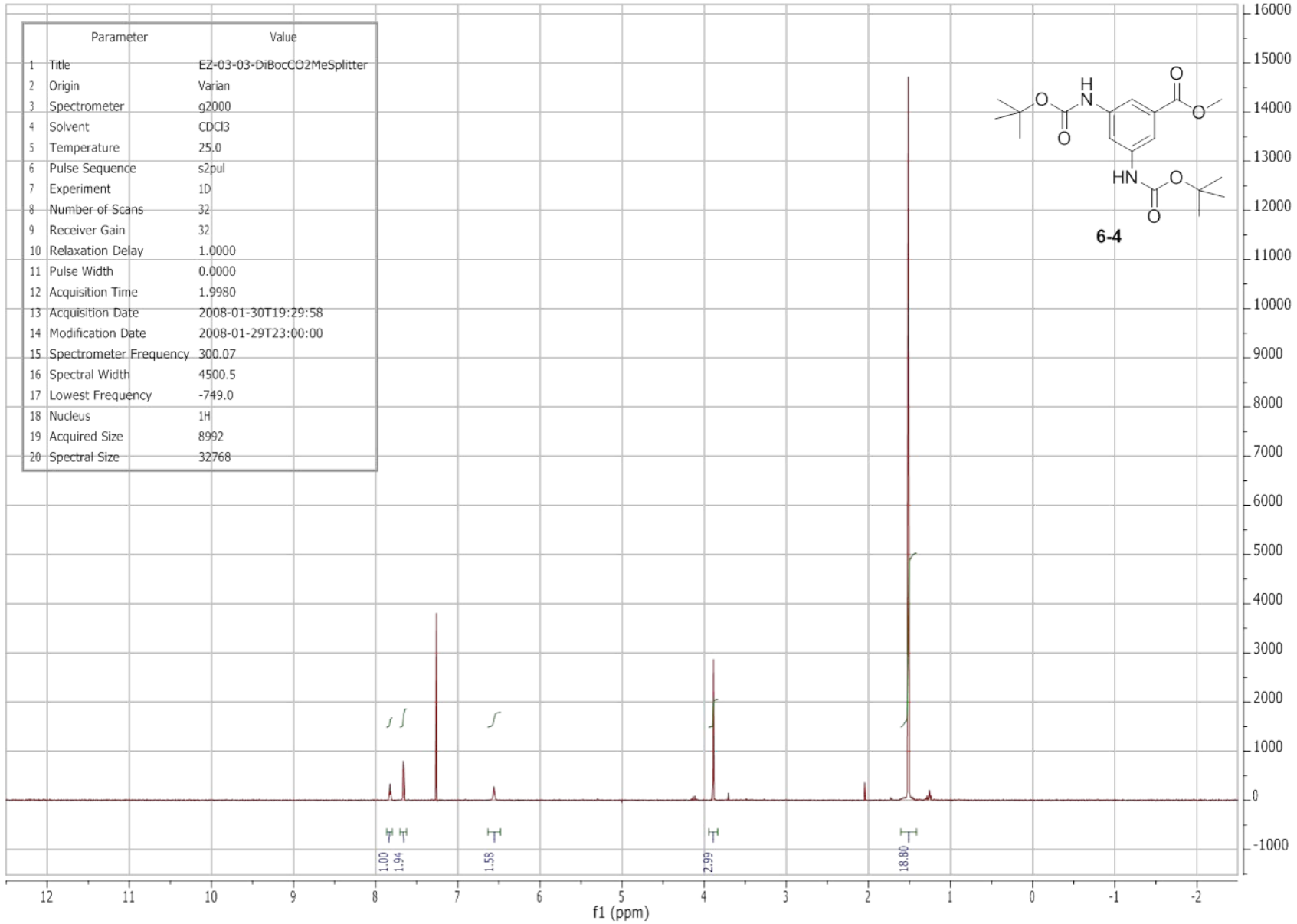
Parameter Value
1 Title EZ-03-03-DiBocCO2MeSplitter
2 Origin Varian
3 Spectrometer g2000
4 Solvent CDCl3
5 Temperature 25.0
6 Pulse Sequence s2pul
7 Experiment 1D
8 Number of Scans 32
9 Receiver Gain 32
10 Relaxation Delay 1.0000
11 Pulse Width 0.0000
12 Acquisition Time 1.9980
13 Acquisition Date 2008-01-30T19:29:58
14 Modification Date 2008-01-29T23:00:00
15 Spectrometer Frequency 300.07
16 Spectral Width 4500.5
17 Lowest Frequency -749.0
18 Nucleus 1H
19 Acquired Size 8992
20 Spectral Size 32768
6-4
1.00
1.94
1.58
2.99
18.80
f1 (ppm)

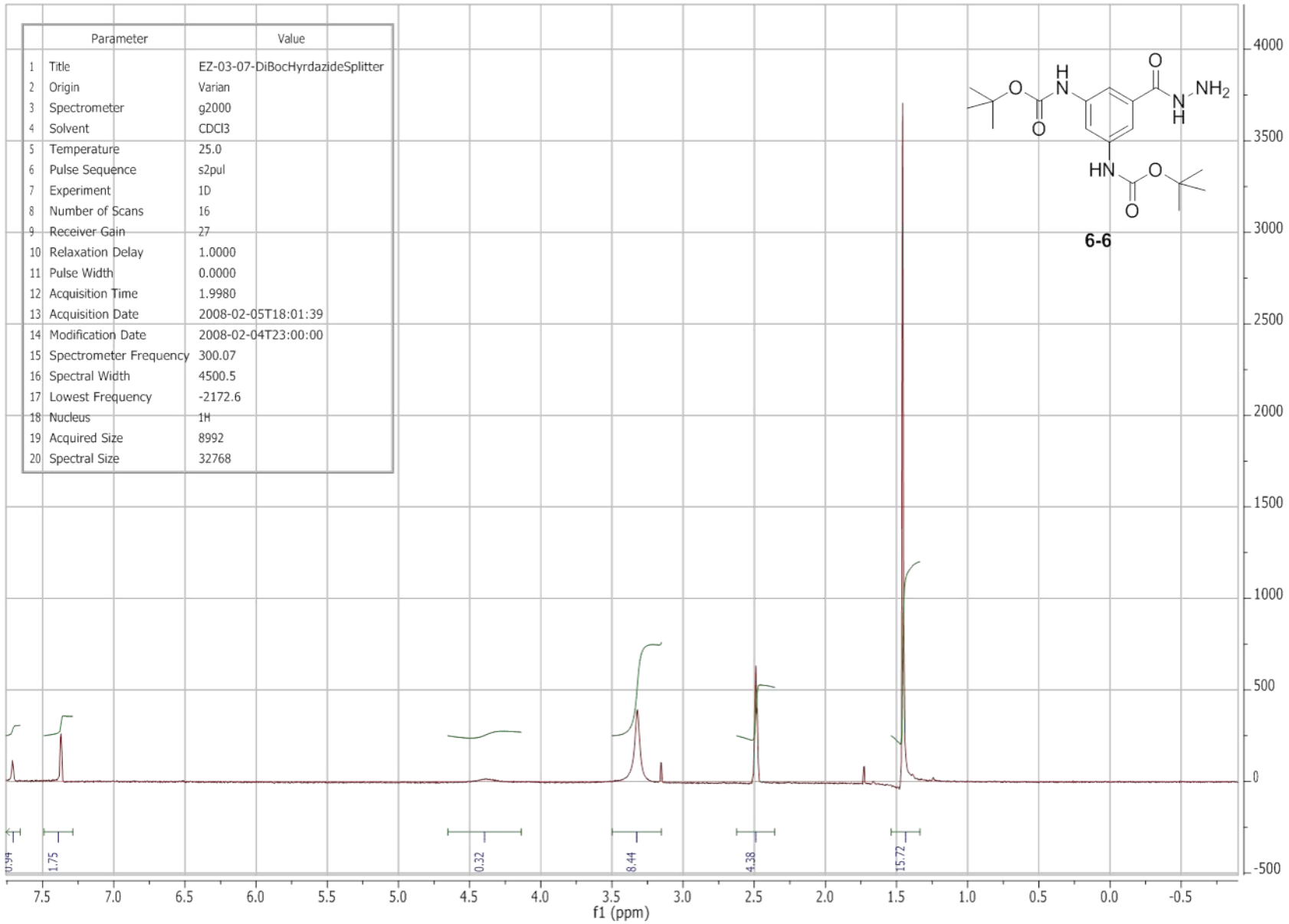
Parameter Value
1 Title EZ-03-07-DiBocHyrdazideSplitter
2 Origin Varian
3 Spectrometer g2000
4 Solvent CDCl3
5 Temperature 25.0
6 Pulse Sequence s2pul
7 Experiment 1D
8 Number of Scans 16
9 Receiver Gain 27
10 Relaxation Delay 1.0000
11 Pulse Width 0.0000
12 Acquisition Time 1.9980
13 Acquisition Date 2008-02-05T18:01:39
14 Modification Date 2008-02-04T23:00:00
15 Spectrometer Frequency 300.07
16 Spectral Width 4500.5
17 Lowest Frequency -2172.6
18 Nucleus 1H
19 Acquired Size 8992
20 Spectral Size 32768
6-6
f1 (ppm)
0.94
1.75
0.32
8.44
4.38
15.72

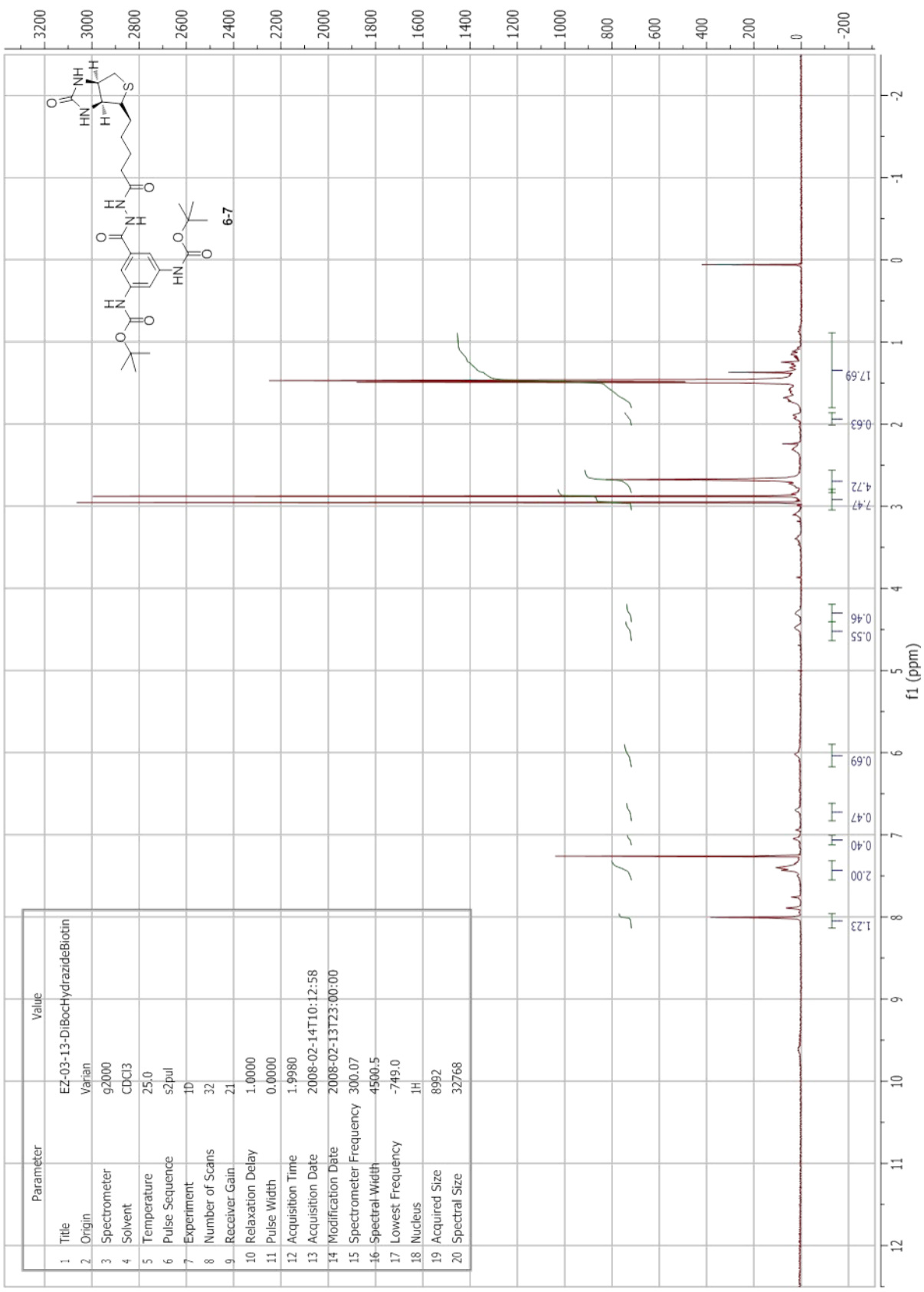

	Parameter	Value
1	Title	EZ-03-13-DiBocHydrazideBiotin
2	Origin	Varian
3	Spectrometer	g2000
4	Solvent	CDCl3
5	Temperature	25.0
6	Pulse Sequence	s2pul
7	Experiment	1D
8	Number of Scans	32
9	Receiver Gain	21
10	Relaxation Delay	1.0000
11	Pulse Width	0.0000
12	Acquisition Time	1.9980
13	Acquisition Date	2008-02-14T10:12:58
14	Modification Date	2008-02-13T23:00:00
15	Spectrometer Frequency	300.07
16	Spectral Width	4500.5
17	Lowest Frequency	-749.0
18	Nucleus	1H
19	Acquired Size	8992
20	Spectral Size	32768

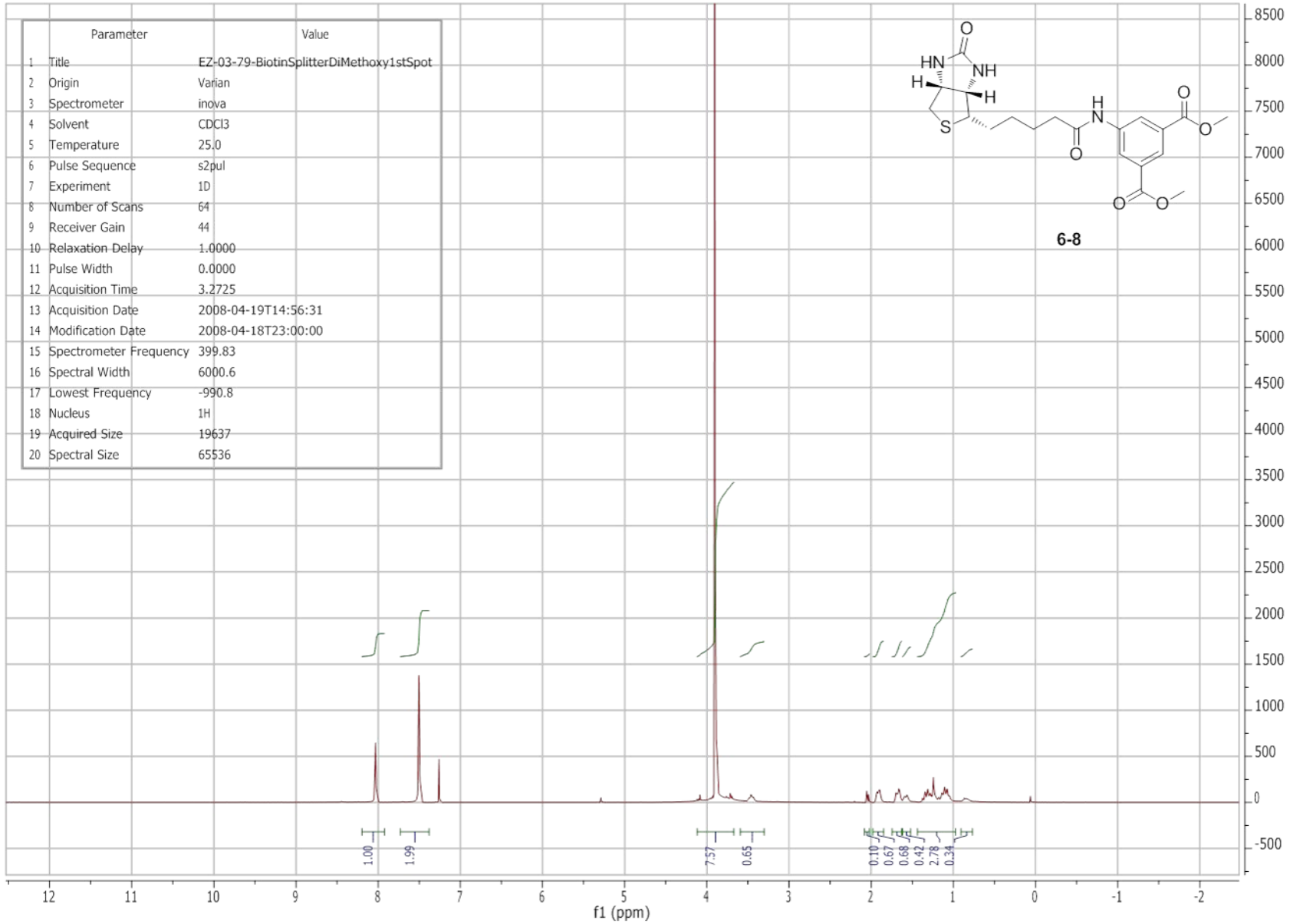
Parameter Value
1 Title EZ-03-79-BiotinSplitterDiMethoxy1stSpot
2 Origin Varian
3 Spectrometer inova
4 Solvent CDCl3
5 Temperature 25.0
6 Pulse Sequence s2pul
7 Experiment 1D
8 Number of Scans 64
9 Receiver Gain 44
10 Relaxation Delay 1.0000
11 Pulse Width 0.0000
12 Acquisition Time 3.2725
13 Acquisition Date 2008-04-19T14:56:31
14 Modification Date 2008-04-18T23:00:00
15 Spectrometer Frequency 399.83
16 Spectral Width 6000.6
17 Lowest Frequency -990.8
18 Nucleus 1H
19 Acquired Size 19637
20 Spectral Size 65536
6-8
f1 (ppm)

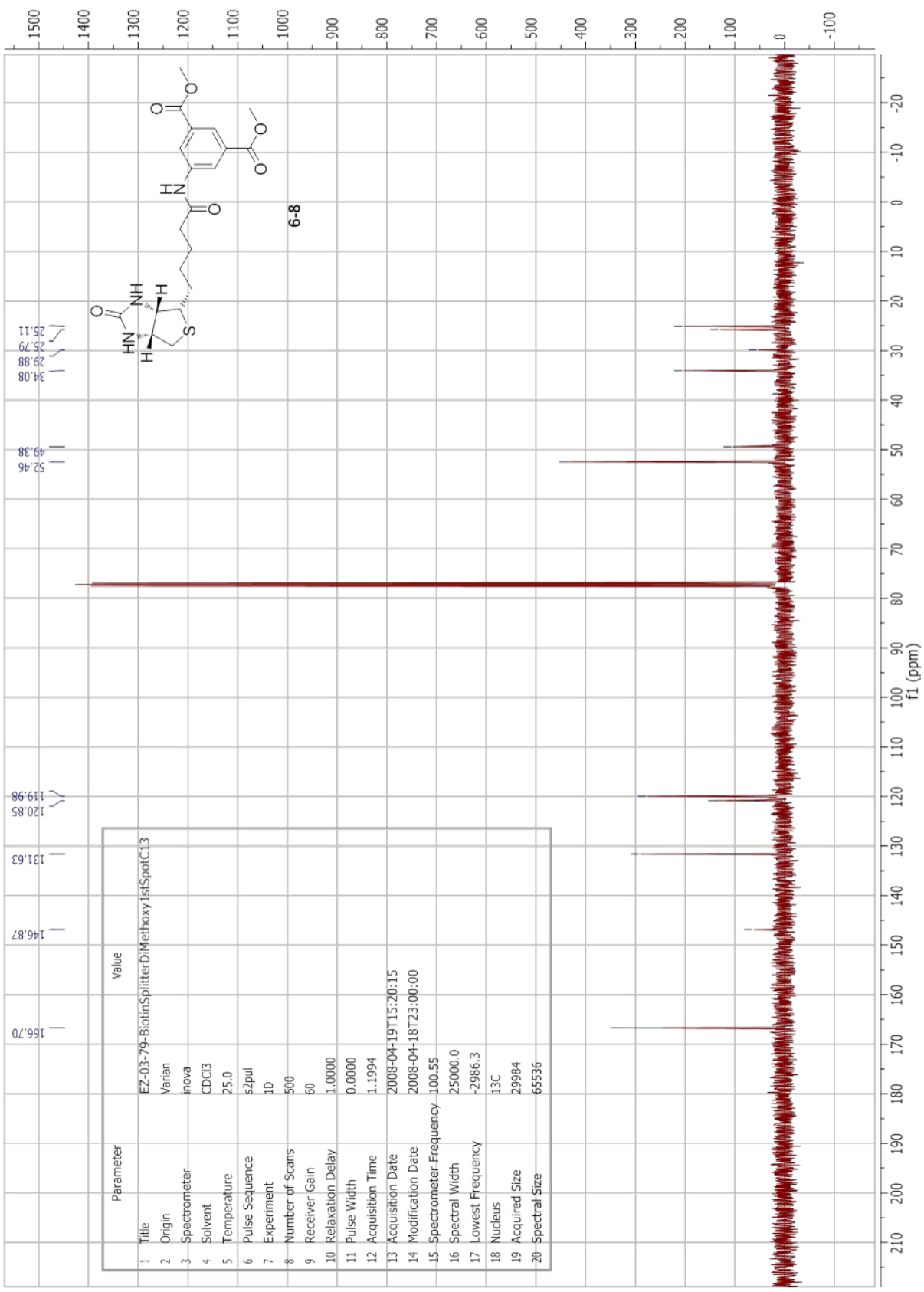
6-8
f1 (ppm)
Parameter Value
1 Title EZ-03-79-BiotinSplitterDiMethoxy1stSpotC13
2 Origin Varian
3 Spectrometer Inova
4 Solvent CDCl3
5 Temperature 25.0
6 Pulse Sequence s2pul
7 Experiment 1D
8 Number of Scans 500
9 Receiver Gain 60
10 Relaxation Delay 1.0000
11 Pulse Width 0.0000
12 Acquisition Time 1.1994
13 Acquisition Date 2008-04-19T15:20:15
14 Modification Date 2008-04-18T23:00:00
15 Spectrometer Frequency 100.55
16 Spectral Width 25000.0
17 Lowest Frequency -2986.3
18 Nucleus 13C
19 Acquired Size 29984
20 Spectral Size 65536
166.70
146.87
131.63
120.85
119.98
52.46
49.38
34.08
29.88
25.79
25.11

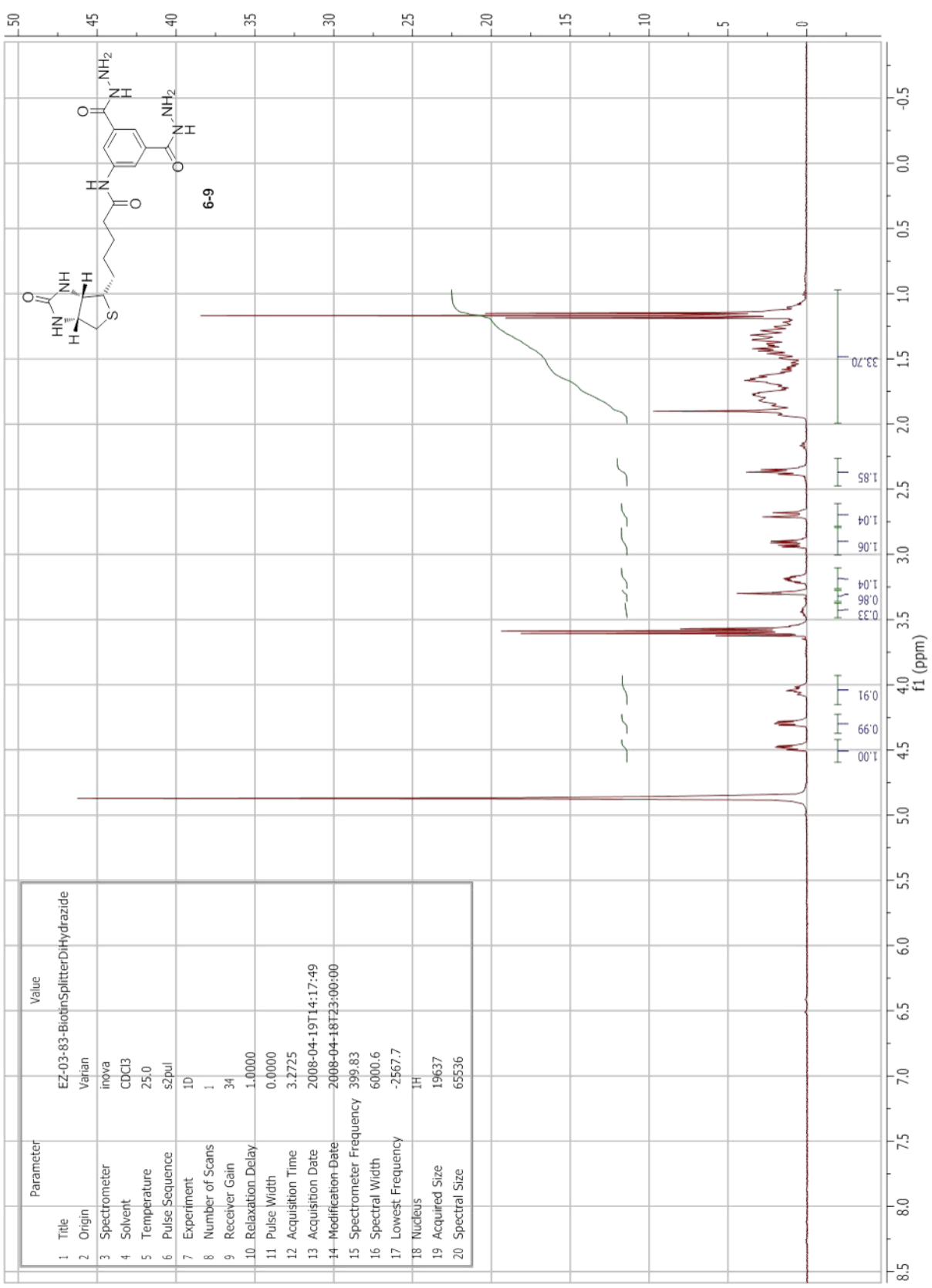
Parameter | Value
1 Title | EZ-03-83-BiotinSplitterDiHydrazide
2 Origin | Varian
3 Spectrometer | inova
4 Solvent | CDCl3
5 Temperature | 25.0
6 Pulse Sequence | s2pul
7 Experiment | 1D
8 Number of Scans | 1
9 Receiver Gain | 34
10 Relaxation Delay | 1.0000
11 Pulse Width | 0.0000
12 Acquisition Time | 3.2725
13 Acquisition Date | 2008-04-19T14:17:49
14 Modification Date | 2008-04-18T23:00:00
15 Spectrometer Frequency | 399.83
16 Spectral Width | 6000.6
17 Lowest Frequency | -2567.7
18 Nucleus | 1H
19 Acquired Size | 19637
20 Spectral Size | 65536
6-9
1.00
0.99
0.91
0.33
0.86
1.04
1.06
1.04
1.85
33.70
f1 (ppm)

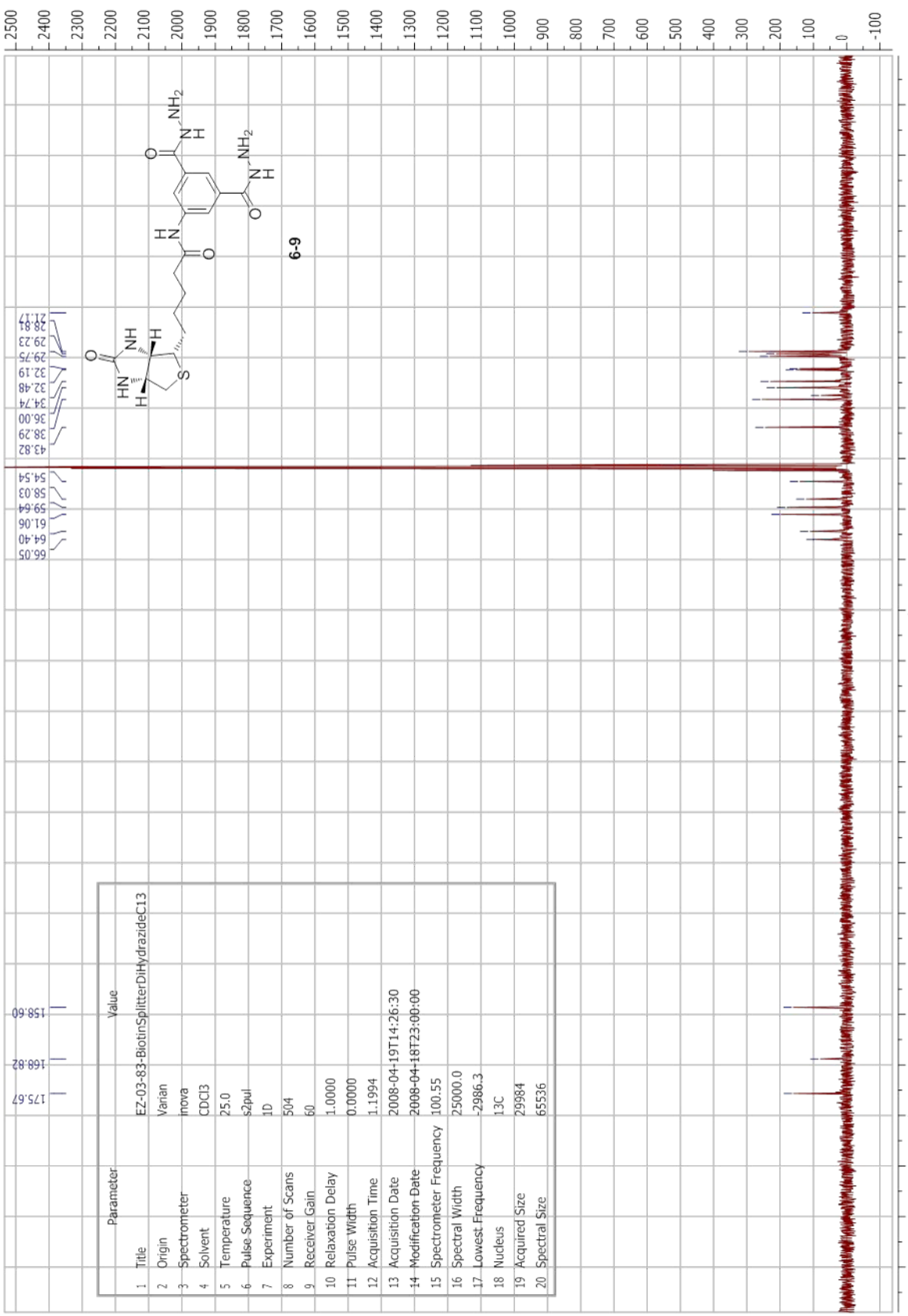
6-9
f1 (ppm)
Parameter
Value
1 Title EZ-03-83-BiotinSplitterDiHydrazideC13
2 Origin Varian
3 Spectrometer inova
4 Solvent CDCl3
5 Temperature 25.0
6 Pulse Sequence s2pul
7 Experiment 1D
8 Number of Scans 504
9 Receiver Gain 60
10 Relaxation Delay 1.0000
11 Pulse Width 0.0000
12 Acquisition Time 1.1994
13 Acquisition Date 2008-04-19T14:26:30
14 Modification Date 2008-04-18T23:00:00
15 Spectrometer Frequency 100.55
16 Spectral Width 25000.0
17 Lowest Frequency -2986.3
18 Nucleus 13C
19 Acquired Size 29984
20 Spectral Size 65536

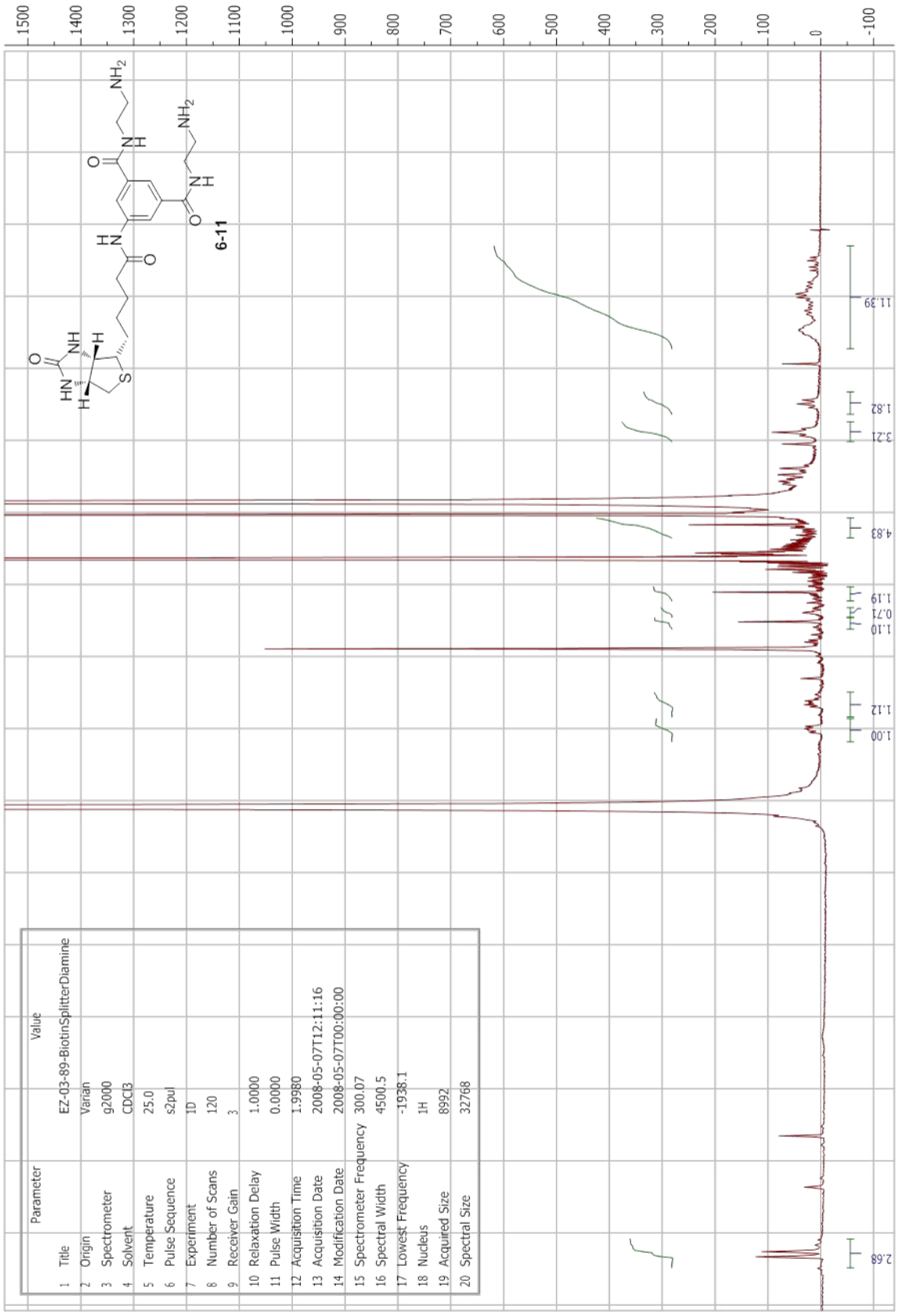
Parameter | Value
1 Title | EZ-03-89-BiotinSplitterDiamine
2 Origin | Varian
3 Spectrometer | g2000
4 Solvent | CDCl3
5 Temperature | 25.0
6 Pulse Sequence | s2pul
7 Experiment | 1D
8 Number of Scans | 120
9 Receiver Gain | 3
10 Relaxation Delay | 1.0000
11 Pulse Width | 0.0000
12 Acquisition Time | 1.9980
13 Acquisition Date | 2008-05-07T12:11:16
14 Modification Date | 2008-05-07T00:00:00
15 Spectrometer Frequency | 300.07
16 Spectral Width | 4500.5
17 Lowest Frequency | -1938.1
18 Nucleus | 1H
19 Acquired Size | 8992
20 Spectral Size | 32768
6-11
f1 (ppm)
2.68
1.00
1.12
1.10
0.71
1.19
4.83
1.82
3.21
11.39

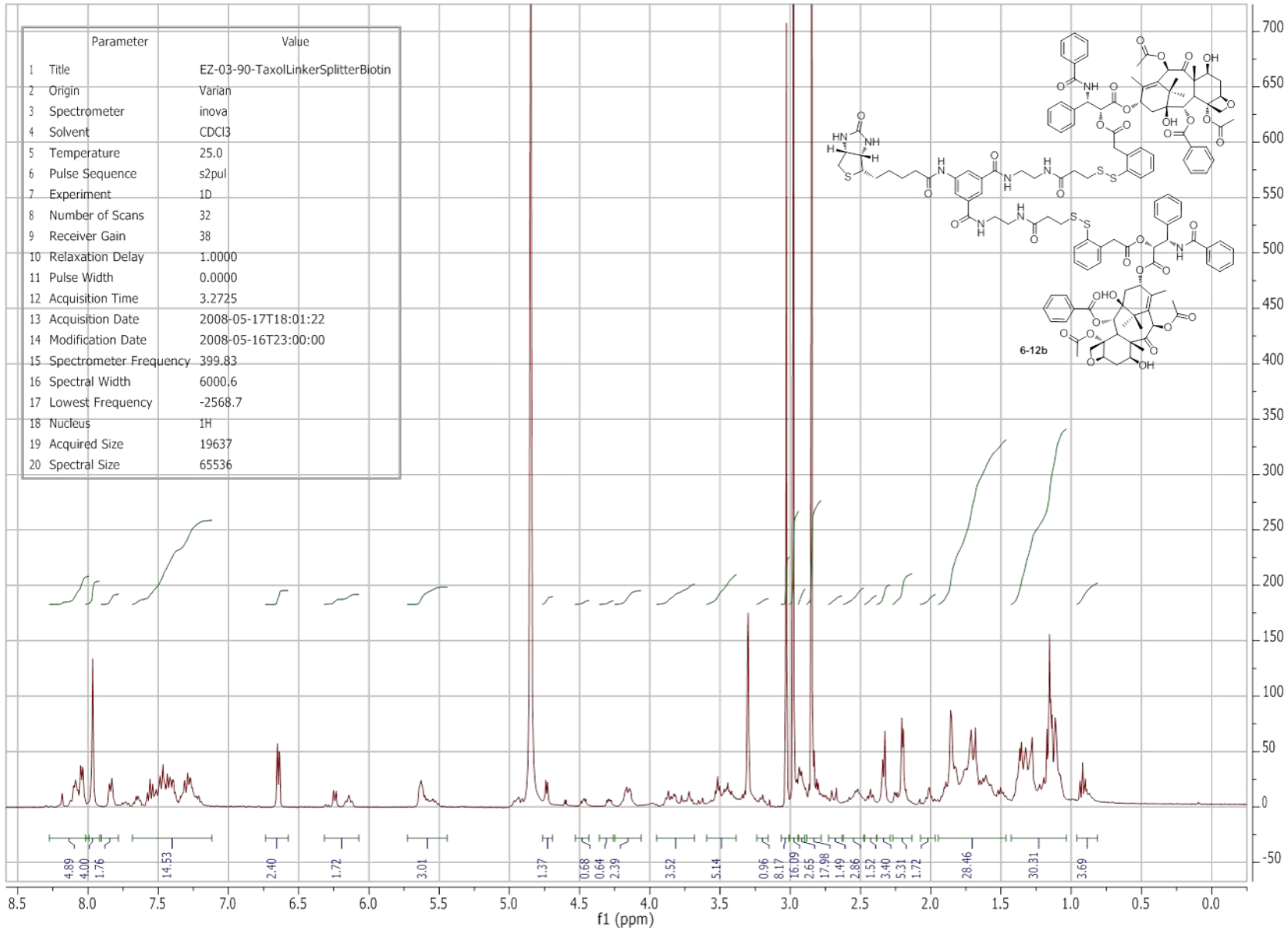
Parameter Value
1 Title EZ-03-90-TaxolLinkerSplitterBiotin
2 Origin Varian
3 Spectrometer inova
4 Solvent CDCl3
5 Temperature 25.0
6 Pulse Sequence s2pul
7 Experiment 1D
8 Number of Scans 32
9 Receiver Gain 38
10 Relaxation Delay 1.0000
11 Pulse Width 0.0000
12 Acquisition Time 3.2725
13 Acquisition Date 2008-05-17T18:01:22
14 Modification Date 2008-05-16T23:00:00
15 Spectrometer Frequency 399.83
16 Spectral Width 6000.6
17 Lowest Frequency -2568.7
18 Nucleus 1H
19 Acquired Size 19637
20 Spectral Size 65536
6-12b
f1 (ppm)

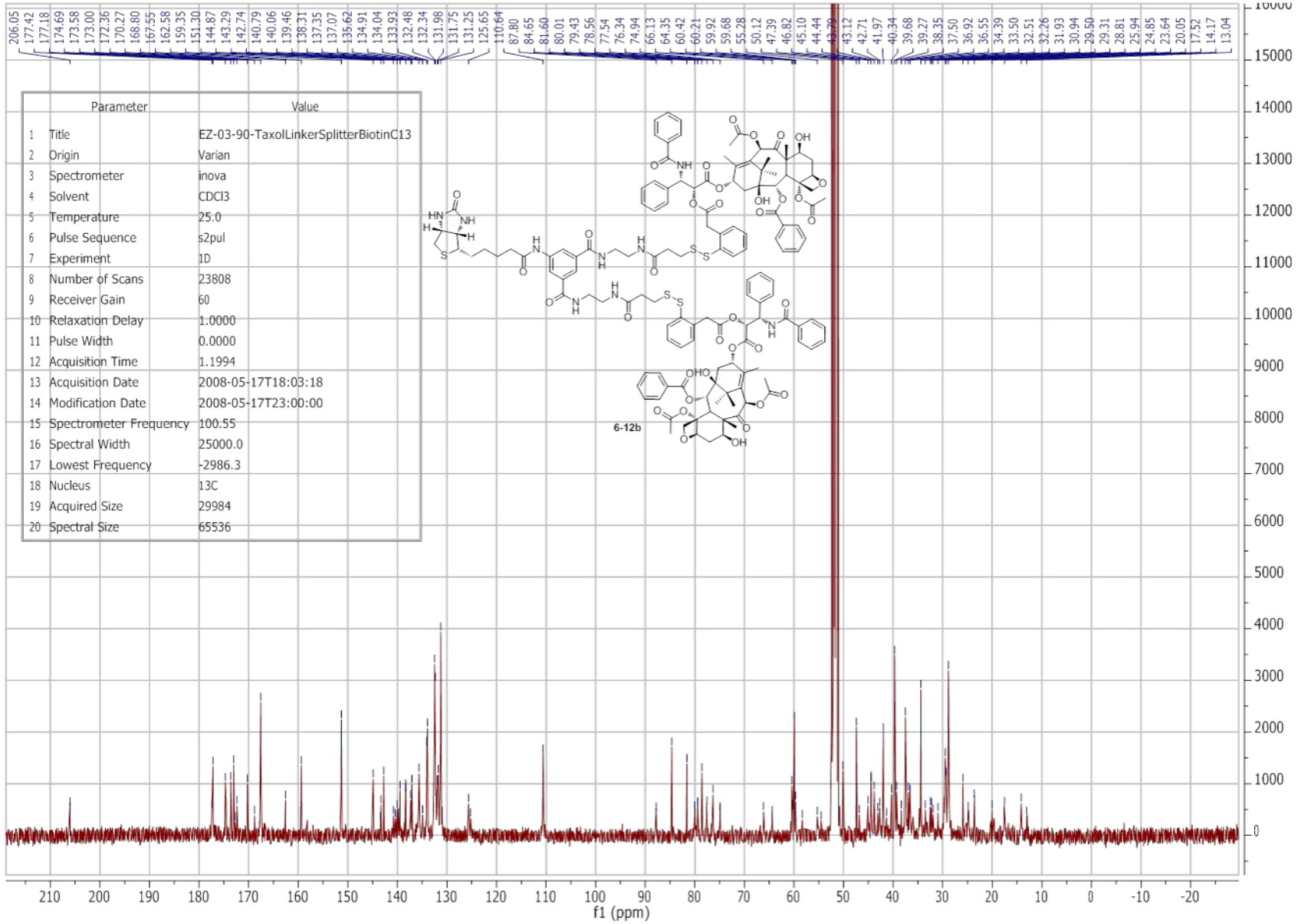
206.05 177.42 177.18 174.69 173.58 173.00 172.36 170.27 168.80 167.55 162.58 159.35 151.30 144.87 143.29 142.74 140.79 140.06 139.46 138.31 137.35 137.07 135.62 134.91 134.04 133.93 132.48 132.34 131.98 131.75 131.25 125.65 110.64 87.80 84.65 81.60 80.01 79.43 78.56 77.54 76.34 74.94 66.13 64.35 60.42 60.21 59.92 59.68 55.28 50.12 47.39 46.82 45.10 44.44 43.79 43.12 42.71 41.97 40.34 39.68 39.27 38.35 37.50 36.92 36.55 34.39 33.50 32.51 32.26 31.93 30.94 29.50 29.31 28.81 25.94 24.85 23.64 20.05 17.52 14.17 13.04
Parameter Value
1 Title EZ-03-90-TaxolLinkerSplitterBiotinC13
2 Origin Varian
3 Spectrometer inova
4 Solvent CDCl3
5 Temperature 25.0
6 Pulse Sequence s2pul
7 Experiment 1D
8 Number of Scans 23808
9 Receiver Gain 60
10 Relaxation Delay 1.0000
11 Pulse Width 0.0000
12 Acquisition Time 1.1994
13 Acquisition Date 2008-05-17T18:03:18
14 Modification Date 2008-05-17T23:00:00
15 Spectrometer Frequency 100.55
16 Spectral Width 25000.0
17 Lowest Frequency -2986.3
18 Nucleus 13C
19 Acquired Size 29984
20 Spectral Size 65536
6-12b
f1 (ppm)

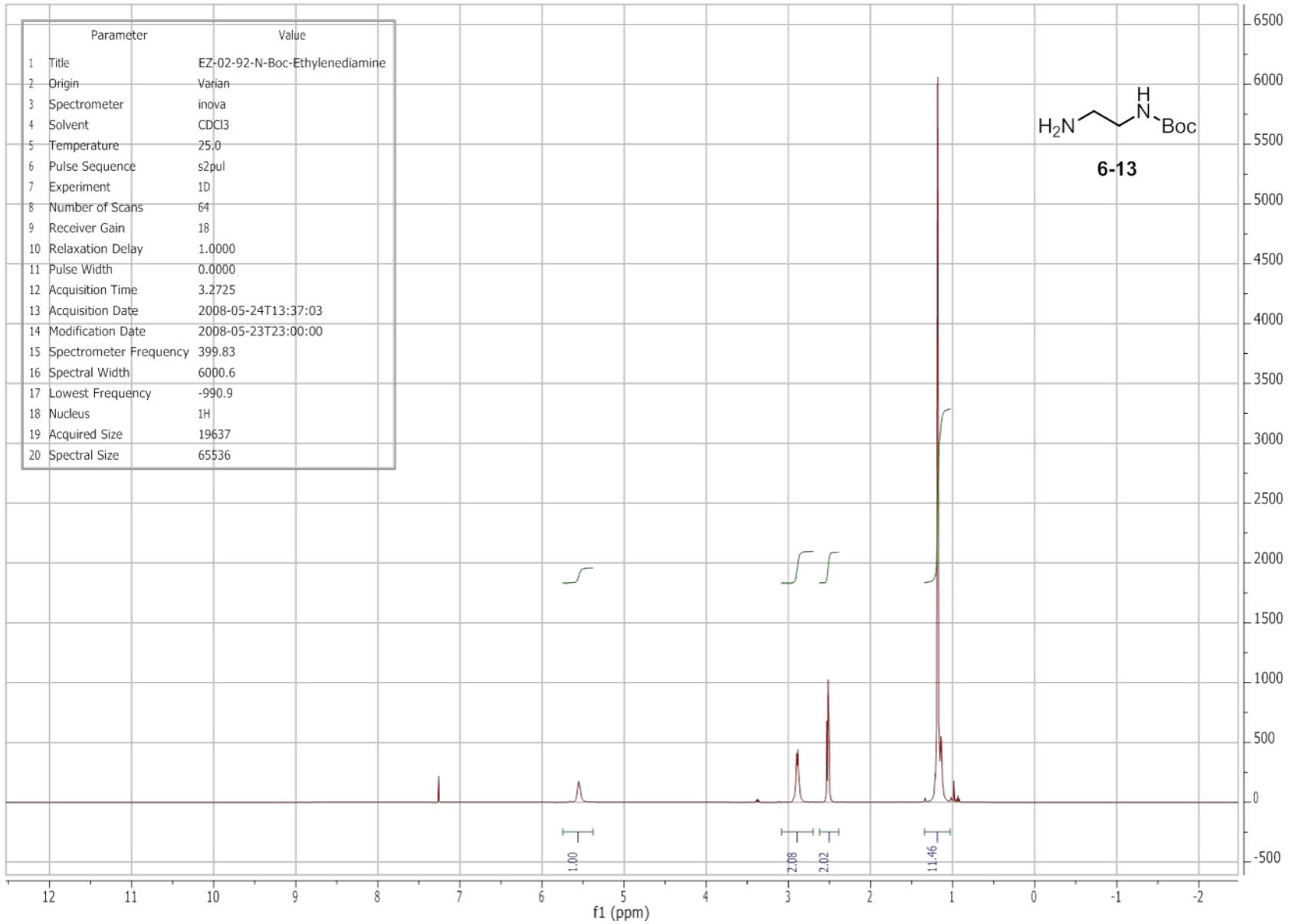
Parameter Value
1 Title EZ-02-92-N-Boc-Ethylenediamine
2 Origin Varian
3 Spectrometer inova
4 Solvent CDCl3
5 Temperature 25.0
6 Pulse Sequence s2pul
7 Experiment 1D
8 Number of Scans 64
9 Receiver Gain 18
10 Relaxation Delay 1.0000
11 Pulse Width 0.0000
12 Acquisition Time 3.2725
13 Acquisition Date 2008-05-24T13:37:03
14 Modification Date 2008-05-23T23:00:00
15 Spectrometer Frequency 399.83
16 Spectral Width 6000.6
17 Lowest Frequency -990.9
18 Nucleus 1H
19 Acquired Size 19637
20 Spectral Size 65536
H2N
N
H
Boc
6-13
1.00
2.08
2.02
11.46
f1 (ppm)

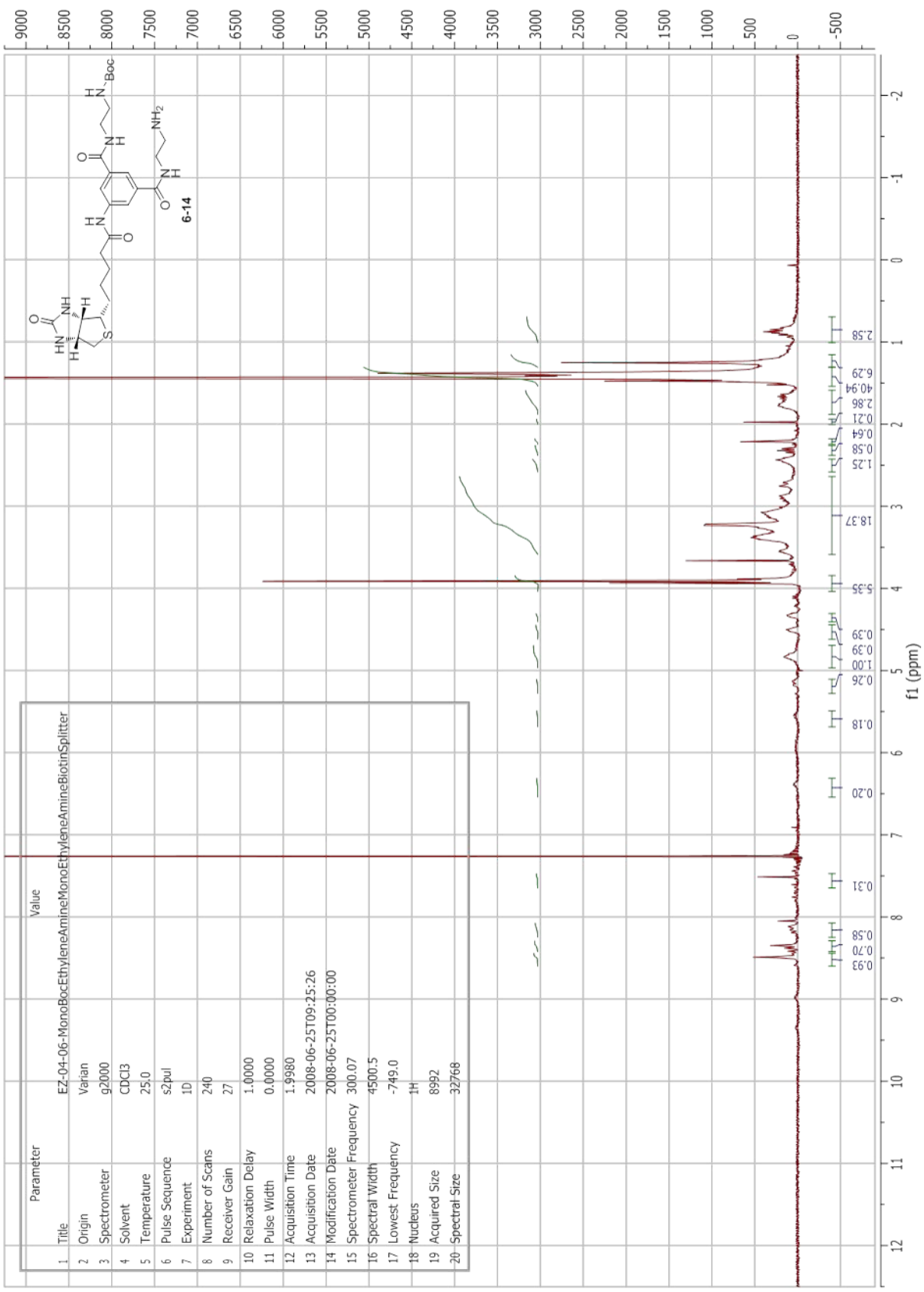

	Parameter	Value
1	Title	EZ-04-06-MonoBocEthyleneAmineMonoEthyleneAmineBiotinSplitter
2	Origin	Varian
3	Spectrometer	g2000
4	Solvent	CDCl3
5	Temperature	25.0
6	Pulse Sequence	s2pul
7	Experiment	1D
8	Number of Scans	240
9	Receiver Gain	27
10	Relaxation Delay	1.0000
11	Pulse Width	0.0000
12	Acquisition Time	1.9980
13	Acquisition Date	2008-06-25T09:25:26
14	Modification Date	2008-06-25T00:00:00
15	Spectrometer Frequency	300.07
16	Spectral Width	4500.5
17	Lowest Frequency	-749.0
18	Nucleus	1H
19	Acquired Size	8992
20	Spectral Size	32768

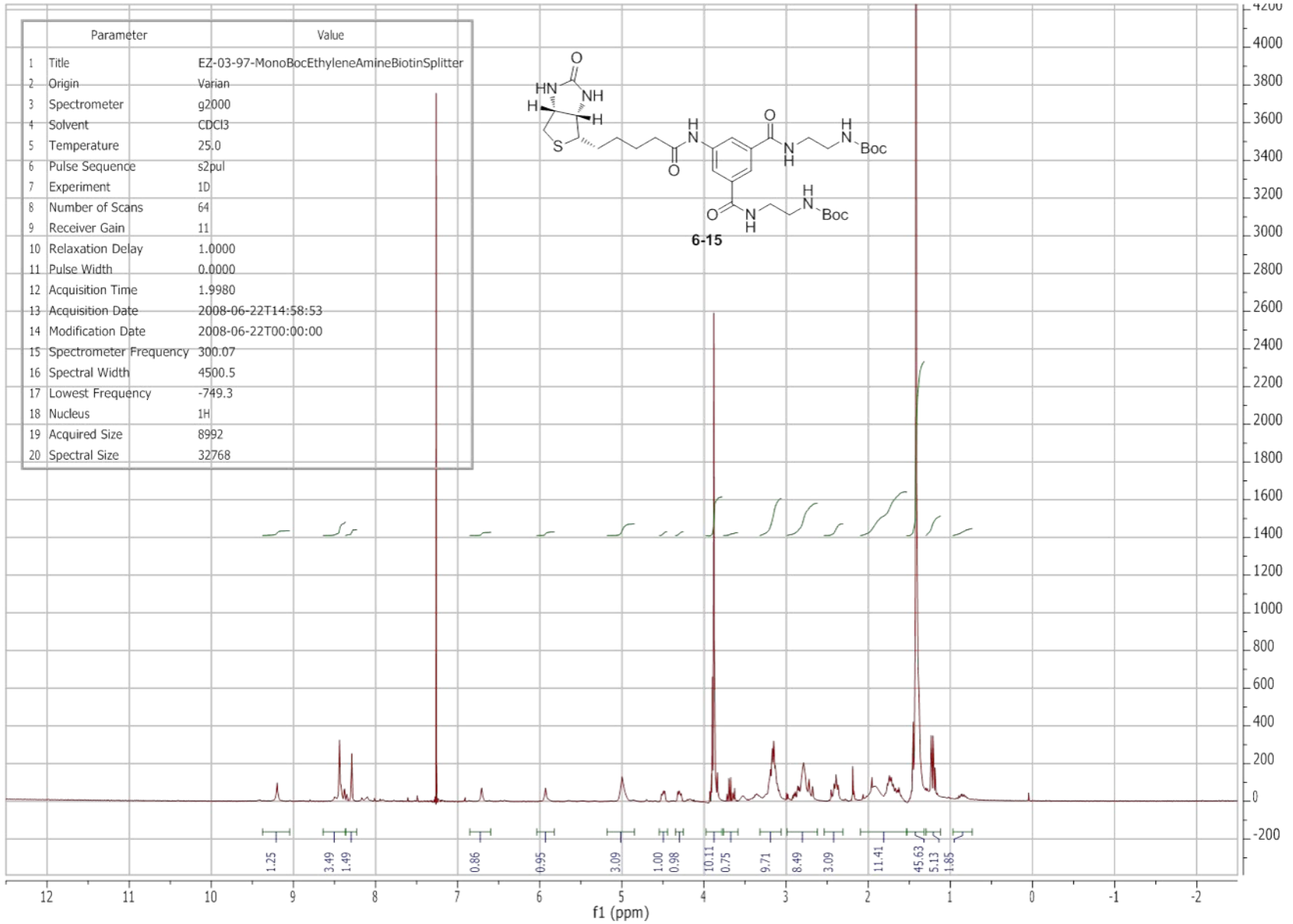
Parameter Value
1 Title EZ-03-97-MonoBocEthyleneAmineBiotinSplitter
2 Origin Varian
3 Spectrometer g2000
4 Solvent CDCl3
5 Temperature 25.0
6 Pulse Sequence s2pul
7 Experiment 1D
8 Number of Scans 64
9 Receiver Gain 11
10 Relaxation Delay 1.0000
11 Pulse Width 0.0000
12 Acquisition Time 1.9980
13 Acquisition Date 2008-06-22T14:58:53
14 Modification Date 2008-06-22T00:00:00
15 Spectrometer Frequency 300.07
16 Spectral Width 4500.5
17 Lowest Frequency -749.3
18 Nucleus 1H
19 Acquired Size 8992
20 Spectral Size 32768
6-15
Boc
Boc
1.25
3.49
1.49
0.86
0.95
3.09
1.00
0.98
10.11
0.75
9.71
8.49
3.09
11.41
45.63
5.13
1.85
f1 (ppm)

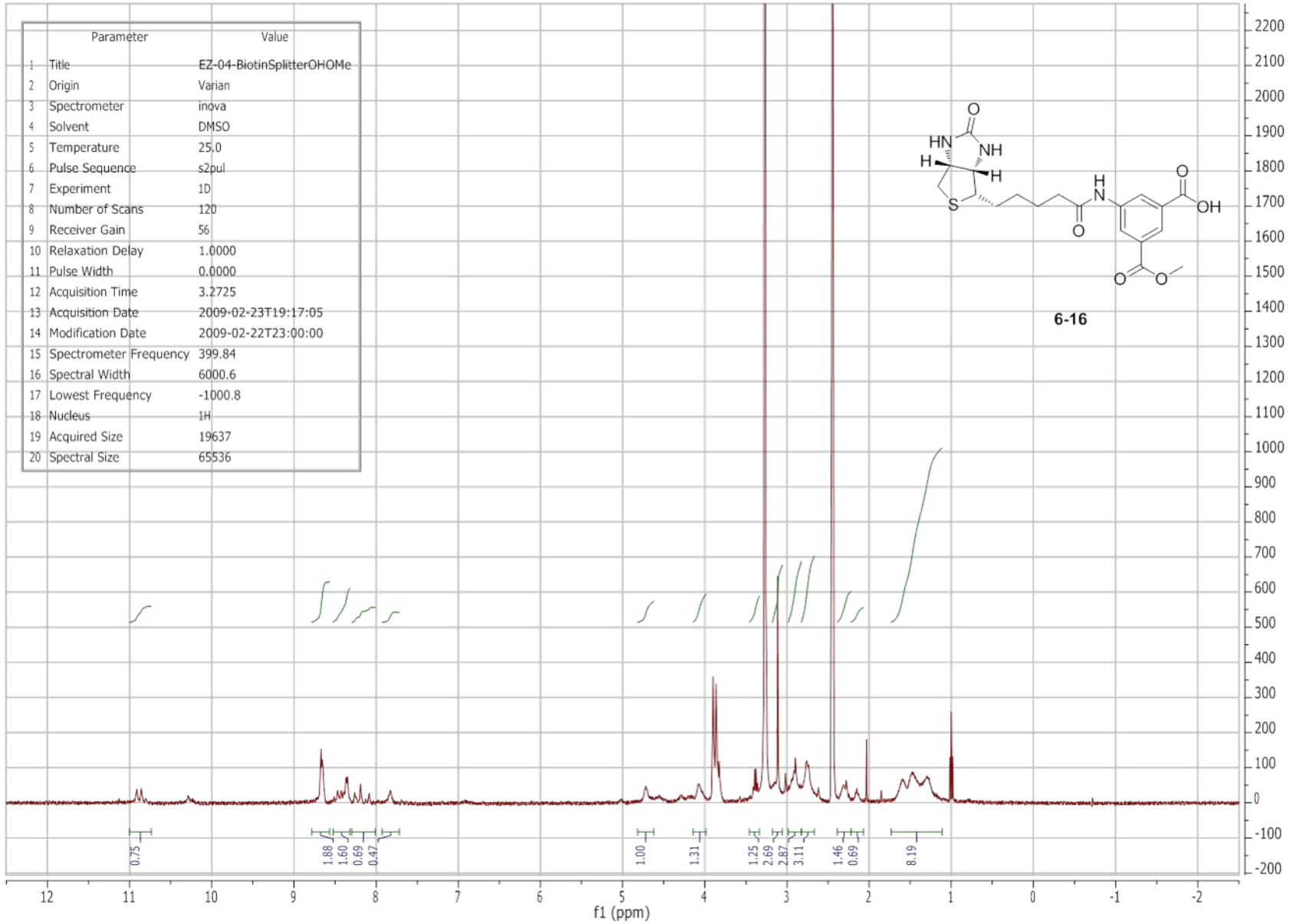
Parameter Value
1 Title EZ-04-BiotinSplitterOHOMe
2 Origin Varian
3 Spectrometer inova
4 Solvent DMSO
5 Temperature 25.0
6 Pulse Sequence s2pul
7 Experiment 1D
8 Number of Scans 120
9 Receiver Gain 56
10 Relaxation Delay 1.0000
11 Pulse Width 0.0000
12 Acquisition Time 3.2725
13 Acquisition Date 2009-02-23T19:17:05
14 Modification Date 2009-02-22T23:00:00
15 Spectrometer Frequency 399.84
16 Spectral Width 6000.6
17 Lowest Frequency -1000.8
18 Nucleus 1H
19 Acquired Size 19637
20 Spectral Size 65536
6-16
0.75
1.88
1.60
0.69
0.47
1.00
1.31
1.25
2.69
2.87
3.11
1.46
0.69
8.19
f1 (ppm)

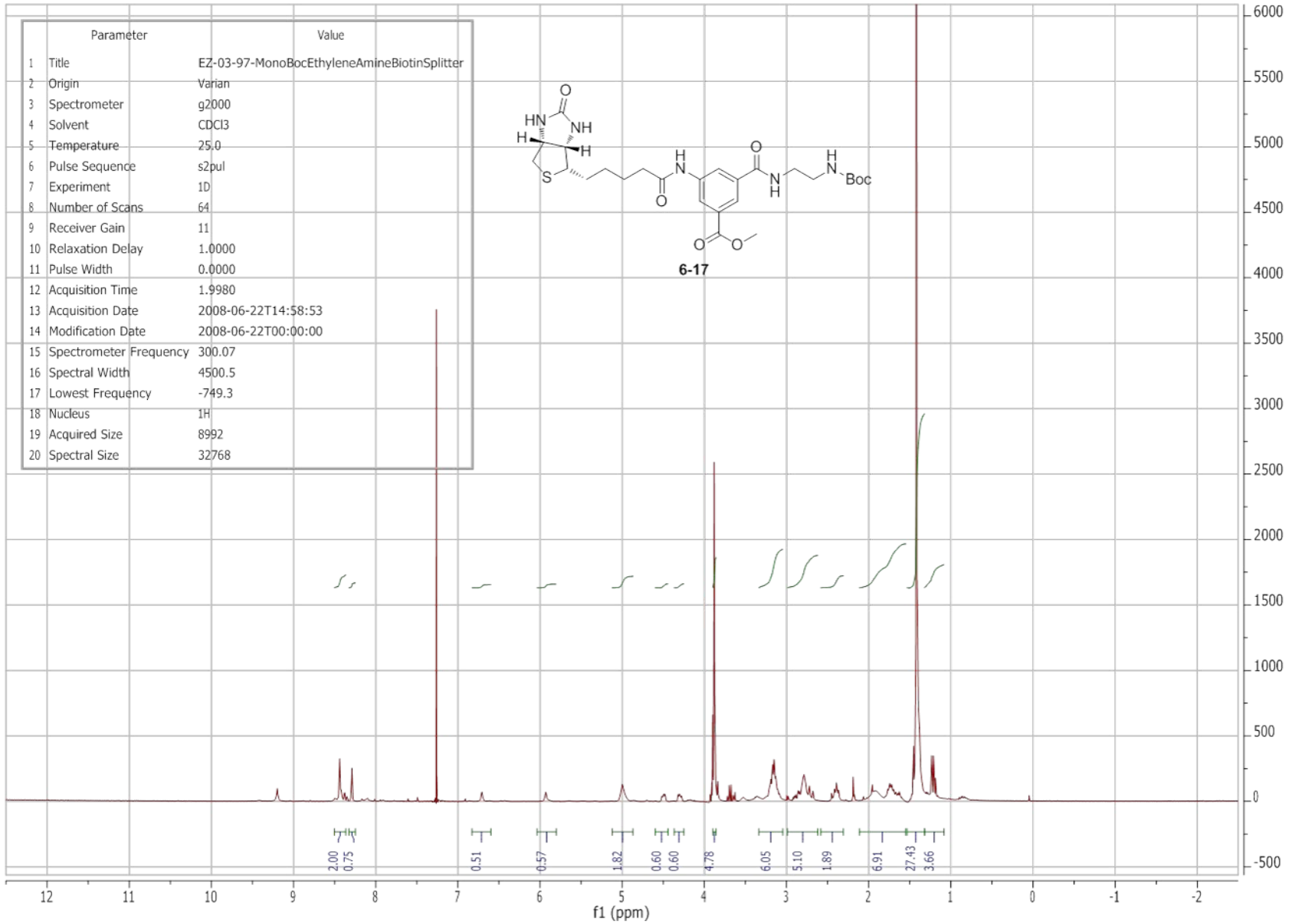
Parameter Value
1 Title EZ-03-97-MonoBocEthyleneAmineBiotinSplitter
2 Origin Varian
3 Spectrometer g2000
4 Solvent CDCl3
5 Temperature 25.0
6 Pulse Sequence s2pul
7 Experiment 1D
8 Number of Scans 64
9 Receiver Gain 11
10 Relaxation Delay 1.0000
11 Pulse Width 0.0000
12 Acquisition Time 1.9980
13 Acquisition Date 2008-06-22T14:58:53
14 Modification Date 2008-06-22T00:00:00
15 Spectrometer Frequency 300.07
16 Spectral Width 4500.5
17 Lowest Frequency -749.3
18 Nucleus 1H
19 Acquired Size 8992
20 Spectral Size 32768
6-17
2.00 0.75 0.51 0.57 1.82 0.60 0.60 4.78 6.05 5.10 1.89 6.91 27.43 3.66
f1 (ppm)

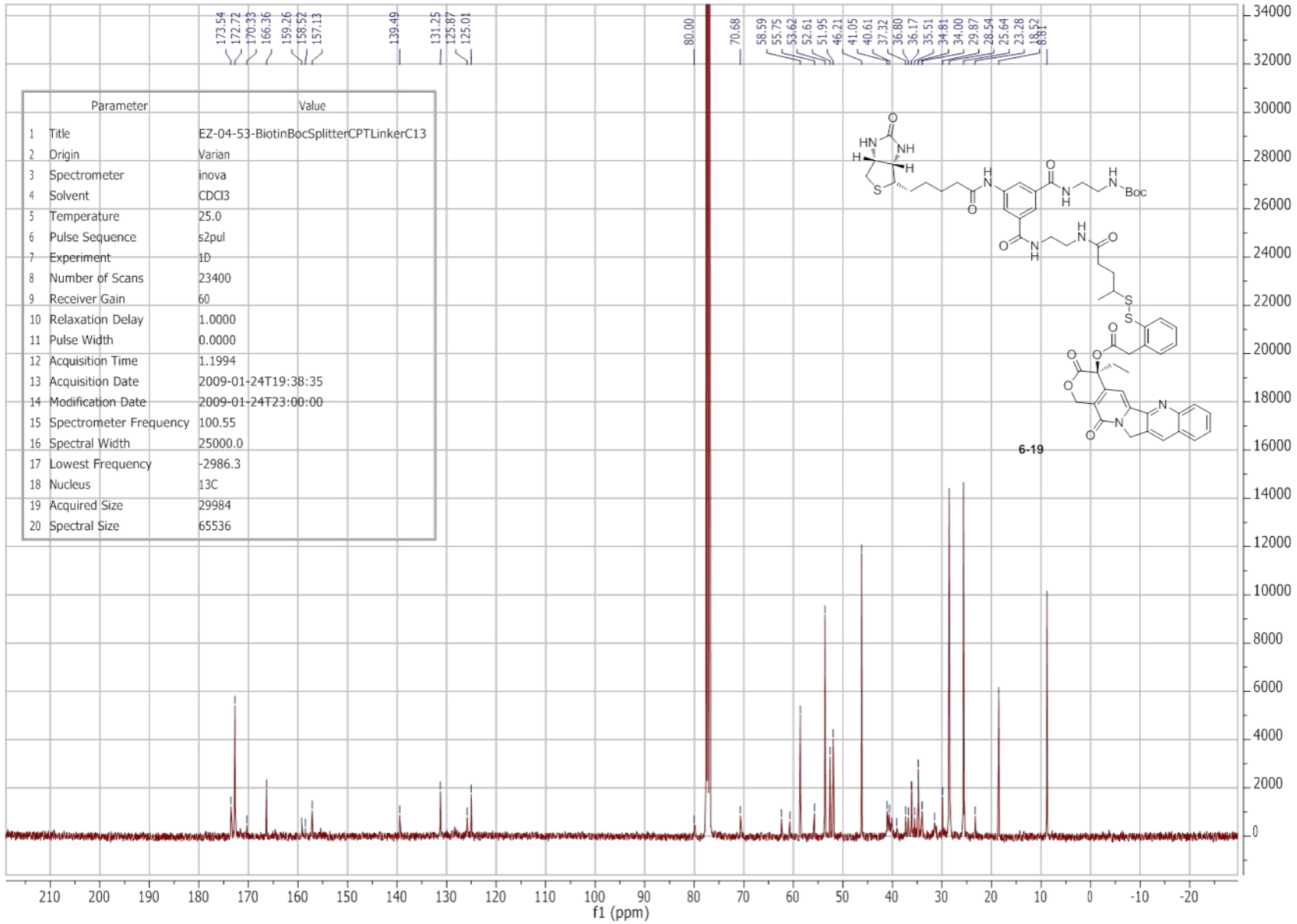

	Parameter	Value
1	Title	EZ-04-53-BiotinBocSplitterCPTLinkerC13
2	Origin	Varian
3	Spectrometer	inova
4	Solvent	CDCl3
5	Temperature	25.0
6	Pulse Sequence	s2pul
7	Experiment	1D
8	Number of Scans	23400
9	Receiver Gain	60
10	Relaxation Delay	1.0000
11	Pulse Width	0.0000
12	Acquisition Time	1.1994
13	Acquisition Date	2009-01-24T19:38:35
14	Modification Date	2009-01-24T23:00:00
15	Spectrometer Frequency	100.55
16	Spectral Width	25000.0
17	Lowest Frequency	-2986.3
18	Nucleus	13C
19	Acquired Size	29984
20	Spectral Size	65536

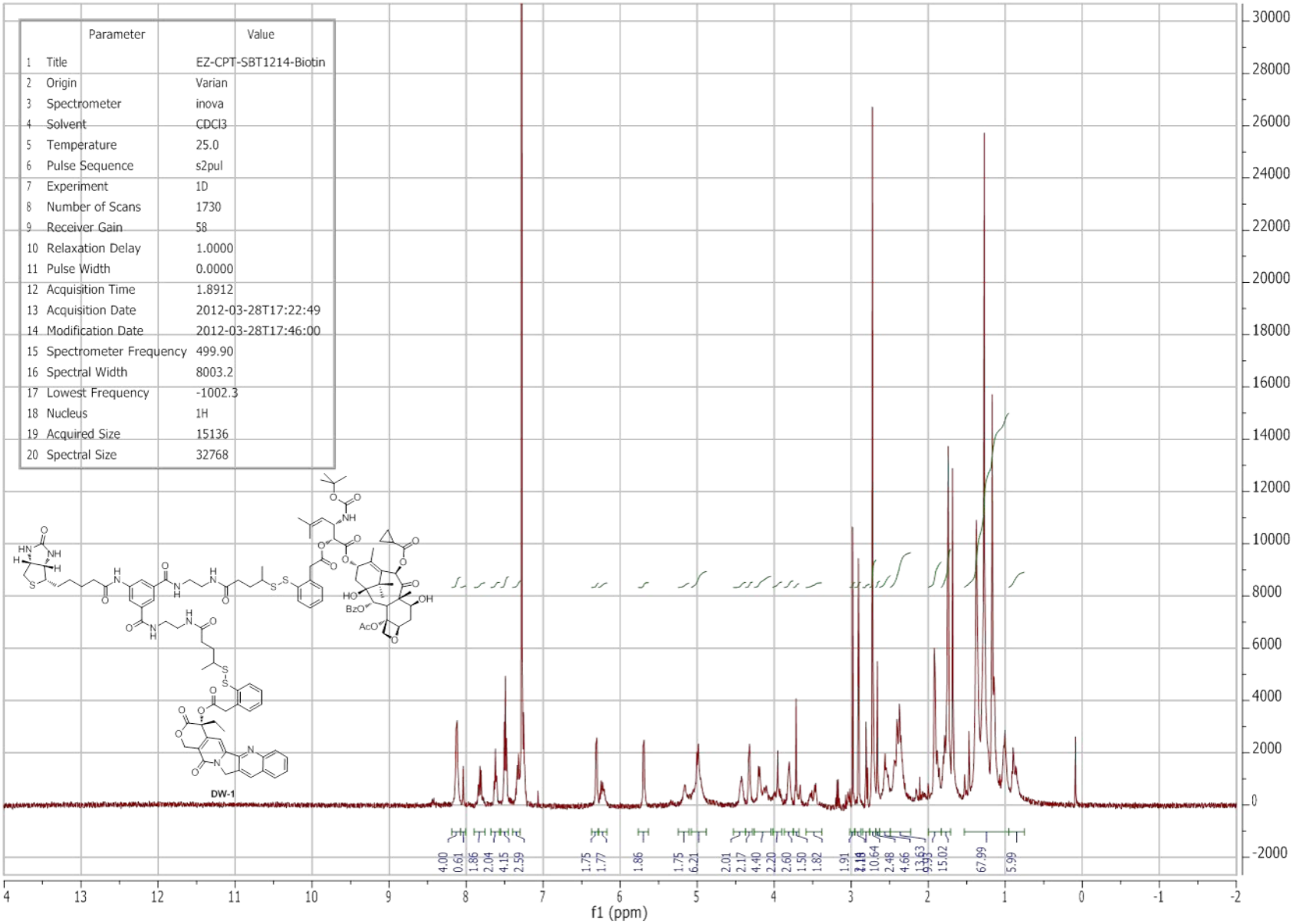
Parameter Value
1 Title EZ-CPT-SBT1214-Biotin
2 Origin Varian
3 Spectrometer inova
4 Solvent CDCl3
5 Temperature 25.0
6 Pulse Sequence s2pul
7 Experiment 1D
8 Number of Scans 1730
9 Receiver Gain 58
10 Relaxation Delay 1.0000
11 Pulse Width 0.0000
12 Acquisition Time 1.8912
13 Acquisition Date 2012-03-28T17:22:49
14 Modification Date 2012-03-28T17:46:00
15 Spectrometer Frequency 499.90
16 Spectral Width 8003.2
17 Lowest Frequency -1002.3
18 Nucleus 1H
19 Acquired Size 15136
20 Spectral Size 32768
DW-1
f1 (ppm)

Appendix 6
Chapter 7 NMR Spectra

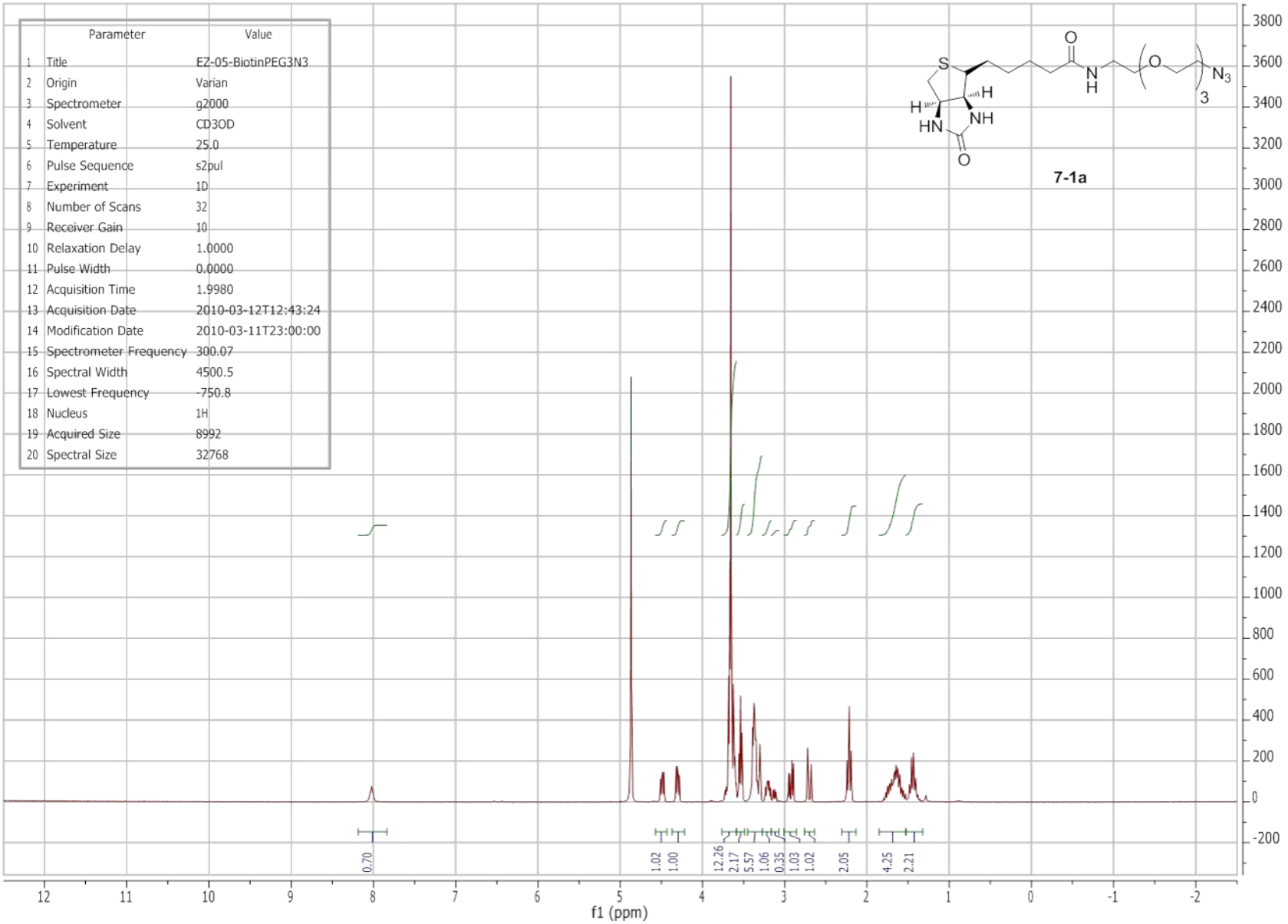
Parameter Value
1 Title EZ-05-BiotinPEG3N3
2 Origin Varian
3 Spectrometer g2000
4 Solvent CD3OD
5 Temperature 25.0
6 Pulse Sequence s2pul
7 Experiment 1D
8 Number of Scans 32
9 Receiver Gain 10
10 Relaxation Delay 1.0000
11 Pulse Width 0.0000
12 Acquisition Time 1.9980
13 Acquisition Date 2010-03-12T12:43:24
14 Modification Date 2010-03-11T23:00:00
15 Spectrometer Frequency 300.07
16 Spectral Width 4500.5
17 Lowest Frequency -750.8
18 Nucleus 1H
19 Acquired Size 8992
20 Spectral Size 32768
7-1a
f1 (ppm)
0.70
1.02
1.00
12.26
2.17
5.57
1.06
0.35
1.03
1.02
2.05
4.25
2.21

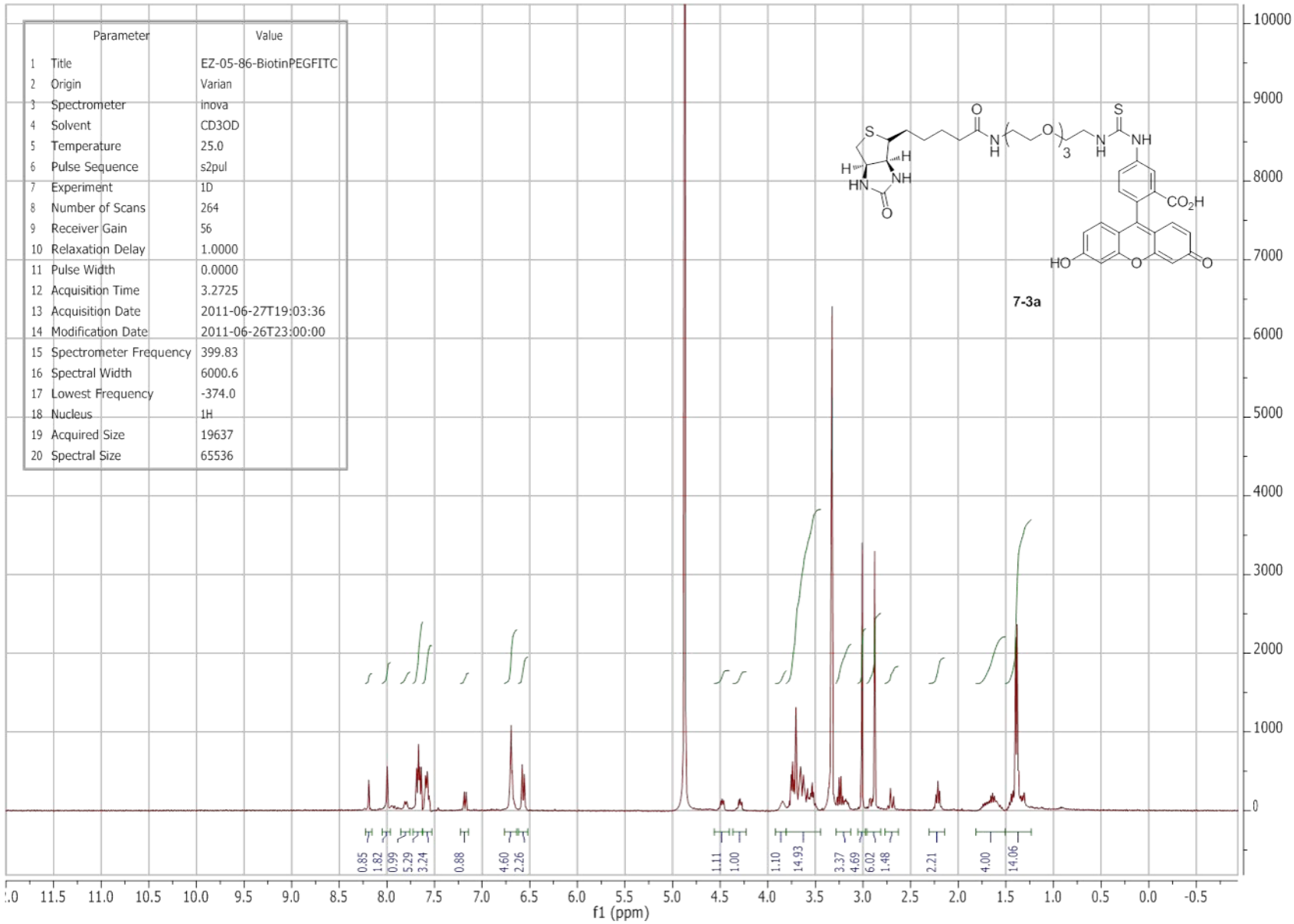
Parameter Value
1 Title EZ-05-86-BiotinPEGFITC
2 Origin Varian
3 Spectrometer inova
4 Solvent CD3OD
5 Temperature 25.0
6 Pulse Sequence s2pul
7 Experiment 1D
8 Number of Scans 264
9 Receiver Gain 56
10 Relaxation Delay 1.0000
11 Pulse Width 0.0000
12 Acquisition Time 3.2725
13 Acquisition Date 2011-06-27T19:03:36
14 Modification Date 2011-06-26T23:00:00
15 Spectrometer Frequency 399.83
16 Spectral Width 6000.6
17 Lowest Frequency -374.0
18 Nucleus 1H
19 Acquired Size 19637
20 Spectral Size 65536
7-3a
f1 (ppm)

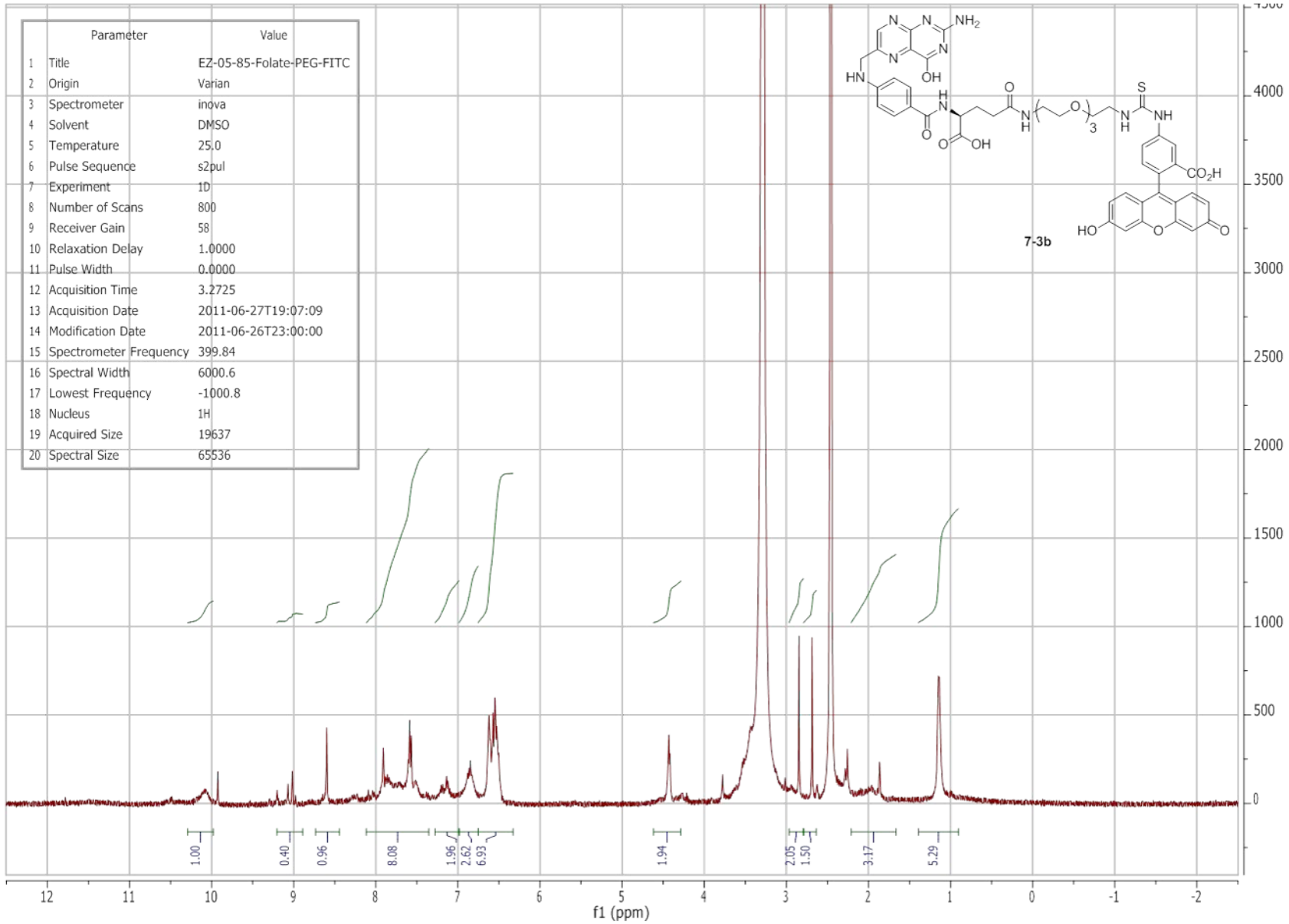
Parameter Value
1 Title EZ-05-85-Folate-PEG-FITC
2 Origin Varian
3 Spectrometer inova
4 Solvent DMSO
5 Temperature 25.0
6 Pulse Sequence s2pul
7 Experiment 1D
8 Number of Scans 800
9 Receiver Gain 58
10 Relaxation Delay 1.0000
11 Pulse Width 0.0000
12 Acquisition Time 3.2725
13 Acquisition Date 2011-06-27T19:07:09
14 Modification Date 2011-06-26T23:00:00
15 Spectrometer Frequency 399.84
16 Spectral Width 6000.6
17 Lowest Frequency -1000.8
18 Nucleus 1H
19 Acquired Size 19637
20 Spectral Size 65536
7-3b
1.00
0.40
0.96
8.08
1.96
2.62
6.93
1.94
2.05
1.50
3.17
5.29
f1 (ppm)

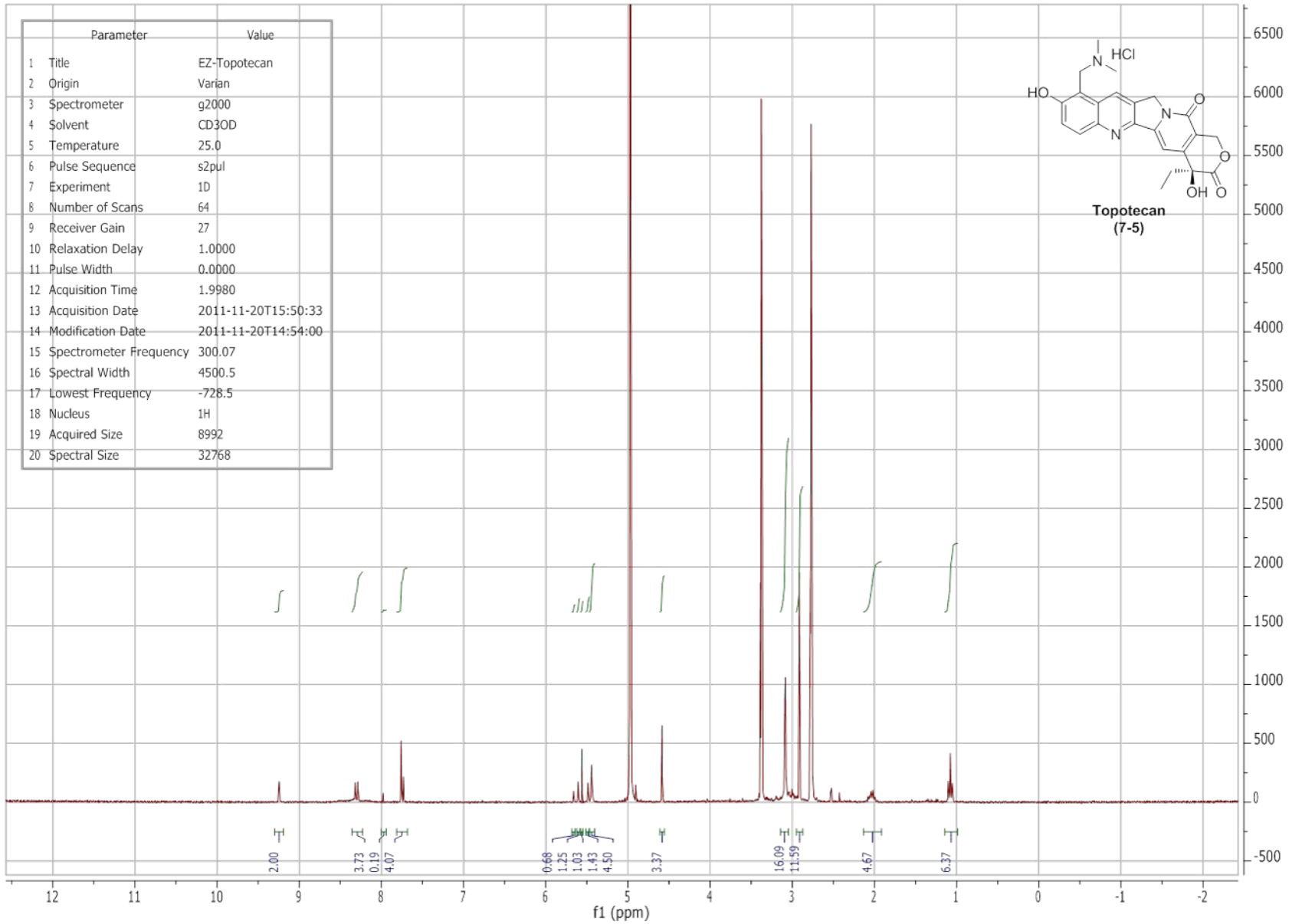
Parameter Value
1 Title EZ-Topotecan
2 Origin Varian
3 Spectrometer g2000
4 Solvent CD3OD
5 Temperature 25.0
6 Pulse Sequence s2pul
7 Experiment 1D
8 Number of Scans 64
9 Receiver Gain 27
10 Relaxation Delay 1.0000
11 Pulse Width 0.0000
12 Acquisition Time 1.9980
13 Acquisition Date 2011-11-20T15:50:33
14 Modification Date 2011-11-20T14:54:00
15 Spectrometer Frequency 300.07
16 Spectral Width 4500.5
17 Lowest Frequency -728.5
18 Nucleus 1H
19 Acquired Size 8992
20 Spectral Size 32768
HCl
HO
N
O
OH
Topotecan
(7-5)
2.00
3.73
0.19
4.07
0.68
1.25
1.03
1.43
4.50
3.37
16.09
11.59
4.67
6.37
f1 (ppm)

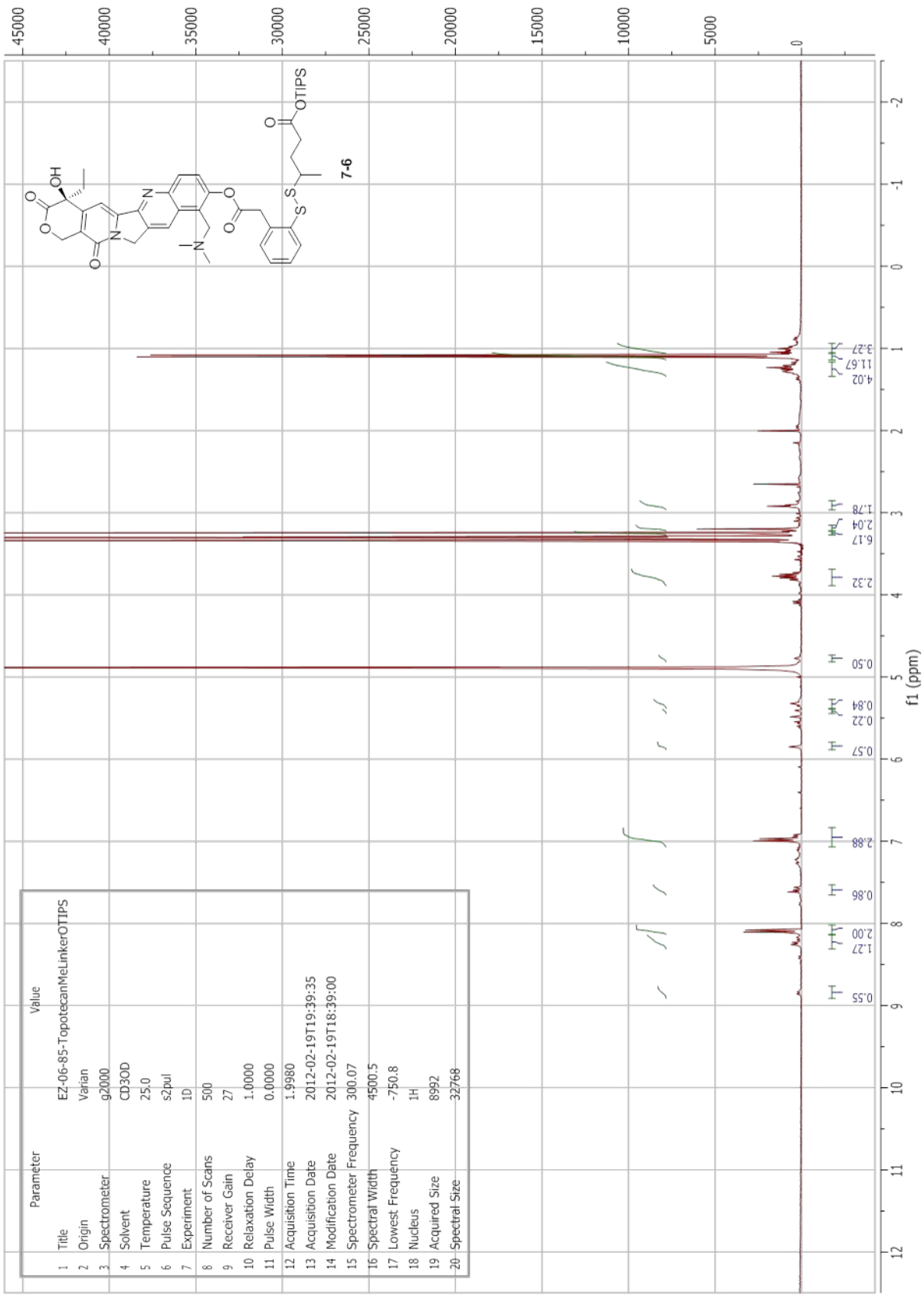
Parameter Value
1 Title EZ-06-85-TopotecanMeLinkerOTIPS
2 Origin Varian
3 Spectrometer g2000
4 Solvent CD3OD
5 Temperature 25.0
6 Pulse Sequence s2pul
7 Experiment 1D
8 Number of Scans 500
9 Receiver Gain 27
10 Relaxation Delay 1.0000
11 Pulse Width 0.0000
12 Acquisition Time 1.9980
13 Acquisition Date 2012-02-19T19:39:35
14 Modification Date 2012-02-19T18:39:00
15 Spectrometer Frequency 300.07
16 Spectral Width 4500.5
17 Lowest Frequency -750.8
18 Nucleus 1H
19 Acquired Size 8992
20 Spectral Size 32768
OTIPS
7-6
f1 (ppm)

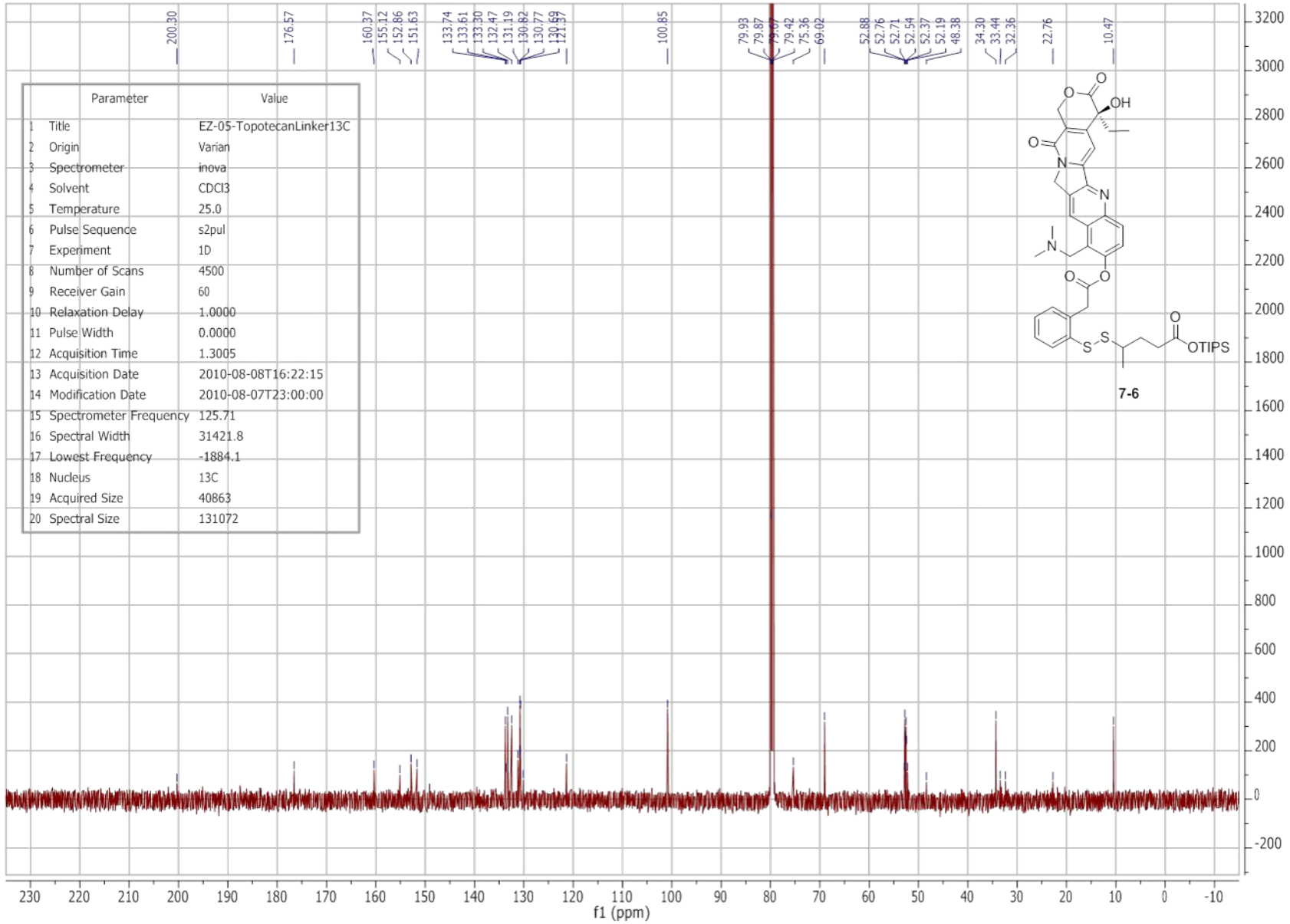
200.30
176.57
160.37
155.12
152.86
151.63
133.74
133.61
133.30
132.47
131.19
130.82
130.77
130.69
121.97
100.85
79.93
79.87
79.07
79.42
75.36
69.02
52.88
52.76
52.71
52.54
52.37
52.19
48.38
34.30
33.44
32.36
22.76
10.47
Parameter Value
1 Title EZ-05-TopotecanLinker13C
2 Origin Varian
3 Spectrometer inova
4 Solvent CDCl3
5 Temperature 25.0
6 Pulse Sequence s2pul
7 Experiment 1D
8 Number of Scans 4500
9 Receiver Gain 60
10 Relaxation Delay 1.0000
11 Pulse Width 0.0000
12 Acquisition Time 1.3005
13 Acquisition Date 2010-08-08T16:22:15
14 Modification Date 2010-08-07T23:00:00
15 Spectrometer Frequency 125.71
16 Spectral Width 31421.8
17 Lowest Frequency -1884.1
18 Nucleus 13C
19 Acquired Size 40863
20 Spectral Size 131072
OH
OTIPS
7-6
f1 (ppm)

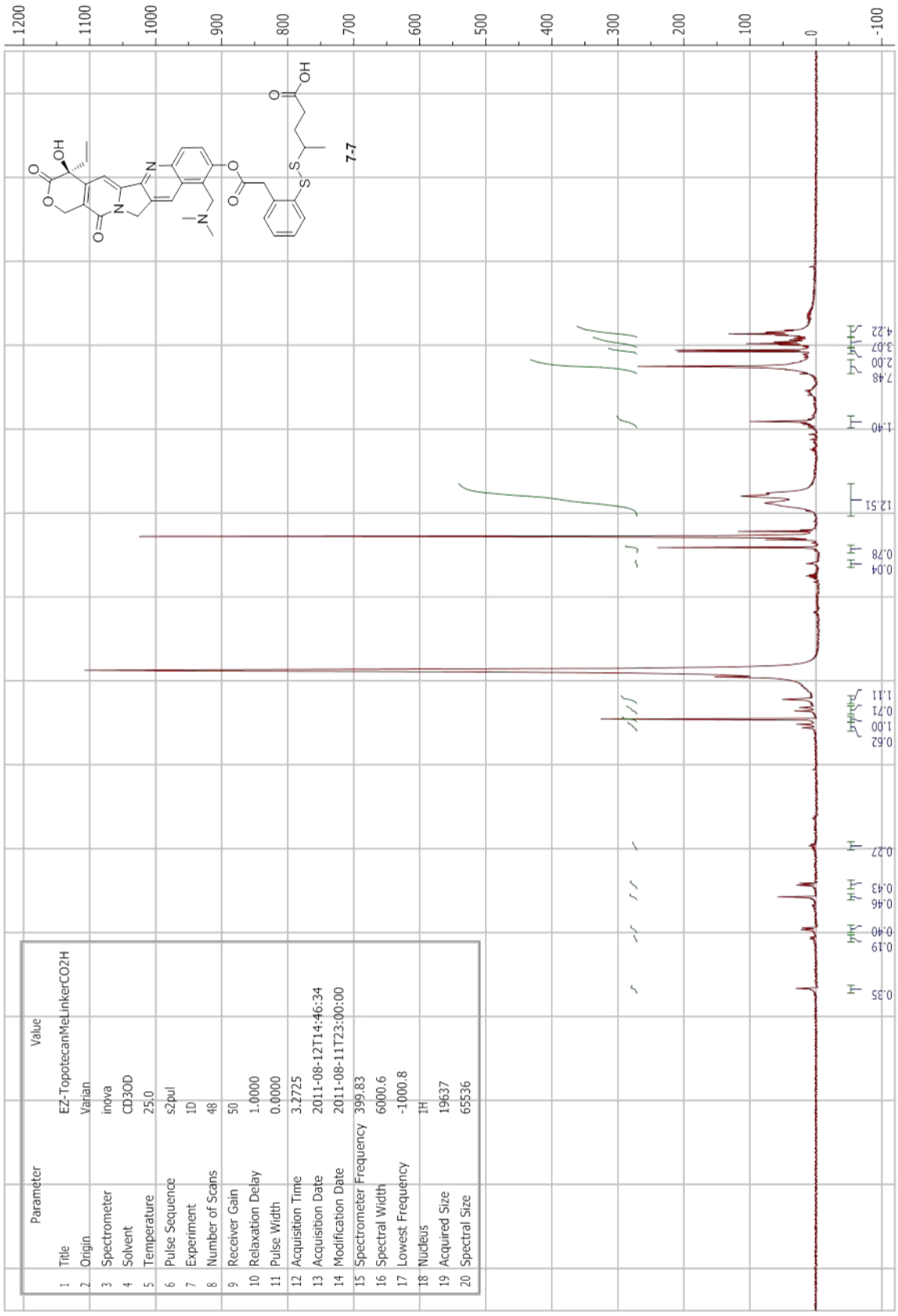

	Parameter	Value
1	Title	EZ-TopotecanMeLinkerCO2H
2	Origin	Varian
3	Spectrometer	inova
4	Solvent	CD3OD
5	Temperature	25.0
6	Pulse Sequence	s2pul
7	Experiment	1D
8	Number of Scans	48
9	Receiver Gain	50
10	Relaxation Delay	1.0000
11	Pulse Width	0.0000
12	Acquisition Time	3.2725
13	Acquisition Date	2011-08-12T14:46:34
14	Modification Date	2011-08-11T23:00:00
15	Spectrometer Frequency	399.83
16	Spectral Width	6000.6
17	Lowest Frequency	-1000.8
18	Nucleus	1H
19	Acquired Size	19637
20	Spectral Size	65536

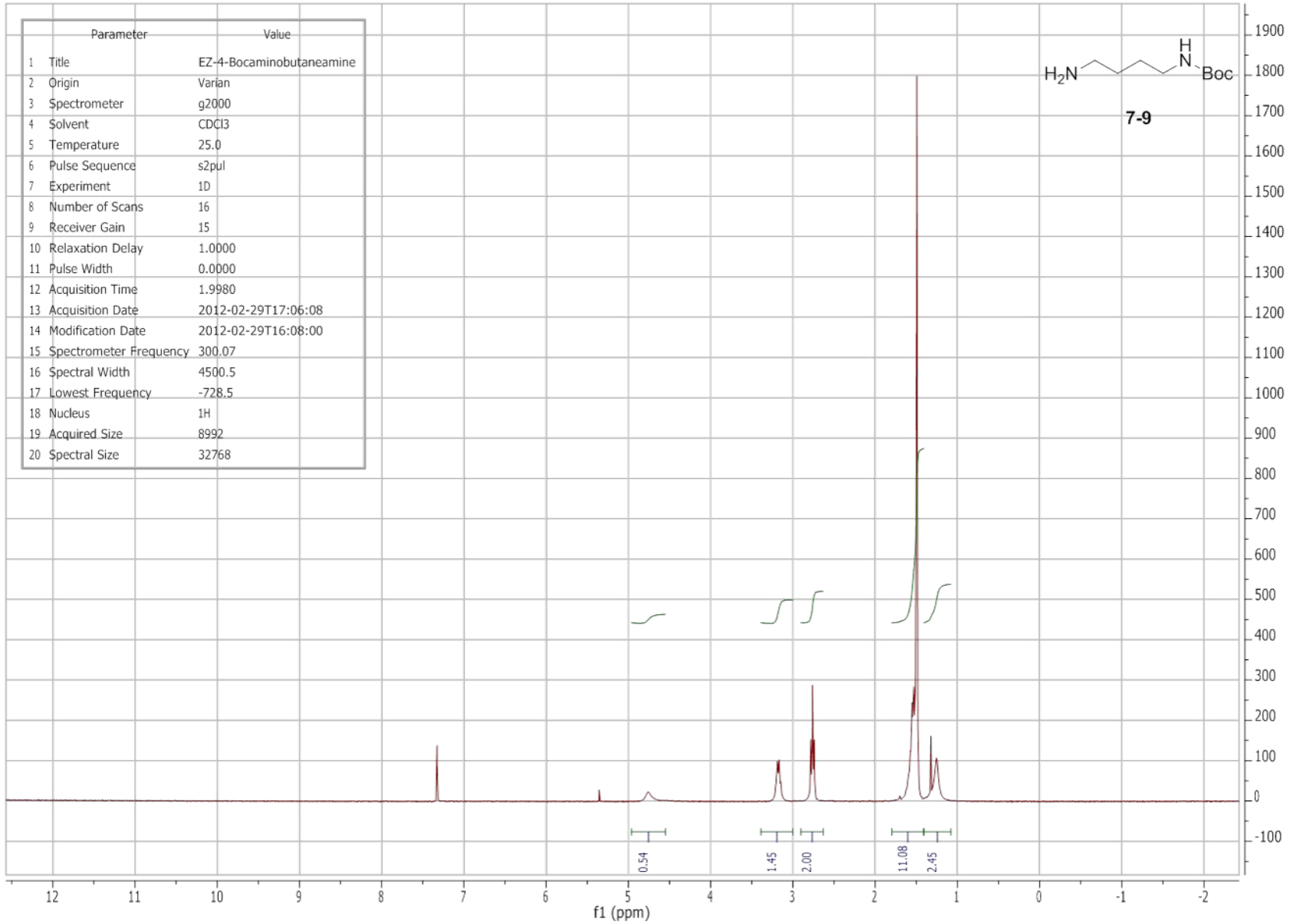
Parameter Value
1 Title EZ-4-Bocaminobutaneamine
2 Origin Varian
3 Spectrometer g2000
4 Solvent CDCl3
5 Temperature 25.0
6 Pulse Sequence s2pul
7 Experiment 1D
8 Number of Scans 16
9 Receiver Gain 15
10 Relaxation Delay 1.0000
11 Pulse Width 0.0000
12 Acquisition Time 1.9980
13 Acquisition Date 2012-02-29T17:06:08
14 Modification Date 2012-02-29T16:08:00
15 Spectrometer Frequency 300.07
16 Spectral Width 4500.5
17 Lowest Frequency -728.5
18 Nucleus 1H
19 Acquired Size 8992
20 Spectral Size 32768
H2N
H
N
Boc
7-9
0.54
1.45
2.00
11.08
2.45
f1 (ppm)

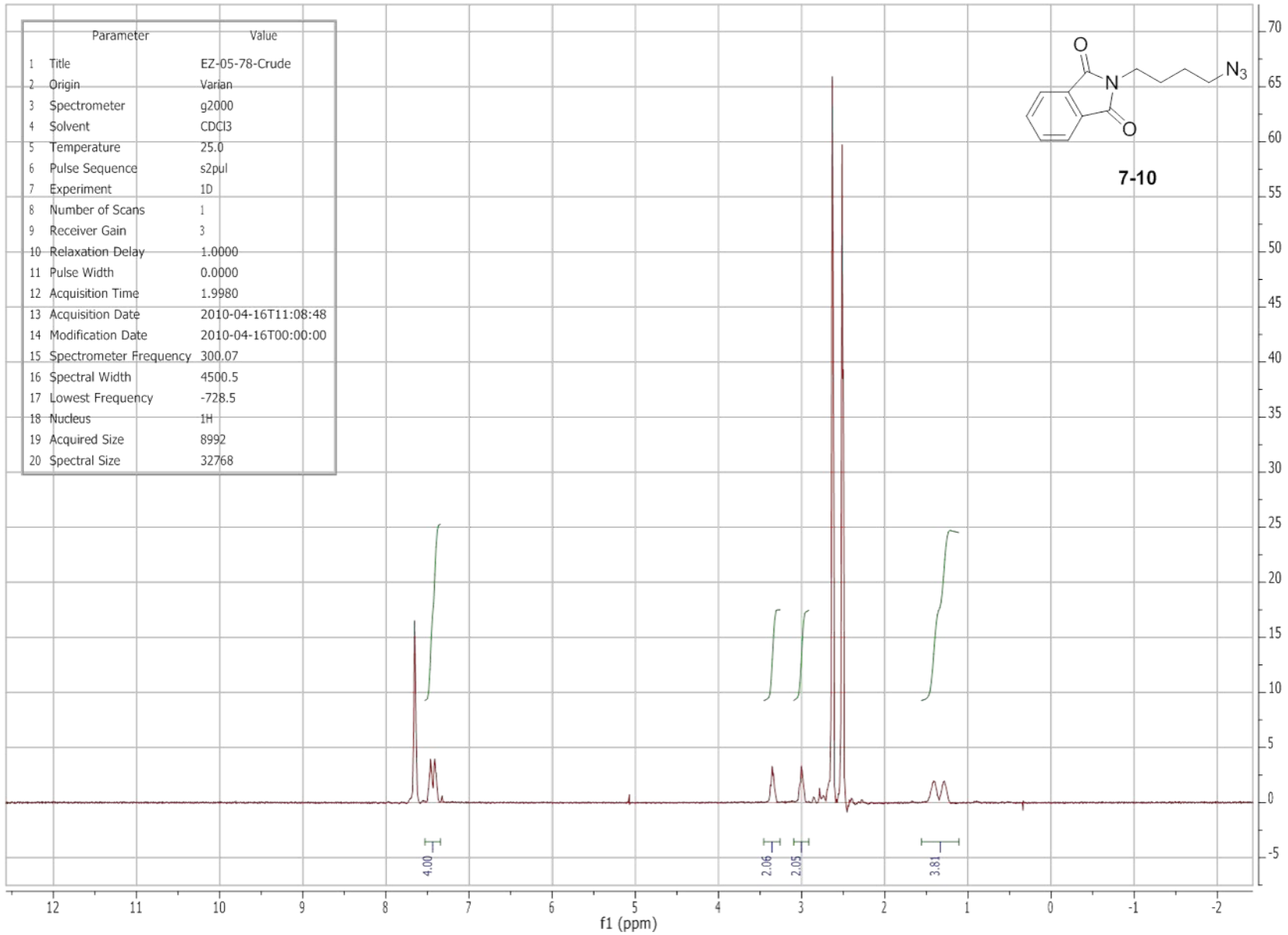
Parameter Value
1 Title EZ-05-78-Crude
2 Origin Varian
3 Spectrometer g2000
4 Solvent CDCl3
5 Temperature 25.0
6 Pulse Sequence s2pul
7 Experiment 1D
8 Number of Scans 1
9 Receiver Gain 3
10 Relaxation Delay 1.0000
11 Pulse Width 0.0000
12 Acquisition Time 1.9980
13 Acquisition Date 2010-04-16T11:08:48
14 Modification Date 2010-04-16T00:00:00
15 Spectrometer Frequency 300.07
16 Spectral Width 4500.5
17 Lowest Frequency -728.5
18 Nucleus 1H
19 Acquired Size 8992
20 Spectral Size 32768
O
N
O
N3
7-10
4.00
2.06
2.05
3.81
12 11 10 9 8 7 6 5 4 3 2 1 0 -1 -2
f1 (ppm)
70 65 60 55 50 45 40 35 30 25 20 15 10 5 0 -5

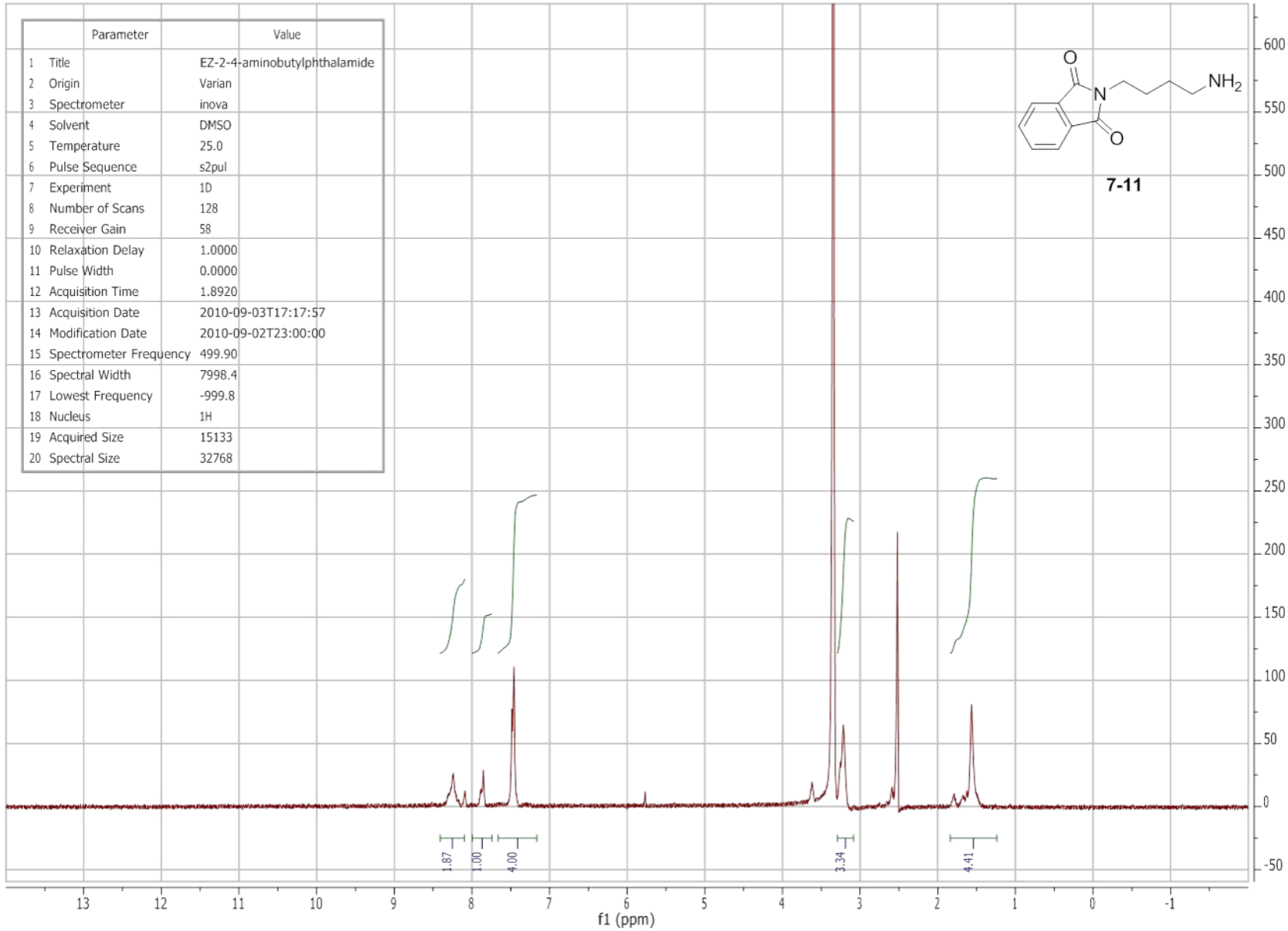
Parameter Value
1 Title EZ-2-4-aminobutylphthalamide
2 Origin Varian
3 Spectrometer inova
4 Solvent DMSO
5 Temperature 25.0
6 Pulse Sequence s2pul
7 Experiment 1D
8 Number of Scans 128
9 Receiver Gain 58
10 Relaxation Delay 1.0000
11 Pulse Width 0.0000
12 Acquisition Time 1.8920
13 Acquisition Date 2010-09-03T17:17:57
14 Modification Date 2010-09-02T23:00:00
15 Spectrometer Frequency 499.90
16 Spectral Width 7998.4
17 Lowest Frequency -999.8
18 Nucleus 1H
19 Acquired Size 15133
20 Spectral Size 32768
O
N
O
NH2
7-11
1.87
1.00
4.00
3.34
4.41
f1 (ppm)

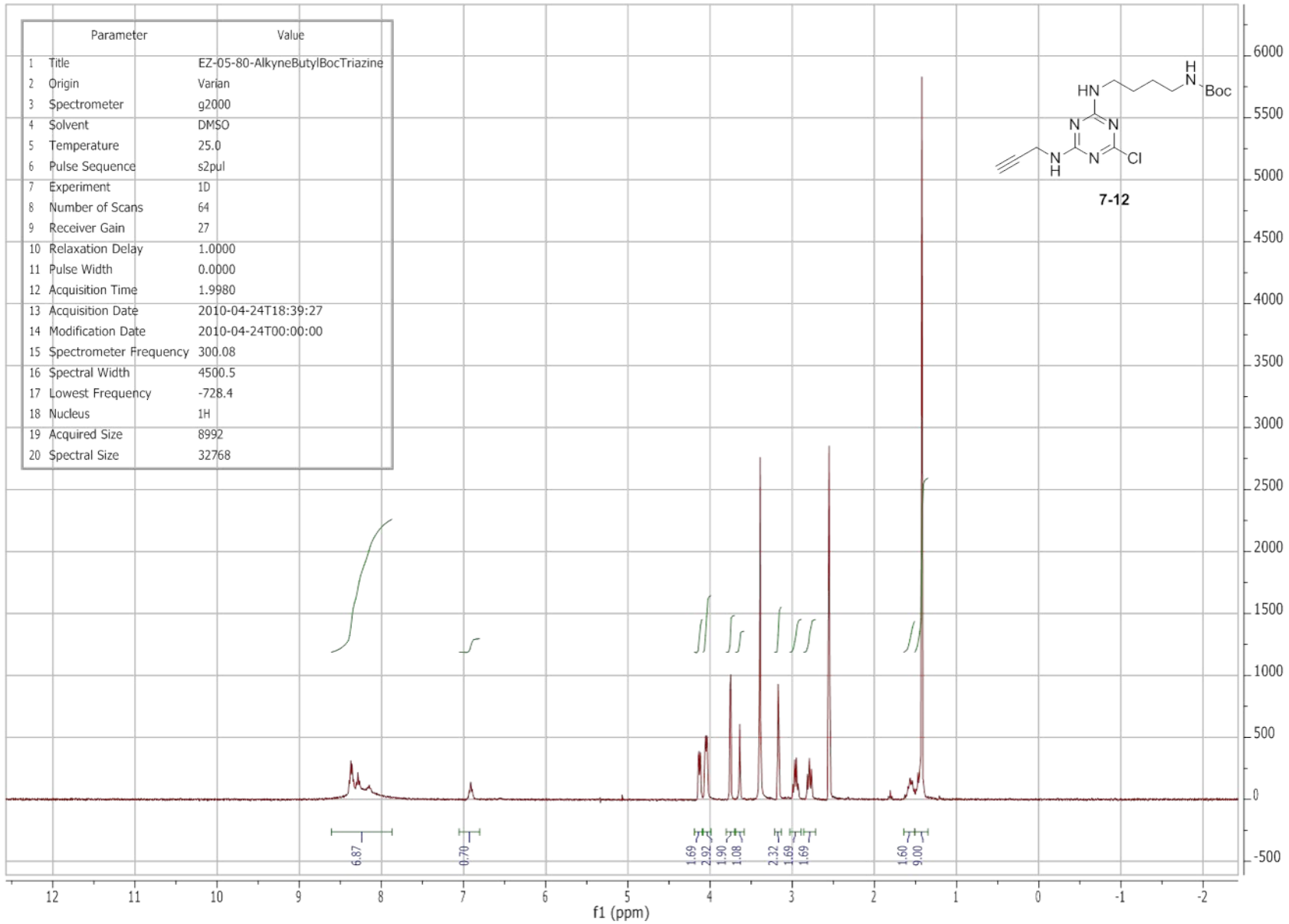
Parameter Value
1 Title EZ-05-80-AlkyneButylBocTriazine
2 Origin Varian
3 Spectrometer g2000
4 Solvent DMSO
5 Temperature 25.0
6 Pulse Sequence s2pul
7 Experiment 1D
8 Number of Scans 64
9 Receiver Gain 27
10 Relaxation Delay 1.0000
11 Pulse Width 0.0000
12 Acquisition Time 1.9980
13 Acquisition Date 2010-04-24T18:39:27
14 Modification Date 2010-04-24T00:00:00
15 Spectrometer Frequency 300.08
16 Spectral Width 4500.5
17 Lowest Frequency -728.4
18 Nucleus 1H
19 Acquired Size 8992
20 Spectral Size 32768
HN
H
N
Boc
N
N
N
N
H
Cl
7-12
6000
5500
5000
4500
4000
3500
3000
2500
2000
1500
1000
500
0
-500
6.87
0.70
1.69
2.92
1.90
1.08
2.32
1.69
1.69
1.60
9.00
12
11
10
9
8
7
6
5
4
3
2
1
0
-1
-2
f1 (ppm)

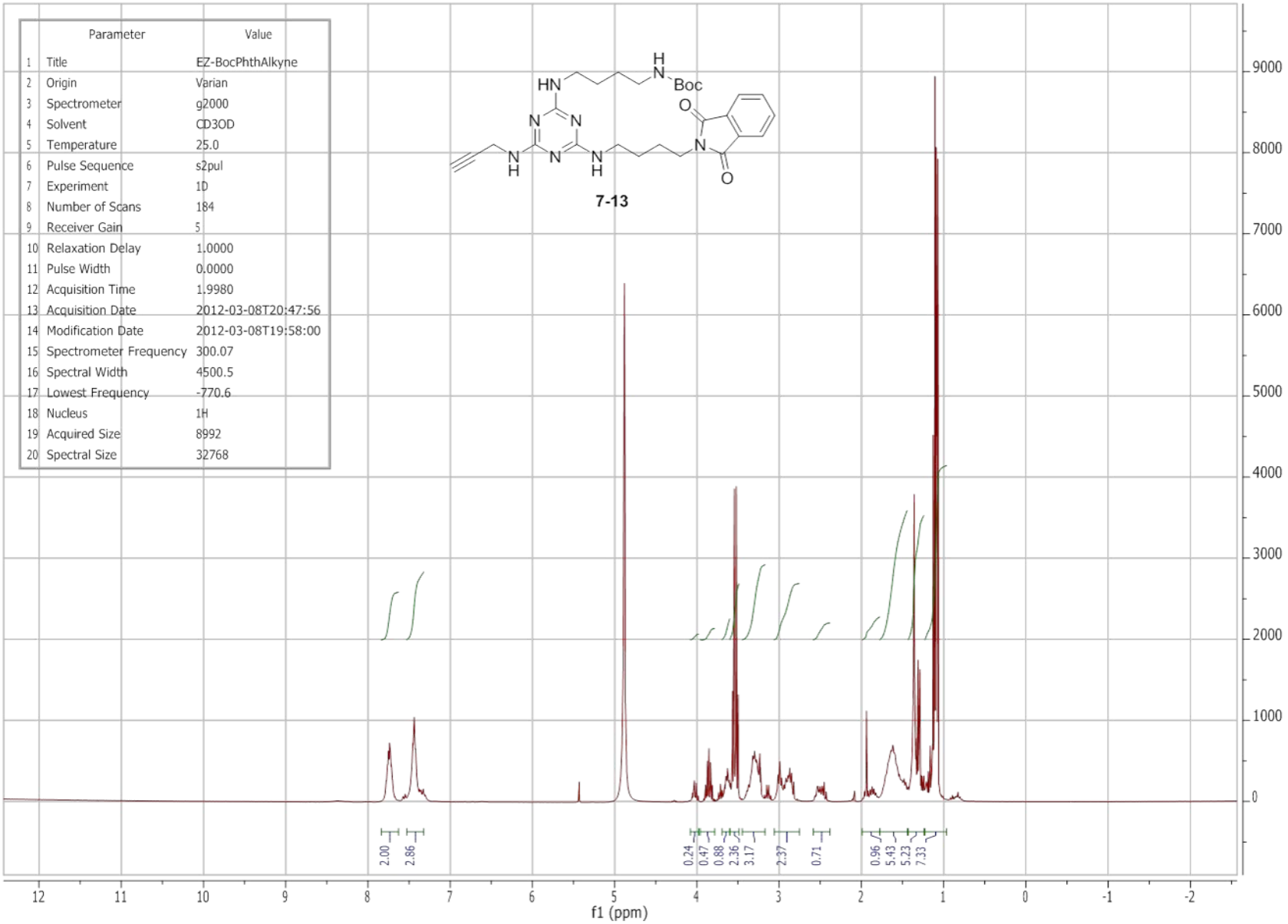
Parameter Value
1 Title EZ-BocPhthAlkyne
2 Origin Varian
3 Spectrometer g2000
4 Solvent CD3OD
5 Temperature 25.0
6 Pulse Sequence s2pul
7 Experiment 1D
8 Number of Scans 184
9 Receiver Gain 5
10 Relaxation Delay 1.0000
11 Pulse Width 0.0000
12 Acquisition Time 1.9980
13 Acquisition Date 2012-03-08T20:47:56
14 Modification Date 2012-03-08T19:58:00
15 Spectrometer Frequency 300.07
16 Spectral Width 4500.5
17 Lowest Frequency -770.6
18 Nucleus 1H
19 Acquired Size 8992
20 Spectral Size 32768
HN
H
N
Boc
O
N
N
N
N
H
N
H
O
7-13
2.00
2.86
0.24
0.47
0.88
2.36
3.17
2.37
0.71
0.96
5.43
5.23
7.33
f1 (ppm)

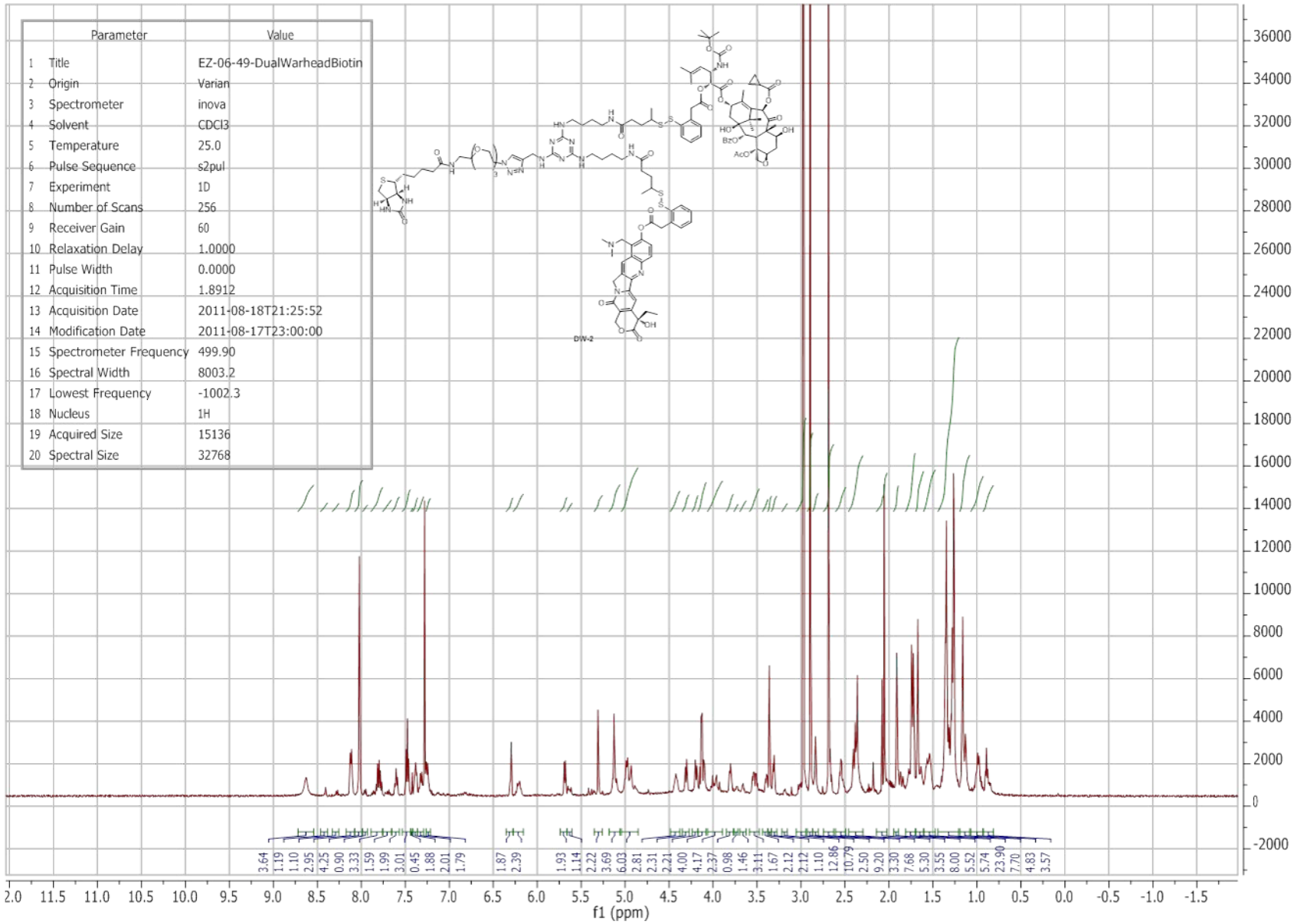
Parameter Value
1 Title EZ-06-49-DualWarheadBiotin
2 Origin Varian
3 Spectrometer inova
4 Solvent CDCl3
5 Temperature 25.0
6 Pulse Sequence s2pul
7 Experiment 1D
8 Number of Scans 256
9 Receiver Gain 60
10 Relaxation Delay 1.0000
11 Pulse Width 0.0000
12 Acquisition Time 1.8912
13 Acquisition Date 2011-08-18T21:25:52
14 Modification Date 2011-08-17T23:00:00
15 Spectrometer Frequency 499.90
16 Spectral Width 8003.2
17 Lowest Frequency -1002.3
18 Nucleus 1H
19 Acquired Size 15136
20 Spectral Size 32768
DW-2
f1 (ppm)

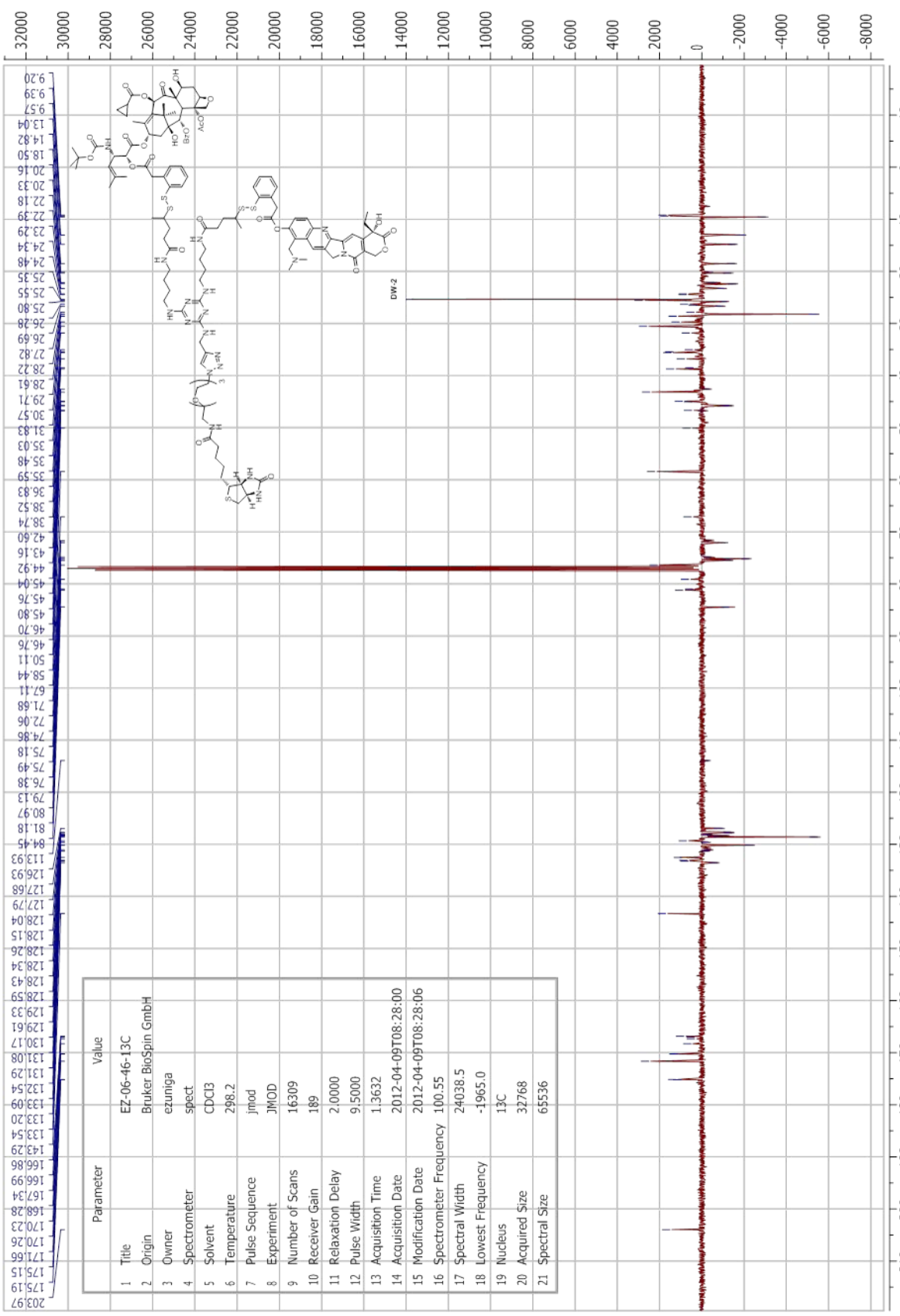

	Parameter	Value
1	Title	EZ-06-46-13C
2	Origin	Bruker BioSpin GmbH
3	Owner	ezuniga
4	Spectrometer	spect
5	Solvent	CDCl3
6	Temperature	298.2
7	Pulse Sequence	jmod
8	Experiment	JMOD
9	Number of Scans	16309
10	Receiver Gain	189
11	Relaxation Delay	2.0000
12	Pulse Width	9.5000
13	Acquisition Time	1.3632
14	Acquisition Date	2012-04-09T08:28:00
15	Modification Date	2012-04-09T08:28:06
16	Spectrometer Frequency	100.55
17	Spectral Width	24038.5
18	Lowest Frequency	-1965.0
19	Nucleus	13C
20	Acquired Size	32768
21	Spectral Size	65536

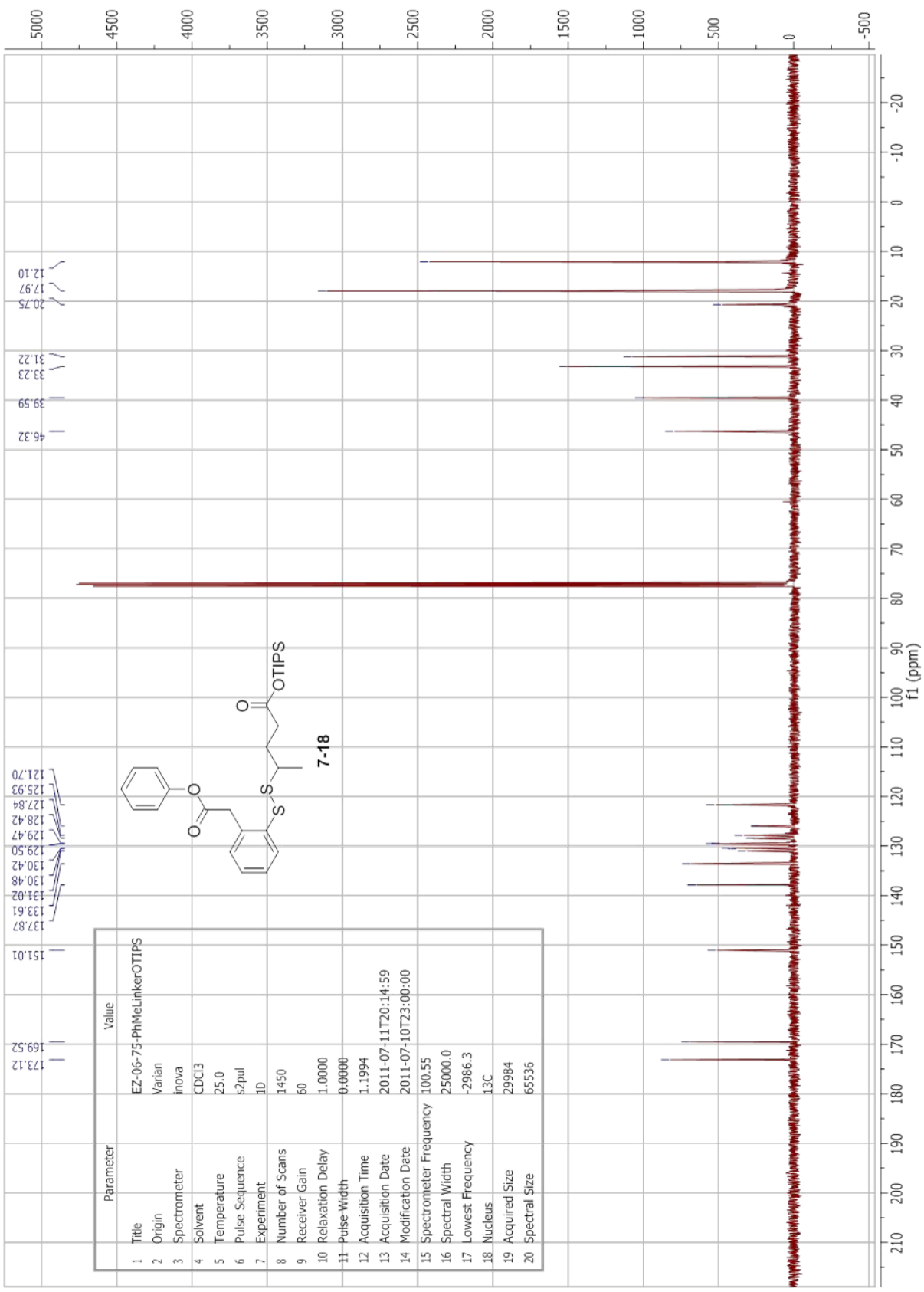
7-18
OTIPS
O
O
S
S
f1 (ppm)
Parameter
Value
1 Title EZ-06-75-PhMeLinkerOTIPS
2 Origin Varian
3 Spectrometer inova
4 Solvent CDCl3
5 Temperature 25.0
6 Pulse Sequence s2pul
7 Experiment 1D
8 Number of Scans 1450
9 Receiver Gain 60
10 Relaxation Delay 1.0000
11 Pulse Width 0.0000
12 Acquisition Time 1.1994
13 Acquisition Date 2011-07-11T20:14:59
14 Modification Date 2011-07-10T23:00:00
15 Spectrometer Frequency 100.55
16 Spectral Width 25000.0
17 Lowest Frequency -2986.3
18 Nucleus 13C
19 Acquired Size 29984
20 Spectral Size 65536

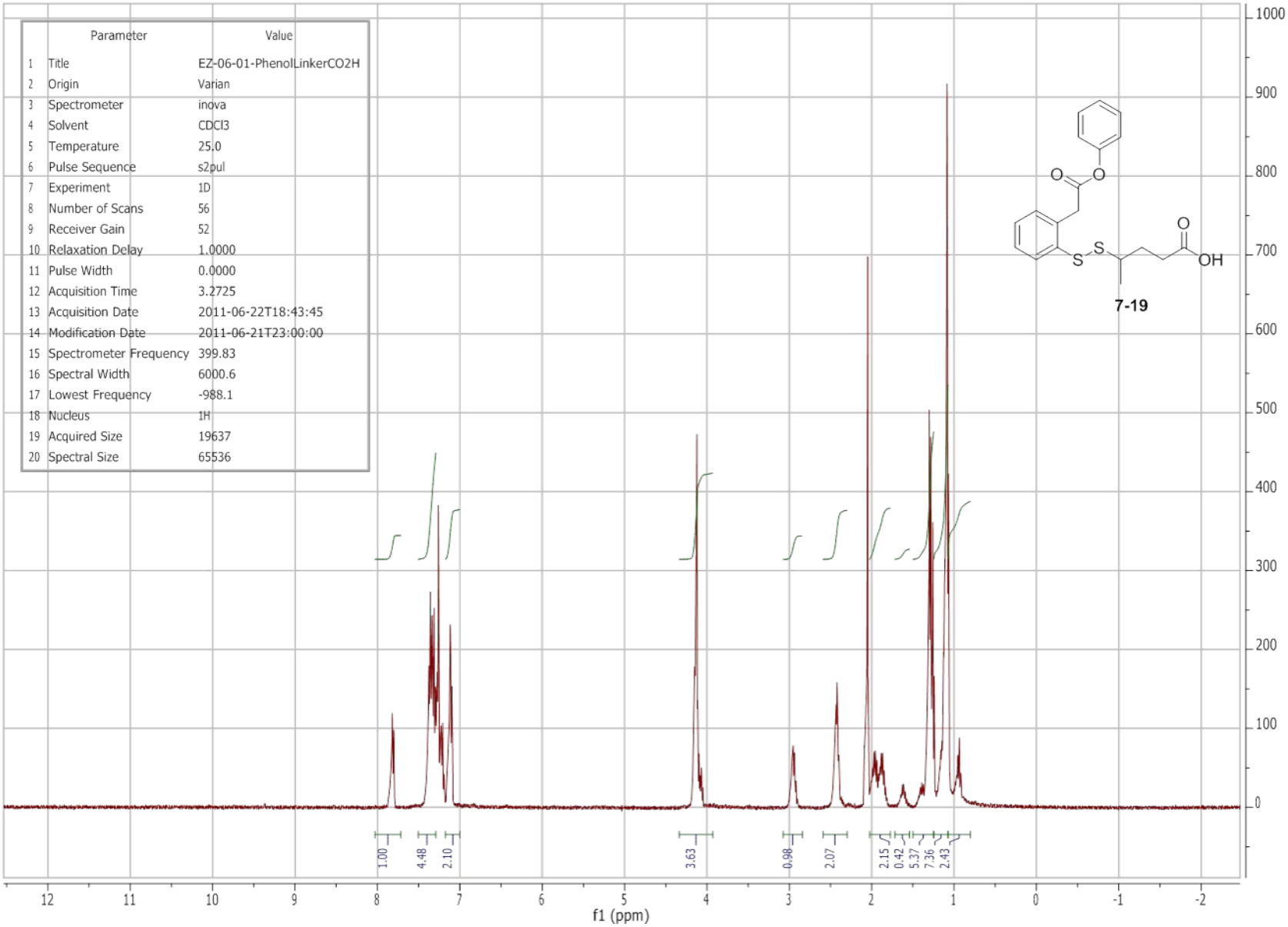
Parameter Value
1 Title EZ-06-01-PhenolLinkerCO2H
2 Origin Varian
3 Spectrometer inova
4 Solvent CDCl3
5 Temperature 25.0
6 Pulse Sequence s2pul
7 Experiment 1D
8 Number of Scans 56
9 Receiver Gain 52
10 Relaxation Delay 1.0000
11 Pulse Width 0.0000
12 Acquisition Time 3.2725
13 Acquisition Date 2011-06-22T18:43:45
14 Modification Date 2011-06-21T23:00:00
15 Spectrometer Frequency 399.83
16 Spectral Width 6000.6
17 Lowest Frequency -988.1
18 Nucleus 1H
19 Acquired Size 19637
20 Spectral Size 65536
O
O
S
S
O
OH
7-19
1.00
4.48
2.10
3.63
0.98
2.07
2.15
0.42
5.37
7.36
2.43
f1 (ppm)

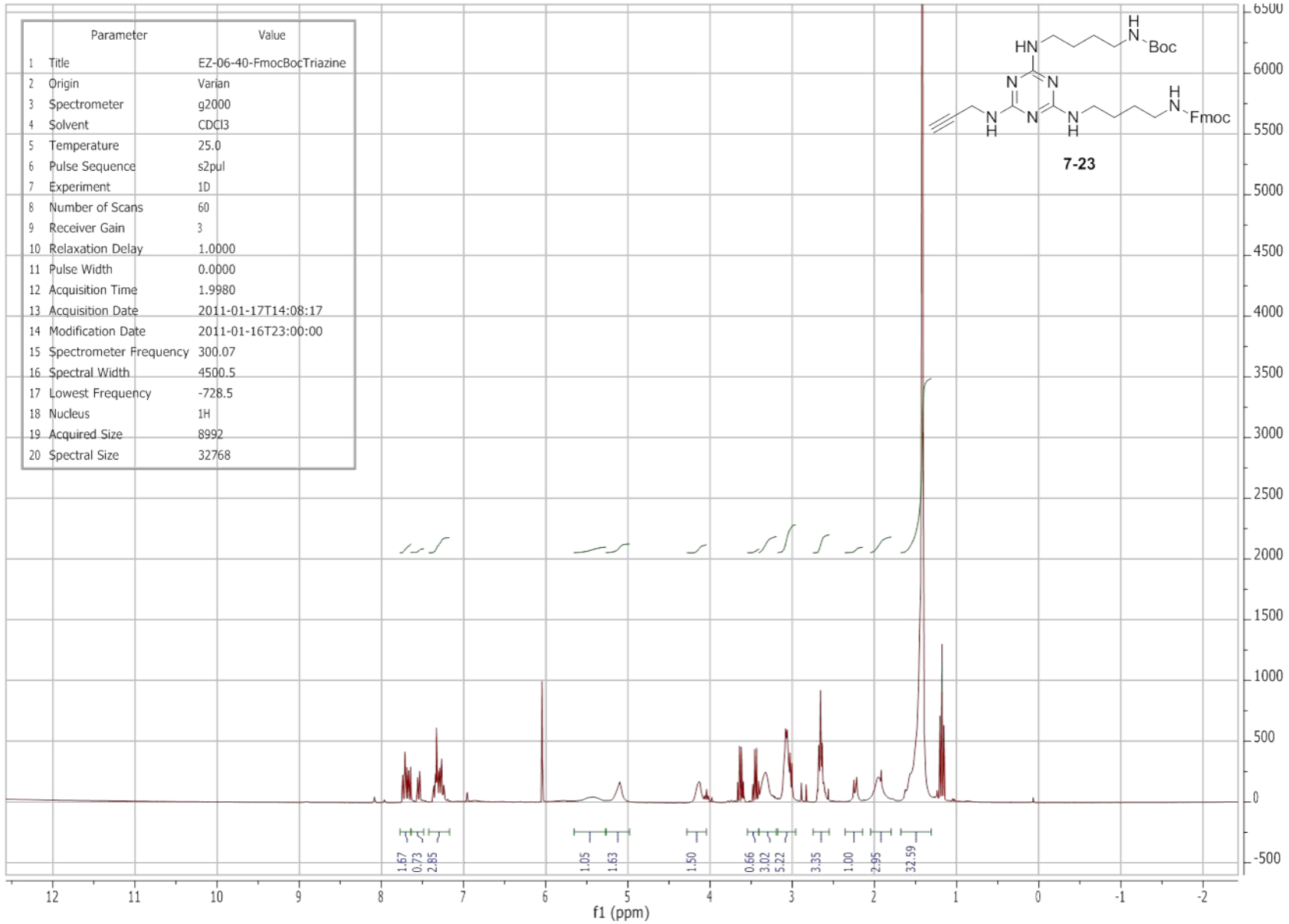
Parameter Value
1 Title EZ-06-40-FmocBocTriazine
2 Origin Varian
3 Spectrometer g2000
4 Solvent CDCl3
5 Temperature 25.0
6 Pulse Sequence s2pul
7 Experiment 1D
8 Number of Scans 60
9 Receiver Gain 3
10 Relaxation Delay 1.0000
11 Pulse Width 0.0000
12 Acquisition Time 1.9980
13 Acquisition Date 2011-01-17T14:08:17
14 Modification Date 2011-01-16T23:00:00
15 Spectrometer Frequency 300.07
16 Spectral Width 4500.5
17 Lowest Frequency -728.5
18 Nucleus 1H
19 Acquired Size 8992
20 Spectral Size 32768
HN
H
N
Boc
N
N
N
N
H
N
H
H
N
Fmoc
7-23
1.67
0.73
2.85
1.05
1.63
1.50
0.66
3.02
5.22
3.35
1.00
2.95
32.59
f1 (ppm)

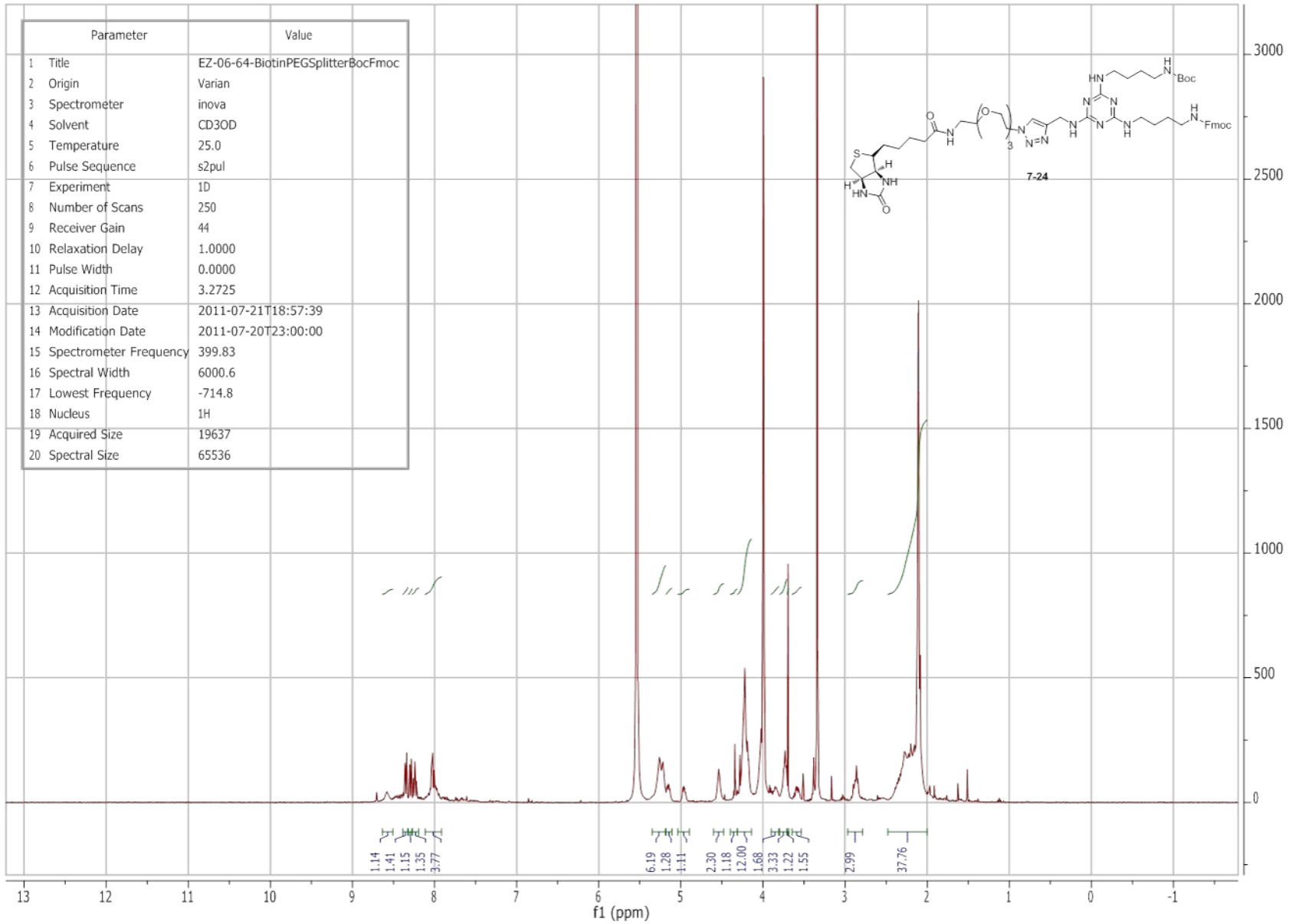
Parameter Value
1 Title EZ-06-64-BiotinPEGSplitterBocFmoc
2 Origin Varian
3 Spectrometer inova
4 Solvent CD3OD
5 Temperature 25.0
6 Pulse Sequence s2pul
7 Experiment 1D
8 Number of Scans 250
9 Receiver Gain 44
10 Relaxation Delay 1.0000
11 Pulse Width 0.0000
12 Acquisition Time 3.2725
13 Acquisition Date 2011-07-21T18:57:39
14 Modification Date 2011-07-20T23:00:00
15 Spectrometer Frequency 399.83
16 Spectral Width 6000.6
17 Lowest Frequency -714.8
18 Nucleus 1H
19 Acquired Size 19637
20 Spectral Size 65536
7-24
Boc
Fmoc
1.14
1.41
1.15
1.35
3.77
6.19
1.28
1.11
2.30
1.18
12.00
1.68
3.33
1.22
1.55
2.99
37.76
f1 (ppm)

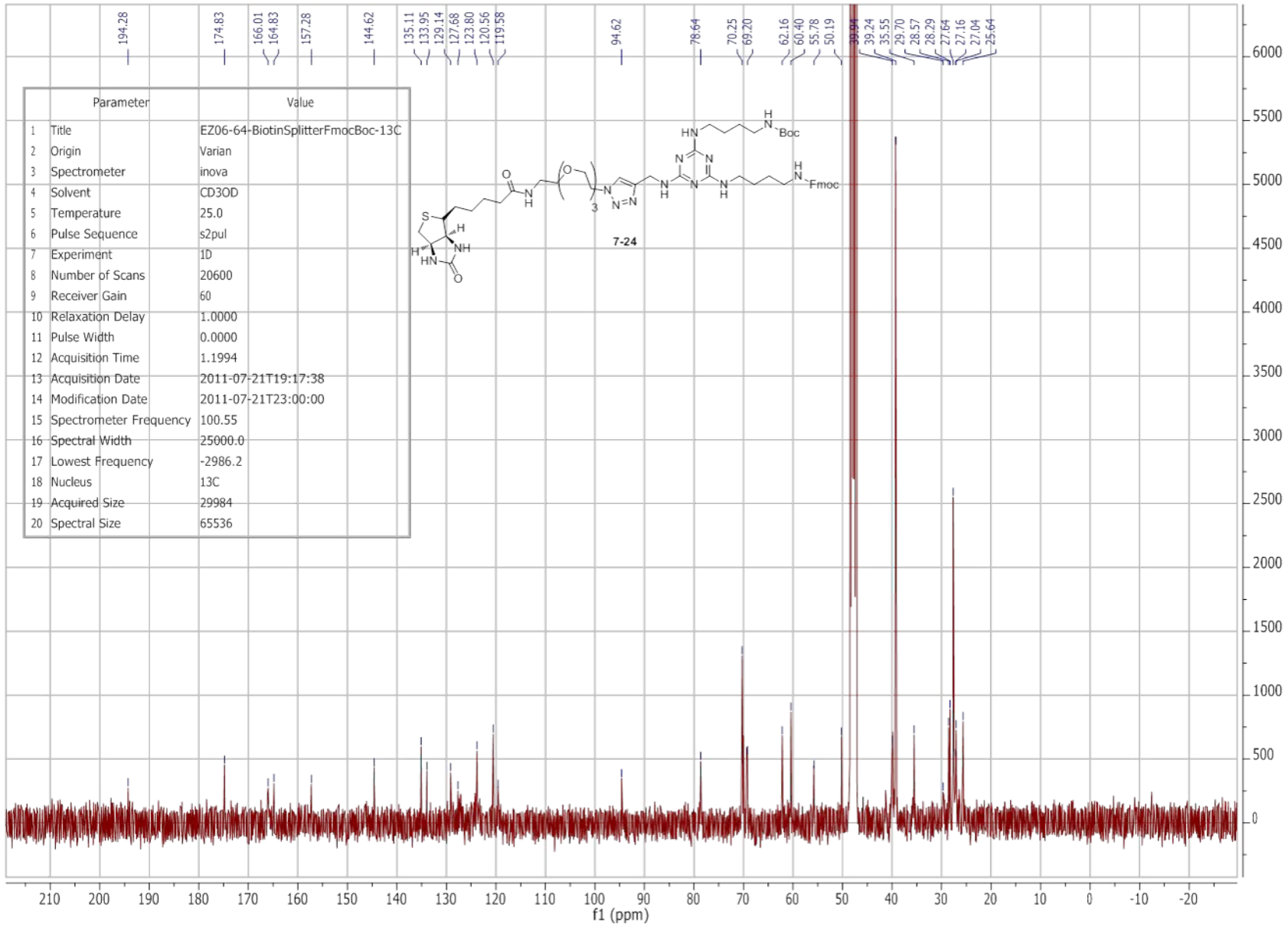
194.28
174.83
166.01
164.83
157.28
144.62
135.11
133.95
129.14
127.68
123.80
120.56
119.58
94.62
78.64
70.25
69.20
62.16
60.40
55.78
50.19
39.24
35.55
29.70
28.57
28.29
27.64
27.16
27.04
25.64
Parameter Value
1 Title EZ06-64-BiotinSplitterFmocBoc-13C
2 Origin Varian
3 Spectrometer inova
4 Solvent CD3OD
5 Temperature 25.0
6 Pulse Sequence s2pul
7 Experiment 1D
8 Number of Scans 20600
9 Receiver Gain 60
10 Relaxation Delay 1.0000
11 Pulse Width 0.0000
12 Acquisition Time 1.1994
13 Acquisition Date 2011-07-21T19:17:38
14 Modification Date 2011-07-21T23:00:00
15 Spectrometer Frequency 100.55
16 Spectral Width 25000.0
17 Lowest Frequency -2986.2
18 Nucleus 13C
19 Acquired Size 29984
20 Spectral Size 65536
7-24
Boc
Fmoc
f1 (ppm)

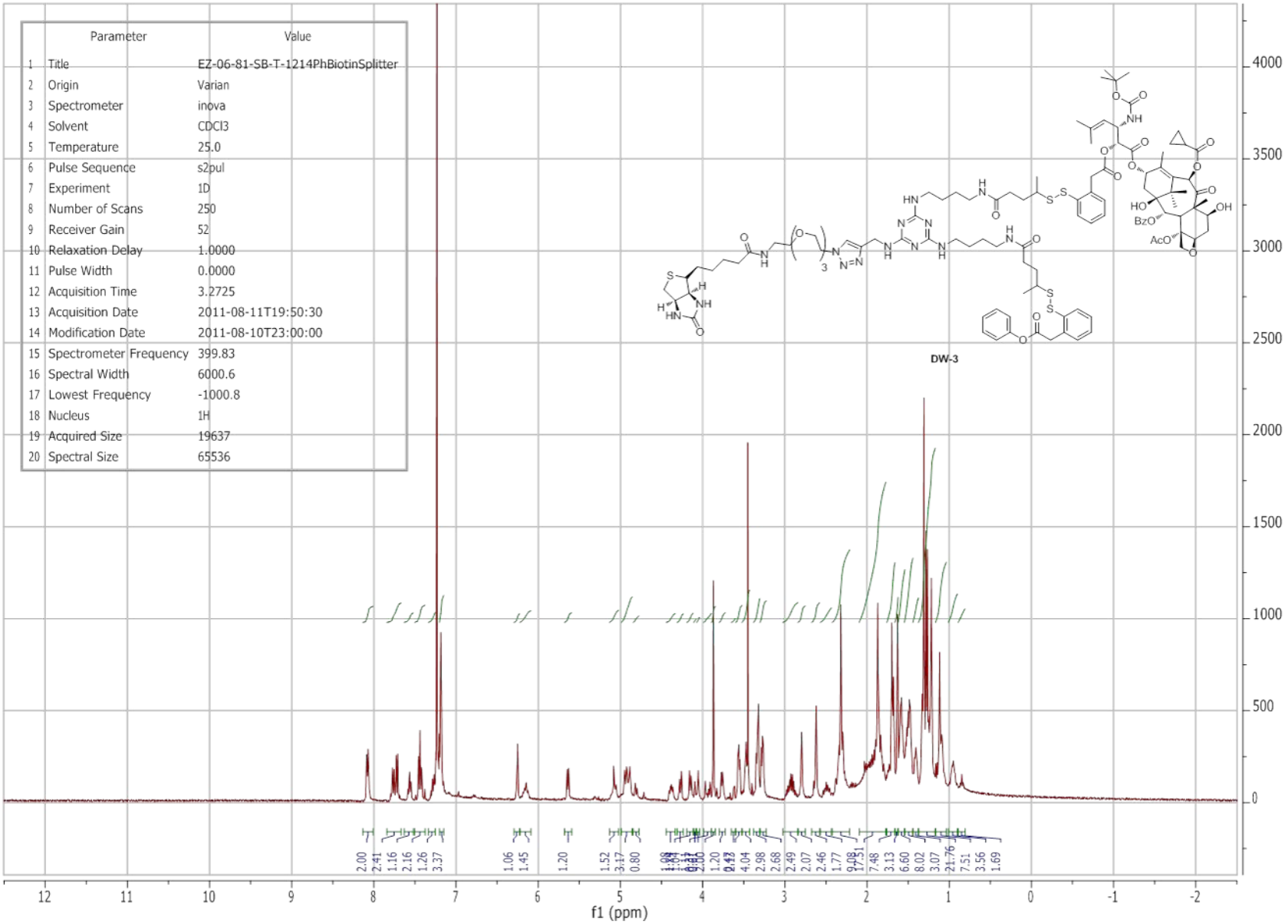
Parameter Value
1 Title EZ-06-81-SB-T-1214PhBiotinSplitter
2 Origin Varian
3 Spectrometer inova
4 Solvent CDCl3
5 Temperature 25.0
6 Pulse Sequence s2pul
7 Experiment 1D
8 Number of Scans 250
9 Receiver Gain 52
10 Relaxation Delay 1.0000
11 Pulse Width 0.0000
12 Acquisition Time 3.2725
13 Acquisition Date 2011-08-11T19:50:30
14 Modification Date 2011-08-10T23:00:00
15 Spectrometer Frequency 399.83
16 Spectral Width 6000.6
17 Lowest Frequency -1000.8
18 Nucleus 1H
19 Acquired Size 19637
20 Spectral Size 65536
DW-3
f1 (ppm)

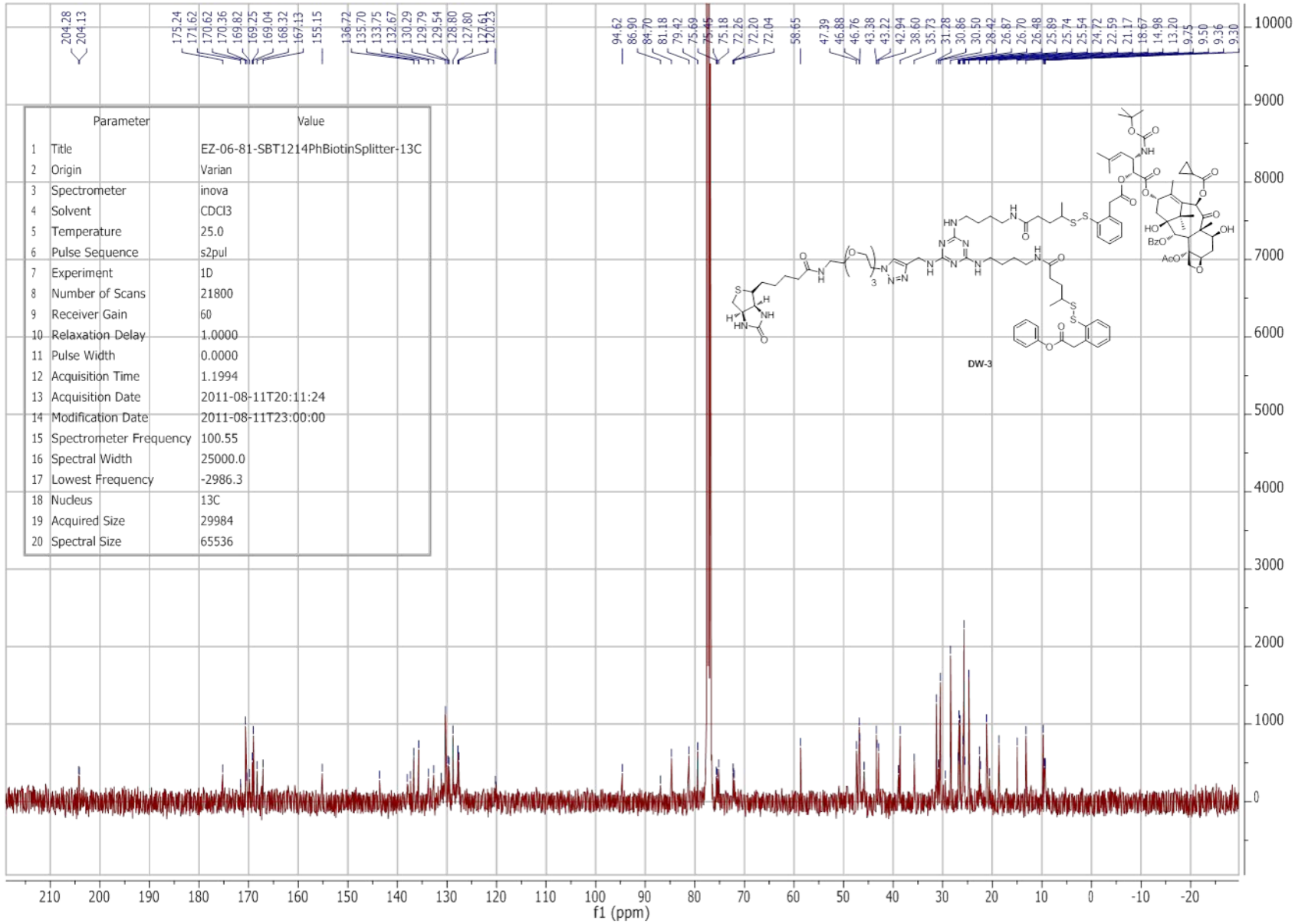
204.28
204.13
175.24
171.62
170.62
170.36
169.82
169.25
169.04
168.32
167.13
155.15
136.72
135.70
133.75
132.67
130.29
129.79
129.54
128.80
127.80
127.61
120.25
94.62
86.90
84.70
81.18
79.42
75.69
75.45
75.18
72.26
72.20
72.04
58.65
47.39
46.88
46.76
43.38
43.22
42.94
38.60
35.73
31.28
30.86
30.50
28.42
26.87
26.70
26.48
25.89
25.74
25.54
24.72
22.59
21.17
18.67
14.98
13.20
9.75
9.50
9.36
9.30
Parameter Value
1 Title EZ-06-81-SBT1214PhBiotinSplitter-13C
2 Origin Varian
3 Spectrometer inova
4 Solvent CDCl3
5 Temperature 25.0
6 Pulse Sequence s2pul
7 Experiment 1D
8 Number of Scans 21800
9 Receiver Gain 60
10 Relaxation Delay 1.0000
11 Pulse Width 0.0000
12 Acquisition Time 1.1994
13 Acquisition Date 2011-08-11T20:11:24
14 Modification Date 2011-08-11T23:00:00
15 Spectrometer Frequency 100.55
16 Spectral Width 25000.0
17 Lowest Frequency -2986.3
18 Nucleus 13C
19 Acquired Size 29984
20 Spectral Size 65536
DW-3
10000
9000
8000
7000
6000
5000
4000
3000
2000
1000
0
210
200
190
180
170
160
150
140
130
120
110
100
90
80
70
60
50
40
30
20
10
0
-10
-20
f1 (ppm)

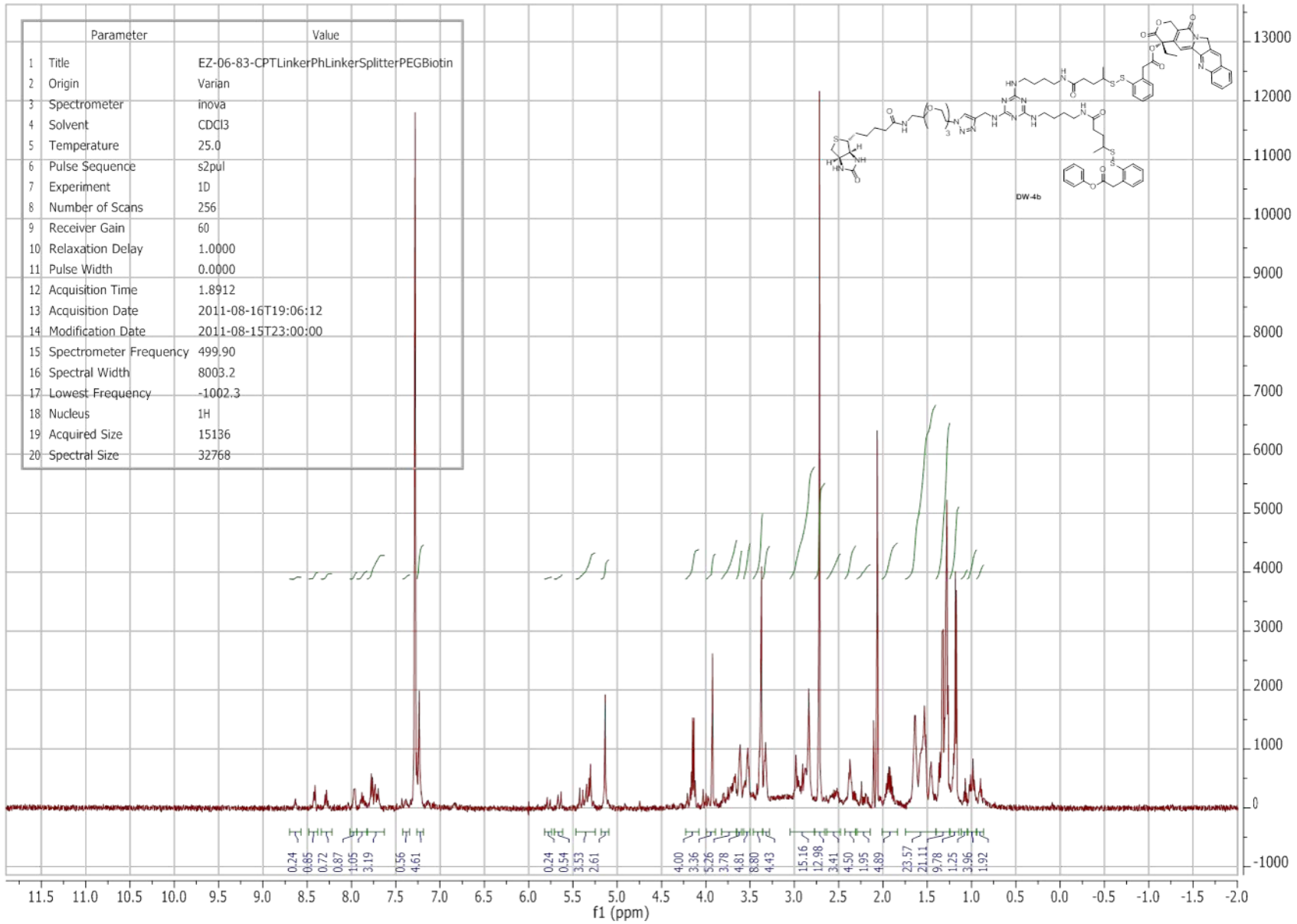
Parameter Value
1 Title EZ-06-83-CPTLinkerPhLinkerSplitterPEGBiotin
2 Origin Varian
3 Spectrometer inova
4 Solvent CDCl3
5 Temperature 25.0
6 Pulse Sequence s2pul
7 Experiment 1D
8 Number of Scans 256
9 Receiver Gain 60
10 Relaxation Delay 1.0000
11 Pulse Width 0.0000
12 Acquisition Time 1.8912
13 Acquisition Date 2011-08-16T19:06:12
14 Modification Date 2011-08-15T23:00:00
15 Spectrometer Frequency 499.90
16 Spectral Width 8003.2
17 Lowest Frequency -1002.3
18 Nucleus 1H
19 Acquired Size 15136
20 Spectral Size 32768
DW-4b
f1 (ppm)

Appendix 7
Chapter 8 NMR Spectra

	Parameter	Value
1	Title	EZ-05-73-BiotinPEGTriazine
2	Origin	Varian
3	Spectrometer	inova
4	Solvent	CDCl3
5	Temperature	25.0
6	Pulse Sequence	s2pul
7	Experiment	1D
8	Number of Scans	32
9	Receiver Gain	56
10	Relaxation Delay	1.0000
11	Pulse Width	0.0000
12	Acquisition Time	1.8920
13	Acquisition Date	2010-04-13T17:53:52
14	Modification Date	2010-04-12T23:00:00
15	Spectrometer Frequency	499.90
16	Spectral Width	7998.4
17	Lowest Frequency	-999.9
18	Nucleus	1H
19	Acquired Size	15133
20	Spectral Size	32768

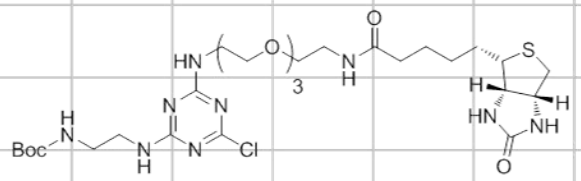

8-1

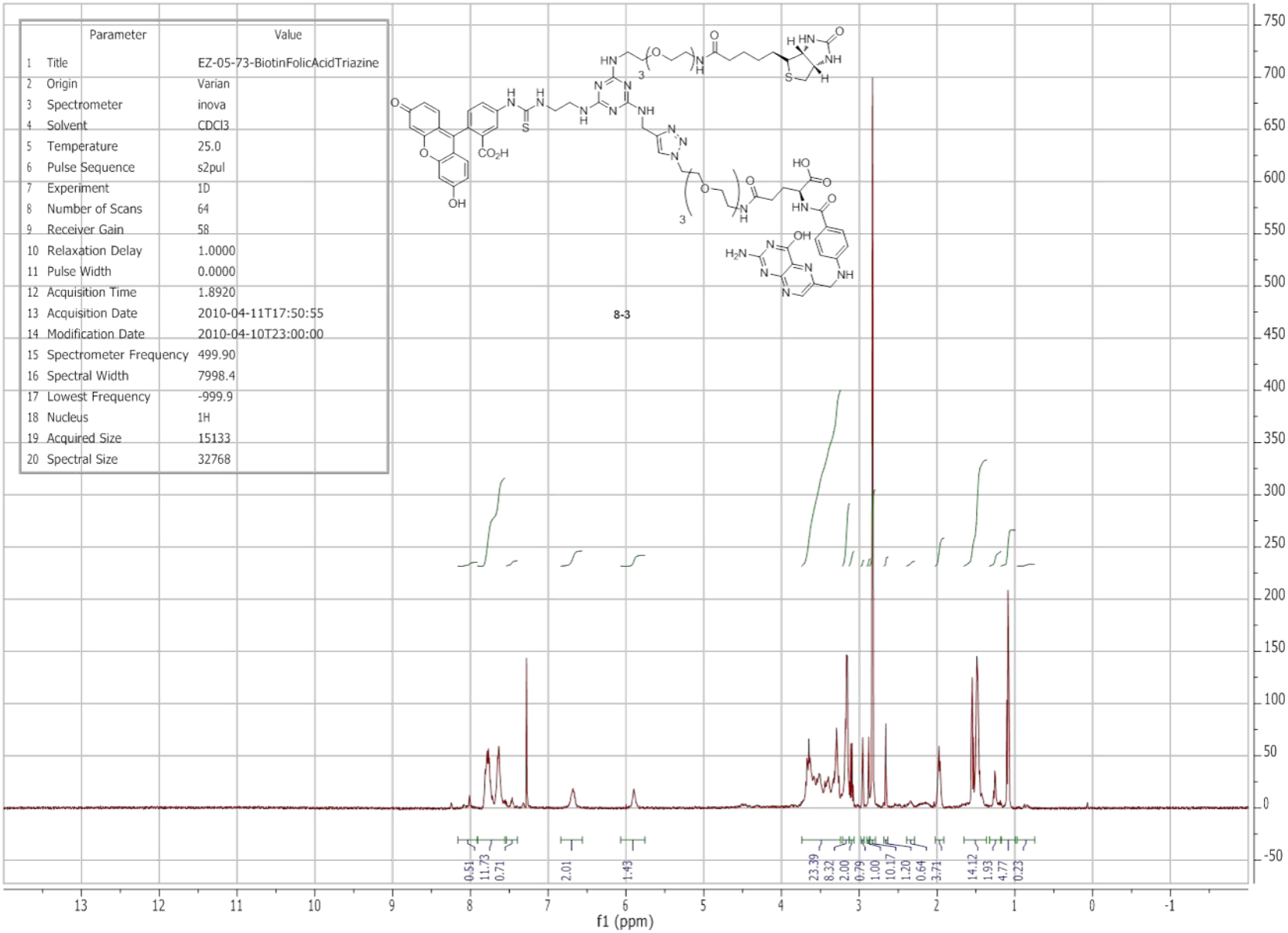
Parameter Value
1 Title EZ-05-73-BiotinFolicAcidTriazine
2 Origin Varian
3 Spectrometer inova
4 Solvent CDCl3
5 Temperature 25.0
6 Pulse Sequence s2pul
7 Experiment 1D
8 Number of Scans 64
9 Receiver Gain 58
10 Relaxation Delay 1.0000
11 Pulse Width 0.0000
12 Acquisition Time 1.8920
13 Acquisition Date 2010-04-11T17:50:55
14 Modification Date 2010-04-10T23:00:00
15 Spectrometer Frequency 499.90
16 Spectral Width 7998.4
17 Lowest Frequency -999.9
18 Nucleus 1H
19 Acquired Size 15133
20 Spectral Size 32768
8-3
f1 (ppm)

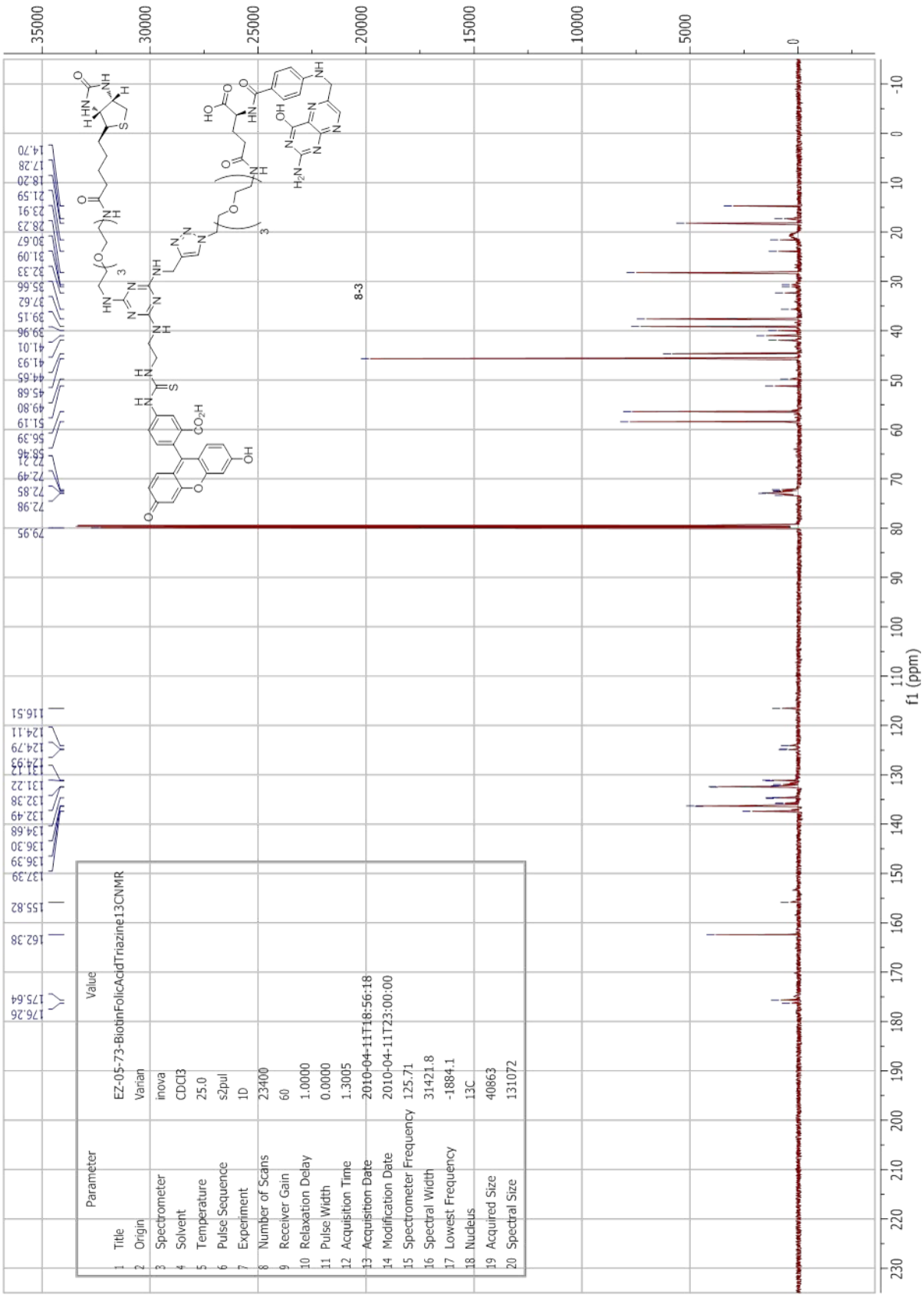
Parameter Value
1 Title EZ-05-73-BiotinFolicAcidTriazine13CNMR
2 Origin Varian
3 Spectrometer inova
4 Solvent CDCl3
5 Temperature 25.0
6 Pulse Sequence s2pul
7 Experiment 1D
8 Number of Scans 23400
9 Receiver Gain 60
10 Relaxation Delay 1.0000
11 Pulse Width 0.0000
12 Acquisition Time 1.3005
13 Acquisition Date 2010-04-11T18:56:18
14 Modification Date 2010-04-11T23:00:00
15 Spectrometer Frequency 125.71
16 Spectral Width 31421.8
17 Lowest Frequency -1884.1
18 Nucleus 13C
19 Acquired Size 40863
20 Spectral Size 131072
8-3
f1 (ppm)

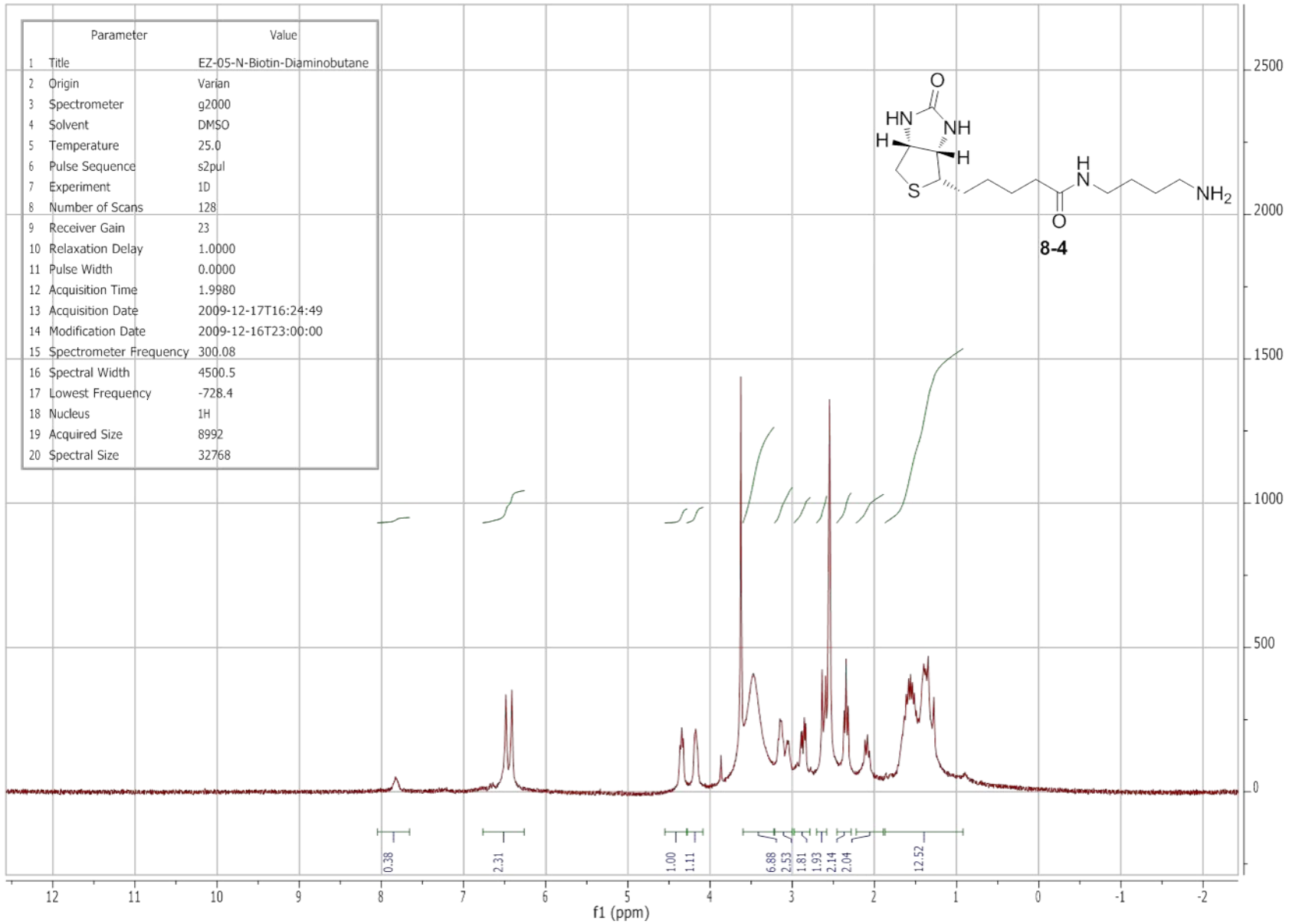
Parameter Value
1 Title EZ-05-N-Biotin-Diaminobutane
2 Origin Varian
3 Spectrometer g2000
4 Solvent DMSO
5 Temperature 25.0
6 Pulse Sequence s2pul
7 Experiment 1D
8 Number of Scans 128
9 Receiver Gain 23
10 Relaxation Delay 1.0000
11 Pulse Width 0.0000
12 Acquisition Time 1.9980
13 Acquisition Date 2009-12-17T16:24:49
14 Modification Date 2009-12-16T23:00:00
15 Spectrometer Frequency 300.08
16 Spectral Width 4500.5
17 Lowest Frequency -728.4
18 Nucleus 1H
19 Acquired Size 8992
20 Spectral Size 32768
O
HN
NH
H
H
S
H
N
O
NH2
8-4
2500
2000
1500
1000
500
0
0.38
2.31
1.00
1.11
6.88
2.53
1.81
1.93
2.14
2.04
12.52
12
11
10
9
8
7
6
5
4
3
2
1
0
-1
-2
f1 (ppm)

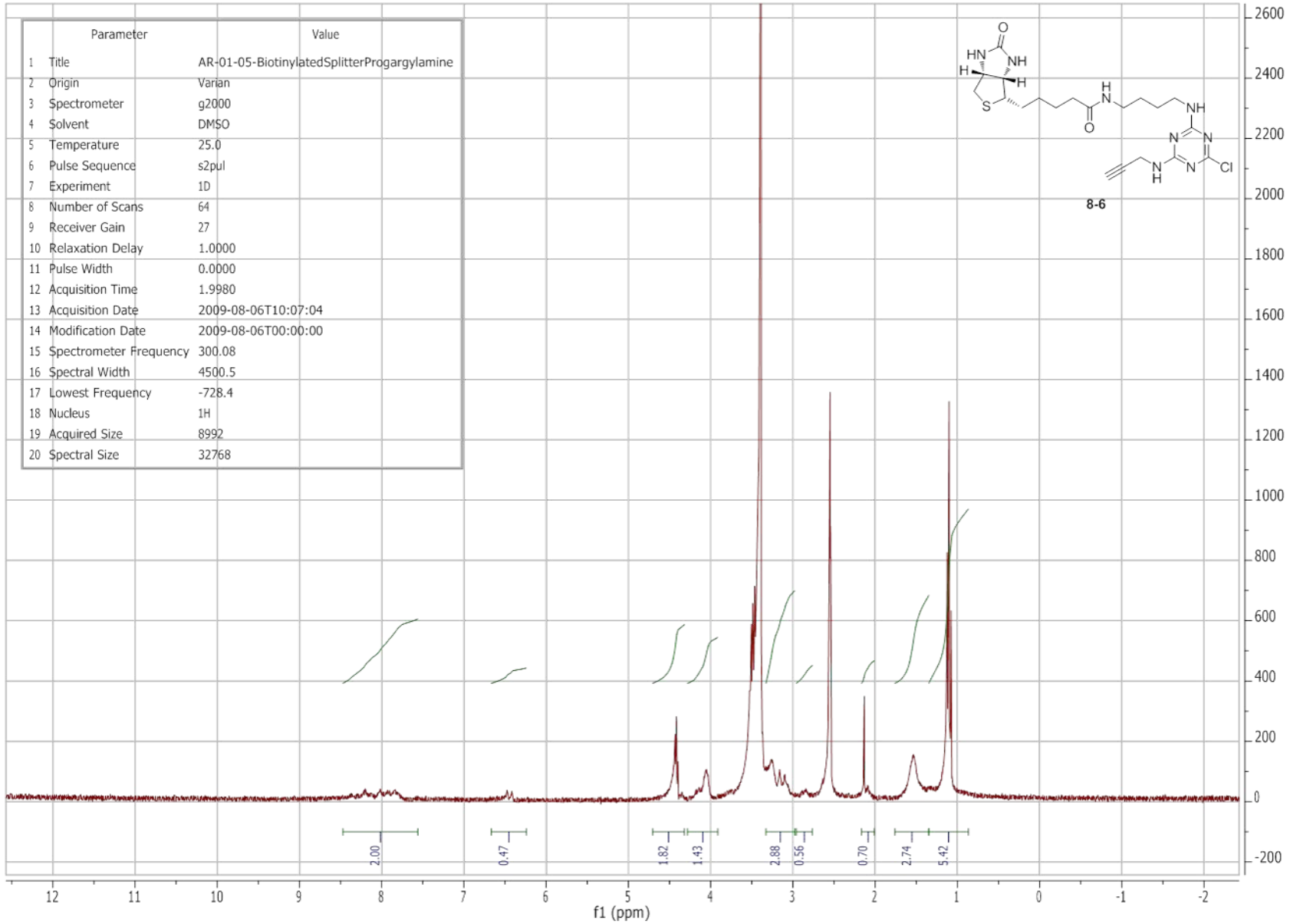
Parameter Value
1 Title AR-01-05-BiotinylatedSplitterProgargylamine
2 Origin Varian
3 Spectrometer g2000
4 Solvent DMSO
5 Temperature 25.0
6 Pulse Sequence s2pul
7 Experiment 1D
8 Number of Scans 64
9 Receiver Gain 27
10 Relaxation Delay 1.0000
11 Pulse Width 0.0000
12 Acquisition Time 1.9980
13 Acquisition Date 2009-08-06T10:07:04
14 Modification Date 2009-08-06T00:00:00
15 Spectrometer Frequency 300.08
16 Spectral Width 4500.5
17 Lowest Frequency -728.4
18 Nucleus 1H
19 Acquired Size 8992
20 Spectral Size 32768
8-6
2.00
0.47
1.82
1.43
2.88
0.56
0.70
2.74
5.42
f1 (ppm)

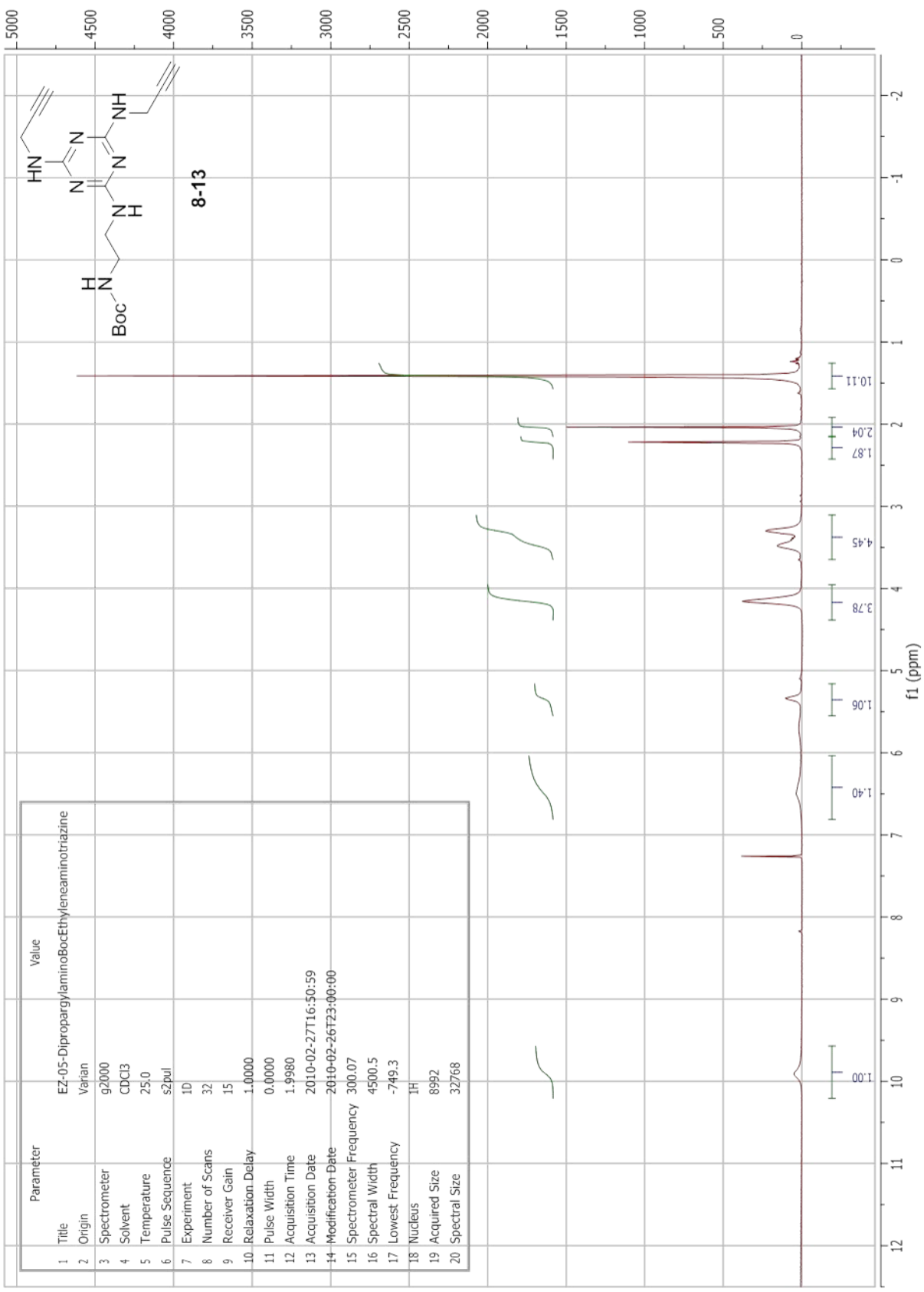

	Parameter	Value
1	Title	EZ-05-DipropargylaminoBocEthyleneaminotriazine
2	Origin	Varian
3	Spectrometer	g2000
4	Solvent	CDCl3
5	Temperature	25.0
6	Pulse Sequence	s2pul
7	Experiment	1D
8	Number of Scans	32
9	Receiver Gain	15
10	Relaxation Delay	1.0000
11	Pulse Width	0.0000
12	Acquisition Time	1.9980
13	Acquisition Date	2010-02-27T16:50:59
14	Modification Date	2010-02-26T23:00:00
15	Spectrometer Frequency	300.07
16	Spectral Width	4500.5
17	Lowest Frequency	-749.3
18	Nucleus	1H
19	Acquired Size	8992
20	Spectral Size	32768

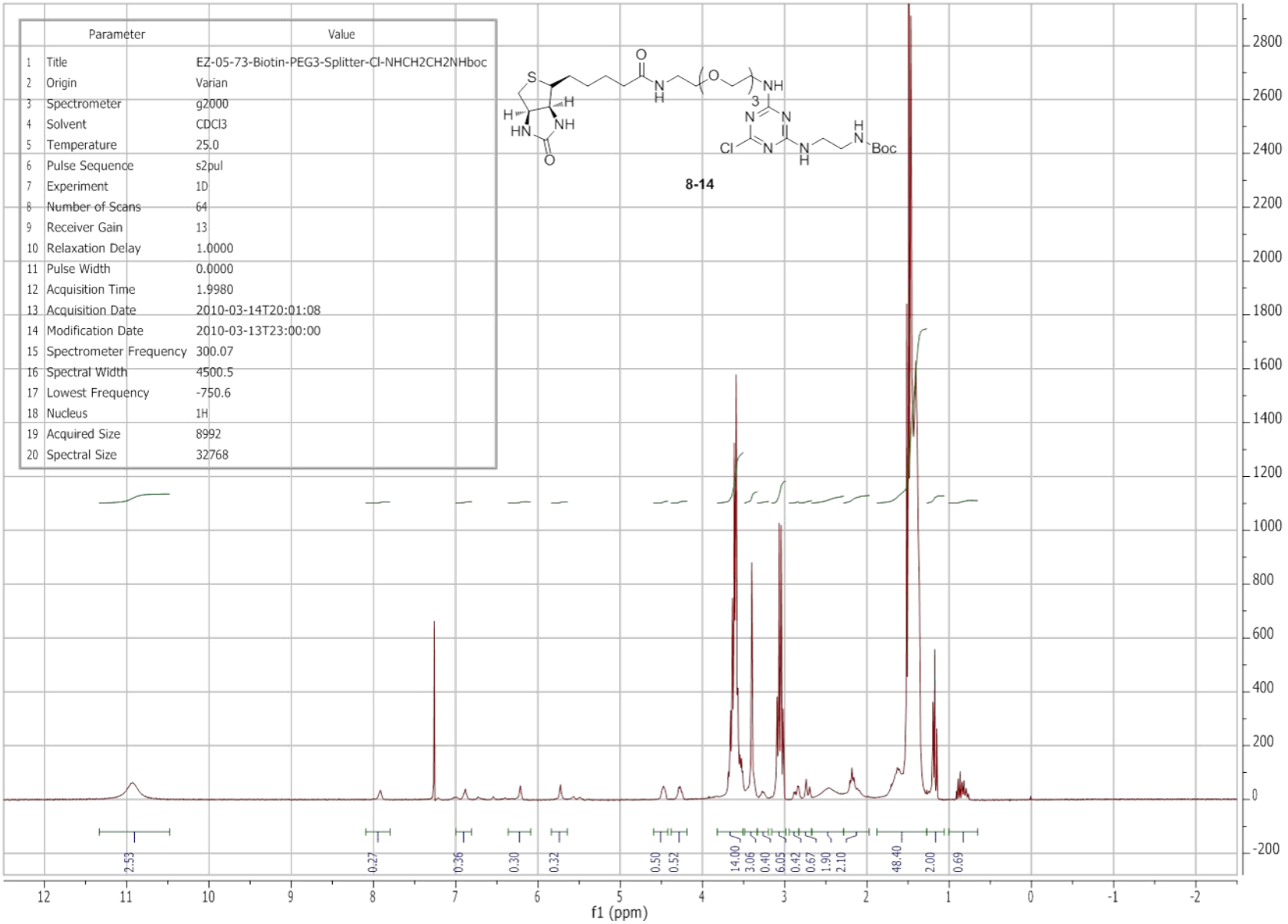
Parameter Value
1 Title EZ-05-73-Biotin-PEG3-Splitter-Cl-NHCH2CH2NHboc
2 Origin Varian
3 Spectrometer g2000
4 Solvent CDCl3
5 Temperature 25.0
6 Pulse Sequence s2pul
7 Experiment 1D
8 Number of Scans 64
9 Receiver Gain 13
10 Relaxation Delay 1.0000
11 Pulse Width 0.0000
12 Acquisition Time 1.9980
13 Acquisition Date 2010-03-14T20:01:08
14 Modification Date 2010-03-13T23:00:00
15 Spectrometer Frequency 300.07
16 Spectral Width 4500.5
17 Lowest Frequency -750.6
18 Nucleus 1H
19 Acquired Size 8992
20 Spectral Size 32768
8-14
2.53
0.27
0.36
0.30
0.32
0.50
0.52
14.00
3.06
0.40
6.05
0.42
0.67
1.90
2.10
48.40
2.00
0.69
f1 (ppm)

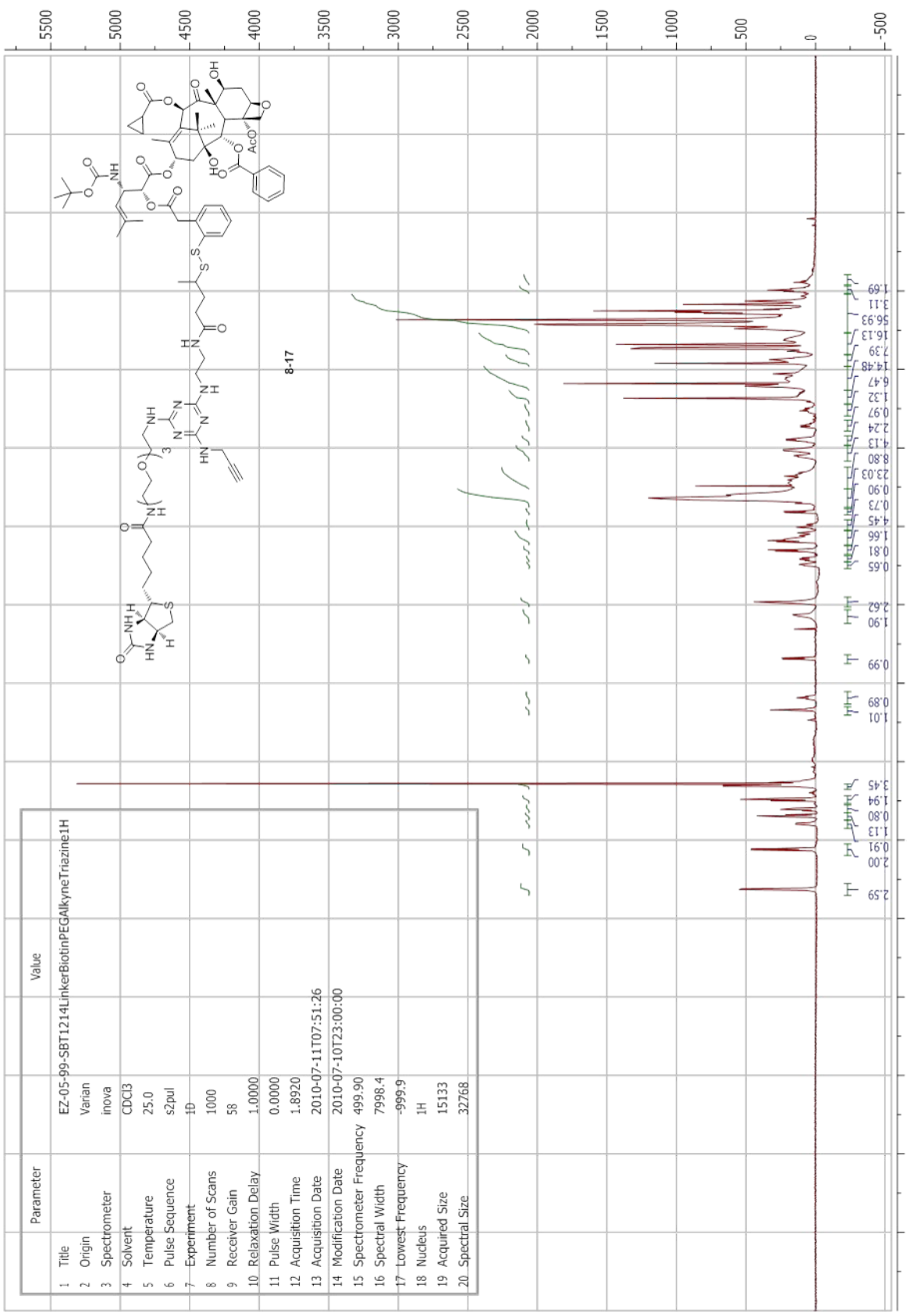
Parameter
Value
1 Title EZ-05-99-SBT1214LinkerBiotinPEGAlkyneTriazine1H
2 Origin Varian
3 Spectrometer inova
4 Solvent CDCl3
5 Temperature 25.0
6 Pulse Sequence s2pul
7 Experiment 1D
8 Number of Scans 1000
9 Receiver Gain 58
10 Relaxation Delay 1.0000
11 Pulse Width 0.0000
12 Acquisition Time 1.8920
13 Acquisition Date 2010-07-11T07:51:26
14 Modification Date 2010-07-10T23:00:00
15 Spectrometer Frequency 499.90
16 Spectral Width 7998.4
17 Lowest Frequency -999.9
18 Nucleus 1H
19 Acquired Size 15133
20 Spectral Size 32768
8-17
f1 (ppm)

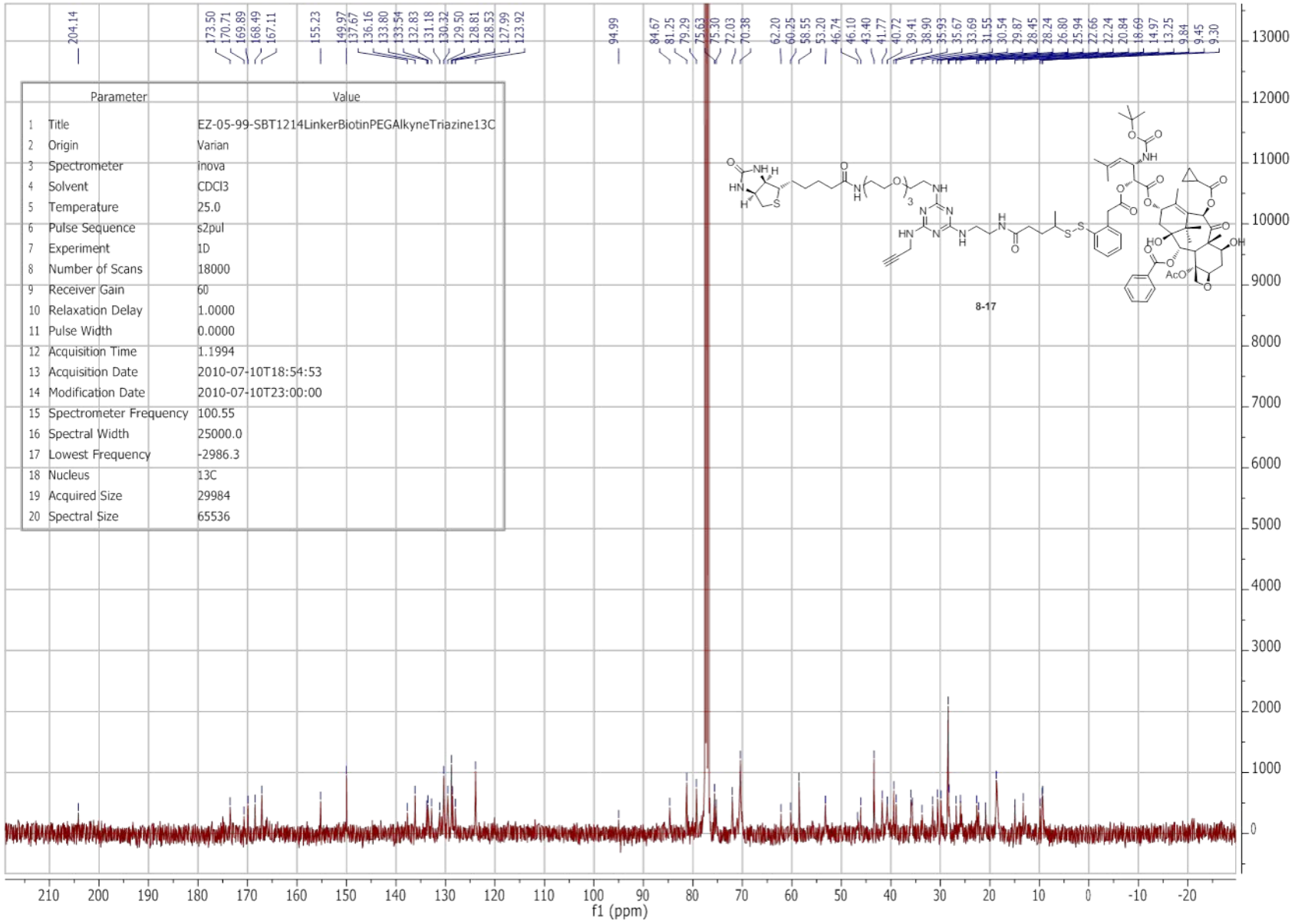
204.14
173.50
170.71
169.89
168.49
167.11
155.23
149.97
137.67
136.16
133.80
133.54
132.83
131.18
130.32
129.50
128.81
128.53
127.99
123.92
94.99
84.67
81.25
79.29
75.63
75.30
72.03
70.38
62.20
60.25
58.55
53.20
46.74
46.10
43.40
41.77
40.72
39.41
38.90
35.93
35.67
33.69
31.55
30.54
29.87
28.45
28.24
26.80
25.94
22.66
22.24
20.84
18.69
14.97
13.25
9.84
9.45
9.30
Parameter
Value
1 Title EZ-05-99-SBT1214LinkerBiotinPEGAlkyneTriazine13C
2 Origin Varian
3 Spectrometer inova
4 Solvent CDCl3
5 Temperature 25.0
6 Pulse Sequence s2pul
7 Experiment 1D
8 Number of Scans 18000
9 Receiver Gain 60
10 Relaxation Delay 1.0000
11 Pulse Width 0.0000
12 Acquisition Time 1.1994
13 Acquisition Date 2010-07-10T18:54:53
14 Modification Date 2010-07-10T23:00:00
15 Spectrometer Frequency 100.55
16 Spectral Width 25000.0
17 Lowest Frequency -2986.3
18 Nucleus 13C
19 Acquired Size 29984
20 Spectral Size 65536
8-17
13000
12000
11000
10000
9000
8000
7000
6000
5000
4000
3000
2000
1000
0
210
200
190
180
170
160
150
140
130
120
110
100
90
80
70
60
50
40
30
20
10
0
-10
-20
f1 (ppm)

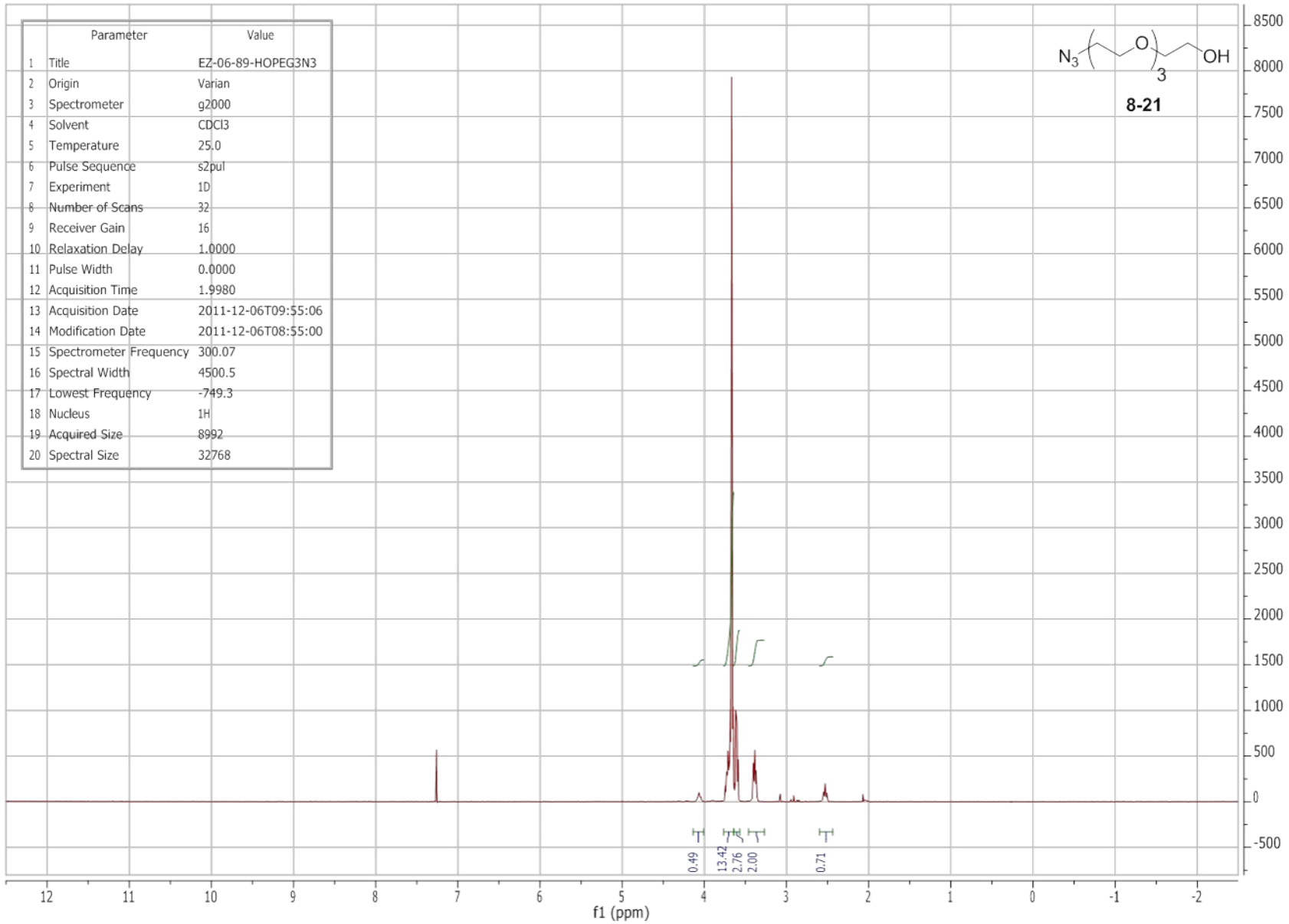
Parameter Value
1 Title EZ-06-89-HOPEG3N3
2 Origin Varian
3 Spectrometer g2000
4 Solvent CDCl3
5 Temperature 25.0
6 Pulse Sequence s2pul
7 Experiment 1D
8 Number of Scans 32
9 Receiver Gain 16
10 Relaxation Delay 1.0000
11 Pulse Width 0.0000
12 Acquisition Time 1.9980
13 Acquisition Date 2011-12-06T09:55:06
14 Modification Date 2011-12-06T08:55:00
15 Spectrometer Frequency 300.07
16 Spectral Width 4500.5
17 Lowest Frequency -749.3
18 Nucleus 1H
19 Acquired Size 8992
20 Spectral Size 32768
N3
O
3
OH
8-21
0.49
13.42
2.76
2.00
0.71
f1 (ppm)

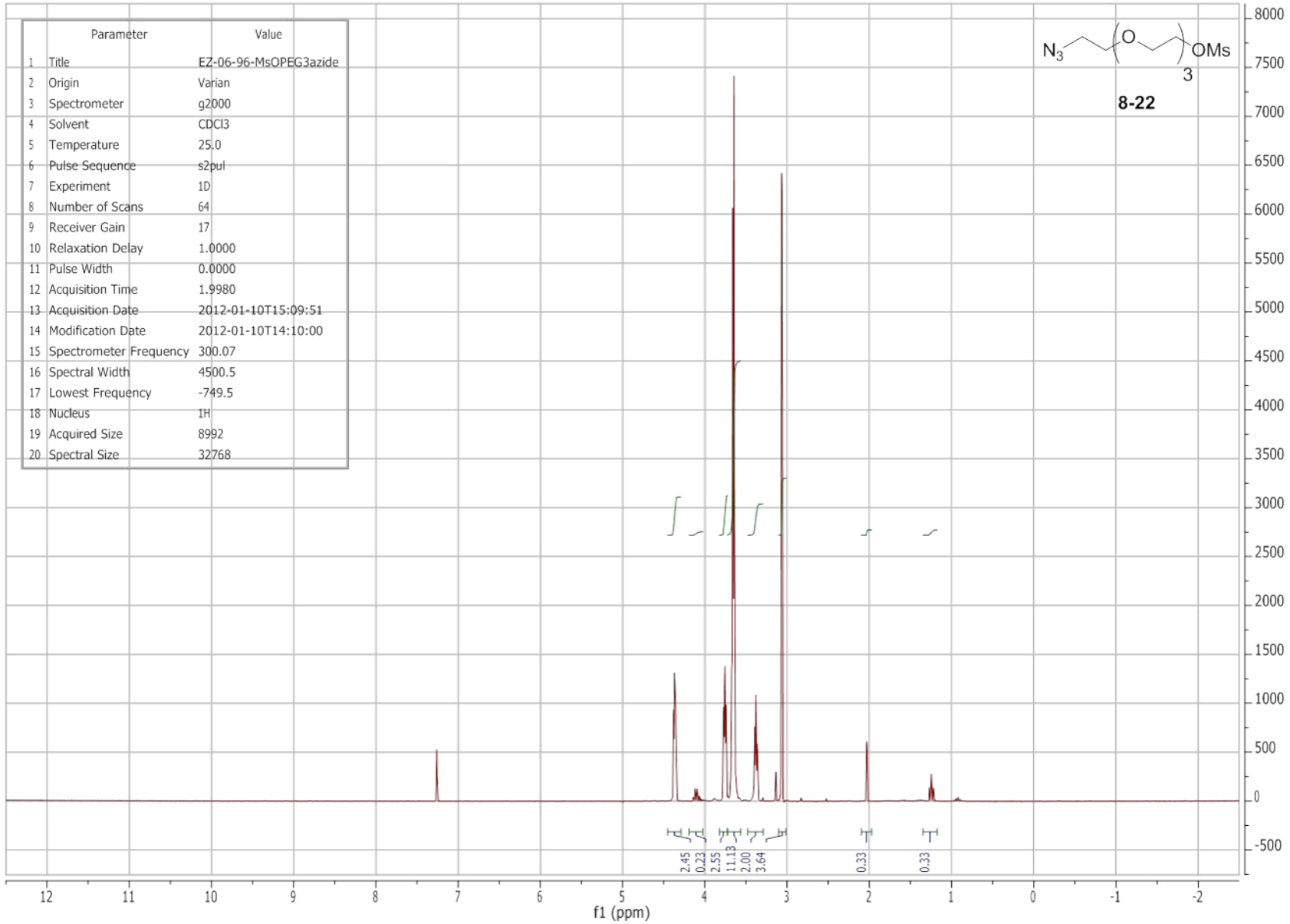
Parameter Value
1 Title EZ-06-96-MsOPEG3azide
2 Origin Varian
3 Spectrometer g2000
4 Solvent CDCl3
5 Temperature 25.0
6 Pulse Sequence s2pul
7 Experiment 1D
8 Number of Scans 64
9 Receiver Gain 17
10 Relaxation Delay 1.0000
11 Pulse Width 0.0000
12 Acquisition Time 1.9980
13 Acquisition Date 2012-01-10T15:09:51
14 Modification Date 2012-01-10T14:10:00
15 Spectrometer Frequency 300.07
16 Spectral Width 4500.5
17 Lowest Frequency -749.5
18 Nucleus 1H
19 Acquired Size 8992
20 Spectral Size 32768
N3
O
OMs
3
8-22
2.45
0.23
2.55
11.13
2.00
3.64
0.33
0.33
f1 (ppm)

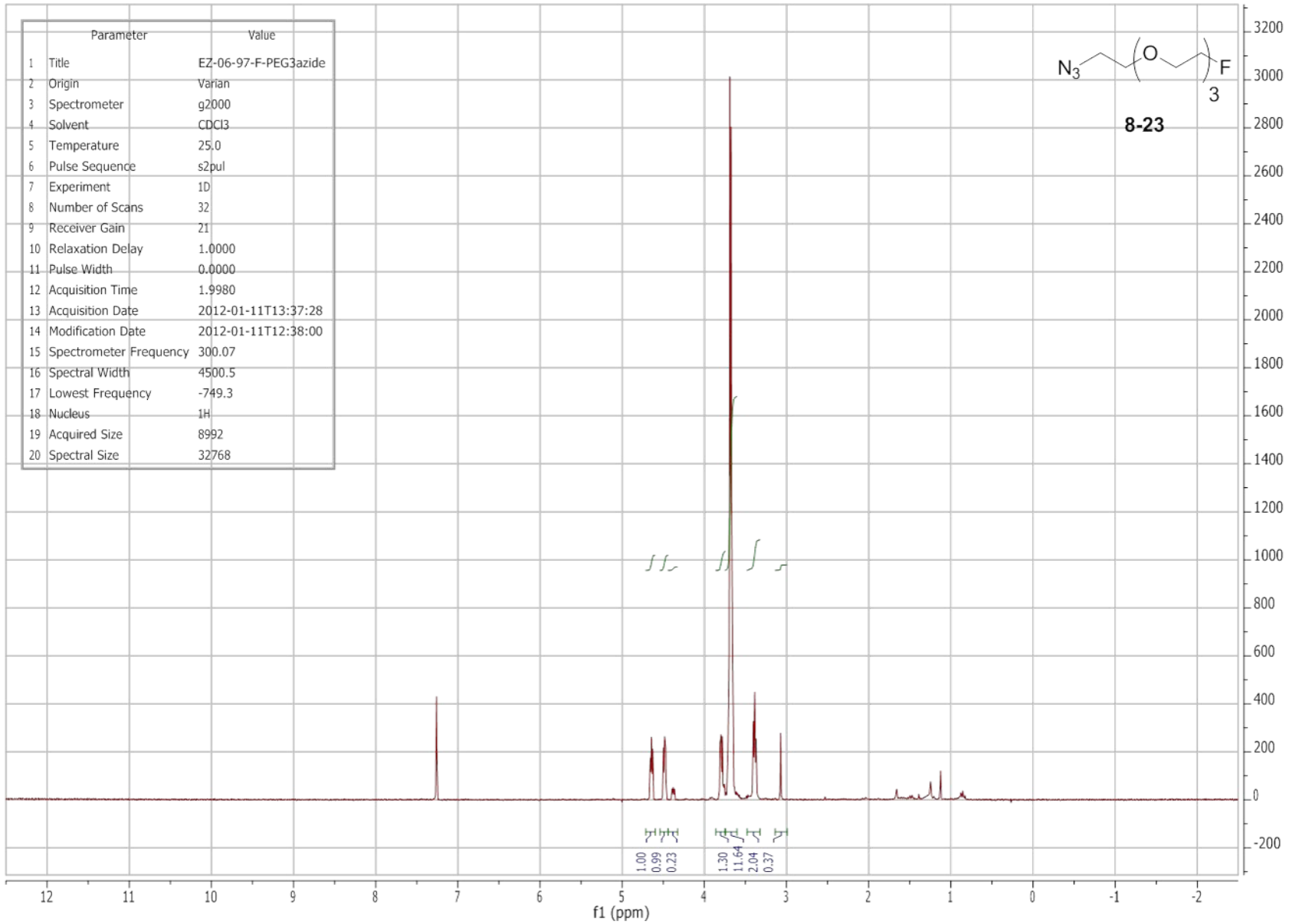
Parameter Value
1 Title EZ-06-97-F-PEG3azide
2 Origin Varian
3 Spectrometer g2000
4 Solvent CDCl3
5 Temperature 25.0
6 Pulse Sequence s2pul
7 Experiment 1D
8 Number of Scans 32
9 Receiver Gain 21
10 Relaxation Delay 1.0000
11 Pulse Width 0.0000
12 Acquisition Time 1.9980
13 Acquisition Date 2012-01-11T13:37:28
14 Modification Date 2012-01-11T12:38:00
15 Spectrometer Frequency 300.07
16 Spectral Width 4500.5
17 Lowest Frequency -749.3
18 Nucleus 1H
19 Acquired Size 8992
20 Spectral Size 32768
N3
O
F
3
8-23
1.00
0.99
0.23
1.30
11.64
2.04
0.37
f1 (ppm)

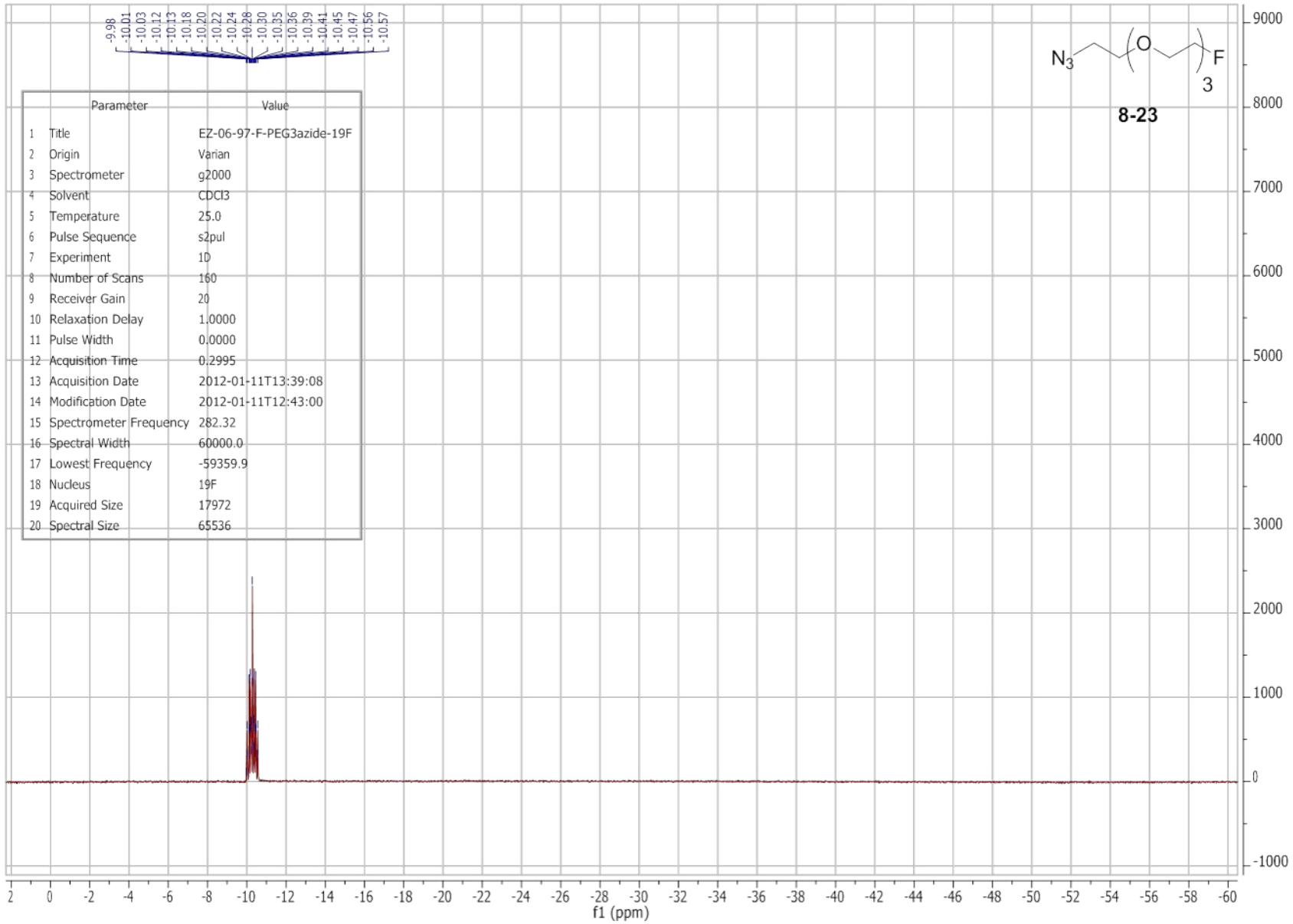
-9.98
-10.01
-10.03
-10.12
-10.13
-10.18
-10.20
-10.22
-10.24
-10.28
-10.30
-10.35
-10.36
-10.39
-10.41
-10.45
-10.47
-10.56
-10.57
Parameter Value
1 Title EZ-06-97-F-PEG3azide-19F
2 Origin Varian
3 Spectrometer g2000
4 Solvent CDCl3
5 Temperature 25.0
6 Pulse Sequence s2pul
7 Experiment 1D
8 Number of Scans 160
9 Receiver Gain 20
10 Relaxation Delay 1.0000
11 Pulse Width 0.0000
12 Acquisition Time 0.2995
13 Acquisition Date 2012-01-11T13:39:08
14 Modification Date 2012-01-11T12:43:00
15 Spectrometer Frequency 282.32
16 Spectral Width 60000.0
17 Lowest Frequency -59359.9
18 Nucleus 19F
19 Acquired Size 17972
20 Spectral Size 65536
N3
O
F
3
8-23
9000
8000
7000
6000
5000
4000
3000
2000
1000
0
-1000
2 0 -2 -4 -6 -8 -10 -12 -14 -16 -18 -20 -22 -24 -26 -28 -30 -32 -34 -36 -38 -40 -42 -44 -46 -48 -50 -52 -54 -56 -58 -60
f1 (ppm)

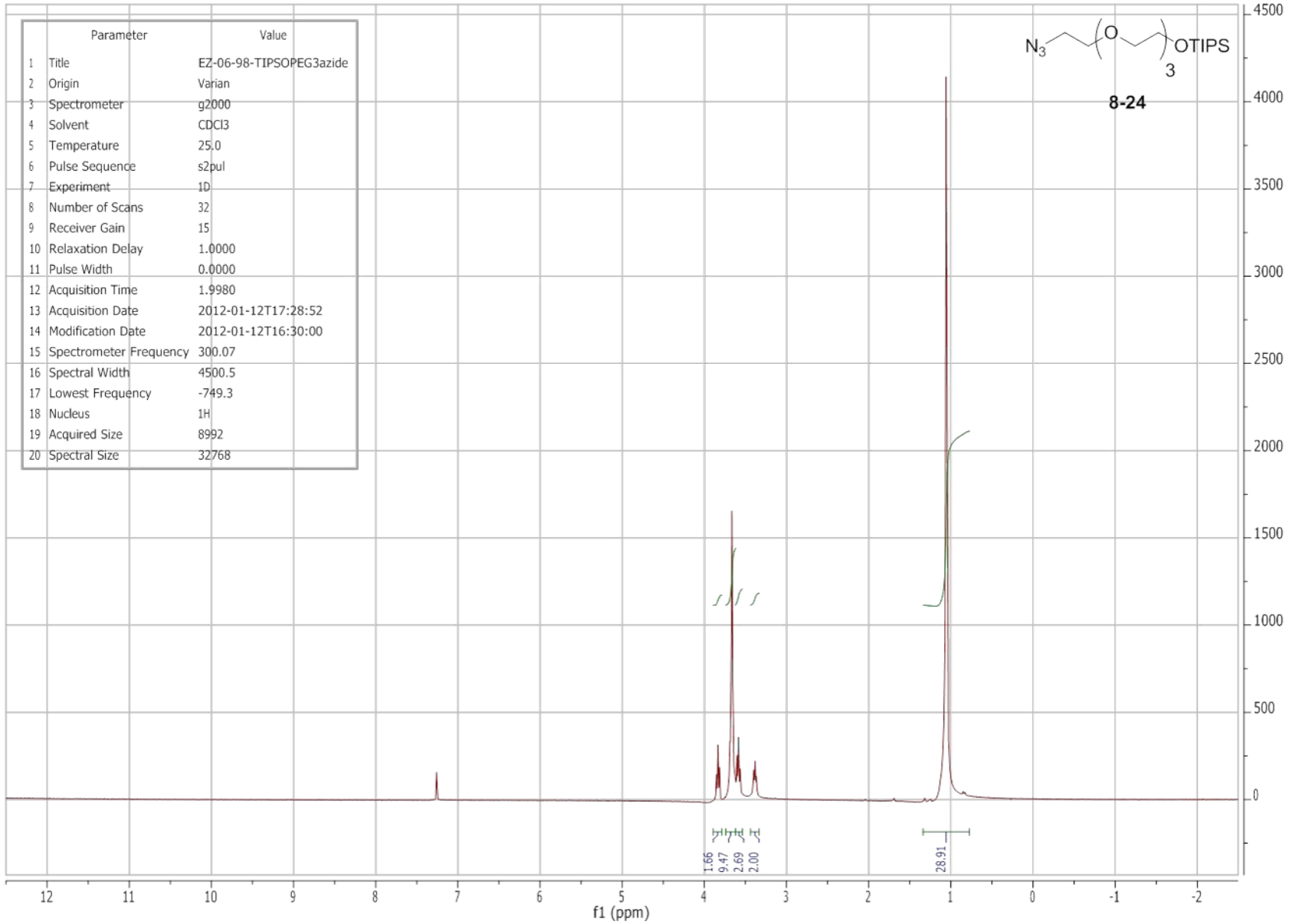
Parameter Value
1 Title EZ-06-98-TIPSOPEG3azide
2 Origin Varian
3 Spectrometer g2000
4 Solvent CDCl3
5 Temperature 25.0
6 Pulse Sequence s2pul
7 Experiment 1D
8 Number of Scans 32
9 Receiver Gain 15
10 Relaxation Delay 1.0000
11 Pulse Width 0.0000
12 Acquisition Time 1.9980
13 Acquisition Date 2012-01-12T17:28:52
14 Modification Date 2012-01-12T16:30:00
15 Spectrometer Frequency 300.07
16 Spectral Width 4500.5
17 Lowest Frequency -749.3
18 Nucleus 1H
19 Acquired Size 8992
20 Spectral Size 32768
N3
O
OTIPS
3
8-24
1.66
9.47
2.69
2.00
28.91
f1 (ppm)

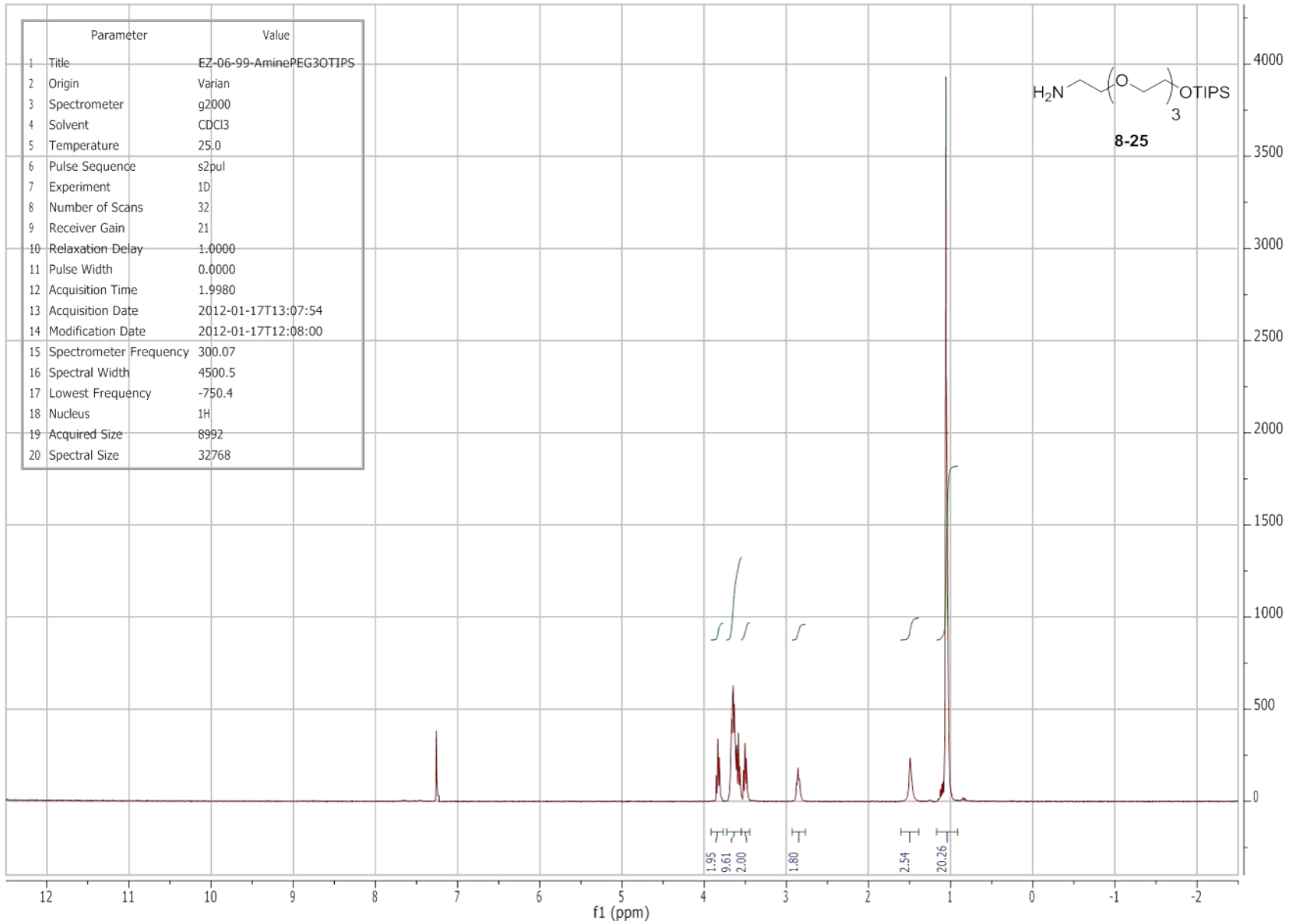
Parameter Value
1 Title EZ-06-99-AminePEG3OTIPS
2 Origin Varian
3 Spectrometer g2000
4 Solvent CDCl3
5 Temperature 25.0
6 Pulse Sequence s2pul
7 Experiment 1D
8 Number of Scans 32
9 Receiver Gain 21
10 Relaxation Delay 1.0000
11 Pulse Width 0.0000
12 Acquisition Time 1.9980
13 Acquisition Date 2012-01-17T13:07:54
14 Modification Date 2012-01-17T12:08:00
15 Spectrometer Frequency 300.07
16 Spectral Width 4500.5
17 Lowest Frequency -750.4
18 Nucleus 1H
19 Acquired Size 8992
20 Spectral Size 32768
H2N
O
3
OTIPS
8-25
1.95
9.61
2.00
1.80
2.54
20.26
f1 (ppm)

Appendix 8
Chapter 9 NMR Spectra

	Parameter	Value
1	Title	EZ-06-19-DiazidePEG3
2	Origin	Varian
3	Spectrometer	g2000
4	Solvent	CDCl3
5	Temperature	25.0
6	Pulse Sequence	s2pul
7	Experiment	1D
8	Number of Scans	16
9	Receiver Gain	3
10	Relaxation Delay	1.0000
11	Pulse Width	0.0000
12	Acquisition Time	1.9980
13	Acquisition Date	2010-11-06T18:00:30
14	Modification Date	2010-11-06T00:00:00
15	Spectrometer Frequency	300.07
16	Spectral Width	4500.5
17	Lowest Frequency	-749.5
18	Nucleus	1H
19	Acquired Size	8992
20	Spectral Size	32768

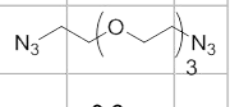

9-2

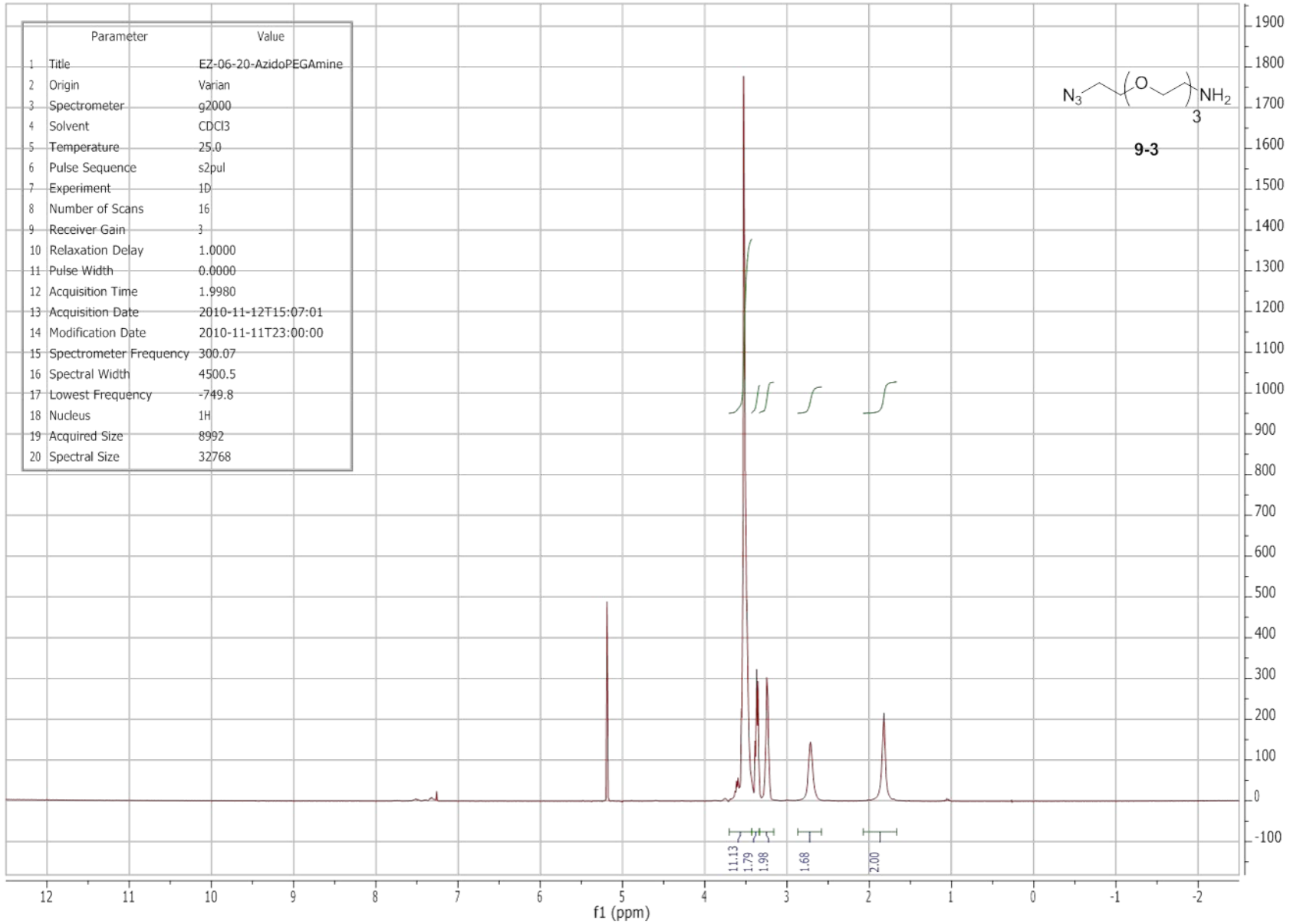
Parameter Value
1 Title EZ-06-20-AzidoPEGAmine
2 Origin Varian
3 Spectrometer g2000
4 Solvent CDCl3
5 Temperature 25.0
6 Pulse Sequence s2pul
7 Experiment 1D
8 Number of Scans 16
9 Receiver Gain 3
10 Relaxation Delay 1.0000
11 Pulse Width 0.0000
12 Acquisition Time 1.9980
13 Acquisition Date 2010-11-12T15:07:01
14 Modification Date 2010-11-11T23:00:00
15 Spectrometer Frequency 300.07
16 Spectral Width 4500.5
17 Lowest Frequency -749.8
18 Nucleus 1H
19 Acquired Size 8992
20 Spectral Size 32768
N3
O
NH2
3
9-3
11.13
1.79
1.98
1.68
2.00
f1 (ppm)

	Parameter	Value
1	Title	EZ-06-21-AzidePEGAcid
2	Origin	Varian
3	Spectrometer	g2000
4	Solvent	CDCl3
5	Temperature	25.0
6	Pulse Sequence	s2pul
7	Experiment	1D
8	Number of Scans	64
9	Receiver Gain	15
10	Relaxation Delay	1.0000
11	Pulse Width	0.0000
12	Acquisition Time	1.9980
13	Acquisition Date	2010-11-17T16:55:27
14	Modification Date	2010-11-16T23:00:00
15	Spectrometer Frequency	300.07
16	Spectral Width	4500.5
17	Lowest Frequency	-749.3
18	Nucleus	1H
19	Acquired Size	8992
20	Spectral Size	32768

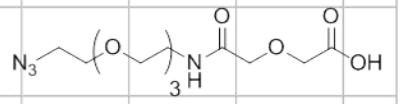

9-4

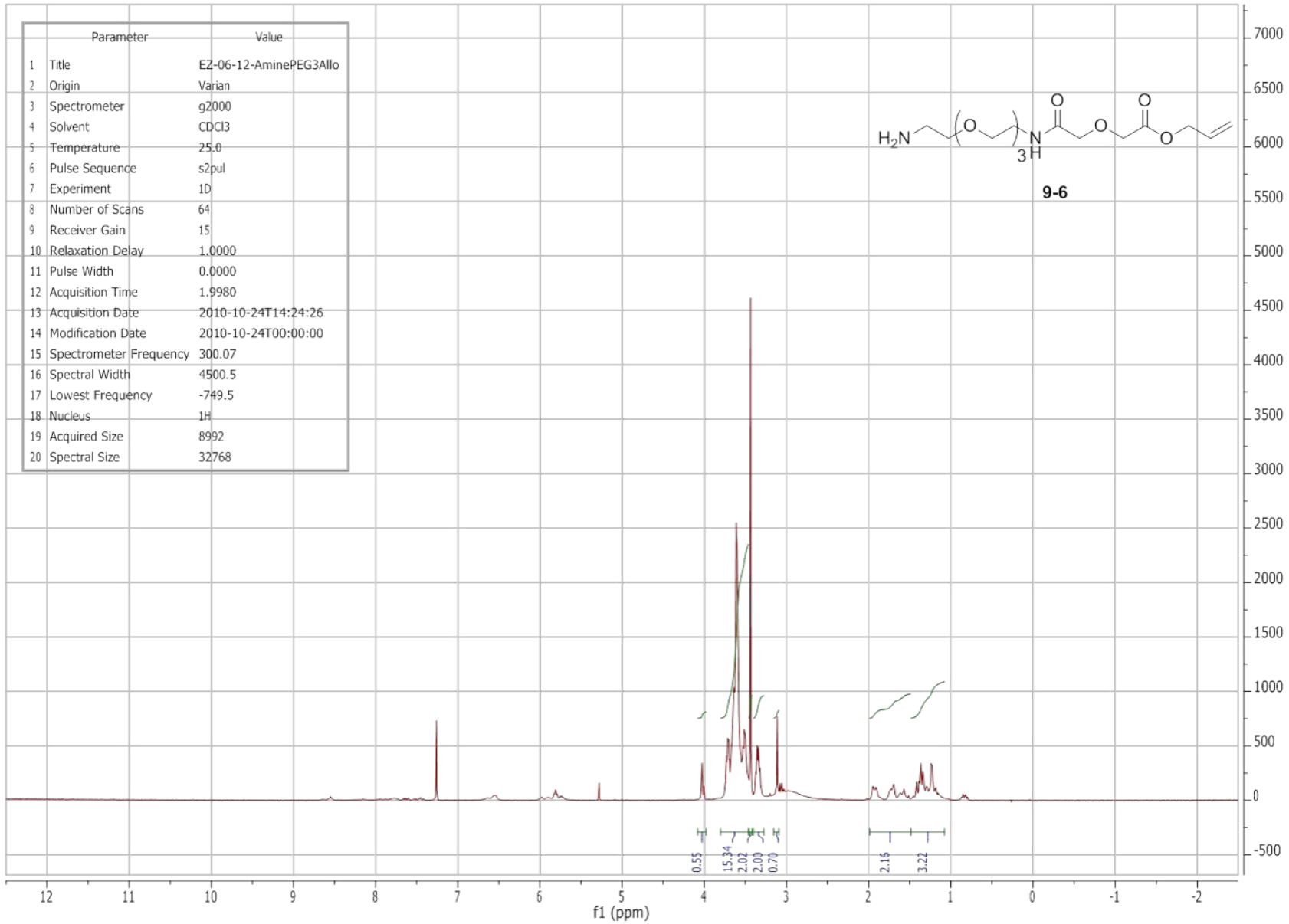
Parameter Value
1 Title EZ-06-12-AminePEG3Allo
2 Origin Varian
3 Spectrometer g2000
4 Solvent CDCl3
5 Temperature 25.0
6 Pulse Sequence s2pul
7 Experiment 1D
8 Number of Scans 64
9 Receiver Gain 15
10 Relaxation Delay 1.0000
11 Pulse Width 0.0000
12 Acquisition Time 1.9980
13 Acquisition Date 2010-10-24T14:24:26
14 Modification Date 2010-10-24T00:00:00
15 Spectrometer Frequency 300.07
16 Spectral Width 4500.5
17 Lowest Frequency -749.5
18 Nucleus 1H
19 Acquired Size 8992
20 Spectral Size 32768
9-6
0.55
15.34
2.02
2.00
0.70
2.16
3.22
f1 (ppm)

	Parameter	Value
1	Title	EZ-06-17-AcidPEG3Allo
2	Origin	Varian
3	Spectrometer	g2000
4	Solvent	CDCl3
5	Temperature	25.0
6	Pulse Sequence	s2pul
7	Experiment	1D
8	Number of Scans	128
9	Receiver Gain	11
10	Relaxation Delay	1.0000
11	Pulse Width	0.0000
12	Acquisition Time	1.9980
13	Acquisition Date	2010-10-30T16:21:20
14	Modification Date	2010-10-30T00:00:00
15	Spectrometer Frequency	300.07
16	Spectral Width	4500.5
17	Lowest Frequency	-749.3
18	Nucleus	1H
19	Acquired Size	8992
20	Spectral Size	32768

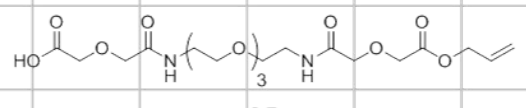

9-7

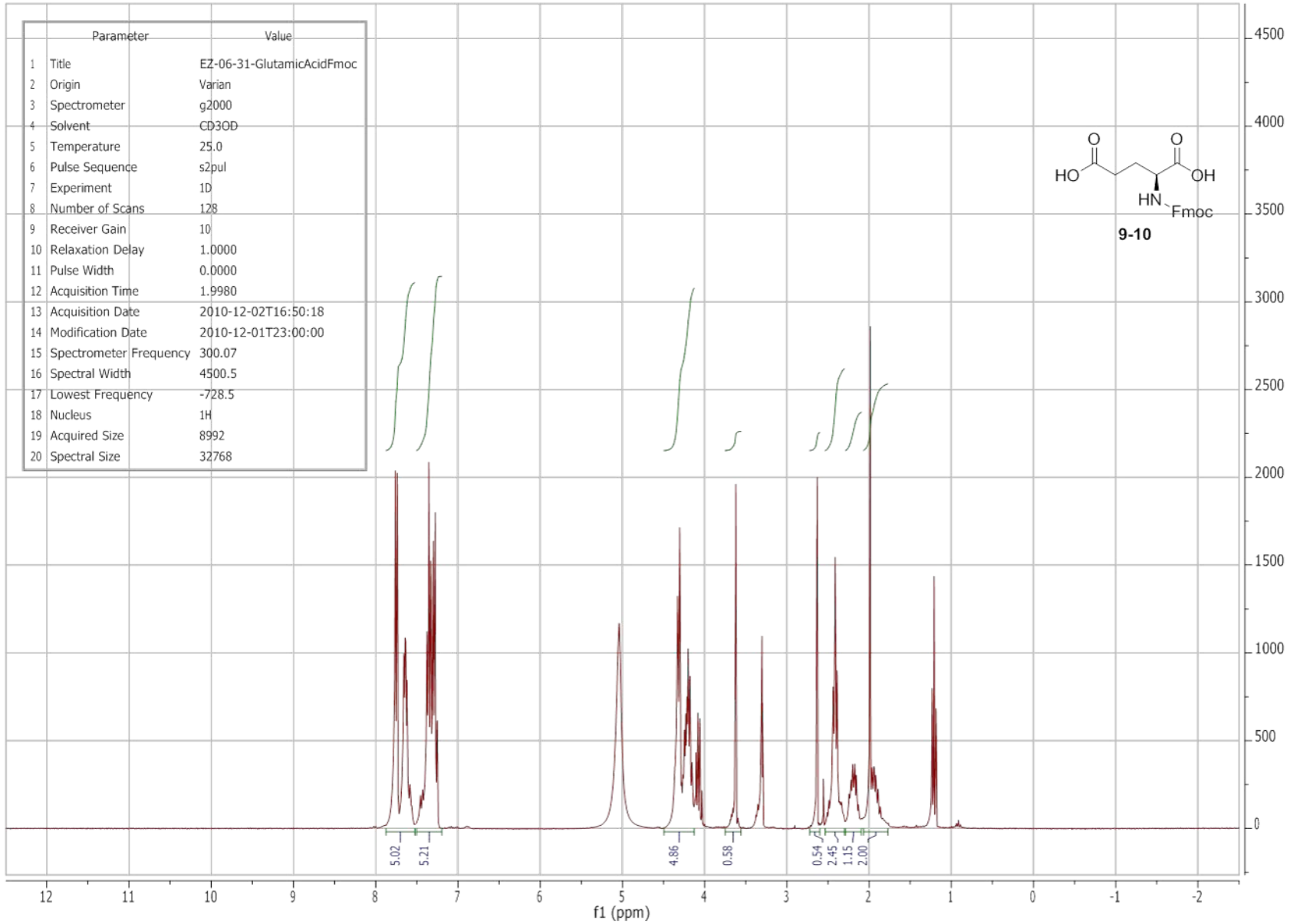
Parameter Value
1 Title EZ-06-31-GlutamicAcidFmoc
2 Origin Varian
3 Spectrometer g2000
4 Solvent CD3OD
5 Temperature 25.0
6 Pulse Sequence s2pul
7 Experiment 1D
8 Number of Scans 128
9 Receiver Gain 10
10 Relaxation Delay 1.0000
11 Pulse Width 0.0000
12 Acquisition Time 1.9980
13 Acquisition Date 2010-12-02T16:50:18
14 Modification Date 2010-12-01T23:00:00
15 Spectrometer Frequency 300.07
16 Spectral Width 4500.5
17 Lowest Frequency -728.5
18 Nucleus 1H
19 Acquired Size 8992
20 Spectral Size 32768
HO
O
O
OH
HN
Fmoc
9-10
5.02
5.21
4.86
0.58
0.54
2.45
1.15
2.00
f1 (ppm)

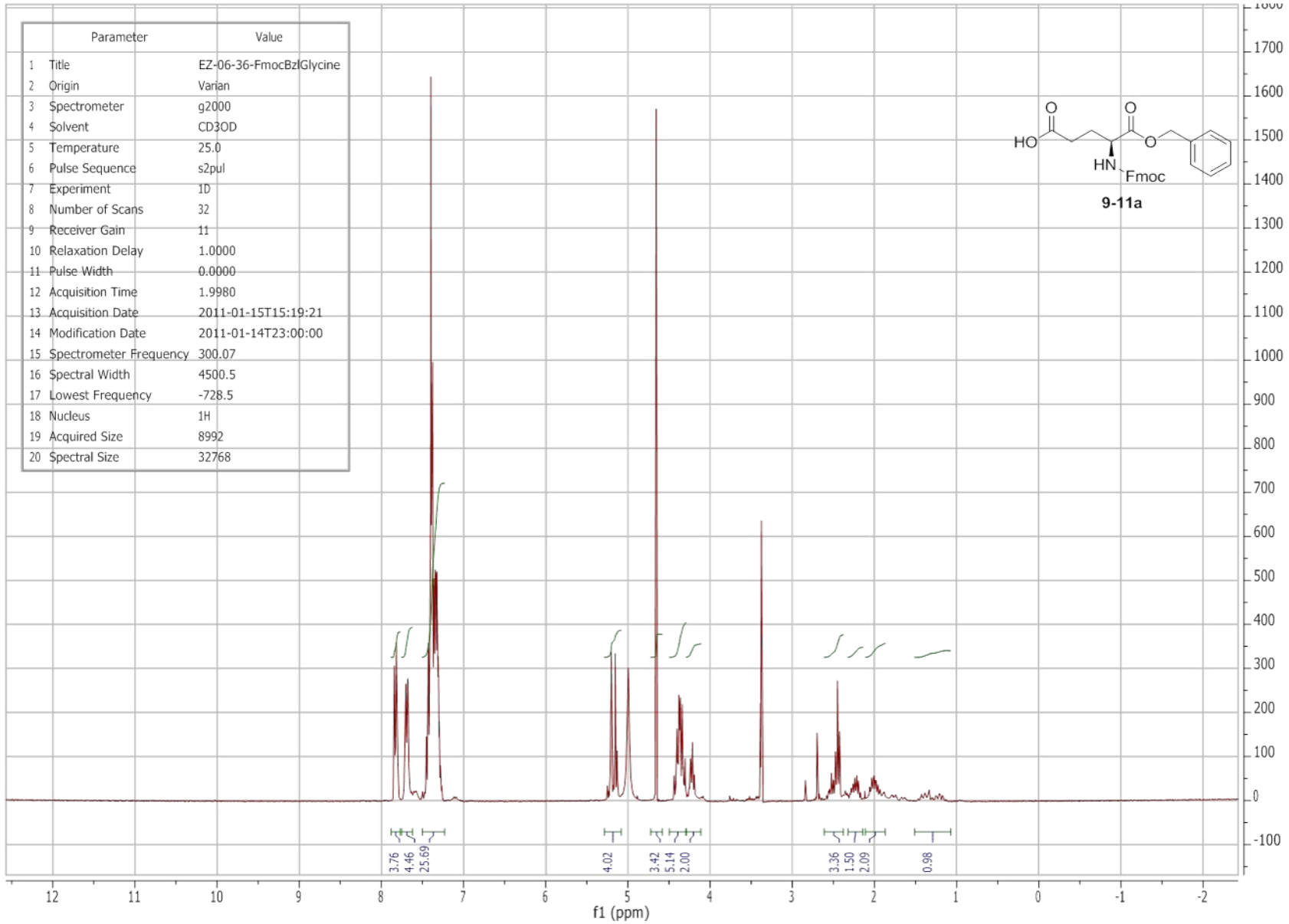
Parameter Value
1 Title EZ-06-36-FmocBzlGlycine
2 Origin Varian
3 Spectrometer g2000
4 Solvent CD3OD
5 Temperature 25.0
6 Pulse Sequence s2pul
7 Experiment 1D
8 Number of Scans 32
9 Receiver Gain 11
10 Relaxation Delay 1.0000
11 Pulse Width 0.0000
12 Acquisition Time 1.9980
13 Acquisition Date 2011-01-15T15:19:21
14 Modification Date 2011-01-14T23:00:00
15 Spectrometer Frequency 300.07
16 Spectral Width 4500.5
17 Lowest Frequency -728.5
18 Nucleus 1H
19 Acquired Size 8992
20 Spectral Size 32768
HO
O
O
O
HN
Fmoc
9-11a
3.76
4.46
25.69
4.02
3.42
5.14
2.00
3.36
1.50
2.09
0.98
f1 (ppm)

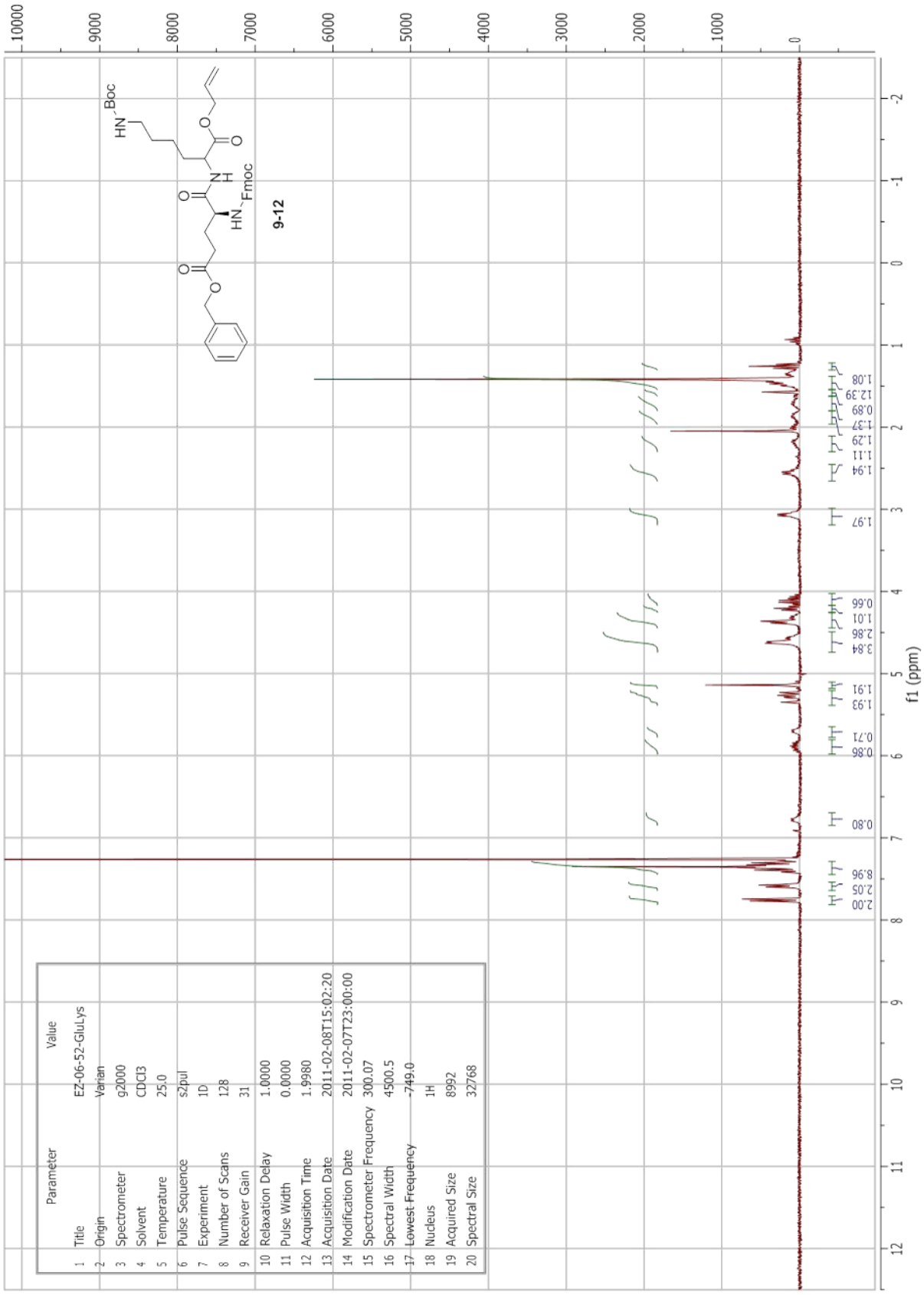

	Parameter	Value
1	Title	EZ-06-52-GluLys
2	Origin	Varian
3	Spectrometer	g2000
4	Solvent	CDCl3
5	Temperature	25.0
6	Pulse Sequence	s2pul
7	Experiment	1D
8	Number of Scans	128
9	Receiver Gain	31
10	Relaxation Delay	1.0000
11	Pulse Width	0.0000
12	Acquisition Time	1.9980
13	Acquisition Date	2011-02-08T15:02:20
14	Modification Date	2011-02-07T23:00:00
15	Spectrometer Frequency	300.07
16	Spectral Width	4500.5
17	Lowest Frequency	-749.0
18	Nucleus	1H
19	Acquired Size	8992
20	Spectral Size	32768

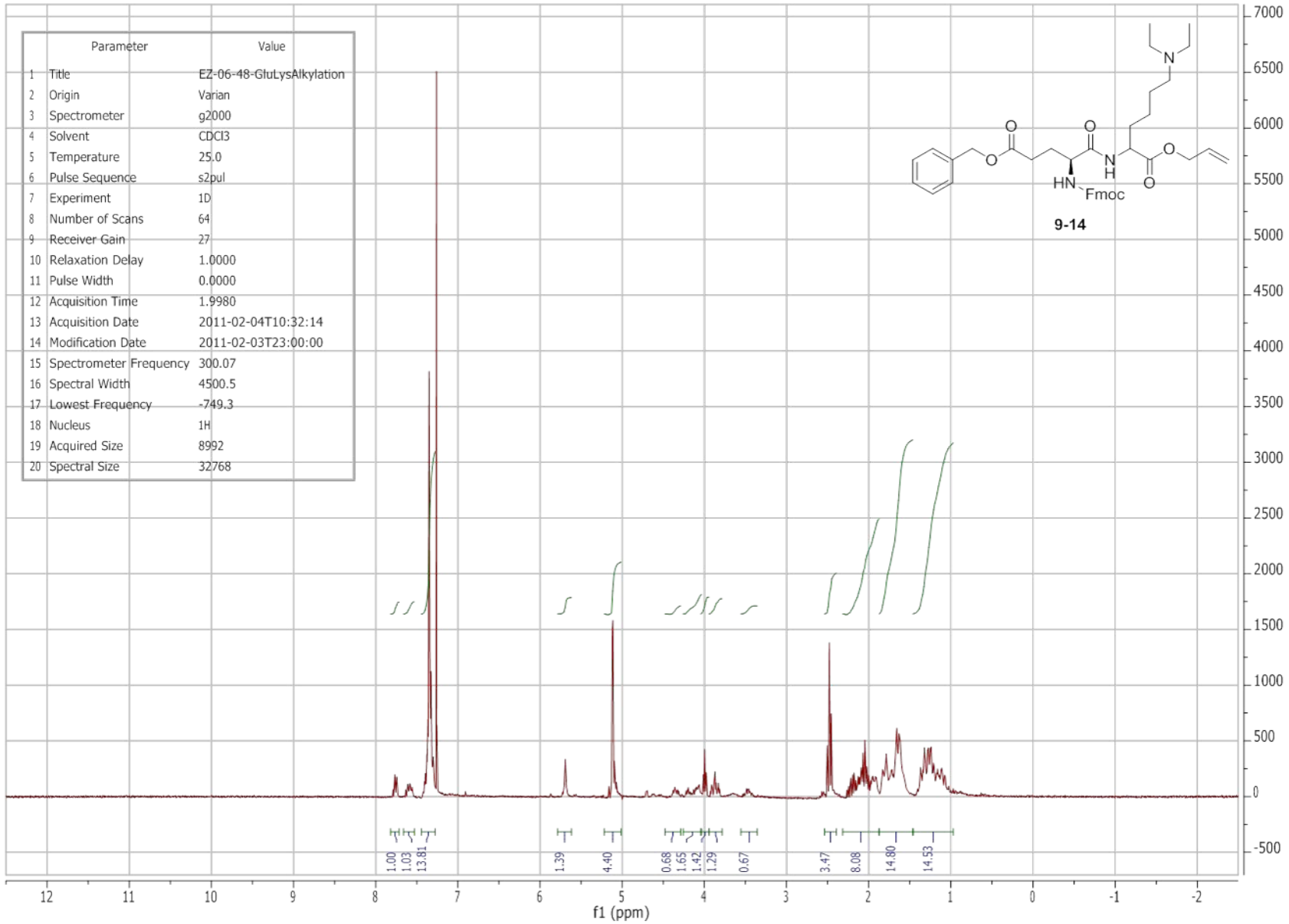
Parameter Value
1 Title EZ-06-48-GluLysAlkylation
2 Origin Varian
3 Spectrometer g2000
4 Solvent CDCl3
5 Temperature 25.0
6 Pulse Sequence s2pul
7 Experiment 1D
8 Number of Scans 64
9 Receiver Gain 27
10 Relaxation Delay 1.0000
11 Pulse Width 0.0000
12 Acquisition Time 1.9980
13 Acquisition Date 2011-02-04T10:32:14
14 Modification Date 2011-02-03T23:00:00
15 Spectrometer Frequency 300.07
16 Spectral Width 4500.5
17 Lowest Frequency -749.3
18 Nucleus 1H
19 Acquired Size 8992
20 Spectral Size 32768
9-14
f1 (ppm)

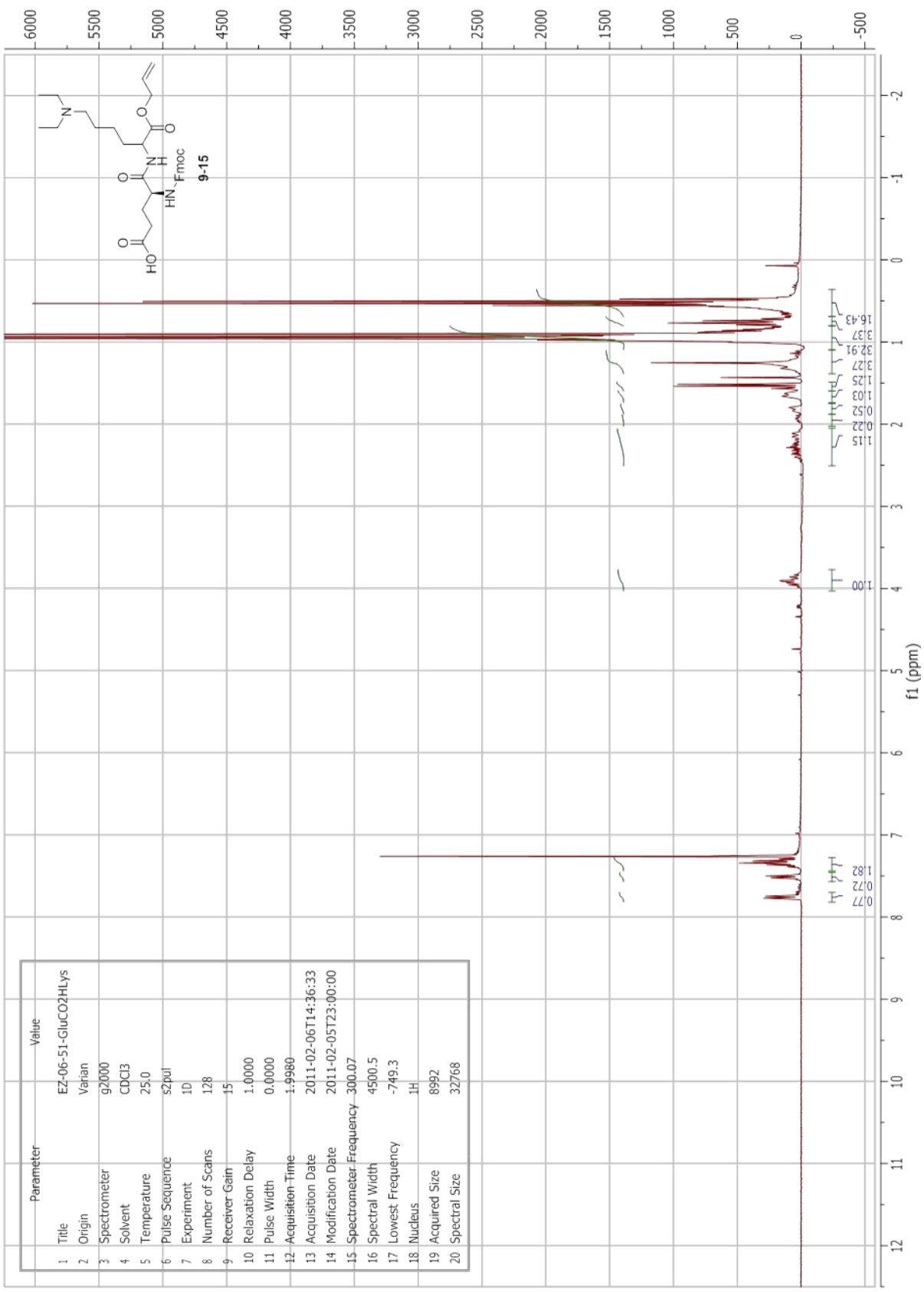
Parameter Value
1 Title EZ-06-51-GluCO2HLys
2 Origin Varian
3 Spectrometer g2000
4 Solvent CDCl3
5 Temperature 25.0
6 Pulse Sequence s2pul
7 Experiment 1D
8 Number of Scans 128
9 Receiver Gain 15
10 Relaxation Delay 1.0000
11 Pulse Width 0.0000
12 Acquisition Time 1.9980
13 Acquisition Date 2011-02-06T14:36:33
14 Modification Date 2011-02-05T23:00:00
15 Spectrometer Frequency 300.07
16 Spectral Width 4500.5
17 Lowest Frequency -749.3
18 Nucleus 1H
19 Acquired Size 8992
20 Spectral Size 32768
9-15
Fmoc
f1 (ppm)

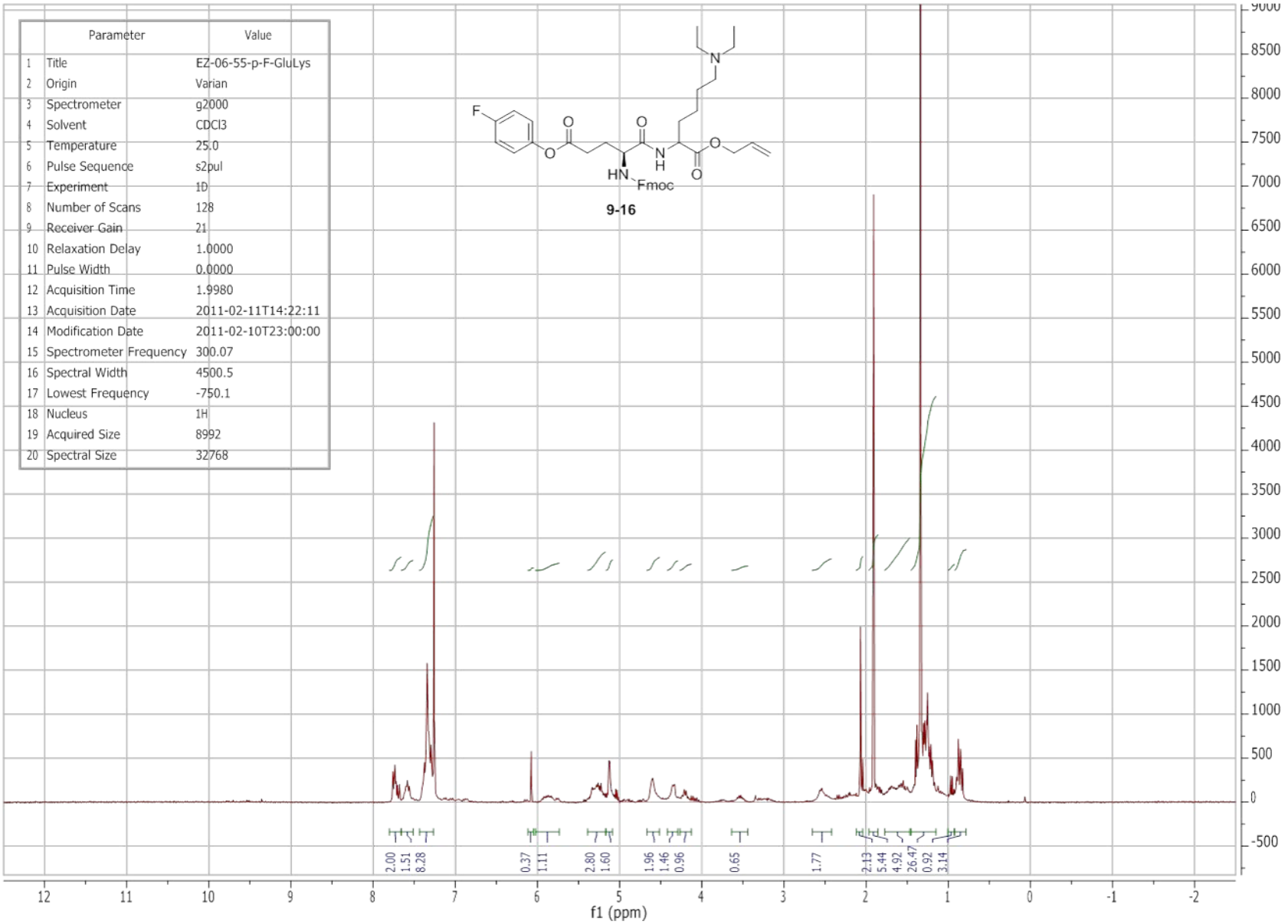
Parameter Value
1 Title EZ-06-55-p-F-GluLys
2 Origin Varian
3 Spectrometer g2000
4 Solvent CDCl3
5 Temperature 25.0
6 Pulse Sequence s2pul
7 Experiment 1D
8 Number of Scans 128
9 Receiver Gain 21
10 Relaxation Delay 1.0000
11 Pulse Width 0.0000
12 Acquisition Time 1.9980
13 Acquisition Date 2011-02-11T14:22:11
14 Modification Date 2011-02-10T23:00:00
15 Spectrometer Frequency 300.07
16 Spectral Width 4500.5
17 Lowest Frequency -750.1
18 Nucleus 1H
19 Acquired Size 8992
20 Spectral Size 32768
F
O
O
O
N
H
HN
Fmoc
N
O
O
9-16
2.00
1.51
8.28
0.37
1.11
2.80
1.60
1.96
1.46
0.96
0.65
1.77
2.13
5.44
4.92
26.47
0.92
3.14
f1 (ppm)

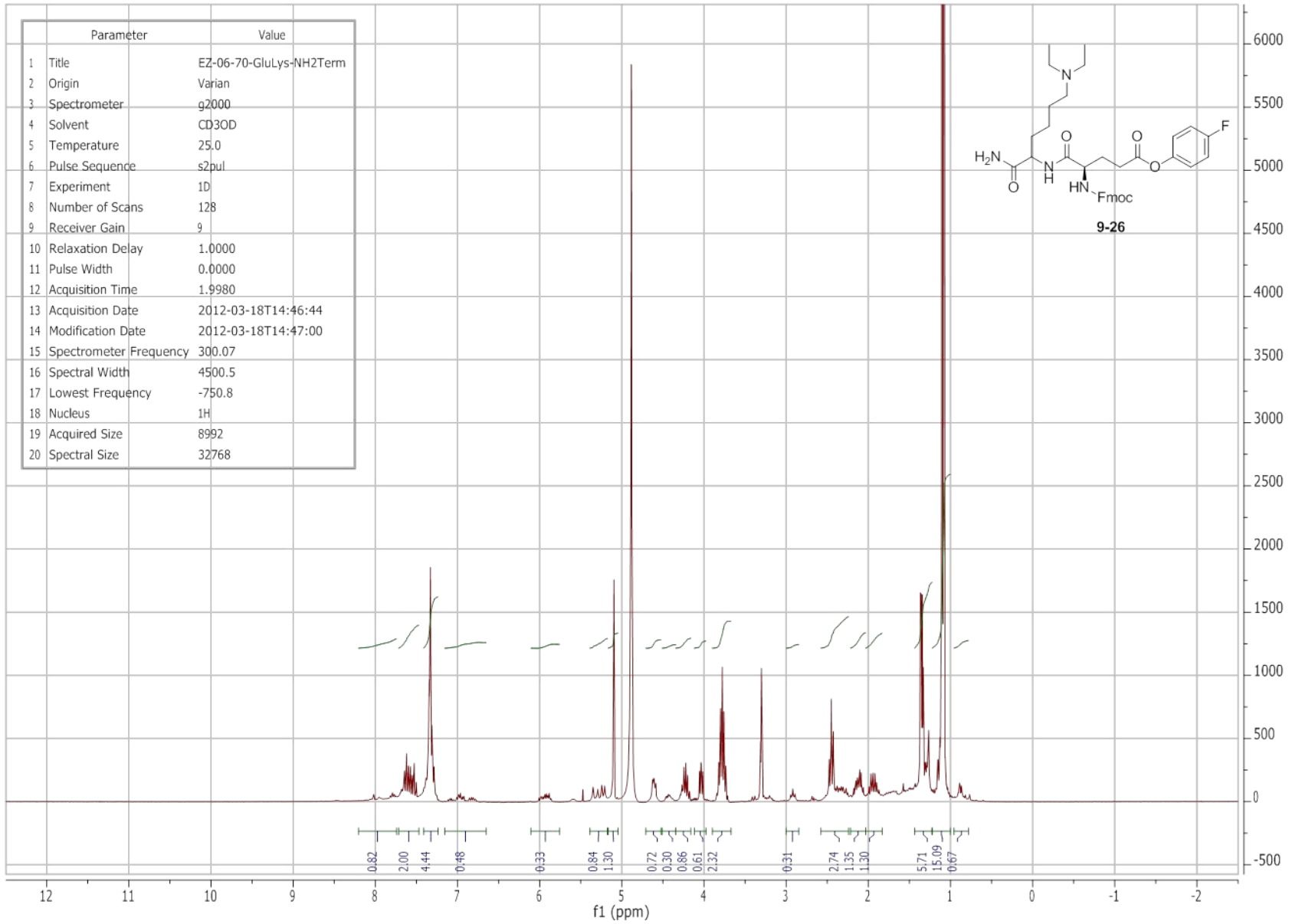
Parameter Value
1 Title EZ-06-70-GluLys-NH2Term
2 Origin Varian
3 Spectrometer g2000
4 Solvent CD3OD
5 Temperature 25.0
6 Pulse Sequence s2pul
7 Experiment 1D
8 Number of Scans 128
9 Receiver Gain 9
10 Relaxation Delay 1.0000
11 Pulse Width 0.0000
12 Acquisition Time 1.9980
13 Acquisition Date 2012-03-18T14:46:44
14 Modification Date 2012-03-18T14:47:00
15 Spectrometer Frequency 300.07
16 Spectral Width 4500.5
17 Lowest Frequency -750.8
18 Nucleus 1H
19 Acquired Size 8992
20 Spectral Size 32768
9-26
f1 (ppm)

	Parameter	Value
1	Title	EZ-05-108-AzidePEGPentynoate
2	Origin	Varian
3	Spectrometer	inova
4	Solvent	CDCl3
5	Temperature	25.0
6	Pulse Sequence	s2pul
7	Experiment	1D
8	Number of Scans	64
9	Receiver Gain	32
10	Relaxation Delay	1.0000
11	Pulse Width	0.0000
12	Acquisition Time	3.2725
13	Acquisition Date	2010-08-07T14:36:15
14	Modification Date	2010-08-06T23:00:00
15	Spectrometer Frequency	399.83
16	Spectral Width	6000.6
17	Lowest Frequency	-990.6
18	Nucleus	1H
19	Acquired Size	19637
20	Spectral Size	65536

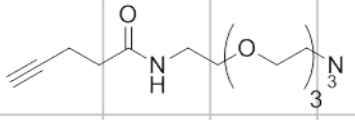

9-27

	Parameter	Value
1	Title	EZ-05-110-Alkyne-PEG-Amine
2	Origin	Varian
3	Spectrometer	inova
4	Solvent	CDCl3
5	Temperature	25.0
6	Pulse Sequence	s2pul
7	Experiment	1D
8	Number of Scans	128
9	Receiver Gain	32
10	Relaxation Delay	1.0000
11	Pulse Width	0.0000
12	Acquisition Time	3.2725
13	Acquisition Date	2010-08-08T18:06:26
14	Modification Date	2010-08-07T23:00:00
15	Spectrometer Frequency	399.83
16	Spectral Width	6000.6
17	Lowest Frequency	-989.3
18	Nucleus	1H
19	Acquired Size	19637
20	Spectral Size	65536

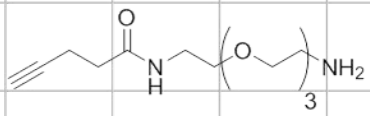

9-28

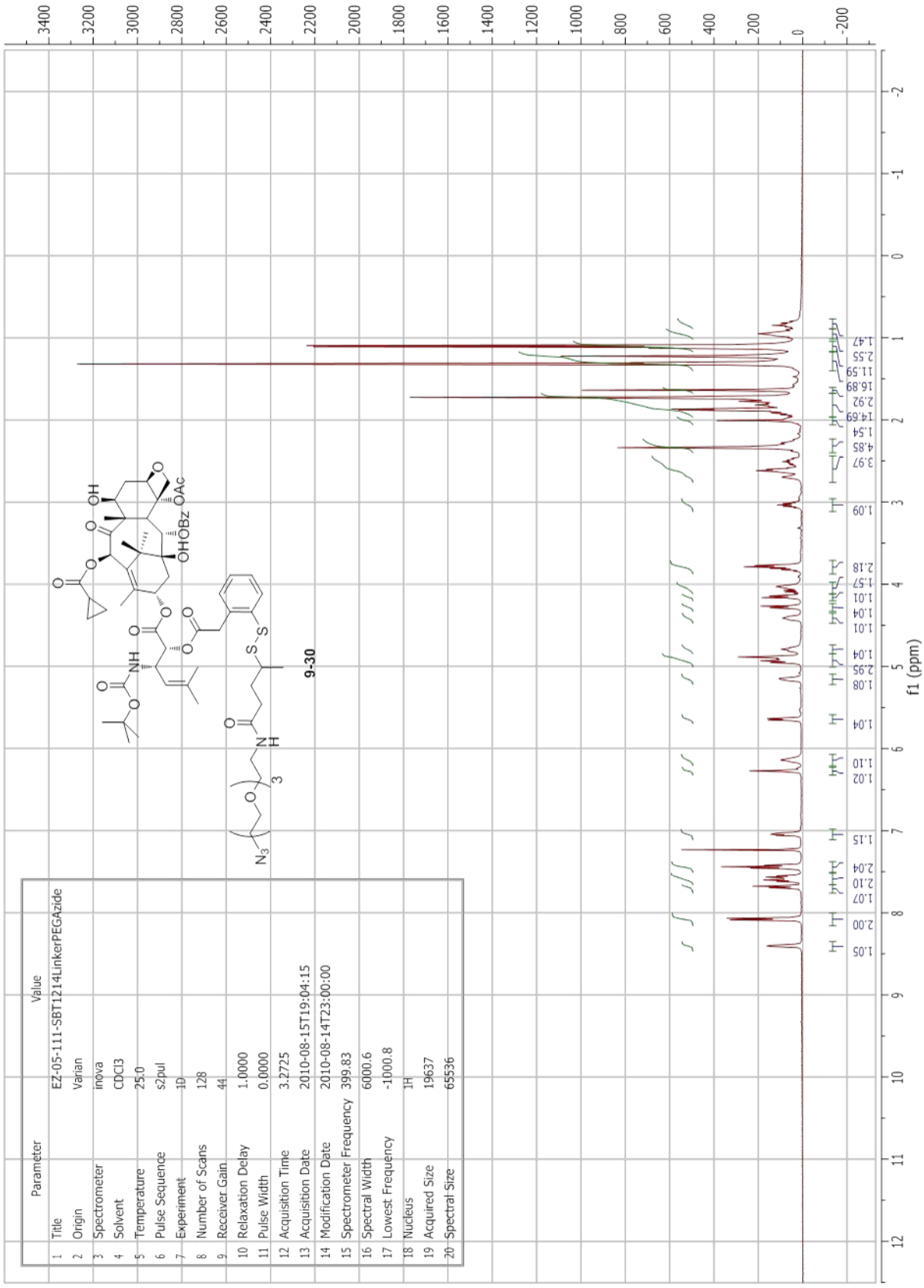
Parameter Value
1 Title EZ-05-111-SBT1214LinkerPEGAzide
2 Origin Varian
3 Spectrometer inova
4 Solvent CDCl3
5 Temperature 25.0
6 Pulse Sequence s2pul
7 Experiment 1D
8 Number of Scans 128
9 Receiver Gain 44
10 Relaxation Delay 1.0000
11 Pulse Width 0.0000
12 Acquisition Time 3.2725
13 Acquisition Date 2010-08-15T19:04:15
14 Modification Date 2010-08-14T23:00:00
15 Spectrometer Frequency 399.83
16 Spectral Width 6000.6
17 Lowest Frequency -1000.8
18 Nucleus 1H
19 Acquired Size 19637
20 Spectral Size 65536
9-30
f1 (ppm)